Molecular and Isotopic Constraints on Oil Accumulation in Tertiary Deltas

Olukayode James SAMUEL, B.Sc.

A thesis submitted to the Newcastle University in partial fulfilment of the requirements for the award of the degree of doctor of philosophy in Petroleum Geochemistry in the faculty of Science, Agriculture and Engineering

School of Civil Engineering and Geosciences, Newcastle University, Newcastle upon Tyne, UK

January 2008

CONTAINS

PULLOUTS

THESIS CONTAINS CD/DVD

DECLARATION

I hereby certify that this work is my own, except where otherwise acknowledged, and that this work has not been submitted previously for a degree at this, or any other university.

Olukayode James SAMUEL

ABSTRACT

Deltaic basins of Tertiary age constitute a significant percentage of the sedimentary environments of the world's known hydrocarbon reserves and with more prospects of huge discoveries, renewed exploration activities are on-going in the progressively deeper waters of the continental shelf of deltaic basins (e.g. Gulf of Mexico, Niger Delta and Beaufort-Mackenzie Delta). Hydrocarbon exploration success depends on the knowledge of the petroleum systems (source rock, migration pathways, reservoirs, traps and seal) contributing to an oil accumulation. Although oil continues to be found in Tertiary delta reservoirs, multidimensional interpretation of literature data on crude oil geochemistry from these deltaic basins reveals a paradox in the geochemical characteristics of some of the reservoired oils with respect to the alleged Tertiary delta source rocks. Consequently there is no consensus on the origin of most of the deltaic petroleum accumulations.

A poor understanding of the petroleum system (in particular the source rocks) escalates the risk of exploration as the presence, let alone the composition and phases, of petroleum could prove difficult to predict in undrilled prospects. Fairly representative crude oil samples taken from accumulations in Tertiary reservoirs of the Assam Delta (India), Beaufort-Mackenzie Delta (Canada), Gulf of Mexico (USA), Niger Delta (Nigeria) and the Kutei Basin (Indonesia) have been characterised for the purpose of predicting their source rock organic facies (organic matter type, depositional environment, age and thermal maturity). Biomarker and stable carbon isotopes analyses have been conducted on 120 samples from these basins in order to better understand the petroleum systems producing them.

All the oils contain the angiosperm higher plant biomarker oleanane, in addition to other biomarkers like bicadinane and lupane which are not ubiquitous, thus providing evidence of higher plant inputs. Novel terpenoid biomarkers were discovered in many of the oils, whose relative abundances correlate strongly with those of conventional terrigenous biomarkers. Oils from Assam and the Kutei Basin are compositionally similar with pronounced terrigenous biomarker and stable carbon isotope characteristics that suggest expulsion from coaly to delta top shales deposited under

highly oxygenated environments. Conversely, oils from the Gulf of Mexico show mixed marine-terrigenous and high marine algae source input biomarker and stable carbon isotopes signatures that suggest limited higher plant contribution to their organic matter. Source rock deposition was under sub-oxic conditions (pristane/phytane) below a stratified water column (presence of gammacerane). On the basis of biomarker and stable carbon isotope data, oil accumulations from the Beaufort–Mackenzie and the Niger Deltas show greater diversity, grouping as dominantly terrigenous and dominantly marine algae sourced end-members, reflecting expulsion from source rocks deposited under oxic non-stratified and sub-oxic stratified water column conditions, respectively.

These clear variations in the geochemistry of the oil accumulations can be attributed to oil sourcing from two discrete units: 1) Oils expelled from within the lean but thick source rock volume of deltas (intra-delta) which are characterised by abundant terrigenous biomarkers and stable carbon isotope signatures; 2) Oils expelled from source rocks rich in marine algal kerogen and envisaged as being laid down prior to the delta prograde, hence now buried below the Tertiary delta (sub-delta). The evidence suggests that sub-delta source rocks charge oil accumulations in the Gulf of Mexico, Beaufort-Mackenzie Delta and the deepwater Niger Delta. Bitumen extracts of core samples of the organic-rich late Cretaceous Araromi shale, from the Gbekebo well drilled in the Dahomey Basin on the western margin of the Niger Delta, are comparable both molecularly and isotopically to the deepwater Niger Delta oil set. This provides confirmatory evidence that similar sub-delta source facies may charge the deepwater Niger Delta accumulations.

ACKNOWLEDGEMENTS

I am grateful to God almighty, the giver of life, hope and destiny for His unfailing love and grace over my life. For God has made my ordinary hands and eyes to behold the extraordinary.

I am most grateful to my supervisors, Drs. Martin Jones and Chris Cornford for their efforts and valuable contributions towards the success of this thesis.

My unreserved gratitude goes to the management and staff of the petroleum technology development fund (PTDF), Nigeria for providing the funds for this research. Dr. John Zumberge (GeoMark Research) and Dr. Joe Curiale (Chevron Corporation) are gratefully acknowledged for their efforts during sample acquisitions for this project. I am grateful to Prof. Lisa Pratt for inviting me as a visiting scientist to carry out compound specific stable isotope analyses at her stable isotopes laboratory at Indiana University, USA. I would like to acknowledge Dr. Peter Nytoft of GEUS for collaborative research in the elucidation of the yet unknown compounds and Dr. Chidi Eneogwe (ExxonMobil) for inspiration to do research in Petroleum Geochemistry and his morale support during this research. I am indebted to Dr. Olabisi A. Adekeye (Unilorin) and Prof. S.O. Akande (Unilorin) for their timely upbringing, useful discussions and encouragement during this research. Special acknowledgement goes to Paul Donohoe, Ian Harrison, Berni Bowler, John Fong, Peter Sauer and Arndt Schimmelmann for their analytical assistance and useful discussions during this research.

I am grateful to staff and management of the Integrated Geochemical Interpretations limited (IGI), especially the director, Dr. Chris Cornford, for accepting me "as a member of the family" through software provision (p; IGI-2.7- used for most of the graphics in this thesis) and for financial supports and technical trainings.

I am highly indebted to my parents (Mr. J.O Samuel and Mrs. Mary Samuel) and my siblings for their enduring morale supports. I acknowledge as always the efforts and contributions of the "Rule of Twelve" who continuously shapes my word: Mr. J.O Samuel, Mrs. Mary Samuel, Mrs. Fola Bobinihi, Dr. Olabisi Dare, Engr. Jerome Bello, Mrs. Alice Ameobi, Mr. Irewole Ayodele (Okunrin náá), Dr. Olabisi Adekeye, Dr. Chidi Eneogwe, Miss Petra Onaiyekan, Pastor John Ameobi and Elder Micheal Eniojukan.

My gratitude goes to my friends who have contributed towards the success of this thesis. I appreciate all the spiritual, material and moral supports of the family of Pastor John and Auntie Margaret Ameobi during my stay in the UK and the fruitful fellowship that I was privileged to have had with brothers and sisters at the Apostolic Church, Newcastle upon Tyne. The memory of our time together will always be on my mind. Auntie Margaret's countless dishes of Jollof rice and Egusi soup, and Oiza's moi-moi did a great job!

DEDICATION

I dedicate this thesis to Mrs. Fola Bobinihi - my high school chemistry teacher, for her timely inspiration during my penultimate year at St. Augustine's College and to many people who fail to outshine their peers because of dearth of counsellors.

...people fall because of no counsellors, but in the multitude of counsellors there is safety- Proverbs. 11:14.

TABLE OF CONTENTS

DECLARATION 2
ABSTRACT 3
DEDICATION 6
TABLE OF CONTENTS 7
PREFACE 26
CHAPTER ONE 27
INTRODUCTION 27
1.0. Introduction 27
1.1. The Problem 28
1.2. Concepts 35
1.2.1. New models for oil sourcing in deltas 35
1.3. Deltas 37
1.4. Delta formation 38
1.5. Types of Delta 41
1.6. Structure of Deltas 42
1.7. Coal as a Petroleum Source Rock in Deltas 43
1.8. The Petroleum System Concept 47
1.9. Tertiary Deltaic Petroleum Systems; present understanding and background to this study 50
1.10. Common Biomarkers in Deltaic oils and Sediments 53
1.11. Aim and Objectives 61
SUMMARY OF THE PETROLEUM SYSTEMS OF CASE STUDY DELTAS 64
2.0. Introduction 64
2.1. Assam Delta 64
2.1.1. Evolution and stratigraphy 64
2.1.2. Characteristics of petroleum systems elements 68
2.1.2.1 Source rocks 69
2.1.2.2. Reservoir rocks 69
2.1.2.3. Traps and seal mechanism 70
2.2. Beaufort-Mackenzie Basin 71
2.2.1. Geological setting and stratigraphy 71
2.2.2. Characteristics of the petroleum systems elements 75
2.2.2.1. Source rocks 75
2.2.2.2. Families of oils and oil-source rock correlations 78
2.2.2.3. Reservoirs, traps and seals 82
2.3. Gulf of Mexico 83
2.3.1. Introduction 83
2.3.2. Characteristics of the petroleum systems elements 86
2.3.2.1. Source rocks 91
2.3.2.2. Reservoirs Traps and seals 93
2.4. Niger Delta 94
2.4.1. Evolution and stratigraphy 94
2.4.2. Characteristics of the petroleum systems elements 96
2.4.2.1. Source rocks 100
2.4.2.2. Reservoir Rock 103
2.4.2.3. Trap and sealing mechanism 104
2.5. Kutei Basin 105

2.5.1. Geological evolution and stratigraphy 105
2.5.2. Characteristics of the petroleum systems elements 110
2.5.2.1. Source rocks 110
2.5.2.2. Reservoir and hydrocarbon trapping mechanisms 111
CHAPTER THREE 113
EXPERIMENTAL METHODS 113
3.0. Introduction 113
3.1. Solid Phase Extraction (SPE) Separation 113
3.2. Gas Chromatography (GC) 115
3.3. Gas Chromatography- Mass Spectrometry (GC-MS) 116
3.4. Gas Chromatography-Mass Spectrometry/Mass Spectrometry (GC-MS-MS) 118
3.5. Gas Chromatography Isotope Ratio Mass Spectrometry (GC-IRMS) 119
3.6. Urea Clathration 121
3.7. Total organic carbon (TOC) analyses 122
3.8. Source rock pyrolysis 123
3.9. Soxhlet extraction of core samples 124
3.10. Separation of pure fractions of compounds A_1, A_2, B_1, B_2 and C 124
CHAPTER FOUR 127
INTERPRETATION OF PETROLEUM GEOCHEMICAL DATA IN THE LITERATURE 127
Summary 127
4.0. Introduction 128
4.1. Crude oil geochemistry 130
4.2. Source organic matter 131
4.2.1. Biomarkers 131
4.2.2. Stable carbon isotopes 136
4.3. Discussion of Tertiary deltaic petroleum systems 141
4.3.1. Compositional-alteration: migration-contamination (leaching), fractionation, and oil mixing as key geochemical processes 142
4.3.2. Source rock groups charging Tertiary delta petroleum systems 144
4.3.2.1. Delta top source rocks (land plants and swamps) 145
4.3.2.2. Sub-marine delta top source rocks 146
4.3.2.3. Pro-delta source rocks 147
4.3.2.4. Sub-delta source rocks 148
4.4. Conclusions 151
CHAPTER FIVE 153
MOLECULAR GEOCHEMISTRY I: OIL CHARACTERIZATION USING CONVENTIONAL MOLECULAR PARAMETERS 153
Summary 153
5.0. Introduction 154
5.1. Methods 155
5.2. Molecular Characteristics of Oils from Assam Delta 155
5.2.1. Normal (n-alkanes) and isoprenoid alkanes 155
5.2.2. Steranes 160
5.2.3. Pentacyclic terpanes 164
5.2.4. Tricyclic and tetracyclic terpanes 168
5.2.5. Aromatic hydrocarbons 169
5.2.6. Summary of source facies and thermal maturity 171
5.3. Molecular characteristics of Beaufort-Mackenzie oils 174

5.3.1. N-alkanes and isoprenoid alkanes 174
5.3.2. Steranes 174
5.3.3. Pentacyclic triterpanes 180
5.3.4. Tricyclic and tetra cyclic terpanes 181
5.3.5. Aromatic hydrocarbons 186
5.3.6. Summary of source facies and thermal maturity 190
5.4. Molecular characteristics of Gulf of Mexico oils 191
5.4.1 N-alkanes and isoprenoid alkanes 191
5.4.2. Steranes 191
5.4.4. Tricyclic and tetracyclic terpanes 199
5.4.5. Aromatic hydrocarbons 199
5.4.6. Summary of source facies and thermal maturity 205
5.5. Molecular Characteristics of the Niger Delta oils 209
5.5.1. N-alkanes and isoprenoid alkanes 209
5.5.2. Steranes 209
5.5.3 Pentacyclic terpanes 216
5.5.4. Tricyclic and tetra cyclic terpanes 219
5.5.5. Aromatics 226
5.5.6. Summary of source facies and thermal maturity 228
5.6. Geochemical Characteristics of oils from Kutei Basin 236
5.6.1. N-alkanes and isoprenoid alkanes 236
5.6.2. Steranes 236
5.6.3. Pentacyclic, tricyclic and tetracyclic terpanes 239
5.6.4. Aromatics 240
5.6.5. Summary of source facies and thermal maturity 242
5.7. Comparative biomarker organofacies signals in the studied oils and their source implications 247
5.7.1. Source rock organic matter type 247
5.7.2. Source rock depositional environment 251
5.7.3. Thermal Maturity 255
5.8. Conclusions 257
CHAPTER SIX 259
MOLECULAR GEOCHEMISTRY II: OIL CHARACTERIZATION USING NOVEL COMPOUNDS 259
Summary 259
6.0. Introduction 260
6.1. Samples 261
6.2. Results and Discussion 262
6.2.1. Gas chromatographic characteristics 262
6.2.2. Distributions in deltaic oils of Tertiary reservoir age 263
6.2.2.1. Niger Delta 264
6.2.2.2. Assam Delta 266
6.2.2.3. Beaufort-Mackenzie Delta 267
6.2.2.4. Gulf of Mexico 267
6.2.2.5. Kutei Basin 269
6.3. Structural Elucidation 270
6.3.1. Mass spectra characteristics of compounds A_1, A_2, B_1, B_2 and C 270
6.3.2. Laboratory experiment to synthesise compounds A_1, A_2, B_1 and B_2 275
6.4. Origin and Predicted Utility of the Novel Compounds 282
6.5. Conclusions 286

CHAPTER SEVEN 291
ISOTOPE GEOCHEMISTRY 291
Summary 291
7.0. Introduction 292
7.1. Sample rationale 294
7.2. Bulk Stable Carbon Isotope Results and Discussion 295
7.2.1. Assam Delta 295
7.2.2. Gulf of Mexico 297
7.3. Compound Specific Stable Carbon isotopes (CSIA) 297
7.3.1. Assam Delta 297
7.3.2. Beaufort-Mackenzie Delta 298
7.3.3. Gulf of Mexico 300
7.3.3. Niger Delta 301
7.4. Controls on the shape of CSIA Plots 303
7.4.1. Investigating the effects of thermal maturity on CSIA profiles 304
7.4.2. Effect of *n*-alkane abundance (short vs. long chain compounds) on CSIA profiles 307
7.4.3. Effect of original organic matter on CSIA profiles 308
7.5. Conclusions 309
CHAPTER EIGHT 314
THE SEARCH FOR SUB-DELTA SOURCE ROCKS: A NIGER DELTA CASE STUDY 314
Summary 314
8.0. Introduction 315
8.1. Samples 318
8.2. Hydrocarbon Source Potential 320
8.3. Comparison of biomarker compositions 322
8.4. Comparison of stable carbon isotope compositions 327
8.5. Summary and source implications 328
CHAPTER NINE 333
CONCLUSIONS AND FUTURE WORK 333
9.0. Introduction 333
9.1. Biomarker compositions 333
9.2. Novel terpane compounds 340
9.3. Stable carbon isotopes characteristics 342
9.4. Model to explain source rock types charging Tertiary deltas as indicated by oil properties 345
9.5. Future work 349
REFERENCES 352

LIST OF TABLES

Chapter One

Table 1. 1: Summary of the petroleum geology and geochemistry of some of the world's major petroleum producing Tertiary deltas.

Chapter Four

Table 4.3. Summary of intra-delta and sub-delta source rocks for some deltas

Chapter Five

Table 5.1: Characteristic isoprenoid and n-alkane ratios for Assam oils

Table 5.2 Source and maturity sterane biomarker parameters for Assam oils

Table 5.3. Source and maturity triterpanes molecular parameters for Assam oils

Table 5.4. Selected thermal maturity and source molecular indicators from aromatic hydrocarbon fractions.

Table 5.5. N-alkane and isoprenoid alkane ratios from the Beaufort-Mackenzie oils

Table 5.6. Source and maturity sterane biomarker parameters for Beaufort-Mackenzie oils.

Table 5.7. Source and maturity triterpanes molecular parameters for Beaufort-Mackenzie oils.

Table 5.8. Selected thermal maturity and source molecular indicators from aromatic hydrocarbon fractions.

Table 5.9. Summary of source facies biomarker parameters for Beaufort-Mackdenzie Delta oils

Table 510. *n*-alkane and isoprenoid alkane ratios for the Gulf of Mexico oil samples

Table 5.11. Sterane source and maturity parameters for the Gulf of Mexico oils

Table 5.12. Characteristic terpane ratios for source and thermal maturity parameters calculated for Gulf of Mexico oils.

Table 5.13. Thermal maturity and source molecular indicators from aromatic hydrocarbon fractions of the Gulf of Mexico oils.

Table 5.14. *n*-alkane and isoprenoid ratios in the Niger Delta oils.

Table 5.15. Sterane source and maturity molecular parameters measured for the Niger Delta oil set.

Table 5.16. Terpane source and maturity parameters measured for the Niger Delta oils

Table 5.17. Selected aromatic thermal maturity and source parameters from the Niger Delta oils.

Table 5.18. *N*-alkanes and isoprenoid alkane ratios in the Kutei Basin oils.

Table 5.19. Sterane source and maturity parameters measured for the Kutei Basin oil set.

Table 5.20. Terpane source and maturity parameters of the oils from the Kutei Basin

Table 5.21. Aromatic hydrocarbon thermal maturity and source indicators from the Kutei Basin oils

Chapter Six

Table 6.1. Source and thermal maturity molecular parameters measured for the selected oils analysed for novel terpane compounds.

Chapter Seven

Table 7.1. Bulk saturated and aromatic hydrocarbon stable carbon isotopes data for Assam and Gulf of Mexico

Table 7.2. Compound Specific stable carbon isotope data of selected Assam crude oil samples

Table 7.3. Compound Specific stable carbon isotope data of selected crude oil samples from Beaufort-Mackenzie Delta

Table 7.4. Compound Specific stable carbon isotope data of selected crude oil samples from the Gulf of Mexico

Table 7.5. Compound Specific stable carbon isotope data of selected Niger Delta crude oil samples.

Chapter Eight

Table 8.1. Bulk geochemical and selected biomarker parameters for the analysed Araromi shale in Dahomey Basin

Table 8.2. Compound specific stable carbon isotope data for representative deepwater and oils and Araromi shale extracts.

Chapter Nine

Table 9.1. Summary of the Biomarker composition of oils from the Basins of study

LIST OF FIGURES

Chapter One

Figure 1.1. Bimodal distribution of Total Organic Carbon (TOC) values from 338 samples with >2%TOC from 21 published accounts of Tertiary deltas worldwide. (Source: 'World Data' p:IGI-2, Version 2.3, IGI Ltd., 2006).

Figure 1.2. Kerogen types of Tertiary coals and carbargillites (>12 wt% TOC) taken from 15 published studies with TOC and Rock-Eval analyses. (Source: 'World Data' p:IGI-2, Version 2.3, IGI Ltd., 2006).

Figure 1.3. Visual kerogen types from coals and shales from 8 publications in a world-wide literature database. (Source: 'World Data' p:IGI-2, Version 2.3, IGI Ltd., 2006).

Figure1.4. Cartoon illustrating how high expulsion and migration efficiencies made possible by interconnected faults and sand and shale couplets of deltaic sedimentary architecture.

Figure 1.5. Cartoon illustrating the charging of Tertiary reservoirs by sub-delta source kitchens

Figure 1.6. A block diagram showing some sedimentary depositional environments. The red arrow highlights the deltaic setting among other environments.

Figure 1. 7. A cartoon showing the components of a river system feeding sediments to the receiving basin where delta is formed.

Figure1.8. Map showing the location of major deltas of the world and their solid sediment discharge capacity.

Figure1.9. Galloway's Ternary diagram classifying deltas using the relative influence of wave, tide and river processes.

Figure 1.10. Map of the world shows the global distribution of major Tertiary deltaic basins with known hydrocarbon potential. The name in bracket is the draining river. Red squares denote selected case studies.

Figure1.11. Representative reaction pathway for the formation of oleanane from higher plant triterpenoids. Large arrows indicate biogenic input(Source; Killops & Killops, 2005).

Figure1.12. Representative reaction pathway for the formation of polymethylnaphthalenes from terpenoidal precursors.(Source; Killops & Killops, 2005)

Figure 1.13. Representative reaction network showing triterpenoid aromatization reactions and products from α-amyrin(source: Killops & Killops, 2005).

Chapter Two

Figure 2.1. Map showing the location of Assam in the north-eastern corner of India (red box). Map taken from:http://www.mapsofindia.com)

Figure 2.2. Generalised stratigraphy of Assam (Source: Raju & Mathur, 1995).

Figure 2.3. Location map of Canadian Beaufort and Mackenzie River Delta in north-western Canada. Map shows location of some oil wells where samples have been collected (adapted from Curiale, 1991).

Figure 2.4. Generalised stratigraphy of the Beaufort Mackenzie Basin (from Tang & Lerche, 1991, after Dixon & Dietrich, 1988).

Figure 2.5.Map showing the location of the Gulf of Mexico Basin.
Source: http://student.britannica.com/eb/art/print?id=54971&articleTypeId=0

Figure 2.6. Generalized stratigraphy of the northern Gulf of Mexico showing the Mesozoic and Cenozoic sequences after Fails, (1990).

Figure 2.7. Map of the Gulf of Guinea showing the approximate location of the Niger Delta (red box) in the south western Nigeria coast on the Gulf of Guinea (Source: http://news.bbc.co.uk/olmedia/1275000/images/_1275867_africa_west_map300.gif). Note map not drawn to scale

Figure 2.8. Generalized stratigraphy of the Niger Delta. Modified from Shannon & Naylor (1989) and Doust & Omatsola (1990). (Source: Tuttle *et al.*, 1999).

Figure 2.9. Map showing the mega sedimentary units (depobelts) and their respective ages in the Niger Delta basin. Source: Ejedawe *et al.*, 1984.

Figure 2.10. Sequence stratigraphic model for the central portion of the Niger Delta showing the relationship between source rocks, migration pathways and hydrocarbon traps related to growth faults. Modified from Tuttle *et al.*, 1999, after Stacher, 1995).

Figure 2.11. Location map showing the approximate outline of the Kutei Basin in the Eastern Kalimantan in the Island of Borneo (after Curiale *et al.*, 2005).

Figure 2.12. The geological map of the Kutei Basin. Note the location of the Mahakam River Delta in the easteen coast of the Kutei Basin (after Moss *et al.*, 1997)

Figure 2.13.Generalised stratigraphy of the Kutei Basin (after Moss *et al.*, 1997)

Chapter Four

Figure 4.1. Ternary diagram showing the plot of C27 C28 and C29 steranes (based on 5 α(H), 14 α(H), 17 α(H)-sterane peaks from m/z 217 mass chromatograms) interpreted in terms of likely kerogen precursor (interpretational overlay from IGI's

p:IGI-2 software modified after Huang and Meinschein, 1979). Data source: Assam: Raju and Mathur, (1995); Goswami et al., (2005). Gulf of Mexico: Geomark Research. Kutei Basin: Curiale et al., (2005). Mackenzie: Brooks (1986a, 1986b); Curiale, (1991). Mahakam Delta: Peters et al. (2000). Niger Delta: Eneogwe and Ekundayo, (2003).

Figure 4.2. Cross plot of canonical variable (CV) and a ratio of sterane 29 and 27 carbon numbers with ααα stereochemistry at the 5, 14 and 17 carbon positions. The plot discriminates samples based on the likely source rock organic matter facies as either marine, terrigenous or intermediate (mixed oils). Data source: Assam: Goswami *et al.* (2005). Gulf of Mexico: Geomark Research. Mackenzie: Curiale, (1991). Mahakam Delta: Peters *et al.* (2000). Niger Delta dataset mostly from western oil accumulations: Eneogwe and Ekundayo, (2003).

Figure 4.3. An histogram of canonical variable (CV) separates samples into land plant dominated coal and associated delta top carbonaceous shale- sourced oils and marine organic matter- sourced oils. Data source: Assam: Goswami *et al.* (2005). Gulf of Mexico: GeoMark Research. Mackenzie: Curiale (1991). Mahakam Delta: Peters *et al.* (2000). Niger Delta dataset mostly from western oil accumulations: Eneogwe and Ekundayo (2003).

Figure 4.4. Cross plot of canonical variable (CV) and the ratio of steranes with 29 and 27 carbon numbers having 5α(H),14α(H),17α(H) stereochemistry. The plot discriminates samples based on the likely source rock organic matter facies as either marine, terrigenous or intermediate (mixed oils). Note some samples e.g. some Beaufort-Mackenzie oils having marine sterane composition incorrectly plot in the terrigenous facies because of their elevated CV (>0.47)

Figure 4.5. Hypothetical Section through a delta showing source rocks indicated by oil properties

Figure 4.6. Rock-Eval characterisation for source and non-source rocks from Mackenzie, Mississippi and Niger deltas showing kerogen type (Hydrogen Index) and maturity (Tmax) and richness (TOC – symbol size). Data from USGS public web database (2003).

Chapter Five

Figure 5.1. Representative gas chromatogram of samples of oils from Assam Delta (India). Numbers on peaks refer to n-alkanes with that number of carbon atoms.

Figure 5.2: Source rock anoxia inferred from the histogram of pristane and phytane ratios for the Assam oils. Overlay field after IGI's p: IGI 2.7 geochemical interpretation software.

Figure 5.3. Cross plot of C29 20S/S+R sterane isomerisation maturity parameter and pr/ph ratio to investigate effects of thermal maturity on the pr/ph ratios for the Assam oils.

Figure 5.4. Representative GC-MS-MS mass chromatogram from sample AS-13 showing sterane distributions typical of Assam oils. Peak identities are in Appendix IIIa. Note absence of detectable peak for m/z 414→217 diagnostic of C_{30} steranes.

Figure 5.5. Ternary diagram showing the distribution of the 27, 28 and 29 carbon number regular steranes with 5α(H), 14α(H), 17α(H)- 20R configuration from GC-MS-MS analysis. Interpretational overlay from IGI's p: IGI-2 software modified after Huang and Meinschein (1979).

Figure 5.6. Representative partial m/z 191 mass chromatogram showing pentacyclic terpane distribution in a crude oil sample (sample AS-15) from Assam Delta. Peak identification is given in appendix IIIb. The increase in the retention time difference and peak broadening for compounds eluting after C_{32} bishomohopane is a common chromatographic effect resulting from the use of a 60m column.

Figure 5.7. GC-MS-MS mass chromatogram showing the C_{30} bicadinanes (m/z 412→369) and methylbicadinanes (m/z 426→383) in sample AS-13 of the Assam sample set. Peak identification is by retention time and comparison of chromatogram with published data. T, T1 and R are C_{30} bicadinanes with the trans-trans-trans configuration and MeT and MeT1 are their methylated homologues, while W2 is the cis-cis-trans C_{30} bicadinane isomers (van Aarssen *et al.*, 1990).

Figure 5.8. Representative partial m/z 191 mass chromatogram showing the distributions of tricyclic and tetra cyclic terpanes in sample AS-13. Peak identifications are presented in appendix IIIc

Figure 5.9. GC-MS m/z 128, 142, 156 and 170 mass chromatograms showing the distributions of naphthalene and alkylnaphthalenes in a representative crude oil (sample AS-13) from Assam. Note integers denote the position of methylation in each isomer, EN represents ethylnaphthalene.

Figure 5.10. GC-MS m/z 178 and 192 showing the distributions of phenanthrene and methylphenanthrenes in a representative oil (sample AS-13) from Assam. P = phenanthrene, and 2-MP, 3-MP, 9-MP and 1-MP are methylphenanthrenes with the integers denoting the position of methyl substitution on the phenanthrene ring.

Figure 5.11. Representative gas chromatograms for samples of crude oil from Beaufort-Mackenzie Delta. Integers refer to *n*-alkane chain length while pr = pristane and ph = phytane.

Figure 5.12. Source rock anoxia inferred from the histogram of pristane and phytane ratios. Histogram show the two distinct distributions for oils from the Beaufort-Mackenzie Delta. Overlay field after IGI's p: IGI 2.7 geochemical interpretation software

Figure 5.13. Representative GC-MS-MS mass chromatograms showing the distribution of steranes in terrigenous type samples (high C_{29} and absence of C_{30} sterane) of the Beaufort-Mackenzie Delta, from sample BM-3. Note high noise in m/z 414-217 transition diagnostic of C_{30} 24-*n*-propyl cholestane. Peak identity in appendix IIIa.

Figure 5.14. Representative GC-MS-MS mass chromatograms from sample BM-4 showing the distribution of steranes in Beaufort-Mackenzie Delta marine type oils. Note presence of peaks labelled 22, 23, 24,25,26,27&28 in the m/z 414→217 transition diagnostic of C_{30} diasteranes and regular steranes. Peak identity in appendix IIIa.

Figure 5.15. Ternary diagram showing the plot of C_{27} C_{28} and C_{29} steranes (based on 5α(H),14α(H),17α(H) 20R sterane peaks from appropriate GC-MS-MS transitions) interpreted in terms of likely kerogen precursor. Interpretational overlay from IGI's p: IGI-2 software modified after Huang and Meinschein (1979).

Figure 5.16. Partial m/z 191 mass chromatogram showing triterpane distribution in a typical marine organofacies oil (sample BM-2) of the Beaufort-Mackenzie Delta. Peak identity in appendix IIIb

Figure 5.17. Partial m/z 191 showing triterpane distributions in a typical terrigenous organofacies oil (sample BM-11) of the Beaufort-Mackenzie Delta. Peak identity in Appendix IIIb.

Figure 5.18. Partial m/z 191 mass chromatograms showing the distributions of tricyclic and tetracyclic terpanes in a marine organofacies type oil (upper chromatogram, sample BM-2) and terrigenous facies oil (lower chromatogram, Sample BM-11) from the Beaufort-Mackenzie Delta. Compound Y1 is the unknown compound Y1 also found in Assam and Niger Delta oils. Peak identifications in Appendix IIIc.

Figure 5.19. GC-MS m/z 128, 142, 156 and 170 showing the distributions of naphthalene and alkylnaphthalenes in representative oil (sample BM-12) from the Beaufort-Mackenzie Delta. Note integer denotes the position of alkylation in each isomer. EN represents ethylnaphthalene

Figure 5.20. GC-MS m/z 178 and 192 showing the distributions of phenanthrene and methylphenanthrenes in representative oil (sample BM-12) from the Beaufort-Mackenzie Delta. P = phenanthrene, and 2-MP, 3-MP, 9-MP and 1-MP are methylphenanthrenes with the integers denoting the position of methyl substitution on the phenanthrene ring.

Figure 5.21. Representative gas chromatograms showing the distributions of *n*-alkanes and isoprenoid alkanes in Tertiary deltaic oils from Gulf of Mexico.

Figure 5.22. Source rock anoxia inferred from the histogram of pristane and phytane ratios calculated for the oils of Gulf of Mexico. Overlay field after IGI's p: IGI 2.7 geochemical interpretation software.

Figure 5.23. Representative GC-MS-MS mass chromatograms from sample GOM-4 showing the distribution of steranes typical of deltaic Gulf of Mexico oils. Note presence of peaks in m/z 414→217 transition chromatogram diagnostic of C_{30} 24-*n*-propyl cholestane. Peaks identity in Appendix IIIa.

Figure 5.24a. Ternary diagram showing the distribution of the 27, 28 and 29 carbon number regular steranes with 5α(H),14α(H),17α(H) 20R configuration from GC-MS-MS analysis. Interpretational overlay from IGI's p: IGI-2 software modified after Huang and Meinschein (1979).

Figure 5.24b. Histogram of the ratio of % ($C_{29}/C_{29}+C_{27}$) for 5α(H),14α(H),17α(H) 20R sterane configuration separates the Gulf of Mexico oils into two groups. Base depth refers to the reservoir depths.

Figure 5.25. Representative partial m/z 191 mass chromatogram showing pentacyclic terpanes in a crude oil (sample GOM-4) from the Gulf of Mexico. Peak identification is given in Appendix IIIb.

Figure 5.26. Partial m/z 191 mass chromatogram showing the distribution of tricyclic and tetra cyclic terpanes in sample GOM-4 which is representative of the Gulf of Mexico oils analysed. See Appendix IIIc for peak annotations.

Figure 5.27. GC-MS m/z 128, 142, 156 and 170 showing the distributions of naphthalene and alkylnaphthalenes in a representative oil (GOM-4) from the Gulf of Mexico. Note integers denote the position of alkylation in each isomer. EN represents ethylnaphthalene.

Figure 5.28. GC-MS m/z 178 and 192 showing the distributions of phenanthrene and methylphenanthrene in representative oil (sample GOM-4) from the Gulf of Mexico. P = phenanthrene, and 2-MP, 3-MP, 9-MP and 1-MP are methylphenanthrenes with the integers denoting the position of methyl substitution on the phenanthrene ring

Figure 5.29a. Plot of Ts/Tm against C29S/S+R thermal maturity paramters shows that the analysed Gulf of Mexioc oils are early- mid-mature. Sample symbols are based on Pr/Ph ratios.

Figure 5.29b. Plots of St29S/R (5α(H),14α(H), 17α(H)- C_{29} 20S/20S+20R sterane isomerisation maturity), St29 I/R (5α(H), 14β(H), 17β(H)- 20S +20R / 5α(H), 14β(H), 17β(H) + 5α(H), 14α(H), 17α(H)- 20S+20R C29 steranes) and Ts/Tm thermal maturity parameters against reservoir depths. Plot show no apparent thermal maturity variation with reservoir depths.

Figure 5.30. Plot of % St29S/R(% 5α(H),14α(H), 17α(H)- C_{29} 20S/20S+20R sterane isomerisation maturity versus C_{29} iso/regular ((5α(H), 14β(H), 17β(H)- 20S +20R / 5α(H), 14α(H), 17α(H)- 20S+20R) steranes shows evidence of likely migration fractionation of the primary oils.

Figure 5.31. Representative gas chromatograms showing the distributions of *n*-alkanes and isoprenoid alkanes in samples of oils from Niger Delta. The upper chromatogram is typical of terrigenous facies(sample NDO10), while the middle chromatogram is representative of the deepwater (marine organofacies, sample NDO14) and the lower chromatogram is intermediate, (sample NDO45).

Figure 5.32. Source rock anoxia inferred from pr/ph ratios of the Niger Delta oil set. The wide range of pr/ph ratio reflects variable source rock depositional conditions. Overlay field after IGI's p:IGI 2.7 geochemical interpretation software.

Figure 5.33. Representative GC-MS-MS mass chromatograms showing the distributions of C_{27} (m/z 372→217) C_{28} (m/z 386→217), C_{29} (m/z 400→217) and C_{30} (m/z 414→217) steranes in marine organofacies (deepwater sample NDO12) crude oil samples from the Niger Delta. Peak annotation in Appendix IIIa

Figure 5.34. Representative GC-MS-MS mass chromatogram showing the distributions of C_{27} (372→217) C_{28} (386→217), C_{29} (400→217) and C_{30} (414→217) steranes typical of a terrigenous organofacies (sample NDO03) oil of the Niger Delta. Note absence of C_{30} (414→217) steranes. Peak annotation in Appendix IIIa

Figure 5.35. Ternary diagram showing the distribution of the 27, 28 and 29 carbon number regular steranes with 5α(H), 14α(H), 17α(H)- 20R configuration from GCMS/MS analysis. Interpretational overlay from IGI's p: IGI-2 software modified after Huang and Meinschein (1979). Note North Sea oil permits a comparison of marine sterane distribution with the deepwater oils.

Figure 5.36. Partial m/z 191 mass chromatogram from sample NDO03 showing distribution of pentacyclic terpanes in a terrigenous organofacies oil of the Niger Delta. Peak identities are given in Appendix IIIb.

Figure 5.37. Partial m/z 191 mass chromatogram of a deepwater oil (sample NDO12) representative of marine organofacies oils of Niger Delta. Peak identities are presented in Appendix IIIb.

Figure 5.38. Cross plot of oleanane index against C_{30} 24-*n*-propyl cholestane relative abundance. The plot separates oils into three families; namely, A= marine superfamily dominated by the deepwater oils B = intermediate family of mixed marine and terrigenous and C = terrigenous superfamily dominated by shallow water oils.

Figure 5.39.Cross plot of pr/ph ratios (redox) against gammacerane index (salinity stratification) which separates oils into families consistent with their depositional environments and organic matter source. Note the clustering of significant proportion of the western oils with the deepwater oils, suggestive of similar depositional conditions.

Figure 5.40. Representative partial m/z 191 showing the distributions of tricyclic and tetracyclic terpanes in typical terrigenous oil (sample NDO02, upper) and marine organofacie type oil (sample NDO23, lower). Peak identity is provided in Appendix IIIc.

Figure 5.41. Partial m/z 191 mass chromatogram showing the distribution of common tricyclic terpanes and unknown compounds X Y, Y_1, Z and Z_1 in oils of the three families. Peaks annotation TC_{19}- TC_{29} = C_{19}-C_{29} tricyclic terpanes. Tet = tetracyclic terpane

Figure 5.42. Cross plot of the X/X+TC_{20} and Y/Y+TC_{23} tricyclic terpanes terrigenous index (TTTI). X and Y are two unknown tricyclic terpanes, while TC_{20} and TC_{23} are the well characterized tricyclic terpanes containing 20 and 23 carbons in their ring structures.

Figure 5.43. Cross plot of oleanane index against Y/Y+TC23 showing a positive correlation between the two parameters. OL Index = oleanane index (18 α(H) +18 β(H)-oleanane/ 17α(H), 14 β(H)-C_{30} hopane. Y is the unknown tricyclic terpane compound Y in figure 5.39. TC_{23} = tricyclic terpane containing 23 carbons in its ring structure

Figure 5.44. Mass spectrum of compound X

Figure 5.45. Mass spectrum of compound Y

Figure 5.46. Mass spectrum for compound Y1

Figure 5.47. Mass spectrum for compound Z

Figure 5.48. Mass spectrum for compound Z1

Figure 5.49. GC-MS m/z 128, 142, 156 and 170 showing the distributions of naphthalene and alkylnaphthalenes in representative oil (sample NDO17) from the Niger Delta. Note integer denotes the position of alkylation in each isomer.

Figure 5.50. GC-MS m/z 178 and 192 showing the distributions of phenanthrenene and methylphenanthrenes in a representative oil (sample NDO17) from the Niger Delta. P = phenanthrene, and 2-MP, 3-MP, 9-MP and 1-MP are methylphenanthrenes with the integers denoting the position of methyl substitution on the phenanthrene ring structure.

Figure 5.51. Representative gas chromatograms showing the distributions of *n*-alkanes and isoprenoid alkanes in samples of oils from Kutei Basin.

Figure 5.52. GC-MS-MS mass chromatogram showing the distributions of steranes in oil sample KT-5 from the Kutei Basin. GC-MS-MS chromatograms shown are: m/z 372→217 (C_{27} steranes), 386→217(C_{28} steranes), 400→217 (C_{29} Steranes) and 414→217(C_{30} steranes). Peak annotation is in Appendix IIIa.

Figure 5.53. Ternary diagram showing the distribution of the Kutei oils 27, 28 and 29 carbon number regular steranes with 5α(H),14α(H),17α(H) 20R configuration, from GC-MS-MS analyses. Interpretational overlay from IGI's p: IGI-2.27 software modified after Huang and Meinschein (1979).

Figure 5.54. Partial m/z 191 mass chromatogram showing the distribution of pentacyclic terpanes in a representative Kutei oil sample (KT-5). Peak annotation is in Appendix IIIb

Figure 5.55. GC-MS m/z 128, 142, 156 and 170 mass chromatograms showing the distributions of naphthalene and alkylnaphthalenes in a representative oil (sample KT-

5) from the Kutei Basin. Note integer denotes the position of alkylation in each isomer. EN represents ethylnaphthalene.

Figure 5.56. GC-MS m/z 178 and 192 mass chromatograms showing the distributions of phenanthrene and methylphenanthrenes in a representative oil (sample KT-5) from the Kutei Basin. P = phenanthrene, and 2-MP, 3-MP, 9-MP and 1-MP are methylphenanthrenes with the integers denoting the position of methyl substitution on the phenanthrene ring.

Figure 5.57. Ternary diagram showing the distribution of the 27, 28 and 29 carbon number regular steranes with 5α(H),14α(H),17α(H) 20R configuration from GC-MS-MS analyses of oils from the case study deltas. Interpretational overlay from IGI's p: IGI-2 software modified after Huang and Meinschein (1979). Note the North Sea oil permits a comparison of marine organofacies with the oils.

Figure 5.58. Novel plot of oleanane index against the C_{30} 24-*n*- propyl cholestane parameter defines oils into various zones determined by their primary source rock organic matter inputs

Figure 5.59. Source rock anoxia inferred from pr/ph ratios. The wide range of values for the crude oil samples reflects variable source rock depositional conditions for the oils.

Figure 5.60. Cross plot of pr/ph (redox) against gammacerane index (salinity stratification) separates oils into families consistent with their depositional environments and organic matter source. Gammacerane index = 10*gammacerane / C_{30} 17α(H),21β(H) hopane

Figure 5.61. Oil source rock anoxia inferred from pristane/nC_{17} and ph/nC_{18} ratios. These parameters are sensitive to biodegradation (generally increase in values), thus biodegraded oils have been excluded from the plot.

Figure 5.62. Cross plot of the ratio of dibenzothiophene/ Phenanthrene (DBT/P) versus the pristane/phytane ratio (pr/ph) provides a means of making inference on the oils source rock depositional environments and lithology after Hughes *et al.* (1995). Dotted fields are not fixed boundaries as exceptions can occur and each zone is as defined by Hughes *et al.* (1995).

Figure 5.63. Plot of C29 abb (C_{29} αββ/αββ+ααα) against C29 aaa S/S+R (5α(H),14 α(H),17α(H) ethyl cholestane 20S and 20R sterane thermal maturity parameters show the wide range of thermal maturity of the oils.

Figure 5.64. Plot of MPI-1= 1.5*(2-MP+ 3-MP)/ (P + 1-MP + 9-MP); Radke *et al.*, (1982a) versus C32 ab S/S+R(17α(H), 21β(H)-bishomohopane) thermal maturity parameters. Most oils tend to have narrow range of values for the bishomohopane parameter but there is a considerable variation in their MPI-1 values.

Chapter Six

Figure 6.1: Map of the world showing the distribution of the Tertiary deltaic basins where the novel terpanes have been detected (block shape). Marine oils from Trinidad and North Sea basins lack A and B isomers (oval shape). Blank map taken from http://wps.ablongman.com/wps/media/objects/579/592970/BlankMaps/World%20Map.gif

Figure 6.2 Representative mass chromatograms showing the distributions of compounds A_1, A_2, B_1, B_1 and C in m/z 123 and m/z 414 GC-MS mass chromatograms. The m/z 414→123 parent-daughter ion transitions GC-MS-MS (bottom chromatogram) afforded the selective monitoring of the compounds from interfering peaks. Note the absence or very low abundance of these novel compounds in the m/z 191 chromatogram. Peak identities are provided in table 6. 2

Figure 6.3. GC-MS-MS 414→123 transition MRM chromatograms showing the distribution of the novel terpanes in representative Niger Delta oils. The North Sea oil permits a comparison of the distribution of the compounds in non-oleanane bearing oil with those of the Niger Delta oils

Figure 6.4. GC-MS-MS 414→123 transition showing the distribution of the novel terpanes in representative Assam oils. "OL" refers to oleanane.

Figure 6.5. GC-MS-MS 414→123 transition chromatograms showing the distribution of the novel terpanes in two representative Beaufort-Mackenzie oils. The low oleanane concentration parallels the low relative abundance of A and B compounds.

Figure 6.6. Upper GC-MS-MS m/z 414→123 chromatogram showing the distribution of compounds A_1, A_2, B_1, B_2 and C in sample GOM-2 from the Gulf of Mexico. Lower chromatogram shows the oleanane concentration in m/z 412→191 MRM chromatogram. The low oleanane concentration parallels the low level of A and B compounds.

Figure 6.7. Upper MRM m/z 414→123 chromatogram shows the distribution of compounds A_1, A_2, B_1, B_2 and C in a representative oil sample (KT-5) from the Kutei Basin. Lower chromatogram shows the oleanane concentration in the MRM m/z 412-191 chromatogram. X, Y, Z are peaks 10, 12 and 13 identified as C_{30} unknown triterpanes in Woolhouse *et al.* (1992). Peak OL refers to oleanane.

Figure 6.8. Mass spectrum of compound A_1

Figure 6.9. Mass spectrum of compound A_2

Figure 6.10. Mass spectrum of compound B_1.

Figure 6.11.Mass spectrum of compound B_2.

Figure 6.12. Mass spectrum of Compound C.

Figure 6.13. Total ion current (full scan) showing the mixtures of oleanenes formed after isomerisation. Peaks labelled 1, 2, 3 and 4 are olean-13(18)-ene, olean-12-ene, oleane-18-ene, and 18α-olean-12-ene respectively.

Figure 6.14. Mass spectrum of olean-13(18)-ene (Peak H, Figure 6.13) obtained from isomerisation of lup-20(29)-ene from birch tree.

Figure 6.15. Mass spectrum of olean-12-ene (Peak I, Figure 6.13) obtained from isomerisation reaction of lup-20(29)-ene from birch tree.

Figure 6.16. Mass spectrum of olean-18-ene (Peak J, Figure 6.13) obtained from isomerisation reaction of lup-20(29)-ene from birch tree.

Figure 6.17. Mass spectrum of 18α-olean-12-ene (Peak K, Figure 6.13) obtained from isomerisation reaction of lup-20(29)-ene from birch tree.

Figure 6.18. M/z 414 mass chromatogram showing the mixture of compounds formed from hydrogenation of oleanenes.

Figure 6.19. Mass spectrum of synthetic B2 (Peak 4, Figure 6.18) obtained from hydrogenation of oleanane. Note the similarity of the spectrum with natural B2 in Niger Delta oil (Figure 6.11).

Figure 6.20. M/z 414→123 mass chromatogram showing the distribution of compounds A_1, A_2, B_1, and B_2 in Kutei oil (above) and similar distribution with co-injected synthetic B_2(below).Note the similarity of retention time between synthetic B_2 and natural B_2 and the increase in the area of peak B_2 in the lower chromatogram.

Figure 6.21. Cross plot of K-Index and Oleanane index shows a positive correlation.

Figure 6.22. Plot of K-Index against C_{29} ααα (20S/20S+20R) sterane thermal maturity parameter reveals no data trend, thus suggesting no thermal maturity influence on K-Index.

Figure 6.23. Plot of K-Index against methyl phenanthrene index (1.5*(2-MP+3-MP)/ phenanthrene+ 9-MP+1-MP) molecular thermal maturity parameter shows no data trend and indicates an absence of maturity influence on K-Index.

Chapter Seven

Figure 7.1. Plot of the $\delta^{13}C$ values of the bulk saturated and aromatic hydrocarbon fractions of the Assam oils.

Figure 7.2. Plot of the $\delta^{13}C$ values of the bulk saturated and aromatic hydrocarbon fractions of the Gulf of Mexico oils

Figure 7.3. The *n*-alkane stable carbon isotope plot for representative samples of oil from Assam Delta.

Figure 7.4. The *n*-alkane stable carbon isotope plot for representative samples of oil from the Beaufort-Mackenzie Delta.

Figure 7.5. The *n*-alkane stable carbon isotope plot for representative samples of oil from the Gulf of Mexico.

Figure 7.6. A negatively sloping *n*-alkane stable carbon isotope profile of samples of oil from the Niger Delta showing terrigenous source facies

Figure 7.7. Nearly flat n-alkane stable carbon isotope profile of deepwater and some western shallow water Niger Delta oils typical of oils expelled from source rock rich in marine kerogen.

Figure 7.8. Plot of C_{29} S/S+R (5α(H), 14α(H), 17α(H) - ethyl cholestane (20S and 20R configurations) versus sterane C29 abb (5α(H),14β(H), 17β(H) 20S +20R / 5α(H),14β(H), 17β(H) + 5α(H),14α(H), 17α(H) 20S+20R for C29 steranes) thermal maturity parameters.

Figure 7.9. Cross plot of C_{29} aaaa S/S+R sterane thermal maturity parameter and Ts/Ts+Tm. C_{29} S/S+R = 5α(H), 14α(H), 17α(H) - ethyl cholestane (20S and 20R configurations). Ts= 18α(H)- 22, 29, 30- Trisnorneohopane. Tm = 17α(H) - 22, 29, 30-trisnorhopane.

Figure 7.10. A gas chromatogram showing the n-alkane distribution in a representative deepwater Niger Delta crude oil (sample NDO14).

Figure 7.11. A gas chromatogram showing the *n*-alkane distribution in a representative terrigenous source facies, shallow water Niger Delta crude oil (sample NDO10).

Chapter Eight

Figure 8.1. Map showing the sedimentary basins of Nigeria. The arrow points to location of the Dahomey Basin on the south-western margin of the Niger Delta. (modified after Adekeye, 2004).

Figure 8.2. Outline Geological map of Dahomey Basin showing the location of the Gbekebo well (red dotted ring) on the eastern margin of Dahomey (west of the Niger Delta). Map modified after Adekeye (2004).

Figure 8.3. Geochemical log of the Gbekebo well. Two organic rich intervals are apparent (A and B). Only one sample within the interval "A" contain oleanane whereas most samples in the interval "B" contain oleanane, with oleanane index values as high as 0.21, despite the high marine algae biomarker composition of interval B

Figure 8.4. Plot of HI against Tmax indicating the kerogen types and their respective hydrocarbon potentials in the analysed Araromi Formation sediments. Overlay field

after Integrated Geochemical Interpretations Ltd p: IGI 2.7 geochemical interpretation software.

Figure 8.5. Representative gas chromatogram of the Araromi shale (samples GB314 and GB 307) extracts and a deepwater Niger Delta oil (sample NDO14) showing how *n*-alkane and isoprenoid distributions in the Araromi shale can vary as to resemble deepwater distributions upon maturation (upper chromatogram) and the apparent contrast in the distribution with the deepwater oils (lower Araromi shale extract chromatogram).

Figure 8.6. Ternary diagram showing the plot of C_{27} C_{28} and C_{29} steranes (based on 5α(H),14α(H),17α(H) 20R sterane peaks from appropriate GC-MS-MS transitions) interpreted in terms of likely kerogen precursor. Interpretational overlay from IGI's p: IGI-2 software modified after Huang and Meinschein (1979).

Figure 8.7. GCMS m/z 217 mass chromatograms showing the distribution of C_{27}-C_{29} steranes in representative intervals within the Araromi shale and a typical distribution in deepwater Niger Delta oil. Note the downhole variation in the sterane distributions within the Araromi shale extracts.
Figure 8.8. Plot of oleanane index versus C_{30} 24-*n*-propyl cholestane shows variability in the compositions of these biomarkers in the Araromi shale extracts.

Figure 8.9. CSIA profile of *n*-alkanes in representative deepwater Niger Delta oils and the bitumen extracts of the Araromi shale.

Chapter Nine

Figure 9.1. Model showing positions of various source rocks charging deltaic petroleum system, their stratigraphic relationships and the summary of their inferred geochemical properties

LIST OF APPENDICES

Appendix I. Tables of published biomarker and stable carbon isotope data from the literature on the selected case study deltas.

Appendix II: Appendix of complete biomarker data for the analysed oils on the attached CD.

Appendix IIIa, IIIa, IIIc: Peak annotations to figures in chapter five.

PREFACE

This thesis is structured to develop new ideas from existing literature on Tertiary deltaic petroleum systems (Chapters 1 and 2) and to extend these ideas by applying fairly standard analytical methods (Chapter 3) to a carefully assembled set of representative oils from Tertiary deltas worldwide. The new ideas generated from the existing literature have been interpreted in the context of petroleum systems in Tertiary deltas as presented in Chapter four. In chapter five, results of biomarker analyses of the representative oils are presented and interpreted. Chapter five also presents comparative interpretations of the oils from all the case study deltas in the context of organofacies (source rock type, age, organic matter type, oil thermal maturity etc.). Chapter six discusses novel compounds and some uncommon biomarkers that are characteristic of terrigenous-deltaic oils and the potential utility of these compounds in unravelling the complex oil systems in deltaic basins. The interpretation of the bulk stable carbon isotopes and compound class isotope measurements as well as the compound specific stable carbon isotope characteristics of these oils are discussed in Chapter seven. In Chapter eight, an attempt is made to test the proposed sub-delta oil sourcing model by correlating deepwater Niger Delta oils with late Cretaceous shale of the Araromi Formation in the Dahomey Basin, south-western Nigeria on the basis of their similarity in biomarker and compound specific isotope characteristics. Based on the successive discussions of the data presented in chapters' four to eight, Chapter nine concludes the discussions and proffers recommendation for future works.

CHAPTER ONE

INTRODUCTION

1.0. Introduction

As the world population grows at an alarming rate, the technological demand to satisfy human needs drives accelerating economic growth that is largely dependent on energy. According to the United States' agency (EIA, 2007), the global energy demand will rise by as much as 54% over the next two decades. Notable is the fact that oil consumption constitutes 40% of this energy demand. The apparent truth that the energy that drives our economy in the face of the technological demands prompted by the world's population growth is largely fossil fuel energy resources (coal, crude oil and gas) offers stimulus for the development of existing reserves and the discovery of more petroleum. This increased demand for more oil encourages exploration and production of more petroleum resources despite the recent political campaign related to global climate change, which discourages a global energy demand that is largely dependent on fossil fuel in favour of the development of renewable energy resources (e.g. wind, solar, hydroelectricity).

Subsurface delta deposits constitute one of several sedimentary environments where hydrocarbons are being actively explored since drilling in a few kilometres depth of deltaic reservoir rocks has become commercially viable and with the prospects of huge discoveries in progressively deeper water explorations (Peters *et al.*, 2000). Today, deltas constitute a significant percentage of the sedimentary environments of the world's known hydrocarbon reserves (Peters *et al.*, 2000; Peters *et al.*, 2005b, pp.762). The business of petroleum exploration requires knowledge of the origin of the oil (and of its source rock in particular) so as to permit the prediction of volumes,

composition, phase and quality of petroleum in undrilled prospects in a sedimentary basin. Such knowledge of the origin of an oil accumulation forms the basis of the petroleum systems concept (Magoon & Dow, 1994, 2000) and it helps to reduce petroleum exploration risk (Cornford, 2000). Poor petroleum system understanding (source rocks in particular) therefore escalates the risk of exploration as the presence, let alone the composition and phases of petroleum could prove difficult to predict in undrilled prospects (Cornford, 2000).

Despite huge petroleum reserves in Tertiary deltaic basins, little is known of the origin of most of the petroleum accumulations in deltaic basins of Tertiary age as the knowledge of the regional and stratigraphic distributions of the source rocks is limited (Peters *et al.*, 2000). The poor petroleum system knowledge is evident in the paucity of published work on oil-source rock correlation studies in most deltas (e.g. Beaufort-Mackenzie, Gulf of Mexico, Niger Delta).

1.1. The Problem

The organic matter of tropical deltas is mainly found in delta-top sediments comprising shale via associated carbonaceous shale to coals which may be humic or perhydrous (hydrogen rich). Considering 388 samples from 21 studies of Tertiary deltas included in IGI's (Integrated Geochemical Interpretations Ltd) 'World Database' supplied with the commercial interpretation software p:IGI-2 (Release 2.3, 2006), a bimodal distribution of TOC values is observed (Figure 1.1), suggesting that coals and shale (but not intermediates) as end members constituting potential oil source rocks. Thus in a river-dominated delta, the petroleum source rocks are expected to consist of high proportions of terrigenous organic matter as reflected in the abundant allocthonous land derived woody and structured (vitrinite) particles,

some cuticles, pollen and spores (liptinites) and generally low 'amorphous' organic matter as seen in optical microscopic studies (Durand & Parratte, 1983; Bustin, 1988).

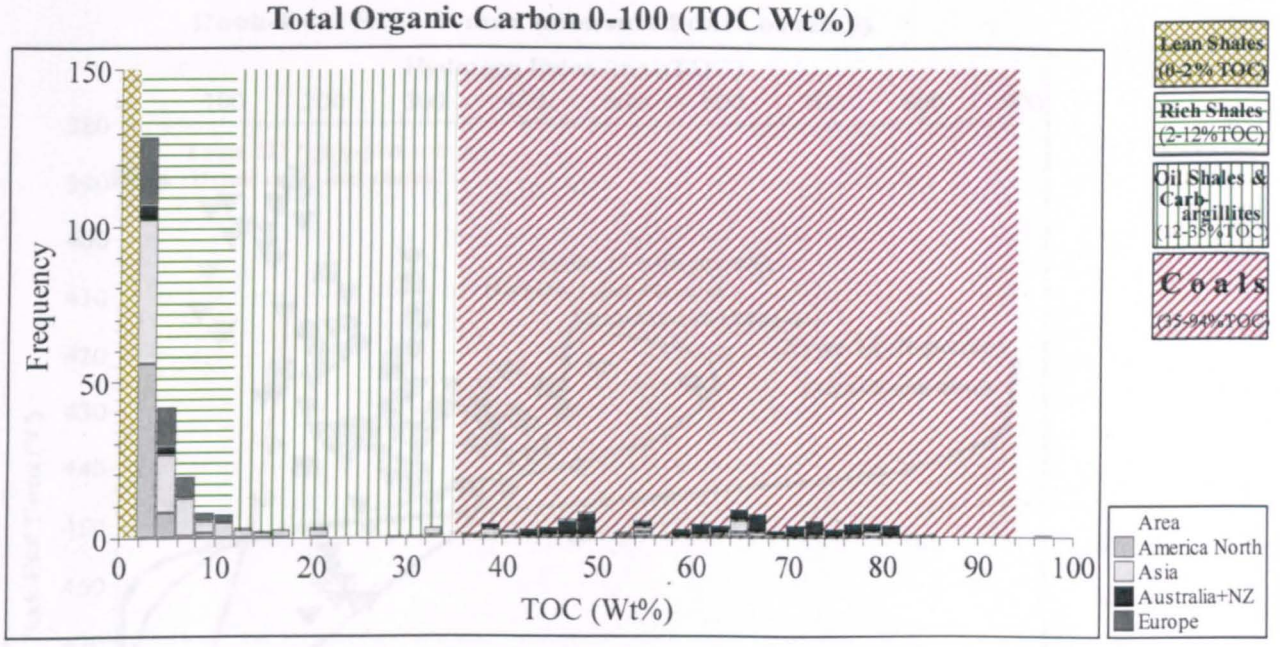

Figure 1.1. Bimodal distribution of Total Organic Carbon (TOC) values from 338 samples with >2%TOC from 21 published accounts of Tertiary deltas worldwide. (Source: 'World Data' p:IGI-2, Version 2.3, IGI Ltd., 2006).

This is in contrast with the algal-bacterial 'amorphous' kerogens seen in typical marine shale source rock, and which might be expected in the mudstones of interdistributary bays of wave-dominated deltas. In terms of pyrolysis (Rock-Eval) characteristics, the typical river-dominated delta facies usually has an abundance of Type III kerogen (rich in gas-prone vitrinitic macerals) with minor liptinites (Huc *et al.*, 1986; Bustin, 1988).

However, many Tertiary deltas contain a portion of more hydrogen rich 'perhydrous' coals, characterised by unusually high hydrogen indices (Figure 1.2), which contain unusually high contents of liptinite macerals (Figure 1.3), typically comprising resinite, suberinite, cutinite and sporinite. This figure also shows that while the coals mainly contain a mix of vitrinite and liptinite, the lower TOC shales contain abundant

inertinite suggesting that globally coals and not the shales are the dominant oil source, assuming equivalent expulsion efficiencies.

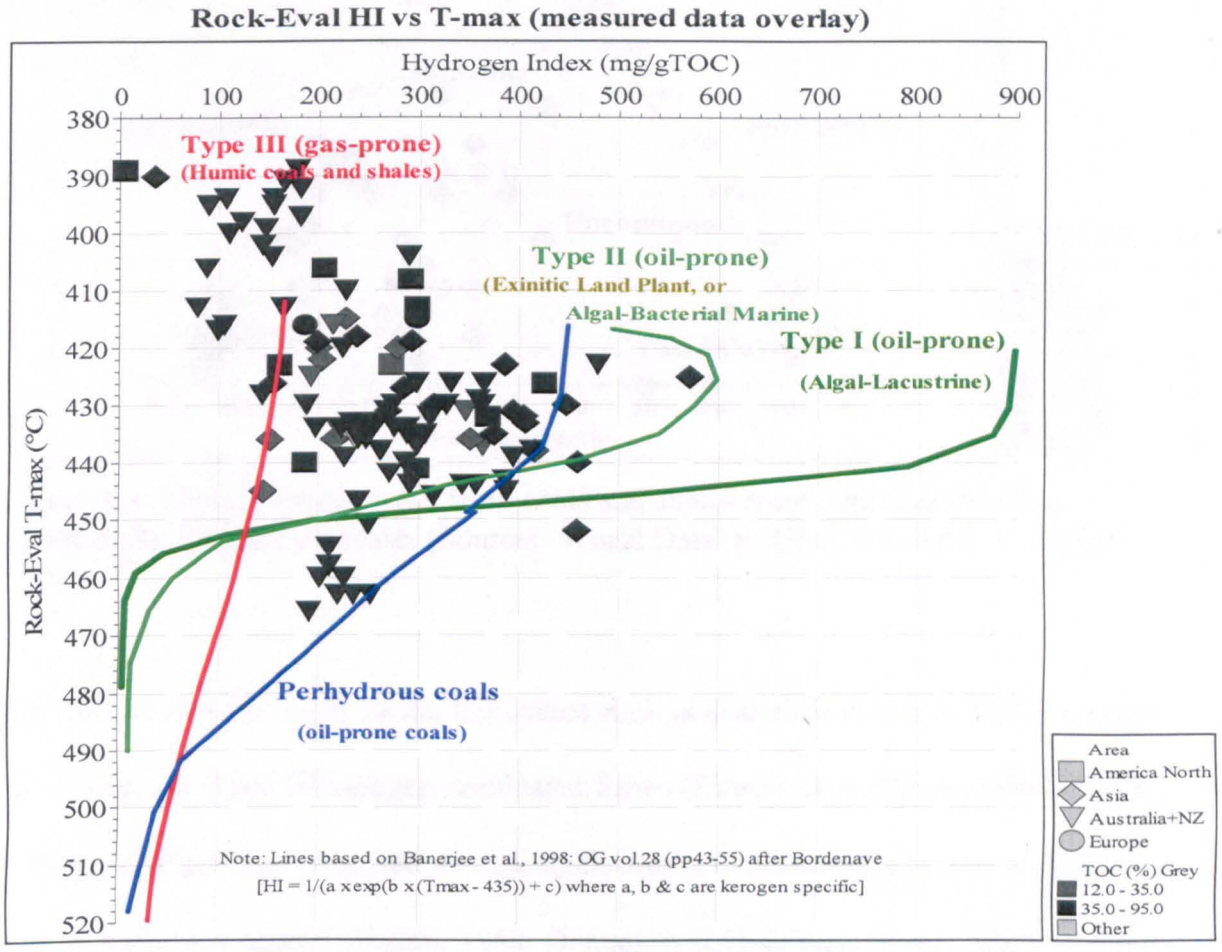

Figure 1.2. Kerogen types of Tertiary coals and carbargillites (>12 wt% TOC) taken from 15 published studies with TOC and Rock-Eval analyses. (Source: 'World Data' p:IGI-2, Version 2.3, IGI Ltd., 2006).

It would thus be expected that the biomarker distribution of the produced oil should be dominated by compounds derived from terrigenous higher plants. From the published accounts, oil-source rock correlation studies in these aforementioned deltas are highly disputatious. A number of workers have carried out individual studies on both source rock characterisation and the crude oil geochemistry in these deltas (see Table 1.1). Common to all of these deltas is that significant proportions of the oils reservoired in the Tertiary sands do not share geochemical affinity with the so called delta source rock samples.

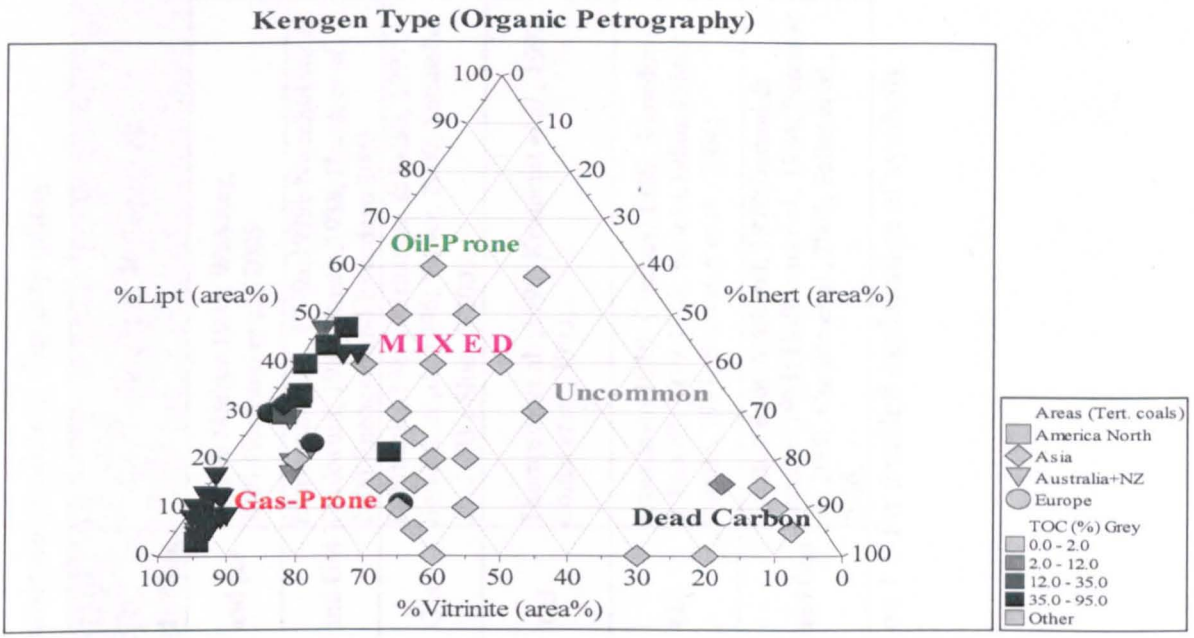

Figure 1.3. Visual kerogen types from coals and shales from 8 publications in a world-wide literature database. (Source: 'World Data' p:IGI-2, Version 2.3, IGI Ltd., 2006).

For instance, in the Niger Delta, the source rock is described as a low TOC (average ca. 1.5%), and Type III kerogen dominated facies (Ekweozor & Okoye, 1980; Bustin, 1988) and it has been proposed that the thick source rock interval compensates for the poor source rock quality (Bustin, 1988; Demaison & Huizinga, 1994). That the huge volume of oil accumulated within the Niger Delta is sourced from such analysed organic-lean Tertiary sediments demands high transformation, expulsion and migration efficiencies.

Table 1. 1. Summary of the petroleum geology and geochemistry of some of the world's major petroleum producing Tertiary deltas

Region/Province	Basin	Major Source rock	Major kerogen type	Main Reservoirs	Principal Maturation Stage	Petroleum system	Main HC production	Selected References
India/Asia	Assam	Barail coal, Kopili shale	III, coal	Tertiary. Deltaic sst.	Neogene	Barail-Bokabil (!) Kopili-Sylhet (!)	Oil and gas.	Raju & Mathur 1995; Wandrey, 2004;Goswami *et al.*, 2005
Nigeria /Sub-Sahara Africa	Niger	Akata Fm. Agbada Fm.	III, coal	Neogene Deltaic sst.	Late Tertiary - Recent	Akata-Agbada (.)	Oil and Gas	Ekweozor *et al.*, 1979a;1979b Nwachukwu & Chukwura, 1986; Bustin,1988; Haack *et al.*, 2000;Eneogwe and Ekundayo 2003
Egypt/North Africa	Nile			Neogene sst	Neogene - Recent		Gas	Rohrback , 1983; Alsharhan & Salah, 1997; Barakat *et al.*, 1996; Wever, 2000; Samuel *et al.*, 2003 ; Sharaf, 2003.
Gulf of Mexico/North America	Mississippi	Tertiary deltaic shale? Pre Tertiary source rocks			Tertiary - Recent		Oil	Thompson et al. ,1990; Kennicutt *et al.*, 1992; Comet *et al.*, 1993;
Canada/North America	Beaufort-Mackenzie Delta	Tertiary deltaic shale? Pre- Tertiary source rocks.	III	Neogene Deltaic sandstone.	Late Tertiary - Recent		Oil	Snowdown 1980; Creaney, 1980; Snowdown & Powell, 1979;1982; Brooks,1986a,1986b; Curiale, 1991; Snowdon et al., 2004;
Indonesia/Asia	Kutei Basin (Mahakam Delta)	Miocene deltaic coals and shales	III, coal	Miocene			Oil and Gas	Combaz & de Matharel, 1978;Durand & Parratte, 1983; Hoffman *et al.*, 1984; Peters *et al.*, 2000; Curiale *et* al., 2005; Saller *et al.*, 2006.

(!) denotes a known petroleum system, while (.) refers to hypothetical petroleum system- see section 1.8 for detailed explanation of symbols.

As a speculative example using data from Haack *et al.* (2000), the Niger Delta covers some 75,000 km^2 and an estimated average thickness of mature (i.e. below 3.2 km) post-rift sediment of 3.6 km, and hence contains a rock volume of 270,000 km^3. Taking 50% of this rock volume to be shale, gives 135,000 km^3 or 350 x 10^{12} tonnes of shale (rock density = 2.6 tonne/m^3). With an optimistic average of 1.5%TOC and HI of 300mg/gTOC the average pyrolysis yield is 4.5kg/tonne, 2kg/tonne of which remains in the source rock and 2.5kg/tonne is optimistically available for expulsion as oil or gas (55% expulsion efficiency). The estimated expelled petroleum (as oil equivalent, density 0.86 tonne/m^3) is thus 158 x 10^9 tonnes (1,158 x 10^9 bbls). The 26.8 billion bbls of (oil equivalent) reserves in the Niger Delta (Haack *et al.*, 2000) equates to some 80 billion bbls (10.9 x 10^9 tonnes) in place. This implies a migration-entrapment efficiency ('in place' oil/ expelled oil) of 6.9% based on a thick lean source rock model, and illustrates the sensitivity of the calculation to the expulsion efficiency.

However, it has been shown that a significant proportion of oil accumulations in the Tertiary reservoirs to the west of the Niger Delta do not exhibit molecules indicative of a land plant dominated source rock organofacies (Haack *et al*, 2000; Eneogwe & Ekundayo, 2003). This divergence in the geochemistry of some of the produced oils and the Tertiary source rocks also operates in the Beaufort-Mackenzie Delta (e.g. Li *et al.*, 2005) among several other deltas thus rendering impossible an unequivocal correlation of produced oils to their source rock(s). However, in the tectonically inverted (thrust-related) Assam-Barail Delta, source rocks are accessible by drilling and from outcrop within the Naga Hills thrust belt to the south.

The observation of a poor geochemical match between some produced oils and the Tertiary source rock character within a delta appears to be a global phenomenon, particularly for deltas building out on passive continental margins with river drainage focussed by tectonic lineaments (e.g. Benue Trough for the Niger Delta and Canada Basin mid ocean ridge for the Mackenzie Delta). This raises some key questions:

1. Do deltas really act primarily as sedimentary overburden to mature the organic rich rocks buried below, and as a reservoir to accommodate expelled oils from source rocks outside of the delta sequence?
2. How much of the oil in a deltaic accumulation is truly generated by and expelled efficiently from the lean and generally mixed gas and oil-prone kerogens seen in deltaic source rocks?

1.2. Concepts

1.2.1. New models for oil sourcing in deltas

With the exception of some delta-top coals, typical deltaic sediments are organic lean and not particularly oil-prone. This leads to consideration of three possible models for sourcing of oil and gas reservoired within deltaic sediments where there is poor biomarker correlation between the coals and oils:

1. An intra-delta source rock exists, but, other than perhydrous coals, has yet to be reliably identified - a popular model that has gained currency!
2. The relatively lean source rocks encountered can account for the observed oil and gas volumes, implying exceptionally high expulsion and migration efficiencies (e.g. Demaison & Huizinga, 1994), see Figure 1.4.
3. Oils are generated outside the 'wedge' of deltaic sediments and migrate into deltaic reservoirs from pre-existing (sub-delta) Cretaceous and older source unit(s) (Figure 1.5).

In this thesis, the term sub-delta is used exclusively to describe source rocks of Cretaceous or older age, typically rich in marine algae and containing high TOC, which are not part of the Tertiary delta *sensu-stricto* but whose oils have migrated into the Tertiary delta reservoirs. Similarly, the term intra-delta refers to Tertiary delta source rocks within the Tertiary delta prograde, which are commonly characterised by significant land plant organic matter inputs.

Unfortunately, partly as a function of the high sedimentation rates and low geothermal gradients in delta prograde, mature source rocks are rarely encountered in exploration wells. Thus the most secure information concerning source rock occurrence derives from the molecular and isotopic signals carried by the oils migrating within the delta.

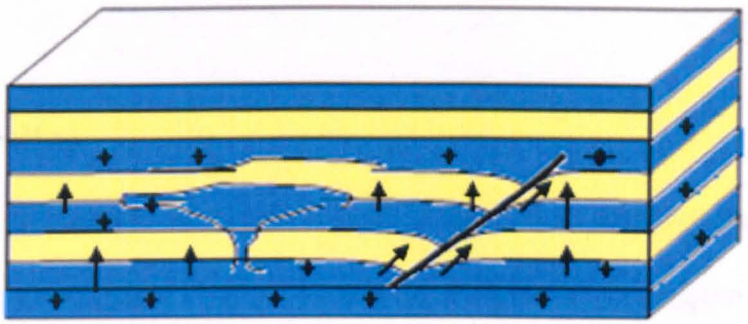

Figure1.4. Cartoon illustrating how high expulsion and migration efficiencies are made possible by interconnected faults and sand and shale couplets of deltaic sedimentary architecture.

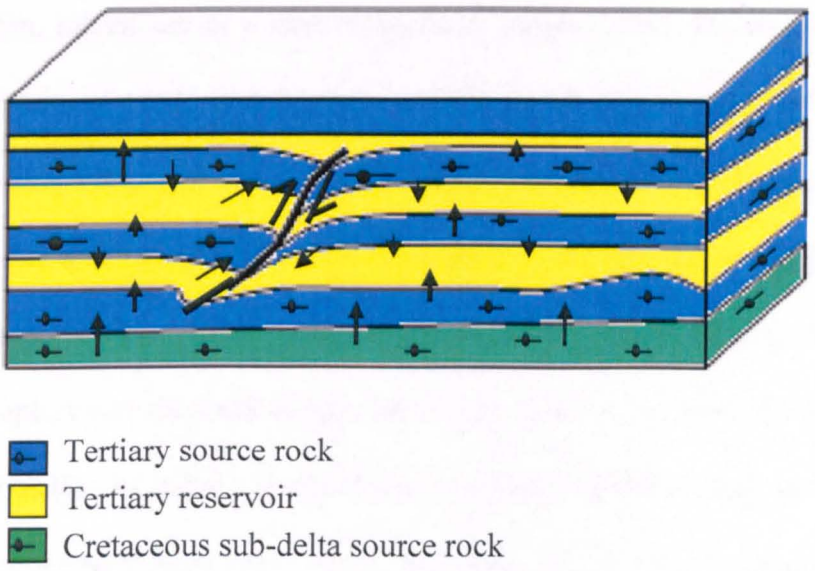

Figure 1.5. Cartoon illustrating the charging of Tertiary reservoirs by sub-delta source kitchens

Having set the problems with Tertiary deltaic Petroleum systems in the previous discussions, it can thus be seen that there exists a paradox between the geochemical characteristics of some of the produced oils and the alleged delta source rocks (Samuel *et al.*, 2006a). The primary objective of this research is to investigate this

geochemical paradox, and to develop an improved understanding of the petroleum systems operating in Tertiary deltaic sedimentary basins of the world.

1.3. Deltas

Deltas are formed where river borne clastics are emptied into a larger water body. (Moore & Asquith, 1971; Coleman & Wright, 1971) (Figure 1.6). The larger water body that receives the sediment is often referred to as the receiving basin (Figure 1. 7) and it forms the base level for the incoming fluvial system. The receiving basin is a depression with accommodation for the incoming river-fed sediments and this may be an ocean, inland sea or a lake (Reineck & Singh, 1980). Deltas were first recognised as agricultural lands and this provoked the curiosity of early scholars like Homer, Herodotus, Plato and Aristotle. Herodotus was in fact the first to suggest the name delta after a close observation of the course of the Nile River, approximately 450 BC (Coleman, 1976). Since several dynamic processes (wave, tide, climate, and topography) and fluctuating base level (e.g. relative sea level change) interact during the deposition of deltaic facies, deltas are best defined as '*subaqueous and subaerial deposits derived from river borne sediments*' (Coleman & Wright, 1971; Coleman, 1976).

Coleman (1976) recognised the following environments where modern deltas are formed:

- Coastal environments ranging from where wave and tidal actions are minimal (e.g. Mississippi Delta) to coasts of extreme wave action and tidal activity (e.g. Nile Delta).

- Tropical rainforest with thick vegetation and intense interaction of biological and chemical processes, e.g. Amazon and Niger deltas,
- Arid or arctic environments with minimal biological activities, although these are rare e.g. Beaufort-Mackenzie Delta.

1.4. Delta formation

Regardless of the environment where a delta is formed, all deltas have a common characteristic and that is the presence of a river which supplies clastic sediments to the receiving basin at a rate faster than it can be removed by erosional (marine) processes (e.g. waves, tides). The rivers feeding deltas thus requires large drainage basin (Figure 1. 7) (Reineck & Singh, 1980). The density of the river sediment discharge greatly depends on the climate, geology and topography of the drainage basin (Reineck & Singh, 1980).

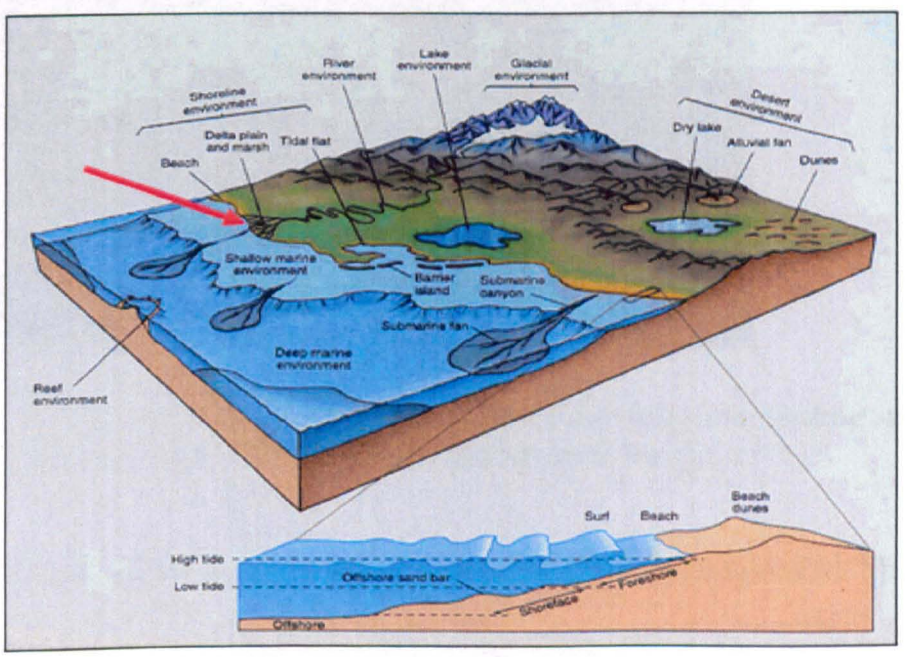

Figure 1.6. A block diagram showing some sedimentary depositional environments. The red arrow highlights the deltaic setting among other environments. (http://academic.brooklyn.cuny.edu/geology/grocha/monument/images/deposit.gif).

A river that feeds a receiving basin often receives sediment supply from tributaries draining a large area of highland. As the tributaries flow down slope, they merge into one or sometimes more than one major river channel, which actively develops an alluvial valley (Reineck & Singh, 1980). Over the course of time, the river matures and begins to flow through its own valley and over sediment loads deposited within its valley as this builds up. As the river matures further down slope, it changes its activity from a predominantly transporting to deposition medium, and dispersion of its sediment load. This dispersed sediment accumulates and spreads over a considerable extent of plain land to form the delta plain (Reineck & Singh, 1980).

Figure 1.7. A cartoon showing the components of a river system feeding sediments to the receiving basin where delta is formed (Coleman & Wright, 1971).

Deltaic deposits compose of the subaerial and sub-aqueous components. The subaerial delta represents that part of the delta plain lying above the low-tide limit. The subaerial delta deposits are a thin layer on top of much thicker strata of the sub-aqueous deltaic successions (Coleman, 1976). The sub-aqueous delta is that part of

the delta plain that lies below the low-tide level. In all cases, it acts as the base level/foundation over which the subaerial delta prograde (Coleman, 1976). The waning energy of the river as it approaches its receiving basin, results in much coarser sediments being deposited from suspension in the water column near the river mouth, followed by medium and finest sediments settling further offshore. This sequence of deposition characterises the subaerial delta and is referred to as the seaward fining of sediments (Reineck & Singh, 1980).

According to Reineck and Singh (1980), where the most rapid deposition of heavy particles (coarse grained) occur, within a short distance from the river mouth, is termed the distributary mouth bar. Seaward of the distributary mouth bar, less coarse materials (silts, and fine sands) are deposited by the progressively waning river flow, in the form of interfingering sands, silts and clays. This distal deposit is called the deltafront (Reineck & Singh, 1980). The finest sediments accumulating from suspension seaward of the deltafront consisting essentially of silts and clays are called the prodelta deposits (Reineck & Singh, 1980).

Due to a steady supply of clastics by the river, sediments are rapidly deposited at a rate faster than that can be removed by wave and tidal processes. Over a considerable period of time, geologically speaking, such a delta begins to build seaward of the receiving basin in a classical manner termed delta progradation (Reineck & Singh, 1980). As the delta progrades in a new sequence of deposition, coarser sediments are laid over the finer sediments laid in the previous cycle of deposition. This results in the characteristic coarsening upward sequence typical of all deltas (Coleman, 1976; Reineck & Singh, 1980). Figure 1.8 shows the global distribution of deltas and their current sediment discharge capacity in units of 10^6 tons.

1.5. Types of Delta

Several classification schemes have evolved for deltas (Fisher *et al.*, 1969; Galloway, 1975; Coleman & Prior, 1980; Wright, 1985). The most popularly accepted classification which considers the influence of sediment input (fluvial process), waves and tides is that of Galloway (1975). Based on the identification of three idealized end-member dominant processes, Galloway (1975) classified deltas into; fluvial-dominated, wave-dominated and tide dominated (Figure 1.9). As an improvement to Galloway's classification, Coleman and Prior (1980) classified deltas using models that not only incorporate Galloway's triangular classification scheme, but also consider other variables such as climate, topography, littoral currents and tectonics of the receiving basin. The varying influence of one or more of these factors has resulted in the formation of different types of deltaic deposits over geological time (Reineck & Singh, 1980).

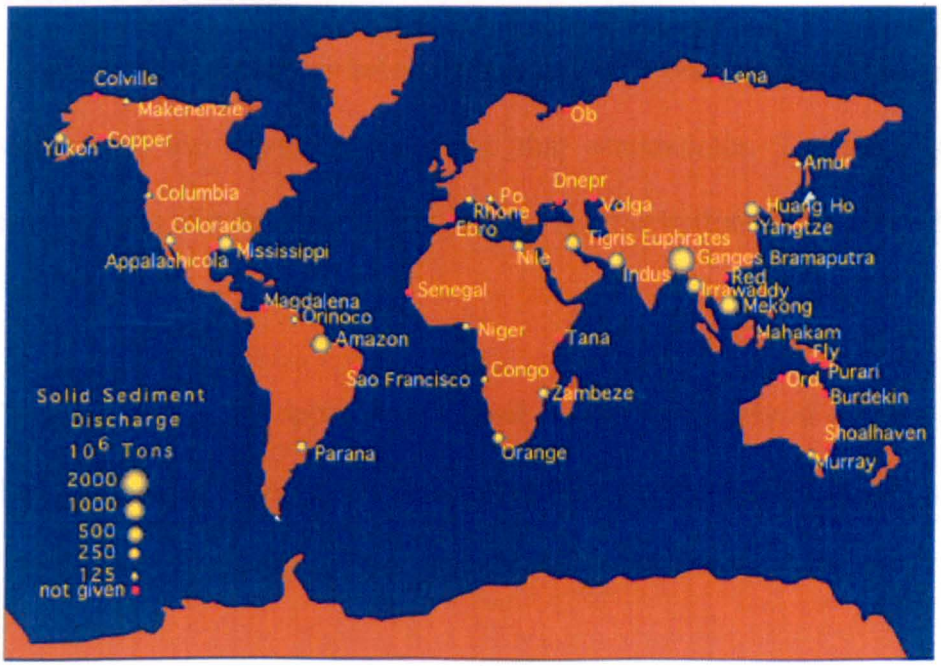

Figure 1.8. Map showing the location of major deltas of the world and their solid sediment discharge capacity (after Coleman & Wright, 1971).

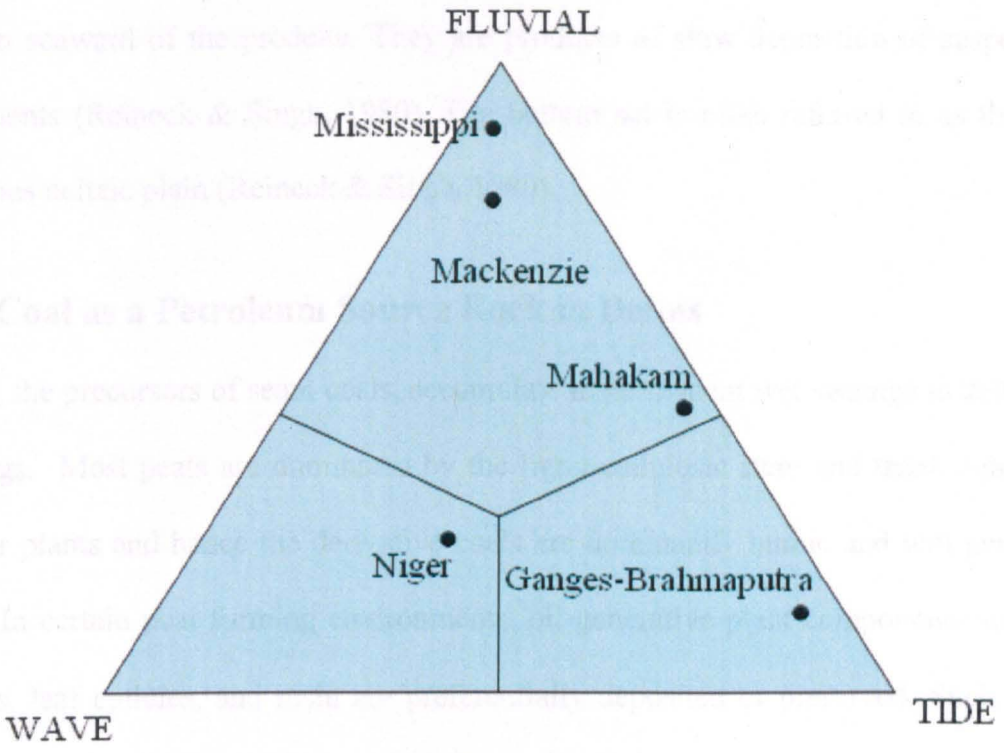

Figure1.9. Galloway's Ternary diagram classifying deltas using the relative influence of wave, tide and river processes(Modified after Galloway, 1975).

1.6. Structure of Deltas

A delta consists of three major sets of deposits, each bearing the influence of the water regime and the sediment grain size that accumulates. The three generally recognized deposits of a delta are topset, foreset and the bottomset (Reineck & Singh, 1980).

Topset Deposit: Forms the uppermost deposit consisting mainly of marshy deposits and shallow water river channel and lagoonal sediments. The deltafront silts and sands are also components of the topset beds (Reineck & Singh, 1980).

Foreset Deposit: Typically consists of prodeltaic clays, silts and coarse sand deposits. This deposit is also known as delta front slope sediments or lower deltaic plain.

Bottomset Deposit: Consist essentially of offshore clays (silts and shelly clays) in the region seaward of the prodelta. They are products of slow deposition of suspended sediments (Reineck & Singh, 1980). The bottom set is often referred to as the sub aqueous deltaic plain (Reineck & Singh, 1980).

1.7. Coal as a Petroleum Source Rock in Deltas

Peats, the precursors of seam coals, accumulate in permanent wet swamps in delta top settings. Most peats are dominated by the ligno-cellulosic stem and trunk debris of higher plants and hence the derivative coals are dominantly humic and will generate gas. In certain peat forming environments, oil-generative plant components such as spores, leaf cuticles, and resin are preferentially deposited or preserved. Such coals have long been considered as a source of oil in addition to some associated lean shales in most deltas (e.g. Mukhopadhyay *et al.*, 1989). The oil generative potential of coals in general has been discussed extensively by numerous workers (Thomas, 1982; Durand & Paratte, 1983; Thompson *et al.*, 1985; Shanmugam, 1985; Saxby & Shibaoka, 1986; Khavari-Khorasani, 1987; Murchison, 1987; Horsfield *et al.*, 1988; Snowdon, 1991; Clayton, *et al.*, 1991;Boreham & Powell, 1993; Law & Rice., 1993; Katz, 1994; Bagge & Keely, 1994; Curry *et al.*, 1994; Killops *et al.*, 1998; Petersen, *et al.*, 2000; Petersen, 2002; Wilkins & George, 2002; Sykes & Snowdon 2002; Boreham *et al.*, 2003; Sykes, 2004; Sykes *et al.*, 2004; Petersen *et al.*, 2005, 2006; Pedersen *et al.*, 2006). Coals are typically dominated by terrigenous kerogen as reflected in the abundance of vitrinite macerals (Durand & Parratte, 1983). According to Curry *et al.* (1994), major contributors to terrigenous kerogen are land plant biomass, microbial biomass-added during diagenesis and fresh water algae.

Since coals were usually thought to be only gas prone until recently, considerations on oil sourcing from coal are built on what makes a coal oil prone. To answer this question, previous workers (e.g. Durand & Parratte, 1983; Murchison, 1987; Macgregor, 1994; Collison *et al.*, 1994; Powell & Boreham, 1994) have discussed different factors that control the oil proneness of coals. Macgregor (1994) asserts that palaeogeographic distribution and age of coaly strata are factors controlling its oil generative potential, and defined two categories of oil bearing coals, which are Tertiary coal bearing basins within 20° of the palaeo-equator, and Late Jurassic-Eocene basins that are located on the Australian and associated continental plates.

However, other workers argue against latitude control and in favour of the nature of the organic mater input and the depositional environmental factors. In a study of New Zealand's coals, Newman *et al.* (1999) demonstrate that floral compositions of coal beds have a strong influence on their petroleum source potential. For instance, more oil prone coals have been discovered within Cretaceous to Tertiary coal sequences regardless of geographical location around the world and this age marked the proliferation of angiosperm and gymnosperm flora. Additionally, within the level of floral control (e.g. mainly gymnosperm or angiosperm dominated plant matters), variation in land plant biomass composition and the early diagenetic conditions of coals may significantly influence their liquid petroleum generation and expulsion potentials (Sykes, 2004, and references therein). Sykes (2004) noted that such variability can be addressed by examining the liquid petroleum potential of each coal on its own merit and not by standard or conventional comparisons with coals within the same basin or from other basins. In a study of Late Cretaceous humic coals of the Pukeiwitahi Formation in Canterbury Basin, New Zealand, Sykes (2004), observed

that despite similar plant organic matter derived mainly from gymnosperms, the amount of leaf-derived liptinites (cutinite and liptodetrinite) controls the paraffinic oil-generating potential of the coals and not the hydrogen (hydrogen index: HI) values. This conclusion was based on the high paraffinic oil potential associated with low HI and high leaf-derived liptinite coals and conversely, low paraffinic oil potential with coals of low leaf-derived liptinite despite high HI values. Isaksen *et al.* (1998) assert that the main control on the oil generating potential of humic coals is the concentration of the aliphatic (straight chain) hydrocarbons components i.e. cutan and suberan. Notable is the fact that the aliphatic hydrocarbon component is strongly influenced by the type of coal macerals; vitrinite is aromatic, and resinites of the liptinite maceral group yield high HI Rock-Eval pyrolysis value but are poor in aliphatic hydrocarbon components (Horsfield *et al.*, 1988; Isaksen *et al.*, 1998), thus a heavy reliance on HI values to predict oil proneness of coals could be misleading (Sykes, 2004).

A well reasoned argument aimed at uniting both organic matter input and the depositional condition controlling factors was that of Cawley and Fleet (1987). The Cawley and Fleet (1987) view unites both Thomas' (1982) stand of the organic matter factor and the Thompson *et al.*, (1985) proposition of depositional environment as being a critical factor. Cawley and Fleet (1987) note that the main sites for the deposition of oil-prone coal-bearing strata are the Cretaceous and younger tropical-subtropical lower delta plain environments where abundant oil-prone detritus (mostly exinite land plant matter) are preserved.

Contrary to the above views, another school of thought believes that coals of all age and environment are capable of sourcing liquid petroleum if sufficient hydrogen-rich

organic constituents (macerals) are present, but the critical factor is the expulsion efficiency (e.g. Hunt, 1991; Collinson *et al.*, 1994). Additionally, Isaksen *et al.* (1998) concluded that the adsorptive capacity of coal matrix controls the expulsion and the composition of expelled products. In a review of adsorption capacity estimates of coals, Durand and Paratte (1983) concluded that all coals are good expellers. This conclusion was drawn because the observed adsorption capacity of the coal matrix is below what could effectively prevent petroleum expulsion from coals before the onset of secondary cracking, when petroleum generation capacity is compared with the observed retained petroleum volume.

Using a mass balance approach, Pepper (1991) concluded that the expulsion efficiencies in coals could vary from very low to very high in response to the influence imposed by a convergence of hydrogenicity (hydrogen richness) and thermal maturity factors. Michelsen and Khavari-Khorasani (1999) examined the mass loss and volumetric changes of coals during petroleum generation and showed that coal beds are effective petroleum expellers and that the low amount of oil deposits associated with coals around the world may be connected with other factors besides coals expulsion efficiency. From the above arguments, it thus shows that the quantity of bitumen required to saturate the coal porous matrix, depends on the hydrogen richness and is critical for the expulsion of liquid petroleum. Snowdon (1991) put the bitumen saturation threshold (BST) of coal to be 30kg hydrocarbon/tonne of rock while Pepper and Corvi (1995) ascribed a BST of 5kg hydrocarbon/tonnes to shale petroleum source rocks. Snowdon (1991) concluded that any coal rich in liptinites will exceed the BST and will expel liquid petroleum upon sufficient burial to the oil generation window, given that a migration pathway exists.

In simple terms, the BST refers to the minimum amount of bitumen required to saturate the pore volume of the coal micro-porosities and above which fluid expulsion will occur. This implies that any bitumen content lower than the BST in a coal bed will lead to self adsorption by the coal matrix and delayed expulsion and/or thermal cracking to gaseous petroleum under the temperature and pressure effects of increasing thermal maturation of the coaly bed.

Deltas (e.g. Assam, Ganges-Brahmaputra, Mahakam, and Beaufort-Mackenzie) usually consist of coaly source rock facies, and coals were previously believed to be mainly gas prone until Durand and Paratte's (1983) work in the Mahakam Delta showed that coal beds are volumetrically capable of sourcing commercial liquid petroleum. Today, it is generally agreed that coals can generate oils and the Barail coals in the Assam Basin (India) is a testament to this as well as the huge oil accumulation from the coals of Mahakam Delta in Indonesia. Further, unusual concentrations of higher plant-derived exinites (cutinites and suberinites in particular) in addition to hydrogen rich vitrinite (desmocollinite, now known as collodetrinite) in the dominantly terrestrially sourced organic matter in these coaly facies accounts for the ability of these deltaic coal sequences to exhibit a potential for oil as well as gaseous hydrocarbons (Combaz & de Matharel., 1978; Durand & Paratte, 1983; Peters *et al.*, 2000).

1.8. The Petroleum System Concept

According to Perrodon (1992) as well as Magoon and Dow (1994), a petroleum system comprises of a "*pod of active or spent source rock, related hydrocarbon accumulations and all the geologic elements and processes that are critical to the*

occurrence of petroleum accumulation in a basin". That is, the petroleum system elements consist of a single source rock that generates the oil and gas, the migration pathways that connect the source to any number of reservoirs, the reservoir rocks that accommodates the oil and the traps and seals that entrap and prevent further migration of the hydrocarbon accumulations in the reservoir (Magoon & Beaumont, 1999).

Mello and Katz (2000, pp.3) pointed out that it is critical that each of the petroleum system elements share temporal and spatial relationships in order that commercial amounts of hydrocarbons be generated and preserved. Such a temporal and spatial relationship is commonly shown in the form of an event chart that shows how each key petroleum system element has evolved over geological time as well as the critical time of trap formation, and the overburden necessary for the source rock maturation. A well-defined petroleum system as summarised by Peters *et al.* (2005, pp. 751) includes a formal name for the pod of active source rock formation followed by a hyphen and the name of the effective reservoir rock formation. In a simple term, a petroleum system can be named from a single source rock and the major reservoir-rock where most of the accumulation is accommodated.

Magoon (1988) proposed three levels of certainty for a petroleum system as summarised below:

1. Known (!): where definitive geochemical correlation has been established between the source rock and the oil accumulations.
2. Hypothetical (.): where no convincing correlation exists between the source rock and the oil accumulations. Hypothetical level of certainty is always the case when samples of the true source rock are not available or the samples are of poor quality as is the case in most deltas.

3. Speculative (?): A questionable system in which the presence of a source rock and its character has only been inferred from geological and geophysical data. In this case petroleum may occur in the same geographic location or within the same stratigraphic interval as the putative source rock, but no geochemical data support a possible correlation.

According to Mello & Katz (2000, pp.3 & 4), the level of certainty of a petroleum system grows over time if not already established as being proven (known) i.e. a once speculative system may become hypothetical and even proven over the course of time as the knowledge base increases from availability of the source rock samples, supportive geochemical, geological and geophysical data.

Other important components of a well-defined petroleum system as outlined by Peters *et al.* (2005, pp. 752) are a:

- summary of the geochemical correlations used to derive the level of certainty;
- burial history chart for a key depocentre;
- petroleum system map showing the geographic extent of the accumulations;
- petroleum system cross-section;
- events chart showing the geologic evolution of the elements of the system; and
- a table of hydrocarbon accumulations.

Nearly all petroleum systems defined for Tertiary deltas have been assigned hypothetical levels of certainty (Peters *et al.*, 2005, pp. 752). This is because the actual oil-prone source rocks are rarely encountered in most of the drilled wells in any deltaic basin. In order to solve this problem, the geochemistry of the reservoired oils is believed to reflect the source rock organofacies (organic matter type as well as the

depositional environment) (e.g. Peters *et al.*, 2000; Haack *et al.*, 2000). This approach of drawing inference of deltaic source rock facies from the basin's regional oil accumulation rests on the assumption that the oils have not been significantly altered during migration through adjacent beds if indeed they have been sourced by the alleged delta source rock(s) (Curiale, 2002).

1.9. Tertiary Deltaic Petroleum Systems; present understanding and background to this study

Tertiary deltas are relatively young subsiding parallic basins which prograde seaward and commonly grade vertically and laterally in sedimentary succession from thick basal shale, mud and clay rich rocks to interfingering sandstone, siltstones and shales, and sandstone units (Curtis, 1982). In most deltas along the Atlantic margin (US Gulf of Mexico, Niger) and also the Beaufort-Mackenzie Delta, there is an orderly and often predictable interrelationship of sedimentation, stratigraphy, depositional environment, and structure, with the characteristics, ages, and distribution of the producing trends (Curtis, 1982). According to Curtis (1986), the Niger Delta, Gulf of Mexico and Beaufort-Mackenzie Basin are comparable geologically because all of these basins have been influenced by major delta sediment supply and similar tectonic events during the Tertiary. Additionally, the Neogene sand units of these three aforementioned basins form excellent reservoir rocks because of their relatively young age, which mean that there is limited deformation of traps by tectonism, and they are thus highly favoured for accumulation of recently generated hydrocarbons (Curtis, 1982).

However, there are marked differences in these deltas, which can be attributed to differences in the geological settings and histories. For example, US Gulf Coast

sedimentary facies and structures are different because of the presence of salt which led to the formation of a variety of salt-dome related traps (Curtis, 1982; Winker & Booth, 2000; Rowan *et al.*, 2001), in addition to the shale diapirs and rollover anticlines common to other Atlantic-type deltas and some other deltas elsewhere in the world. Furthermore, in most Tertiary deltas, there is a marked difference in structural trends which are largely dependent on the pre-Tertiary tectonic histories, which in turn influences the depositional systems and sequences (i.e. sedimentation rate to rate of subsidence, sandstone geometries; Curtis, 1982).

Tropical deltas are typically dominated by delta-top sediments containing shale through to perhydrous coal (with abundant hydrogen rich exinites, e.g. Assam-Barail, Mahakam), and associated carbonaceous shale source rock facies consisting of high proportions of terrigenous organic matter as reflected in the abundant allocthonous land derived woody and structured kerogen particles, some cuticles, pollen and spores and generally low amorphous organic matter in optical microscopic studies (Durand & Parratte, 1983; Bustin, 1988). In terms of visual kerogen petrological characteristics, the typical delta facies usually have an abundance of Type III kerogen (rich in gas-prone vitrinitic macerals) with minor liptinites (Huc *et al.*, 1986; Bustin, 1988). It would thus be expected that the biomarker distribution of the produced oil should be dominated by compounds derived from terrigenous higher plants. From current literature knowledge, except for the Assam-Barail delta, which is a "fringe" delta in an overthrust setting with a metamorphic basement (Goswami *et al.*, 2005), oil-source rock correlation studies in most Tertiary deltas are highly disputatious.

In general, Tertiary deltas world wide have seen active petroleum exploration and production in the last three decades, but whether most of the so called 'deltaic oils' are sourced within (intra-delta) or from below the delta (sub-delta) remains unclear. Previous studies have characterized oils and source rocks from single deltas (Snowdon, 1978, 1984, 1987; Ekweozor *et al.*, 1979a, 1979b; Ekweozor & Okoye, 1980; Hoffman *et al.*, 1984; Brooks, 1986a, 1986b; Curiale, 1991; Woolhouse *et al.*, 1992; Raju & Mathur, 1995; Haack *et al.*, 2000; Peters *et al.*, 2000; Eneogwe & Ekundayo, 2003; Goswami *et al.*, 2005; Curiale *et al.*, 2005), and the petroleum geochemical data from these studies may be difficult to compare retrospectively because of the different analytical goals, approaches (methods) as well as instrumental conditions used in each and partly because of continuing analytical advances. Further, it is worthy of note that palaeographical factors (location in space and time) – which control palaeo floral distributions, play a key role in the geochemical characteristics of oils from deltas. Because of their variable palaeo floral distributions (discussed in next section), the Assam, Beaufort-Mackenzie, Gulf of Mexico, Niger and the Mahakam delta have been selected as case studies (Figure 1.5).

1= Beaufort –Mackenzie (Mackenzie). 2 = Gulf of Mexico (Mississippi). 3 = Orinoco (Orinoco). 4= Niger (Niger-Benue). 5= Ogooué (Congo). 6 = Nile (Nile). 7 = Rhone (Rhone). 8 = Rhine (Rhine). 9 = Assam (Ganges-Bralumaputra). 10 = Ganges-Bralumaputra (Ganges-Bralumaputra). 11= Lena (Lena).12 =Amur- (Amur-Darya).13 = Mekong (Mekong). 14 =Sabah (Sabah). 14= Baram (Baram). 16 = Balingian (Balingian). 17 = Mahakam (Mahakam). 18 =Tarakan (Tarakan).

Figure 1.10. Map of the world shows the global distribution of major Tertiary deltaic basins with known hydrocarbon potential. The name in bracket is the draining river. Red squares denote selected case studies. (Plain map from: http://www.mapsinternational.co.uk)

1.10. Common Biomarkers in Deltaic oils and Sediments

The last three decades have seen advances in our understanding of the biosynthetic pathways of many classes of organic molecules and their application to petroleum exploration and production. Because some of these organic compounds that occur in oils and sediments possess basic carbon skeleton can be linked unmistakably to a known natural product in the biosphere, they are called biological markers or biomarkers for short (Mackenzie, 1984). Briefly, biomarkers are molecular compounds (chemical fossils) found in the geosphere with preserved and recognisable chemical structures that maintain a link to the biosphere. Key examples are discussed below.

The non-hopanoid triterpane biomarkers of the oleananoid family have been reported in the oils derived from most deltas, and are a testament to angiosperm land plant source inputs e.g. the Assam (Raju & Mathur, 1995; Goswami *et al.*, 2005), Beaufort-Mackenzie, (Brooks, 1986a; Curiale, 1991), Niger Delta (Ekweozor *et al.*, 1979a, 1979b; Ekweozor & Udo, 1988; Haack *et al.*, 2000; Eneogwe & Ekundayo, 2003) and Kutei Basin and associated Mahakam Delta (Peters *et al.*, 2000; Curiale *et al.*, 2005). Oleananes (18α(H) and 18β(H)- oleanane) are formed as diagenetic product from the β-amyrin precursor of angiosperm origin (Killops & Killops, 2005, pp. 191) via the pathway summarised in Figure 1.11. Oleanane is a marker of angiosperm higher plant input to the source rock organic matter (Ekweozor & Udo, 1988) and oleanane is used to provide geochemical information in form of the oleanane index, which is the concentrations of 18α(H) and 18β(H) isomers normalised to C_{30} 17α(H),21β(H)-hopane. The oleanane index is routinely used in conjunction with other age-specific biomarkers, to infer the age of sediment or source rock from which oil has been expelled and an oleanane index generally greater than 0.2 tentatively suggests Cretaceous or younger source rock age (Moldowan *et al.*, 1994). The relative concentration of oleanane in the oils sourced from these deltas is thought to be diagnostic of the level of contribution of angiosperm land plants to the sedimentary organic matter which has generated the oils. However, Murray *et al.* (1997) suggest that oleanane abundance could result from formation of oleanenes and preferential preservation as oleananes at the expense of the competing diagenetic reaction pathways that favour the formation of aromatic products from the β-amyrin precursor compounds (Figure 1.12). Common aromatic products that could be formed as diagenetic products from the β-amyrin precursor are the 1,2,5,6,-tetramethylnaphthalene and 1,2,7-trimethylnaphthalene (Killops & Killops,

2005,pp.195, and references therein), while 1,2,9-trimethylpicene and 3,6,7-trimethylchrysene form from α-amyrin precursor (Figure 1.13). Under common gas chromatograph conditions, oleanane can co-elute with lupane(Nytoft *et al.*,2002), thus making oleanane index sometimes difficult to interprete without caution. The widespread occurrence of oleanenes (olefin hydrocarbon of the oleananoid family) has also been reported in the literature on most deltaic oils (e.g. Woolhouse *et al.*, 1992; Eneogwe *et al.*, 2002; Goswami *et al.*, 2005; Curiale *et al.*, 2005; Curiale, 2006). In a critical review of the occurrence of olefins in oils, Curiale and Frolov (1998) suggest a primary origin involving derivation from the source rocks which expelled the oils.

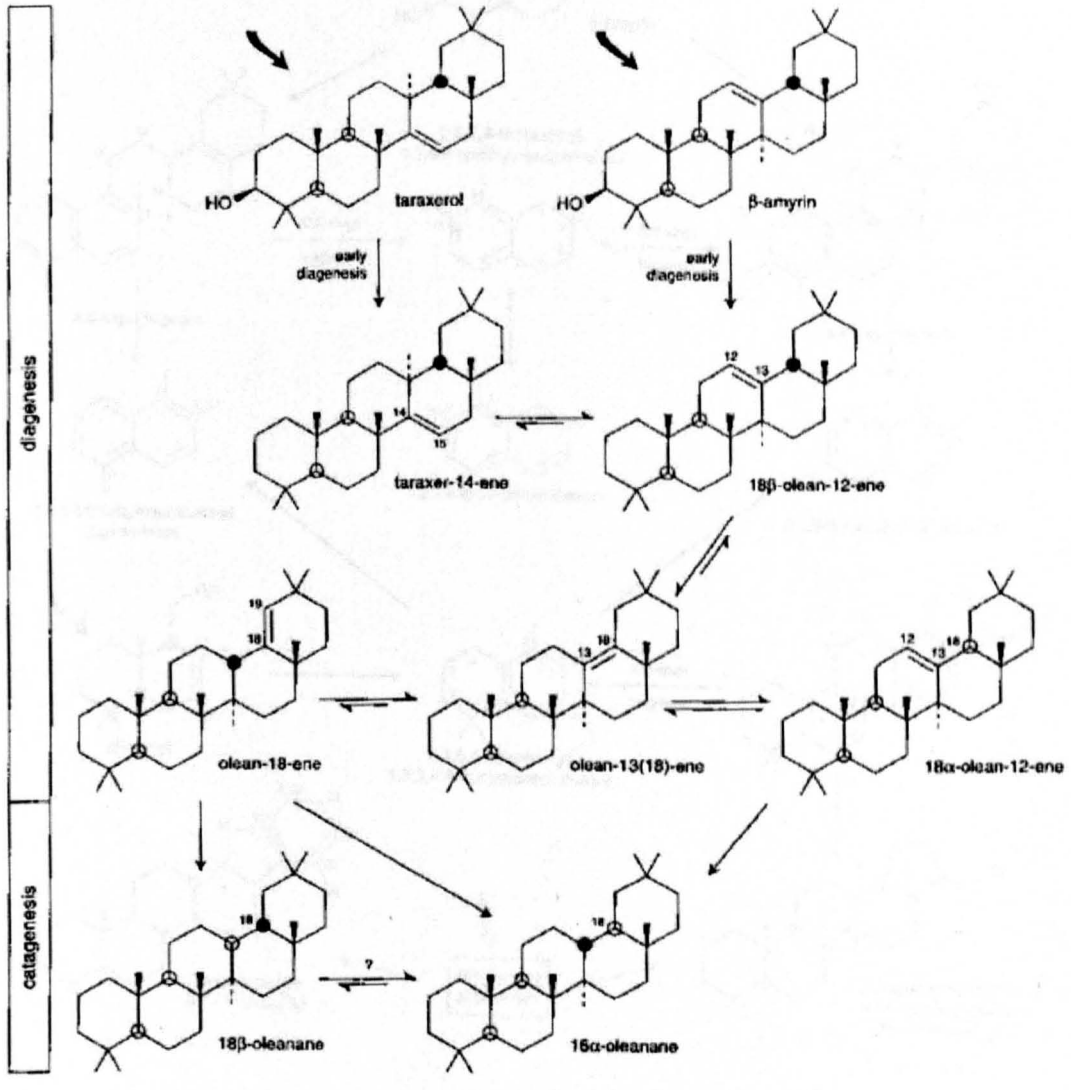

Figure1.11. Representative reaction pathway for the formation of oleanane from higher plant triterpenoids. Large arrows indicate biogenic input(Source: Killops & Killops, 2005).

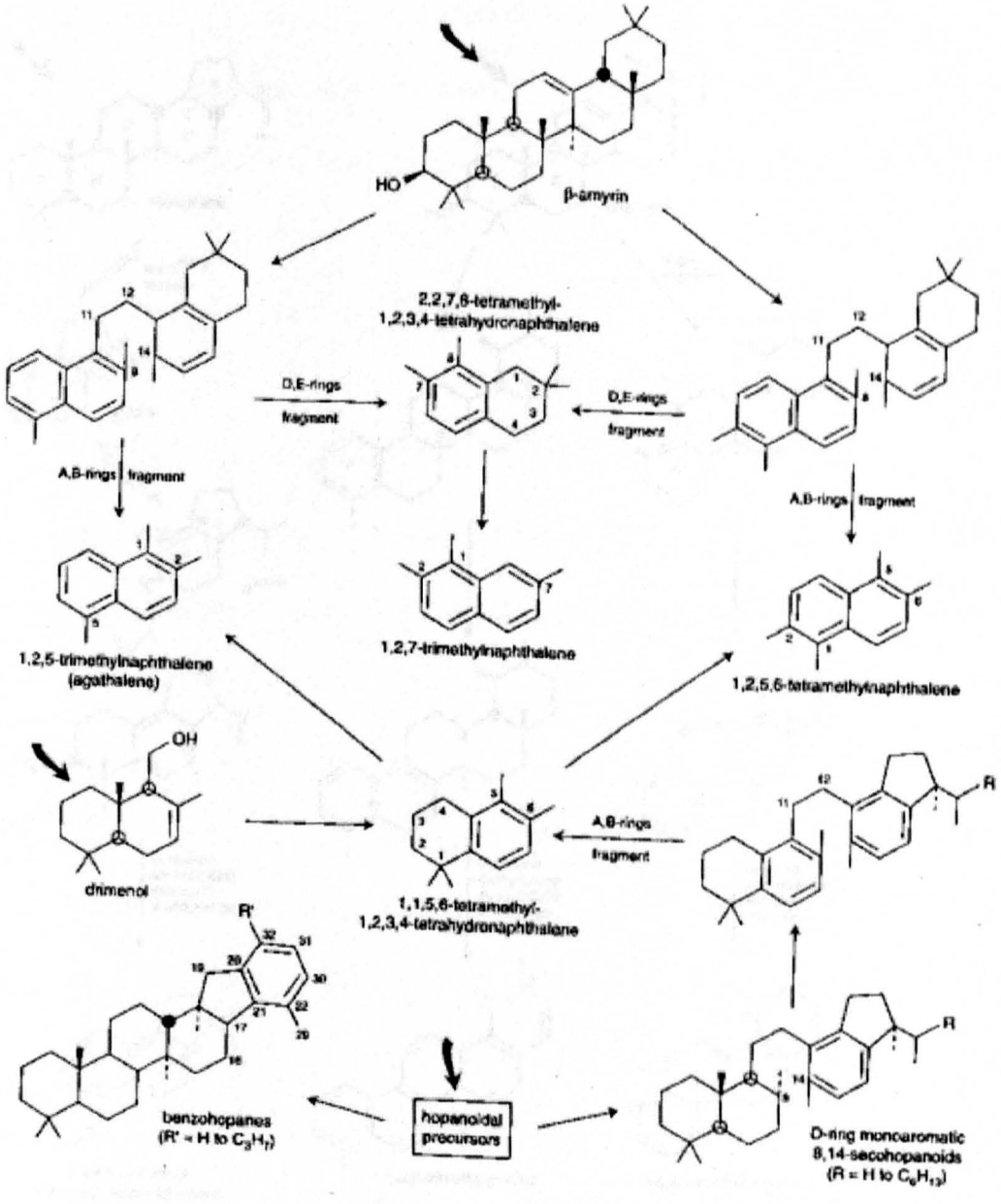

Figure1.12. Representative reaction pathway for the formation of polymethylnaphthalenes from terpenoidal precursors. Large arrows indicate biogenic input (Source: Killops & Killops, 2005).

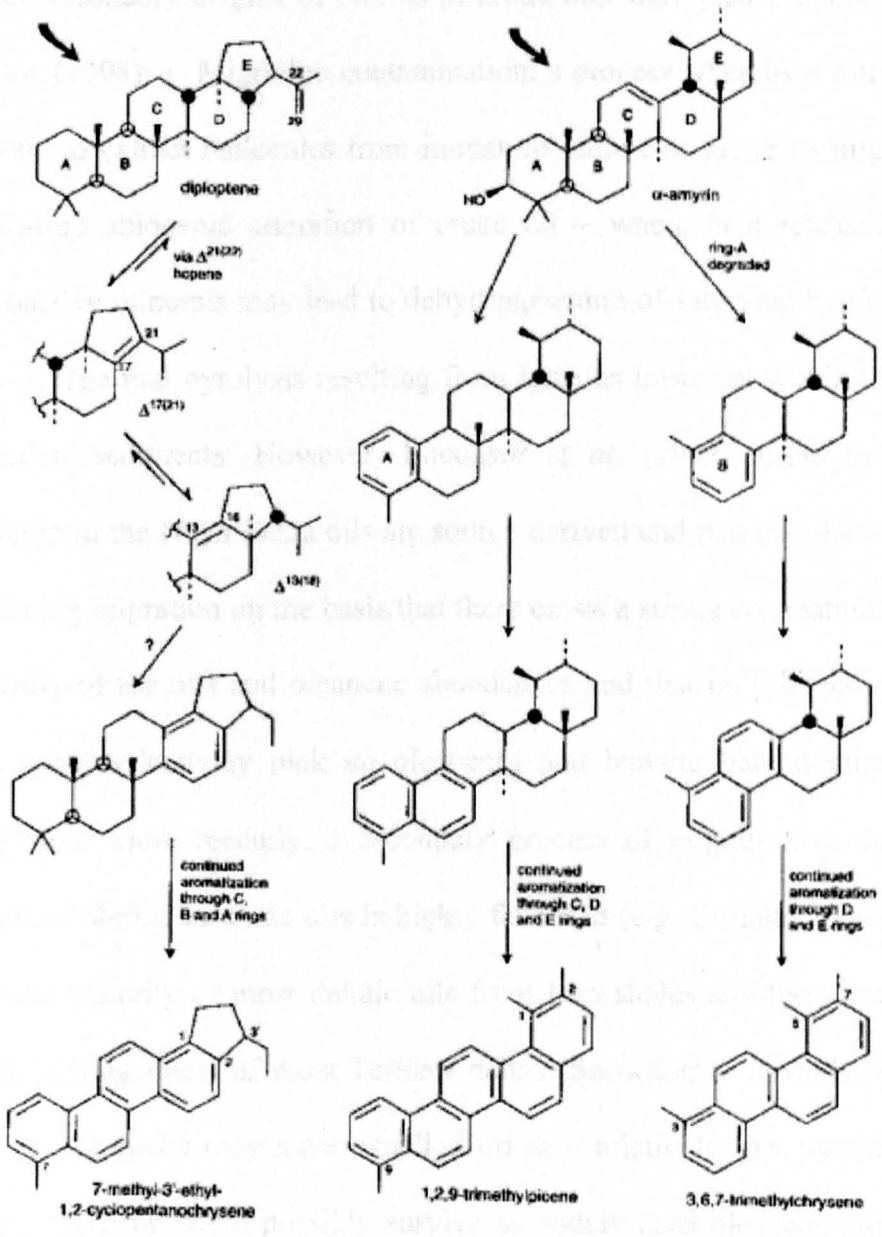

Figure 1.13. Representative reaction network showing triterpenoid aromatization reactions and products from α-amyrin. Large arrows indicate biogenic input (Source: Killops & Killops, 2005).

Three secondary origins of olefins in crude oils were also proposed by Curiale and Frolov (1998); 1. Migration contamination: a process whereby a migrating oil acts as solvent to extract molecules from immature sediments along its migration pathways. 2. In-trap abiogenic alteration of crude oil – where heat released from decaying radioactive minerals may lead to dehydrogenation of saturated hydrocarbons in crude oils. 3. Thermal pyrolysis resulting from igneous intrusion within the vicinity of the reservoir sediments. However, Eneogwe *et al.* (2002) argue that the oleanenes reported in the Niger Delta oils are source-derived and that they have not been picked up during migration on the basis that there exists a strong correlation between thermal maturity of the oils and oleanene abundances and that no process has been reported that could selectively pick up oleanenes and leaving behind other olefins during migration. More recently, a secondary process of migration contamination as the origin of olefins in crude oils is highly favoured (e.g. Curiale, 2006). Given the low thermal maturity of most deltaic oils from lean shales and the short thermal history (high heating rates) of most Tertiary deltas (Snowdon & Powell, 1982), it could be that source rocks may have expelled oil at a relatively low thermal maturity level where oleanene could possibly survive as widely used oleanane index maximises at vitrinite reflectance level of 0.55Ro(Ekweozor & Telnaes,1990), which coincides with the onset of oil window. As such, whether or not the olefins are sourced-derived or migration contamination products, is yet to be unequivocally established.

Despite the commonality shared by these deltas in terms of oleananes (18 α(H)- and 18 β(H)- isomers) and their unsaturated counterparts (oleanenes), it is noteworthy that there is evidence of differences in the molecular characteristics of the oils from these deltas. Brooks (1986a, 1986b) as well as Curiale (1991) reported significant

concentration of lupane and its isomers in the Mackenzie Delta oils. A widespread occurrence of lupanoid hydrocarbons (norlupanes and biosnorlupanes) has been reported in crude oils from the Beaufort-Mackenzie Basin, Canada (Brooks 1986a, 1986b; Curiale 1991; Piggot & Abrams, 1996), Great North Slope Basin, Northeast Alaska, USA, (Curiale 1995), Kutei Basin, Indonesia (Curiale *et al.*, 2005), Sakhalin Island, east Russia (Aref'yev *et al.*, 1996), Washington State, USA (Kvenvolden *et al.*, 1989,1991) and Western Greenland (Christiansen *et al.*, 1994,1996; Nytoft *et al.*, 2002). Further, Curiale (2006) noted that only norlupane (24-norlaupane) occurrence was reported for crude oils from South China Sea (Zhou *et al.*, 2003) and Egypt (Trendel *et al.*, 1991). Several higher plant lupanoids such as lupeol (lup-20(29)-en-3β-ol) and betulin (lup-20(29)-en-3β,28-diol) are considered as possible precursors for lupanoid hydrocarbons in oils (Peters *et al.*, 2005b, pp.580). Additionally, lupanoids can be derived from a wide variety of fucntionalised angiosperm-derived natural products occurring in living organism e.g. lupeol in bark of birch tree (Curiale 2006, and references therein). It is noteworthy that the occurrence of lupanoid hydrocarbons does not appear to have been reported in Tertiary deltaic oils from Assam and Niger Delta. Curiale (2006) in a review of the occurrence of lupane and norlupanes in oils and sediments proposed that although there is widespread occurrence of lupanoids in crude oils from around the world, the relative differences in the distributions of the isomers could be useful for correlation purposes and as a migration indicator. However, the discovery of lupane in oil from the Niger Delta, Nigeria was recently confirmed (Nytoft, H.P. Pers. Comm., 2007). The relatively scarcity with the occurrences of lupane in crude oils may be related to the difficulty in its positive identification as it often co-elutes with oleanane under common gas chromatograph column conditions (Nytoft *et al.*, 2002). A-ring degradational product of lupane

(10β-de-A-lupane) have been reported in oils together with the 10β-de-A-ursane, which are likely derived from α-amyrin precursor (Woolhouse *et al.*, 1992).

The Assam Delta, like other basins in the Southeast Asia with significant contributions of terrigenous material to the source rock organic matter, has a high concentration of bicadinanes. Bicadinanes are pentacyclic hydrocarbon biomarkers thought to be derived from catagenetic dissociation of polycadinene of the angiosperm dipterocarpaceae dammar resins (van Aarssen *et al.*, 1990). Until recently, it was thought that bicadinanes occurrence followed the limited occurrence and distribution of the dipterocarpaceae in the Asia and Indo-Australian continents, but Nytoft *et al.* (2005) reported for the first time the discovery of bicadinanes in oils from central west Greenland and the Beaufort Mackenzie Delta, Canada. This latest discovery of bicadinanes in high latitude oils suggests that resin-forming families of angiosperms other than the dipterocarpaceae may also be sources of bicadinanes. Additionally, However, the discovery of bicadinanes in Permian coals of terrigenous origin (Moldowan, 2002, unpublished data, cited in Peters *et al.*, 2005b, pp.548) casts doubt on angiosperms as the sole precursors. Palaeogeographical factors which give rise to the paleobotanical provinciality of plants (i.e. restriction of various paleofloras, which are precursors to oleananes, lupanes, etc., to localities in time and space) seem to be the primary control on the biomarker distribution disparity in the oils sourced from Assam, Beaufort-Mackenzie, Niger, Mahakam and other Tertiary deltas of the world.

1.11. Aim and Objectives

As modern deltaic environments are presently being intensively explored for oil and gas and since drilling in progressively deeper (kilometre depth) water has become commercially viable, there is a need to carry out more work that will improve the

current inadequate understanding of the petroleum systems operating in Tertiary deltas. In the exploration for oil and gas, particularly in Tertiary deltaic systems, there are a number of fundamental questions that remain unanswered. For instance, why is it so difficult to correlate deltaic oils to their true source rocks? Do we attribute the geochemical divergence between some Tertiary delta reservoired oils and their putative source rocks to indicate that the true source rock is in part of the delta but has yet to be drilled or sampled, or that the source rock is outside of the delta wedge? Could other post generation processes, such as leaching (migration-contamination), mixing and biodegradation be contributing significantly to the alteration of "primary oils" (original oil composition) thus making oil-source rock correlations difficult? How can we categorize deltaic oil accumulation in terms of the numbers of source kitchens and relate this to the levels of the efficiency (i.e. how much of the reservoired oils come from a particular source rock group) of these source rocks?

The primary aim of this project is to characterize, compare and synthesise the common factors of oils from Tertiary deltas using Assam, Niger, Mackenzie, Mahakam (Kutei Basin) and Mississippi (Gulf of Mexico) deltas as case studies.

The workflow required to meet the objectives of this project is:

- To select and obtain samples of oils representative of Tertiary deltas worldwide.
- To analyse these oils at bulk, molecular and isotopic levels in order to characterise them in terms of inferred source rock depositional environment, lithology and age, maturity at expulsion, migrational fractionation (±leaching) and intra-reservoir alteration.

- To use predictive multivariate statistics to search for new biomarkers and other geochemical parameters capable of further characterising these Tertiary deltaic oils.
- To generate geochemical-stratigraphic models that will answer key questions as to why it is so difficult to correlate Tertiary deltaic oils to their alleged source rocks.
- To use graphical analysis and multivariate statistics to identify genetically related oil families within these basins as well as to recognise the signatures from different primary bioproducers contributing to source rock kerogens.
- In a broader sense, to generate an internally consistent data set characterising Tertiary deltaic petroleum systems on a global scale.

CHAPTER TWO

SUMMARY OF THE PETROLEUM SYSTEMS OF CASE STUDY DELTAS

2.0. Introduction

This chapter describes and discusses currently available information on the petroleum systems of the basins that are studied in this thesis. A short review is given on the geological evolution and stratigraphy of each of the case study deltas. For each delta, a summary is made of the published crude oil geochemistry and the established petroleum system(s) based on the genetic relationships between the oils and their putative source rock(s).

2.1. Assam Delta

2.1.1. Evolution and stratigraphy

The Assam sedimentary basin (a part of the Assam-Arakan province) is situated in the north-eastern segment of the Indian subcontinent (Figure 2.1). In India, the Assam geological province covers an estimated area of 74,000km^2 (Wandrey, 2004).

The present day Assam Delta (often referred to in literature as Assam Valley) is an intermontane basin that is margined by the major draining river Brahmaputra and the Himalayan mountain ranges in the north/north-west, and on the south and east by the Indo-Burman Ranges and the Naga folded and thrust zone (Wandrey, 2004; Goswami *et al.*, 2005).

Tectonically, the evolution of the Assam delta is closely associated with the Gondwana break-up in the Late Jurassic (145Ma). The Indian plate is an outgrowth of the break up of the southern hemisphere super-continent called Gondwana (Africa, South America, Antarctica, Australia and India) (Wandrey, 2004). Prior to the rift,

India was at a latitude that reflects a cold paleoclimate. Following the Gondwana rifting, the Indian plate drifted northward into a warmer climate during the early Cretaceous through the Late Cretaceous time (65 Ma) at an accelerated rate of 15-20 cm/yr (Wandrey, 2004). The northward movement culminated in the formation of the sea floor, and opening of the Indian Ocean in the south, contraction of the Tethyan Ocean in the north as well as the collision of the Indian and the Eurasian plates to form the Himalayan mountain ranges and the subsequent block faulting and development of a south-easterly dipping shelf called the Assam Shelf

Figure 2.1. Map showing the approxiamte location of Assam in the north-eastern corner of India (red box). Plain map taken from: http://www.mikelockett.com/cp/we7/uploads/1000/india.jpg)

Following the rising of the Himalayan mountain ranges as the Indian plate was subducted beneath the Eurasian plate, weathering of the frontal ranges formed

sediments which were transported down the slope. The Ganges, Brahmaputra and several other rivers that drain the Himalayan orogenic belt began to develop extensive deltas in response to the sediment supplies (Wandrey, 2004).

Stratigraphically, the Assam shelf was on a passive continental margin during the Late Cretaceous to early Tertiary time. Figure 2.2 shows the generalized Tertiary stratigraphy of the Assam Basin. The depositional environment was a shallow marine setting during this time and this was documented in the sedimentation of more than 500m of sandstones and shales of the upper Cretaceous Dergaon Formation (Raju & Mathur, 1995; Wandrey, 2004). The medium-grained massive Paleocene sandstone bed of Langpar and Tura formations lies unconformably on the Dergaon Formation. The over 250m of these dominantly sandstone beds were laid down in a fluvial to marginal marine environment. Overlying the Langpar Formation is the Sylhet and Kopili formations of the Jaintia Group. The Eocene Sylhet Formation consists of three-member lithostratigraphic units that are well differentiated on the basis of their depositional environments; the oldest member is the Lakadong (thin sandstone, interbedded shelf-lagoonal shales, coals and shallow water platform calcareous sandstone), Clay stone and siltstone beds of the Narputh Member overlay the Lakadong Member. The essentially shelf carbonate with minor siltstone and clay interbeddings of the Prang Member forms the uppermost member of the Sylhet Formation (Mathur *et al.*, 2001; Wandrey, 2004)

Subsequent to the deposition of the Sylhet Formation, was a regional unconformity that transcends the entire basin and over which has accumulated middle Eocene shallow marine shales and interbedded limestone of the Kopili Formation. The Kopili Formation has an estimated thickness of about 500m (Wandrey, 2004). The Barail

Group rocks (Upper Eocene-Oligocene) were deposited on top of the Kopili Formation.

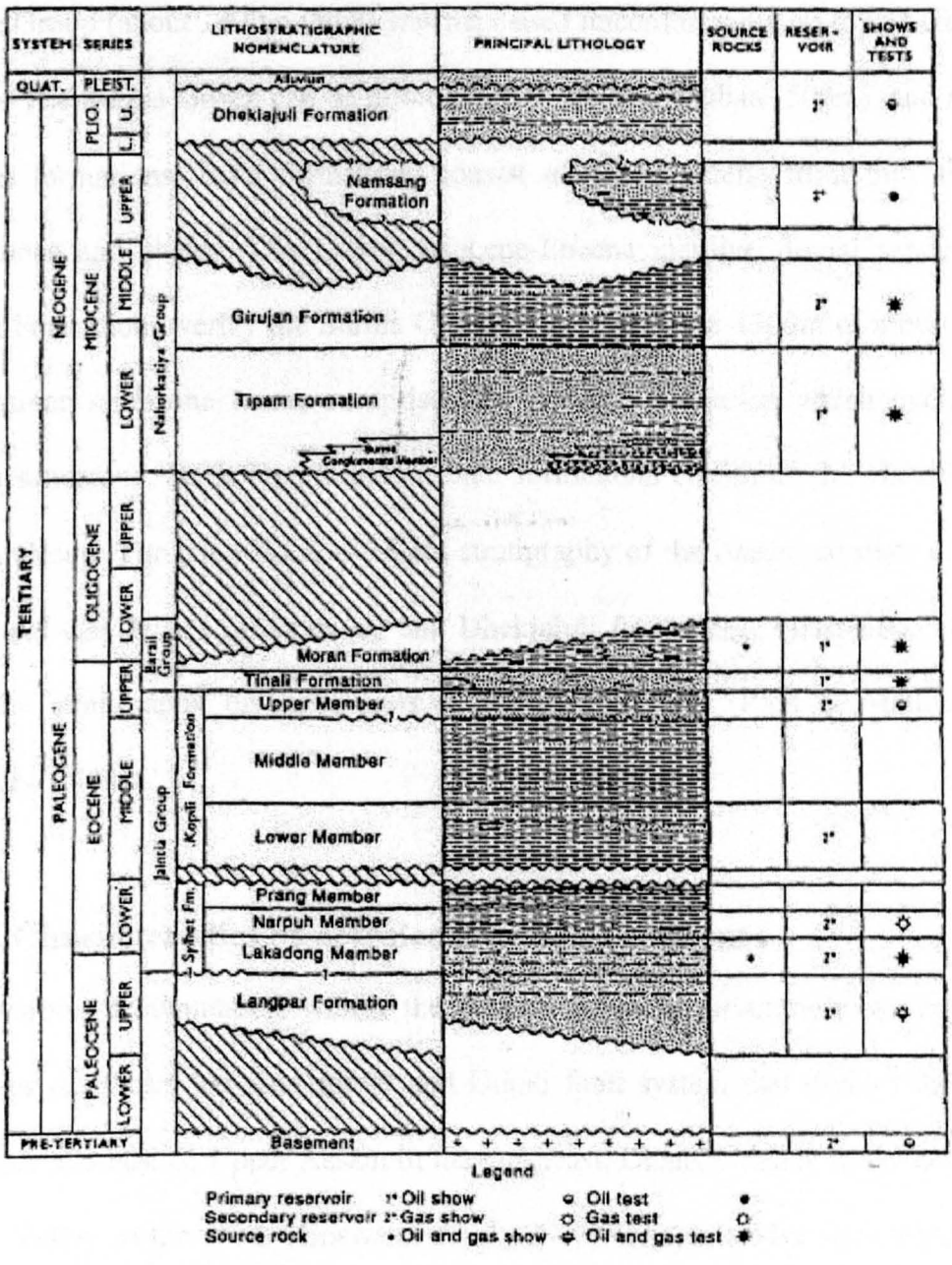

Figure 2.2. Generalised stratigraphy of Assam (Source: Raju & Mathur, 1995)

The Barail Group is divided into the lower (essentially 900m thick delta front sandstone, also known in some parts of Assam as the Tinali Formation), and the upper Barail Group (more than 1200m of delta plain coal and shale unit equivalent to the

Rudrasagar Formation elsewhere). The Barail Group is again separated from its overlying stratigraphic units by a major unconformity that is probably connected with the uplift initiated by the crustal shortening event (Wandrey, 2004). The Miocene Surma Group (about 1400m thick) was deposited unconformably on top of the Barail Group. The Surma Group can be differentiated into the Bhuban (500m), and Bokabil (900m) formations. Both formations consist of prodelta-delta front thin siltstone, sandstones and shales. The Lower Miocene-Eocene massive fluvial sandstone of Tipam Formation overlay the Surma Group sediments. Over 1300m of mottled clays with minor sandstone lenses comprises the Girujan Formation which overlies the Tipam sandstone. Both Tipam and Girujan formations constitute the Nahorkatiya / Tipam Group. The late Miocene-Recent stratigraphy of the Assam consists of fluvial sands and clay lenses of Namsong and Dhekiajuli formations. Pleistocene alluvium caps the stratigraphy on most parts of the Assam shelf (Raju & Mathur 1995; Wandrey, 2004).

2.1.2. Characteristics of petroleum systems elements

Hydrocarbon accumulation within the Assam Basin is structurally controlled by northwest-southeast trending Jorhat and Dunki fault system that divides the region into three sub-basins; Upper Assam in the northeast, Dhansri Valley in the center and Surma Valley in the south (Goswami *et al.*, 2005). The extensive fault system also permits mixing of hydrocarbons from multiple sources. Despite efforts to better define the Assam petroleum systems, the oil-source rock relationships are not yet fully understood (Raju & Mathur, 1995; Mathur *et al.*, 2001; Goswami *et al.*, 2005). Goswami *et al.* (2005) recognised two petroleum systems (the Barail-Bokabil and the Kopili-Sylhet) using only a few samples of oils and source rocks, and up to four

possible petroleum systems (Barail-Bokabil and the Kopili-Sylhet, Barail-Barail? and Kopili-Barail?) were also proposed. The possibility of three or more petroleum systems and/or one composite system in the Assam Basin cannot be excluded (Wandrey, 2004). To date, no oil-oil correlation studies have been published for the Assam Basin.

2.1.2.1 Source rocks

Major source rocks contributing to the petroleum systems include the deltaic coal and shale of the Eocene-Oligocene Barail Group, together with Eocene prodeltaic shales of Kopili Formation (Wandrey, 2004; Goswami *et al.*, 2005). The Barail Group coals and associated shale have proven to be the primary contributor to the basin's petroleum system (Goswami *et al.*, 2005). Shales of the Lakadong member (oldest source rock in the basin) are a minor contributor to the oil generated in the basin (Mathur *et al.*, 2001). TOC values range between 0.8 wt.% - 12 wt % within the Barail Group (Wandrey, 2004) though interbedded coals have values in the 60-75%TOC range. Organic matter within the Kopili Shale Formation includes Type II and III kerogens and TOC ranges from 0.5wt.% to 1.5wt.%.

2.1.2.2. Reservoir rocks

Reservoir rocks of the Assam basin can be divided into primary and secondary reservoirs based on the volume of hydrocarbon they hold. The massive sandstone of Tipam Group and the Barail main pay sands are the most productive reservoir units (primary reservoir) (Wandrey, 2004; Goswami *et al.*, 2005). The Tipam Group sandstone permeability ranges from less than 8 millidarcies to as much as 800 millidarcies with porosities of about 7% to 30 % (Wandrey, 2004). Secondary

reservoir rocks are the limestone and sandstone of the Sylhet Formation (Jaintia Group), and interbedded sandstone of the Kopili Formation (Wandrey, 2004).

2.1.2.3. Traps and seal mechanism

The widespread occurrence of numerous fault systems and structural highs in the Assam Basin produce anticlinal and faulted anticlinal traps as the major traps. Other traps are stratigraphic including sandstone lenses within the Barail Group.Although some minor seals occur within the interbedded shales and clays of the Oligo-Miocene sequences, the marine shale and clays of the Girujan Formation (Nahorkatiya/Tipam Group) acts as a regional seal for the traps (Wandrey, 2004).

2.2. Beaufort-Mackenzie Basin

2.2.1. Geological setting and stratigraphy

The Beaufort-Mackenzie Basin is located in the northern coast of Canada. The basin occupies an area of 92,000km^2 (Figure 2.3) and is built up of sedimentary discharge of River Mackenzie into the Beaufort Sea of the Artic Ocean (Greiner & Chi, 1995). The Beaufort Mackenzie Basin constitutes one of Canada's major oil, gas and gas hydrate provinces (Ondrak *et al.*, 2005), though due to remoteness and political & environmental factors, current production is limited to the Norman Wells Field in the Mackenzie Valley delivering through a small 60 year old pipeline. The Mackenzie Delta, the Tuktoyaktuk Peninsula and the Beaufort Shelf constitute the Beaufort-Mackenzie Basin (Greiner & Chi, 1995). In terms of local geography, the Beaufort Mackenzie Basin is margined in the North by the deep Artic Ocean, in the southwest by the northern segment of the Richardson Mountains and by the Aklavik Arch in the southeast (Greiner & Chi, 1995, and references therein).

The evolution of the Beaufort-Mackenzie Basin is closely associated with the Arctic plate tectonic events (Young *et al.*, 1976). Two views have emerged on the structural evolution of the Beaufort-Mackenzie Basin and the differences in views are mainly on the timing of specific events: Dietrich *et al.* (1989a) suggested an Early Jurassic to Early Cretaceous extension followed by compressional events that lasted up to the present, while another proposal, favouring a period of extension that lasted untill the Mid-Miocene (14 Ma), followed by a period of subsidence consequential to the accumulation of about 16km of Cretaceous to Recent sediments, was made by Enachescu (1990).

According to Greiner and Chi (1995), the Beaufort-Mackenzie Basin developed over Precambrian to Devonian truncated terrain and the basin is filled with at least 12km of Jurassic, Cretaceous and Tertiary clastics that thicken seaward. The pre-Tertiary sediments of the basin are constituted by transgressive shallow marine clastics, minor regressive sands and organic rich marine shales (Figure 2.4). Several workers (e.g. McWhae, 1986; Lawver & Scotese, 1990), believe that the interaction between rift tectonics, Cordilleran compressional deformation, and the thermal subsidence of the continental margin gave rise to the present day structural and stratigraphic characteristics of the Beaufort-Mackenzie Basin. Several tectonostratigraphic phases of basin filling have been recognised (Dixon, *et al.*, 1985; Dixon *et al.*, 1992).

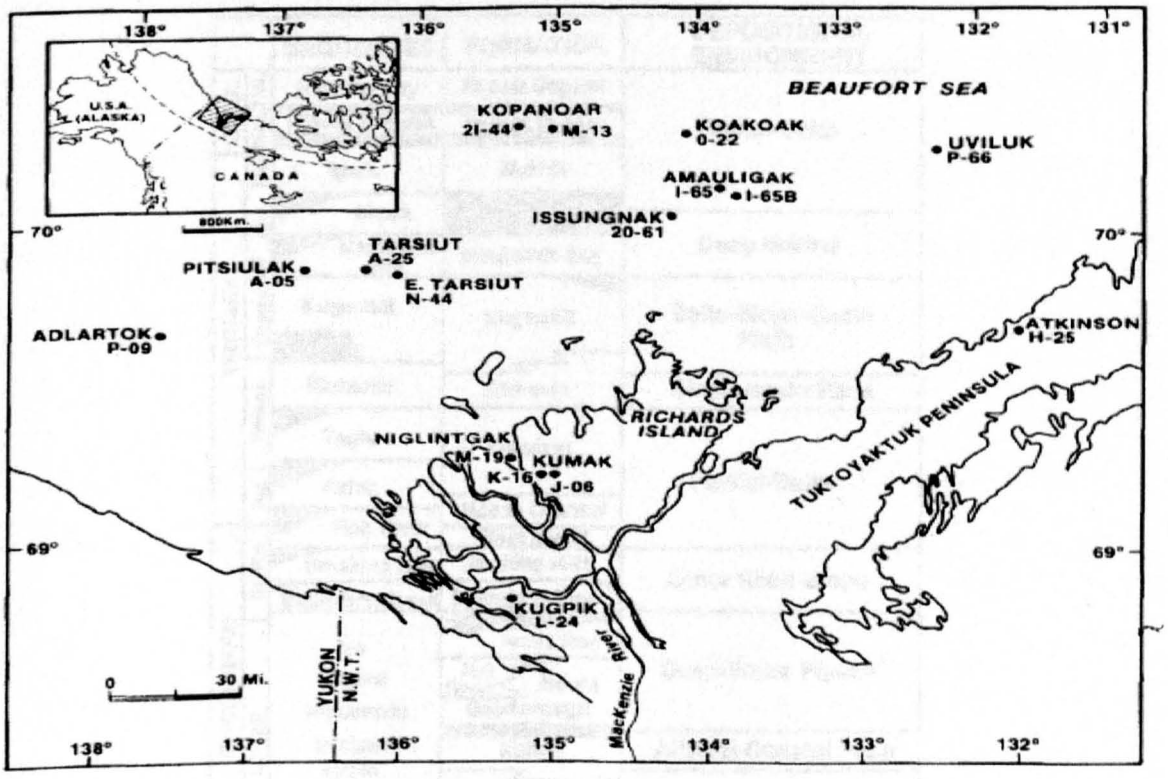

Figure 2.3. Location map of Canadian Beaufort and Mackenzie River Delta in north-western Canada. Map shows location of some oil wells where samples have been collected (adapted from Curiale, 1991).

In an analysis of the Beaufort-Mackenzie Basin's burial and thermal histories, Tang and Lerche (1991) described two of these tectono-stratigraphic episodes that occur in

the pre-Cretaceous sediments: firstly, a Jurassic to Middle Hauterivian phase marked by the deposition of mainly epicontinetal shelf deposits of the Bug Creek Group, organic rich shale of the Husky Formation, and the sandstones of Parsons Formation (Dixon *et al.*, 1985, cited in Tang & Lerche, 1991); secondly a Late Hauterivian-Albian episode marked by deposition of low energy shelf and deepwater flysch of the Atkinson and Arctic Red formations. (Tang & Lerche, 1991, and references therein). A major regional unconformity separates the tectonostratigraphic episodes one and two (Tang & Lerche, 1991). According to Dixon *et al.* (1992), the Late Cretaceous to Pleistocene sediments of the Beaufort-Mackenzie Basin are divisible into four major tectonostratigraphic assemblages as follows:

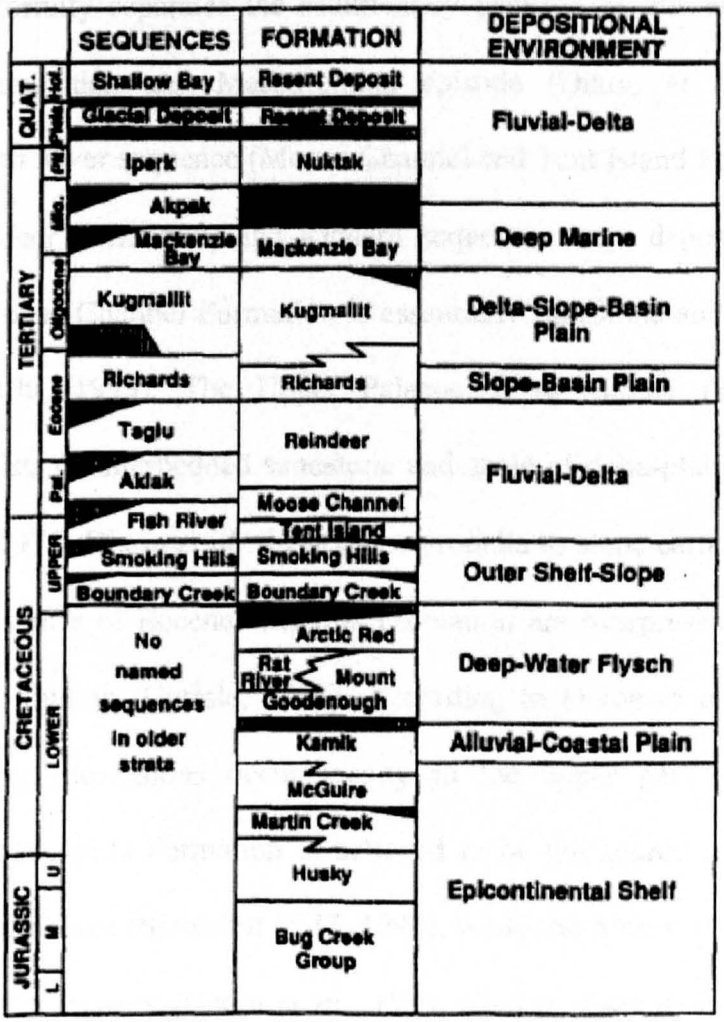

Figure 2.4. Generalised stratigraphy of the Beaufort Mackenzie Basin (from Tang & Lerche, 1991, after Dixon & Dietrich, 1988).

Cenomanian – Campanian and Maastrictian:

This episode was marked by drifting and subsidence of the Canadian continental margins (Dixon *et al.*, 1992). The outer shelf-slope and deep basin sediments of the organic rich Boundary Creek and Smoking Hill formations that were deposited under low energy and anoxic marine conditions represent this tectonostratigraphic episode (Dixon *et al.*, 1985, cited in Dixon *et al.*, 1992).

Maastrichtian- Middle Eocene:

This episode marked the onset of deltaic sequence and occurred during a major northward shift in deposition towards the Canadian basin's continental margin and a regional unconformity separates the sedimentary package of this episode from the Cenomanian-Campanian and Maastrichtian episode (Dixon *et al.*, 1992). The sediments of Fish River sequence (Moose Channel and Tent Island Formation), Taglu sequence (Reindeer Formation) and Richard sequences were deposited during this episode. The Moose Channel Formation is essentially sandstone and mudstone units (Greiner and Chi, 1995). The Upper Palaeocene to Middle Eocene Reindeer Formation consists of interbedded sandstone and shale of delta-plain and delta-front origin (Young, 1975; Dixon *et al.*, 1992). The prodelta to slope carbonaceous marine mudstones and shales of Eocene Richards Formation are overpressured and overlay the Reindeer Formation (Curiale, 1991). According to Dixon *et al.* (1992), minor sandstone-bearing successions occur locally in the upper part of the Richards Formation. The Richards Formation is believed to be the source rock unit for this stratigraphic assemblage (Snowdon 1987, 1990), while the Moose Channel sands are considered to be reservoirs (Dixon *et al.*, 1985, cited in Tang & Lerche, 1991, pp. 512).

Late Eocene- Late Miocene:

During this episode, the sediment depocenter moved further basin-ward (Dixon *et al.*, 1992), and the marine and non-marine sandstones and mudstones of late Eocene-Oligocene Kugmallit Formation (delta plain to distal slope) were deposited. The Oligocene-Miocene deep marine Mackenzie Bay Formation overlies the Kugmallit Formation and is a dominantly shale sequence that is up to 2000m thick in the western Canadian Beaufort Sea (Dixon *et al.*, 1992). This tectonostratigraphic episode was marked by compressional deformation that lasted into the Miocene (Dixon *et al.*, 1992). A major unconformity separates this phase from the overlying Pliocene to Pleistocene strata.

Pliocene- Lower Pleistocene:

The prevailing depositional environment during this phase was essentially fluvio-deltaic and was marked by the deposition of the Ipark and younger sequences of the Beaufort Formation (Miocene-Pliocene). Finally, the Pleistocene alluvium and glacial deposits) were laid unconformably on these younger sequences (Dixon *et al.*, 1992).

A comprehensive review of the stratigraphic and structural evolution of the Beaufort-Mackenzie Basin is provided in Dixon *et al.* (1992).

2.2.2. Characteristics of the petroleum systems elements

2.2.2.1. Source rocks

Several studies have been carried out to identify the true source rocks for the hydrocarbons reservoired within the Mackenzie Delta. Potential source rocks for the oils discovered in the basin are the Jurassic Husky Formation (Dixon *et al.*, 1985; Xiong *et al.*, 2005), Late Cretaceous shales of Boundary Creek and Smoking Hill formations (Snowdon, 1978,1980; Creaney, 1980), shales of the Late Cretaceous Tent

Island Formation (Snowdon, 1987), Paleocene- Eocene Reindeer Formation (Snowdon, 1987), Eocene Richard Formation (Snowdon & Powell, 1982; Snowdon, 1987, 1990; Curiale, 1991). The pre-Tertiary source rock units are organic rich and contain abundant marine algal organic matter (Snowdon, 1978, 1979; Creaney 1980).

At outcrop, the Cenomanian-Turonian Boundary Creek and Santonian-Campanian Smoking Hill formations contain hundreds of meters of organic rich shales (TOC up to 4-6% with bentonite interbedding (Dixon *et al.*, 1992), and organic matter mostly derived from algal and other marine organisms (Snowdon, 1980). Creaney (1980) described the organic matter within the Boundary Creek shales to be bituminous because of the high concentration of alginite within the liptinite macerals and few resinites. Additional evidence for high hydrocarbon potential of the Boundary Creek shale is evident in the positive geochemical correlation of oils in the Imnak, Mayogiak and Kugpik wells with extracts of Boundary Creek shales (Snowdon, 1980). The shale extracts and the oils are characterised by low pristane/phytane (pr/ph) ratios and the Boundary Creek Formation represents the only sequence of known low pr/ph ratios that reflects reducing depositional conditions (Snowdon, 1978). Geochemical evidence shows limited land plant contribution to the organic matter in the Boundary Creek Formation (Snowdon, 1980). The controls on Boundary Creek's hydrocarbon prospectivity in any part of the basin are its burial depths (Snowdon, 1980) and lateral extent, and based on this, if intervals within the shale are present and buried to oil generation depths, the shale has high potential to expel liquid petroleum (Creaney, 1980; Snowdon, 1980).

In a study of 276 samples from six wells, Snowdon (1987) reported average TOC values of 1.84% (standard deviation 0.80) for the shales of Late Cretaceous Tent Island Formation. The hydrogen index (HI) is generally low for these shale samples (average, 200mgHC/gTOC) and they are dominated by Type III kerogen (Snowdon, 1987). However, the slightly more algal rich intervals within the Tent island shales have HI values as high as 255mgHC/gTOC (Snowdon, 1987). The overlying shales of Reindeer Formation are characterised by intervals rich in higher plant-derived Type III kerogen (Snowdon, 1987). Snowdon (1987) reported in a study of 134 samples an average TOC of 2.34% (standard deviation of 1.86) for the Reindeer Formation. Sterane compositions in the bitumen extracts are dominated by C_{29} sterane homologues, consistent with a higher plant source for the organic matter in Reindeer Formation (Snowdon, 1987). The presence of resinite Type III organic matter and few alginites led to the conclusion by Snowdon (1987) that the Reindeer and Tent Island formations have limited potential to generate liquid petroleum. The lower part of the Eocene Richards Formation is considered as the source rock for most of the terrigenous oils in Tertiary reservoirs based on positive geochemical correlation of oils and the bitumen extracts of the basal section of the Richards Formation (Brooks, 1986a, 1986b). However the source rock potential of the Richards Formation is very low, and by conventional standard, the formation has a limited hydrocarbon generation potential (Snowdon, 1984, 1987; Dietrich *et al.*, 1989; Issler & Snowdon, 1990).

Dieckmann *et al.* (2005) proposed additional generation of hydrocarbons from neo-formed macromolecular organic matter (organic matter formed from the transformation of residual kerogen), which degrades beyond the conventional oil window in the deep Mackenzie Delta overmature sequences. It is estimated that

hydrocarbons derived from neo-formed organic matter could upgrade the potential of deep Mackenzie Delta Basin by up to 20% compared with the previously accepted estimates (Dieckmann *et al.*, 2005). This postulation is well supported by the fitting of carbon isotope values of methane generated from these neo-formed sources with natural gas samples from the Mackenzie Delta (Dieckmann *et al.*, 2005).

2.2.2.2. Families of oils and oil-source rock correlations

Using a combination of geological models and constraints and limited geochemical data, Snowdon and Powell (1979) identified four distinct families of oils in the Beaufort-Mackenzie Basin. However, using a more powerful analytical approach that incorporated the use of biomarkers for oil-oil correlation, Brooks *et al.* (1986a) restricted this to three oil families that reflect three distinct source units. These oil families are:

A. Oils showing expulsion from a source rock of marine organofacies, which correlate with Boundary Creek shale extracts (Brooks, 1986a). They are the most mature oil group.

B. Terrigenous organic matter derived oils (category II and IV of Snowdon and Powell, 1979), and which are distinguishable from those of the third family on the basis of triterpane distributions.

C. Terrigenous organic matter sourced oils that are divisible to further sub-groups based on diasterane/sterane contents. They contain oleanane and biosnorlupanes.

Families B and C oils have been derived from source rock(s) rich in terrigenous organic matter typical of deltaic successions (Brooks, 1986a). The Eocene Richards Formation has been inferred as one of the sources for the terrigenous oils in the Tertiary sequence on the basis of the occurrence of bisnorlupanes in the Richards

Shale extracts (Brooks, 1986a; Curiale, 1991). Other Palaeocene age shales contain 28,30-bisnorhopane, but this compound is absent in the Tertiary oils, thus providing evidence for a more probable Eocene Richards contribution to the terrigenous oils in the Tertiary reservoirs (Snowdon, 1988). Additionally, a consideration for a Kugmallit contribution to the terrigenous oil accumulations is less favoured because of its high stratigraphic position, thus implying low thermal maturity (Dixon *et al.*, 1992). However, on geochemical evidence, the Kugmallit source cannot be ruled out as a contributor to the terrigenous oil pool, because extracts of an organic rich interval within the Kugmallit formation contains similar biomarkers (biosnorlupanes), to those found in the oils and which were also observed in the lower Richards Formation (Dixon *et al.*, 1992).

Curiale (1991) asserts that the Cretaceous-reservoired oils are indeed distinctly sourced as earlier demonstrated by Brooks (1986a), but Curiale (1991) further suggested that the Tertiary-reservoired oils can be separated into three families on the basis of compositional differences among oils in Kugmallit/Richards, Reindeer and Moose Channel reservoirs or two genetic families on the basis of the presence or absence of bisnorlupanes, noroleanene and norursene. The basis of Curiale's (1991) grouping of Tertiary oils into two groups differs from previous workers (e.g. Brooks, 1986a), because Brooks (1986a) grouped the Tertiary oils into a super family that is divisible into two sub-groups on the basis of diasterane/regular sterane content. However, Curiale (1991) noted that the diasterane/regular sterane content of the studied oils only reflect maturity differences rather than genetic control. More importantly, although the bitumen extracts of the basal part of the Richards Formation correlate well with the Tertiary oils based on bisnorlupanes occurrence, Curiale

(1991) made a tentative conclusion that the poor hydrocarbon source potential of the Richards Formation based on conventional criteria, implicates oil sourcing from additional source rock intervals (different from Richards Formation) that are more organic rich within the Palaeogene sequence, and are yet to be identified in the basin. In what could be seen as confirmation of Curiale's (1991) conclusion, Snowdon *et al*, (2004) reported the discovery of the 17α(H) and 17β(H), 23,28-bisnorlupane in a coaly interval within the lower Taglu sequence (early Eocene). That report thus improved our understanding that additional source rocks contributing to the Tertiary-reservoired oils exist other than the Richards Formation, as the bisnorlupanes present in the Tertiary-reservoired oils were only previously known to occur in the basal part of the Richards Formation. Snowdon *et al.* (2004) thus concluded that previous oil-source rock correlation studies may be incorrect and that coals in the Taglu sequence may be the principal source rock for oils reservoired in Palaeocene and early Eocene sequences in the southern part of the Mackenzie Delta.

Xiong *et al.* (2005) show that, based on compound specific stable carbon and hydrogen isotopes (CSIA) of *n*-alkanes in source rock bitumen extracts, the Mesozoic marine and non-marine source rocks can be distinguished from the Tertiary deltaic source rocks. Nearly constant *n*-alkane isotope values were obtained for the Mesozoic source rock extracts and using a combination of the CSIA data and biomarkers, Xiong *et al.* (2005) successfully correlated the Kamik, Parsons, and Siku oils to mature Jurassic-Lower Cretaceous source rocks, such as the Husky Formation. Conversely, Tertiary-reservoired terrigenous oils have more negative *n*-alkane isotope values with increasing carbon number and these correlate with source rocks in the Taglu sequence.

There is evidence of biodegradation in some of the oils because of their low reservoir temperatures (Powell & Snowdon, 1975; Snowdon & Powell, 1982; Snowdon, 1988; Brooks, 1986a). Additionally, the oils are characterised by low molecular thermal maturity values (odd over even predominance of *n*-alkanes, triterpane and sterane maturity parameters), suggesting early oil generation (Snowdon and Powell, 1982; Brooks, 1986a). The low thermal maturity of the terrigenous oils is thought to be a result of early oil generation from source rocks containing abundant resinitic organic matter (Snowdon, 1980b, Snowdon & Powell, 1982). Snowdon and Powell, (1982) show geochemical evidence (pr/nC_{17} ratios, stable isotopes and diterpenoid compounds) to support a proposal that oils and condensates of the Beaufort-Mackenzie Basin are characteristically immature to low maturity corresponding to vitrinite reflectance value of 0.4-0.6%R_0.

The significant occurrence of resinite in source rocks has been used to explain the huge hydrocarbon accumulation despite low TOC contents of some of the shale intervals (e.g. Isaksen *et al.*, 1998). On the basis of the low thermal maturity of resinite-derived oils and condensates, Snowdon and Powell (1982) proposed the modification of conventional hydrocarbon generation models of Tissot *et al.* (1974) and Harwood (1977) to give consideration to early generation of oils and condensates from resinite-rich terrigenous organic matter. Such a proposal for the modification of oil generation model will incorporate a new Type III organic matter suggested by Snowdon and Powell (1982) to be described as Type IIIa (resinite rich 10-15%). The subsequent recognition of the leaching process during migration has provided an

alternative explanation of the low maturity signature observed in reservoired oils. I.e. the oils pick up biomarkers from immature units during migration.

2.2.2.3. Reservoirs, traps and seals

The principal reservoirs occur in Oligocene sandstones of the Kugmallit sequence (Enachescu, 1990; Dixon *et al.*, 1992), and the overlying shales of the Miocene Mackenzie Bay sequence provide seals (Enachescu, 1990). The oil and gas discoveries of the Amauligak field are located within the upthrown rotated fault block within the Tarsiut-Amauligak fault zone of the Kugmallit sandstone reservoirs (Dixon *et al.*, 1992). The thermal and subsidence history suggest multiple phases of hydrocarbon generation and reservoir filling (Dixon *et al.*, 1992). Hydrocarbons are trapped in structural and stratigraphic traps (Dixon *et al.*, 1992).

Based on thermal maturation pattern in seven studied wells, Tang and Lerche (1991) proposed that the hydrocarbons in Cretaceous reservoirs probably migrated vertically from the Husky Formation and that the hydrocarbons in Tertiary reservoirs may have been sourced by means of lateral migration from more mature offshore equivalents of the onshore Richards Formation. Snowdon (1988) observed that oils in offshore reservoirs are thermally more mature than their reservoir host rocks, whereas oils in onshore reservoirs have similar maturity ranges to those of their reservoir rocks. This observation led to the conclusion that extensive vertical migration along faults may be prevalent in the northernmost oils than for nearshore and onshore oils in the south.

2.3. Gulf of Mexico

2.3.1. Introduction

The United State's sector of the Gulf of Mexico Basin (Figure 2.5) is the most important petroleum producing basin in the country, accounting for about 31% and 48% of the produced oil and gas respectively (Fails, 1990). The basin is one of the most extensively studied sedimentary basins in the world (Weimer *et al.*, 1998). Despite these extensive studies, there is a lack of agreement on the basins' petroleum systems and this primarily results from the combination of the basin's large size, thickness of its sedimentary strata, and complex structural evolution (McBride *et al.*, 1998a).

Figure 2.5.Map showing the location of the Gulf of Mexico Basin.
Source: http://student.britannica.com/eb/art/print?id=54971&articleTypeId=0

2.3.2 Tectonic Evolution and Stratigraphy

The evolution of the Gulf of Mexico has been discussed in numerous articles (e.g. Pilger, 1981; Pindell, 1985; Schumacher & Perkins, 1990; Fails, 1990, and references

therein; Weimer *et al.*, 1998; McBride *et al.*, 1998a; 1998b). The basin's evolution is associated with the crustal attenuation and rifting resulting from the separation of the North American plate from the South American and African plates during the late Triassic–early Jurassic. According to Weimer *et al.* (1998) the evolution of the Gulf of Mexico is closely linked with two major rifting episodes resulting from widespread mantle upwelling and extension;

A late Triassic rifting as documented by the Eagle Mills deposits in the east Texas of the southern United States.

A mid-Jurassic rifting episode represented by half graben commonly seen in the deep portion of the basin. The mid-Jurassic crustal rifting generated areas of thin and thick transitional crust within the basin (Dobson & Buffler, 1997). The early rift fills were initially composed of upper Triassic-lower Jurassic red shales and siltstone beds of the Eagle Mills Formation (Heydari *et al.*, 1997; Dobson & Buffler, 1997).

A middle Jurassic (Bathonian-Callovian) marine incursion gave rise to precipitation of a thick succession of salt (Louann Salt Formation) over the transitional crust (Salvador, 1987, 1991). The movement of the salt deposits gave rise to widespread formation of salt structures (diapirs, rollers and pillows) in the basin (MacRae, 1991; MacRae & Watkins, 1993). During the Upper Middle Jurassic (Bathonian-Callovian) localised basal conglomerates, red clastics and Werner anhydrite were deposited in the basin. (Salvador, 1991). The continued rifting after the salt deposition led to the separation of the salt deposits into two Jurassic salt basins that are separated by over 300km of non salt bearing basin (Fails, 1990, and references therein). Additionally, the subsequent sea floor spreading marked the time during which alluvial sandstones, conglomerates and aeolian sandstones of the Oxfordian Norphlet Formation were

deposited during relative sea level lowstand (Wade & Moore, 1993). Subsequent transgression of the sea led to the deposition of the Smackover carbonates in the Upper Jurassic (Oxfordian) (Fails, 1990; Heydari *et al.*, 1997). The Haynesville Formation (Kimmeridgian), overlies the Smackover carbonates and represents evaporates and transitional/marine clastics and limestones deposited as regression commenced (Fails, 1990). The Haynesville Formation consists of the Buckner Member in the lower part and dominantly Gilmer Limestone in the upper part (Claypool & Mancini, 1989). The sandstone unit of the Cotton Valley Group (Kimmeridgian-Berriassian) conformably overlies the Haynesville Formation (Claypool & Mancini, 1989; Heydari *et al.*, 1997). Fine to medium-grained sandstones, minor shale, limestone and thin anhydrite of Sligo and Glen Rose of Texas groups constitute the Lower Cretaceous rock units in the basin (Fails, 1990). The Upper Cretaceous stratigraphy is composed of the Tuscaloosa Group (sandstone and marine shale), the Eutaw Formation (shale with shale and glauconitic sands interbeddings) and the Selma Group chalk (Claypool & Mancini, 1989, and references therein). The occurrence of evaporates with carbonates in the Mesozoic stratigraphic sequence of the Gulf of Mexico is interpreted to be a result of the absence of clastic influx being sometimes more important than the water depth during the transgressive events (Fails, 1990). The Cenozoic sedimentary package is composed mainly of terrigenous clastics that were derived from river-born sediments from the Tertiary uplift of the Cordilleran mountain and the sediments represent the regressive basin filling sequences which are progressively younger basin-ward (Thompson *et al.*, 1990). The cordilleran-derived clastic forms prograding deltaic sequences layed in deltaic, inter-deltaic, shelf and slope environments (Fails, 1990). The Tertiary and Quaternary stratigraphy is thus composed of marine shale facies (pro-delta and shelf-

slope deposits) and shale-sand facies of delta plain deposits consisting of sandstones, shales, lignites, limestones, clays, gravels, and sands (Claypool & Mancini, 1989; Curtis, 1989; Thompson *et al.*, 1990).

2.3.2. Characteristics of the petroleum systems elements

The origin of most petroleum accumulations in the northern Gulf of Mexico (United States sector) is as yet unresolved because of the different source facies, hydrocarbon generation potential and varying thermal histories of oil prone sequences in various parts of the basin (Kennicutt *et al.*, 1992). The structural geometry and evolution of allochthonous salt systems in the northern Gulf of Mexico and its control on the petroleum systems was discussed by McBride *et al.* (1998b). Briefly, the salt bodies have high thermal conductivity and this retards thermal maturation of the subsalt petroleum source rocks. Additionally, vertical migration of petroleum from subsalt source rocks are impeded by the impervious nature of the salt bodies, thus causing migrating petroleum to deflect laterally up dip along the base salt (McBride *et al.*, 1998b).

From multivariate statistical analyses of about 150 crude oil samples from the Jurassic to Tertiary reservoirs in the Gulf Coast, Landrum and Sutton (1988) identified four main oil families which may reflect different source facies (source rock organic matter type, depositional conditions and age of source rocks); Group I oils are consistent with Smackover source units and are characterized by highly reducing marine conditions reflecting expulsion from Carbonate rich source rock.

Group II oils are expelled from clastic (clay-rich rocks) in a paralic/deltaic environment. The Cretaceous oils of southwestern Mississippi also belong to this oil family. Group III oils includes the Tertiary-reservoired oils of southwestern Mississippi and southern Louisiana that were generated by source rocks deposited in a rapidly subsiding, marginal-marine environment. Group IV oils are generated by open-marine, carbonate source rocks containing varying proportions of terrigenous organic matter.

Based on the geological evidence and similarity in the molecular and isotopic characteristics of the extractable organic matter from Smackover carbonates and the Jurassic-sourced oils, Claypool and Mancini (1989) asserted that the main source of oils and condensates in Mesozoic reservoir rocks in southwestern Alabama is the Jurassic Smackover Formation.

Additionally, from the geochemical analyses of 355 petroleum samples (oils and condensates), Thompson *et al.* (1990) identified five groups of petroleum which broadly represents one superfamily in the offshore Gulf of Mexico on the basis of the stable carbon and sulphur isotope content and trace metal (nickel and vanadium) content:

Group 1A: constituted by oils presumably derived from clastic source rocks, account for about 80% of the analysed oils. The oils have low sulphur content and enriched in nickel relative to vanadium. Thompson *et al.* (1990) observed that the coefficient of variation of the $\delta^{13}C$ values of the oils in this group (1.5%) compares favourably with the oils from Phosphoria and Smackover formations.

Group 1B: The oils can not be distinguished from the Group 1A on the basis of their carbon and sulphur isotope compositions but they are very rich in sulphur and vanadium relative to nickel and contain low pristane/phytane ratios (<1). This source facies characteristic suggests strongly reducing conditions of source rock deposition, which is often associated with carbonate and clastic poor source rock. A Jurassic-Cretaceous carbonate source rock (probably Smackover carbonate source rock) is thus inferred. Thompson *et al.*(1990) suggest that Group 1A and 1B may be derived from different facies of the same source rock.

Group 2 petroleums are constituted by condensates in Miocene and Pliocene reservoirs in offshore Texas. They are isotopically heavier and are considered as supermature equivalents of Group 1A petroleums.

Group 3: Oils of this group are produced from Lower Cretaceous Sunninland limestone. The oils are similar to the Smackover Formation oils in Alabama and northeast Florida on the basis of their carbon and sulphur isotope composition.

Group 4: Condensates from the Brazos region, offshore Texas constitutes this group. A Jurassic carbonate source rock was inferred as the source for these condensates on the basis of C_{29} norhopane/C_{30} hopane ratios >1 (a common characteristic of carbonate-sourced petroleum) and different sulphur and carbon isotope compositions as compared with the rest of the petroleum groups.

Further to the work of Thompson et al. (1990), Kennicutt *et al.* (1992) identified four genetic oil families based on the biomarker and stable carbon isotope compositions of oils from the northern Gulf of Mexico. The four families are;

1. Smackover oil family: This family of oil is derived mainly from Jurassic Smackover carbonates and characterized by low pr/ph ratio (<1), high sulphur

content and high extended hopane (C_{35}>C_{34}). This characteristics is consistent with previous reports (e.g. Landrum & Sutton, 1988; Thompson *et al.*, 1990)

2. Flexure-reservoired oils having similar biomarker compositions to Jurassic Smackover but an upper Jurassic/Lower Cretaceous source interval is inferred. According to Kennicutt *et al.* (1992), this oil family is similar to the Type II Smackover oils from Alabama and Florida discussed in the work of Sassen (1989).
3. Upper Cretaceous oil family: These oils are characterized by a distinct suite of biomarker compositions in comparison with the Smackover and flexure oil families. Oils of this family occur across central Texas and Louisiana. They have abundant non-hopanoid triterpanes, such as oleananes, closely associated with Tertiary and older land plant origin (Kennicutt *et al.*, 1992, and references therein). Additionally, they have an abundance of C_{24}-C_{30} triterpanes. This family is constituted by the Austin Chalk, some Woodbine and Tuscaloosa oils as described by Comet *et al.* (1993).
4. Paleogene-reservoired oils: This family is distinguishable by the presence of oleanane, low abundances of extended hopanes and presence (though not always) of bisnorlupane. These oils occur in south Texas, central and southern offshore Louisiana. According to Kennicutt *et al.* (1992), the Texas oils of Thompson and Kennicutt (1992) constitute this group/family.

Each of these oil families can be further divided into sub-groups on the basis of the variation in the abundances of certain biomarkers which may represent source facies difference within a single source bed or multiple source beds.

A lacustrine-sourced oil family was recognized in several Norphlet/Werner and Smackover reservoirs in northeast Texas and northwestern Louisiana by Alan *et al.* (1993).

Comet *et al.* (1993) classified 481 Gulf of Mexico oils into nine major families on the basis of their sterane and triterpane characteristics. The identified oil families were confined within age-specific producing trends that comprises the Kimmeridgian-Oxfordian (Smackover and Norphlet formation), Aptian (Pipe Island, Bexar and Sunninland formations), Albian (Paloxy Formation), Cenomanian-Turonian (Eagle Ford and Tuscaloosa formations), Coniacian-Santonian (Eagle Ford and Austin Chalk) and Paleocene (Wilcox, Midway and Sparta formations). Five of these oil families have been described previously (e.g. Landrum & Sutton, 1988; Thompson *et al.* 1990; Kennicutt *et al.*, 1992). The nine families' classifications of Comet *et al.* (1993) are:

1. Carbonate-derived oils which occur in Jurassic-Cretaceous reservoirs of northern Texas, Arkansas, Northern Louisiana, Alabama and Mississippi.

2. Austin Chalk oils- distinct and homogenous and occur in upper Cretaceous Austin Chalk and younger rocks in Texas. They are isotopically light ($\delta^{13}C$ average -28‰) and contain low levels of oleanane.

3. Tuscaloosa derived oils and some non-indigenous (migrated) oils.

4. Wilcox reservoired oils rich in oleanane and or bisnorhopane.

5. South Texas Paleogene reservoired oils also rich in oleanane or bisnorhopane and reservoired in Wilcox, Yegua and Vicksburg formation.

6. Mississippi oils constitute oils in the modern Mississippi delta and contain low/absence of oleanane.

7. Post mature oils of unknown origin.

8. Migrated-contaminated oils.

9. Oils and condensate lacking biomarkers.

2.3.2.1. Source rocks

Three source rock models have evolved for the Gulf of Mexico and these have been summarized by Bissada *et al.* (1990) as follows:

1. Cenozoic source rock consisting of marine deltaic shales that is in contact with the reservoir sands (Clark & Rouse, 1971).
2. Dissociated Neogene organic rich source rocks formed in an anoxic salt layer under conditions favoring restricted oceanic circulation (William & Lerche, 1988).
3. Mesozoic (Jurassic and Cretaceous) and early Tertiary (Paleogene) source rocks. (Bissada *et al.*, 1990; Thompson *et al.*, 1990; Sassen *et al.*, 1988; Thompson & Kennicutt, 1992; Kennicutt *et al.*, 1992; Palacas *et al.*, 1984a, 1984b).

Several source rocks ranging in age from Mesozoic to Tertiary have been proposed as major source of oil and gas in the Gulf of Mexico. Prolific source rocks are present in the Upper Jurassic, Lower Cretaceous, Upper Cretaceous, and Paleogene strata (Kennicutt *et al.*, 1993). According to Bissada *et al.* (1990) the Miocene and early Tertiary sediments are presently buried to the oil window in many parts of the basin and this suggests that the Mesozoic strata may be buried too deeply to currently generate oil (but mainly gas) in the offshore part of the basin. However, Cretaceous and Jurassic sequences are mostly favoured as major contributors to the vast petroleum accumulation in the basin based on two stand points;

1. The world-wide occurrence and abundance of good source rocks of Jurassic and Cretaceous age renders credence for oil generation from the equivalent age strata in the Gulf of Mexico (Kennicutt *et al.*, 1992, and references therein; Heydari *et al.*, 1997), providing that the generated hydrocarbons are able to escape zone of the thermal destruction from the present day deeply buried level of Jurassic strata (Bissada, *et al.*, 1990).
2. Evidence from vast petroleum accumulations containing geochemical source signatures of Jurassic Smackover carbonate source rock contribution (e.g. Pr/Ph<1, C_{35}/C_{34} hopane >1, abundant extended hopanes (C_{31}-C_{35}), low diasteranes, high sulphur content and high vanadium relative to Nickel (Thompson *et al.*, 1990; Kennicutt *et al.*, 1992; Comet *et al.*, 1993).

Significant oil and gas generation potential is present in the Late Paleocene/ early Eocene (Wilcox) sequences in southern Louisiana (Sassen *et al.*, 1988; Sassen *et al.*, 1990a). Additionally some onshore oil accumulations have been correlated with the Tertiary Wilcox, Frio and Jackson sequences (Kennicutt *et al.*, 1992, and references therein).

Overall, potential source rocks are identified based on oil geochemistry and these source rocks range from Mesozoic to Cenozoic age as follows:

Jurassic Smackover: oils generated from the Jurassic Smackover (Oehler, 1984; Claypool & Mancini, 1989; Sassen, 1990b; Wenger *et al.*, 1990). The Smackover source rock is also considered as a probable source for some Flexure trend family oils (Thompson *et al.*, 1990; Bissada *et al.*, 1990). Heydari *et al.* (1997) believe that the lime mudstones of the Smackover Formation sourced all hydrocarbons in Jurassic

reservoirs, and much of the oil and gas in younger overlying strata. Subsequent studies (e.g. Oehler, 1984; Sassen *et al.*, 1987a) generally concluded that the Smackover Formation is the primary source of the Jurassic oils in the Gulf of Mexico Basin. According to Kennicutt *et al.* (1993), the Paleogene source units are the primary source of coastal and continental shelf oils while the Mesozoic (including Smackover) sources the onshore and the deep water northern Gulf of Mexico oils.

2.3.2.2. Reservoirs Traps and seals

The vast hydrocarbon production in the Gulf of Mexico is owed in part to the clean, well sorted, high porosities and permeability sands in producing intervals which occur within the Mesozoic and lower Tertiary rocks (Fails, 1990; Kennicutt *et al.*, 1992; Kennicutt *et al.*, 1993). The Woodbine and Tuscaloosa sandstone Group forms major producing Cretaceous intervals (Fails, 1990) as well as Neogene reservoirs in the Tertiary sequence (Kennicutt *et al.*, 1992).

The salt movement forms many important petroleum producing structures in the Gulf of Mexico, particularly in the interior salt basins in which most hydrocarbons are trapped in salt diapiric structures (Fails, 1990; McBride *et al.*, 1998b). Truncated traps, stratigraphic traps faulted anticlines and tilted fault blocks are important structures for trapping petroleum in the basin especially within the Smackover oil fields (Fails, 1990).

2.4. Niger Delta

2.4.1. Evolution and stratigraphy

The Niger Delta is located in the Gulf of Guinea. It is margined in the east by the Cameroon volcanic line and in the North-western part by the Okitipupa ridge of the Dahomey embayment (Figure 2.6). The Niger Delta sedimentary basin covers an area of about 75,000 km^2 (Haack *et al.*, 2000). The delta evolution is closely associated with the formation of a rift triple junction (an aulacogen known as the Benue Trough in Nigeria) during the separation of the continental crusts of the South America and Africa in the Late Jurassic (Burke, 1972; Whiteman, 1982).

Figure 2.6. Map of the Gulf of Guinea showing the approximate location of the Niger Delta (red box) in the south western Nigeria coast on the Gulf of Guinea (Source: http://news.bbc.co.uk/olmedia/1275000/images/_1275867_africa_west_map300.gif). Note map not drawn to scale.

Following the separation of the continental plates of South America and the Africa, the opening of the Atlantic Ocean in turn gave rise to marine incursion as marked by

marine sedimentation in the Benue Trough and the Anambra Basin during the Cretaceous period in Nigeria (Doust & Omatsola, 1990). As the Niger River increasingly fed clastics from the adjacent highlands during the early Tertiary, the Niger Delta began to form at the point where the Benue Trough adjoins the Atlantic Ocean (Doust & Omatsola, 1990).

The Niger Delta consists of a subsurface sedimentary sequence up to 12 km thick in places that represents a progradational package, which has been extensively described and discussed (e.g. Short & Stauble, 1967; Avbovbo, 1978; Doust & Omatsola, 1990; Kulke, 1995). The sedimentary sequence represents prograding facies that are separable on the basis of the sand-shale ratio and are divisible into three (Figure 2.7) diachronous lithostratigraphic units. The overpressured basal Palaeocene-Miocene Akata Formation (Knox & Omatsola, 1989) represents a deep marine shale sequence of prodeltaic facies approximately 6000m thick. The Akata Formation is a lowstand system, at which time terrestrial organic materials and clays were transported to the deepwater part of the receiving basin by low energy conditions and less oxygenated water (Stacher, 1995). The Akata Formation is overlain by over 4000m of alternating sandstones and shales of parallic facies (Short & Stauble, 1967; Avbovbo, 1978). This interbedded sandstone and shale unit is called the Agbada Formation (Eocene-Recent). The Agbada Formation represents the deltaic system (deltafront, fluvio-deltaic facies) of the sedimentary sequence (Tuttle *et al.*, 1999). The Benin Formation (Late Eocene-Holocene) overlies the Agbada Formation and is a sequence of about 2000m of fluviatile sands and alluvium which represents the youngest bed in the sequence (Avbovbo, 1978).

2.4.2. Characteristics of the petroleum systems elements

Structure exerts great influence on the hydrocarbon accumulations and production in the Niger Delta (Haack *et al.*, 2000). Based on a regional study of source rocks and oils from the Niger Delta region (south-west and southern Nigeria in general), Haack *et al.* (2000) informally inferred the possibility of three petroleum systems in the Niger Delta. The systems defined by their source rock age and environments of deposition are:

- Lower Cretaceous petroleum system (lacustrine);
- Upper Cretaceous –Palaeocene petroleum system (marine); and
- Tertiary petroleum system (deltaic).

It is worthy of note, however that of the three systems proposed for the Niger Delta region, only the Tertiary system is proven within the scale of the Niger Delta oil accumulations *sensu stricto*. The oils of Tertiary system contain abundant C_{29} steranes relative to other sterane homologues, thus suggesting a dominantly higher plant input (Ekweozor *et al.*, 1979a; Huang & Meinshein, 1979). Additionally, oleanane, a marker of angiosperm higher plant input to source rock organic matter occurs copiously in the oils (Ekweozor *et al.*, 1979a; Ekweozor & Udo, 1988). The other two systems described by Haack *et al.* (2000) are speculative and have been drawn mainly from the studies of oil seeps and source rocks in the adjoining Dahomey Basin. Using the invariance in the isoheptanes light hydrocarbon parameter as proposed by Mango (1987), Eneogwe (2004) reported the occurrence of at least two petroleum systems in the Niger Delta from a study of over eighty six oils from the western and eastern Niger Delta. Most studies of source rock and oil characterization in the Niger Delta have mainly covered the Tertiary petroleum system (Ekweozor *et al.*, 1979a, 1979b; Ekweozor & Okoye, 1980; Lambert-Aikhionbare & Ibe, 1984; Ekweozor & Daukoru,

1984; Udo *et al.*, 1988; Ekweozor & Daukoru, 1994; Eneogwe *et al.*, 2002; Eneogwe & Ekundayo, 2003; Eneogwe, 2003, 2004; Akinlua & Torto, 2006; Akinlua *et al.*, 2005; 2006, 2007a, 2007b). This Tertiary system is formally recognised as the Akata-Agbada (!) petroleum system. The Tertiary petroleum system is seen as the principal source for most of the discovered accumulations. The Upper Cretaceous-Palaeocene system has been proposed to be the likely system to dominate the deepwater areas. This requires sufficient hydrocarbon charge through migration pathways that connect the pre-growth source intervals (below the regional décollement) with the overlying traps of the Tertiary growth strata, and trap formation (in particular seal development) contemporaneous with or pre-dating the generation of hydrocarbon (Haack *et al.*, 2000).

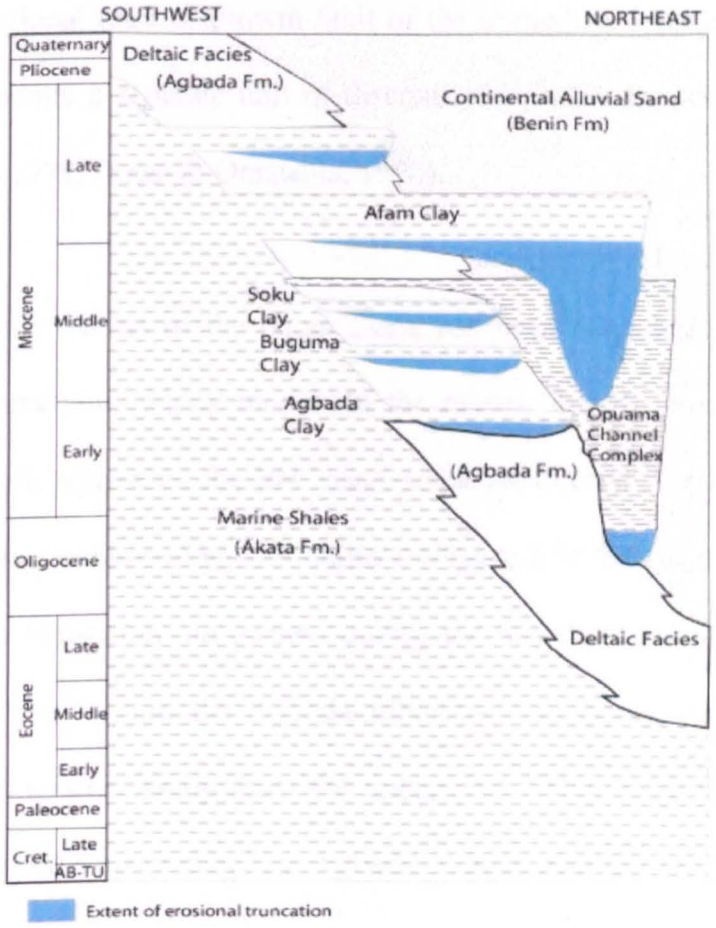

Figure 2.7. Generalized stratigraphy of the Niger Delta. (Source: Tuttle *et al.*, 1999).

As earlier described, the Niger Delta lithostratigraphy consists of three formations; the Akata, Agbada and Benin formations. These formations were deposited in five sedimentary cycles, described as "depobelts", within the Niger Delta (Stacher, 1995). These belts are about 30-60 kilometres wide and prograded in a southerly direction by 250 kilometres over the oceanic crust into the Gulf of Guinea (Stacher, 1995). The formation of the depobelts is closely associated with the interplay of crustal subsidence and sediment supply rate, usually when the depression created by crustal subsidence can no longer accommodate any more sediment supply. In effect, the site of sediment deposition shifted seaward to form a new depobelt in the adjacent depression (Doust & Omatsola, 1990) (Figure 2.8). Each of the depobelts recognised within the Niger Delta is bounded in a landward direction by a growth fault and seaward by regional fault or growth fault of the immediate seaward depobelt. Each depobelt represents a separate unit of discontinuity in the regional dip of the delta (Evamy *et al.*, 1978; Doust & Omatsola, 1990).

The hydrocarbon habitat of the Niger Delta has been described by Stacher (1995) using a sequence stratigraphy model. In the model, the oil prone marine shale of Akata Formation represents the low stand sequence deposit in a deep water setting under low energy and low oxygen conditions (Figure 2.9). Hydrocarbon bearing sands of the Agbada Formation are formed during the highstand system tracts while the sealing shale layer within the Agbada represents the transgressive system tracts. Hydrocarbon migration updip from the underlying Akata shale is enhanced by the extensive fault systems within the Agbada, which also act as structural traps in addition to the rollover growth fault structures that accumulate petroleum (Tuttle *et al.*, 1999).

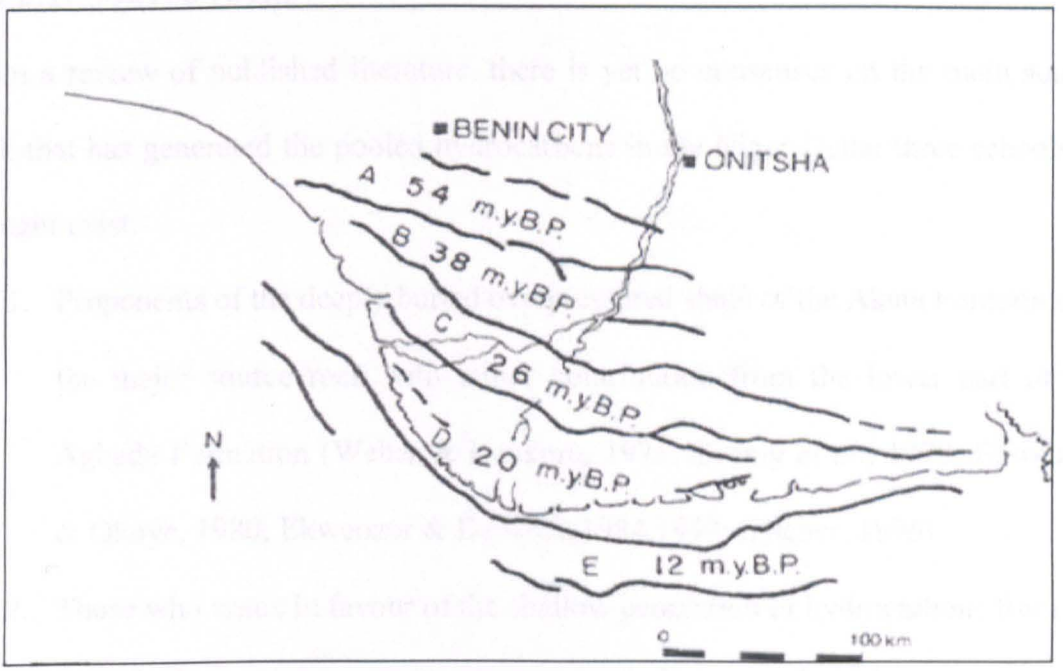

Figure 2.8. Map showing the mega sedimentary units (depobelts) and their respective ages in the Niger Delta basin. Source: Ejedawe *et al.*, 1984.

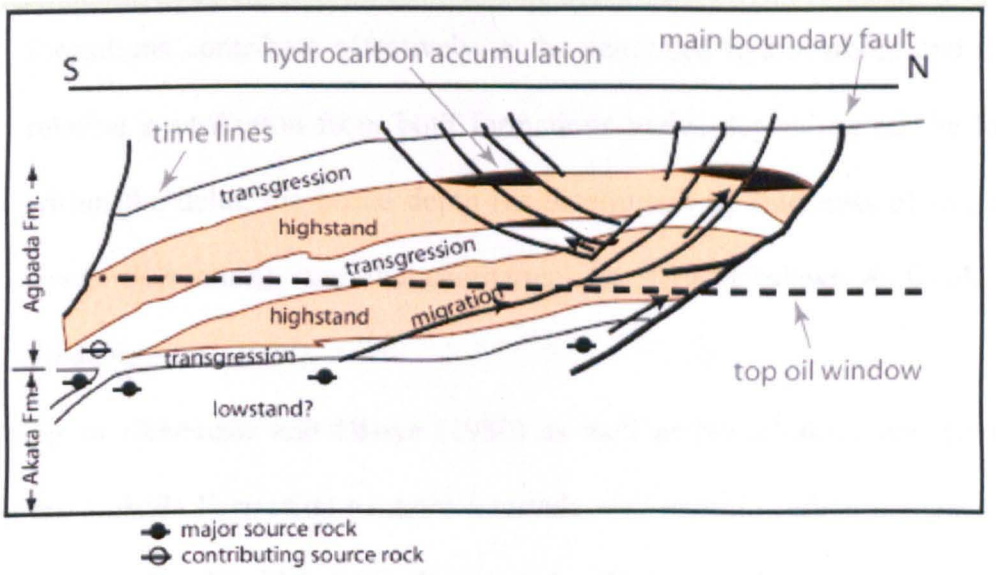

Figure 2.9. Sequence stratigraphic model for the central portion of the Niger Delta showing the relationship between source rocks, migration pathways and hydrocarbon traps related to growth faults. Modified from Tuttle *et al.*, 1999, after Stacher, 1995).

2.4.2.1. Source rocks

From a review of published literature, there is yet no consensus on the main source rock that has generated the pooled hydrocarbons in the Niger Delta: three schools of thought exist:

1. Proponents of the deeply buried overpressured shale of the Akata Formation as the major source rock with minor contribution from the lower part of the Agbada Formation (Weber & Daukoru, 1975: Evamy *et al.*, 1978; Ekweozor & Okoye, 1980; Ekweozor & Daukoru,1984,1994; Stacher, 1995)
2. Those who argue in favour of the shallow generation of hydrocarbons from the Agbada Formation as the main source rock rather than the overpressured marine shale of Akata Formation (Frankl & Cordry, 1967; Short & Stauble, 1967; Reed, 1969; Lambert-Aikhionbare & Ibe, 1984).
3. The third school of thought believes that both the Akata and Agbada formations contribute effectively to the generated hydrocarbon, and that the relative contribution from both formations varies depending on the location within the delta, the burial depth (as determined by thickness of overburden Benin Formation), and the geothermal gradient (Ejedawe & Okoh, 1981; Ejedawe *et al.*, 1984).

According to Ekweozor and Okoye (1980) as well as Nwachukwu and Chukwura (1986), the Agbada Formation contains intervals with organic carbon content that are capable of sourcing liquid hydrocarbon, but the thickness of these intervals are not sufficient to classify the Agbada Formation as a world-class source rock.

TOC values ranging from 0.4 to 4.4wt.% were reported for shales of Akata and Agbada formations studied in two onshore and two offshore wells by Ekweozor and Okoye, (1980). Based on variations in maturation parameters used to assess the source

rocks, Ekweozor and Okoye (1980) placed the threshold depth for onset of mature source beds (i.e. oil generation depth) to be 3375m and 2900m for the onshore and offshore parts respectively. However, Nwachukwu and Chukwura (1986) reported TOC values as high as 6.5 wt. % in Agbada shale samples studied in three wells from western Niger Delta fields. In a fairly recent and most comprehensive source rock study to date, Bustin (1988) observed a trend of decreasing mean TOC values with sediment age (average 2.2 wt.% in Late Eocene and 0.9 wt.% in Pliocene sediments). Bustin (1988) believed that this trend was a result of increased dilution of terrestrial organic matter under prevailing high sedimentation rates. HI values are generally low as reported by Bustin (1988) and values as high as 200mgHC/gTOC only recorded in coal samples. Udo *et al.* (1988) reported HI values as high as 232 mg HC/g TOC in kerogen isolates from immature Akata-Agbada boundary shale sequence samples of the western Niger Delta.

Most geochemical studies on the Niger Delta source rocks have been done predominantly on the Agbada Formation and the upper section of the Akata (e.g. Ekweozor & Okoye, 1980; Bustin 1988). A paucity of data on the source rock character of the Akata shale may be connected with the deep level of its burial. Uniform terrigenous organic matter content occurs in the Agbada and the upper Akata formations (Bustin, 1988). The dominant kerogen maceral type in both the studied sections of the Akata and Agbada formations is the land derived vitrinite (85-98 %), small amounts of associated liptinite, resinite, alginite and a very low level of inertinite macerals (Ekweozor & Okoye, 1980; Bustin, 1988). The amorphous or structureless organic matter in the Niger Delta source rock samples studied have been shown not to be of marine origin by Stacher (1995), but may be bacteria-derived.

However, recent work of Haack *et al.* (2000) reported a minor contribution of marine organic matter to the source rock kerogen of oils from the western Niger Delta on the basis of bulk isotopic and molecular marker characteristics of the oils in their study.

Lambert-Aikhionbare and Ibe (1984) argue that the Akata Formation is immature and would not have sourced the bulk of Niger Delta oil. According to Lambert-Aikhionbare and Ibe (1984), chemical reactions that occur during organic matter maturation are accompanied by a small volume increase as well documented by Barker (1972) and Sengupta (1974) and because the deeply buried Akata shale is overpressured, the maturity of the shale will be greatly inhibited by the high pressure effect. In addition, Lambert-Aikhionbare & Ibe (1984) also drew a line of reasoning from the work of Neglia (1980) who concluded from studies of kerogen from overpressured Triassic shales in Western Germany that pressure inhibits kerogen maturation.To support their hypothesis, Lambert-Aikhionbare & Ibe (1984) constructed a different maturity profile that favours an upward increase in maturity from deepest to the shallowest part of the stratigraphic sequence, and that the migration efficiency from the over-pressured Akata shale would be less than 12%, suggesting a low fluid expulsion from the formation. However, such a maturity profile is counter-conventional. Ejedawe *et al.* (1984) drew a conclusion based on maturation models that the Agbada shale sources the oil in the central part of the delta while the Akata shale sources the gas. They also concluded that co-sourcing of the oil in other parts of the delta occurs.

Notwithstanding the above mentioned report by Lambert-Aikhionbare & Ibe (1984), it has been well documented that temperature overrides pressure in the kinetic scheme

of organic matter maturation, and in the Niger Delta, high temperature is closely associated with areas of overpressure (Ekweozor & Daukoru, 1984), it is therefore consistent with the established maturation trend to support the conclusion of Ekweozor and Daukoru (1984) that the deeply buried Akata shales could be the major source rock of the Niger Delta. By conventional standards, there is no mappable petroleum source rock in Niger Delta. Based on published geochemical data, the poor source rock quality is believed to have been compensated for by the thickness of the source rock (Bustin, 1988; Demaison & Huizinga, 1994). Source potential index (SPI) of 14t HC/m^2 has been calculated for the Niger Delta by Demaison and Huizinga (1994). Although Type III organic matter dominates in the Niger Delta, Demaison and Huizinga (1994) believe that the high source potential index (SPI) results from the thickness of the source rock interval. However, to conclude that the huge volume of oil accumulated within the Niger Delta is sourced from such analysed Tertiary sediments demands very high transformation, expulsion and migration efficiencies. In summary, whether regionally extensive and prolific hydrocarbon source rock is proven or not, huge petroleum accumulations occur in the Niger Delta. Sourcing for the recently discovered deepwater accumulations is even more poorly understood. The characteristics of the oils, if insignificantly altered by migration contamination, may help describe and locate the effective source rock, which may exist within or outside the delta wedge.

2.4.2.2. Reservoir Rock

Deltaic sandstone of the parallic Agbada Formation is the primary reservoir for the produced hydrocarbon in the Niger Delta. Reservoir depths vary and range from 5000 to as much as 14000 feet (Stacher, 1995). The age of the producing sand intervals ranges from Eocene to Pliocene (Ejedawe, 1981). Reservoir types as described by

Kulke (1995) are point bars, distributary channel and coastal barrier bars that are in places occasionally truncated by sand-filled channels.

2.4.2.3. Trap and sealing mechanism

The Agbada Formation, which houses the hydrocarbon accumulation intervals within the Niger Delta has been affected by synsedimentary deformations resulting in a system of mainly east-west and northwest-southeast growth faults often in close association with rollover anticlines, which together forms the dominant trap types in Niger Delta (Weber & Daukoru, 1975; Ejedawe, 1981). The growth faults besides acting as trap also connect the proposed source intervals within the Akata and the lower Agbada formations with the reservoirs in the Agbada Formation, thus acting as migration pathways (Weber & Daukoru, 1975). In addition, fault bound structural traps (Nwangwu, 1995), collapsed crest structures and other stratigraphic traps (truncation traps, channels, etc.) also contribute to the trap types in the Niger Delta (Douts & Omatsola, 1990; Stacher, 1995). The interbedded shale within the Agbada Formation provides excellent seal for the reservoired hydrocarbons within the Agbada sand intervals. The interbedded shale seals the traps in form of vertical seals, clay smears along faults, etc. (Doust & Omatsola, 1990).

2.5. Kutei Basin

2.5.1. Geological evolution and stratigraphy

The Kutei Basin is located on the east coast of Kalimantan on and offshore of the Island of Borneo, Indonesia (Figure 2.10) (Combaz & de Matharel., 1978; Peters *et al.*, 2000). The Tertiary Mahakam Delta lies within the Kutei Basin (Figure 2.11), and the Kutei Basin, covering an approximate area of 60,000 km^2, is regarded as the deepest Tertiary basin in Indonesia and the western region of Australia with sedimentary sequence as thick as 15 km in the deepest part of the basin (Rosé & Hartono, 1978; Hutchison, 1989; Chambers & Daley, 1995; Moss *et al.*, 1997). The Kutei Basin is margined by the Schwaner Mountains in the southwest and by the Late Cretaceous/early Tertiary turbidites of the Rajang and Embaluh Groups to the northwest (Figure 2.11) (Moss *et al.*, 1997). The Kutei Basin is probably underlain by ophiolites, deep-sea sediments that represent facies of a subduction zones (van de Weerd & Armin, 1992). According to van de Weerd & Armin (1992), the subsidence of the greater Kalimantan Basin began during the Eocene. A comprehensive discussion on the pre-Kutei Basin inception and tectonic evolutions of the Indonesia basins are available in numerous works (e.g. Van Bemmelen, 1949; Rosé & Hartono, 1978; Hamilton, 1979; Hutchsion, 1989; Moss *et al.*, 1997). A generalised stratigraphy of Kutei Basin after Moss *et al.* (1997) is presented in Figure 2.12.

According to Moss *et al.* (1997), the exact timing of the beginning of the Kutei Basin evolution is poorly understood. This is due largely to the paucity of biostratigraphic age markers in the dominantly terrestrial-derived earliest basin fill sediments (Moss *et al.*, 1997, and references therein).

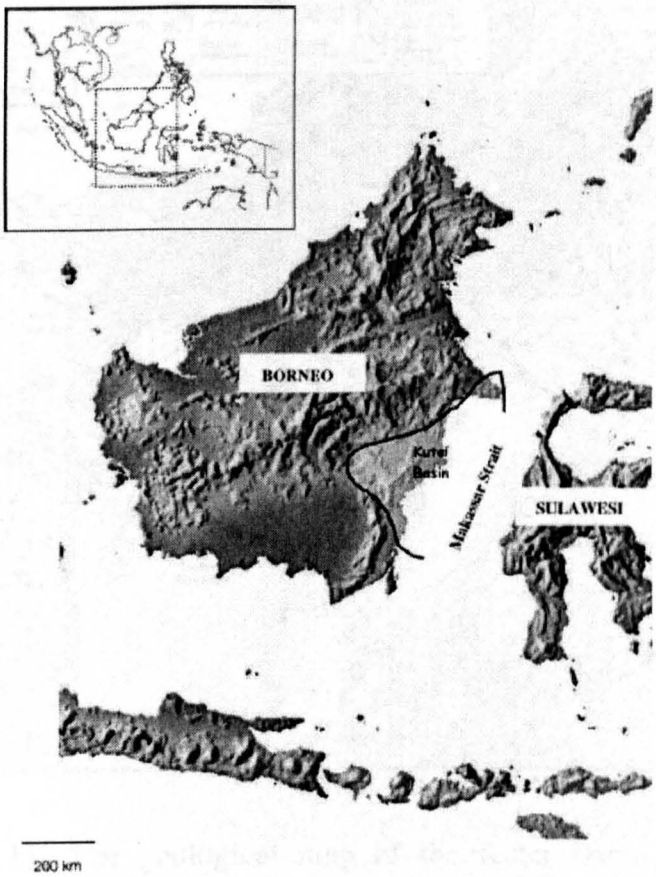

Figure 2.10. Location map showing the approximate outline of the Kutei Basin in the Eastern Kalimantan in the Island of Borneo (after Curiale *et al.*, 2005).

Additionally, synrift sequences are poorly represented in well samples because of a lack of well penetration into the deeper part of the basin. Nonetheless, a Middle-Upper Eocene base sediment age is mostly favoured (van de Weerd & Armin, 1992; Pieters *et al.*, 1993; Moss *et al.*, 1997). The evolution of the Kutei Basin is associated with crustal extension and rifting followed by a stage of tectonic inversion (Moss *et al.*, 1997). On this basis of varying tectonism, the stratigraphic successions within the Kutei Basin are divisible into a synrift phase (mid Eocene), a sag phase (Late Eocene-Oligocene) and a subsidence phase (Oligocene to Miocene) (Moss *et al.*, 1997).

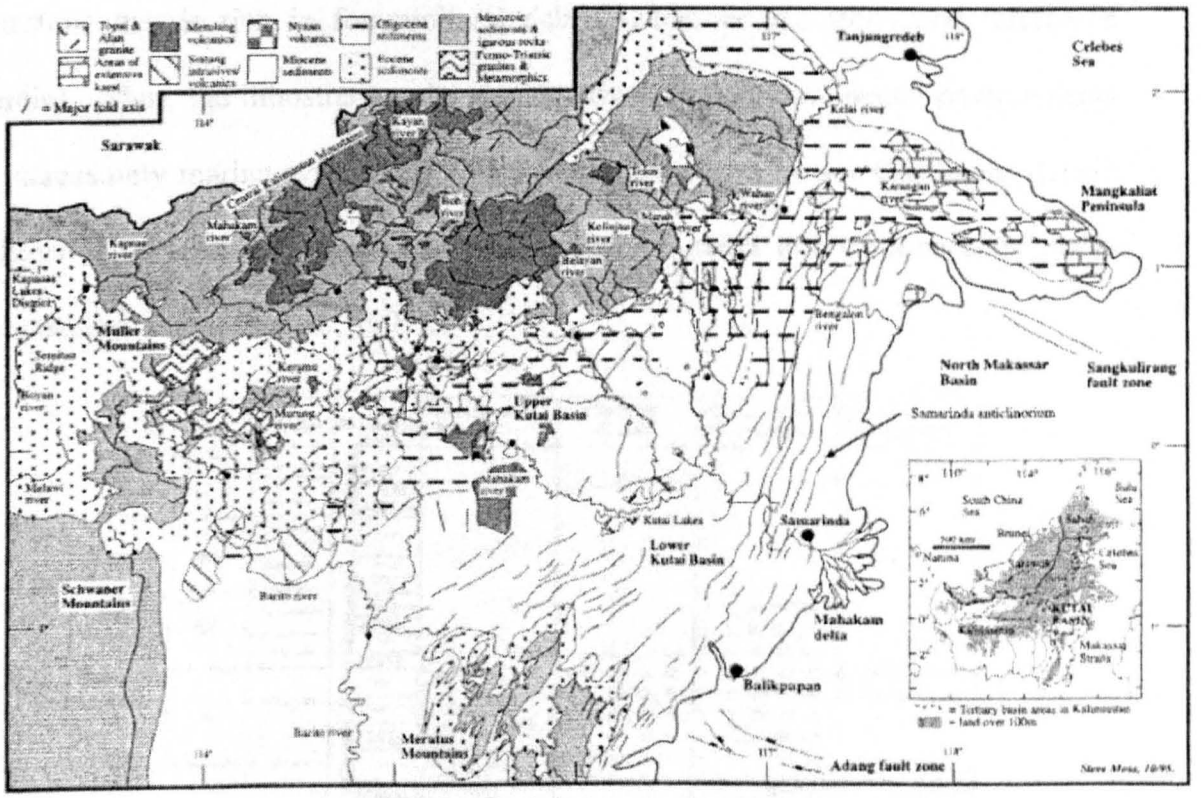

Figure 2.11. The geological map of the Kutei Basin. Note the location of the Mahakam River Delta in the eastern coast of the Kutei Basin (after Moss *et al.*, 1997)

The earliest middle Eocene synrift bed is the basal conglomerate that is seen in most parts of the basin. The conglomerate unit has different formation names in different parts of the Kalimantan region. For instance, in the Barito and southern Kutei, the formation is called Tanjung, whereas the equivalent stratigraphic unit is known as Kuaro Formation and the Kiham Haloq sandstone Formation in the southern part of the Kutei and western basin margin respectively (Moss *et al.*, 1997, and references therein). The conglomerates are composed of sub-angular to rounded pebble- sized clasts that typify alluvial fan deposits (Moss *et al.*, 1997). During the Upper Eocene to Lower Oligocene of Kutei, sedimentation shifted from fluvial to bathyal system with the deposition of shales and foraminiferal bearing sandstones in the deeper part of the basin (Moss *et al.*, 1997). In the northern and southern margins as well as the upper Mahakam area, the bathyal shale is overlain by middle-upper Eocene shallow marine

limestone that is rich in foraminiferal debris (Moss *et al.*, 1997, and references therein). Thus, the lithostratigraphy changes from beds of continental environments to increasingly marine systems. During the late Eocene to Lower Oligocene, deltaic sedimentation with occasional coal seams, channel sands and carbonaceous shales were deposited (Moss *et al.*, 1997).

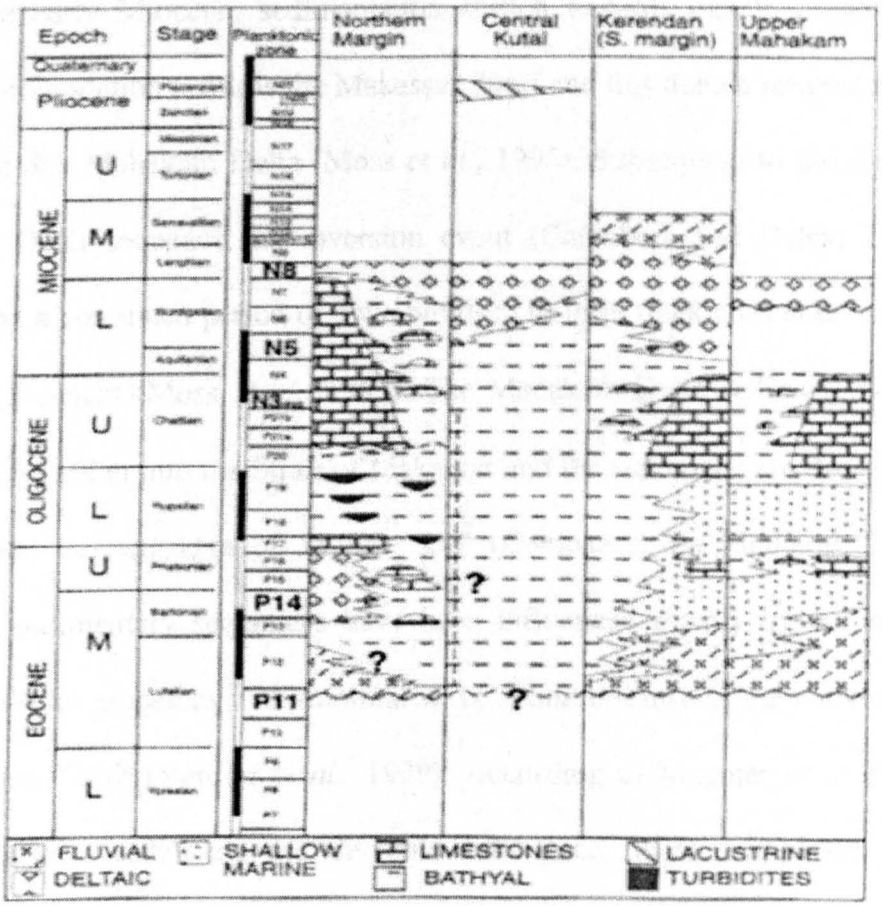

Figure 2.12.Genralised stratigraphy of the Kutei basin (after Moss *et al.*, 1997).

Locally, especially on the northern margin of the basin, turbidites were deposited during the upper Eocene to Lower Oligocene period (Figure 2.12). Turbidite packages are well exposed at outcrop in the northern part of the Kutei Basin (Moss *et al.*, 1997). These turbidites have different lithostratigraphic names in several parts of Kutei. The names include Batu Kelau Formation, Atan Formation, Bongan Formation (van der Weerd *et al.*, 1987) and Morah Formation (Supritana, 1990). Much of the Upper Oligocene is documented by thick carbonate platform development in the Kutei

Basin. Foraminiferal evidence in the limestone suggests an upper Oligocene-Lower Miocene age. This carbonate sedimentation extended up to the Lower Miocene and is marked in places within the Kutei Basin by related limestone breccia deposits (Moss *et al.*, 1997).

During the early Miocene, sedimentation shifted towards deltaic clastics with an eastward progradation towards the Makassar Strait and this deltaic progradation forms the present day Mahakam Delta (Moss *et al.*, 1997). Subsequent to the formation of Mahakam Delta sequence, an inversion event (Chambers and Daley, 1995), was followed by a continued period of delta build-up to form thick coastal deltaic plain of about 3000 meters (Moss *et al.*, 1997). The Mahakam Delta sedimentary sequence extends up to 50km into the Strait of Makassar and the sediments are derived from an approximate drainage area of 75,000 km^2 (Combaz & de Matharel, 1978). The Mahakam sedimentary sequences have been influenced mainly by combination of fluvial and tidal processes with minimal wave action because of the narrow nature of the Makassar Strait (Verdier *et al.*, 1979). According to Magnier *et al.* (1975), the Mahakam Delta sediments are divisible into three major complexes that have accumulated through time (at least since the delta began to form as far back as Miocene, 20Ma), and are still actively prograding because of the high rate of sediment supply. The three major complexes as described by Magnier *et al.* (1975) as well as Combaz and de Matharel (1978) are:

Middle Miocene delta complex, Miocene-Pliocene delta complex and Holocene Delta Complex. These three complexes are separated by marine transgressive events and the recent transgression occurred in Holocene time (Combaz & de Matharel, 1978). The sediment supplies for the prograding delta are possibly derived from erosion of the

lower Miocene deltaic sediments (Chambers & Daley, 1995) and erosion of the central hinterlands (Moss *et al.*, 1997). According to Moss *et al.* (1997), Pliocene to Recent age lakes (e.g. Anap Formation) occur locally, particularly in the west of the Samarinda area. The evolution of the lakes is attributed to the ponding of the Pliocene Mahakam River drainage basin caused by the uplift of the Samarinda anticlinorium (Moss *et al.*, 1997).

2.5.2. Characteristics of the petroleum systems elements

2.5.2.1. Source rocks

Terrestrial organic matter derived from the hinterland is the precursor for oils in the Kutei Basin and associated Mahakam Delta (Combaz & de Matharel., 1978). The source rocks are mainly marine shales and coaly sequences of the upper deltaic top to deltaic plain environments (Verdier *et al.*, 1979). The source rocks for most of the crude oils in the Mahakam Delta are believed to be deeply buried Miocene shales and coals of the Balikpapan Group (Schoell *et al.*, 1983; Robinson, 1987). TOC values ranging between 3 to 10 wt.% and 1.5 to 4wt.% were reported for shale by Combaz and de Matharel, (1978) and Verdier *et al.* (1979) respectively. Additionally, 45-70 wt.% TOC were reported for coals by Verdier and co workers (1979). Petrographic analyses of the source rocks revealed abundance of vitrinite macerals (70 to 90%) and low levels of exinites (10-20%) and inertinites (2 to 20%) (Verdier *et al.*, 1979; Combaz & de Matharel, 1978). The oil generative potential of the coals is thought to be due to its hydrogen richness (high exinite contents), thus the term perhydrous coals (coals containing hydrogen rich vitrinite formerly termed desmocollinite, now known by the term collodetrinite; Sykes *et al.*, 2004, and references therein) is often used (Combaz &de Matharel., 1978; Durand & Paratte, 1983; Peters *et al.*, 2000). The organic matter has been derived mostly from the hinterland vegetation with few

pollen and spores (Combaz & Matharel., 1978; Saller *et al.*, 2006). The organic matter for the deepwater oils is land plant exinites (leaf fragments) arguably deposited with and preserved in deepwater turbidite sands (Saller *et al.*, 2006).

Peters *et al.* (2000) developed a new geochemical sequence-stratigraphic model for the Mahakam Delta and the Makassar Strait. Under this new model, three source rock sequence-stratigraphic frameworks were recognised:

1. Highstand systems tract coastal plain coals deposited during high sea level intervals.
2. Lowstand systems tract coaly shales formed in outer shelf to slope environments where terrigenous organic matter eroded from the delta coastal plain and inner shelf exposed during low sea levels were deposited
3. Transgressive systems tracts source rocks bounded by the maximum flooding surface (MFS) at the top and the transgressive boundary at the base in a less turbulent water conditions favouring accumulation of algal rich organic matter.

The new sequence stratigraphic model developed by Peters *et al.* (2000) places the shelf margin farther offshore than previously accepted in the Total IFP model, thus favouring source rock deposition in the outer shelf and slope environments. Additionally, the Peters *et al.*'s (2000) model favours oil-window maturity levels for source rocks previously believed to have been deeply buried.

2.5.2.2. Reservoir and hydrocarbon trapping mechanisms

The reservoir rocks are mainly sandstones. According to Verdier *et al.* (1979), at least three reservoir types reflecting quality diffrences are present in the basin:

1. High quality sands having low clay content and shale laminations, thus high porosity and permeability.

2. Reservoir sands of intermediate quality dominated by shaly sandstone.

3. Poor reservoir shaly sandstones of low porosities because of high clay content.

Hydrocarbons are commonly found in structural highs along major anticlinal axes, and structural traps (Combaz & de Matharel, 1978; Verdier *et al.*, 1979; Peters *et al.*, 2000). Fault-bounded traps also provide significant trapping mechanisms in the Kutei Basin (Combaz & de Matharel., 1978). Additionally, toe thrusts in Miocene reservoirs act as traps (Curiale *et al.*, 2005).

CHAPTER THREE

EXPERIMENTAL METHODS

3.0. Introduction

Two methods were utilized to achieve the objectives of this research:

a. Collection of published geochemical data from peer reviewed journal articles, and public data resources (such as that of the United States Geological Survey). The data were interpreted to develop new ideas on the petroleum systems (particularly source rock organic matter type and origin) from the work carried out on case study deltaic basins.

b. The application of standard petroleum geochemical analytical techniques to characterise a carefully assembled global set of representative Tertiary deltaic oils from Assam, Beaufort-Mackenzie, Gulf of Mexico, Niger, and Kutei Basin.

For the analysed crude oil sample set, the following analytical techniques were utilized.

3.1. Solid Phase Extraction (SPE) Separation

SPE is a rapid and inexpensive method for the separation of hydrocarbon and non-hydrocarbon compound classes from crude oils and sediment extracts. It is based on a method described by Bennet and Larter (2000). Briefly, commercially available 3ml C_{18} bonded non-endcapped silica columns (Kinensis UK, Ltd) were pre-cleaned with approximately 6ml dichloromethane (DCM), surplus DCM was removed from each column using a gentle air flush and the columns were left overnight to dry on top of an oven set at about 60 °C. Following this pre-extraction of the columns, about 3ml hexane was used to pre-condition each column. After elution of hexane, the surplus

absorbed on the column sorbent bed was removed using gentle air flush. Approximately 60-80mg of whole oil was weighed directly onto the frit of the column and allowed to adsorb onto the sorbent. Care was taken not to get oil onto the sides of the column. A 10ml glass vial was placed under the column after sample addition, and the oil sample was eluted using hexane (5ml). Oil stains to the inside walls of the column were washed down into the column and the entire sample was transferred onto the solid phase. The samples were allowed to elute through the column. After gentle addition of the 5ml hexane, the remaining hexane in the column was removed with a gentle air flush and the column tip was washed with more hexane. The fraction obtained was capped and stored. This fraction contained the aliphatic and aromatic hydrocarbons, dibenzofurans and dibenzothiophenes.

The hexane fraction collected from above was carefully evaporated to approximately 1ml under nitrogen gas. About 100µl was taken from the 1ml hexane fraction for further separation into saturated and aromatic hydrocarbons using a Ag^+ impregnated silica gel (KieselGel 60G) packed 3ml column. To prepare the Ag^+ impregnated silica columns (say for 40 columns), about 30g Kieselgel silica (60G) was weighed into a conical flask followed by addition of 60ml distilled water into which 3g silver nitrate has been dissolved. The slurry was thoroughly mixed by vigorous shaking. The flask was covered with foil and left to dry in an oven set at 60 °C for about 7 days. After drying, the lumps were transferred into a clean mortar and crushed into powder using a pestle.

A clean frit was placed into the base of an empty 3ml cartridge barrel to be used for column separation. This was followed by addition of about 550mg of the powdered

Ag^+ impregnated silica. The Ag^+ impregnated silica bed was compacted carefully using a clean glass rod. After compaction, the second frit was added and compacted further to a depth of about 13-15mm using a specially-designed glass rod.

After pre-cleaning with hexane (5ml) using positive pressure (syringe and adaptor) for the solvent to pass through the column, the solvent was removed with a gentle air flush. An aliquot (100µl) of the hexane fraction containing the aliphatic and aromatic hydrocarbons was carefully added to the frit of the packed Ag^+ impregnated silica column. 4ml of hexane was used to elute the aliphatic hydrocarbons assisted by gentle air pressure and excess solvent in the column bed after self-elution was removed by gentle air flush and this was collected in clean 10 ml vial. The aromatic hydrocarbon fraction was recovered into another 10 ml vial by subsequent elution with 4ml DCM. After elution and collection of the fractions in vials, the aliphatic and aromatic hydrocarbon fractions were evaporated to 500 µl under nitrogen gas and transferred to auto sampler vials prior to gas chromatograph (GC) and gas chromatography-mass spectrometry (GC-MS) analyses.

3.2. Gas Chromatography (GC)

Gas chromatography was performed on the aliphatic hydrocarbon fractions in order to obtain *n*-alkane and acyclic isoprenoid data as well as to determine the molecular concentrations and complexity (by looking at visual GC fingerprint and compare whether injected amount of sample was optimal for the capacity of the detector) before gas chromatography- mass spectrometry (GC-MS) and gas chromatography-isotope ratio mass spectrometry (GC-IRMS) analyses. An HP 5890 series II gas chromatograph equipped with an HP-5 capillary column (60m x0.25mm, 0.25µm film thickness) was used. The GC oven was initially set at 50°C for 2mins and then the

temperature was ramped from 50°C at 4°C/min to 300°C and held at final temperature for 20 minutes. Hydrogen was used as the carrier gas with a flow rate of approximately 2ml/min and an initial pressure of 100kPa.

3.3. Gas Chromatography- Mass Spectrometry (GC-MS)

Gas chromatography-mass spectrometry (GC-MS) analyses of aliphatic hydrocarbon fractions were performed on a Varian CP3800 GC equipped with a split/splitless injector (280°C) linked to a Varian 1200 Triple Quadrupole mass spectrometer (electron voltage 70eV, filament current 50μA, source temperature 230°C, quadrupole temperature 40°C, multiplier voltage 1400V, interface temperature 300°C). The acquisition was controlled by a Dell GX150 computer and Varian software MS workstation (Version 6.42). After addition of 5β-cholane internal standard (approximately 200ng), samples were analysed in SCAN mode 50-550 atomic mass units /second (AMU/S) or in selected ion monitoring mode (SIM) mode for 30 ions (dwell time 35ms per ion). The sample (1μl) in hexane was injected by a Varian CP8400 auto sampler and the split opened after 1 minute. After the solvent peak had passed, the GC temperature programme and data acquisition commenced. Separation was performed on a fused silica capillary column (60m x 0.32mm i.d) coated with 0.25μm methylsilicone (HP-1). The GC was temperature programmed over 3 ramps from 40°C- 300°C (40°C - 175°C at 10°C/ min, held for 1min at 175°C, followed by 175°C-225°C at 6°C/min and held for 1 min at 225°C, and 225-300 at 4 °C/min) and held at final temperature for 20 minutes with helium as the carrier gas (flow approx 1ml/min with an initial pressure of 30kPa, split at 30 ml/min). The 30 ions monitored in the selected ion monitoring modes for the saturated hydrocarbon fractions were: m/z 85 (for *n*-alkanes and isoprenoid alkanes), m/z 109 (diterpanes), m/z 123

(diterpanes and tetracyclic terpanes), m/z 149 (trisnorhopanes), m/z 163 (bisnorhopane), m/z 177 (demethylated hopanes), m/z 183 (acyclic isoprenoids), m/z 191 (triterpanes), m/z 205 (methylhopanes), m/z 217 (regular steranes); m/z 218 (iso-steranes), m/z 219 (isosteranes), m/z 231 (methyl steranes), m/z 238 (botryococcanes), m/z 257 (17α-steranes), m/z 259 (diasteranes), m/z 318 (C_{23} tricyclic terpane), m/z 330 (C_{24} tetracyclic terpane), m/z 358 (C_{26} sterane), m/z 369 (triterpanes), m/z 370 (C_{27} triterpanes), m/z 372 (C_{27} steranes), m/z 384 (C_{28} triterpanes), m/z 386 (C_{28} steranes), m/z 398 (C_{29} triterpanes), m/z 400 (C_{29} steranes), m/z 410 (hopenes) m/z 412 (C_{30} triterpanes), m/z 414 (triterpanes), and m/z 426 (homohopanes).

The aromatic hydrocarbon fractions were analysed on a Hewlett-Packard 6890 GC split/splitless injector (280°C) linked to a Hewlett-Packard 5973MSD (electron voltage 70eV, source temperature 230°C, quad temperature 150°C multiplier voltage 2000V, interface temperature 310°C). The acquisition was controlled by a HP Kayak xa pc chemstation computer, initially in full scan mode (50-550 amu/sec) or in selected ion mode (30 ions 0.7cps 35ms dwell) for greater sensitivity. The sample (1ul) in DCM was injected by an HP7683 auto sampler and the split opened after 1 minute. After the solvent peak had passed the GC temperature programme and data acquisition commenced. Separation was performed on a fused silica capillary column (30m x 0.25mm i.d.) coated with 0.25μm 5% phenylmethylpolysiloxane (HP-5) phase. The GC was temperature programmed for the aromatics from 40°C (held for 5 min), ramped at 4°C/min to 300°C and held at final temperature for 20 minutes with helium as the carrier gas (flow approx 1ml/min, initial pressure of 50kPa, split at 30 ml/min).

3.4. Gas Chromatography-Mass Spectrometry/Mass Spectrometry (GC-MS-MS)

Gas chromatography mass spectrometry/ mass spectrometry analyses of the aliphatic hydrocarbon fractions were performed on a Varian CP3800 GC equipped with a split/splitless injector (280°C) and fitted with fused silica capillary column (60m x 0.32mm i.d) coated with 0.25μm methylsilicone (HP-1). This was linked to a Varian 1200 Triple Quadrupole mass spectrometer (electron voltage 70eV, filament current 50uA, source temperature 230°C, quad temperature 40°C, multiplier voltage 1400V, and interface temperature 300°C). The acquisition was controlled by a Dell GX150 computer (Varian software MS Workstation version 6.42) and up to 8 parent/daughter transitions of interest for steranes and triterpanes were monitored using argon as the collision gas at a pressure of 2mTorr, with collision energy of -10ev. The sample (1μl) in hexane was injected by a Varian CP8400 auto sampler and the split opened after 1 minute. After the solvent peak had passed, the GC temperature programme and data acquisition commenced. The following GC-MS-MS parent-to-daughter ion transitions were undertaken for the following compounds:

M/z 330→217 (5β cholane standard), m/z 368→217 (C_{26} steranes), m/z 372→217 (C_{27} steranes), 386→217 (C_{28} steranes), m/z 400→217(C_{29} steranes), m/z 414→217 (C_{30} steranes), m/z 398→177 (norlupanes), m/z 386→177 (bisnorlupanes), m/z 412→191 (C_{30} triterpanes), m/z 412→369 (C_{30} hopane, lupane and bicadinanes), m/z 414→123 (onoceranes and unknown triterpane compounds A, B and C), m/z 414→259 (tetracyclic polyprenoid), m/z 412→205 (methylated hopane). Most of the data for the calculated biomarker parameters presented in this work were generated using the GC-MS/MS mode. Because of the variation in instrument sensitivity which results from commonly occurring sagging filament problems and/or dirty ion source over extended run times during GC-MS/MS experiments, samples were run in batches

of 10 samples with a well characterised North Sea oil as reference standard to check variations in ratios involving the relative peak heights or areas of certain compounds for desired measurements. The reference standard oil was run at the beginning and end of each batch to check the reproducibility of the biomarker data.

3.5. Gas Chromatography Isotope Ratio Mass Spectrometry (GC-IRMS)

Isotope ratio measurements were performed on individual *n*-alkanes in the saturated hydrocarbon fractions at the Stable Isotope Research Facility (SIRF) of Department of Geological Sciences, Indiana University, USA. In the absence of unresolved complex mixture, Sofer *et al.* (1991) as well as Bjorøy *et al.* (1994) show that $\delta^{13}C$ isotope ratios measured on *n*-alkanes either in saturated hydrocarbon fractions or in whole oil samples are comparable in values. Briefly, samples were co-injected into the GC with a mixture of three reference standards consisting of decanoic, icosanoic and tricontanoic fatty acid methyl esters (FAME) of known chromatographic behaviour as well as $\delta^{13}C$ isotope values. The FAME standards were prepared by Dr. Arndt Schimmelmann of Indiana University. A Thermo Electron Trace GC Ultra connected to AS 2000 autosampler and fitted with an HP-5 fused silica capillary column (30m x0.25mm, 0.25μm film thickness) was used for sample separation. The temperature program was 50°C for 2mins, followed by a ramp of 3°C/min to 320°C and final temperature was held for 30 minutes. Helium was used as the carrier gas (flow rate of approx1.4ml/min). The eluting compounds were transferred to a standard Thermo Finnigan GC Combustion III (GCC III) interface consisting of Cu/Ni/Pt metal at temperature of 940°C. The GCC III is fitted with a Nafion purge trap to remove water, thus preventing protonation of the generated CO_2. The CO_2 generated from the combustion of individual *n*-alkane and isoprenoid compounds in the reactor was

transferred by means of helium gas through a capillary linked to a Finnigan MAT 252 isotope ratio mass spectrometer, where $\delta^{13}C$ isotope ratios were determined for the CO_2 representative of each *n*-alkane and isoprenoid peaks.

Instrument accuracy: The accuracy of the instrument was tested by co-injection of the FAME standard with another standard (mixture A2) containing mixture of nC_{16} to nC_{30} *n*-alkanes of known $\delta^{13}C$ isotopic values. This experiment was carried out at the beginning and end of three sample analyses each day in order to ascertain if any systematic errors occur in peak sample definition and to account for instrument drift. The FAME standard was used in this experiment as the reference standard to assign isotope values to the compounds in the *n*-alkane mixture. An acceptable deviation level of ± 0.8 per mil was set for each *n*-alkane peak. In each case where samples were analysed, the isotopic variation in the standards were found to be below ± 0.5 per mil in most cases and it was ensured that samples were only run when there was no apparent trend in enrichment or depletion in the $\delta^{13}C$ isotope values of the nC_{16} to nC_{30} *n*- alkane standard mixture.

Data reproducibility: The reproducibility of measured *n*- alkane $\delta^{13}C$ isotope data is a critical factor in data quality for interpretation purposes. To overcome any problem associated with this, an initial experiment was performed to determine the optimum sample concentration required for data reproducibility under our analytical conditions. In general, compound peaks generating an ion of 44 amu ($^{12}C^{16}O_2$) amplitude between 1 and 5 volts proved to be very reproducible in the various runs. Most samples were analysed twice to check again for data reproducibility.

In addition to the above analytical conditions utilised for the suite of oil samples analysed at Indiana University, USA, three deepwater oil samples together with bitumen extracts from Late Cretaceous Araromi shale samples were also analysed for

their *n*-alkane carbon isotope compositions (after urea adduction were performed on the saturated hydrocarbon fraction of oil samples and the Araromi shale bitumen extracts to isolate the *n*-alkanes from multibranched alkanes) under the same experimental conditions using the stable isotope analytical facilities at the Newcastle University's Institute for Research on Environment and Sustainability (IRES). Briefly, GC-IR-MS analysis of the *n*-alkanes was performed on a Thermo Electron Trace Ultra GC splitless injector (300°C) via a Combustion III Interface linked to a Thermo Electron Delta V+ IR-MS (HT voltage 3-5kV, Trap current 0.75mA, Box current 0.7mA). The acquisition was controlled by a Dell computer using Isodat software in carbon mode monitoring the CO_2 m/z 44:45 ($\delta^{13}C$) ratio. The sample (1μl) in hexane was injected by a CTC autosampler and the split opened after 1 minute. The chromatographic separation was performed on a fused silica capillary column (30m x 0.25mm i.d) coated with 0.25um 5% phenylmethylpolysiloxane (DB-5) phase, and the GC was temperature programmed from 50 to 320°C at 5°C/min and held at final temperature for 6 mi, with helium as the carrier gas (flow 1ml/min, initial pressure of 50kPa, split at 20 mls/min). The solvent peak was diverted to the FID and CO_2 reference gas was pulsed into the mass spectrometer and after 7 minutes the back flush valve directed the split sample via the combustion furnace (940°C) and reduction furnace (650°C) into the mass spectrometer and the isotope ratio measured. The acquired data was processed to give the peak retention times and isotope ratios.

3.6. Urea Clathration

The urea clathration method, popularly called urea adduction, was used to separate *n*-alkanes from multi-branched and cyclic alkanes in the saturated hydrocarbon fractions of the three deepwater crude oil samples and the Late Cretaceous Araromi shale

extracts prior to their GC-IRMS analyses. An approximately weighed (ca. 5-10 mg) sample of a saturated hydrocarbon fraction was added to 4ml of a hexane/acetone (2:1) solution in a centrifuge tube. A saturated solution of urea in methanol (2ml) was added drop wise, with vigorous shaking of the centrifuge tube. A precipitate was formed in which urea adducts the unbranched (normal) and some of the monomethyl branched alkanes. Solvent above the precipitate was removed by evaporating to dryness in a stream of nitrogen without heating. This operation was repeated twice. Following repeated addition of the hexane/acetone solution and saturated solution of urea in methanol and solvent blow down, hexane (~ 4ml) was added to the centrifuge tube to dissolve the oily, non-adducted hydrocarbons and this was centrifuged (3000 rpm – 5 min). After centrifugation, the supernatant liquid was carefully removed with a pasteur pipette. This operation was again repeated two more times. The washings were collected in 10ml vials and evaporated under a stream of nitrogen gas, to provide the non-adducted multibranched and cyclic hydrocarbons.

The urea precipitate in the centrifuge tube was dissolved using a small amount of distilled water (~ 2ml). The urea solution was then transferred carefully into a test tube, to which was added hexane (~2ml). The mixture in the test tube was capped using a stopper and shaken vigorously. Removal of the upper hexane layer was done with a Pasteur pipette after the mixture was allowed to settle, to provide the adducted straight chain and some monomethyl hydrocarbon fractions. This step was repeated three times for thorough extraction of *n*-alkanes from the mixture.

3.7. Total organic carbon (TOC) analyses

Total organic carbon (TOC wt. %) values were determined on powdered core samples of the Araromi shale using a LECO LS-244 Carbon Analyser. Briefly, approximately

100mg of sample was weighed into a non-porous crucible. The samples in the crucible were then treated with 1mL of hydrochloric acid solution (HCl; 37%HCl in water) to remove all inorganic carbon ($CaCO_3$), prior to TOC measurement. The crucibles were allowed to dry for about 4 hours and later transferred into an oven at 60°C overnight to dry prior to TOC measurements. Prior to sample analysis, the instrument was calibrated using a steel standard of known carbon content. In order to facilitate combustion (at 1500°C), some iron chips (metal accelerator) were added to the samples. The carbon present in the sample is then oxidized to CO_2 in the presence of oxygen and the CO_2 is is measured by a thermal conductivity detector. Results were reported as sample weight percent carbon.

3.8. Source rock pyrolysis

Rock pyrolysis was performed on approximately 100mg of powdered source rock samples. A Delsi oil show analyser fitted with Delsi Rockplus software was used. Weighed rock samples in crucibles were heated under controlled temperature program in an inert atmosphere. The temperature program used by the machine consists of three phases of heating. Firstly, sample was heated at 100°C for a period of three minutes, during which free volatile hydrocarbons (gas) are released (S_0). This was followed by a phase marked with increase in furnace temperature to 300°C and held for a period of three minutes to allow the expulsion of heavier free hydrocarbons (oil) from the sample (S1). The furnace temperature was then ramped from 300°C to 550°C at a rate of 25°C/min and then held at 550°C for two minutes. During this phase the kerogens in the sample is pyrolysed to generate hydrocarbons (S2). The temperature at which maximum petroleum generation occurred, Tmax (°C) was also recorded during this ramp.

3.9. Soxhlet extraction of core samples

Weighed amounts of powdered core samples of the Araromi Formation (about 20 grams) were placed into pre-extracted cellulose thimbles. The thimbles containing samples, plugged with pre-extracted cotton wool, were then placed into the soxhlet apparatus and extracted using azeotropic mixture of redistilled dichloromethane/ methanol (93:7, v/v) for 24 hours. Activated copper turnings were added to the solvent mixture to absorb elemental sulphur. After extraction of bitumen from the samples, the whole extracts were fractionated into saturated and aromatic hydrocarbon fractions using the SPE separation method prior to GC, GC-MS and GC-MS-MS analyses.

3.10. Separation of pure fractions of compounds A_1, A_2, B_1, B_2 and C

Purified fractions containing the compounds A_1, A_2, B_1, B_2 and C were obtained by means of a reverse phase high performance liquid chromatography (HPLC) analyses of Niger Delta sample ND10 oil, selected as having the highest abundance of compounds A_1, A_2, B_1, B_2 and C). About half a gram (412.9 mg) of the oil was separated into saturated hydrocarbons, aromatic hydrocarbons and polar compounds using medium pressure liquid chromatography (MPLC) technique. The oil has very low asphaltene content and was injected directly (0.12 ml at a time). The branched and cyclic hydrocarbons elute slightly later than the *n*-alkanes. The late half of the saturate peak (sat 2) was collected separately and injected again. The separation was repeated for the second half (sat. 22) finally giving a fraction (13.9 mg, sat. 222) highly enriched in hopanes and other cyclic compounds.

Sat 1:	102.0 mg
Sat 21 + sat 221:	88.2 mg
Sat 222:	**13.9 mg**

Sat 3	1.2 mg
Aro 1	10.7 mg
Aro 2	45.0 mg
Polar fraction (NSO)	30.6 mg
Loss (mainly evaporation)	121.3 mg

The cycloakyl biomarker concentrate (sat 222) was separated using reverse phase HPLC. The pump used was a Waters Model 590 and the detector a Shimadzu RID-10A refractive index detector with a Waters M730 Data Module recorder. Approximately 10.5 ml of the concentrate was separated on a large reverse phase HPLC column. 42 fractions (P01-P42) were collected. The column used was a Phenomenex C18, 10 x 250 mm, 5μm, and mobile phase was acetone at 2 ml/min flow rate. Fractions P10-P32 were analysed using GC-MS in full scan mode. The fractions containing compounds of interest (P25, P26, P28 and P29) were separated on a smaller column (column: Vydac 201TP, C18, 4.6 x 250 mm, 5μm.) using acetone 70 %, acetonitrile 30 %, vol/vol mobile phase and flow rate approximately at 0.8 ml/min. Fraction P25 was separated into 26 fractions (vy01 - vy26). Vy03-vy22 were analysed using GC-MS in full scan mode. Fraction P26 was separated into 21 fractions (vy01 - vy21). Vy03-vy13 were analysed using GC-MS in full scan mode. Fraction P28 was separated into 31 fractions (vy01 – vy31). Vy06-vy31 were analysed using GC-MS in full scan mode. Fraction P29 was separated into 32 fractions (vy01 – vy32). Vy05-vy23 were analysed using GC-MS in full scan mode.

The GC-MS analyses were performed using an Agilent 6890N gas chromatograph connected to a Waters (Micromass) Quattro Micro GC tandem quadrupole mass spectrometer. A Phenomenex ZB-5 capillary column (30 m x 0.25 mm i.d., film thickness 0.10 μm) was used. The temperature program was 30°C/min from 70 °C to

100°C and 4°C/min from 100°C to 308°C followed by 8 min at 308°C. The mass spectrum of A_1 was obtained from fraction P26 vy07. The mass spectrum of A_2 was obtained from fraction P25 vy10. The mass spectrum of B_1 was obtained from fraction P29 vy16. The mass spectrum of B_2 was obtained from fraction P29 vy12. The mass spectrum of compound C was obtained from fraction P26 vy05.

In addition to clean mass spectra generated for compounds A_1, A_2, B_1, B_2 and C using the procedures described above, mass spectra for several hundred other compounds were obtained. Minor compounds having mass spectra similar to those of A_1, A_2, B_1, B_2 were detected as well as C_{31} and C_{32} compounds which appear to be higher molecular weight homologoues of the A and B isomers. Notable is the fact that Fazeelat *et al.* (1994) also reported the occurrence of extended 8, 14- secohopanes that are related to the C_{30} 8, 14- secohopane compound in seep oils from Pakistan. The North Sea sample, ND09, ND10 and the Kutei sample were all analysed by GC-MS-MS (total saturated fraction only with Argon used as collision gas). The mass spectra obtained for compounds A_1, A_2, B_1, B_2 and C are discussed in the section 6.3.2.

CHAPTER FOUR

INTERPRETATION OF PETROLEUM GEOCHEMICAL DATA IN THE LITERATURE

Summary

This chapter presents a précis of published geochemical data relating to oils and source rocks of Tertiary deltas and the deficiencies that have led to the current poor petroleum system understanding. Certain processes which have previously been recognised in the literature in various non-deltaic basins have been reviewed and new ideas presented as to how these processes in addition to poor source rocks knowledge may combine to account for low level of petroleum systems understanding in Tertiary deltas. Three models for souring of oil and gas reservoired in Tertiary deltas earlier set out in chapter one were tested using statistical analyses performed on data of about 250 crude oil samples reservoired in Tertiary deltas from Beaufort-Mackenzie, Niger, Assam-Barail and Kutei Basin (Mahakam and Sulawesi). Additionally, the interpretation of this geochemical data provides evidence for at least four source rock groups charging Tertiary delta reservoirs. The initial conclusion based on this data set forms the premise of ideas that have been tested in subsequent chapters of this thesis using geochemical data from the newly analysed set of representative oils from the case study deltas.

4.0. Introduction

Petroleum occurrences in sedimentary basins are routinely described in relation to the source rock from which they have been generated. This concept of looking at petroleum occurrence in terms of the physical and temporal processes of generation in, and expulsion from a single pod of mature source rock is termed a petroleum system (Magoon, 1988; Perrodon 1992; Magoon & Dow 1994). By various migration pathways, a single petroleum source rock may charge a number of accumulations with reservoirs at various stratigraphic levels and traps (structure and seal) of various types. By emphasising the efficiencies of generation, expulsion, migration and entrapment, the petroleum system concept encourages prediction of origin, volumes and composition in undrilled prospects. Arguably this approach is least easy to apply for oil and gas exploration in river-mouth Tertiary deltas.

The understanding of source rock deposition in deltas has been dominated by three models, two of which have proved to be unrepresentative of the global norm:

i. The Westphalian coals measures of NW Europe and North America dominated the industrial revolution of the 19th and first half of the 20th Century and hence have tended to dominate coal studies (van Krevelen & Schuyer,1957; van Krevelen, 1993). Westphalian coals are unusually gas-prone, containing low levels (typically less than 8%) of oil-prone macerals (mainly sporinite and cutinite), and they source major gas provinces such as the Southern North Sea (Tissot, 1984; Glennie, 1997). By extrapolation, an assumption that 'coals generate gas' spread worldwide.

ii. Early studies of gas-prone organic matter were based on samples from the Douala Basin, Cameroon (Albrecht & Ourisson, 1969; Albrecht, *et al.*, 1976; Durand & Espitalie, 1976; Vandenbroucke *et al.*, 1976; Huc *et al.*, 1986). The analysed section of the studied well contained lean and gas prone kerogen, and led to the assumption that this is another typical gas-prone delta. However, the Douala area and Sanaga River Delta are now known to contain abundant oil seeps and significant oil accumulations.

iii. French studies of the oil-rich Mahakam Delta of Indonesia (Connan & Cassou 1977; Combaz & de Matharel, 1978; Durand & Oudin,1979; Oudin & Picard 1982; Durand & Parrate, 1983) have suggested that oil may be generated from liptinite-rich or 'perhydrous' coals, a proposal that has been supported by Curiale and co-workers in the Mackenzie Delta, Canada (Curiale, 1991; Snowdon *et al.*, 2004) and the Kutei Basin, East Kalimantan, Indonesia (Peters *et al.*, 2000; Curiale *et al.*, 2005; 2006). These more recent studies have supported oil generation from some delta-top coals (Wilkins & George, 2002) and indeed, have suggested that prodelta sands may co-sediment with leaf cuticle which acts as a source for deep water waxy oils (Saller, 2006).

The concept of oil generation within deltas has thus been skewed by these coal generative models. In the last three decades, deltas have become one of the spotlights of renewed hydrocarbon exploration. This is arguably because of relatively easy access offered by the flat topography and a ready market provided by the large and ever-expanding populations living on the world's delta tops. Most recently,

exploration has been spurred by the large size of deepwater discoveries. Oil and gas reservoired within deltaic sediments constitute a significant percentage of the world's known hydrocarbon reserves, but whether these accumulations are truly generated from source rocks within the delta remains unproven.

Based on an extensive review of the published data on bulk, molecular and isotopic properties of crude oils (Appendix I), this chapter attempts to throw light on the poorly understood genesis of oil within and adjacent to Tertiary deltas. Collecting published but previously uncollated data permits a summary of what is known and not known about the geochemical processes occurring in Tertiary deltaic basins, and how these processes affect our understanding of the deltaic petroleum systems. This leads to a reduction of the technical risk associated with oil and gas exploration in present and palaeo-deltaic systems.

4.1. Crude oil geochemistry

In order to discriminate between the three models presented in chapter one, the geochemistry of the reservoired oils is studied at the molecular and isotopic level to infer the source rock '*organofacies*' (organic matter type as well as the depositional environment) (e.g. Peters *et al.*, 2000; Haack *et al.*, 2000). This approach of drawing inferences concerning the deltaic source rock facies from the basin's petroleum accumulations rests on the assumption that the oil's molecular composition has been little (or predictably) altered during migration through intervening beds and possibly within the reservoir. Molecular (biomarker) and isotopic properties of some 250 Tertiary delta-reservoired oils (Appendix I) were used to identify their likely source rocks in terms of organic matter source, depositional environment and maturity.

These latter three deductions are then used to place limits on the likely stratigraphic age of the source rock from which the deltaic oils were expelled.

4.2. Source organic matter

Petroleum is generated from kerogen in source rocks, and the approach adopted here accepts that the molecular characteristics of the organic matter in the source rock and its conditions of accumulation are carried, relatively unaltered, with the migrated hydrocarbons to the reservoir and can be recognised in the produced oil. For this interpretation, oils may be characterised from both biomarker and isotopic properties

4.2.1. Biomarkers

Following the work of Huang and Meinschein (1979) on the relationship of the steroidal compound carbon number distribution in sediments and their precursor organisms and the more recent review of microalgal lipid compositions by Volkman *et al.* (1998), the distributions of the C_{27}, C_{28} and C_{29} steranes compounds in sediments and crude oils can be used to infer dominant organic matter contributor (marine phytoplanktons and zookplanktons vs. terrigenous higher plants) (e.g. Moldowan *et al.*, 1985; Peters *et al.*, 1986). In marine settings, the C_{27} steranes dominate largely because of the zookplanton input (as in most animals, cholesterol dominates; Killops & Killops, 2005, pp.171), while the C_{27} steranes dominates in terrigenous higher plants.

The C_{27}-C_{29} sterane distribution, when plotted on a ternary diagram (Figure 4.1) provides useful visual assessment of a large dataset. Organofacies fields, modified from the initial concept of Huang and Meinshein (1979), are indicated on the triangle plot.

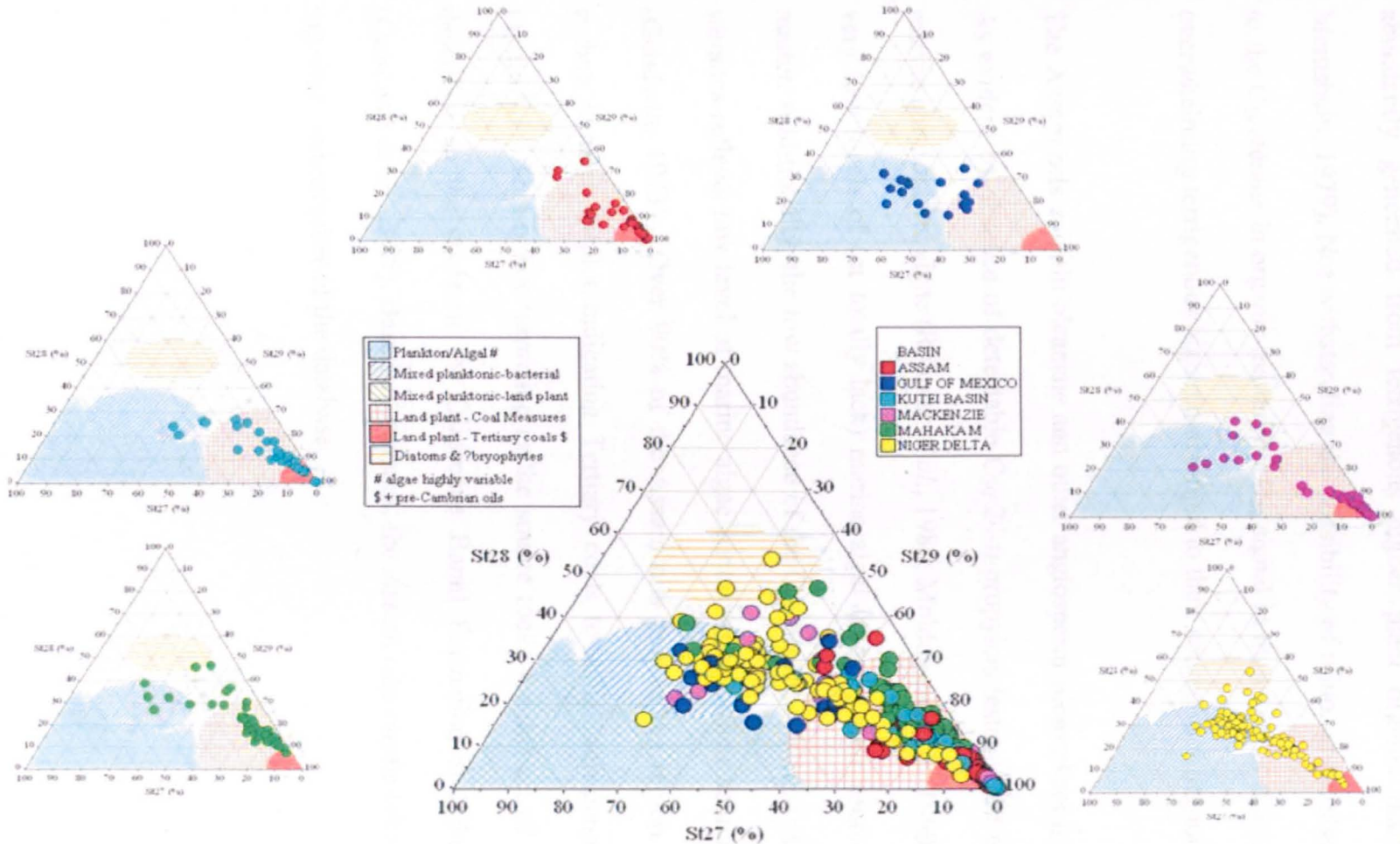

Figure 4.1. Ternary diagram showing the plot of C_{27} C_{28} and C_{29} steranes (based on 5α(H), 14α(H), 17α(H)-sterane peaks from m/z 217 mass chromatograms) interpreted in terms of likely kerogen precursor (interpretational overlay from IGI's p:IGI-2 software modified after Huang and Meinschein, 1979). Data source: Assam: Raju and Mathur, (1995); Goswami et al., (2005). Gulf of Mexico: GeomarkResearch. Kutei Basin: Curiale et al., (2005). Mackenzie: Brooks (1986a, 1986b); Curiale, (1991). Mahakam Delta: Peters et al. (2000). Niger Delta: Eneogwe and Ekundayo, (2003)

The Assam-Barail samples group closely within the regions marked as coaly and delta top source rock facies as expected. In Assam, the post-Paleocene section sits on metamorphic Basement, so no sub-delta source rock is plausible. Generally, sterane compositions of Assam oils are dominated by stigmastane, a C_{29} compound that is abundantly generated from terrigenous higher plant organic matter (Huang & Meinshein, 1979). Not withstanding the possibility of minor green algae contribution to the C_{29} sterane in organic matter, the C_{29} signal in these oils is considered to reflect overwhelming terrigenous higher plant input to their source rock organic matter.

The Assam oils contain oleanane and other angiosperm biomarkers like bicadinanes. As evident by absence of detectable C_{30} 24-*n*-propylcholestane that is diagnostic of marine chrysophyte algae (Rohmer *et al.*, 1980; Moldowan *et al.*, 1990), the oils have very low levels of (or totally lack) marine algal input to their source rock organic matter. Additionally, the low abundance of the C_{27} sterane relative to the C_{28} and C_{29} steranes reflects low level of marine algae contribution to their source rock kerogen (Goodwin, 1973). Over 90% of the Assam oils plot in the region of the sterane carbon number tri-plot indicating Tertiary coals to deltaic-terrigenous samples in Figure 4.1. This is not surprising as the source rocks for this set of oils have been described as the coals of the Oligocene Barail Formation and the Kopili shale (Goswami *et al.*, 2005). Based on steranes, the Assam oils can be taken as the 'delta-top coal' end-member of the database.

Conversely, samples of oils from the Beaufort-Mackenzie separate into two groups based on their sterane compositions (Figure 4.1). The group plotting into the C_{29} sterane apex implicates expulsion from terrigenous higher plants organic matter source units while the oil group contain higher C_{27} sterane content are thus presumably expelled from source units with abundant marine algae input. The occurrence of marine and terrigenous end-member oils within oil accumulations in the Tertiary deltaic reservoir in Beaufort-Mackenzie Delta has been reported by previous workers (e.g. Brooks, 1986a; Curiale, 1991; Li *et al.*, 2005). The marine oils are believed to have been expelled from Cretaceous source units with the Late Cretaceous Smoking Hills and Boundary Creek formations as candidate source rocks, while the terrigenous oils are sourced from Tertiary source units within the Eocene Richards Formation (Brooks, 1986a; Curiale, 1991) and coaly interval within the lower (early Eocene) Taglu Sequences (Snowdon *et al.*, 2004). Thus the marine oils are considered as being sub-delta sourced and in effect, the Beaufort-Mackenzie oil set provides a means of establishing the truly terrigenous organic matter dominated intra-delta sourced and non-terrigenous sub-delta derived oils within Tertiary delta accumulations.

Oils from Gulf of Mexico allegedly sourced from Tertiary deltaic source rocks have mixed marine and terrigenous source signatures with high marine algae content on occasions (moderately high C_{27} sterane and presence of C_{30} 24-*n*-propyl cholestane). The oils contain relatively low level of oleanane (oleanane index generally less than 0.2, figure not shown), which suggests limited angiosperm higher plant contribution and/or source rock age older than Tertiary (Moldowan *et al.*, 1994).

The Mahakam Delta within the greater Kutei Basin was one of the first major basins where coal has been demonstrated to be volumetrically capable of sourcing commercial oil (Durand & Parratte, 1983; Huc *et al.*, 1986). However, based on sterane carbon number, samples of oils from the Mahakam split into two groups; the first group as seen in Figure 4.1 is a coaly facies sourced oil which characterizes the majority of the Mahakam sample set and co-plots with the Assam oils at high C_{29} sterane content apex. In contrast, the second minor group plots in the planktonic-bacterial or mixed planktonic-land plant kerogen fields characteristic of shallow marine to open marine depositional environments. It is significant to add that the planktonic-bacterial (shallow-open marine) group of oils contains the C_{30} 24-*n*-propylcholestane molecule (up to 5.1% as detected by GCMS/MS as was reported in the dataset; Peters *et al.*, 2000), which is associated with marine chrysophyte algae precursor (Moldowan *et al.*, 1990). This establishes a second end-member of the oils discovered in Tertiary deltas, those expelled from planktonic-bacterial kerogens in marine source rock.

Furthermore, unlike the organofacies homogeneity displayed by oils from the Assam and Gulf of Mexico as being expelled from source rocks containing dominantly terrigenous and marine algae rich kerogen respectively, samples of oils from the Niger Delta contain oils from both marine and terrigenous end-members based on their sterane compositions (Figure 4. 1). Oils having intermediate marine and terrigenous organic matter source signatures either reflect mixed accumulations or expulsion from source rocks laid in distal deltaic setting (pro-delta shales) that received significant marine algae and terrigenous organic matter inputs. The published Niger Delta

database is dominated by oils from reservoirs located in the western section of the delta and may not fairly represent the entire Niger Delta oil sterane signature.

4.2.2. Stable carbon isotopes

The stable carbon isotope ratios of whole crude oil, together with those of its saturated and aromatic hydrocarbon fractions offer useful information as to the origin of the source rock organic matter. The carbon isotopic signatures of source rock extracts and oils provide reliable kerogen type discrimination since they can be measured to a high degree of repeatability, and are little altered by most other processes such as generation, migration and intra-reservoir alteration (especially biodegradation). The isotope information is useful to distinguish oils of terrigenous and marine origin when combined with other geochemical data (e.g. Sofer, 1984). Figure 4.2 is a cross-plot of stable carbon isotope $\delta^{13}C$ ratio values for saturated and aromatic hydrocarbon fractions. From the plot, the marine groups and terrigenous groups of oils from Assam, Gulf of Mexico, Mahakam, Beaufort-Mackenzie and Niger Delta are separated about the best statistical line of separation defined as canonical variable (CV) of 0.47 where CV is defined (Sofer, 1984) as:

$$CV = -2.53(\delta 13C \text{ sat.}) + 2.22(\delta 13C \text{ arom.}) - 11.65$$

The oil group having dominantly marine characteristics based on the biomarker data (Gulf of Mexico and some western Niger Delta oils) plot on the marine side of the CV= 0.47 line (Figure 4.2), overall, the entire western Niger Delta dataset plots in the marine region of the CV (Figure 4.2), thus supporting the earlier observation from molecular data that marine source rocks may be generating some of the oils reservoired within these deltas. A histogram of canonical variables (CV) provides a separation of the crude oil samples into those derived from marine organic matter and

those derived from terrigenous land plant dominated perhydrous coals to delta top shales (Figure 4.3). Arguably the distribution is tri-modal, with the marine end member being more negative than CV = -1, the terrigenous more positive than CV = +1, with an intermediate (or mixed) population of oils in the central mode (CV ranging from -1 to +1).

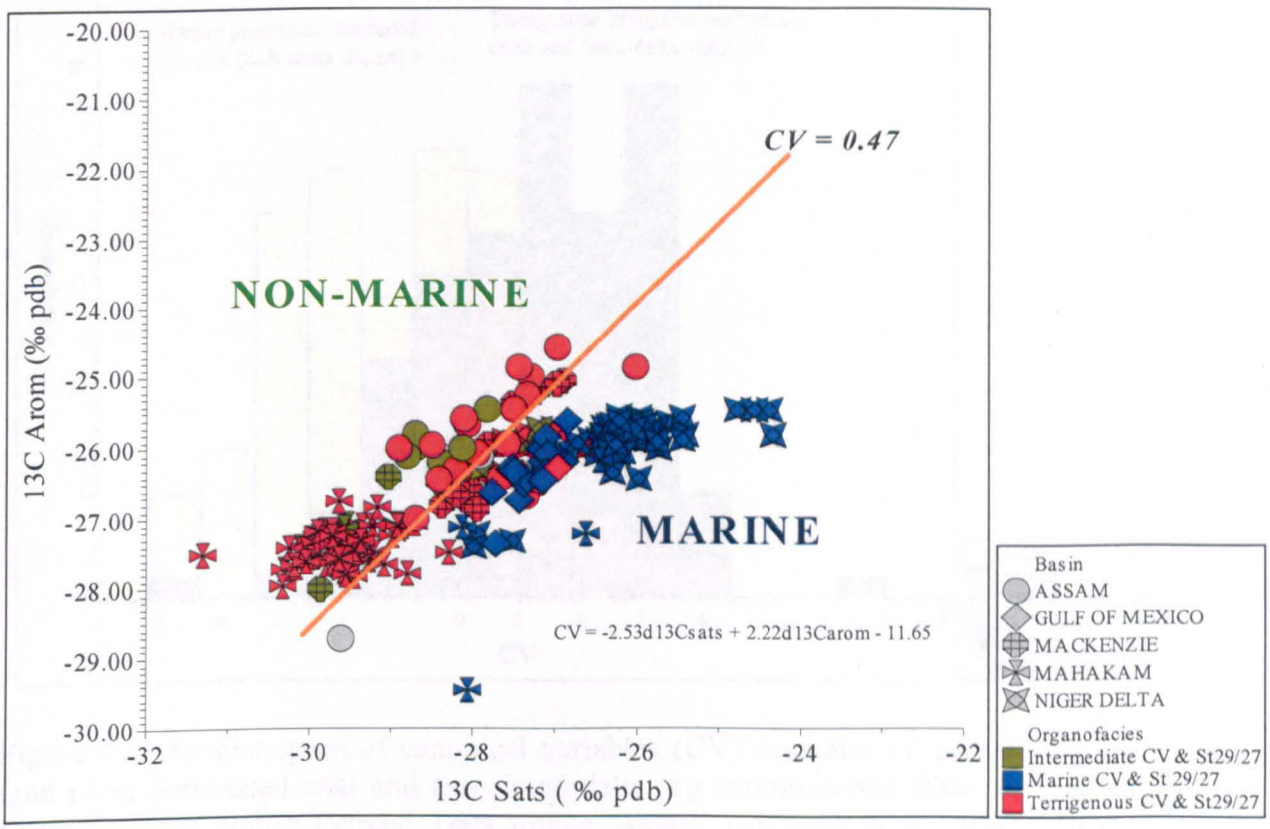

Figure 4.2. Cross plot of stable carbon isotope ratios for saturate ($\delta^{13}C_{sats}$) and aromatic ($\delta^{13}C_{arom}$) fractions of deltaic oils from the literature. The plot discriminates samples based on the likely source rock organic matter facies as either marine, terrigenous or intermediate (mixed oils). Data source: Assam: Goswami *et al.* (2005). Gulf of Mexico: Geomark Research. Mackenzie: Curiale, (1991). Mahakam Delta: Peters *et al.* (2000). Niger Delta dataset mostly from western oil accumulations: Eneogwe and Ekundayo, (2003).

Overall, saturates and aromatics hydrocarbon fractions from marine organisms are from a bicarbonate carbon pool dissolved in seawater. Generally, phytoplankton organic matter derives mainly from dissolved CO_2, which is isotopically lighter than bicarbonate, but the $CO_2 \leftrightarrow HCO_3^- \leftrightarrow CO_3^{2-}$ equilibria causes the dissolved CO_2 to be a little heavier than atmospheric CO_2, which terrestrial plant utilizes, hence the marine

organic matter saturates and aromatics are isotopically heavier than the terrestrial components. The canonical variable (CV) measures the difference between the saturated and aromatic hydrocarbons of these two different kerogen precursors (Sofer, 1984).

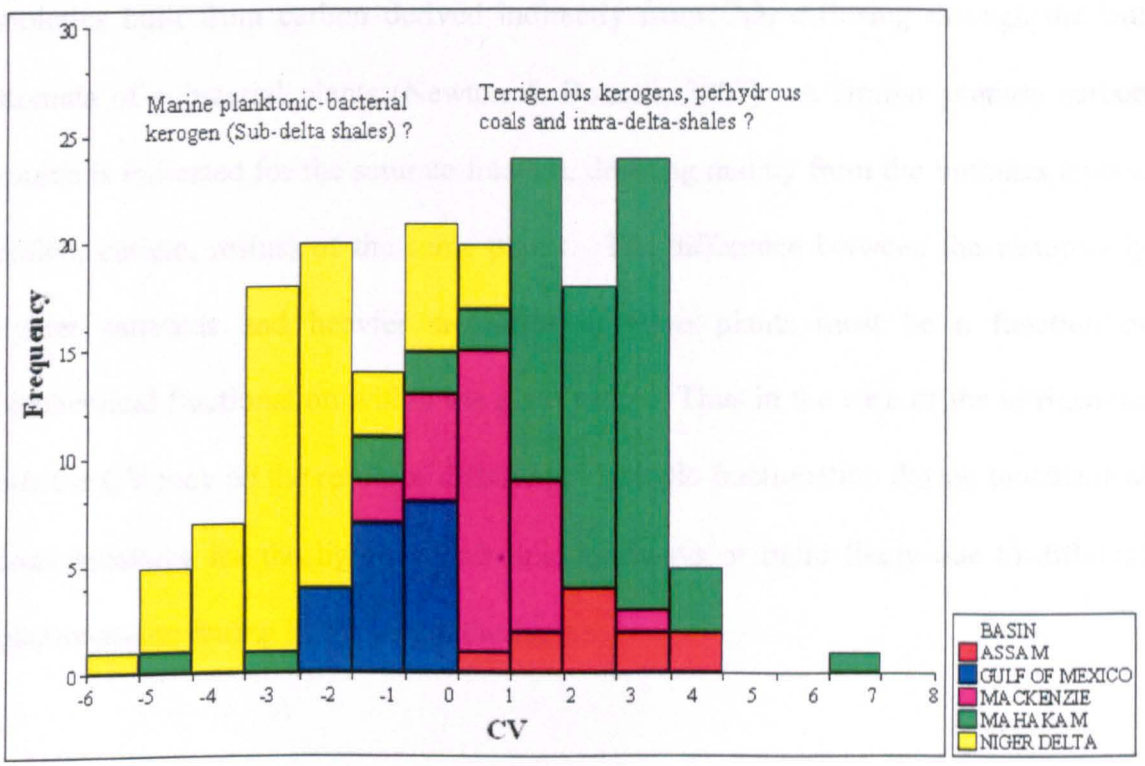

Figure 4.3. An histogram of canonical variables (CV) separates oil provenance into land plant dominated coal and associated delta top carbonaceous shale sourced and marine organic matter sourced. Data source: Assam: Goswami *et al.* (2005). Gulf of Mexico: GeoMark Research. Mackenzie: Curiale (1991). Mahakam Delta: Peters *et al.* (2000). Niger Delta dataset mostly from western oil accumulations: Eneogwe and Ekundayo (2003).

Independent of absolute values, the increasingly negative CV values of the marine oils reflect that the aromatics of marine kerogens (of uncertain origin) tend to be isotopically lighter than the saturated hydrocarbons, which derive mainly from planktonic algal lipids. The origin of marine humic acids which are reported as being isotopically heavier than terrigenous humic acids (Galimov, 1980) is poorly

understood (Rashid, 1985). The consensus is that they form from the polymerization of sugars and amino acids via the melanoidin pathway (Ertel & Hedges, 1980).

In contrast, the aromatics of the delta-top coals are sourced mainly from lignin moieties built from carbon derived indirectly from CO_2 diffusing through the leaf stomata of sub-aerial plants (Newton & Bottrell, 2007). A similar primary carbon source is indicated for the saturate fraction, deriving mainly from the liptinites (spore, pollen, cuticle, resins) of the same plants. The difference between the isotopically lighter saturates and heavier aromatics of these plants must be a function of biochemical fractionation within the plant tissue. Thus in the case of the terrigenous oils the CV may be the result of differential isotopic fractionation during biochemical bond breakage for the lignin versus lipid pathways or more likely due to different fractionantion during lignin biosynthesis.

The Assam-Barail samples show evidence of overwhelming terrigenous sourced oil (positive CV values) and thus provide further proof of the use of these oils as an end member for derivation from a delta top (coaly and associated carbonaceous shale) organofacies. The other stable carbon isotope end member of the worldwide database of Tertiary delta oils comprises the western Niger Delta oils where most samples are indicated as being sourced from kerogens with major amount of marine algae (Figure 4.8). Both positive stable carbon isotope canonical variables and smaller amounts of C_{29} steranes both point towards expulsion from a more marine organofacies. Within the assembled database, this constitutes the 'marine' end member of the Tertiary deltaic oil provenance. Using this model, the Beaufort-Mackenzie Delta oil samples

show two distinct groups as noted from the steranes; those from a coal and delta top sourced facies and an arguably marine sourced oil group.

From the measured sterane data (Figure 4.1), most of the Mahakam oils show characteristics of sourcing from mainly terrigenous organic matter, but a minority of the oils show marine aspect, this dichotomy being supported by their stable carbon isotopes compositions (Figure 4.2): the majority is again from mainly terrigenous organic matter. On the other hand, the stable carbon isotopes compositions of oils from the Gulf of Mexico show marine aspect that is in accord with the marine algae organic facies inferred from their biomarker characteristics.

To summarise the separation of deltaic oil families, a plot showing a combination of steranes carbon number (ratio of C_{29}/C_{27} from the 5α,14α,17α sterane peaks) and stable carbon isotope CV (canonical variable) was created (Figure 4.4). The plot separates samples in the Tertiary delta oils dataset into groups that may define their likely source rock organic matter origin as either marine, terrigenous and intermediate organofacies or mixed oils. What is noticeable is that using this separation, 4 of the 5 deltas reported have a number of oils that show marine characteristics. This is taken as evidence that most deltas have both intra-delta source rocks with terrigenous oil-prone kerogens and sub-delta source rocks containing marine oil-prone kerogens.

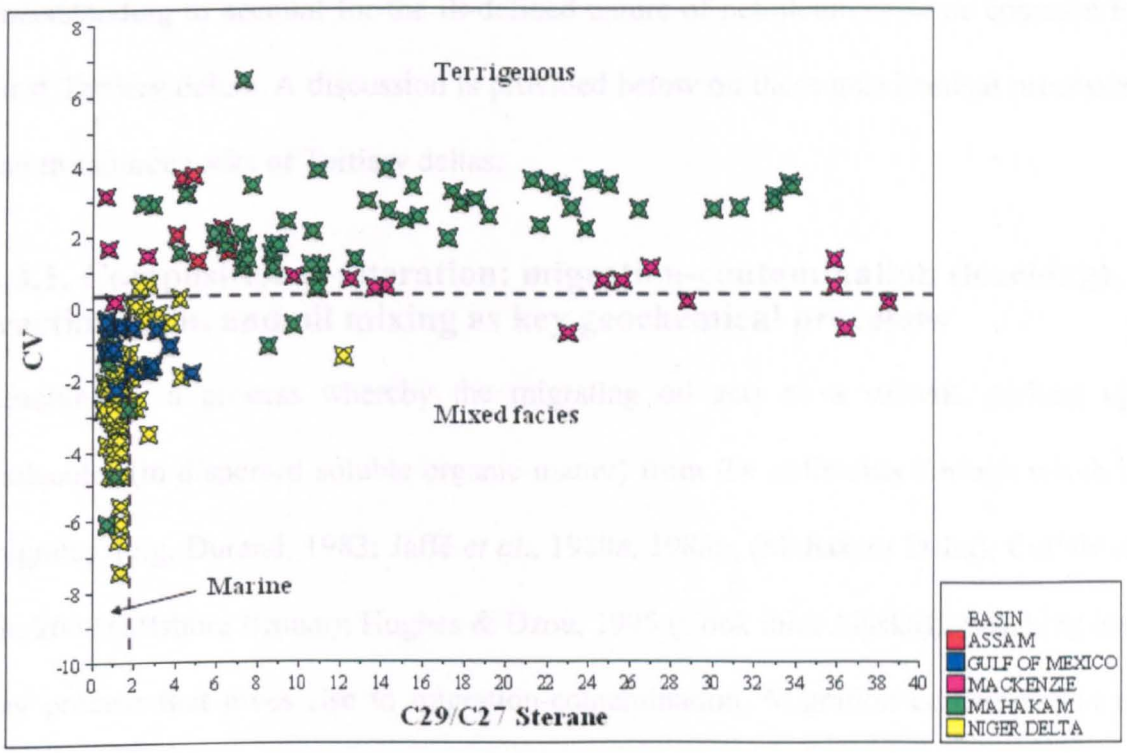

Figure 4.4. Cross plot of canonical variable (CV) and the ratio of steranes with 29 and 27 carbon numbers having 5α(H),14α(H),17α(H) stereochemistry. The plot discriminates samples based on the likely source rock organic matter facies as either marine, terrigenous or intermediate (mixed oils). Note some samples e.g. some Beaufort Mackenzie oils having marine sterane composition incorrectly plot in the terrigenous facies because of their elevated CV (>0.47).

Furthermore, because of large inconsistencies in the biomarker parameters measured by different workers from which this database has been harvested (Appendix I), more biomarker parameters could not be utilised to further establish variations in source facies among the oils.

4.3. Discussion of Tertiary deltaic petroleum systems

In terms of sediment body geometries, with channels, over bank deposits, inter-distributary bays, canyons, and in deep water, multiple lobes of mass-flow deposits, deltas represent a complex stratigraphic system deriving from a rapid rate of sediment supply and hence high accumulation rates in an open continental margin setting. Additionally, several geochemical processes combine with the poor source rock

understanding to account for the ill-defined nature of petroleum systems common to most Tertiary deltas. A discussion is provided below on these geochemical processes and the source rocks of Tertiary deltas.

4.3.1. Compositional-alteration: migration-contamination (leaching), fractionation, and oil mixing as key geochemical processes

Leaching is a process whereby the migrating oil acts as a solvent, picking up molecules (in dispersed soluble organic matter) from the sediments through which it migrates. (e.g. Durand, 1983; Jaffé *et al.*, 1988a, 1988b, (Mahakam Delta); Curiale *et al.*, 2000 (offshore Brunei); Hughes & Dzou, 1995 (Cook inlet Alaska)). Leaching is a key process that gives rise to migration-contamination. Migration contamination is said to have occurred when "foreign" molecules, picked up en-route during migration, have mixed with the original sourced-derived molecular compounds in the oils and thus confuses oil-source rock correlations (Curiale, 2002 and references therein; Curiale, 2006). A critical review of the process of migration-contamination has been provided by Curiale (2002). Compositional alteration also occurs when migrating "composite oil" has undergone fractionation in which some molecules have been preferentially remobilised into various fractions under the new migration and in-reservoir temperature and pressure conditions. Such alteration can be fractionation favouring more mobile molecules in distal migrated products (Curiale & Bromley, 1996).

In rift basins (passive margins) and basins formed in thrusted settings that have been tectonically unstable in the geological past, extensive faults and fractures are commonly developed to enhance vertical migration of petroleum fluids over considerable distance (Allen & Allen, 2005, pp.410). In deltas, vertical migration is

prevalent as a result of active tectonics and associated faults during rapid sedimentation, and the delta sedimentary architecture of proximal sands and shales interbeds. The relatively long oil migration journey via vertical routes favours the leaching of molecules from non oil-contributing source rocks, hence the more commonly observed migration-contamination, which may confuse oil-source rock correlations and as a consequence, lead to a poor understanding of petroleum systems (e.g. Li *et al.*, 2007).

The occurrence of olefins (unsaturated hydrocarbons) in oils of Tertiary deltas is often taken as evidence of migration contamination (Curiale & Frolov, 1998; Curiale, 2002; Curiale 2006). Although Eneogwe *et al.* (2002) argue that the oleanenes reported in the Niger Delta oils are source-derived (from the same kitchen as the oils) and that they have not been picked up during migration, on the basis that no process has been reported that could selectively pick up oleanenes and leaving behind other olefins during migration. In addition, given the low thermal maturity of most deltaic oils containing oleanenes (e.g. Eneogwe *et al.* 2002) in and the short thermal history (high heating rate) of most Tertiary basins, it could be that if hydrogenation of double bonds is a slower reaction than oil generation, then source rocks may have expelled oil at a relatively low thermal maturity level where olefins survive. Whether or not the olefins are sourced derived or a migration contamination product is yet to be unequivocally established.

In summary contamination and fractionation of composite oils during migration and in the reservoirs are considered as some of the major processes that can account for the poor level of correlation between the reservoired oils in Tertiary deltas and the

alleged delta source rock samples. That all the oil accumulations may not have been similarly contaminated during migration (i.e. the occurrence of a few Tertiary-reservoired oils not contaminated enroute migration) provides a means a to understand source rocks facies variations within the delta and oil sourcing outside the Tertiary delta sediments. This can in fact unlock the seeming geochemical paradox between reservoired oils and the alleged source rock samples as discussed in the next section.

4.3.2. Source rock groups charging Tertiary delta petroleum systems

According to Peters *et al.* (2005b, pp.752), nearly all the petroleum systems defined for Tertiary deltas have been assigned speculative to hypothetical level of certainty. The distribution of TOC and kerogen type data from wells drilled into Tertiary deltas (Figures 1.1 and 1.2) suggests that source rocks are poorly represented in most drilled wells. Thus the speculative to hypothetical level of petroleum system designation may be attributed to the rarity of organic-rich oil-prone source rocks that are regarded as the '*engine*' of the hydrocarbon '*generative machine*' in samples recovered from exploration wells in most deltas.

That source rocks are too deeply emplaced to be sampled when exploration activities were centred on the delta top, coastal swamps and shallow offshore areas of the continental shelf should not hold true now that exploration wells are being drilled in deepwater delta front, toe and pro-delta locations. The potential positions of oil-prone source rocks with a schematic delta are shown in Figure 4.5. Evidence from the assembled literature database of source rock and oil properties suggest that at least four source rock groups may be contributing to Tertiary delta oil accumulations as discussed below in terms of contributions from the sub-aerial delta top, the sub-marine delta top and delta front, and the pro-delta depositional environments, together with pre-existing sub-delta source rocks(Figure 4.5).

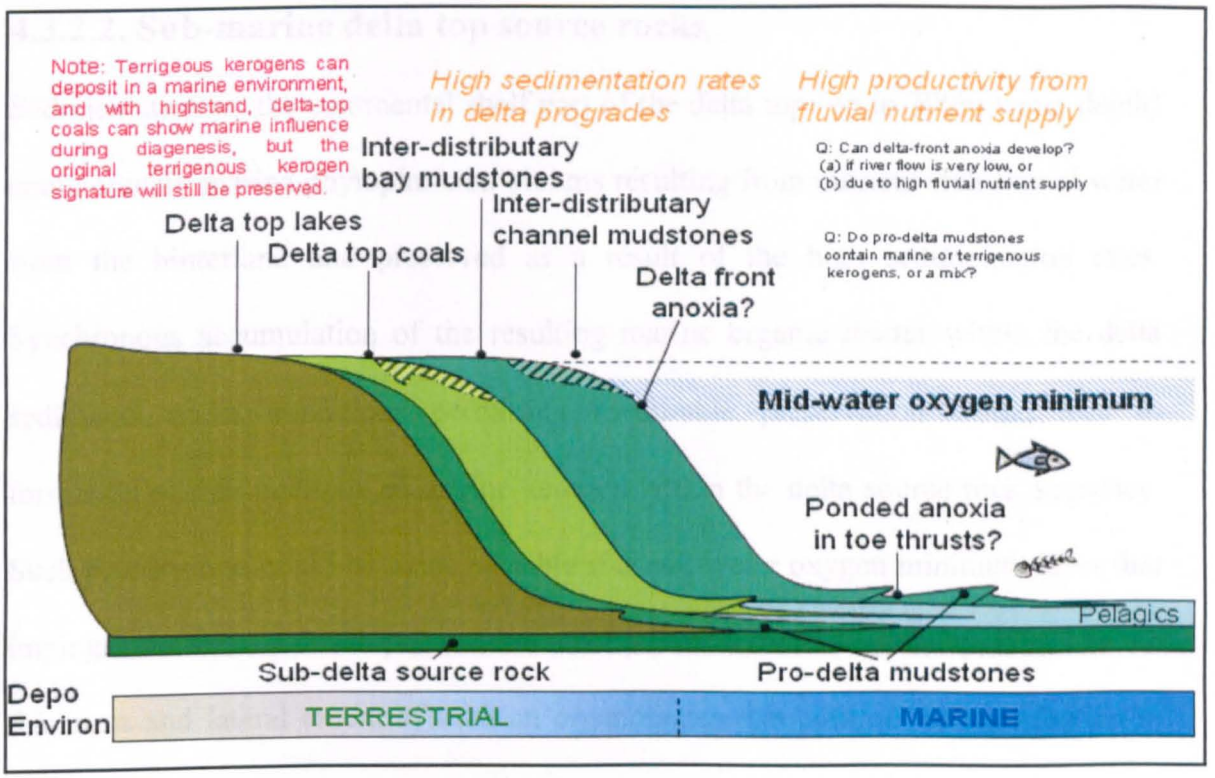

Figure 4.5. Hypothetical Section through a delta showing source rocks indicated by oil properties

4.3.2.1. Delta top source rocks (land plants and swamps)

These source rocks would typically be per-hydrous (oil prone) coals and occasionally lagoonal and lacustrine source rocks. These facies would produce the oils with a dominance of C_{29} steranes and positive CV values. In delta-top lakes and swamps, freshwater algae may contribute significantly to the organic matter, but drilling to date has failed to identify such source rocks as a common facies and in significant rock volumes. On a regional scale, within the delta basin, such lacustrine deposits appear rare and the oils bearing the freshwater algal geochemical signatures (e.g.botryococcane) are unusual. For instance, Ganz *et al.* (2005) reported the presence of botryococcane in some oils from the central Niger Delta, whereas on a basin-wide scale, botryococcane has not been otherwise reported in Niger Delta oils.

4.3.2.2. Sub-marine delta top source rocks

Sedimentation on the continental shelf part of the delta top (up to 200m water depth) could contain marine phytoplankton blooms resulting from nutrient-rich fluvial water from the hinterland and preserved as a result of the high sedimentation rates. Synchronous accumulation of the resulting marine organic matter within the delta sediments under conditions permitting favourable preservation would lead to formation of rich intervals of marine kerogen within the delta source rock sequence. Such preservation could be made possible if a mid-water oxygen minimum layer that impinges the shelf is developed to form a delta front anoxia. Practically, it will be the thickness and lateral extent of such an organofacies that controls its contribution to commercial oil accumulations.

To date no Tertiary source rock interval rich in marine kerogen has been reported within the Mahakam, Beaufort-Mackenzie, and Niger deltaic sequences. A questionable marine Eocene source rock lies at the base of the Tertiary sequence in Assam, though this could be seen as a sub-delta source rock. The kerogen for the source rock samples of the Tertiary thick marine Agbada and Akata shales in the Niger Delta have been described as terrigenous in terms of organic matter provenance with vitrinite being the most abundant macerals ($\geq$ 80%; Ekweozor & Okoye, 1980; Bustin, 1988), yet oils of overwhelming marine characteristics occur in wells drilled in the western (Eneogwe & Ekundayo, 2003) as well as the deepwater Niger Delta accumulations (Samuel *et al.*, 2006b).

Marine (liptinitic) organic-rich source rocks are absent from the delta literature database (Figure 1.3) and the limited distribution of marine-sourced oils in shallow

water deltaic settings suggests that source rocks containing dominantly marine kerogens do not occur or are highly diluted within deltas. This argues that to find the source intervals for the limited number of marine oil accumulations one must look below the delta sediments.

4.3.2.3. Pro-delta source rocks

The typical pro-delta depositional environment comprises mass flow clastics brought down in canyons at global sea level low-stands interbedded with fine grained hemi-pelagics. This results in the deposition of turbidites in the form of a deep sea fan sequence. During high-stands the deltaic sediment supply is captured on the shelf (in shallow water) and a muddy facies dominates the deep water. In the open ocean, pro-delta deposition occurs under oxic conditions. Occasionally, as in the Danube Delta of the Black Sea the receiving water body is anoxic (Huang *et al.*, 2000; Arthur & Sageman, 2004).

Recently, the deepwater oils of the Kutei Basin have been attributed to land plant organic matter in turbidite sands (Saller *et al.*, 2006). It is proposed that the sand grains and terrigenous organic matter have been transported down-slope in suspension in a mass flow to be deposited together in the deepwater. Thus recent publications show that oils sourced from both terrigenous kerogen and marine kerogen may be present in accumulations currently found in deep water marine settings. Source rocks in this location will, with time, become buried by the main body of sediment of the prograding delta and may be confused with sub-delta sources.

4.3.2.4. Sub-delta source rocks

Source rocks which predate Tertiary deltas are commonly (but not exclusively) Cretaceous and may be seen at outcrop in delta margin basins (Table 4.1). These basins typically extend laterally and non-conformably on the Basement rock. Such sub-delta source rocks are organic rich, and more commonly they are very organic rich mudstones having high TOC contents and Type II marine kerogen.

The overlying delta overburden thus provides the necessary sedimentary pile to enhance the thermal maturation of these pre-delta and pre-Tertiary source rocks. With migration showing a strong vertical component, the generated and expelled oil can pass into intra-delta traps. A model to illustrate the stratigraphic relationship of the sub-delta source rocks to the true delta (intra-delta) source rocks is presented in Figure 4.5. To illustrate this point of sub-delta sourcing of oils, Rock-Eval data from 9,548 rock samples from the Mackenzie, Mississippi and Niger delta areas were taken from a large public database of some 66,000 analyses available on the website of the United States Geological Survey (USGS, 2003). The whole 3-delta database is shown on the left of Figure 4.6, where the vast majority of samples fall within a Type II (algal-bacterial) envelope.

Extracting the small number of samples with reliable stratigraphy shows a dominance of leanness and gas-prone Type III kerogen in the Tertiary samples (Figure 4.6, top right). In contrast, the Cretaceous and older samples plot as containing Type II oil-prone kerogen in Figure 4.6 bottom right. Sub-delta Cretaceous and older source sediments below these major Tertiary deltas have historically been too deep to be sampled by drilling.

Table 4.1. Summary of intra-delta and sub-delta source rocks for some Tertiary deltas

DELTA	ORGANIC RICH FORMATIONS	
	Intra-Delta (Tertiary)	**Sub-delta (Cretaceous and older)**
Mackenzie	Kugmalit Formation Richards Formation Reindeer Formation?	Smoking Hills[1] Boundary Creek[1]
Mississippi	Sparta Willcox[1] Midway[1]	'Tithonian marls'[2] Smackover shale & marl[2]
Niger	Agbada Formation. Akata Formation.	Araromi & Afowo Formation[1] (Dahomey Basin) Lokpanta & Nkporo Shale[1] (Lower Benue Trough)

[1]= Cretaceous; [2] = Jurassic

In the case of both the greater Mississippi and Mackenzie delta data sets, Figure 4.6 (left) shows a cluster of very rich but highly immature oil-prone sub-delta Cretaceous samples (indicated by ellipse). In both cases (ODP Site 171B, Bahamas Platform and Amauligak I-65A respectively), these samples derive from wells drilled on or beyond the flanks of the major deltaic prograde. The analogous sub-delta sediments for the Niger Delta outcrop in the Lower Benue Trough and the Dahomey Basins (Ekweozor, 2004; Samuel *et al.*, 2006a, 2006b). The intra- and sub-delta units for the three locations are summarised in Table 4.1.

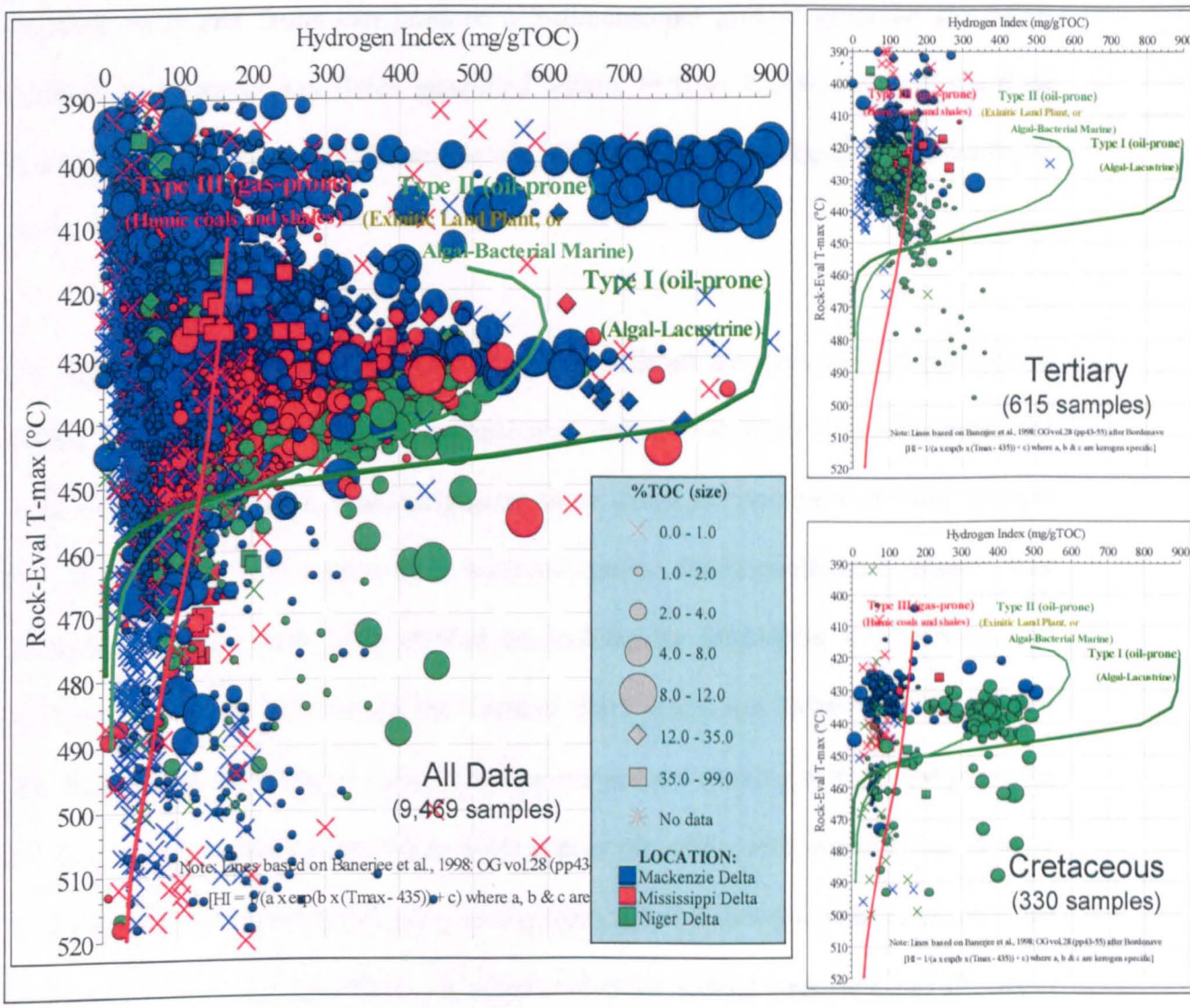

Figure 4.6. Rock-Eval characterisation for source and non-source rocks from Mackenzie, Mississippi and Niger deltas showing kerogen type (Hydrogen Index) and maturity (Tmax) and richness (TOC– symbol size). Data from USGS public web database (2003); http://www.usgs.gov/pubprod/

Deltaic sedimentation typically produces interbeds of mud and sand, producing the potential for sub-vertical (up dip) migration of fluids in the coarser clastic layers. High sedimentation and hence delta growth rates favours instability and the initiation of gravity tectonics, and this tectonic activity often results in a network of sub-vertical fault and fracture systems. Faults often show low angle listric detachments, dying out within over pressured fine-grained beds. Excess pressures and fine grain size are characteristics of source rocks, so the loss of pressure from such beds will require fluids to move along fault lanes. These fluids can be water, oil or gas. Taken

together, beds and faults can produce a 3-dimensional grid of potential migration conduits to transport any fluids generated within, or from below, deltas if the fault systems are well connected (Burrus *et al.*, 1993; Caillet & Batiot, 2003; Corredor *et al.*, 2005).

As predicted, possibilities thus abound that significant amounts of oils reservoired within the sands of most South Atlantic-type deltas have been sourced outside the delta sedimentary wedge, thus designating some deltas as "*receivers of*" and "*donors to*" oil accumulations within their reservoir sands. Traditionally, oil- source rock correlation studies have been centred on looking for intra-delta source rocks and linking them to the oils within the Tertiary delta reservoirs. Where oils have been sourced outside the delta, the reality is that we are not looking at the right place for the true source rocks and that might explain poor oil-source rock correlations. A more recent approach to considering oil sourcing from sub-delta source rocks is exemplified in the work of Li *et al.* (2005), in which sub-delta source rock samples of Upper Cretaceous Boundary Creek and Smoking Hills formations show a good correlation to one of the three oil families in the Beaufort-Mackenzie Basin, while mature source rock samples from Lower Cretaceous and Jurassic Husky Formations are correlatable to a second oil family.

4.4. Conclusions

From discussions of published opinions and reinterpretation of the merged database, it has been demonstrated that some oils within the Tertiary delta accumulations are not sourced by the alleged intra-delta source rocks containing land plant kerogens, but have been derived from sub-delta source units rich in marine bacterial-algal kerogen.

Common themes of deep burial of true source rocks, localised source organofacies variation, mixing, and migration contamination during migration were previously promoted as being the cause for poor petroleum systems understanding in deltas. Sub-delta sourcing of oil was not given due attention as a major mechanism in resolving the poor understanding of petroleum system in deltas.

Additionally, because of source rock kerogen heterogeneity within Tertiary deltas, oil source rock correlations are often confused due to unrepresentative samples of rocks being utilised. Accepting that the above conclusions were based on studies by different authors, working in different laboratories using a variety of analytical approaches over some 30 years, confirmation is needed. This has been sought by collecting a global oil data set and subjecting them to internally consistent high resolution analyses as detailed in the main body of this thesis.

High resolution molecular and isotopic data from unaltered oil samples can potentially permit the recognition of the sources of oils as either sub-delta or intra-delta within any deltaic basin when coupled with regional source rock geochemical and geological data. More work needs be done on deltaic oil samples, particularly on compound specific isotope analyses (CSIA) which could potentially permit the recognition of contributions from several organic bioproducers (e.g. marine vs. terrigenous) to the hydrocarbon compositions of crude oils. In the following chapters, the CSIA approach will be combined with biomarker data from analyses of representative oils from case study deltas to show further evidence of sub-delta contributions to oil accumulations in Tertiary delta reservoirs.

CHAPTER FIVE

MOLECULAR GEOCHEMISTRY I: OIL CHARACTERIZATION USING CONVENTIONAL MOLECULAR PARAMETERS

Summary

This chapter presents the results of routine biological marker (biomarker) and non-biomarker analyses performed on fairly representative samples of crude oils from each basin of study. Crude oils have been analysed to provide information on the type of source rock organic matter (marine or terrigenous), the source rock depositional environments, thermal maturity at expulsion, and post generation alteration processes. This chapter thus focuses on the molecular geochemical characteristics of oils from Assam, Niger, Beaufort-Mackenzie, Gulf of Mexico and Kutei basins. Additionally, the implication of the results in the context of organofacies (source rock depositional conditions, the organic matter type and stratigraphic age of source rocks) and insights into the petroleum systems of the basins are discussed comparatively in the later part of this chapter.

5.0. Introduction

In most deltaic basins building on the passive continental margins (e.g. Gulf of Mexico, Niger Delta), the source rock regarded as the hydrocarbon generating *machine* is believed to be deeply buried, and as such the representative source rocks have not been sampled in exploration wells (Peters *et al.*, 2005b, pp. 751).

Nonetheless, because oil inherits organic molecules expelled concomitantly with the bitumen from its source rock kerogen. The bulk, molecular and isotopic composition of oil is primarily a function of the type and maturity of source rock from which it has been expelled, while the source rock type reflects both the conditions of its deposition (e.g. fresh versus salt water, oxic versus anoxic, etc.) and the nature of the precursor organisms (e.g. marine algae vs. terrigenous higher plants, level of bacterial degradation) that contributed to the kerogen (e.g. Moldowan *et al.*, 1985; Peters *et al.*, 1986). The resulting source rock organic facies or 'organofacies,' (Jones, 1987) often lead to characteristic biomarker and isotopic signals in the expelled oils (e.g. Peters *et al.*, 1999; Janardhanan *et al.*, 2000).

Therefore, in keeping with the concept of crude oil molecular inheritance from its source rock(s), in the absence of source rock samples, the crude oil samples can provide valuable information that can be used to make inference on the nature of their source rocks (e.g. Peters *et al.*, 2000; Haack *et al.*, 2000). However, this assumes that the oils have not been significantly altered by migration-contamination, fractionation or intra-reservoir alteration processes (Curiale, 2002). The objectives of this chapter is to characterise the representative crude oil samples from the Assam-Barail, Beaufort-Mackenzie, Gulf of Mexico, Kutei Basin and the Niger Delta using organic

molecules (biomarker) and to ultimately predict the depositional environments and the organic matter characteristics of the potential source rock(s) for these oils.

5.1. Methods

The *n*-alkane and isoprenoid alkane data have been generated using the gas chromatograph experimental conditions discussed in Chapter Three. Sterane data are of high resolution and their acquisition were made possible by the advantage offered by the GC-MS-MS technique using appropriate parent to daughter transitional ions as described in the same chapter. In addition, data for tricyclic, tetracyclic and pentacyclic terpanes were generated from the m/z 191 mass chromatogram by GC-MS analyses together with terpanes data generated using diagnostic parent to daughter ion transition GC-MS-MS technique (Chapter Three). The detailed results of all these analyses are tabulated in Appendix II on the CD attached to this thesis. In all of the analysed crude oils, only few aromatic compounds were monitored for the purpose of obtaining thermal maturity parameters. Of particular note are aromatised terpenoids, particularly oleanoids, which were not monitored because of the assumption that the steranes and terpanes could give sufficient information on the organofacies of the oils.

5.2. Molecular Characteristics of Oils from Assam Delta

5.2.1. Normal (n-alkanes) and isoprenoid alkanes

The analysed crude oil samples from the Assam Delta generally possess high relative abundances of > C_{20} *n*-alkanes and they extend to as high as nC_{40} alkane under these analytical conditions. The samples are generally waxy solids at room temperature. The representative gas chromatograms for the Assam oil sets are presented in Figure 5.1. A number of the samples shows a bi-modal *n*-alkane distribution diagnostic of

dual sourcing from algal/bacterial and terrigenous higher plants organic matter (e.g. Bray & Evans, 1961). Table 5.1 shows the characteristic *n*-alkane and isoprenoid ratios of the Assam oil samples.

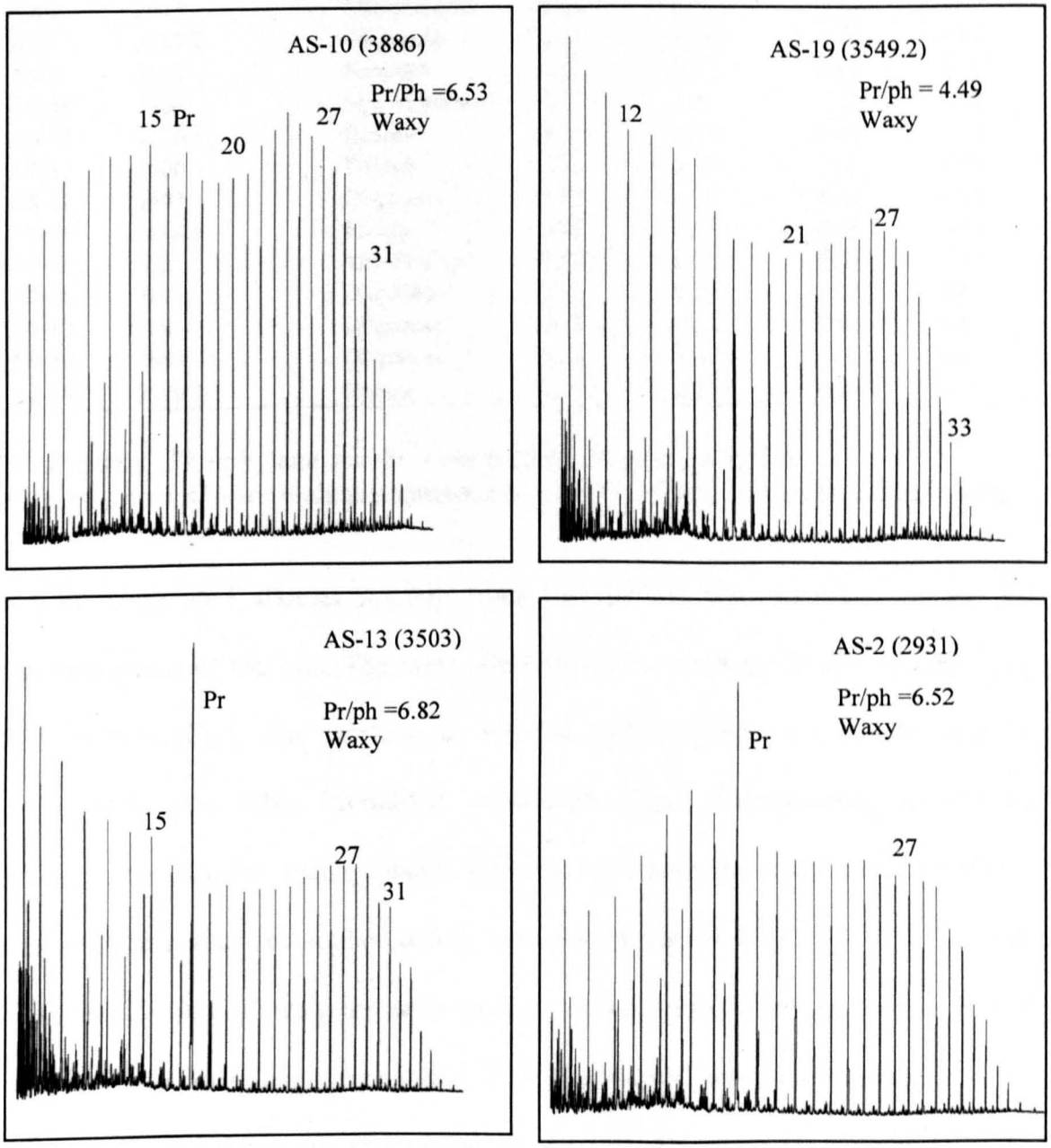

Figure 5.1. Representative gas chromatogram of samples of oils from the Assam Delta (northeast India). Numbers on peaks refer to the n-alkanes carbon number (chain length).

Table 5.1: Characteristic isoprenoid and n-alkane ratios for Assam oils

Sample	Base Depth (m)	Reservoir Age	Pr/Ph	norPr/Pr	Pr/nC_{17}	Ph/nC_{18}	nC_{17}/nC_{27}
AS-1	3125	Oligocene	5.92	0.18	8.53	1.41	2.31
AS-2	2931	Oligocene	6.52	0.21	2.24	0.37	0.76
AS-3	3150	Mio-Pliocene	6.90	0.20	3.01	0.48	0.80
AS-4	1396.5	Mio-Pliocene	6.20	0.25	2.88	0.50	0.64
AS-5	2964.2	Oligocene	6.16	0.21	2.46	0.42	0.94
AS-6	3453	Mio-Pliocene	5.92	0.29	1.03	0.18	0.83
AS-7	2715	Mio-Pliocene	5.04	0.25	9.32	1.92	1.41
AS-8	2647.2	Oligocene	5.71	0.20	3.45	0.64	0.90
AS-9	3522	Eocene?	4.82	0.27	0.87	0.19	0.77
AS-10	3886	Mio-Pliocene	6.53	0.21	1.51	0.23	0.98
AS-11	4676.5	Eocene	4.20	0.33	0.64	0.16	0.65
AS-12	3500	Eocene	5.31	0.25	1.03	0.21	0.77
AS-13	3503	Oligocene	6.82	0.20	3.48	0.55	1.03
AS-14	4494.5	Eocene	5.78	0.29	0.68	0.14	0.29
AS-15	762	Mio-Pliocene	4.42	0.27	9.89	5.51	0.55
AS-16	3241	Oligocene	5.88	0.20	3.45	0.64	1.09
AS-17	3263	Oligocene	6.36	0.20	3.68	0.63	0.92
AS-18	2684	Oligocene	6.04	0.24	24.01	4.32	1.52
AS-19	3549.2	Eocene	4.49	0.28	0.82	0.19	0.94

Pr= Pristane. Ph =phytane. NorPr = nor pristane (C_{18}) isoprenoids.
nC_{17}, nC_{18} and $_nC_{27}$ are *n*-alkane compounds with 17, 18 and 27 carbon chain lenghts.

Acyclic isoprenoid alkanes ranging from C_{13} to C_{20} were identified in the gas chromatograms of the oils. The most abundant of the isoprenoids are pristane (C_{19}) and phytane (C_{20}). The pristane to phytane ratio (pr/ph) is routinely used in conjunction with other biomarker parameters (e.g. gammacerane) in organic geochemistry to infer redox conditions occurring within the environment of source rock organic matter accumulation and preservation (Didyk *et al.*, 1978;Volkman & Maxwell, 1986). Following the early work of Brooks *et al.* (1969) as well as Powell and McKirdy (1973), the interpretation of the redox conditions of sediment deposition is based on the believe that pr/ph in sediments and oils, is mainly derived from the phytol side chain of chlorophyll of photosynthetic organism and, in specific depositional environments, of purple sulphur bearing bacteriochlorophyl a and b. Briefly, oxic to suboxic depositional conditions favour generation of more pristane

from the phytol side chain precursor, while reducing (anoxic) conditions favours generation of more phytane. Thus the pr/ph reflects the redox potential of the source rock depositional system under competing oxic and reducing conditions. However, several other workers (e.g. Chappe *et al.*, 1982; Illich, 1983; Goosens *et al.*, 1984; Rowland, 1990) provide evidence for additional sources for pristane and phytane, thus in this thesis, care has been taken in the interpretation of the redox conditions of sediment-water interface during organic matter accumulation based on pr/ph ratios alone. The pr/ph ratios are generally high for the Assam sample set and range from 4.2 to 6.9 (Figure 5.2). Pr/ph ratios less than 1 are commonly accepted to indicate anoxic depositional conditions (Didyk *et al.*, 1978). The pr/ph ratios for the Assam oil samples are generally high and above the boundary value of ~3 this being typical of petroleum derived from terrigenous organic matter deposited under oxic source rock depositional conditions, particularly coaly source rocks (Peters *et al.*, 2005b. pp.499). Furthermore, pr/ph ratios have been shown to be sensitive to the level of thermal maturation of the sediment and oils (Peters *et al.*, 2005b, pp.500), with increases in pr/ph ratios with elevated maturity level resulting from generation of relatively more pristane from kerogen and/or cracking of the C_{20} phytane to C_{19} pristane. However, samples of oils from Assam analysed in this study do not show these effect of maturation on the pr/ph ratios (Figure 5.3). For instance sample AS-2 has sterane isomerisation thermal maturity ratio ($C_{29}S/S+R$) of 0.65, suggesting a relatively high maturity (although the $C_{29}S/S+R$ isomerisation parameter only shows at least early oil window before full equilibrium is reached), yet it has pr/ph ratio of 6.5, on the other hand, sample AS-3 has pr/ph ratio of 6.9 despite being comparatively less mature ($C_{29}S/S+R = 0.51$).

Pr/nC_{17} and Ph/nC_{18} range from 0.64 to 24.01 and 0.14 to 5.51 respectively, which is typical of most terrigenous organic matter derived oils (Peters *et al.*, 2005b, pp.489).

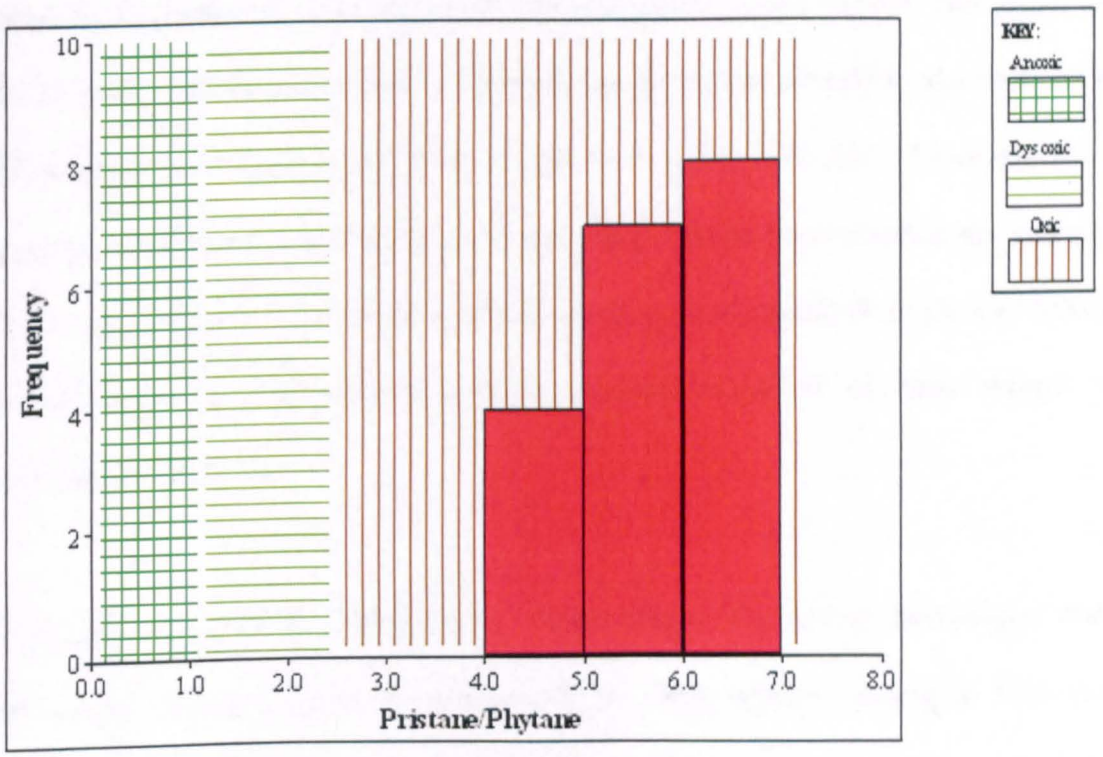

Figure 5.2: Degree of source rock anoxia inferred from the histogram of pristane and phytane ratios for the Assam oils. Overlay field after IGI's p: IGI 2.7 geochemical interpretation software.

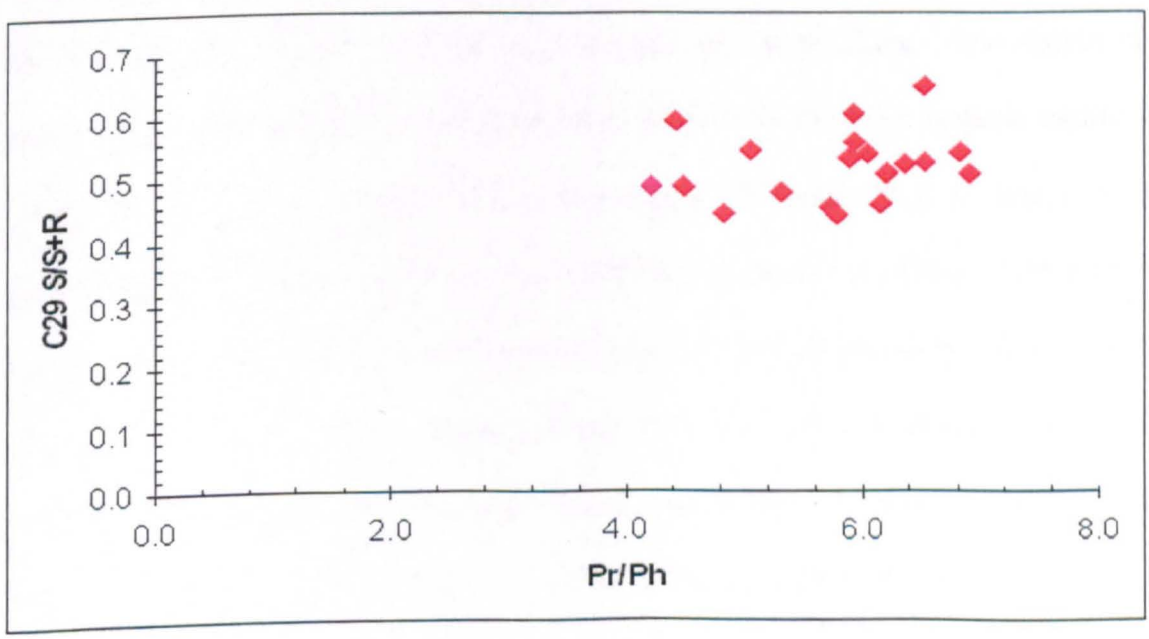

Figure 5.3. Cross plot of C_{29} 20S/S+R sterane isomerisation maturity parameter and pr/ph ratio to investigate effects of thermal maturity on the pr/ph ratios for the Assam oils.

5.2.2. Steranes

Regular steranes and iso-steranes in the Assam oils were quantified using appropriate parent to daughter ions for the GC-MS-MS analyses (Chapter Three). The use of GC-MS-MS afforded the generation of superior data to that obtainable by the routine GC-MS selected ion monitoring (SIM) of ions m/z 217, 218, and 259 diagnostic of steranes, isosteranes and diasteranes respectively. The measured ratios are presented in Table 5.2. Figure 5.4 shows a mass chromatogram obtained from the GC-MS-MS analysis showing characteristic sterane distribution typical of most Assam oils analysed in this study.

Generally, steranes are dominated by stigmastane, a C_{29} carbon homologue that is abundantly generated from terrigenous higher plant matters (Huang & Meinshein, 1979). Notwithstanding the possibility of minor green algae contribution to the C_{29} steranes in organic matter, the C_{29} signal in these oils is considered to reflect overwhelming terrigenous higher plant input to their source rock organic matter as will be supported by other source specific molecular biomarkers. The Assam oils have very low or lack of marine algal input to their source rock organic matter as evident by absence of detectable C_{30} 24-*n*-propyl cholestane that is diagnostic of marine chrysophyte algae (Rohmer *et al.*, 1980; Moldowan *et al.*, 1990). Additionally, the low abundance of the $\%C_{27}$ steranes (Figure 5.5), which generally reflects marine phytoplankton contribution to organic matter (Goodwin, 1973; Volkman *et al.*, 1998) relative to the C_{28} and C_{29} steranes renders support for a terrigenous higher plant dominated organic source inputs. Over 99% of the oils plot in the region marked for Tertiary coals to deltaic-terrigenous samples in Figure 5.5, which is not surprising as

perhydrous coals and associated carbonaceous shales have been reported as the source rocks for most of the oils in the Assam region (Goswami *et al.*, 2005).

In an assessment of global sterane literature on marine and terrigenous organic matter sourced oils, one ratio derived from sterane data in oils particularly useful for separating oils of marine and terrigenous organic matter origins is the ratio of the C_{29}/C_{27} 5α(H),14α(H),17α(H) 20R steranes. Assam oils generally have values that range from 2.11 to as high as 63.82. a value greater than 2 seems to be characteristic of terrigenous organic matter dominated oils.

In addition to the regular steranes, the oil samples are very rich in diasteranes (rearranged steranes), which are diagenetic products derived by clay mineral acid catalysed backbone rearrangement of sterols to diasterenes and subsequent reduction to diasteranes (Rubistein *et al.*, 1975; Moldowan *et al.*, 1986; Brincat & Abbott, 2001). The rearrangement reaction is reported to be catalysed by low pH (acid) and high Eh (oxic) conditions, this being typical for the depositional environment for coals. Under the more oxic conditions of coal swamps, there is greater degradation, and steranes/ sterenes are more susceptible, leading to higher diasterane/sterane ratios, although steroid levels aoverall are lower than in most marine settings. This could be due to where most of the steroids are located in plant (leaf) tissue(e.g. Killops & Frewin, 1994, and references therein; Killops *et al.*, 1994). The limited amount of clay minerals in coals may thus be overprinted by these favourable conditions. Thus, the oxic nature of the organic matter accumulation during deposition of the coaly source rocks for these oils as reflected in the high pr/ph ratios is paralleled by the relatively high diasterane concentrations. The diasterane/regular sterane ratio ranges from 1.84 to 5.69 (Table 5.2).

Table 5.2. Source and maturity sterane biomarker parameters for Assam oils

Sample	%C_{27} Reg	%C_{28}Reg	%C_{29} Reg	%C_{27} Dia	%C_{28} Dia	%C_{29} Dia	$C_{29}\beta\beta$	$C_{29}\alpha\alpha$	Dia/Reg	C_{29}/C_{27}	Hop/Ster
AS-1	7.51	5.31	87.18	2.81	9.01	88.18	0.56	0.56	3.12	11.61	1.66
AS-2	4.44	16.91	78.65	3.28	10.88	85.84	0.55	0.65	4.02	17.71	1.69
AS-3	4.87	20.32	74.81	3.99	10.04	85.97	0.51	0.51	3.10	15.37	2.46
AS-4	7.92	27.66	64.41	4.46	15.24	80.30	0.73	0.51	2.06	8.13	2.57
AS-5	5.70	11.03	83.27	2.44	10.22	87.34	0.58	0.46	3.04	14.60	1.47
AS-6	8.31	19.44	72.25	6.76	6.76	86.49	0.63	0.60	1.87	8.69	
AS-7	5.97	14.39	79.64	2.18	11.09	86.73	0.61	0.54	3.26	13.33	1.34
AS-8	1.38	10.32	88.30	2.19	10.40	87.40	0.56	0.45	2.88	63.82	1.27
AS-9	6.79	19.88	73.33	4.82	27.65	67.53	0.33	0.44	5.69	10.80	9.53
AS-10	14.35	14.96	70.68	3.95	15.52	80.53	0.58	0.52	1.84	4.92	4.74
AS-11	21.99	31.52	46.48	9.58	35.36	55.05	0.72	0.49	2.04	2.11	5.93
AS-12	7.89	39.55	52.56	8.33	33.86	57.81	0.40	0.48	4.00	6.66	7.02
AS-13	3.35	14.23	82.41	2.17	11.33	86.50	0.59	0.54	3.01	24.58	1.28
AS-14	13.14	22.63	64.22	10.38	22.05	67.57	0.55	0.44		4.89	3.00
AS-15	6.17	11.29	82.54	3.78	16.48	79.74	0.64	0.59	2.28	13.38	2.43
AS-16	6.22	13.71	80.07	2.43	10.26	87.31	0.53	0.53	3.53	12.88	1.49
AS-17	7.59	13.25	79.16	2.13	12.98	84.89	0.56	0.52	3.57	10.43	1.28
AS-18	4.29	13.31	82.40	3.26	10.19	86.54	0.58	0.54	3.12	19.21	1.41
AS-19	20.47	33.45	46.08	9.27	32.90	57.83	0.50	0.49	3.59	2.25	7.00

% C_{27} Reg, C_{28} Reg and C_{29} Reg = C_{27}, C_{28}, C_{29} as a percentage of sum 27-29 for 5α(H),14α(H), 17α(H)- 20R sterane. % C_{27}Dia = %C_{27} to sum 27-29 for 13β(H) 17α(H)- 20S+R diasteranes. C_{29} ββ = 5α(H),14β(H), 17β(H) 20S +R / 5α(H),14β(H), 17β (H) + 5 α(H),14α(H), 17 α(H)- 20 S+R C_{29} steranes. $C_{29}\alpha\alpha$ = 5 α(H),14α(H), 17α(H)- C_{29} 20S/20S+20R sterane isomerisation maturity parameter. Dia/ Reg = Sum of 13 β(H), 17α(H) and 13α(H), 17β(H)- 20S+20R diasteranes/ sum of 5α(H), 14α(H), 17α(H) and 5α(H), 14β(H), 17β(H)- 20S+20R for all the 27, 28 and 29 compounds obtained from GC-MS-MS. C_{29}/C_{27} = ratio of C_{29}/C_{27} carbon number compounds for 5α(H),14α(H), 17α(H)-20R sterane. Hop/Ster = 17α(H), 21β(H)- hopane/ sum of all C_{27}-C_{29} steranes (regular, isosterane and diasterane). All data were obtained from appropriate GC-MS-MS transitions.

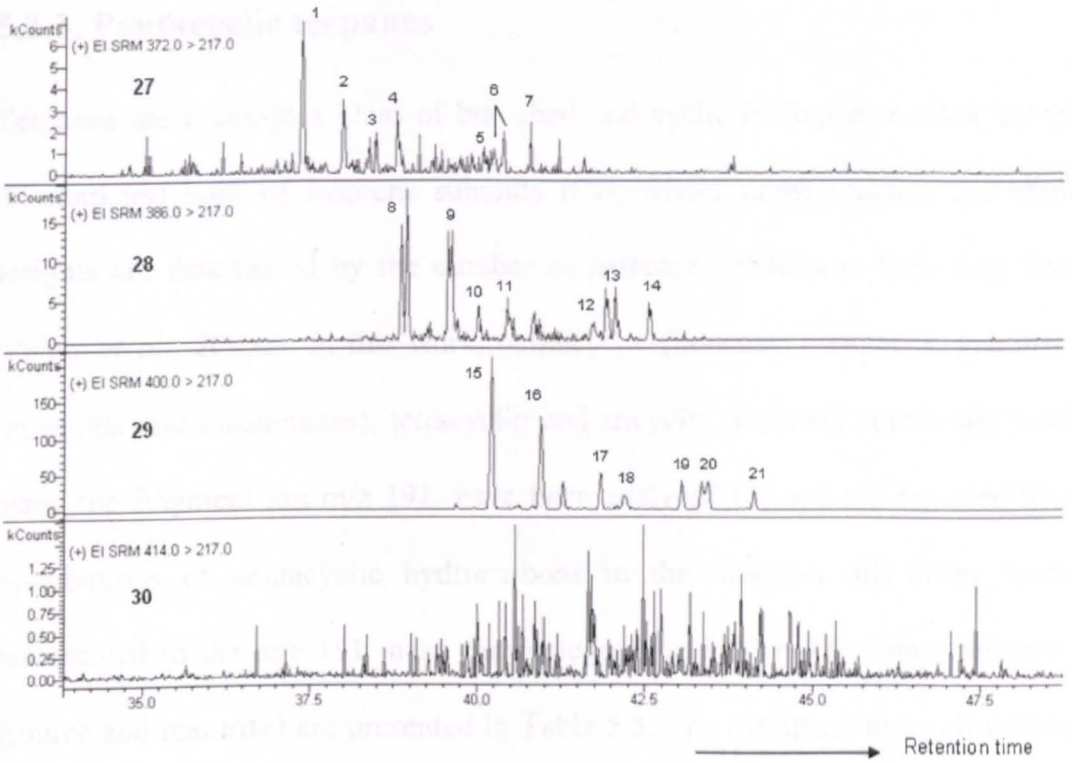

Figure 5.4. Representative GC-MS-MS mass chromatogram from sample AS-13 showing sterane distributions typical of Assam oils. Peak identities are in Appendix IIIa. Note absence of detectable peak for m/z 414➔217 diagnostic of C_{30} steranes.

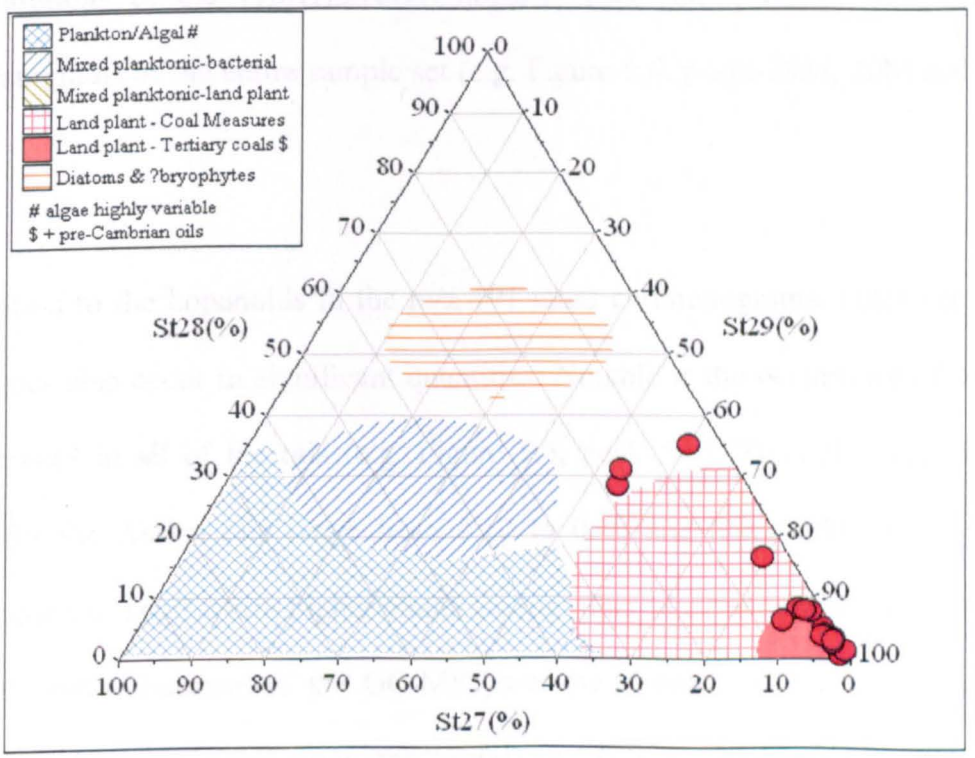

Figure 5.5. Ternary diagram showing the distribution of the 27, 28 and 29 carbon number regular steranes with 5α(H), 14α(H), 17α(H)- 20R configuration from GC-MS-MS analysis. Interpretational overlay from IGI's p:IGI-2 software modified after Huang and Meinschein (1979).

5.2.3. Pentacyclic terpanes

Terpanes are a complex class of branched and cyclic biological marker compounds (biomarkers) built of isoprene subunits (C_5), whose nomenclatures and molecular weights are determined by the number of isoprene subunits in their ring structures (Peters *et al.*, 2005a). In this work, pentacyclic (hopanes, oleananes, gammacerane, lupanoids and bicadinanes), tetracyclic and tricyclic terpanes, commonly monitored using the fragment ion m/z 191, have been analysed for and are reported here. The distributions of pentacyclic hydrocarbons in the nineteen oils from Assam are represented in the m/z 191 mass chromatogram in Figure 5.6. Characteristics ratios (source and maturity) are presented in Table 5.3. The triterpane mass chromatograms show the presence of series of hopanoid hydrocarbons with the 17α(H),21β(H) isomeric configuration ranging from C_{27} to C_{35}. There are also relatively high concentrations of the 17β(H),21α(H) hopanes (moretanes) in the m/z 191 mass chromatograms of the entire sample set (e.g. Figure 5.6, peaks 29M, 30M and 31S, R M)

In addition to the hopanoids in the m/z 191 mass chromatograms, other pentacyclic triterpanes also occur in significant quantities. Notable is the occurrence of oleanane and lupane? in all of the oils (e.g. Figure 5.6, peak OL). The calculated oleanane index for the Assam oils range from 0.12 to 0.40 and this could reflect variable contribution of angiosperm higher plants among other plant matters to the source rock organic matter. Because of the GC-MS parameters (principally column phase, see Chapter three) used in this study, the 18α(H) and 18β(H) oleanane isomers could not be resolved, hence the oleanane peak measured is the sum of the concentration of the 18α(H) and 18β(H) isomers.

Table 5.3. Source and maturity triterpanes molecular parameters for Assam oils.

Sample	OL Index	C35/C34	Bicad Index	23T/24T	Tet/Hop	23T/21T	19T/23T	Tet/23	C_{32} αβ	Hop/ Hop+Tet	30 αβ / αβ + βα	29Ts/ 29Ts+29βα
AS-1	0.21	0.61	0.927	0.99	0.06	0.73	3.57	3.70	0.57	0.99	0.86	0.23
AS-2	0.21	0.49	0.002	0.98	0.07	0.94	3.61	3.07	0.56	0.98	0.85	0.14
AS-3	0.18	0.51	0.001	1.36	0.05	0.66	3.15	3.26	0.57	0.99	0.83	0.12
AS-4	0.16	0.70	3.387	1.40	0.13	0.88	5.31	3.90	0.59	0.98	0.86	0.17
AS-5	0.22	0.59	0.311	1.07	0.07	1.05	2.92	3.40	0.56	0.98	0.84	0.21
AS-6	0.22	0.41	5.650	1.16	0.15	0.81	6.11	3.24	0.52	0.96	0.82	0.23
AS-7	0.24	0.76	0.173	1.17	0.06	0.71	2.47	2.21	0.58	0.98	0.83	0.19
AS-8	0.23	0.51	1.090	0.97	0.06	0.92	2.61	2.85	0.55	0.98	0.84	0.14
AS-9	0.29	0.72	0.418	0.00	0.14	1.04	7.76	8.60	0.55	1.00	0.83	0.37
AS-10	0.12	0.43	0.370	0.71	0.12	1.68	8.35	9.02	0.56	0.98	0.83	0.15
AS-11	0.40	0.77	1.234	1.16	0.32	0.58	14.04	10.99	0.55	0.98	0.91	0.59
AS-12	0.28	0.73	4.630	0.84	0.12	0.65	6.42	6.82	0.58	0.98	0.80	0.31
AS-13	0.21	0.63	1.808	1.12	0.06	0.78	2.82	3.14	0.56	0.98	0.82	0.25
AS-14	0.10	0.62	8.256	0.00	0.00	0.00	0.00	0.00	Nm	nm	Nm	Nm
AS-15	0.16	0.64	3.403	1.61	0.12	0.97	5.26	4.33	0.58	0.98	0.85	0.21
AS-16	0.22	0.61	0.119	0.85	0.05	0.65	3.99	4.58	0.67	0.99	0.86	0.23
AS-17	0.27	0.55	1.024	0.73	0.06	0.56	2.54	2.83	0.54	0.97	0.84	0.20
AS-18	0.23	0.56	0.728	1.22	0.07	0.97	3.24	2.99	0.56	0.98	0.83	0.18
AS-19	0.35	0.72	0.927	0.94	0.14	0.36	8.77	10.13	0.58	0.99	0.86	0.36

OL Index= 18α(H) + 18β(H) oleanane/(18α(H) + 18β(H) oleanane+ C_{30} 17α(H)21β(H) hopane). 35/34 = ratio of 17α(H),21β(H) pentakishomohopane (22S+ 22R)/ 17α(H),21β(H) tetrakishomohopane (22S +22R). Bicad Index = sum 100* (T + T_1 + R C_{30} bicadinanes)/ (T+T_1+R bicadinanes +17α(H),21β(H) hopane. 23T/24T = C_{23} tricyclic terpane/ C_{24} tricyclic terpane. Tet/Hop = tetracyclic terpane (24-de-E-hopane)/ C_{30} 17α(H) 21β(H) hopane.23T/21T = C_{23} tricyclic terpane/ C_{21} tricyclic. 19T/23T = C_{19} tricyclic terpane/ C_{23} tricyclic. Tet/ 23T = tetracyclic terpane(24-de-E-hopane)/ / C_{23} tricyclic. C32αβ = 17α(H),21β(H)-bishomohopane 22S/ 22S+ 22R thermal maturity parameter. Hop/hop+ Tet = 17α(H),21β(H) hopane /17α(H),21β(H) hopane + Tetracyclic terpane. 30 αβ /30 αβ +βα= 17α(H),21β(H) hopane/ sum 17α(H),21β(H) hopane + 17β(H),21α(H) hopane (moretane). 29Ts/ 29Ts+29αβ = 18α(H)-norneohopane/ 18α(H) norneohopane + 17α(H),21β(H) norhopane. Nm=data not measured.

As mentioned earlier in Section 1.10, lupane commonly co-elute with oleanane peak, and the oleanane index may not be wholly representative of oleanane alone.

Bicadinanes are present in all of the Assam oils and can be monitored using m/z 217, m/z191 and m/z 412 ions in the GC-MS analyses. However, to avert the problems of co-elution with other triterpanes in m/z 191 and steranes in m/z 217, and because of the relatively low level of abundance compared with other terpanes in m/z 191, parent to daughter ion transitions GC-MS-MS analyses (m/z 412→369 for C_{30} bicadinanes and m/z 426→383 for methyl-bicadinanes) were carried out to accurately detect and quantify bicadinanes with little interference (Figure 5.7) using the GC-MS-MS condition reported in Chapter Three of this study and following procedures described for the identification of bicadinanes in Assam oils by GC-MS-MS analyses by Goswami *et al.* (2005). In the m/z 414→369 distributions for bicadinanes, the *cis-cis-trans* isomers (V, W, W1 and W2; van Aarssen *et al.*, 1990) occur in very low concentrations such that accurate peak measurements were not possible in most samples and data for these isomers were not reported. However, *trans-trans-trans* (T, T1 and R) bicadinanes (Cox *et al.*, 1986) occur in high concentrations and were successfully quantified (Figure 5.7). The peak labelled T in Figure 5.6 is tentatively identified as 19α(H)-taraxastane on the basis of its retention time and comparison with published chromatogram of oils from South East Asia (Sosrowidjojo *et al.*, 1993; Rullkötter *et al.*, 1994) and in the Marraat-1 oil, West Greenland (Nytoft *et al.*, 2002 and references therein).

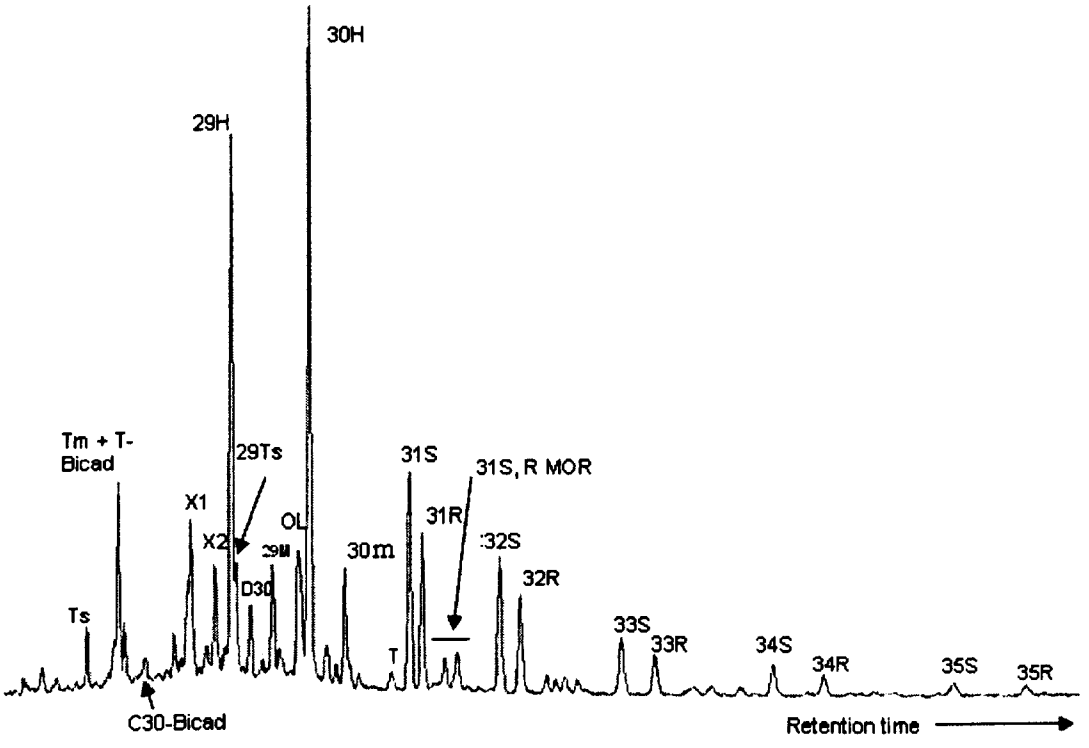

Figure 5.6. Representative partial m/z 191 mass chromatogram showing pentacyclic terpane distribution in a crude oil sample (sample AS-15) from the Assam Delta. Peak identification is given in Appendix IIIb. The increase in the retention time difference and peak broadening for compounds eluting after C_{32} bishomohopane is a common chromatographic effect resulting from the use of a 60m column.

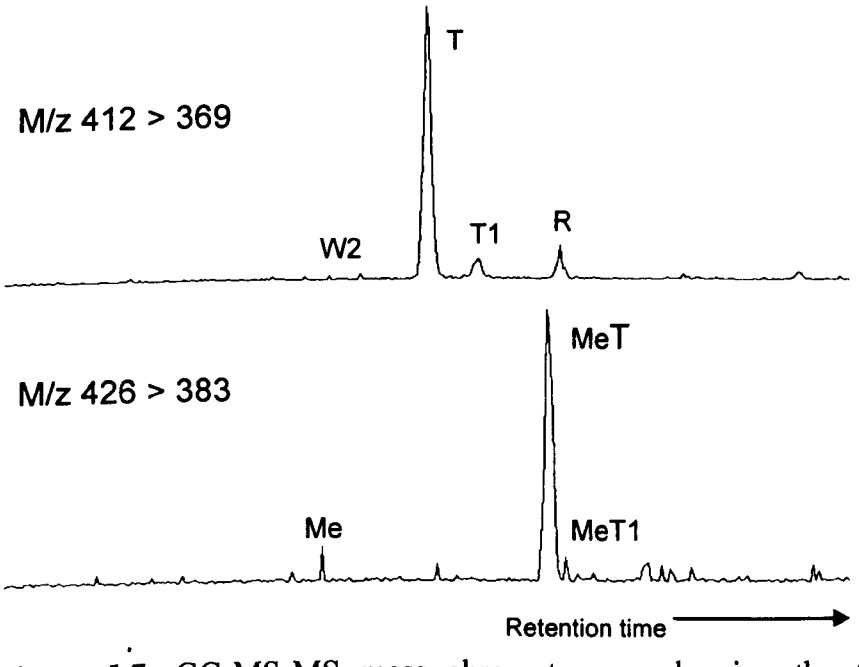

Figure 5.7. GC-MS-MS mass chromatogram showing the C_{30} bicadinanes (m/z 412➔369) and methylbicadinanes (m/z 426➔383) in sample AS-13 of the Assam sample set. Peak identification is by retention time and comparison of chromatogram with published data. T, T1 and R are C_{30} bicadinanes with the *trans-trans-trans* configuration and MeT and MeT1 are their methylated homologues, while W2 is the *cis-cis-trans* C_{30} bicadinane isomers (van Aarssen *et al.*, 1990).

5.2.4. Tricyclic and tetracyclic terpanes

Several tricyclic terpanes ranging from C_{19} to C_{29} as well as tetracyclic terpanes were detected with confidence in measurable amounts in the Assam oils (Figure 5.8). The distributions of tricyclic and tetracyclic terpanes in the Assam oils are relatively unusual when compared to samples from other basins investigated in this study (Figure 5.8). The complex distribution is a result of occurrence of several peaks, perhaps of land plant origin eluting between the tricyclic terpanes. The peaks are labelled X, Y1, Z and Z1(Figure 5.8). Compounds Y1 and Z have been identified by Woolhouse *et al.* (1992) as A-ring-degraded oleanane and ursane respectively, while the peak poorly resolved on the shoulder of peak Y1 (Figure 5.8) may be the de-A-lupane. These compounds also occur in Niger Delta oils (see Figure 5.41) and their mass spectra obtained from GC-MS analyses of pure triterpane concentrate recovered from a Niger Delta crude oil sample (ND10) by high performance liquid chromatography (HPLC) technique are presented in Figures 5.42, 5.44-5.48.

In general, the Assam oils are not very rich in tricyclic terpanes. Unlike in most distributions of tricyclic terpanes in oils where C_{23} tricyclic terpane is usually most abundant, in Assam oils the tetracyclic and C_{19} tricyclic terpanes are the most abundant peaks in the distributions (Figure 5.8). Also notable is the elevated concentration of C_{22} tricyclic terpane relative to other tricyclic terpanes in the Assam oils, which is quite uncommon with most tricyclic terpanes distributions in crude oils.

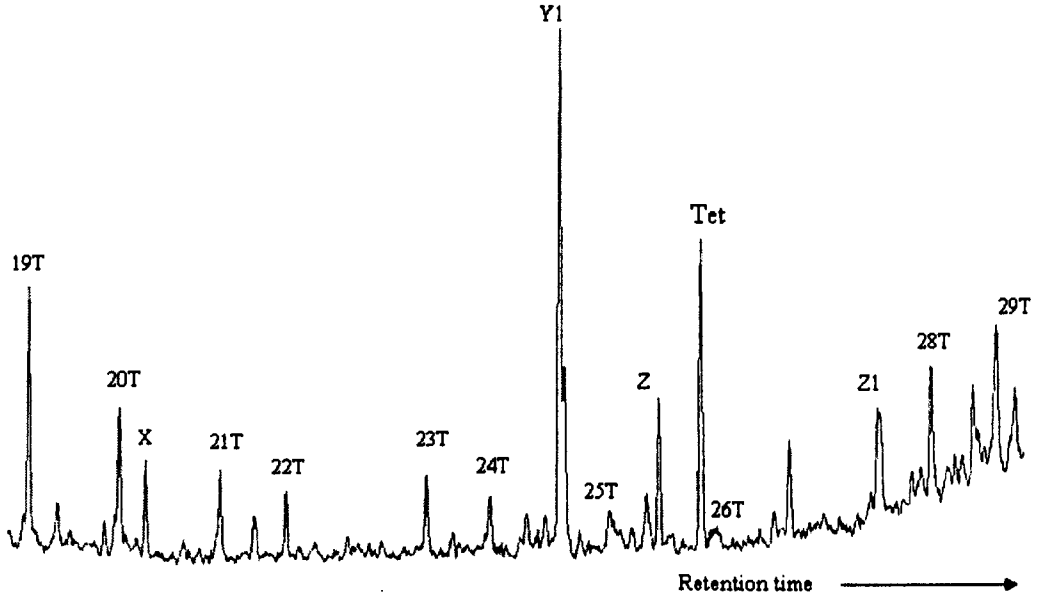

Figure 5.8. Representative partial m/z 191 mass chromatogram showing the distributions of tricyclic and tetra cyclic terpanes in sample AS-13. Peak identifications are presented in Appendix IIIc. Mass spectra of PeaksX, Y1, Z and Z1 are presented in Figures 5.44-5.48.

5.2.5. Aromatic hydrocarbons

Aromatic hydrocarbon fractions obtained from SPE separation of whole oil were analysed by GC-MS technique as described in Section 3.4. Although the aromatic hydrocarbon fraction of the oils contains many compounds, only the alkylnaphthalene, alkylphenanthrene and alkyldibenzothiophene were quantified and utilised for thermal maturity and organic source assessments. The data generated are presented in Table 5.4. Figures 5.9 and 5.10 show a typical distribution of alkylnaphthalene and alkylphenanthrene in Assam oils.

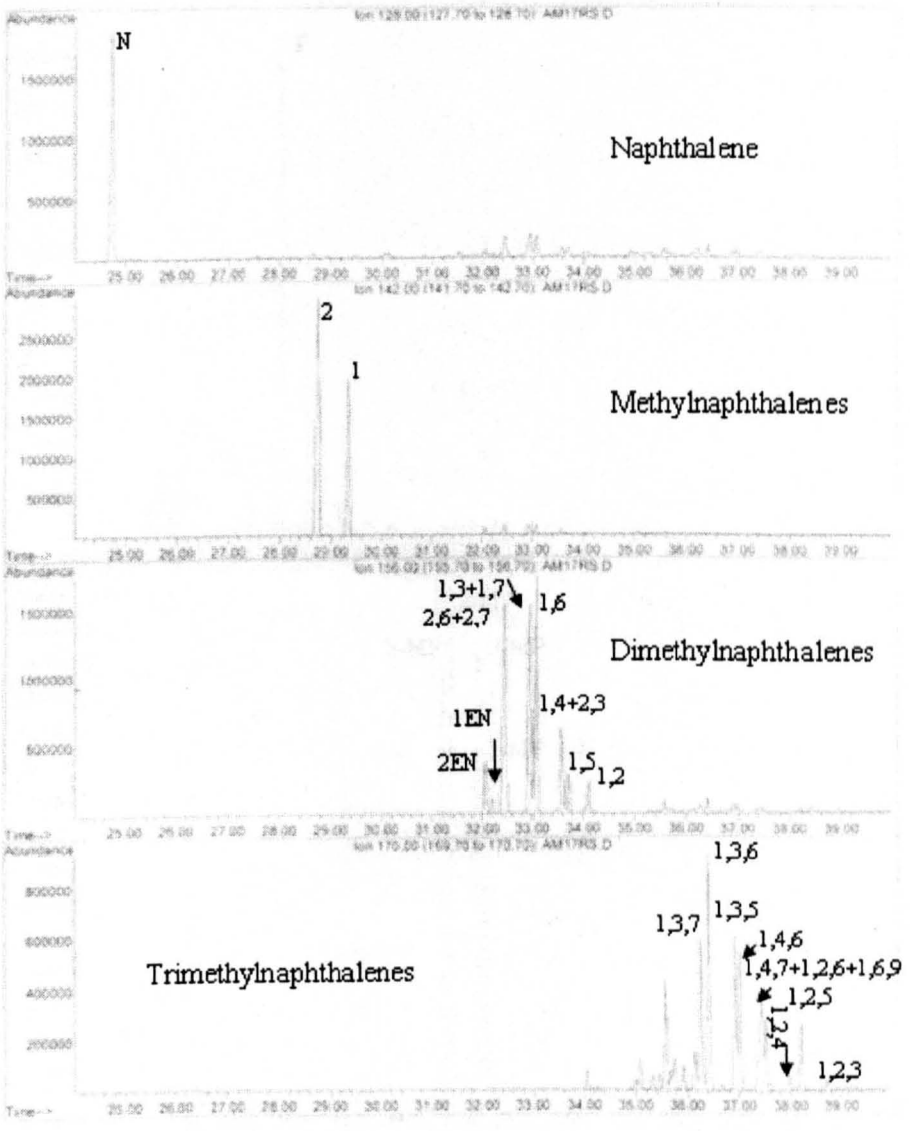

Figure 5.9. GC-MS m/z 128, 142, 156 and 170 mass chromatograms showing the distributions of naphthalene and alkylnaphthalenes in a representative crude oil (sample AS-13) from Assam. Note integers denote the position of methylation in each isomer, EN represents ethylnaphthalene.

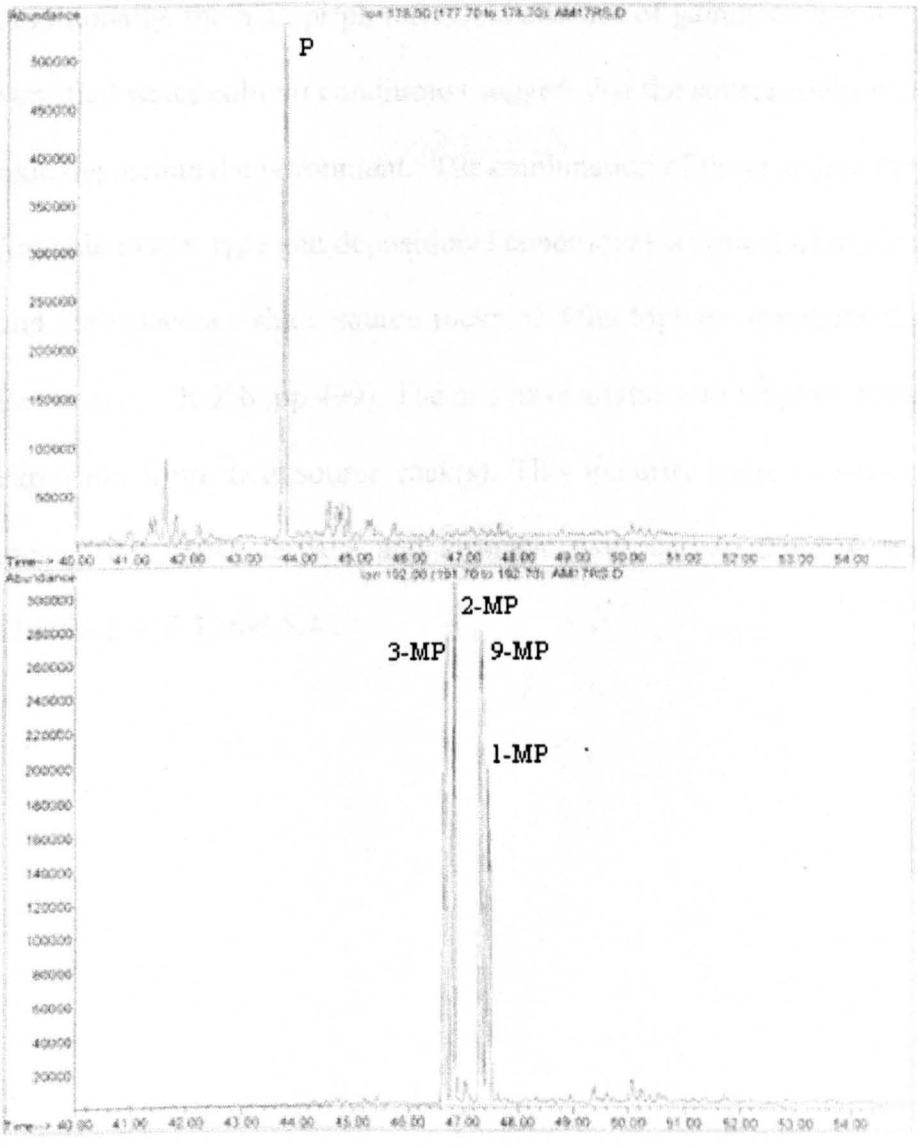

Figure 5.10. GC-MS m/z 178 and 192 showing the distributions of phenanthrene and methyl-phenanthrenes in a representative oil (sample AS-13) from Assam. P = phenanthrene, and 2-MP, 3-MP, 9-MP and 1-MP are methylphenanthrenes with the integers denoting the position of methyl substitution on the phenanthrene ring.

5.2.6. Summary of source facies and thermal maturity

On the basis of the molecular properties of the analysed Assam crude oil samples in this study, the oils have been derived overwhelmingly from source rock facies that received abundant terrigenous higher plants organic input as evident in the high wax content (abundant *n*-alkanes >C_{21} and, see C_{17}/C_{27} ratio, Table 5.1), high C_{29} sterane contents, high oleanane indices and absence of C_{30} 24-*n*-propylcholestane.

Additionally, the high pr/ph ratios and absence of gammacerane in the oils (marker of stratified water column conditions) suggest that the source rocks were laid down in an oxic depositional environment. The combination of these source facies characteristics (organic matter type and depositional conditions) is typical of oils expelled from coaly and carbonaceous shale source rocks of delta tops environment (Peters *et al.*, 2000; Peters *et al.*, 2005b. pp.499). The oils have attained oil window maturity at the time of expulsion from their source rock(s). This maturity stage is evident in the ratios of measured sterane, terpane and aromatic hydrocarbon thermal maturity parameters (Tables 5.2, 5.3. and 5.4).

Table 5.4. Selected thermal maturity and source molecular indicators from aromatic hydrocarbon fractions

Sample	MPI-1	MPI-2	MNR	ENR	DNR-1	TNR-1	DBT/P	MDR	MDR-1
AS-1	0.62	0.67	4.35	2.79	6.76	0.71	0.17	5.69	0.18
AS-2	0.79	0.83	2.03	7.73	9.04	0.76	0.11	8.32	0.14
AS-3	0.79	0.83	1.76	3.04	8.74	0.74	0.12	8.01	0.15
AS-4	0.55	0.54	1.18	2.51	5.13	0.56	0.18	3.53	0.13
AS-5	0.76	0.79	1.85	2.98	8.77	0.74	0.16	7.67	0.13
AS-6	0.98	0.98	1.80	2.56	9.55	0.77	0.16	13.91	0.08
AS-7	0.43	0.47	1.08	3.87	7.03	0.33	0.11	3.07	0.20
AS-8	0.67	0.70	3.31	3.18	8.35	0.65	0.15	6.00	0.17
AS-9	0.66	0.71	1.61	3.74	7.64	0.74	0.30	0.00	0.00
AS-10	0.72	0.77	1.61	2.72	5.93	0.67	0.13	7.23	0.15
AS-11	0.79	0.88	1.84	4.24	9.68	0.77	0.23	9.46	0.15
AS-12	0.60	0.63	1.56	2.88	7.30	0.71	0.23	0.00	0.00
AS-13	0.74	0.77	1.65	2.75	8.32	0.74	0.12	8.11	0.14
AS-14	0.76	0.80	1.85	3.27	10.03	0.75	0.12	0.00	0.00
AS-15	0.59	0.71	1.76	1.44	3.73	0.75	0.69	2.93	0.69
AS-16	0.58	0.63	1.70	2.39	6.44	0.73	0.11	7.24	0.17
AS-17	0.62	0.66	1.64	2.33	6.51	0.75	0.09	0.00	0.00
AS-18	0.75	0.79	0.00	0.00	0.00	0.69	0.12	6.46	0.14
AS-19	0.68	0.73	1.57	3.20	7.04	0.75	0.31	0.00	0.00

MPI-1= 1.5*(2-MP+ 3-MP)/ (P + 1-MP + 9-MP); Radke *et al.*, (1982a). MPI-2 = (3* 2-MP/ (P+ 1-MP + 9-MP); Radke *et al.*, (1982a). MNR = (2-MN/ 1-MN); Radke *et al.*, (1982b). ENR = 2-EN/1-EN; Radke *et al.*, (1982b). DNR-1 = (2,6-DMN+ 2,7-DMN)/ 1,5-DMN; Radke *et al.*, (1982b). TNR-1 = 2,3,6-TMN/ (1,4,6-TMN + 1,3,5-TMN); Alexander *et al.*, (1985).DBT/P = dibenzothiophene/ phenanthrene (Hughges *et al.*, 1995). MDR = 4-MDBT/1-MDBT; Radke *et al.*, (1986). MDR-1= 1-MDBT/DBT; Radke *et al.*, (1982a). 0.00 = denote samples where data can not be computed because of the low concentration of certain compound in the parameter.

5.3. Molecular characteristics of Beaufort-Mackenzie oils

5.3.1. N-alkanes and isoprenoid alkanes

Unbiodegraded Beaufort-Mackenzie Delta oils in this study generally show a fairly similar *n*-alkane distribution. A few samples exhibit unimodal *n*-alkane distributions that maximize around nC_{15}-nC_{17}. Representative gas chromatograms are shown in Figure 5.11. Based on GC chromatograms, samples BM-3, BM-6, BM-7 and BM-8 were found to be severely biodegraded and most *n*-alkane and isoprenoid parameters were absent and so could not be calculated for these samples. Subsequent analyses for biomarkers were performed but data interpretation for the biodegraded oils were handled with caution. Except for a few samples e.g. BM-4 which shows loss of light oil and gasoline range molecules (Figure 5.11), there is not obvious wax richness in the *n*-alkane distributions. Pristane/phytane ratios for this sample set range from 1.22 to 4.91 (Figure 5.12, Table 5.5) with a bimodal distribution suggesting expulsion from source rocks accumulated under either dysoxic (lower mode) or oxic conditions (higher mode).

5.3.2. Steranes

The distribution of steranes is variable in the Beaufort-Mackenzie oils and can generally be classified into two groups. A group of oil samples contain high proportion of C_{29} steranes (BM-1, BM-3, BM-6, BM-7, BM-9, BM-11 and BM- 12, and low abundance to absence of C_{30} 24-*n*-propyl cholestane (Figure 5.13, Table 5.6). Based on the interpretation of Huang & Meinshein (1979), these molecular characteristics reflect oil sourcing from an overwhelmingly terrigenous organic matter rich source rock. The second oil group is characterised by low level of C_{29} relative to C_{27} and C_{28} sterane steranes and presence of copious quantities of C_{30} 24-*n*-propyl

cholestane (Figure 5.14). Figure 5.15 is a ternary diagram showing two oil groupings based on the sterane distributions among the oils from Beaufort-Mackenzie Delta.

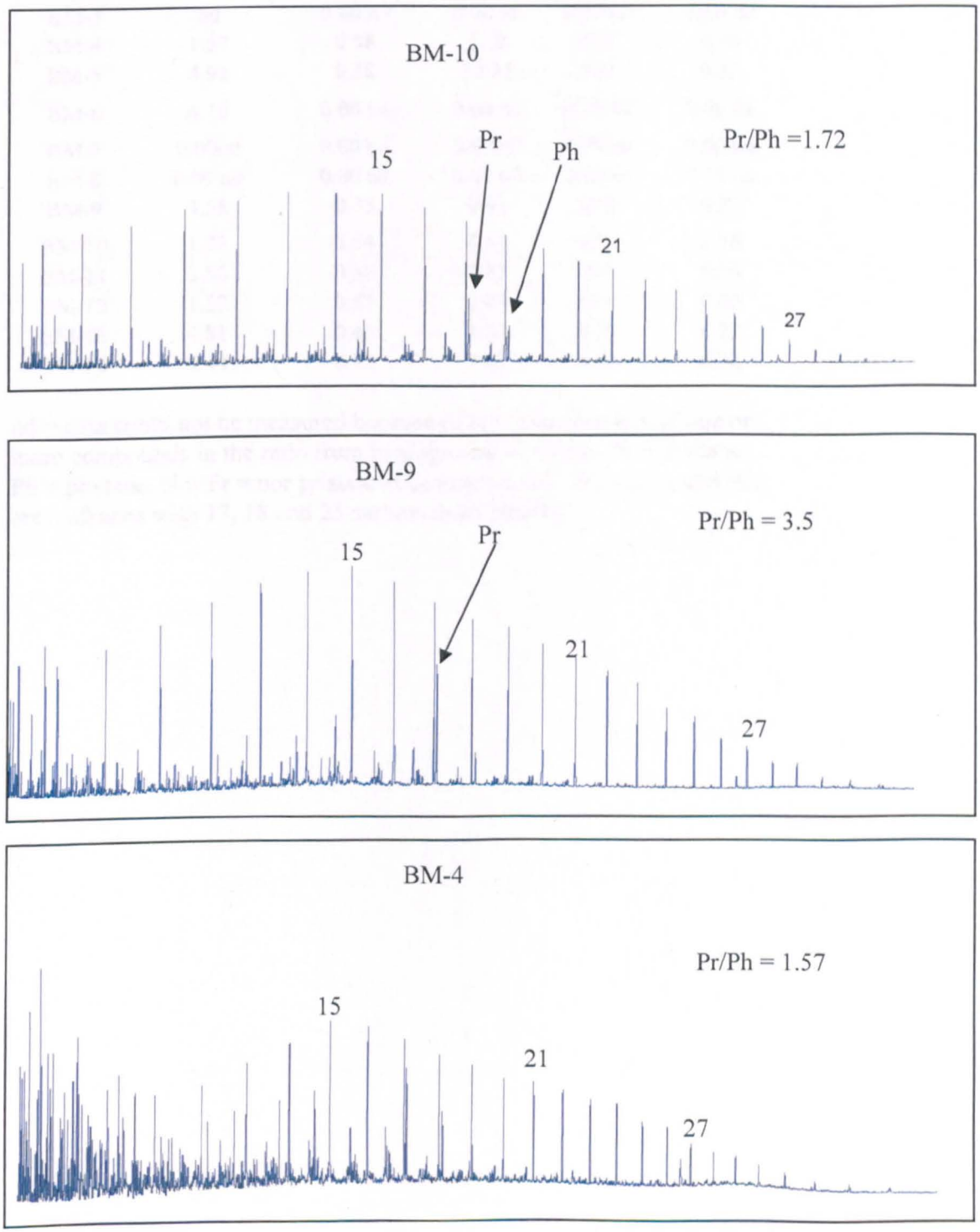

Figure 5.11. Representative gas chromatograms for samples of crude oil from Beaufort-Mackenzie Delta. Integers refer to *n*-alkane chain length while pr = pristane and ph = phytane.

Table 5.5. N-alkane and isoprenoid alkane ratios from the Beaufort-Mackenzie oils

Sample	Pr/Ph	norPr/Pr	pr/nC_{17}	Ph/nC_{18}	nC_{17}/nC_{27}
BM-1	3.46	0.39	3.39	1.32	0.05
BM-2	3.58	0.35	0.92	0.29	0.22
BM-3	nd	0.00 nd	0.00 nd	0.00 nd	0.00 nd
BM-4	1.57	0.58	1.18	0.91	0.30
BM-5	4.91	0.38	19.28	5.61	0.15
BM-6	4.10	0.00 nd	0.00 nd	0.00 nd	0.00 nd
BM-7	0.00nd	0.00 nd	0.00 nd	0.00 nd	0.00 nd
BM-8	0.00 nd	0.00 nd	0.00 nd	0.00 nd	0.00 nd
BM-9	3.58	0.35	0.92	0.29	0.22
BM-10	1.72	0.54	0.64	0.44	0.16
BM-11	3.56	0.30	1.52	0.47	0.26
BM-12	1.22	0.67	0.67	0.66	0.00
BM-13	4.81	0.45	1.52	0.38	6.22
BM-14	4.44	0.39	7.92	2.88	6.32

nd = data could not be measured because of low concentration of one or more compounds in the ratio from biodegradation effects. Pr = pristane. Ph = phytane. Nor Pr = nor pristane (C_{18} isoprenoid). nC_{17}, nC_{18} and nC_{27} are *n*-alkanes with 17, 18 and 25 carbon chain lengths.

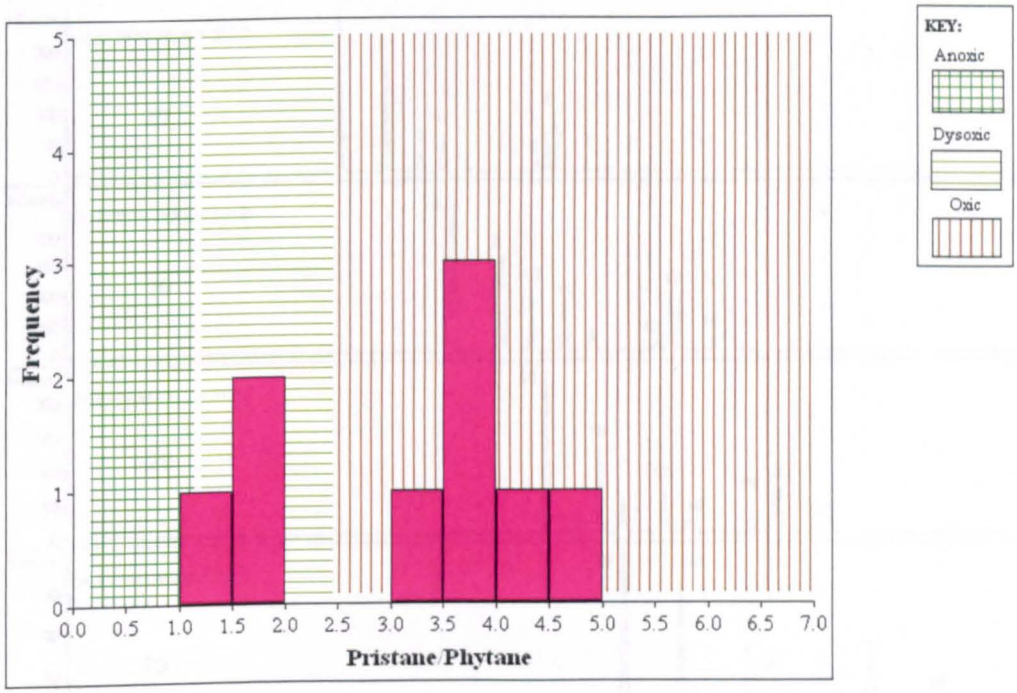

Figure 5.12. Source rock anoxia inferred from the histogram of pristine/phytane ratios. Histogram shows the two distinct distributions for oils from the Beaufort-Mackenzie Delta. Overlay field after IGI's p: IGI 2.7 geochemical interpretation software

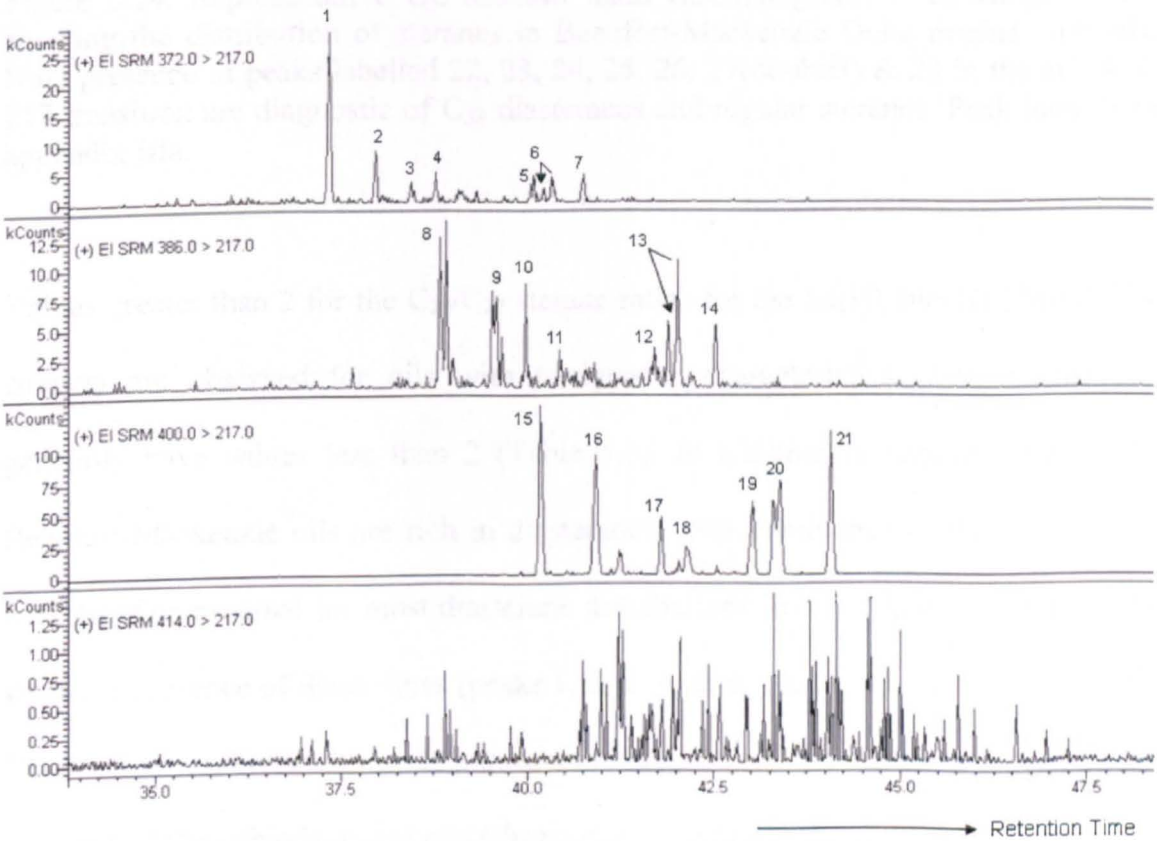

Figure 5.13. Representative GC-MS-MS mass chromatograms showing the distribution of steranes in terrigenous type samples (high C_{29} and absence of C_{30} sterane) of the Beaufort-Mackenzie Delta, from sample BM-3. Note high signal/noise in the m/z 414-217 transition suggests C_{30} 24-*n*-propyl cholestanes are below the detection level. Peak identity in Appendix IIIa.

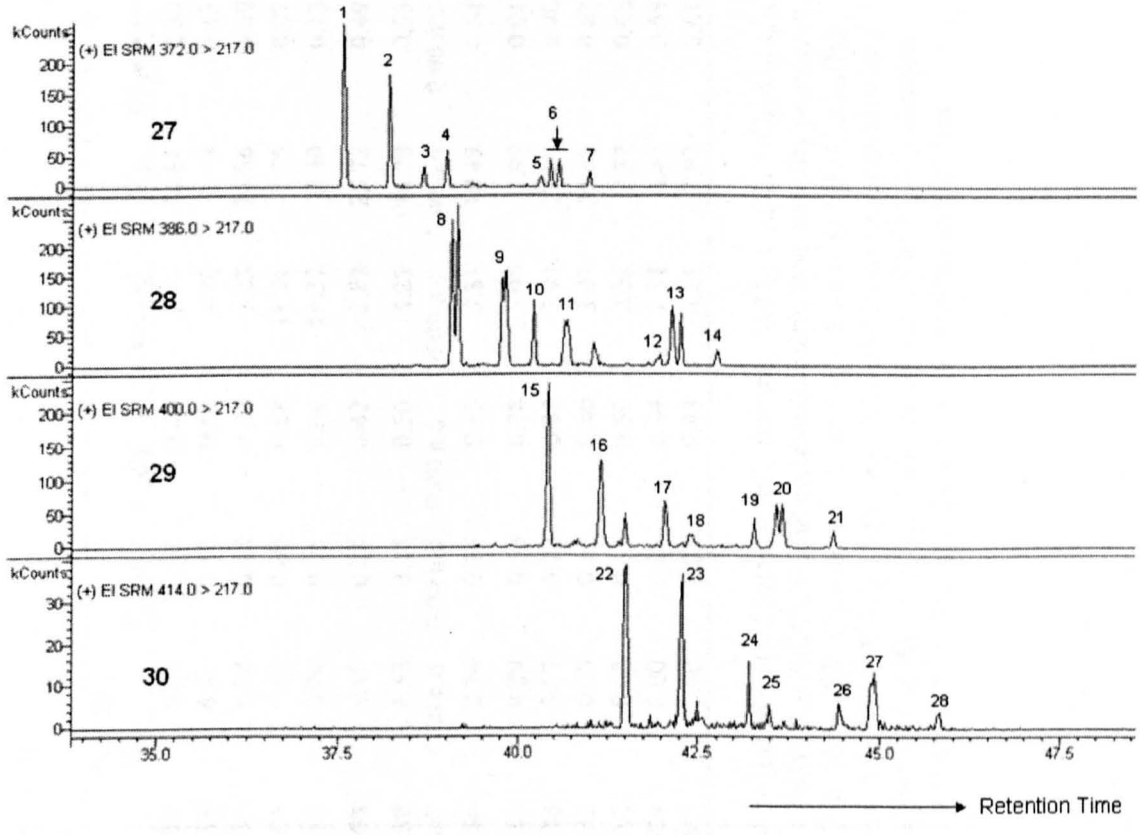

Figure 5.14. Representative GC-MS-MS mass chromatograms from sample BM-4 showing the distribution of steranes in Beaufort-Mackenzie Delta marine type oils. Note presence of peaks labelled 22, 23, 24, 25, 26, 27(doublet) & 28 in the m/z 414-217 transition are diagnostic of C_{30} diasteranes and regular steranes. Peak identity in appendix IIIa.

Values greater than 2 for the C_{29}/C_{27} sterane ratios for the 5α(H),14α(H),17α(H) 20R isomers are observed for oils with terrigenous characteristics, with marine oils generally have values less than 2 (Table 5.6). In addition to regular steranes, all Beaufort-Mackenzie oils are rich in diasteranes, with dominance of the βα isomeric configuration as usual for most diasterane distributions in oils. Figures 5.13 and 5.14 show the presence of diasteranes (peaks 1, 2, 3, 4, 8, 9, 10, 11, 15, 16, 17, 22 and 23) for the C_{27}- C_{30} homologues. The diasterane/sterane ratio ranges from 2.23 to 35.95 for some of the unbiodegraded oils (Peters *et al.*, 2005b).

Table 5.6. Source and maturity sterane biomarker parameters for Beaufort-Mackenzie oils

Sample	%C27 Reg	%C28 Reg	%C29 Reg	%C30 Reg	%C27 Dia	%C28 Dia	%C29 Dia	% C30 Dia	$C_{29}\alpha\alpha$	$C_{29}\beta\beta$	Dia/Reg	C_{29}/C_{27}	Hop/Ster
BM-1	3.74	3.27	92.98	0.00	4.89	5.27	89.84	0.00	0.30	0.41	2.97	24.84	0.60
BM-2	29.91	34.55	35.54	10.19	32.08	38.56	29.36	6.81	0.52	0.56	4.86	1.19	0.13
BM-3	3.82	4.34	91.84	0.00	8.48	9.93	81.59	0.00	0.40	0.47	2.23	24.06	0.00
BM-4	27.30	38.59	34.11	6.22	24.86	47.08	28.06	5.44	0.60	0.68	11.91	1.25	0.07
BM-5	23.61	19.70	56.68	0.00	26.97	23.42	49.61	0.00	0.55	0.54	19.37	2.40	0.10
BM-6	3.38	9.67	86.95	0.49	11.00	18.12	70.88	1.48	0.28	0.42	2.82	25.72	0.49
BM-7	2.71	3.13	94.16	0.00	8.30	12.40	79.30	1.58	0.44	0.50	4.27	34.78	0.53
BM-8	0.00 n.d	0.00 n.d	0.00 n.d	0.00 n.d	0.00 n.d	0.00 n.d	0.00 n.d	0.00 n.d	0.00 n.d	0.00 n.d	0.00 n.d	0.00 n.d	0.00 n.d
BM-9	4.69	8.83	86.49	1.81	14.63	24.81	60.56	2.70	0.25	0.45	3.81	18.45	0.54
BM-10	23.87	28.61	47.51	20.64	28.98	33.20	37.83	4.29	0.53	0.78	35.95	1.99	0.01
BM-11	3.02	12.61	84.37	1.93	18.74	28.38	52.88	3.57	0.22	0.38	2.98	27.89	0.40
BM-12	3.44	9.09	87.47	0.00	8.43	14.25	77.32	0.00	0.15	0.40	3.07	25.42	0.63
BM-13	23.1	10.7	66.2	0.00	21.1	18.7	60.2	0.00	0.35	0.50	2.66	2.87	0.48
BM-14	15.3	16.3	68.4	0.00	13.3	28.3	58.4	0.00	0.26	0.44	2.31	4.47	0.58
BM-15	10.4	7.1	82.5	0.00	8.4	13.1	78.5	0.00	0.33	0.43	4.81	7.93	0.61

% C_{27}, C_{28} ,C_{29} and C_{30} Reg =$C_{27,}$ $C_{28,}$ C_{29} and C_{30} sterane as a percentage of sum 27-30 of 5α(H),14α(H), 17α(H)- 20R sterane. % C_{27}-C_{30}Dia = $C_{27,}$ $C_{28,}$ C_{29} and C_{30} sterane as a percentage of sum 27-30 for βα diasteranes. $C_{29}\alpha\alpha$ = 5α(H),14α(H), 17α(H)- C_{29} 20S/20S+20R sterane isomerisation maturity parameter. C_{29} ββ = 5α(H),14β(H), 17β(H)- 20S +20R / 5α(H),14β(H), 17β(H) + 5α(H),14α(H), 17α(H)- 20 S+20R C_{29} steranes. Dia/ Reg = Sum of (13 β(H), 17α(H) and 13α(H), 17β(H) 20S+20R diasteranes/ sum of 5α(H), 14α(H), 17α(H) and 5α(H),14β(H),17 β(H)- 20S+20R) for the 27,28 and 29 compounds obtained from GC-MS-MS. C_{29}/C_{27} = ratio of C_{29}/C_{27} for 5α(H),14α (H), 17α(H)- 20R sterane. Hop/Ster = 17 α(H), 21 β(H)- C_{30}-hopane/ sum of all C_{27}-C_{29} steranes (regular, isosterane and diasterane). All data were obtained from appropriate GC-MS-MS transitions. nd = data could not be measured because of low concentration of one or more compounds in the ratio.

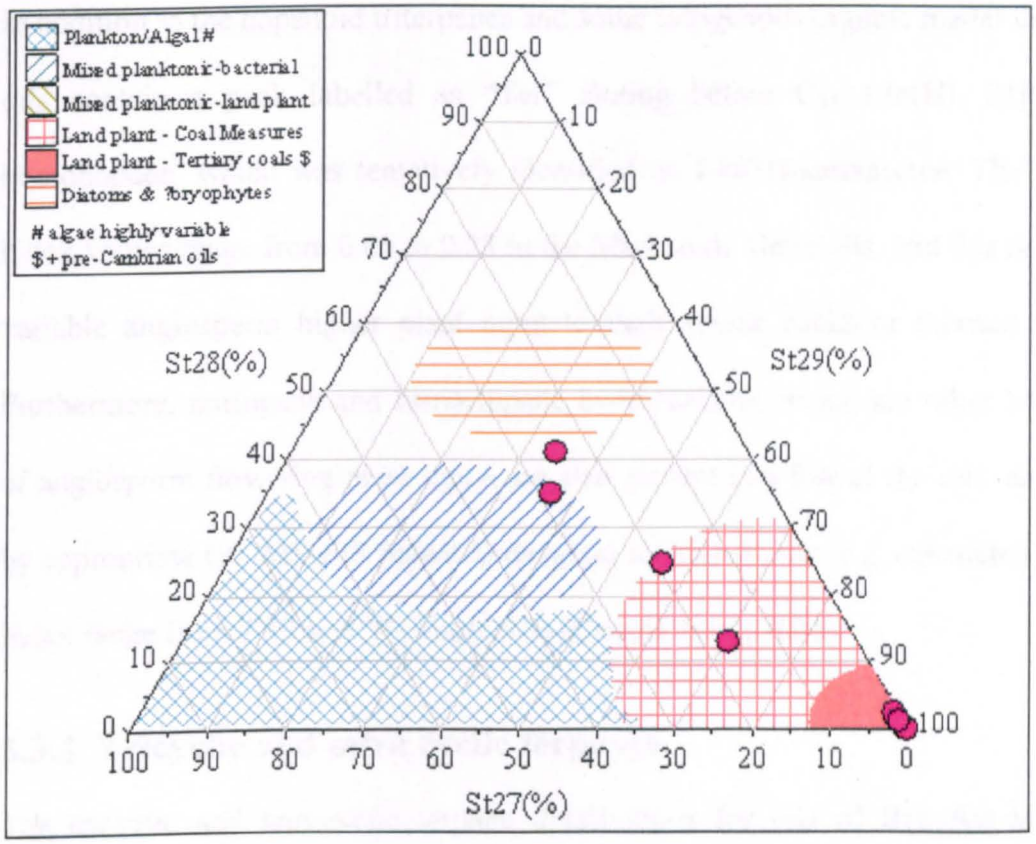

Figure 5.15. Ternary diagram showing the plot of C_{27} C_{28} and C_{29} steranes (based on 5α(H),14α(H),17α(H) 20R sterane peaks from appropriate GC-MS-MS transitions) interpreted in terms of likely kerogen precursor. Interpretational overlay from IGI's p: IGI-2 software modified after Huang and Meinschein (1979).

5.3.3. Pentacyclic triterpanes

Unlike the Assam oils where triterpane distributions appear relatively similar, the triterpane distributions for Beaufort-Mackenzie oils can be classified into two groups consistent with the sterane distributions;

1. Samples showing low level of late Cretaceous-Tertiary higher land plant contribution as reflected in low (but not zero) oleanane content (Figure 5.16)

2. Oils of high angiosperm land plant organic matter input, evident by high oleanane index values and other terrigenous triterpanes (Figure 5.17).

In addition to the hopanoid triterpanes and some terrigenous organic matter dominated oils contain a peak labelled as "Tar" eluting before C_{31} 17α(H), 21β(H) 22S homohopane, which was tentatively identified as 19α(H)-taraxastane. The oleanane index values range from 0.06 to 0.28 in the Mackenzie Delta oils, and this reflects the variable angiosperm higher plant input to their source rocks or thermal maturity. Furthermore, norlupane and bisnorlupane hydrocarbons, which are other biomarkers of angiosperm flowering plant input, are also present in a few of the oils as detected by appropriate GC-MS-MS parent to daughter ion transitions (e.g. calculated lupanoid index range from 2.12 to 6.71, Table 5.7) (Curiale *et al.*, 2005).

5.3.4. Tricyclic and tetra cyclic terpanes

The tricyclic and tetracyclic terpane distributions for oils of Beaufort-Mackenzie Delta, show the same two gross groupings as those based on visual assessment of the gas chromatograms and derivative ratios, the sterane carbon numbers and angiosperm-derived hopanoids. Figure 5.18 shows the distributions of tri- and tetra-cyclic terpanes in representative oils. The upper chromatograms from sample BM-2 represents the distribution in marine organofacies oils and is similar to most distributions commonly observed among oils having least peak interference from unknown terpanes of possibly higher plant origins. The lower chromatogram from sample BM-11 represents those of the terrigenous oil group having several unknown compounds. The peak labelled Y1 is the same as compound Y1 in the Niger Delta oils where it occurs in oils of overwhelming terrigenous signatures in the Niger Delta. Though the biological origin of the tri- and tetra-cyclic terpanes is unclear, the precursor(s) have clearly contributed to both the terrigenous and marine oils of the Mackenzie Delta.

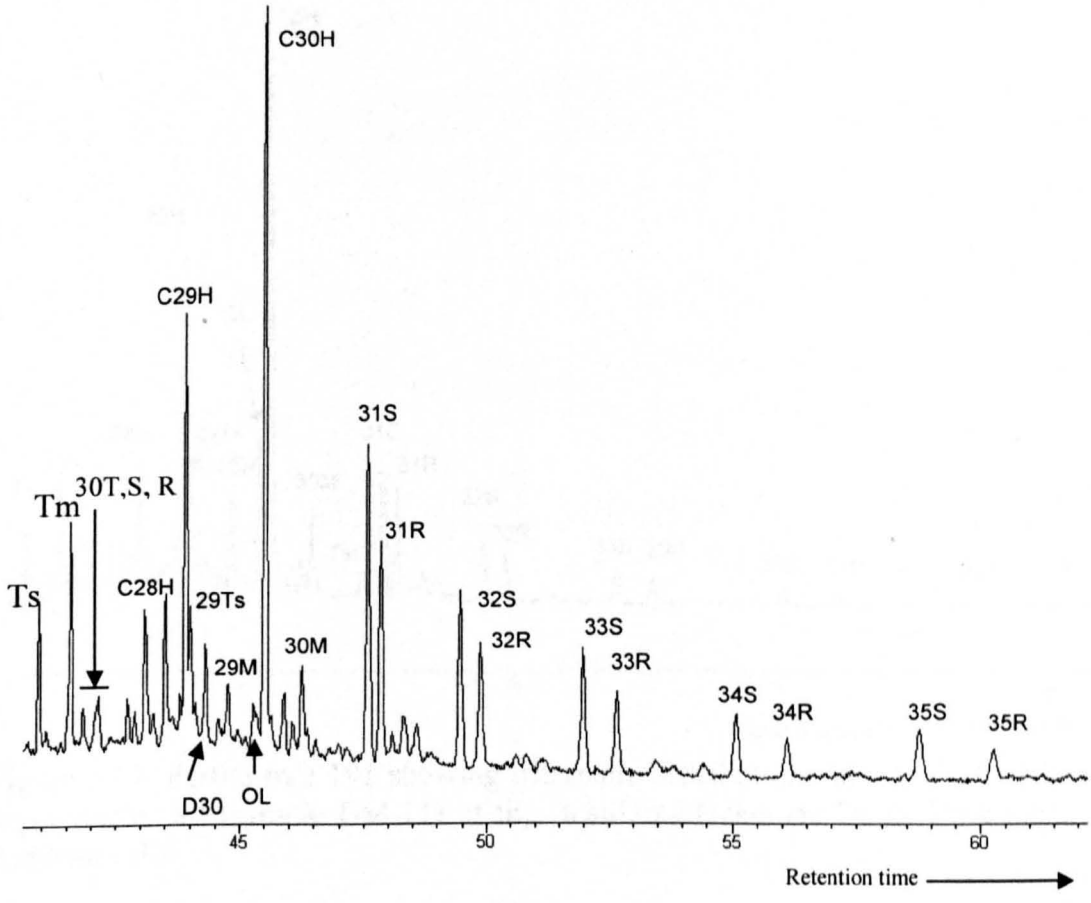

Figure 5.16. Partial m/z 191 mass chromatogram showing triterpane distribution in a typical marine organofacies oil (sample BM-2) of the Beaufort-Mackenzie Delta. Peak identity in Appendix IIIb.

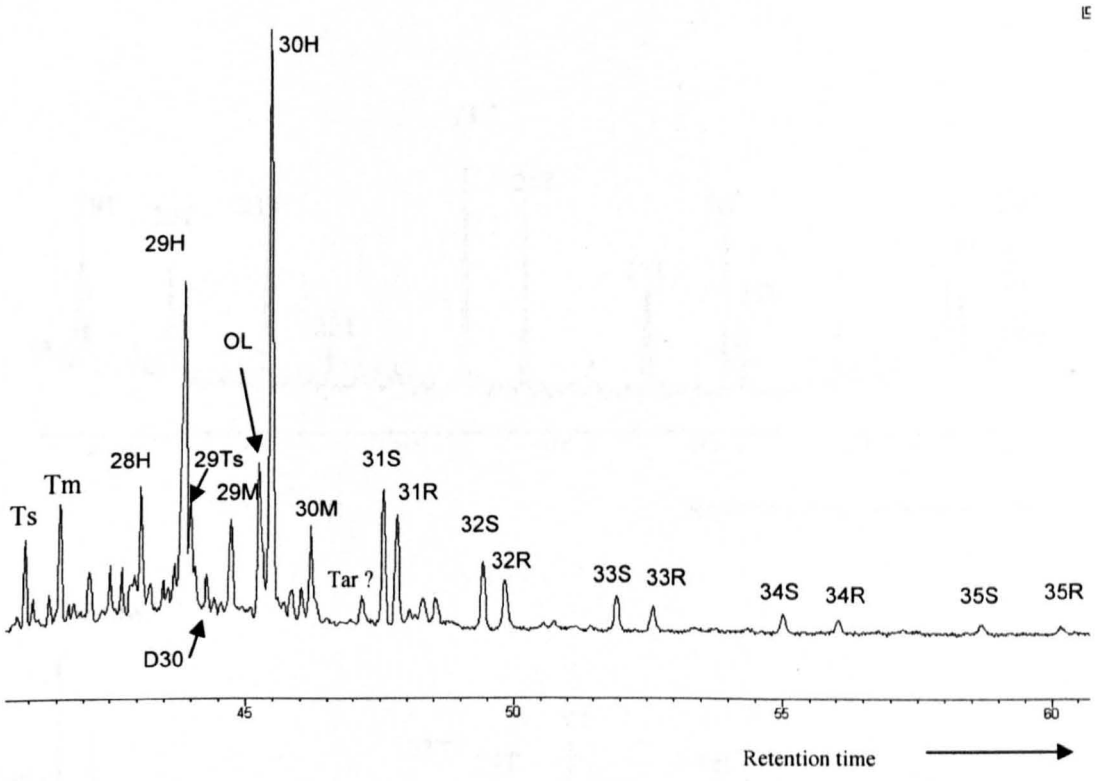

Figure 5.17. Partial m/z 191 showing triterpane distributions in a typical terrigenous organofacies oil (sample BM-11) of the Beaufort-Mackenzie Delta. Peak identity in Appendix IIIb.

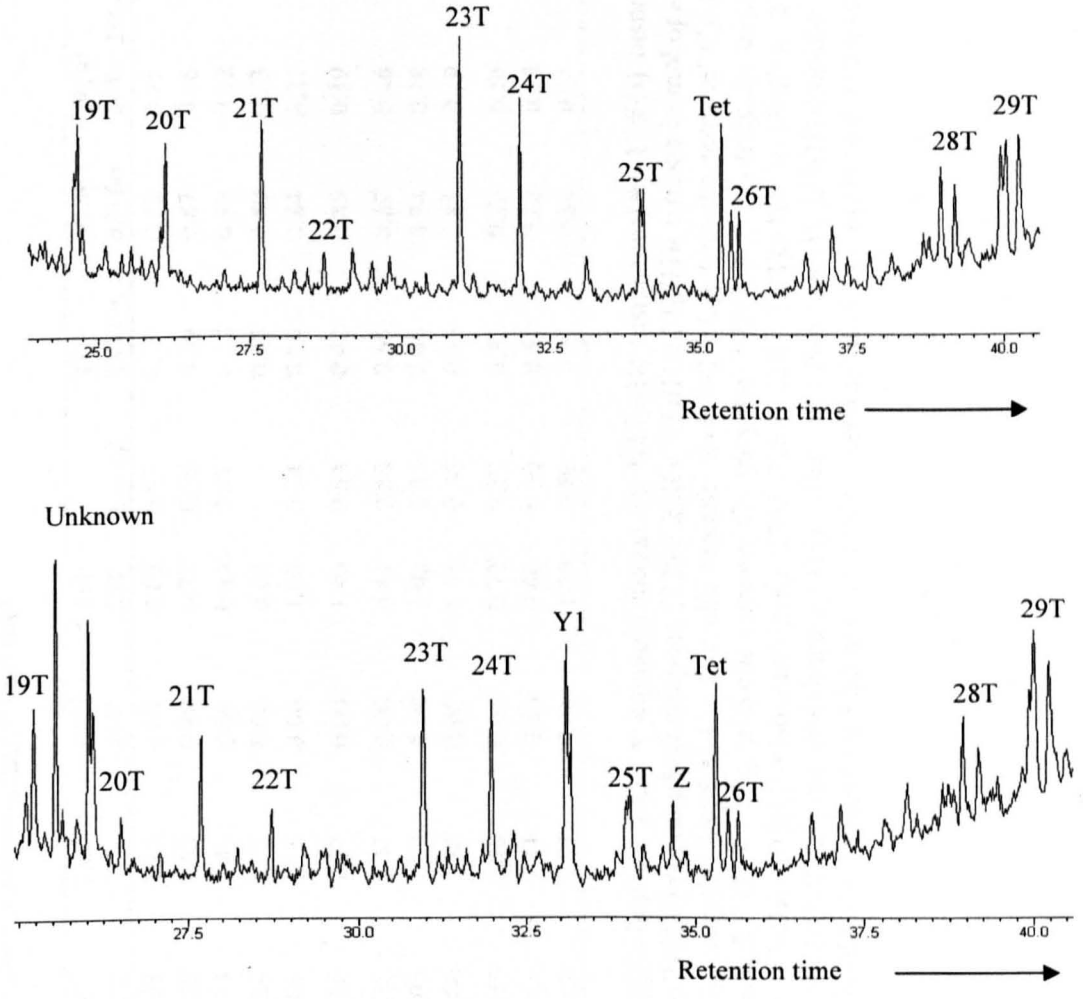

Figure 5.18. Partial m/z 191 mass chromatograms showing the distributions of tri-cyclic and tetra-cyclic terpanes in a marine organofacies type oil (upper chromatogram, sample BM-2) and terrigenous facies oil (lower chromatogram, Sample BM-11) from the Beaufort-Mackenzie Delta. Compound Y1 is the unknown compound Y1 also found in Assam and Niger Delta oils. Peak identifications in Appendix IIIc.

Table 5.7. Source and maturity triterpanes molecular parameters for Beaufort-Mackenzie oils

Sample	OL	LUP	35/ 34	Ga/ Hop	26T/ 25T	23T/ 24T	Tet/ Hop	23T/ 21T	19T/ 23T	Tet/ 23T	C_{32} αβ	Ts/ Ts+Tm	30 αβ / αβ+βα	29Ts/ 29Ts+29βαHop
BM-1	0.14	0.00	0.50	0.11	0.78	1.53	0.08	1.18	0.00	0.85	0.55	0.29	0.85	0.15
BM-2	0.07	0.00	0.98	0.29	0.66	1.21	0.08	1.45	0.80	0.73	0.56	0.39	0.87	0.18
BM-4	0.06	0.00	0.93	0.00	0.70	1.14	0.04	1.45	0.00	0.44	0.57	0.57	0.92	0.32
BM-5	0.20	0.00		0.00	0.56	1.32	0.24	0.75	0.00	0.68		0.43	0.80	0.23
BM-6	0.28	2.31	0.50	0.07	0.74	0.78	0.05	1.15	0.00	1.53	0.54	0.39	0.84	0.21
BM-9	0.20	2.12	0.73	0.00	0.61	1.10	0.06	1.37	0.00	1.40	0.54	0.42	0.85	0.19
BM-10	0.00	5.84	0.87	0.00	0.91	1.20	0.19	1.47	0.00	0.41	0.50	0.69	0.89	0.46
BM-11	0.23	0.00	0.64	0.19	0.78	1.16	0.05	1.27	0.00	1.08	0.53	0.40	0.84	0.18
BM-12	0.21	3.12	0.68	0.00	0.59	1.10	0.06	1.38	0.00	1.41	0.56	0.45	0.85	0.19
BM-13	0.16	4.02	0.51	0.00	0.62	1.41	0.03	1.28	0.00	0.72	0.53	0.32	0.78	0.16
BM-14	0.22	6.71	0.58	0.00	0.68	1.35	0.06	1.41	0.00	0.66	0.50	0.41	0.82	0.18
BM-15	0.21	3.81	0.61	0.00	0.67	1.28	0.07	1.32	0.00	1.20	0.56	0.31	0.84	0.21

OL = Oleanane index; 18α(H) + 18β(H) oleanane/C_{30} 17α(H), 21β(H)-hopane. LUP = lupanoid index; 10 *(17α(H) bisnorlupane+ 17β(H) bisnorlupane +Norlupane)/ C_{30} 17α(H), 21β(H)-hopane. 35/34 = ratio of 17α(H), 21β(H)-pentakishomohopane (22S+ 22R)/ 17α(H), 21β(H)- tetrakis homohopane -22S +22R. Ga /hop = 10*gammacerane / C_{30}αβ Hopane. 26T/25T = C_{26} tricyclic terpane/ C_{25} tricyclic terpane. 23T/24T= C_{23} tricyclic terpane/ C_{24} tricyclic terpane. Tet/Hop = tetracyclic terpane(24-de-E-hopane)/ C_{30}αβ hopane.23T/21T = C_{23} tricyclic terpane/ C_{21} tricyclic. 19T/23T = C_{19} tricyclic terpane/ C_{23} tricyclic. Tet/ 23T = tetracyclic terpane/ C_{23} tricyclic. C_{32} αβ= 17α(H), 21β(H)-bishomohopane 22S/ 22S+ 22R. Ts/Ts+Tm = 18α(H)- 22,29,30-Trisnorneohopane (Ts)/ 18α(H)- 22,29,30- Trisnorneohopane (Ts) + 17α(H)- 22,29,30-trisnorhopane (Tm). 30αβ /αβ + βα= 17α(H), 21β(H)- hopane/ 17α(H), 21β(H) hopane = 17β(H), 21α(H)- hopane (moratane). 0.00 = data could not be measured because of low concentration of one or more compounds in the ratio.

5.3.5. Aromatic hydrocarbons

Aromatic hydrocarbon fractions obtained from SPE separation of whole oils were analysed by the GC-MS technique as described in section 3.4. Although the aromatic hydrocarbon fraction of the oils contain several groups of compounds, only the alkylnaphthalene, alkylphenanthrene and alkyldibenzothiophene were quantified and utilised for thermal maturity and organic source assessments. The data generated are presented in Table 5.8. Figures 5.19 and 5.20 show typical distributions of alkylnaphthalenes and alkylphenanthrenes found in the Beaufort-Mackenzie oils.

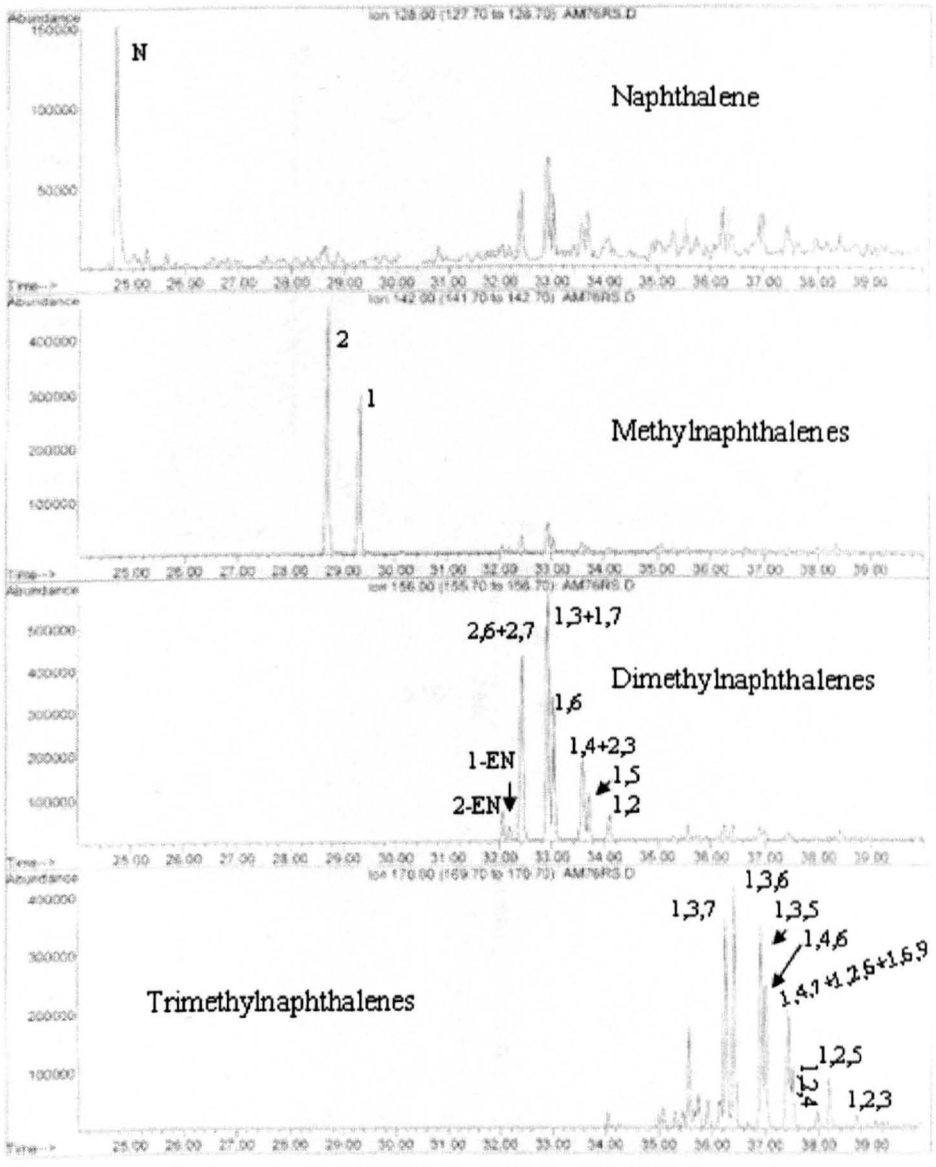

Figure 5.19. GC-MS m/z 128, 142, 156 and 170 showing the distributions of naphthalene and alkylnaphthalenes in representative oil (sample BM-12) from the Beaufort-Mackenzie Delta. Note integer denotes the position of alkylation in each isomer. EN represents ethyl-naphthalene.

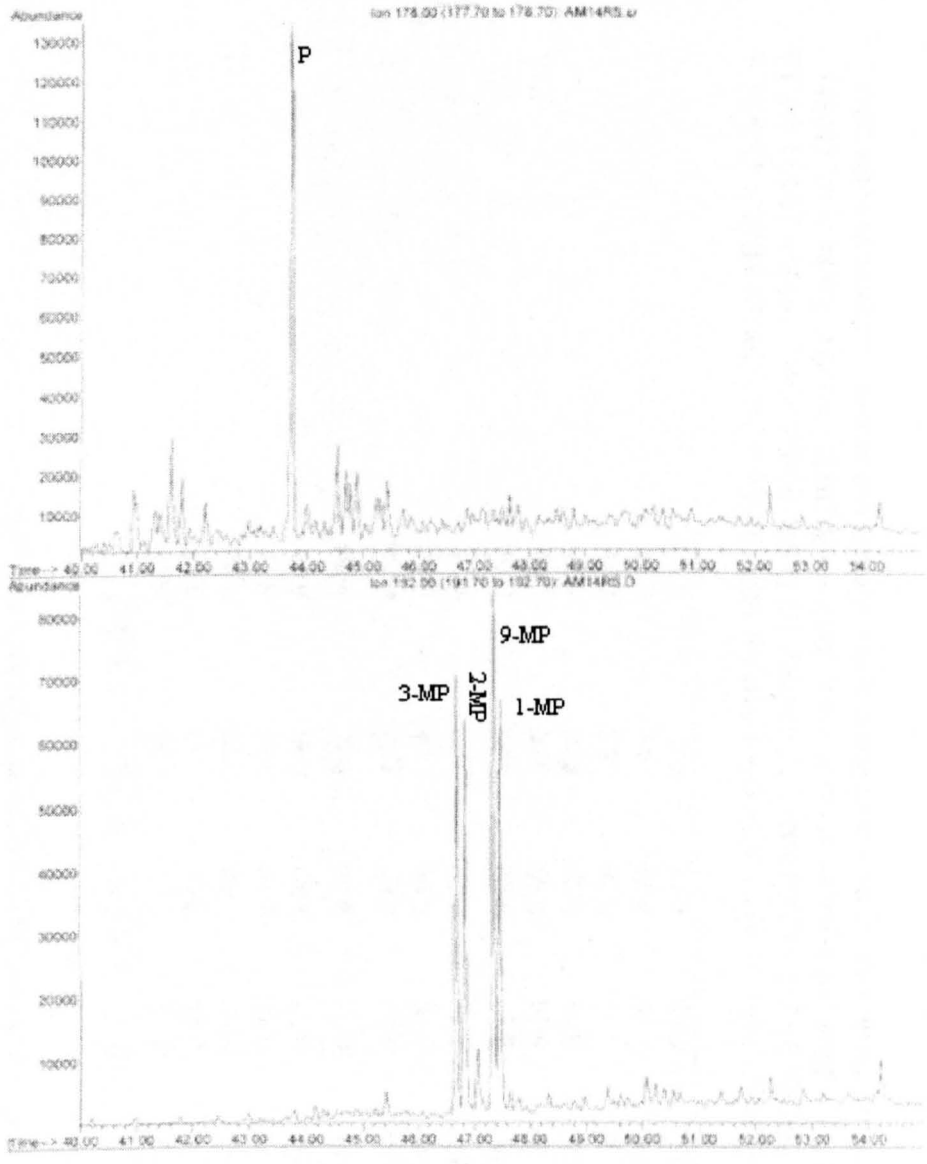

Figure 5.20. GC-MS m/z 178 and 192 showing the distributions of phenanthrene and methyl-phenanthrenes in representative oil (sample BM-12) from the Beaufort-Mackenzie Delta. P = phenanthrene, and 2-MP, 3-MP, 9-MP and 1-MP are methylphenanthrenes with the integers denoting the position of methyl substitution on the phenanthrene ring.

Table 5.8. Selected thermal maturity and source molecular indicators from aromatic hydrocarbon fractions

Sample	MPI-1	MPI-2	MNR	ENR	DNR-1	TNR-1	DBT/P	MDR	MDR-1
BM-1	0.86	0.84	1.67	2.50	7.17	0.72	0.18	10.54	0.15
BM-2	0.86	0.76	1.37	2.71	5.51	0.90	0.46	2.63	0.40
BM-3	0.40	0.48	0.00	0.00	0.00	0.00	0.00	0.00	0.00
BM-4	0.69	0.62	1.11	2.05	3.12	0.87	0.19	5.37	0.41
BM-5	0.93	0.85	1.20	2.18	6.99	0.77	0.23	0.00	0.00
BM-6	0.00	0.00	3.81	2.10	8.40	0.37	0.00	0.00	0.00
BM-7	0.89	0.80	0.00	0.00	0.00	0.00	0.07	5.91	0.39
BM-8	0.00	0.00	0.00	0.00	0.00	0.00	0.00	0.00	0.00
BM-9	0.65	0.63	1.59	2.71	6.92	0.77	0.15	7.72	0.15
BM-10	0.00	0.00	1.86	3.15	8.96	0.80	0.00	0.00	0.00
BM-11	0.57	0.56	1.90	2.57	7.52	0.78	0.00	0.00	0.00
BM-12	1.25	1.34	1.45	3.21	6.81	0.73	0.32	9.52	0.31
BM-13	0.88	0.76	1.42	0	0	0	0.16	6.2	0.21
BM-14	0.85	0.78	0	2.41	7.4	0	0.21	6.2	0.36
BM-15	0.74	0.81	1.51	0	6.81	0.68	0.18	4.81	0.18

MPI-1= 1.5*(2-MP+ 3-MP)/ (P + 1-MP + 9-MP); Radke *et al.*, (1982a). MPI-2 = (3* 2-MP/ (P+ 1-MP + 9-MP); Radke *et al.*, (1982a). MNR = (2-MN/ 1-MN); Radke *et al.*, (1982b). ENR = 2-EN/1-EN; Radke *et al.*, (1982b). DNR-1 = (2,6-DMN+ 2,7-DMN)/ 1,5-DMN; Radke *et al.*, (1982b). TNR-1 = 2,3,6-TMN/ (1,4,6-TMN + 1,3,5-TMN); Alexander *et al.*, (1985).DBT/P = dibenzothiophene/ phenanthrene. MDR = 4-MDBT/1-MDBT; Radke *et al.*, (1986). MDR-1= 1-MDBT/DBT; Radke *et al.*, (1982a). 0.00 = data could not be measured because of low concentration of one or more compounds in the ratio

5.3.6. Summary of source facies and thermal maturity

On the basis of the molecular properties of the analysed Beaufort-Mackenzie crude oil samples in this study, the oils are separable into marine and terrigenous organofacies reflecting expulsion from source rocks having two distinct kerogen types. These two end-member orgaonofacies are typical of Beaufort-Mackenzie oil accumulations as previously observed by Brooks (1986a) and Curiale (1991). The marine oils were assigned Cretaceous source with the Late Cretaceous Smoking Hills and Boundary Creek formations as likely source rocks while the terrigenous oils were believed to have been expelled from Eocene Richards Formation and other Tertiary source units rich in terrigenous organic matter (Table 5.9, below). The source rocks of the marine organofacies oils are thermally more mature than those that expelled the terrigenous oils as evident in the sterane and terpane thermal maturity parameter calculated for the oils (Tables 5.5, 5.6. and 5.7). The marine oils, though reservoired within the Tertiary sands, are therefore considered to have been expelled by sub-delta Cretaceous source rocks.

Table 5.9. Summary of source facies biomarker parameters for Beaufort-Mackdenzie Delta oils

Sample	Pr/Ph	% C_{27} Sterane	% C_{29} Sterane	Oleanane Index	Maturity (MPI/Ts/Tm)	Likely Source
BM-1	3.46	3.74	92.98	0.14	mid/low	Tertiary
BM-2	3.58	29.91	35.54	0.07	mid/mid	Late Cretaceous
BM-3	nd	3.82	91.84	--	low/--	Tertiary
BM-4	1.57	27.30	34.11	0.06	mid/high	Late Cretaceous
BM-5	4.91	23.61	56.68	0.20	high/mid	Tertiary
BM-6	4.10	3.38	86.95	0.28	mid/mid	Tertiary
BM-7	nd	2.71	94.16	--	mid/mid	Tertiary
BM-8	nd	nd	nd	--	mid/mid	?Tertiary
BM-9	3.58	4.69	86.49	0.20	high/mid	Tertiary
BM-10	1.72	23.87	47.51	0.00	mid/high	?mixed
BM-11	3.56	3.02	84.37	0.23	low/mid	Tertiary
BM-12	1.22	3.44	87.47	0.21	high/mid	Tertiary
BM-13	4.81	23.1	66.2	0.16	mid/low	?mixed
BM-14	4.44	15.3	68.4	0.22	mid/mid	Tertiary
BM-15	--	10.4	82.5	0.21	mid/low	

5.4. Molecular characteristics of Gulf of Mexico oils

5.4.1 N-alkanes and isoprenoid alkanes

The analysed crude oil samples from the Gulf of Mexico generally show a unimodal *n*-alkane distribution that maximizes between nC_{12} and nC_{15} (Figure 5.21). Pristane/phytane ratios range from 1.86 to 2.85 with most samples having values greater than 2.20. An average pr/ph ratio for the sample set is 2.50 (Table 5.10), thus reflecting a sub-oxic depositional conditions for the source rock(s) of these oils (Figure 5.22)

5.4.2. Steranes

The characteristic ratios and distributions of steranes and diasteranes are shown in Table 5.11 and Figure 5.23. Based on carbon number, the 17 analysed Gulf of Mexico oils produce an average of approximately one third of each of C_{27}, C_{28} and C_{29} independent of the isomers used to quantify the carbon number. However, based on figures 5.24a and 5.24b the oils fall into two groups and as shown by the C_{29}/C_{27} sterane ratio (see histogram Figure 5.24b taken from C_{29}/C_{27} data in Table 5.11) one containing high $\%C_{27}$ steranes indicating generation from a source rock with a dominance of marine kerogen and a second group with higher levels of C_{29} steranes pointing to a more terrigenous kerogen mix. This reflects a limited input of terrigenous higher plant to the source rock organic matter and conversely an overwhelmingly marine phytoplankton contribution (Goodwin *et al.*, 1973; Volkman *et al.*, 1998). The analysed oils contain input from marine chrysophyte algae as evident in the C_{30} 24-*n*-propyl cholestane abundance (Moldowan *et al.*, 1990) (Figure 5.23, Table 5.11 thus corroborating the interpretation of the strong marine algal contribution. In addition to the regular steranes, the oil set from the Gulf of Mexico

are particularly rich in diasteranes (Figure 5.23, Table 5.11), which may reflect expulsion from a clay rich source rock deposited under sub-oxic environment.

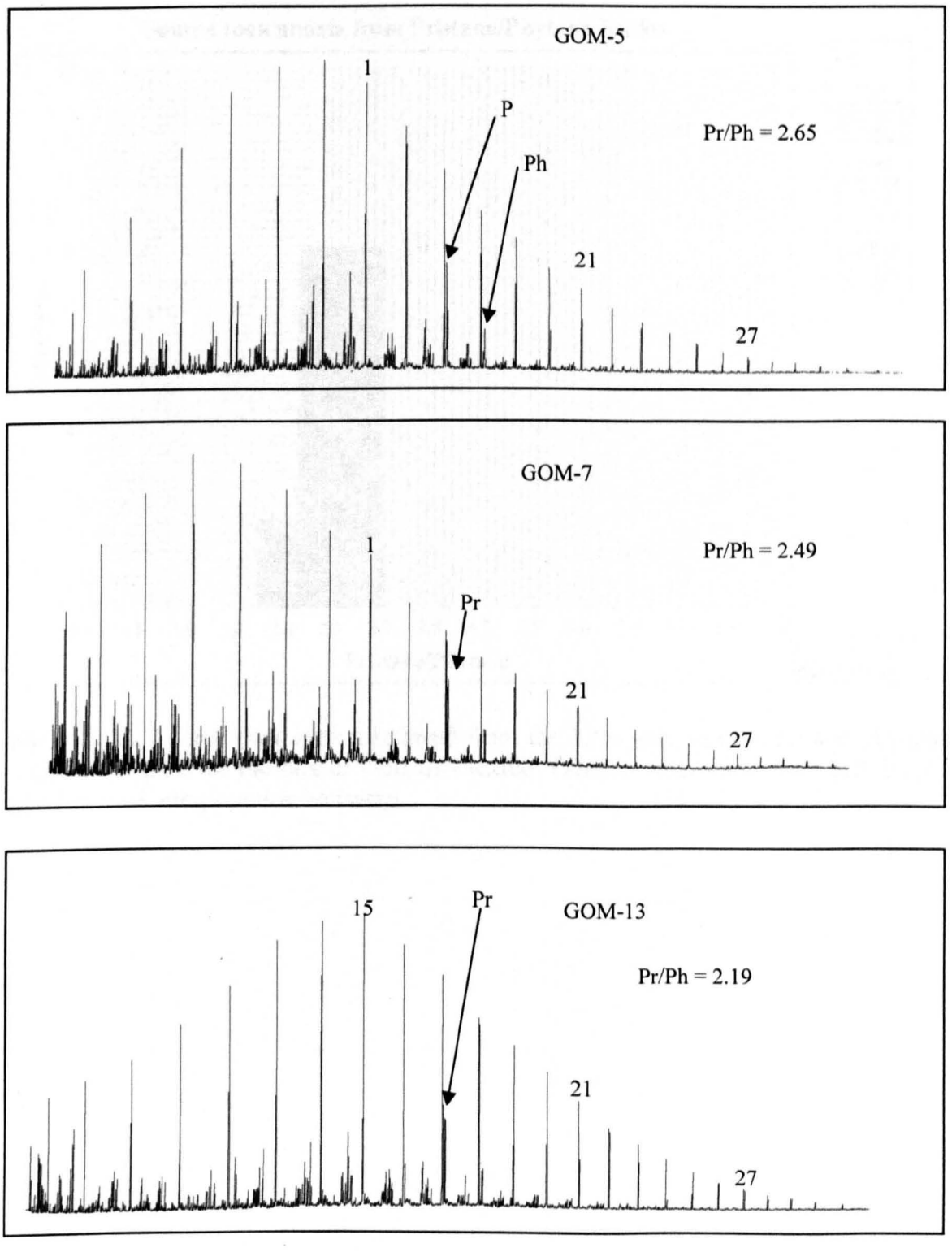

Figure 5.21. Representative gas chromatograms showing the distributions of *n*-alkanes and isoprenoid alkanes in Tertiary deltaic oils from Gulf of Mexico

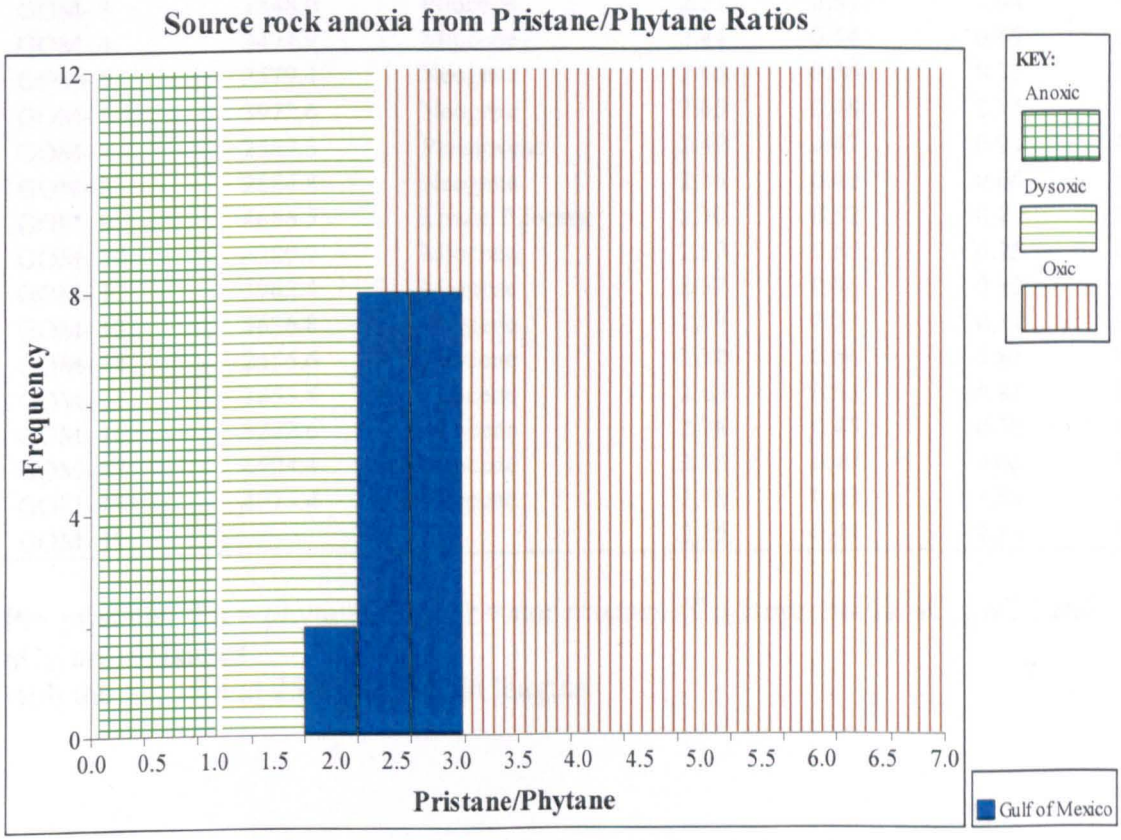

Figure 5.22. Source rock anoxia inferred from the histogram of pristane and phytane ratios calculated for the oils of Gulf of Mexico. Overlay field after IGI's p:IGI 2.27 geochemical interpretation software.

Table 5.10. *n*-alkane and isoprenoid alkane ratios for the Gulf of Mexico oil samples

Sample	Base Depth (m)	Reservoir Age	Pr/Ph	Nor Pr/Pr	Pr/nC_{17}	Ph/nC_{18}	nC_{17}/nC_{27}
GOM- 1	3736.5	Oligocene	2.73	0.51	0.91	0.40	0.16
GOM- 2	2898.0	Oligocene	2.79	0.43	0.75	0.29	0.23
GOM- 3	1848.0	Pliocene	2.27	0.51	1.94	1.28	0.15
GOM- 4	3471.9	Miocene	2.44	0.54	0.69	0.35	0.10
GOM- 5	2579.4	Neogene	2.65	0.56	0.73	0.37	0.07
GOM- 6	3972.6	Neogene	2.65	0.48	0.74	0.32	0.15
GOM- 7	2547.3	Pleistocene	2.49	0.47	0.94	0.48	0.10
GOM- 8	2884.8	Neogene	2.46	0.40	0.66	0.29	0.13
GOM- 9	4666.5	Lower Pliocene	2.70	0.52	0.79	0.38	0.07
GOM- 10	4289.7	Miocene	2.59	0.50	0.75	0.38	0.05
GOM- 12	3962.4	Miocene	2.57	0.46	0.62	0.30	0.06
GOM- 13	4636.8	Pliocene	2.19	0.55	0.51	0.29	0.08
GOM- 14	2556.6	Pliocene	2.72	0.56	0.81	0.40	0.06
GOM- 15	3663.6	Pliocene	2.65	0.52	0.81	0.37	0.13
GOM- 16	3222.6	Miocene	2.28	0.47	0.70	0.36	0.16
GOM- 17	4604.4	Miocene	2.15	0.47	0.65	0.33	0.46
GOM- 18	4073.4	Pliocene	1.86	0.63	1.90	1.12	0.23
GOM- 19			2.85	0.44	0.84	0.37	0.04

Pr= pristane. Ph = phytane. Nor Pr = nor pristane (C_{18} isoprenoid). nC_{17}, nC_{18} and nC_{27} are *n*-alkanes
with the 17, 18 and 25 carbon chain lengths

Table 5.11. Sterane source and maturity parameters for the Gulf of Mexico oils.

Sample	%C_{27} Reg	%C_{28} Reg	%C_{29} Reg	%C_{30} Reg	%C_{27} Dia	%C_{28} Dia	%C_{29} Dia	% C_{30} Dia	C_{29} αββ	C_{29} ααα	Dia/Reg	C_{29}/C_{27}	Hop/Ster
GOM- 1	36.42	23.41	40.16	0.57	38.18	30.56	31.26	2.25	0.44	0.23	6.69	1.10	0.52
GOM- 2	36.88	20.03	43.09	2.14	35.18	32.01	32.81	2.51	0.62	0.59	16.35	1.17	0.22
GOM- 3	26.62	24.11	49.27	1.65	26.04	24.34	49.62	1.92	0.39	0.27	7.47	1.85	0.36
GOM- 4	39.06	32.95	27.98	0.99	38.89	29.15	31.96	2.27	0.35	0.19	3.95	0.72	0.28
GOM- 5	36.19	30.93	32.88	0.62	40.93	29.21	29.86	1.57	0.42	0.20	6.83	0.91	0.22
GOM- 6	35.01	30.39	34.60	0.80	38.16	30.43	31.41	2.52	0.43	0.26	7.68	0.99	0.18
GOM- 7	26.91	22.54	50.56	4.17	29.17	26.13	44.70	1.50	0.64	0.39	24.52	1.88	0.14
GOM- 9	37.83	27.08	35.09	0.97	39.31	30.31	30.38	2.57	0.42	0.23	7.51	0.93	0.15
GOM- 10	39.59	28.38	32.02	0.00	39.07	21.62	39.31	0.00	0.76	0.29	40.50	0.81	0.16
GOM- 12	42.79	23.48	33.72	0.00	42.53	28.28	29.19	1.04	0.48	0.22	12.67	0.79	0.17
GOM- 13	18.32	36.05	45.62	0.00	32.42	33.85	33.73	0.00	0.42	0.17	3.80	2.49	0.51
GOM- 14	35.24	29.54	35.22	1.06	37.64	30.28	32.08	2.73	0.43	0.31	8.16	1.00	0.14
GOM- 15	24.26	27.48	48.26	0.00	29.33	24.91	45.76	2.04	0.39	0.28	8.67	1.99	0.29
GOM- 16	17.42	32.35	50.23	1.21	26.23	25.24	48.52	1.73	0.36	0.26	5.51	2.88	0.35
GOM- 17	32.41	19.81	47.78	3.07	30.44	30.92	38.63	0.00	0.61	0.61	16.98	1.47	0.16
GOM- 18	24.48	25.46	50.07	1.96	27.91	25.21	46.88	1.52	0.55	0.43	10.88	2.05	0.07
GOM- 19	27.69	30.63	41.67	0.70	34.61	25.44	39.95	1.71	0.46	0.25	10.54	1.50	0.19

% C_{27}, C_{28} ,C_{29} and C_{30} Reg = C_{27}, C_{28}, C_{29} and C_{30} sterane as a percentage of sum 27-30 of 5α(H),14α(H), 17α(H)- 20R sterane. % C_{27} – C_{30}Dia = C_{27}, C_{28}, C_{29} and C_{30} sterane as a percentage of sum 27-30 for 13α(H), 17β(H)- diasteranes. C_{29} ββ = 5α(H),14β(H), 17β(H)- 20S +20R / 5α(H),14β(H), 17β(H) + 5α(H),14α(H), 17α(H)- 20S+20R C29 steranes. C_{29}αα = 5α(H),14α(H), 17α(H)- C_{29} 20S/20S+20R sterane isomerisation maturity parameter. Dia/ Reg = Sum of (13β(H), 17α(H) and 13α(H), 17β(H) 20S+20R diasteranes/ sum of 5α(H), 14α(H), 17α(H) and 5α(H), 14β(H), 17β(H) 20S+20R)for the 27,28 and 29 compounds obtained from GC-MS-MS. C_{29}/C_{27} = ratio of C_{29}/C_{27} for 5α(H),14α(H), 17α(H)- 20R sterane. Hop/Ster = C_{30} 17α(H),21β(H)- hopane/ sum of all C_{27}-C_{29} steranes (regular, isosterane and diasterane). All data were obtained from appropriate GC-MS-MS transitions.

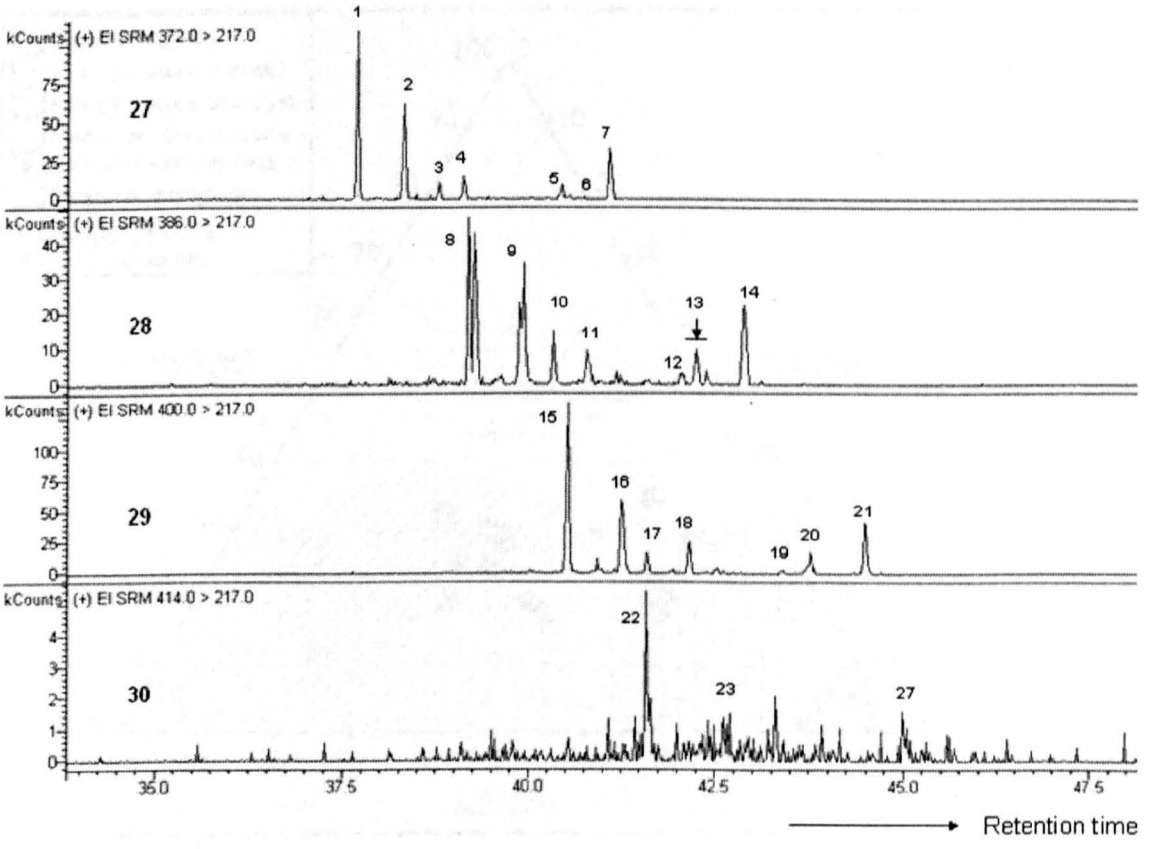

Figure 5.23. Representative GC-MS-MS mass chromatograms from sample GOM-4 showing the distribution of steranes typical of deltaic Gulf of Mexico oils. Note presence of peaks in m/z 414➔217-transition chromatogram diagnostic of C_{30} 24-*n*-propyl cholestane. Peaks identity in appendix IIIa.

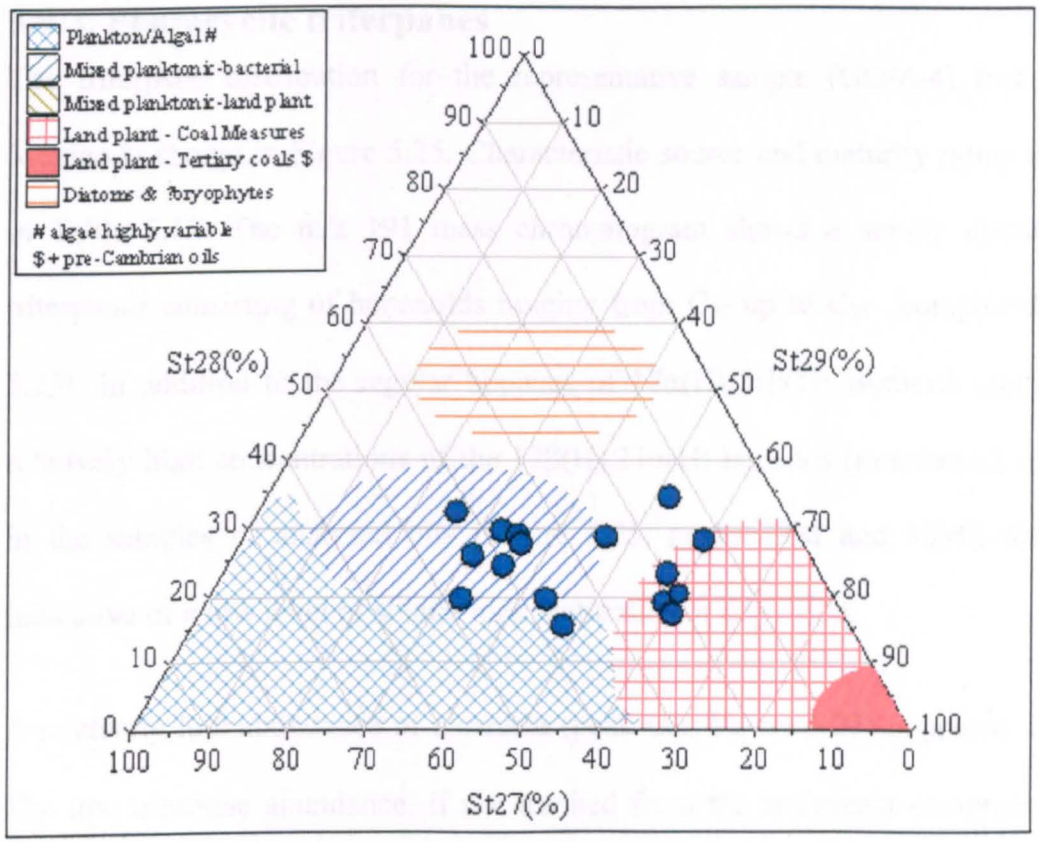

Figure 5.24a. Ternary diagram showing the distribution of the 27, 28 and 29 carbon number regular steranes with 5α(H),14α(H),17α(H) 20R configuration from GC-MS-MS analysis. Interpretational overlay from IGI's p: IGI-2 software modified after Huang and Meinschein (1979).

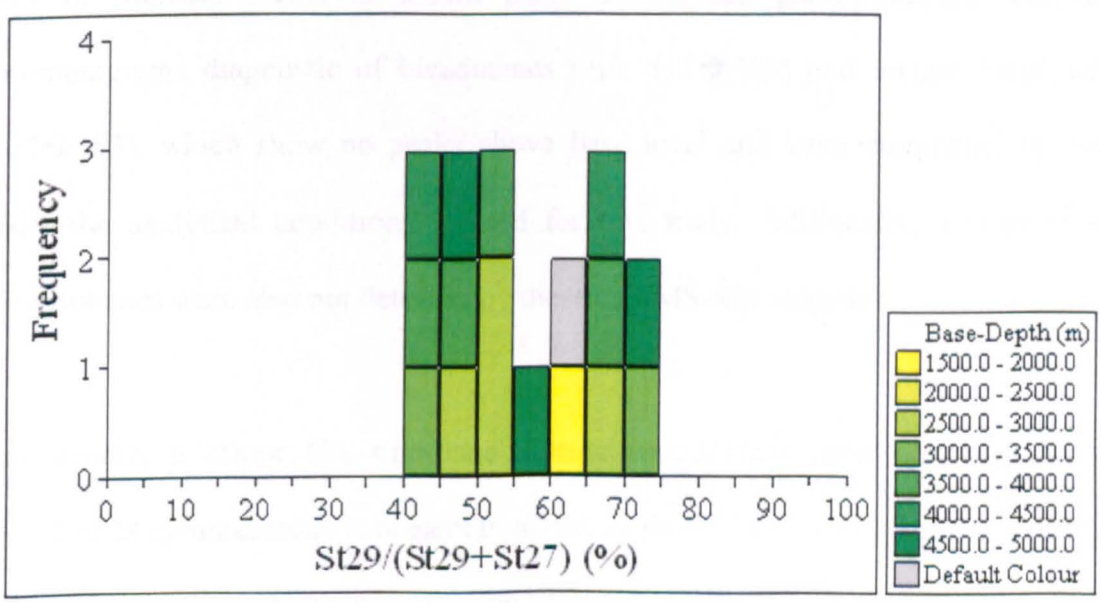

Figure 5.24b. Histogram of the ratio of % ($C_{29}/C_{29}+C_{27}$) for 5α(H),14α(H),17α(H) 20R sterane configuration separates the Gulf of Mexico oils into two groups. Base depth refers to the reservoir depths.

5.4.3. Pentacyclic triterpanes

The triterpane distribution for the representative sample (GOM-4) from Gulf of Mexico is shown in Figure 5.25. Characteristic source and maturity ratios are shown in Table 5.12. The m/z 191 mass chromatogram shows a simple distribution of triterpanes consisting of hopanoids ranging from C_{27} up to C_{35} compounds (Figure 5.25). In addition to the regular hopanes of 17α(H),21β(H) isomeric configuration, relatively high concentrations of the 17β(H),21α(H) hopanes (moretanes) are present in the samples of analysed oils (Figure 5.25, peaks 29M and 30M), these being indicative of a low level of source rock maturation at expulsion.

A relatively low abundance of oleanane (peak OL, Figure 5.25) is present in the oil. The low oleanane abundance, if not leached from the sediments comprising the oil migration path (migration contamination), reflects limited angiosperm higher plants to the source rock organic matter. Oleanane indices range from 0.05 to 0.14 for the oils. Unlike the Assam oils, there is an absence of bicadinanes in the samples from the Gulf of Mexico. This is shown from GC-MS-MS parent-daughter transition chromatograms diagnostic of bicadinanes (m/z 412→369) and methyl bicadinanes (426→383), which show no peaks above base level and were dominated by noise under the analytical conditions utilised for this study. Aditionally, norlupane and bisnorlupanes were also not detected by these GC-MS-MS analyses.

Furthermore, a minor C_{30} triterpane eluting immediately after C_{31} homohopane identified as gammacerane is present in all the analysed Gulf of Mexico oils (peak Ga, Figure 5.25). Gammacerane may be derived from reduction of tetrahymanol (Gammaceran-3β-ol), which is synthesized by *Tetrahymena pyriformis* as lipid substitute for sterols in these bacterivorous ciliated protozoan (Venkatesan, 1989; ten

Haven *et al.*, 1989). Gammacerane is believed to be a marker of stratified water column conditions (Sinninghe Damsté *et al.*, 1995). Taraxastane identified as peak T in the m/z 191 chromatogram of the Assam oil in Figure 5.6 is either present at levels below reliable identification or is absent in the Gulf of Mexico oils. In general, all the analysed Gulf of Mexico oils are compositionally similar in their terpane biomarker characteristics.

5.4.4. Tricyclic and tetracyclic terpanes

The distribution of tricyclic and tetracylic terpanes from sample GOM-4 is shown in Figure 5.26. Unlike the complex distributions in Assam and Niger Delta oils having several unknown compounds, the distribution of tricyclic and tetracylic terpanes for the Gulf of Mexico oils (GOM) is simple and reflect a commonly observed pattern among marine-sourced oils with C_{23} tricyclic being the most abundant tricyclic terpane. This distribution is similar in all the analysed oils.

5.4.5. Aromatic hydrocarbons

Aromatic hydrocarbon fractions obtained from SPE separation of whole oil were analysed by the GC-MS technique as described in Section 3.4. Although the aromatic hydrocarbon fraction of the oils contains several groups of compounds, only the alkylnaphthalene, alkylphenanthrene and alkyldibenzothiophene were quantified and utilised for thermal maturity and organic source assessments. The data generated are presented in Table 5.13. Figures 5.27 and 5.28 show typical distributions of alkylnaphthalene and alkylphenanthrene in the Gulf of Mexico oils.

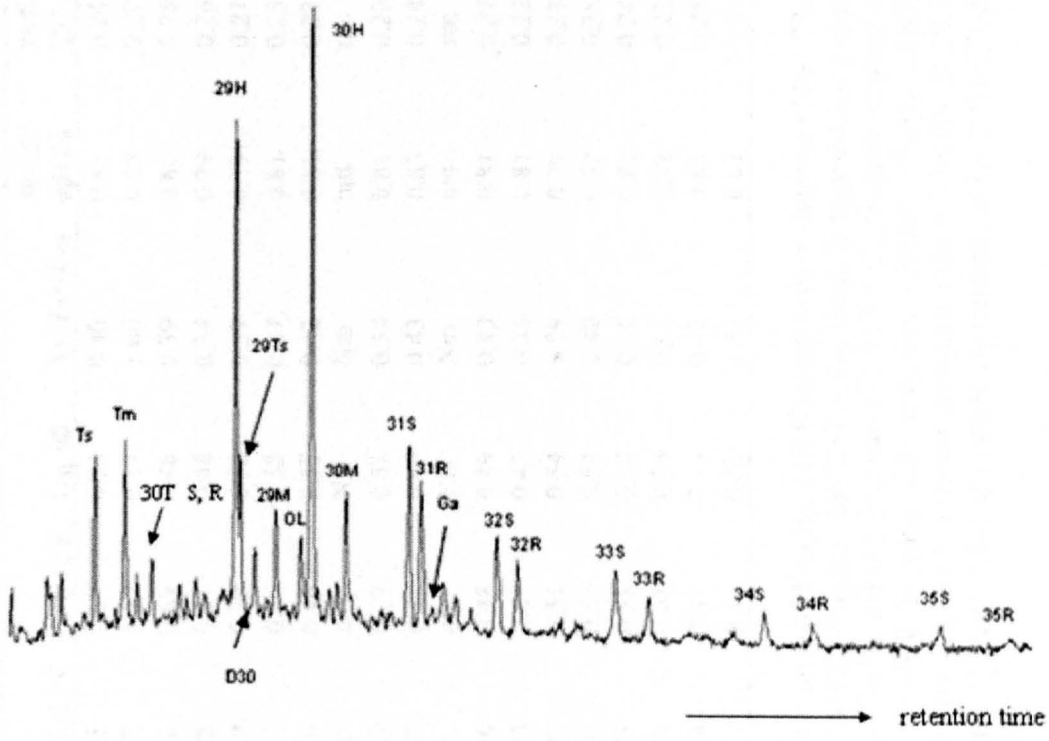

Figure 5.25. Representative partial m/z 191 mass chromatogram showing pentacyclic terpanes in a crude oil (sample GOM-4) from the Gulf of Mexico. Peak identification is given in Appendix IIIb.

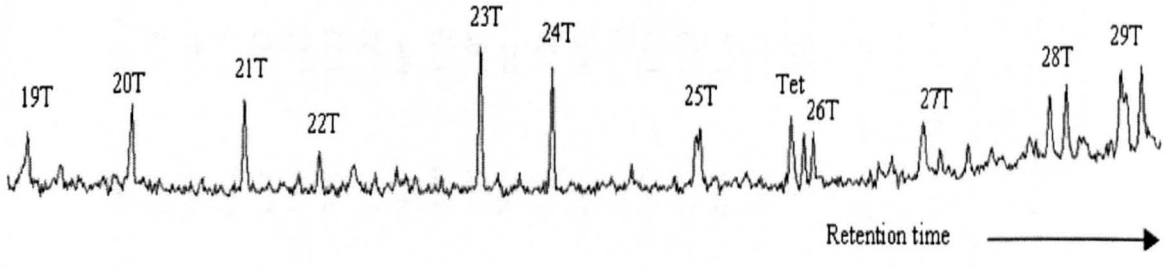

Figure 5.26. Partial m/z 191 mass chromatogram showing the distribution of tricyclic and tetra cyclic terpanes in sample GOM-4 which is representative of the Gulf of Mexico oils analysed. See Appendix IIIc for peak annotations.

Table 5.12. Characteristic terpane ratios for source and thermal maturity parameters calculated for Gulf of Mexico oils.

Sample	OL Index	C35/C34	Ga/Hop	26T/25T	23T/24T	Tet/Hop	23T/21T	19T/23T	Tet/23T	C_{32} αβ	Ts/Ts+Tm	30 αβ / αβ+βα	29Ts/ 29Ts+29βαHop
GOM- 1	0.13	0.34	0.29	1.11	1.08	0.05	1.35	1.63	0.89	0.53	0.40	0.82	0.24
GOM- 2	0.14	0.45	0.12	0.83	1.01	0.05	1.14	3.22	1.52	0.54	1.00	0.85	0.27
GOM- 3	0.14	0.41	0.36	0.92	1.25	0.05	1.37	0.66	0.69	0.48	0.39	0.81	0.25
GOM- 4	0.12	0.61	0.30	1.17	1.27	0.05	1.06	0.95	0.71	0.48	0.34	0.79	0.26
GOM- 5	0.13	0.53	0.36	1.46	1.21	0.06	0.99	0.79	0.70	0.52	0.37	0.79	0.27
GOM- 6	0.11	0.82	0.32	0.89	1.27	0.06	1.53	0.81	0.56	0.53	0.37	0.81	0.25
GOM- 7	0.12	0.80	0.26	0.96	1.23	0.06	1.95	0.54	0.44	0.53	0.42	0.81	0.23
GOM- 8	nm	nm	Nm	Nm	nm	nm	nm	nm	nm	Nm	Nm	nm	nm
GOM- 9	0.11	0.50	0.21	0.89	1.43	0.05	1.52	0.59	0.37	0.52	0.34	0.81	0.22
GOM- 10	0.17	0.47	0.00	0.64	1.08	0.09	1.14	1.12	0.74	0.49	0.43	0.83	0.28
GOM- 11	nm	nm	Nm	Nm	nm	nm	nm	nm	nm	Nm	Nm	nm	nm
GOM- 12	0.12	0.00	0.46	0.86	1.32	0.10	1.08	1.09	0.48	0.49	0.43	0.81	0.27
GOM- 13	0.11	nm	0.39	0.71	0.83	0.06	0.83	2.23	0.89	0.43	0.31	0.81	0.22
GOM- 14	0.12	0.71	0.31	0.92	1.26	0.06	1.52	0.97	0.51	0.54	0.39	0.79	0.23
GOM- 15	0.10	0.73	0.24	0.77	1.07	0.04	1.47	0.55	0.51	0.54	0.40	0.82	0.26
GOM- 16	0.11	0.57	0.80	0.93	1.19	0.05	1.51	0.77	0.58	0.48	0.36	0.82	0.24
GOM- 17	0.13	0.40	0.32	0.98	1.24	0.05	1.99	0.77	0.61	0.56	0.43	0.82	0.23
GOM- 18	0.05	0.76	0.31	1.08	1.27	0.06	1.28	0.43	0.43	0.55	0.42	0.83	0.25
GOM- 19	0.14	0.46	0.35	1.01	1.05	0.04	1.23	0.91	0.44	0.52	0.37	0.82	0.25

OL = 18α(H) + 18β(H) oleanane/(18α(H) + 18β(H) oleanane + 17α(H), 21β(H) hopane). 35/34 = ratio of 17α(H), 21β(H)-pentakishomohopane (22S+ 22R)/ 17α(H), 21β(H)- tetrakis homohopane (22S +22R). Ga /hop = 10*gammacerane / C_{30} 17α(H), 21β(H) -hopane. 26T/25T = C_{26} tricyclic terpane/ C_{25} tricyclic terpane. 23T/24T= C_{23} tricyclic terpane/ C_{24} tricyclic terpane. Tet/Hop = tetracyclic terpane/ C_{30} 17α(H), 21β(H)- hopane. 23T/21T = C_{23} tricyclic terpane/ C_{21} tricyclic. 19T/23T = C_{19} tricyclic terpane/ C_{23} tricyclic. Tet/ 23T = tetracyclic terpane (24-de-E-hopane)/ C23 tricyclic. C32αβ= 17α(H), 21β(H)-bishomohopane 22S/ 22S+ 22R. Ts/Ts+Tm = 18α(H)- 22,29,30- Trisnorneohopane (Ts)/ 18α(H)- 22,29,30- Trisnorneohopane (Ts) + 17α(H)- 22,29,30-trisnorhopane (Tm). 30αβ ab/30 αβ + βα = 17α(H), 21β(H)- hopane/ 17α(H), 21β(H) hopane +17β(H), 21α(H) hopane (moratane). 29Ts/ 29Ts+29αβ = 18α(H)- norneohopane/ 18α(H)-norneohopane + 17α(H), 21β(H)-norhopane. nm= not measured.

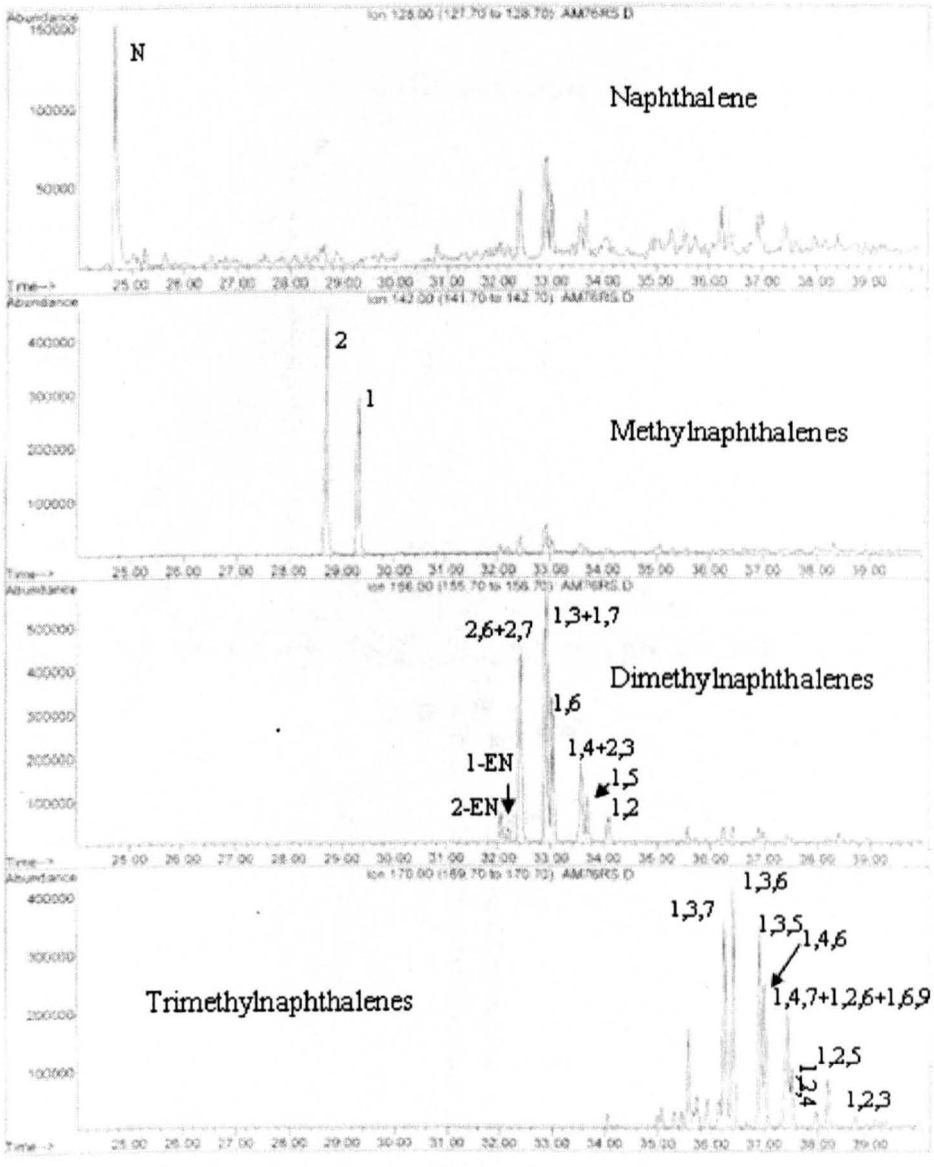

Figure 5.27. GC-MS m/z 128, 142, 156 and 170 showing the distributions of naphthalene and alkyl-naphthalenes in representative oil (GOM-4) from the Gulf of Mexico. Note integers denote the position of alkylation in each isomer. EN represents ethylnaphthalene.

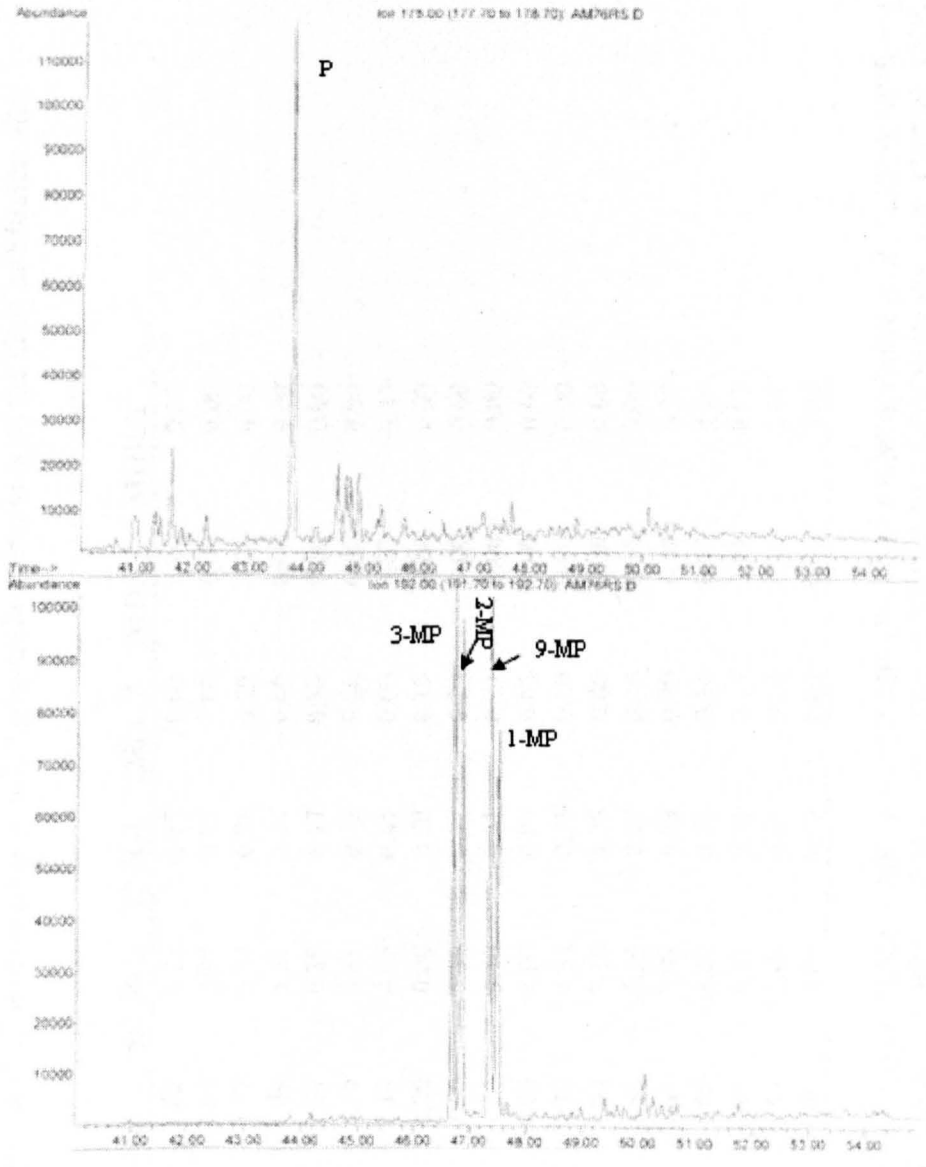

Figure 5.28. GC-MS m/z 178 and 192 showing the distributions of phenanthrene and methyl-phenanthrene in representative oil (sample GOM-4) from the Gulf of Mexico. P = phenanthrene, and 2-MP, 3-MP, 9-MP and 1-MP are methylphenanthrenes with the integers denoting the position of methyl substitution on the phenanthrene ring.

Table 5.13. Thermal maturity and source molecular indicators from aromatic hydrocarbon fractions of the Gulf of Mexico oils.

Sample	MPI-1	MPI-2	MNR	ENR	DNR-1	TNR-1	DBT/P	MDR	MDR-1
GOM- 1	0.38	0.40	0.92	1.82	2.11	0.75	0.00	0.00	0.00
GOM- 2	0.61	0.61	1.08	2.03	5.05	0.75	0.00	0.00	0.00
GOM- 3	0.78	0.79	1.31	1.57	5.62	0.71	0.29	0.00	0.00
GOM- 4	0.86	0.87	1.32	1.49	5.51	0.76	0.00	0.00	0.00
GOM- 5	0.78	0.76	1.32	1.54	6.30	0.77	0.32	0.00	0.00
GOM- 6	0.74	0.72	1.20	1.49	4.61	0.72	0.00	0.00	0.00
GOM- 7	0.00	0.00	1.29	1.39	4.65	0.65	0.00	4.03	0.19
GOM- 8	0.22	0.09	0.00	0.00	0.00	0.00	0.13	0.00	0.00
GOM- 9	0.89	0.86	1.35	1.60	5.39	0.72	0.29	0.00	0.00
GOM- 10	0.70	0.72	1.23	1.53	5.10	0.71	0.21	0.00	0.00
GOM- 11	0.71	0.91	0.00	0.00	0.00	0.00	0.03	0.00	0.00
GOM- 12	0.81	0.80	1.13	1.30	4.55	0.76	0.00	0.00	0.00
GOM- 13	0.88	0.87	1.46	1.90	7.10	0.75	0.00	0.00	0.00
GOM- 14	0.90	0.90	1.33	1.54	6.30	0.73	0.14	0.00	0.00
GOM- 15	0.86	0.86	1.23	1.36	4.83	0.66	0.00	0.00	0.00
GOM- 16	1.11	1.11	1.38	1.88	5.29	0.74	0.34	0.00	0.00
GOM- 17	0.60	0.64	1.07	1.61	4.50	0.72	0.15	3.88	0.05
GOM- 18	0.62	0.62	1.58	1.53	2.89	0.67	0.28	0.00	0.00
GOM- 19	0.00	0.00	0.00	0.00	0.00	0.00	0.00	0.00	0.00

MPI-1= 1.5*(2-MP+ 3-MP)/ (P + 1-MP + 9-MP); Radke *et al.*, (1982a). MPI-2 = (3* 2-MP/ (P+ 1-MP + 9-MP); Radke *et al.*, (1982a). MNR = (2-MN/ 1-MN); Radke *et al.*, (1982b). ENR = 2-EN/1-EN; Radke *et al.*, (1982b). DNR-1 = (2,6-DMN+ 2,7-DMN)/ 1,5-DMN; Radke *et al.*, (1982b). TNR-1 = 2,3,6-TMN/ (1,4,6-TMN + 1,3,5-TMN); Alexander *et al.*, (1985).DBT/P = dibenzothiophene/ phenanthrene.MDR = 4-MDBT/1-MDBT; Radke *et al.*, (1986). MDR-1= 1-MDBT/DBT; Radke *et al.*, (1982a). 000= values of parameters for which one or more compounds could not be integrated.

5.4.6. Summary of source facies and thermal maturity

On the basis of the molecular properties of the analysed Gulf of Mexico crude oil samples in this study, the oils are early - mid-mature (based on sterane and terpane thermal maturity parameters (Figure 5.29a), and show no variation with reservoir depth (Figure 5.29b). Anomalously high iso-sterane thermal maturity ratios (C_{29} ββ = 5α(H), 14β(H), 17β(H)- 20S +20R / 5α(H), 14β(H), 17β(H) + 5α(H), 14α(H), 17α(H)- 20S+20R C29 steranes; Table 5.10) compared with the very low regular 20S/S+R ratios suggest a high degree of migrational fractionation (Figure 5.30).

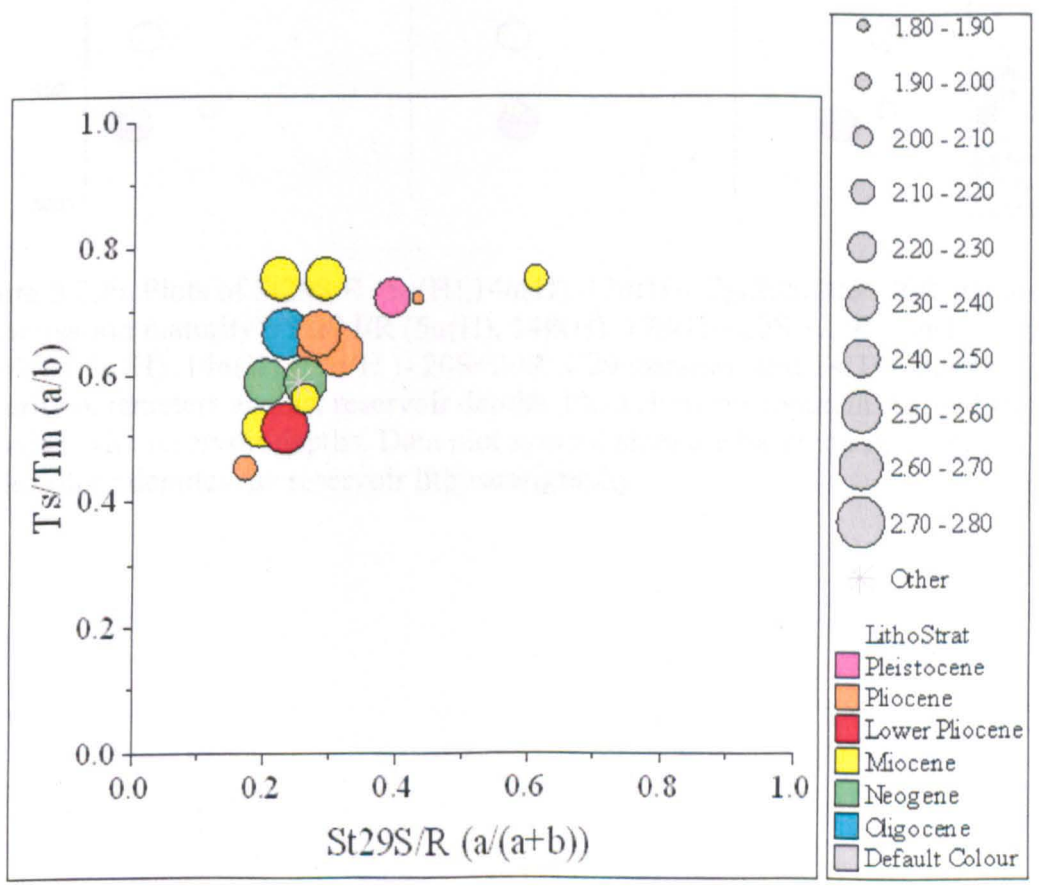

Figure 5.29a. Plot of Ts/Tm against C29S/S+R thermal maturity parameters shows that the analysed Gulf of Mexico oils are early- mid-mature. Data plot symbol sizes are based on Pr/Ph ratios, while colour denotes the reservoir lithostratigraphy.

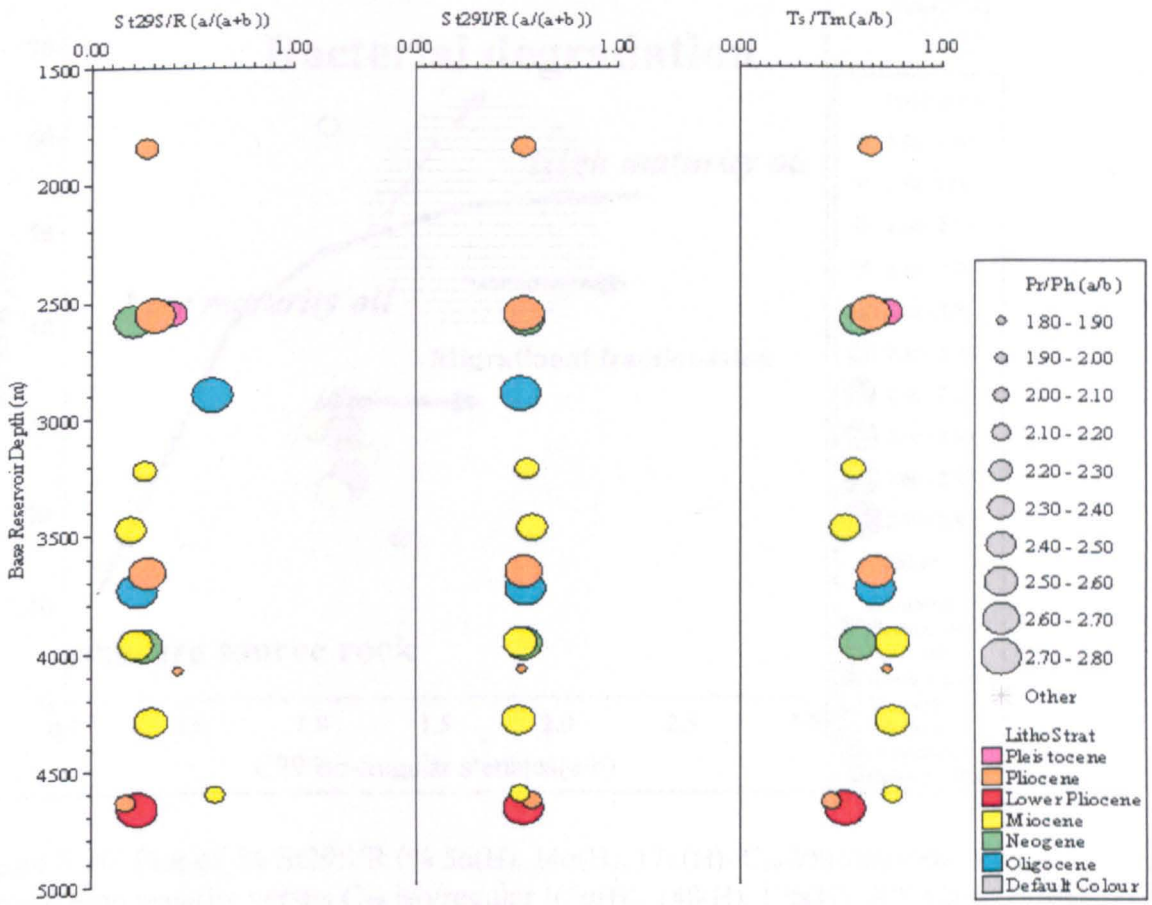

Figure 5.29b. Plots of St29S/R (5α(H),14α(H), 17α(H)- C_{29} 20S/20S+20R sterane isomerisation maturity), St29 I/R (5α(H), 14β(H), 17β(H)- 20S +20R / 5α(H), 14β(H), 17β(H) + 5α(H), 14α(H), 17α(H)- 20S+20R C29 steranes) and Ts/Tm thermal maturity parameters against reservoir depths. Plots show no apparent thermal maturity variation with reservoir depths. Data plot symbol sizes are based on Pr/Ph ratios, while colour denotes the reservoir lithostratigraphy

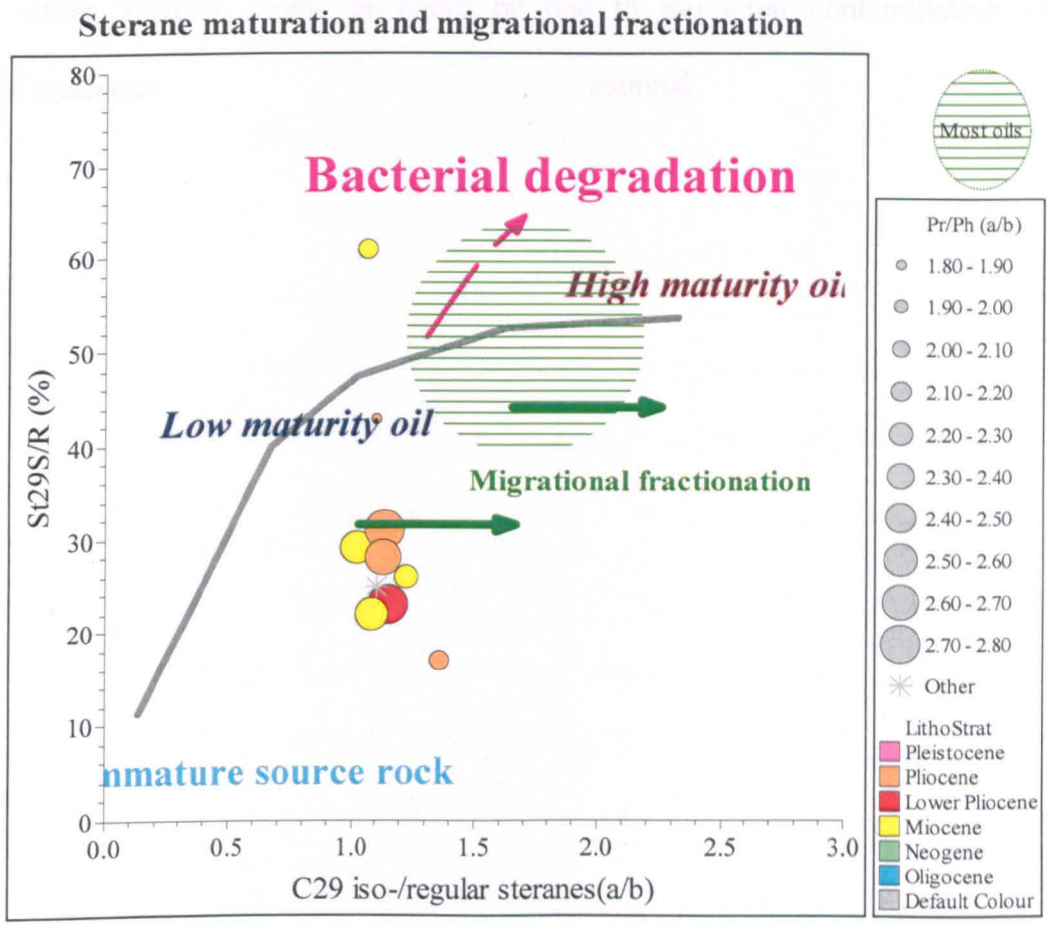

Figure 5.30. Plot of % St29S/R (% 5α(H), 14α(H), 17α(H)- C_{29} 20S/20S+20R sterane isomerisation maturity versus C_{29} iso/regular ((5α(H), 14β(H), 17β(H)- 20S +20R / 5α(H), 14α(H), 17α(H)- 20S+20R) steranes shows evidence of likely migration fractionation of the primary oils. Data plot symbol sizes are based on pr/ph ratios, while colour denotes the reservoir lithostratigraphy

Compositionally, the oils fall into two groups (sterane carbon number) indicating expulsion from a source rock of marine organofacies rich in algal remains, while the second oil family indicates a source rock containing a mix with higher levels of terrigenous higher plant inputs. Both the pr/ph ratio as well as presence of gammacerane suggests that the source rock(s) that expelled these oils was/were deposited under sub-oxic conditions. The low oleanane index could, being an indication of limited angiosperm contribution to the source rock kerogen, points to a source rock depositional age of Late Cretaceous, with the present day reservoirs

within Tertiary sands, or could be due to migration contamination of a Late Cretaceous sourced oil.

5.5. Molecular Characteristics of the Niger Delta oils

5.5.1. N-alkanes and isoprenoid alkanes

The analysed Niger Delta crude oil samples are generally rich in both low and high molecular weight *n*-alkanes. There is evidence of wax richness as reflected in high concentration of *n*-alkanes greater than nC_{21} in most samples (Figure 5.31 and final column of Table 5.14). Under the GC programs used, *n*-alkanes up to C_{34} were resolved and detected where present in sufficient concentrations. Based on gas chromatograms, the samples can be visually separated into two groups, i.e. those rich in low molecular weight *n*-alkanes less than nC_{21}, consisting of deepwater oils and some shallow water accumulations, and another sample set rich in both short and long chain *n*-alkanes (Figure 5.31). The pristane/phytane ratios range from 2.11 to 4.42 (Figure 5.32, Table 5.14) reflecting variable source rock depositional conditions that transcend sub-oxic to oxic environments.

5.5.2. Steranes

Consistent with *n*-alkane envelopes discriminating samples into two groups, sterane distribution also reflect a distribution that spans between samples rich in stigmastane (C_{29} -ethyl cholestane) and lacking C_{30} 24-*n*-propylcholestane (Figure 5.34) through oils that have both marine and terrigenous organofacies characteristics (intermediate geochemical properties). The other end member comprises those crude oil samples having a relatively low C_{29} sterane abundances and significant amounts of C_{30} 24-*n*-propyl cholestane that is diagnostic of marine algae contribution (Moldowan *et al.*, 1990) (Figure 5.33). A ternary diagram showing the distributions of the C_{27}-C_{29} steranes in the oil set is shown in Figure 5.35.

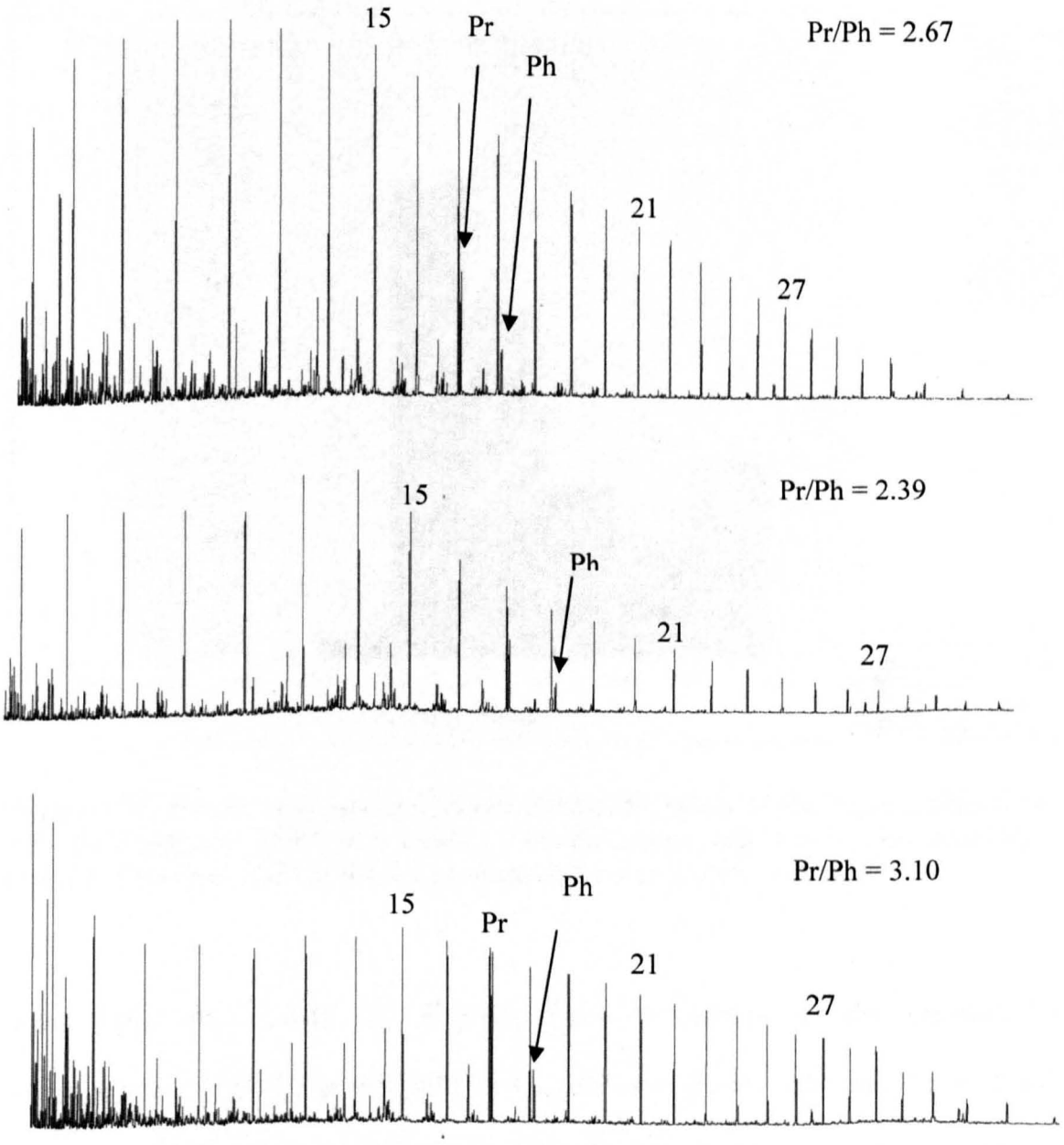

Figure 5.31. Representative gas chromatograms showing the distributions of *n*-alkanes and isoprenoid alkanes in samples of oils from Niger Delta. The upper chromatogram is typical of terrigenous facies(sample NDO10), while the middle chromatogram is representative of the deepwater (marine organofacies, sample NDO14) and the lower chromatogram is intermediate, (sample NDO45).

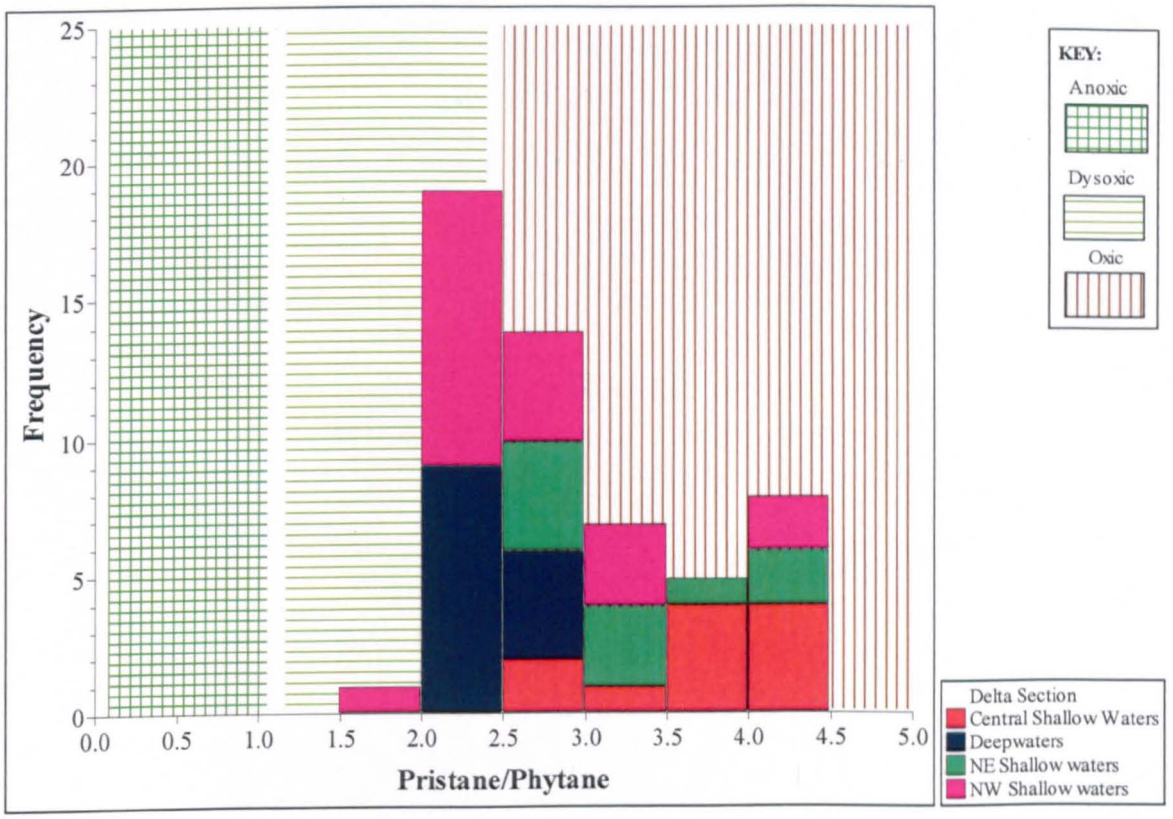

Figure 5.32. Source rock anoxia inferred from pr/ph ratios of the Niger Delta oil set. The wide range of Pr/Ph ratio reflects variable source rock depositional conditions. Overlay field after IGI's p:IGI 2.7 geochemical interpretation software.

In general, most crude oil samples show terrigenous sterane organofacies characteristics (high $\%C_{29}$ and lack of C_{30} steranes; Figure 5.34 and Figure 5.35). However, notable are the samples of oils from the deepwater accumulations and a few oils from the western section of the delta that show sterane organofacies characteristics that reflect expulsion from source rocks that received less terrigenous input and high marine algae contribution and whose depositional conditions are less oxygenated as reflected in their pr/ph ratios (Figure 5.32). The marine organofacies characteristics of a few shallow western oils has earlier been observed by some other workers (Haack *et al.,* 2000; Eneogwe & Ekundayo, 2003) and was thought to reflect oil expelled from source rock of localised organofacies within the delta and which is

Table 5.14. *n*-alkane and isoprenoid ratios in the Niger Delta oils.

Sample	Region	Pr/Ph	norPr/Pr	pr/nC_{17}	Ph/nC_{18}	nC_{17}/nC_{27}
NDO01	East	2.67	0.50	0.51	0.23	0.27
NDO02	East	2.99	0.38	1.41	0.54	0.41
NDO03	East	3.87	0.37	3.02	0.95	0.26
NDO04	East	3.22	0.37	1.52	0.56	0.36
NDO05	East	3.34	0.34	1.53	0.52	0.54
NDO06	East	4.42	0.32	0.93	0.23	0.26
NDO07	East	3.00	0.39	1.29	0.50	0.37
NDO08	East	4.20	0.29	1.46	0.38	0.52
NDO09	East	2.99	0.40	1.67	0.68	0.27
NDO10	East	4.39	0.33	1.21	0.32	0.40
NDO11	East	3.15		1.48	0.55	
NDO13	Deepwater	2.40	0.47	0.77	0.40	0.15
NDO14	Deepwater	2.39	0.51	0.84	0.45	0.17
NDO15	Deepwater	2.38	0.47	0.68	0.36	0.16
NDO16	Deepwater	2.28	0.48	0.46	0.24	0.21
NDO17	Deepwater	2.40	0.47	0.75	0.39	0.16
NDO18	Deepwater	2.36	0.56	0.48	0.26	0.14
NDO19	Deepwater	2.26	0.50	0.92	0.52	0.31
NDO20	Deepwater	2.56	0.62	0.43	0.31	0.11
NDO21	Deepwater	2.47	0.48	0.54	0.32	0.11
NDO22	Deepwater	2.62	0.51	0.26	0.18	0.04
NDO23	Deepwater	2.24	0.51	0.38	0.24	0.25
NDO24	Deepwater	2.57	0.49	0.46	0.27	0.08
NDO26	Deepwater	2.88	0.46	1.28	0.62	0.17
NDO27	Deepwater	2.56	0.52	0.53	0.27	0.13
NDO28	West	0.00	0.00	0.00	0.00	0.00
NDO29	West	2.81	0.44	0.50	0.20	0.47
NDO30	West	2.18	0.51	2.79	1.74	0.34

Sample	Region	Pr/Ph	norPr/Pr	pr/nC_{17}	Ph/nC_{18}	nC_{17}/nC_{27}
NDO31	West	2.99	0.43	0.55	0.22	0.56
NDO32	West	4.06	0.40	0.76	0.22	0.22
NDO33	West	2.46	0.48	0.80	0.38	0.42
NDO34	West	2.61	0.51	0.50	0.25	0.13
NDO35	West	2.28	0.49	1.13	0.61	0.31
NDO36	West	2.29	0.50	0.49	0.24	0.43
NDO37	West	3.26	0.36	19.20	7.18	0.09
NDO40	West	3.10	0.34	1.49	0.55	0.53
NDO41	West	3.08	0.36	1.49	0.55	0.45
NDO42	West	2.18	0.52	0.45	0.24	0.48
NDO43	West	2.24	0.34	4.54	0.92	3.71
NDO45	West	2.12	0.49	0.54	0.29	0.35
NDO46	West	2.11	0.53	0.42	0.23	0.37
NDO47	West	2.12	0.49	0.77	0.43	0.39
NDO48	Central	3.96	0.33	0.51	0.23	0.30
NDO49	Central	4.11	0.38	1.05	0.30	0.10
NDO50	Central	4.01	0.35	0.82	0.23	0.30
NDO51	Central	4.02	0.36	0.80	0.24	0.18
NDO52	Central	3.98	0.36	0.81	0.25	0.20
NDO53	Central	4.02	0.33	0.82	0.23	0.28
NDO54	Central	3.95	0.36	0.79	0.24	0.20
NDO55	Central	3.92	0.38	0.80	0.25	0.20
NDO56	Central	3.28	0.42	1.23	0.44	0.23
NDO57	Central	3.33	0.40	1.72	0.61	0.26
NDO58	Central	2.97	0.47	0.76	0.31	0.26

n.m = data could not be measured because of biodegradation/ water washed *n*-alkane.
0.00 = no data due to either low level of one or more of the compounds in the ratio or biodegradation effects .Pr = pristane. Ph = phytane. Nor Pr = nor pristane (C_{18} isoprenoid).
nC_{17}, nC_{18} and nC_{27} are *n*-alkanes with the 17, 18 and 27 carbon chain lengths.

at variance with the overwhelmingly terrigenous source rocks organofacies of the delta.

The diasterane/ regular sterane ratios range from 0.5 to 1.43, reflecting low levels of the rearranged steranes in the Niger Delta oils when compared to oils from Gulf of Mexico and the Assam. The C_{29}/ C_{27} sterane ratio ranges from 0.63 to 6.07 for this oil set, thus suggesting oil expulsion from source rocks of variable marine (29/27 <2) and more terrigenous (29/27 >2) organofacies (Table 5.15).

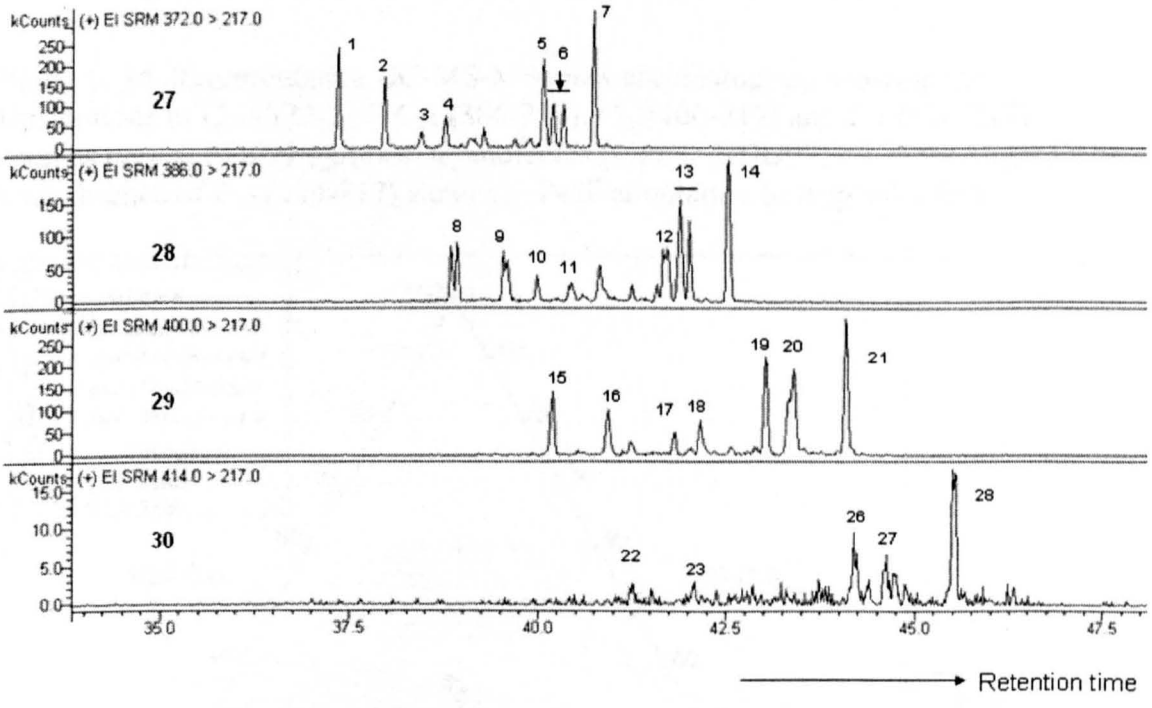

Figure 5.33.Representative GC-MS-MS mass chromatograms showing the distributions of C_{27} (m/z 372-217) C_{28} (m/z 386-217), C_{29} (m/z 400-217) and C_{30} (m/z 414-217) steranes in marine organofacies (deepwater sample NDO12) crude oil samples (from the Niger Delta. Peak annotation in Appendix IIIa

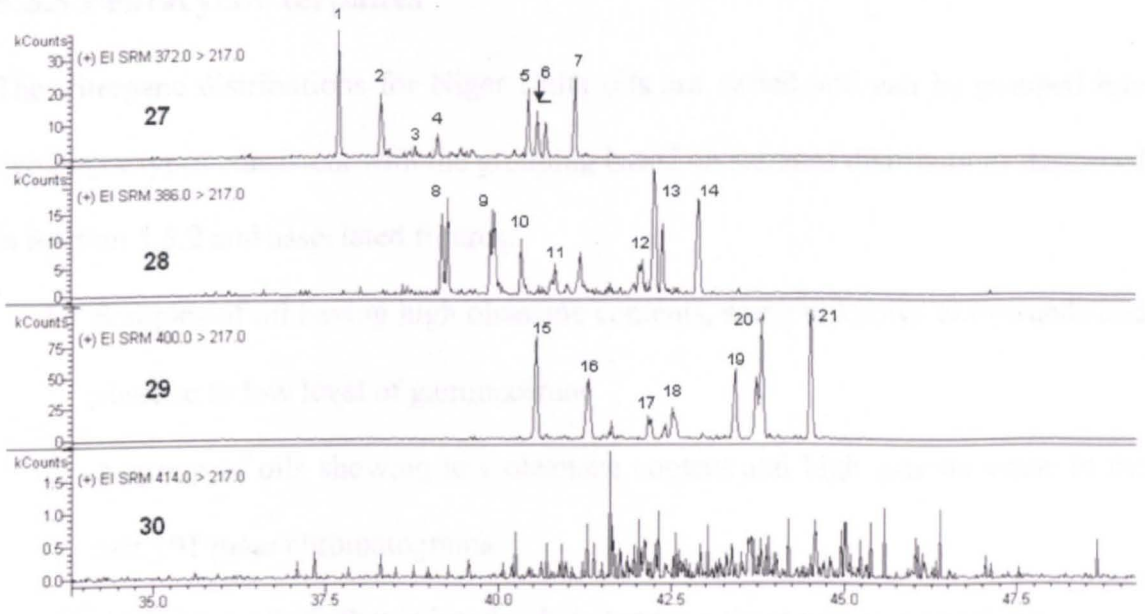

Figure 5. 34. Representative GC-MS-MS mass chromatogram showing the distributions of C_{27} (372-217) C_{28} (386-217), C_{29} (400-217) and C_{30} (414-217) steranes typical of a terrigenous organofacies (sample NDO03) oil of the Niger Delta. Note absence of C_{30} (414-217) steranes. Peak annotation in Appendix IIIa

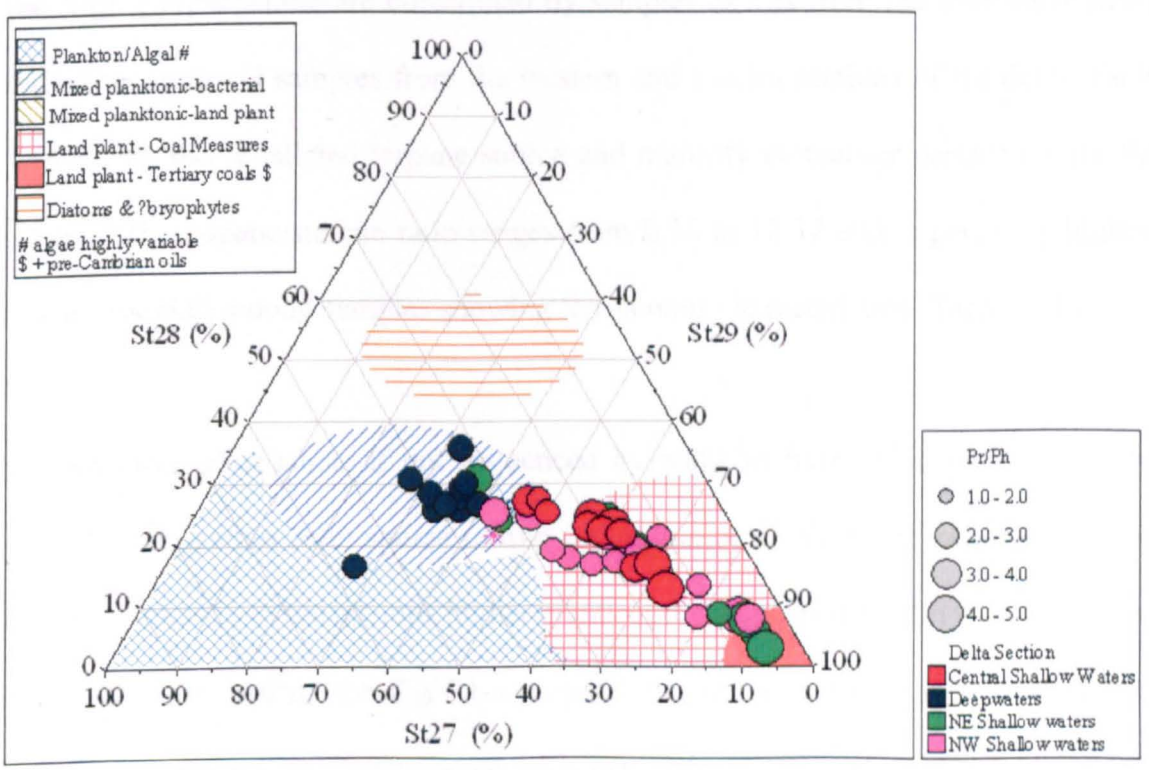

Figure 5.35. Ternary diagram showing the distribution of the 27, 28 and 29 carbon number regular steranes with 5α(H), 14α(H), 17α(H)- 20R configuration from GCMS/MS analysis. Interpretational overlay from IGI's p: IGI-2 software modified after Huang and Meinschein (1979). Note North Sea oil permits a comparison of marine sterane distribution with the deepwater oils.

5.5.3 Pentacyclic terpanes

The triterpane distributions for Niger Delta oils are varied and can be grouped into two major types consistent with the grouping based on steranes distributions described in Section 5.5.2 and associated figures.

1. Samples of oil having high oleanane contents, some unknown compounds and absence to low level of gammacerane
2. A group of oils showing low oleanane content and high gammacerane in the m/z 191 mass chromatograms.

Notable is a group of oils that is intermediate between these two end-members.

These two distinct terpane characteristics in m/z 191 mass chromatograms are shown in Figures 5.36 and 5.37 respectively. The group of oils having low oleanane content and high gammacerane are constituted by samples of oils from the deepwater fields and some crude oil samples from the western and eastern sections of the delta. Table 5.14 shows the calculated terpane source and maturity biomarker parameters for the oil sets. The hopane/sterane ratio ranges from 0.28 to 12.37 and is generally highest (most bacterial) among samples showing terrigenous characteristics (Table 5.16)

The oleanane abundance, if not influenced by addition from adjacent source rocks during oil migration from source to trap (migration contamination), reflects the level of contribution from terrigenous higher plants of the angiosperm family. A plot of the oleanane index against the C_{30} 24-*n*-propylcholestane abundance separates samples into groups defined by their source rock organofacies (Figure 5.38). Additionally, gammacerane occurs in some oils and is labelled as peak "Ga" in Figure 5.37. The gammacerane occurrence and abundance parallels pr/ph ratio changes and samples

having gammacerane generally have low to intermediate pr/ph ratios among the oils of the Niger Delta (Figure 5.39).

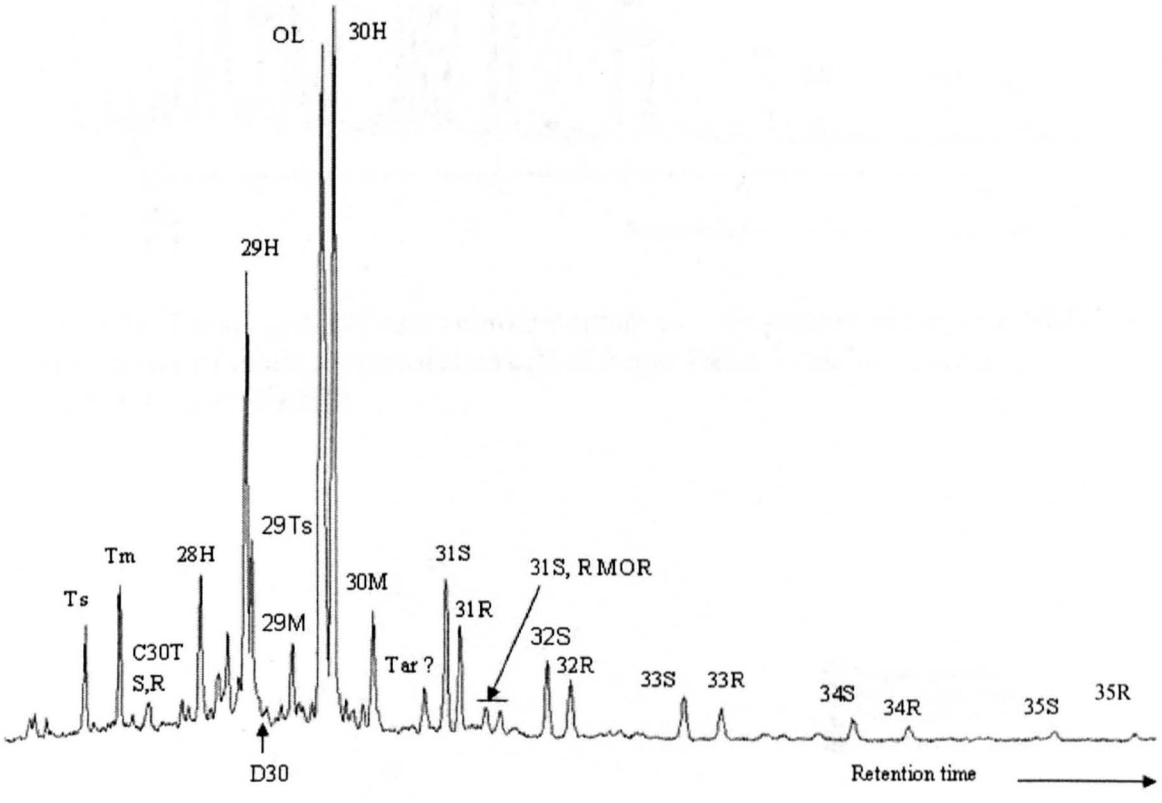

Figure 5.36. Partial m/z 191 mass chromatogram from sample NDO03 showing distribution of terpanes in a terrigenous organofacies oil of the Niger Delta. Peak identities are given in appendix IIIb.

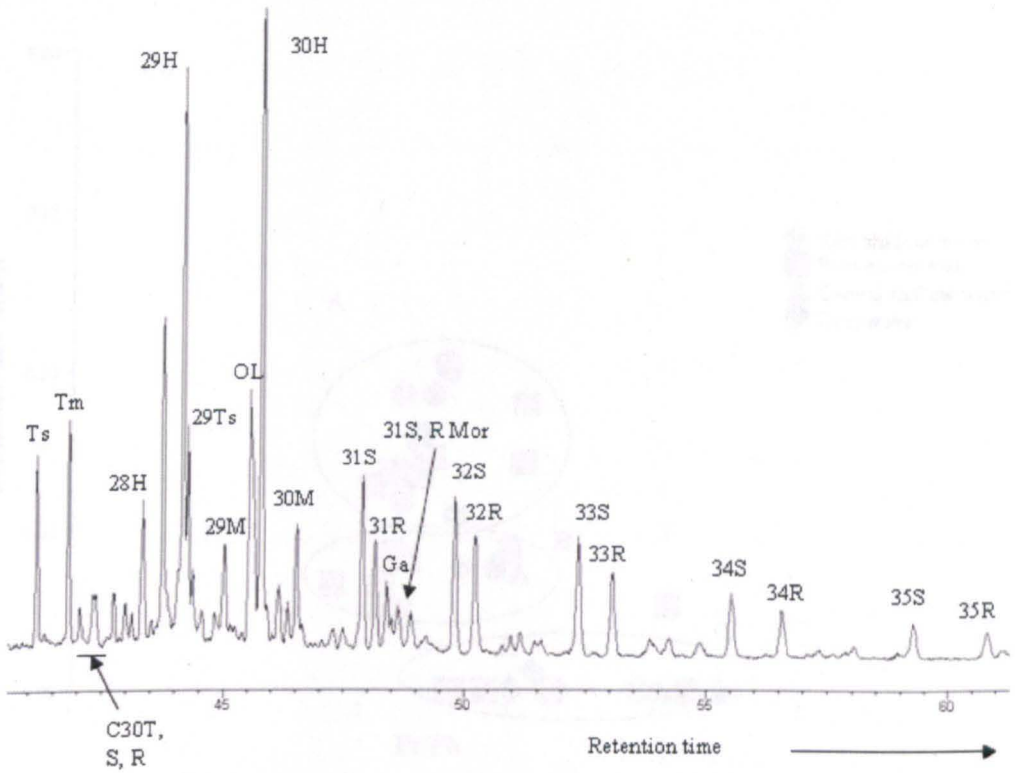

Figure 5.37. Partial m/z 191 mass chromatogram of a deepwater oil (sample NDO12) representative of marine organofacies oils of Niger Delta. Peak identities are presented in appendix IIIb.

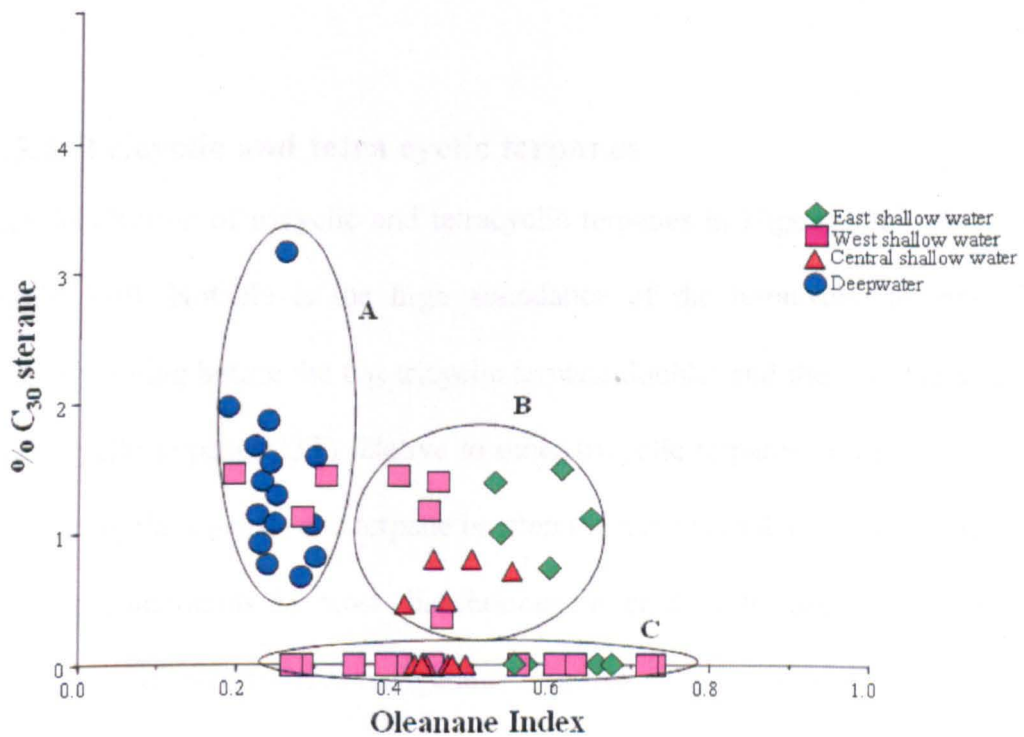

Figure 5.38. Cross plot of oleanane index against C_{30} 24-*n*-propyl cholestane relative abundance. The plot separates oils into three families; namely, A= marine superfamily dominated by the deepwater oils B = intermediate family of mixed marine and terrigenous and C = terrigenous superfamily dominated by shallow water oils.

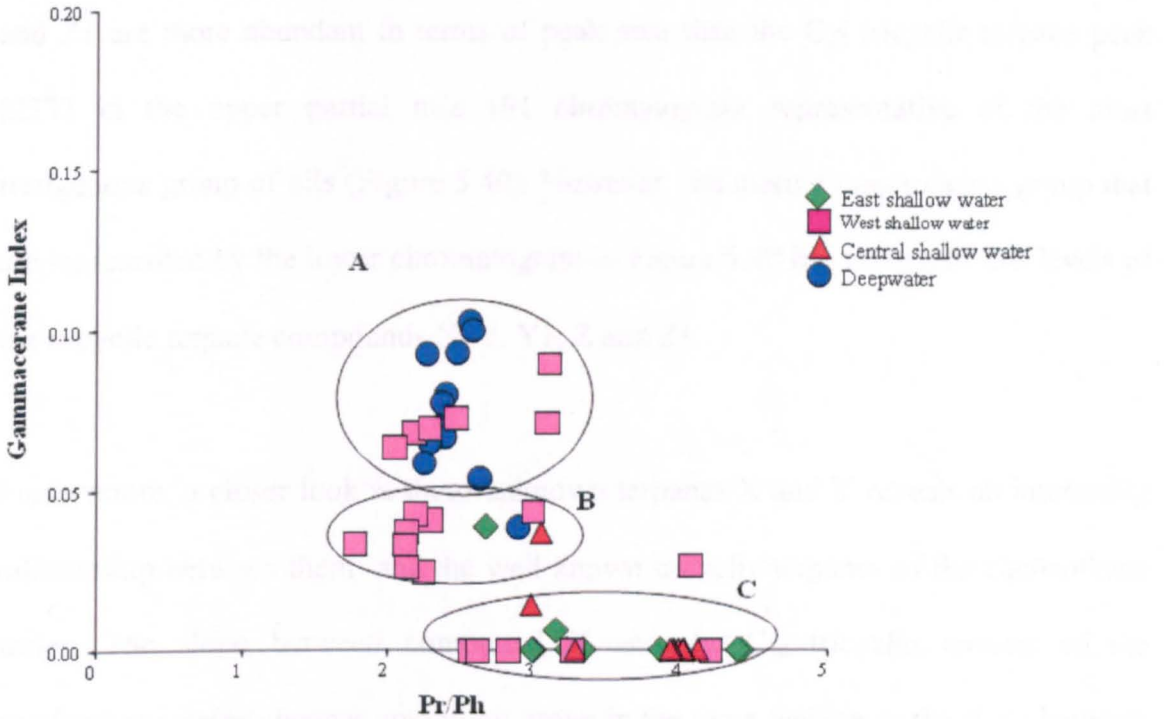

Figure 5.39. Cross plot of pr/ph ratios (redox) against gammacerane index (salinity stratification), which separates oils into families consistent with their depositional environments and organic matter source. Note the clustering of significant proportion of the western oils with the deepwater oils, suggestive of similar depositional conditions.

5.5.4. Tricyclic and tetra cyclic terpanes

The distribution of tricyclic and tetracyclic terpanes in Niger Delta oils is shown in Figure 5.40. Notable is the high abundance of the tetracyclic terpane (24-de-E-hopane) eluting before the C_{26} tricyclic terpane doublet and the variable abundance of C_{23} tricyclic terpane (23T) relative to other tricyclic terpanes in the Niger Delta oils. In contrast, the C_{23} tricyclic terpane is often the most abundant peak amongst the other tricyclic compounds in most distributions in crude oils. Some unknown tricyclic terpenoids believed to have terrigenous origin also appear as significant peaks in the partial m/z 191 showing the tricyclic and tetracyclic terpanes (Figure 5.40). Of these several uncommon compounds, the major peaks labelled X, Y, Y1, Z and Z1 (Figure 5.40) were characterized. Compounds Y1 and Z have been identified by Woolhouse *et*

al. (1992) as des-A-oleanane and des-A-ursane respectively. Compounds X, Y, Y1 and Z1 are more abundant in terms of peak area than the C_{23} tricyclic terpane peak (23T) in the upper partial m/z 191 chromatogram representative of the most terrigenous group of oils (Figure 5.40). However, the marine organofacies group that are represented by the lower chromatogram in Figure 5.40 has relatively low levels of the tricyclic terpane compounds X, Y, Y1, Z and Z1.

Furthermore, a closer look at these unknown terpanes X and Y reveals an interesting relationship between them and the well known tricyclic terpanes of the cheilanthane series. The slope between compound X and the C_{20} tricyclic terpane of the cheilanthane series changes among oil group in the same fashion as the slope between unknown tricyclic compound Y and the C_{23} tricyclic terpane (Figure 5.41). This relationship is systematic and it appears to be source specific. The relationship is also apparent when the peak heights of the compounds Y1, and Z1 are compared with the tricyclic terpane compounds eluting beside them (Figure 5.41). On the basis of variation in the relative abundance of tricyclic compounds X and Y among oils from Niger Delta, a parameter called Tricyclic Terpane Terrigenous Index (TTTI), which proved very powerful in discriminating the marine organofacies oils from the other oil families, has been developed and defined as cross plot of ratios of compounds X/ $X+TC_{20}$ and $Y/Y+ TC_{23}$, (Figure 5.42), where TC_{20} and TC_{23} being the known tricyclic terpane compounds with 20 and 23 carbons in their structures. A plot of one of these ratios against oleanane index provides additional evidence for land plant origin for the unknown tricyclic compounds X and Y (Figure 5.43).

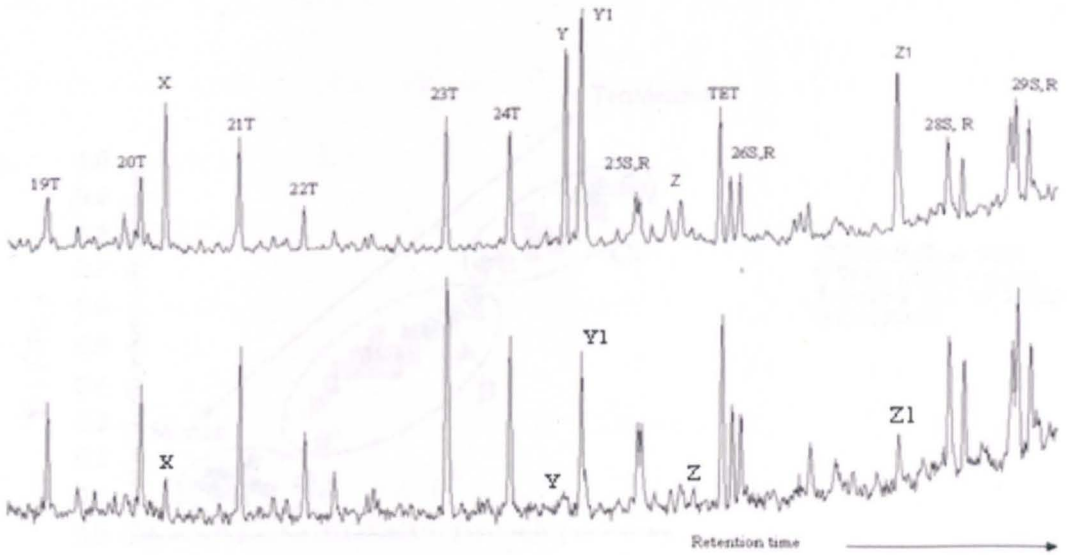

Figure 5.40. Representative partial m/z 191 showing the distributions of tricyclic and tetracyclic terpanes in a typical terrigenous oil (sample NDO02, upper) and marine organofacie type oil (sample NDO23, lower). Peak identity is provided in appendix IIIc.

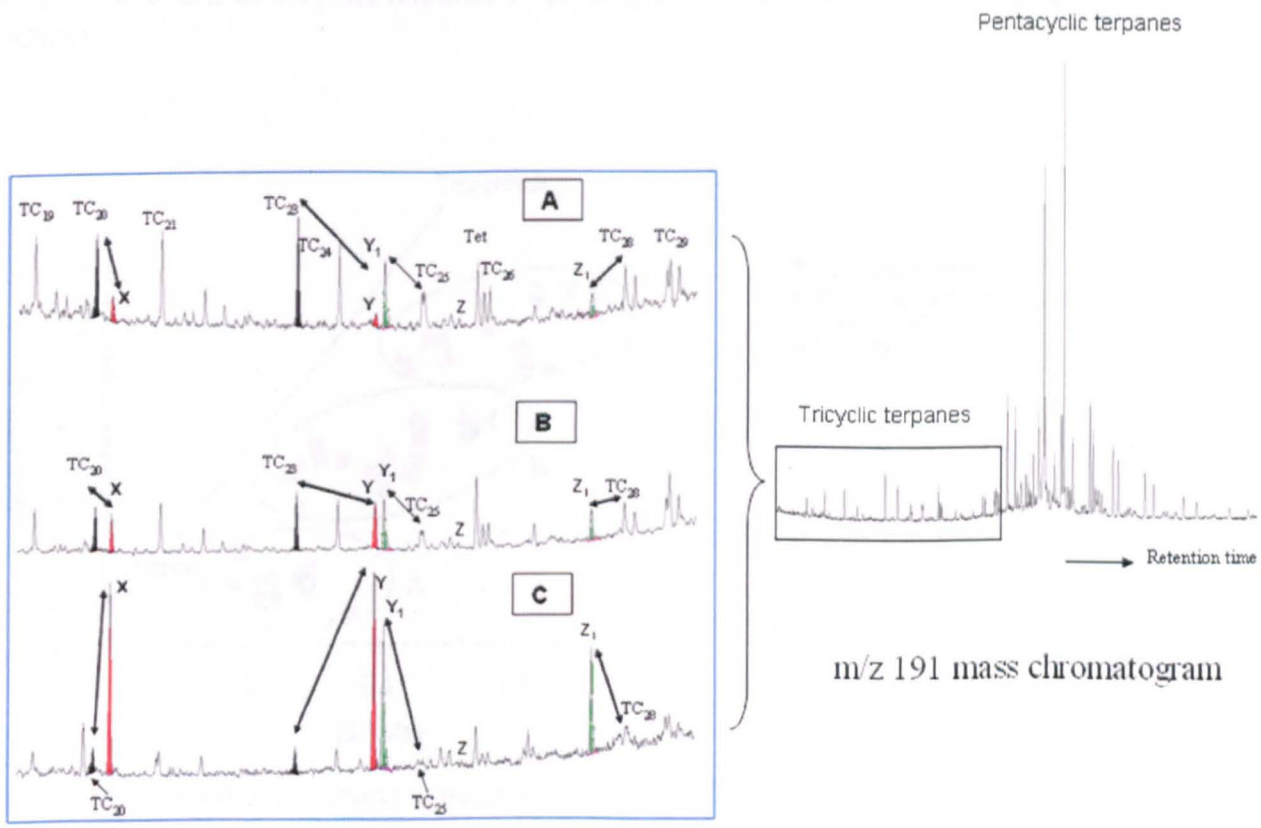

Figure 5.41. Partial m/z 191 mass chromatogram showing the distribution of common tricyclic terpanes and unknown compounds X , Y, Y_1, Z and Z_1 in oils of the three families. Peaks annotation TC_{19}- TC_{29} = C_{19}-C_{29} tricyclic terpanes. Tet = tetracyclic terpane.

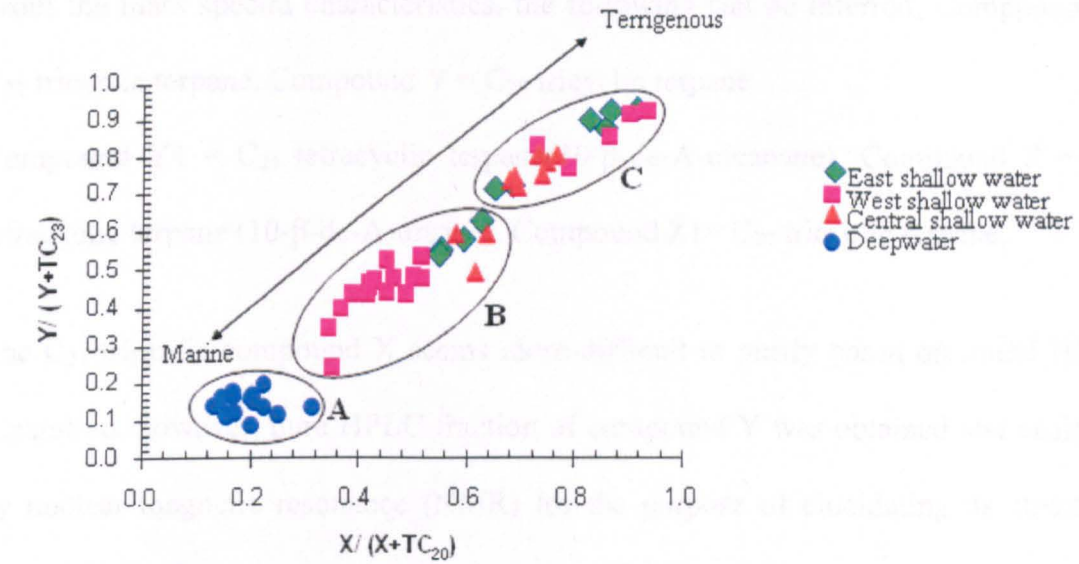

Figure 5.42. Cross plot of the $X/X+TC_{20}$ and $Y/Y+TC_{23}$ tricyclic terpanes terrigenous index (TTTI). X and Y are two unknown tricyclic terpanes, while TC_{20} and TC_{23} are the well-characterized tricyclic terpanes containing 20 and 23 carbons in their ring structures.

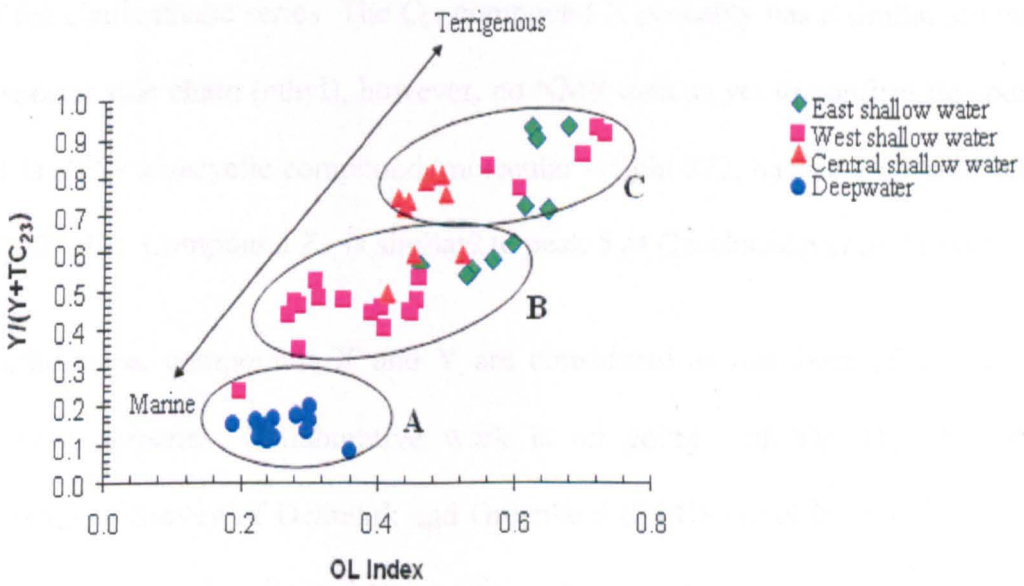

Figure 5.43. Cross plot of oleanane index against Y/Y+TC23 showing a positive correlation between the two parameters. OL Index = oleanane index (18 α(H) +18 β(H)-oleanane/ 17α(H), 14 β(H)-C_{30} hopane. Y is the unknown tricyclic terpane compound Y in figure 5.41. TC_{23} = tricyclic terpane containing 23 carbons in its ring structure.

The mass spectra for compounds X, Y, Y1, Z and Z1 are shown in Figures 5.44- 5.48. From the mass spectra characteristics, the following can be inferred; Compound X= *C_{21} tricyclic terpane.* Compound Y = C_{25} tricyclic terpane

Compound Y1 = C_{24} tetracyclic terpane(10-β-de-A-oleanane). Compound Z = C_{24} tetracyclic terpane (10-β-de-A-ursane). Compound Z1= C_{27} tricyclic terpane.

The C_{21} tricyclic compound X seems more difficult to purify based on initial HPLC separation, however, pure HPLC fraction of compound Y was obtained and analysed by nuclear magnetic resonance (NMR) for the purpose of elucidating its structure. Based on NMR structural data (Figure 5.45), compound Y is a degradational product of oleanane with a schematic proposed formational pathway shown in Figure 5.45. It forms by degradation of rings A and B, leaving rings C, D and E intact in the oleanane structure (Figure 5.45). The structure of compound Y is unlike the tricyclic terpanes of the cheilanthane series. The C_{21} compound X probably has a similar structure with a shorter side chain (ethyl), however, no NMR data as yet to confirm this possibility. Z1 is a C_{27} tetracyclic compound, molecular weight 372, having a C3 side chain (329 = 372 - 43). Compound Z1 is similar? to peak 5 of Czochanska *et al.* (1988).

Furthermore, compounds X and Y are considered as members of a new series of tricyclic terpanes. Collaborative work is on going with Dr. H.P. Nytoft at the Geological Survey of Denmark and Greenland (GEUS) to elucidate the structures of these unknown tricyclic and tetracyclic compounds by a nuclear magnetic resonance (NMR).

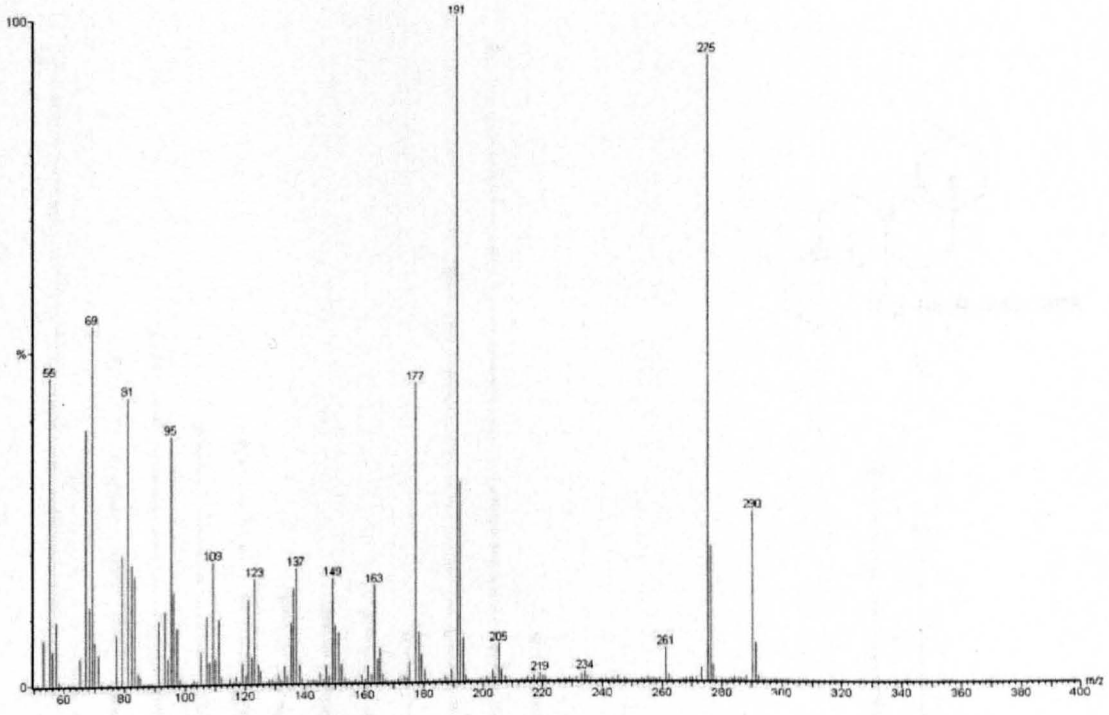

Figure 5.44. Mass spectrum of compound X.

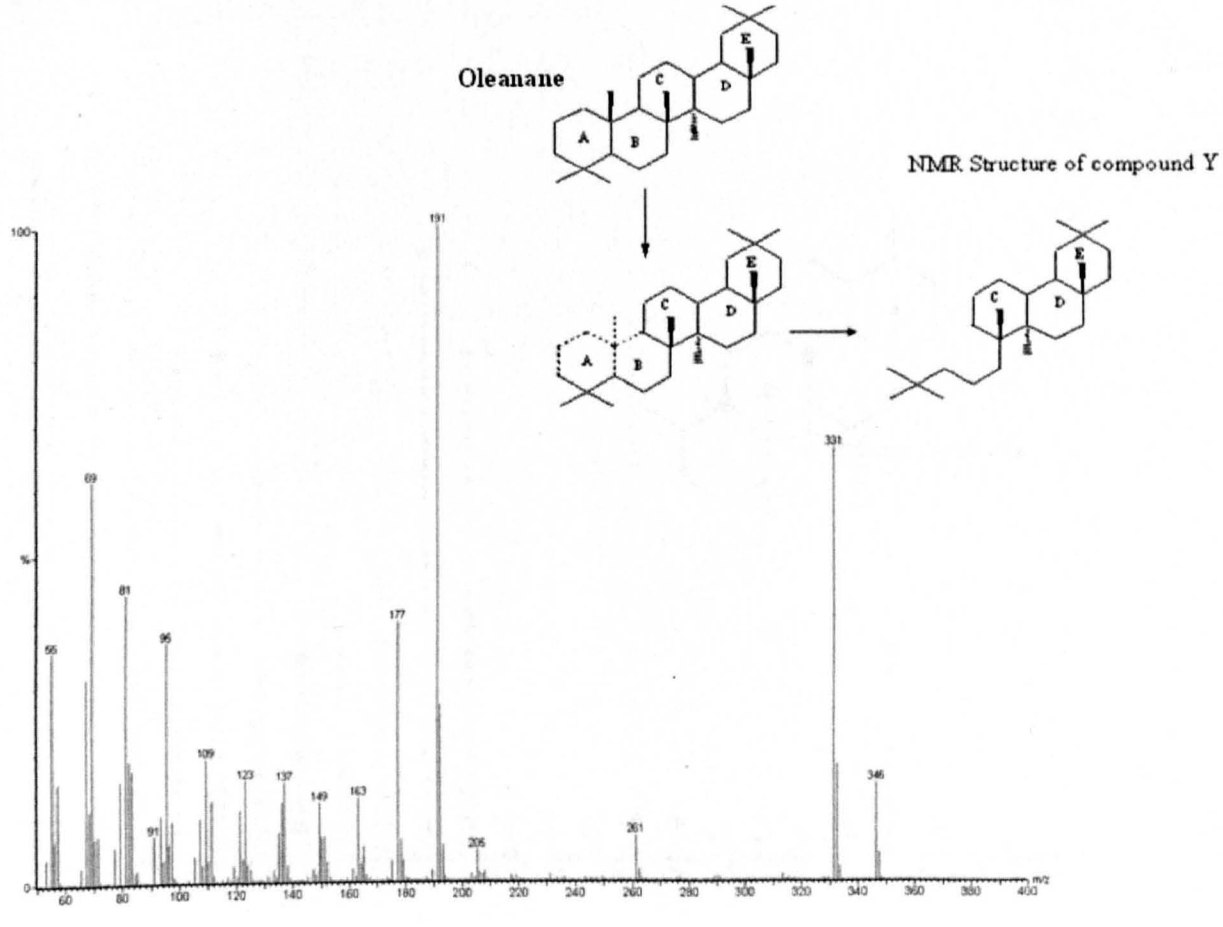

Figure 5.45. Mass spectrum of compound Y

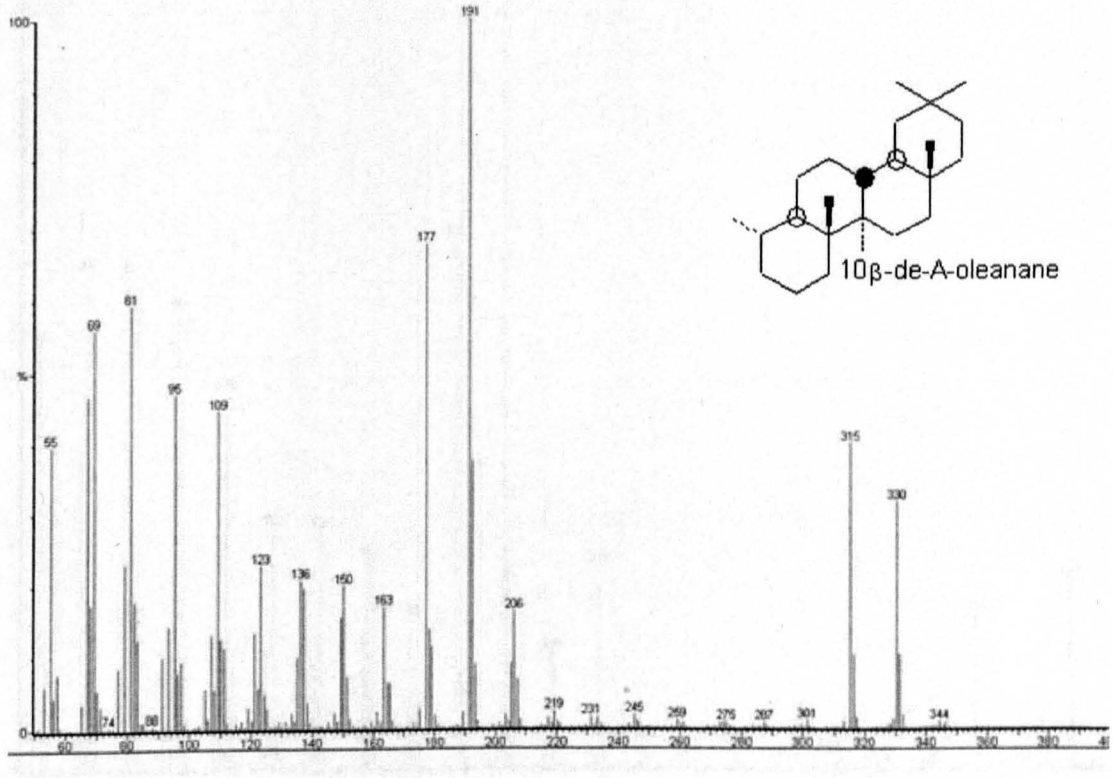

Figure 5.46. Mass spectrum for compound Y1.

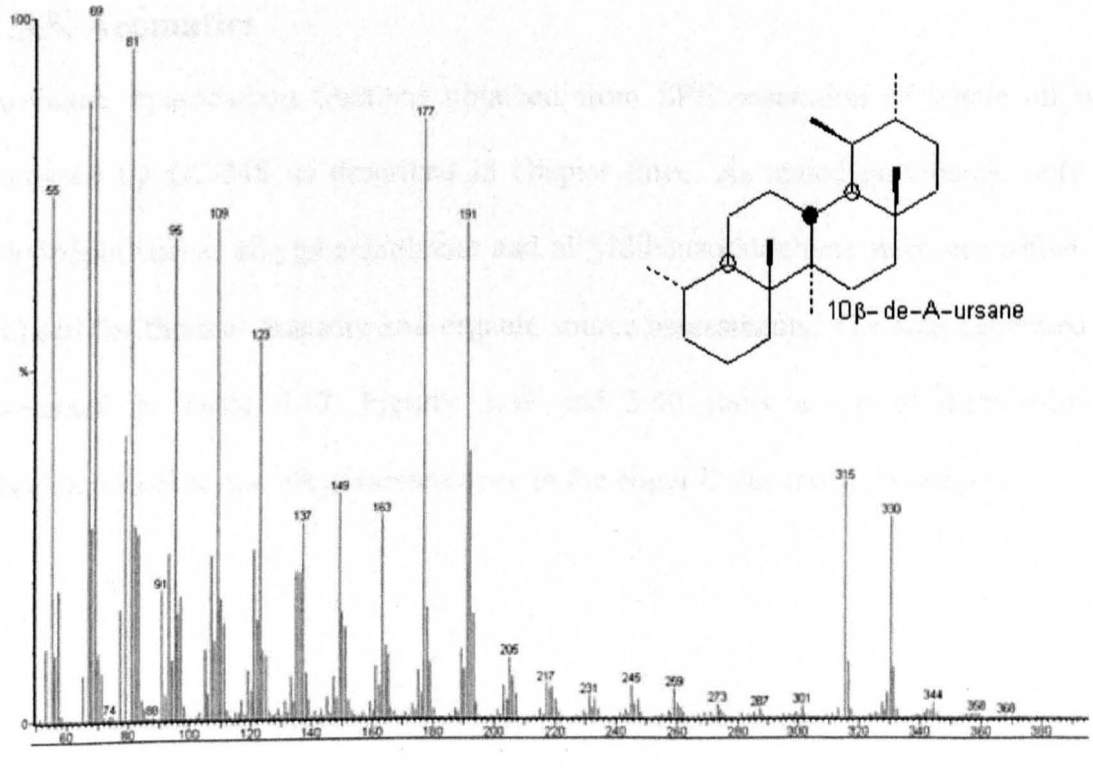

Figure 5.47. Mass spectrum for compound Z

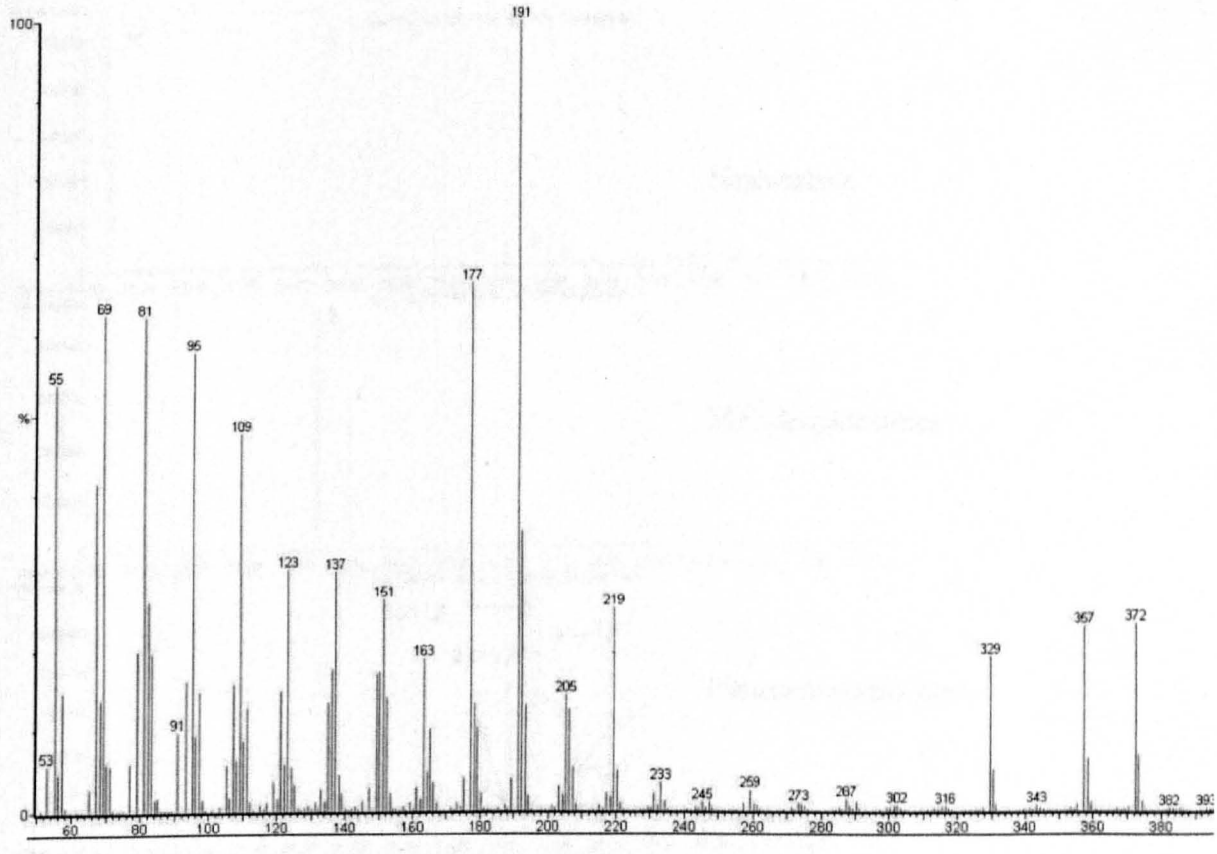

Figure 5.48. Mass spectrum for compound Z1.

5.5.5. Aromatics

Aromatic hydrocarbon fractions obtained from SPE separation of whole oil were analysed by GC-MS as described in chapter three. As stated previously, only the alkylnaphthalene, alkylphenanthrene and alkyldibenzothiophene were quantified and utilised for thermal maturity and organic source assessments. The data generated are presented in Table 5.17. Figures 5.49 and 5.50 show a typical distribution of alkylnaphthalene and alkylphenanthrene in the Niger Delta crude oil samples.

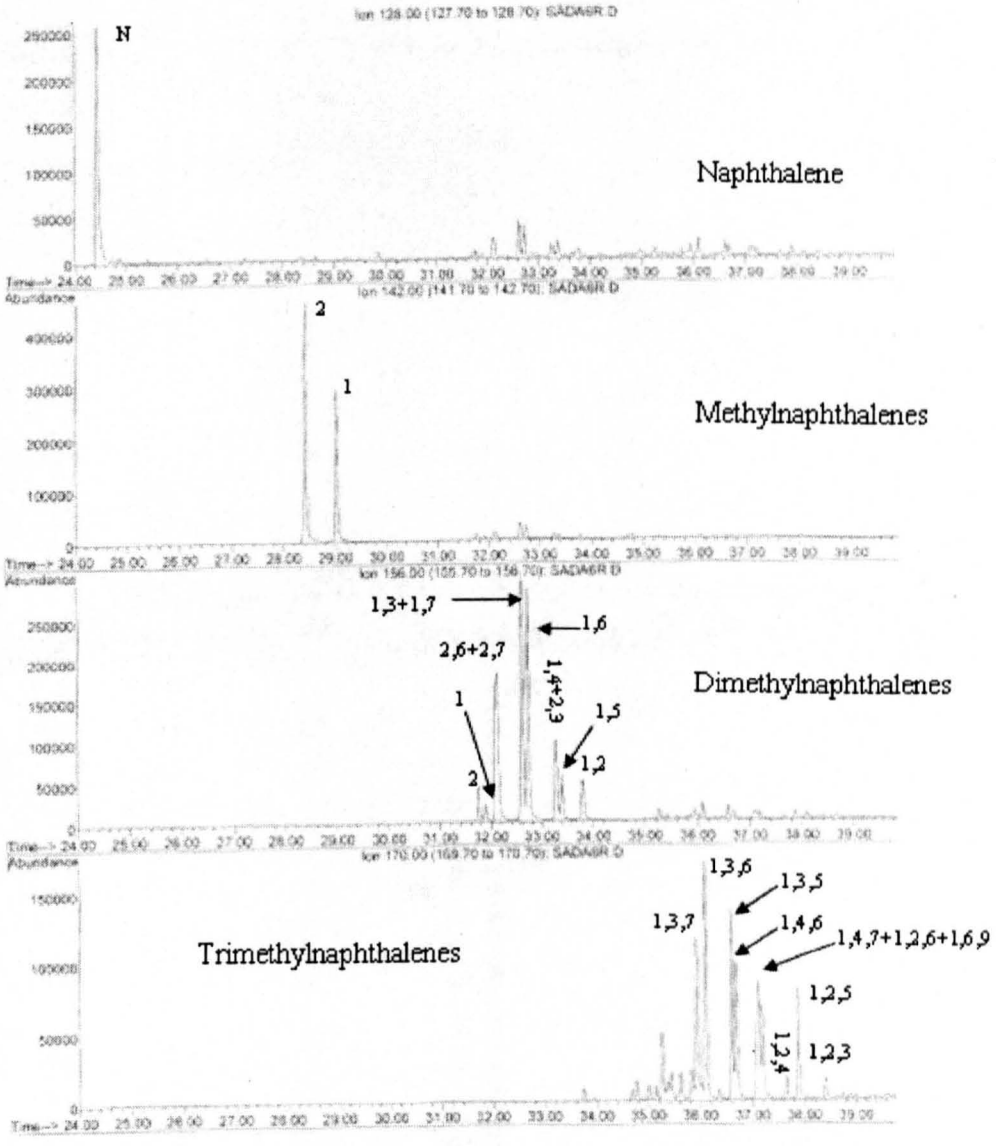

Figure 5.49. GC-MS m/z 128, 142, 156 and 170 showing the distributions of naphthalene and alkylnaphthalenes in a representative oil (sample NDO17) from the Niger Delta. Note integer denotes the position of alkylation in each isomer.

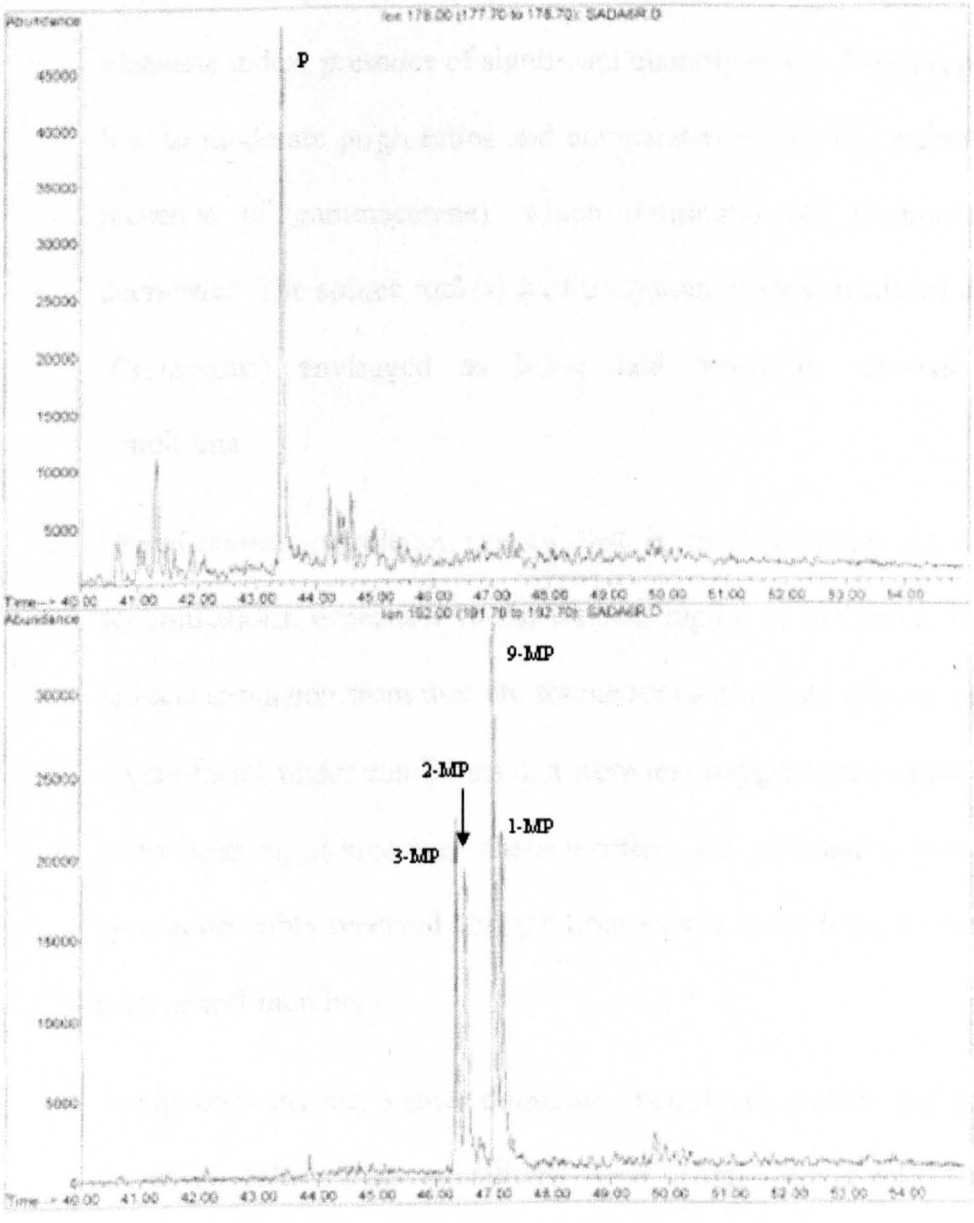

Figure 5.50. GC-MS m/z 178 and 192 showing the distributions of phenanthrenene and methylphenanthrenes in a representative oil (sample NDO17) from the Niger Delta. P = phenanthrene, and 2-MP, 3-MP, 9-MP and 1-MP are methylphenanthrenes with the integers denoting the position of methyl substitution on the phenanthrene ring structure.

5.5.6. Summary of source facies and thermal maturity

The molecular data presented in this study show that two different end-member oil families and an intermediate family reflecting expulsion from at least two distinct bulk source rock organofacies are present within the Niger Delta oil accumulations. The three oil families require three petroleum systems as follows:

1. A petroleum system charged by a source rock rich in marine kerogen (low oleanane index, presence of significant quantity of C_{30} 24-*n*-propyl cholestane, low to moderate pr/ph ratios and comparatively low C_{29} sterane content and presence of gammacerane), which dominates oil accumulations in the deepwater. The source rock(s) for this system is/are considered to be sub-delta (Cretaceous) envisaged as being laid down in sub-oxic depositional conditions.

2. Mixed-marine petroleum system that is most common in shallow water accumulations, especially in the western region of the delta. This oil system reflects expulsion from discrete source rocks of mixed marine and terrigenous organofacies under conditions that were less oxygenated compared to those of overwhelming terrigenous characteristics. An alternative view is that this system probably received charges from source rocks from the terrigenous and marine end-members.

3. Terrigenous organic matter dominated petroleum system that is pervasive in the entire delta oil accumulations. Oils of this system reflect the true delta source rocks described for the Niger Delta in terms of molecular characteristics (high oleanane index, high C_{29} sterane and high pr/ph ratios).

Table 5.15. Sterane source and maturity molecular parameters measured for the Niger Delta oil set

Sample	Region	%C_{27} Reg	%C_{28} Reg	%C_{29} Reg	%C_{30} Reg	%C_{27} Dia	%C_{28} Dia	%C29 Dia	C_{29} ααα	C_{29}αββ	Dia/Reg	C_{29}/C_{27}	Hop/Ster
NDO01	East	17.04	17.07	65.89	0.00	32.55	25.41	42.04	0.20	0.29	0.50	3.87	3.50
NDO02	East	22.36	25.95	51.69	0.00	24.88	26.72	48.40	0.47	0.50	1.05	2.31	1.33
NDO03	East	13.55	14.13	72.32	0.00	17.83	21.59	60.57	0.37	0.47	1.19	5.34	2.83
NDO04	East	21.95	23.88	54.17	1.49	24.50	23.76	51.75	0.46	0.51	1.09	2.47	1.69
NDO05	East	21.20	25.54	53.26	1.11	23.67	23.81	52.52	0.49	0.51	1.41	2.51	1.05
NDO06	East	14.98	9.64	75.38	0.00	17.00	15.64	67.36	0.34	0.39	0.77	5.03	6.43
NDO07	East	21.48	29.19	49.33	1.00	20.65	27.68	51.67	0.47	0.50	1.02	2.30	1.69
NDO08	East	14.05	17.65	68.29	0.00	15.97	15.83	68.19	0.41	0.44	1.38	4.86	3.92
NDO09	East	33.00	26.94	40.06	1.39	34.34	28.34	37.32	0.41	0.43	0.87	1.21	0.98
NDO10	East	13.32	17.03	69.66	0.00	11.25	17.00	71.75	0.40	0.46	0.98	5.23	4.76
NDO11	East	32.66	31.54	35.79	0.73	37.55	29.11	33.34	0.41	0.43	0.86	1.10	0.91
NDO12	Deepwater	32.15	28.32	39.53	3.16	38.73	29.65	31.62	0.43	0.41	0.78	1.23	0.44
NDO13	Deepwater	36.06	28.13	35.81	1.41	42.65	27.97	29.38	0.31	0.35	0.67	0.99	1.86
NDO14	Deepwater	38.16	28.18	33.66	1.15	41.64	31.27	27.09	0.32	0.33	0.88	0.88	1.34
NDO15	Deepwater	33.17	27.78	39.05	1.31	40.64	30.77	28.59	0.32	0.37	0.79	1.18	1.15
NDO16	Deepwater	35.24	29.66	35.10	1.08	36.80	28.05	35.15	0.38	0.40	0.76	1.00	1.39
NDO17	Deepwater	34.01	28.85	37.14	0.77	40.17	29.12	30.71	0.34	0.32	0.67	1.09	1.98
NDO18	Deepwater	37.71	30.09	32.20	0.82	43.72	28.85	27.44	0.37	0.40	0.92	0.85	1.83
NDO19	Deepwater	34.59	30.62	34.79	1.55	43.38	29.32	27.30	0.35	0.38	0.80	1.01	0.78
NDO20	Deepwater	36.85	28.81	34.34	1.88	43.90	28.45	27.66	0.39	0.37	1.04	0.93	1.21
NDO21	Deepwater	38.77	31.77	29.46	1.68	44.34	29.07	26.59	0.36	0.43	1.09	0.76	1.45
NDO22	Deepwater	48.24	21.14	30.62	0.67	45.95	27.31	26.73	0.42	0.38	1.66	0.63	1.46
NDO23	Deepwater	33.85	31.28	34.87	1.09	42.33	29.26	28.40	0.44	0.47	1.25	1.03	1.62
NDO24	Deepwater	28.29	28.74	42.97	0.94	32.36	28.11	39.53	0.32	0.42	1.07	1.52	0.28
NDO26	Deepwater	32.40	35.06	32.54	1.98	35.56	28.73	35.71	0.25	0.37	0.37	1.00	2.44
NDO29	West	21.69	23.79	54.52	0.00	40.54	14.32	45.14	0.24	0.38	0.72	2.51	6.60
NDO30	West	16.29	22.07	61.64	0.00	22.06	30.35	47.59	0.26	0.44	1.00	3.78	3.30
NDO31	West	20.99	18.52	60.49	0.00	31.09	21.00	47.92	0.31	0.43	1.22	2.88	2.53

Sample	Region	%C27 Reg	%C28 Reg	%C29 Reg	%C30 Reg	%C27 Dia	%C28 Dia	%C29 Dia	$C_{29\ \alpha\alpha\alpha}$	$C_{29\alpha\beta\beta}$	Dia/Reg	C29/C27	Hop/Ster
NDO32	West	15.38	16.81	67.81	0.00	19.05	22.48	58.47	0.21	0.36	0.62	4.41	3.35
NDO33	West	29.50	22.66	47.84	1.44	39.41	24.91	35.67	0.32	0.43	1.06	1.62	2.42
NDO34	West	30.37	23.49	46.15	0.00	25.95	21.23	52.82	0.40	0.44	0.37	1.52	0.56
NDO35	West	22.42	25.07	52.52	0.00	25.90	24.62	49.48	0.30	0.40	0.91	2.34	1.87
NDO36	West	21.09	25.36	53.55	0.36	25.14	26.55	48.31	0.36	0.41	0.37	2.54	2.30
NDO37	West	11.59	18.05	70.37	0.00	12.91	18.96	68.14	0.20	0.37	0.79	6.07	5.48
NDO40	West	33.05	27.71	39.24	1.13	38.64	25.29	36.06	0.44	0.47	0.71	1.19	1.32
NDO41	West	29.88	27.73	42.39	1.18	31.96	30.83	37.22	0.38	0.46	1.43	1.42	1.58
NDO42	West	21.04	15.46	63.50	0.00	19.78	40.44	39.78	0.35	0.38	0.46	3.02	2.94
NDO43	West	16.95	27.91	55.13	0.00	21.71	28.59	49.70	0.42	0.47	0.54	3.25	3.23
NDO44	West	27.92	27.77	44.31	1.40	36.31	22.89	40.81	0.57	0.63	0.89	1.59	0.63
NDO45	West	27.74	21.91	50.36	1.45	35.07	17.13	47.81	0.41	0.44	0.81	1.82	2.86
NDO46	West	24.92	22.93	52.15	0.00	26.74	22.51	50.75	0.36	0.49	0.65	2.09	3.13
NDO47	West	23.79	26.00	50.21	1.46	29.05	25.46	45.49	0.53	0.52	1.30	2.11	1.65
NDO48	Central	23.23	22.41	54.36	0.00	27.67	21.67	50.66	0.40	0.46	1.19	2.34	1.33
NDO49	Central	23.73	28.36	47.91	0.00	28.32	23.57	48.11	0.29	0.45	0.85	2.02	1.50
NDO50	Central	20.74	23.63	55.63	0.00	22.58	20.38	57.03	0.40	0.50	1.11	2.68	1.84
NDO51	Central	21.85	27.91	50.23	0.00	25.93	24.73	49.34	0.25	0.40	0.61	2.30	1.50
NDO52	Central	24.96	27.17	47.87	0.00	27.77	19.76	52.47	0.23	0.40	0.63	1.92	1.90
NDO53	Central	21.76	19.78	58.47	0.00	26.50	18.40	55.10	0.40	0.46	1.12	2.69	1.85
NDO54	Central	23.57	27.08	49.35	0.81	28.32	23.79	47.89	0.26	0.40	0.80	2.09	1.68
NDO55	Central	21.70	27.08	51.22	0.48	29.23	23.69	47.08	0.25	0.41	0.59	2.36	1.77
NDO56	Central	29.06	29.50	41.44	0.81	26.31	26.27	47.42	0.40	0.47	0.70	1.43	1.11
NDO57	Central	27.88	29.86	42.25	0.71	23.89	27.35	48.76	0.38	0.47	0.70	1.52	1.13
NDO58	Central	28.04	28.29	43.66	0.47	28.63	24.46	46.91	0.43	0.47	0.59	1.56	1.11

% C_{27} Reg = % C_{27} ααα sterane to sum 27-29 ααα regular steranes also calculated for C_{28}, C_{29} and C_{30} sterane; % C_{27}Dia = %C27 to sum 27-29 βα diasteranes C_{29} ββ = 5 α(H),14β(H), 17β(H) 20S +R / 5α(H),14β(H), 17β(H) + 5α(H),14α(H), 17α(H) 20 S+R C29 steranes. C_{29}αα = 5α(H),14α(H), 17α(H)- C_{29} 20S/20S+20R sterane isomerisation maturity parameter. Dia/ Reg = Sum of 13β(H), 17α(H) and 13α(H), 17β(H) 20S+20R diasteranes/ sum of 5α(H), 14α(H), 17α(H) and 5α(H),14 β(H),17β(H) 20S+20R)for the 27,28 and 29 compounds obtained from GC-MS-MS. C_{29}/C_{27} = ratio of C29/C27 for 5α(H),14α (H), 17α(H) 20R sterane. All data were obtained from appropriate GC-MS-MS transitions. 0.00 = no data due to either low level or absence of one or more of the compounds in the parameter.

Table 5.16. Terpane source and maturity parameters measured for the Niger Delta oils

Sample	Region	OL	35/34	Ga/Hop	26T/25T	23T/24T	Tet/Hop	23T/21T	19T/23T	Tet/23T	C32 αβ	Ts/Ts+Tm	30 αβ / 30 αβ +βα
NDO01	East	0.55	0.68	0.39	1.07	1.19	0.05	0.91	1.09	1.18	0.52	0.45	0.82
NDO02	East	0.57	0.51	0.00	1.12	1.04	0.03	1.02	0.66	1.04	0.53	0.44	0.83
NDO03	East	0.66	0.34	0.00	1.70	1.07	0.04	1.32	1.20	1.45	0.54	0.44	0.82
NDO04	East	0.61	0.52	0.00	0.87	1.18	0.03	1.00	0.70	1.03	0.55	0.40	0.84
NDO05	East	0.65	0.49	0.00	0.92	1.06	0.04	1.05	0.76	1.15	0.55	0.41	0.82
NDO06	East	0.62	0.53	0.00		1.20	0.02	0.43	2.65	2.08	0.52	0.44	0.85
NDO07	East	0.53	0.52	0.00	1.03	1.10	0.04	1.04	0.37	1.02	0.54	0.41	0.84
NDO08	East	0.63	0.39	0.00	0.62	0.82	0.03	0.57	1.62	2.00	0.54	0.42	0.83
NDO09	East	0.53	0.55	0.00	0.97	1.01	0.03	1.00	0.43	1.08	0.54	0.43	0.84
NDO10	East	0.68	0.44	0.00			0.00				0.51	0.44	0.84
NDO11	East	0.60	0.55	0.06	0.85	1.10	0.04	1.09	0.53	1.10	0.54	0.42	0.82
NDO12	Deepwater	0.36	0.72	1.49	1.01	1.59	0.08	1.91	0.39	0.64	0.55	0.45	0.82
NDO13	Deepwater	0.23	0.57	0.73	1.00	1.36	0.05	1.65	0.71	0.98	0.54	0.56	0.87
NDO14	Deepwater	0.23	0.65	0.69	1.06	1.51	0.05	1.72	0.42	0.94	0.53	0.55	0.85
NDO15	Deepwater	0.25	0.71	0.67	1.27	1.28	0.04	1.83	0.35	0.76	0.55	0.54	0.86
NDO16	Deepwater	0.30	0.70	0.65	1.12	1.50	0.04	1.61	0.27	0.75	0.56	0.47	0.86
NDO17	Deepwater	0.24	0.61	0.80	0.99	1.57	0.04	1.41	0.44	0.87	0.55	0.53	0.85
NDO18	Deepwater	0.30	0.63	0.78	1.19	1.26	0.06	1.34	0.57	0.89	0.51	0.51	0.83
NDO19	Deepwater	0.24	0.65	0.93	1.07	1.24	0.06	1.75	0.51	0.72	0.54	0.50	0.85
NDO20	Deepwater	0.24	0.57	1.02	1.01	1.35	0.07	1.69	0.30	0.68	0.53	0.58	0.85
NDO21	Deepwater	0.22	0.74	0.93	0.11	1.35	0.08	1.83	0.64	0.67	0.53	0.58	0.85
NDO22	Deepwater	0.28	0.55	0.54	0.87	1.39	0.10	1.23	0.70	0.58	0.56	0.55	0.88
NDO23	Deepwater	0.25	0.81	0.58	1.76	1.41	0.06	1.29	0.42	0.75	0.54	0.53	0.85
NDO24	Deepwater	0.23	0.67	1.00	1.26	1.52	0.07	1.89	0.55	0.66	0.49	0.63	0.85
NDO26	Deepwater	0.19	0.45	0.39	1.05	1.06	0.06	1.19	0.80	1.51	0.53	0.49	0.84
NDO29	West	0.56	0.59	0.00	1.39	1.61	0.04	0.78	1.09	1.61	0.55	0.50	0.82
NDO30	West	0.41	0.51	0.68	0.91	1.09	0.07	1.26	0.87	1.16	0.56	0.49	0.83
NDO31	West	0.60	0.50	0.43	1.26	1.19	0.06	0.95	1.16	1.09	0.56	0.50	0.82

Sample	Region	OL	35/34	Ga/Hop	26T/25T	23T/24T	Tet/Hop	23T/21T	19T/23T	Tet/23T	C32 αβ	Ts/Ts+Tm	30 αβ / 30 αβ +βα
NDO32	West	0.70	0.53	0.27	0.84	1.01	0.04	0.71	1.17	1.10	0.51	0.48	0.82
NDO33	West	0.40	0.71	0.73	1.19	1.15	0.06	1.20	0.92	1.37	0.56	0.47	0.84
NDO34	West	0.45	0.70	0.00	0.91	1.29	0.05	1.16	0.66	0.83	0.51	0.49	0.83
NDO35	West	0.39	0.61	0.69	0.98	1.13	0.07	1.20	0.95	1.32	0.55	0.45	0.83
NDO36	West	0.46	0.61	0.41	1.03	1.05	0.04	1.20	0.68	0.98	0.57	0.46	0.84
NDO37	West	0.73	0.46	0.00	1.08	1.05	0.03		0.63	1.12	0.48	0.49	0.84
NDO40	West	0.28	0.52	0.90	1.03	1.32	0.07	1.26	1.08	1.57	0.56	0.50	0.86
NDO41	West	0.44	0.66	0.71	0.93	1.19	0.07	1.31	0.80	1.26	0.54	0.52	0.85
NDO42	West	0.28	0.52	0.42	1.22	1.02	0.04	0.96	1.40	2.11	0.55	0.45	0.86
NDO43	West	0.35	0.55	0.24	0.82	0.98	0.05	0.97	1.15	1.17	0.57	0.55	0.88
NDO45	West	0.31	0.63	0.37	1.19	1.24	0.05	1.33	0.81	1.21	0.56	0.52	0.86
NDO46	West	0.27	0.67	0.33	0.95	1.18	0.05	1.17	0.91	1.42	0.57	0.51	0.87
NDO47	West	0.20	0.55	0.26	1.15	1.20	0.04	1.58	0.44	0.94	0.57	0.42	0.86
NDO48	Central	0.44	0.47	0.00	1.32	1.02	0.04	0.74	1.37	1.43	0.54	0.46	0.85
NDO49	Central	0.49	0.48	0.00	1.20	1.11	0.03	0.73	1.68	1.13	0.56	0.49	0.85
NDO50	Central	0.43	0.41	0.00	0.55	1.10	0.03	0.70	1.56	1.29	0.57	0.43	0.84
NDO51	Central	0.47	0.47	0.00	1.64	1.24	0.03	1.05	1.10	1.03	0.53	0.44	0.85
NDO52	Central	0.48	0.26	0.00	1.17	0.97	0.03	0.74	1.75	1.35	0.52	0.44	0.85
NDO53	Central	0.44	0.66	0.00	0.99	0.99	0.04	0.79	1.62	1.40	0.52	0.45	0.85
NDO54	Central	0.50	0.46	0.00	0.73	1.26	0.03	1.04	1.37	0.96	0.56	0.45	0.85
NDO55	Central	0.47	0.64	0.00	1.84	1.21	0.03	0.91	1.37	1.23	0.52	0.44	0.84
NDO56	Central	0.45	0.53	0.00	1.18	1.20	0.03	1.17	0.77	0.76	0.55	0.41	0.85
NDO57	Central	0.88	0.47	1.25	0.98	1.19	0.30	1.19	0.70	0.87	0.53	0.42	0.34
NDO58	Central	0.41	0.47	0.14	1.19	1.21	0.04	1.50	0.51	0.76	0.56	0.45	0.83

OL = 18α(H)+18β(H) oleanane/C_{30} 17α(H), 21β(H)- Hopane. 35/34 = ratio of 17α(H), 21β(H)-pentakishomohopane (22S+ 22R)/ 17α(H), 21β(H)- tetrakis homohopane (22S +22R). Ga /hop = 10*gammacerane / C_{30} 17α(H), 21β(H)- Hopane. 26T/25T = C_{26} tricyclic terpane/ C_{25} tricyclic terpane. 23T/24T= C_{23} tricyclic terpane/ C_{24} tricyclic terpane. Tet/Hop = tetracyclic terpane/ C_{30} 17α(H), 21β(H)- Hopane. 23T/21T = C_{23} tricyclic terpane/ C_{21} tricyclic. 19T/23T = C_{19} tricyclic terpane/ C_{23} tricyclic. Tet/ 23T = tetracyclic terpane (24-des-E-hopane)/ C_{23} tricyclic. C_{32} αβ = 17α(H), 21β(H)-bishomohopane 22S/ 22S+ 22R. Ts/Ts+Tm = 18α(H)-22,29,30- Trisnorneohopane (Ts)/ 18α(H)- 22,29,30- Trisnorneohopane (Ts) + 17α(H)- 22,29,30-trisnorhopane (Tm). 30αβ/30αβ+ βα = 17α(H), 21β(H) hopane/ 17α(H), 21β(H) hopane = 17β(H), 21α(H) hopane (moratane). 0.00 = no data due to either low level or absence of one or more of the compounds in the parameter

Table 5.17. Selected aromatic thermal maturity and source parameters from the Niger Delta oils.

Sample	MPI-1	MPI-2	MNR	ENR	DNR-1	TNR-1	DBT/P	MDR	MDR-1
NDO01	0.79	0.68	1.57	2.59	7.14	0.75	0.15	4.88	0.44
NDO02	0.81	0.77	1.44	2.42	6.49	0.73	0.04	4.80	0.78
NDO03	0.80	0.78	1.55	1.97	7.35	0.80	0.07	6.89	0.26
NDO04	0.84	0.79	1.36	2.49	6.45	0.77	0.08	3.73	0.44
NDO05	0.81	0.79	1.46	2.55	6.36	0.75	0.05	4.59	0.58
NDO06	0.85	0.79	1.37	2.08	6.64	0.77	0.10	8.87	0.30
NDO07	0.80	0.76	1.40	2.47	6.40	0.74	0.09	3.75	0.45
NDO08	0.72	0.60	1.14	2.20	5.03	0.79	0.09	4.52	0.76
NDO09	0.81	0.79	1.01	2.13	4.82	0.76	0.15	5.40	0.37
NDO10	0.80	0.74	1.44	2.23	6.96	0.77	0.10	4.12	0.37
NDO11	0.85	0.81	1.35	2.19	5.95	0.79	0.11	5.28	0.55
NDO12	0.83	0.83	1.61	1.75	1.41	0.17	0.13	3.79	0.61
NDO13	0.60	0.61	1.58	2.26	5.21	0.76	0.06	13.69	0.12
NDO14	0.57	0.56	1.63	2.38	5.24	0.73	0.04	9.06	0.19
NDO15	0.62	0.63	1.47	1.94	5.22	0.74	0.08	8.03	0.20
NDO16	0.61	0.62	1.45	2.14	5.46	0.74	0.08	6.05	0.21
NDO17	0.58	0.57	1.57	2.12	5.41	0.72	0.08	5.62	0.25
NDO18	0.61	0.60	1.46	2.19	5.61	0.75	0.05	10.01	0.15
NDO19	0.78	0.77	1.38	2.12	5.28	0.70	0.10	10.27	0.22
NDO20	0.63	0.65	1.46	2.32	5.60	0.71	0.05	7.26	0.27
NDO21	0.63	0.66	1.37	2.16	5.25	0.68	0.06	8.23	0.24
NDO22	0.64	0.62	1.46	2.85	7.34	0.75	0.04	12.11	0.15
NDO23	0.65	0.66	1.43	2.65	6.16	0.73	0.02	8.81	0.26
NDO24	0.55	0.51	1.49	2.06	5.49	0.69	0.05	10.27	0.20
NDO25	0.70	0.63	1.29	1.74	7.48	0.84	0.08	8.05	0.32
NDO26	0.70	0.62	1.32	1.74	8.35	0.79	0.06	15.71	0.19
NDO29	0.84	0.78	1.50	2.37	6.66	0.78	0.11	8.65	0.23
NDO30	0.88	0.87	1.78	2.97	7.55	0.76	0.07	6.58	0.31
NDO31	0.83	0.81	1.67	2.69	8.37	0.79	0.06	14.59	0.13

Sample	MPI-1	MPI-2	MNR	ENR	DNR-1	TNR-1	DBT/P	MDR	MDR-1
NDO32	0.98	0.99	1.94	3.79	10.53	0.83	0.05	5.75	0.36
NDO33	0.93	0.93	1.38	1.92	6.17	0.76	0.15	3.24	0.31
NDO34	0.56	0.49	1.32	1.94	5.37	0.73	0.04	7.52	0.45
NDO35	0.90	0.88	1.29	2.22	5.59	0.71	0.10	4.75	0.49
NDO36	0.63	0.63	1.36	2.15	5.67	0.73	0.07	5.41	0.29
NDO37	0.78	0.00	0.00	0.00	0.00	0.00	0.07	7.65	0.22
NDO40	0.78	0.78	0.89	0.93	4.08	0.82	0.07	6.49	0.29
NDO41	0.91	0.90	1.38	2.12	7.62	0.77	0.11	6.63	0.31
NDO42	0.82	0.78	1.50	3.67	7.06	0.81	0.06	7.62	0.30
NDO43	0.75	0.72	1.29	2.22	5.59	0.71	0.07	7.36	0.13
NDO45	0.82	0.81	1.32	2.37	5.96	0.79	0.27	4.75	0.35
NDO46	0.71	0.65	1.38	2.12	6.28	0.77	0.04	6.26	0.65
NDO47	0.67	0.68	1.53	2.46	6.98	0.76	0.05	3.88	0.35
NDO48	0.89	0.89	1.47	2.65	8.49	0.78	0.13	8.68	0.16
NDO49	0.87	0.84	1.27	2.45	6.25	0.77	0.16	7.07	0.18
NDO50	0.89	0.89	1.68	2.67	8.52	0.77	0.13	7.89	0.18
NDO51	0.86	0.83	1.37	2.07	6.59	0.75	0.01	12.87	0.15
NDO52	0.87	0.88	1.69	4.05	8.75	0.79	0.16	8.46	0.16
NDO53	0.88	0.87	1.67	2.63	8.51	0.78	0.14	8.69	0.15
NDO54	0.85	0.84	1.64	2.75	8.71	0.79	0.16	10.02	0.12
NDO55	0.86	0.85	1.63	2.73	8.68	0.80	0.17	8.94	0.13
NDO56	0.79	0.79	1.73	2.36	7.00	0.74	0.13	5.35	0.26
NDO57	0.79	0.78	1.30	2.46	3.00	0.84	0.12	6.89	0.24
NDO58	0.63	0.62	1.32	2.03	5.45	0.75	0.12	5.00	0.29

MPI-1= 1.5*(2-MP+ 3-MP)/ (P + 1-MP + 9-MP); Radke *et al.*, (1982a). MPI-2 = (3* 2-MP/ (P+ 1-MP + 9-MP); Radke *et al.*, (1982a). MNR = (2-MN/ 1-MN); Radke *et al.*, (1982b). ENR = 2-EN/1-EN; Radke *et al.*, (1982b). DNR-1 = (2,6-DMN+ 2,7-DMN)/ 1,5-DMN; Radke *et al.*, (1982b). TNR-1 = 2,3,6-TMN/ (1,4,6-TMN + 1,3,5-TMN); Alexander *et al.*, (1985).DBT/P = dibenzothiophene/ phenanthrene. MDR = 4-MDBT/1-MDBT; Radke *et al.*, (1986). MDR-1= 1-MDBT/DBT; Radke *et al.*, (1982a). 0.00 = no data due to either low level or absence of one or more of the compounds in the parameter

5.6. Geochemical Characteristics of oils from Kutei Basin

5.6.1. N-alkanes and isoprenoid alkanes

Samples of oils from the Kutei Basin exhibit waxy *n*-alkane distributions. Most samples in this set are light oils (mostly condensates) and because of this they are particularly low in high molecular weight hydrocarbon components. Figure 5.51 is a typical gas chromatograph of *n*-alkane distribution for the oil/condensate samples, showing both light-end depleted and light-end dominated distributions. The data for *n*-alkane and isoprenoid alkane common ratios are presented in Table 5.18. The pr/ph ratio ranges from 2.51 to 11.01 thus reflecting source rock deposition in oxic depositional environments.

5.6.2. Steranes

Biomarker analyses could only be performed on three samples because most of the fluids are condensates and are inherently therefore low in biomarkers found amongst the higher molecular weight hydrocarbon components. For the analysed samples, the sterane data are presented in Table 5.19. The sterane carbon distribution is dominated by the C_{29} homologues (Table 5.19, Figures 5.52 and 5.53), which may reflect overwhelming terrigenous higher plants contributions. Under the mass spectrometry analytical conditions used, C_{30} 24-*n*- propylcholestane was not detected in the samples as shown by the absence of its peak in the m/z 414→217 transition in Figure 5. 52.

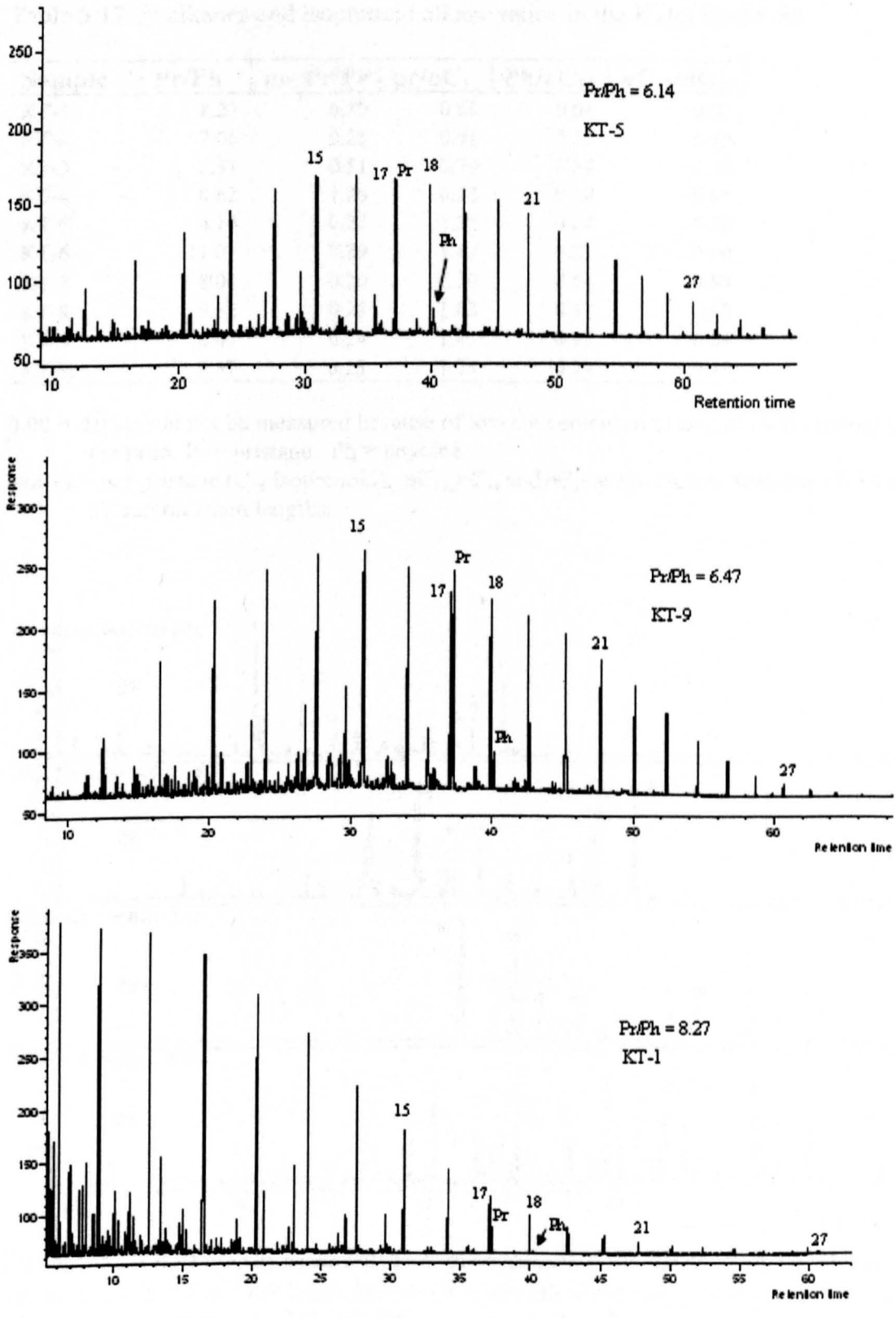

Figure 5.51. Representative gas chromatograms showing the distributions of *n*-alkanes and isoprenoid alkanes in samples of oils from Kutei Basin.

Table 5.17. *N*-alkanes and isoprenoid alkane ratios in the Kutei Basin oils.

Sample	Pr/Ph	norPr/Pr	pr/nC_{17}	Ph/nC_{18}	nC_{17}/nC_{27}
KT-1	8.27	0.30	0.68	0.08	0.03
KT-2	7.66	0.23	0.91	0.11	0.15
KT-3	2.51	0.51	0.79	0.38	0.39
KT-4	8.62	1.26	0.22	0.18	0.01
KT-5	6.14	0.23	1.37	0.24	0.20
KT-6	11.01	0.29	1.47	0.22	0.00
KT-7	8.04	0.20	6.30	0.54	0.88
KT-8	9.52	0.28	1.85	0.32	0.00
KT-9	6.47	0.24	1.43	0.25	0.04
KT-10	7.37	0.25	1.78	0.29	0.19

0.00 = data could not be measured because of low concentration of one or more compounds in the ratio. Pr = pristane. Ph = phytane.

Nor Pr = nor pristane (C_{18} isoprenoid). nC_{17}, nC_{18} and nC_{27} are n-alkanes with the 17, 18 and 27 carbon chain lengths.

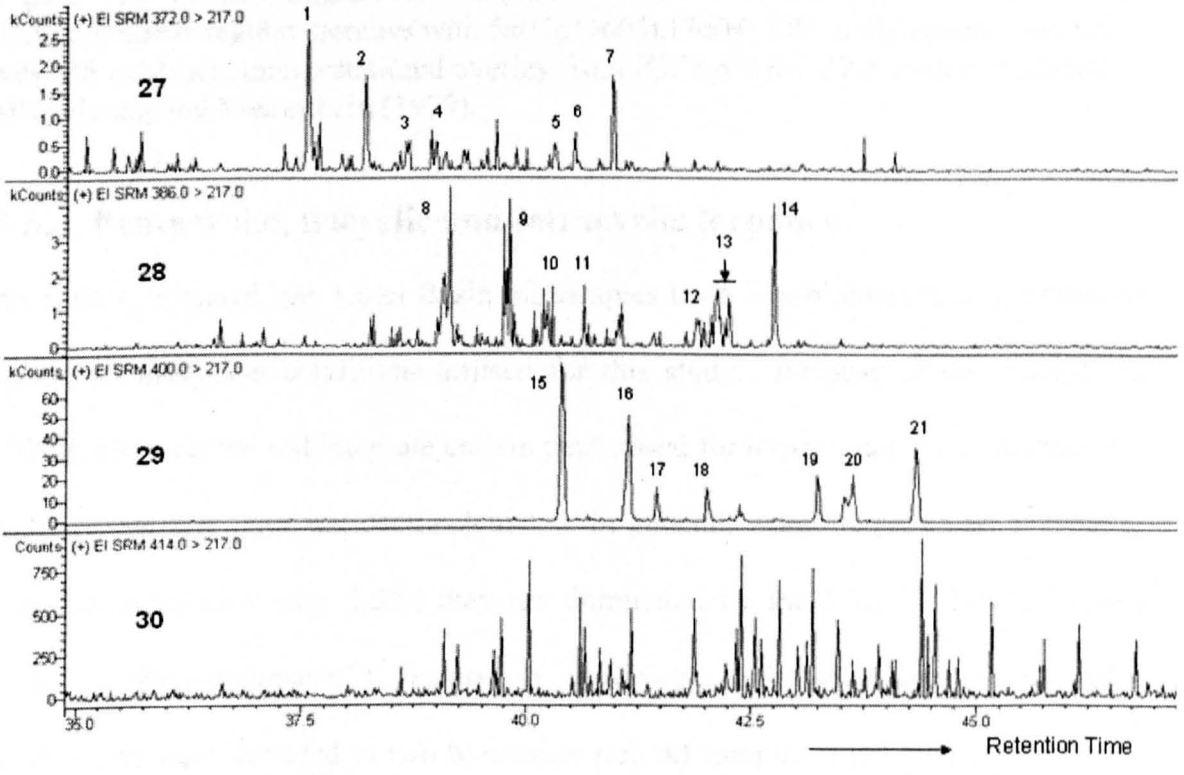

Figure 5.52. GC-MS-MS mass chromatogram showing the distributions of steranes in oil sample KT-5 from the Kutei Basin. GC-MS-MS chromatograms shown are: m/z 372➔217 (C_{27} steranes), 386➔217(C_{28} steranes), 400➔217 (C_{29} Steranes) and 414➔217(C_{30} steranes). Peak annotation is in Appendix IIIa.

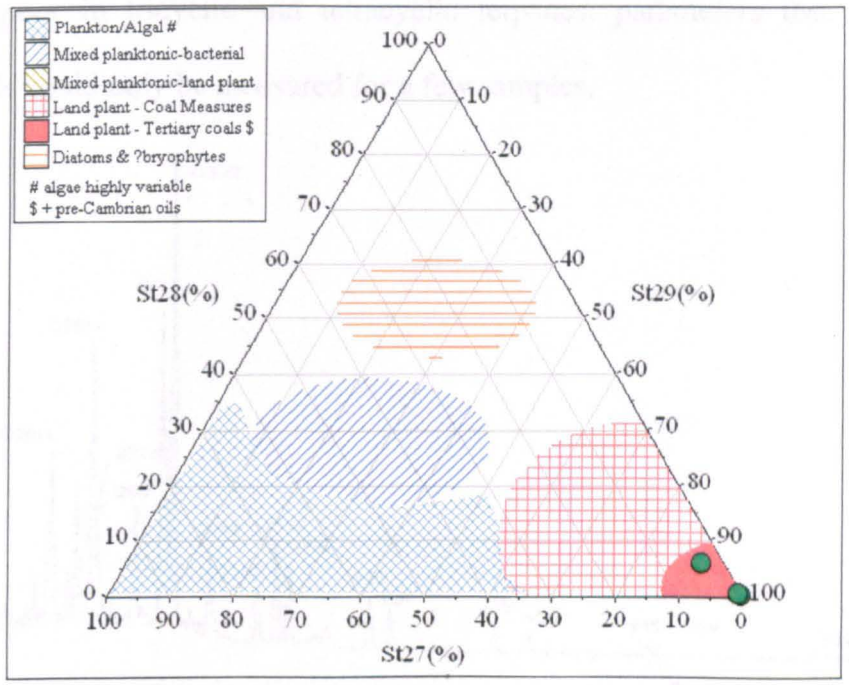

Figure 5.53. Ternary diagram showing the distribution of the Kutei oils 27, 28 and 29 carbon number regular steranes with 5α(H),14α(H),17α(H) 20R configuration, from GC-MS-MS analyses. Interpretational overlay from IGI's p:IGI-2.27 software modified after Huang and Meinschein (1979).

5.6.3. Pentacyclic, tricyclic and tetracyclic terpanes

As earlier indicated, the Kutei Basin oil samples have low biomarker concentrations under the analytical conditions utilised for this study. Because of the inability to effectively separate and integrate certain peaks used for terpane ratios and parameters, some parameters have not been calculated. In general, where terpanes are present in abundance (as in Figure 5.54), they are dominated by the 17α(H), 21β(H)-hopane series. Oleanane+lupane(?) occurs in relatively high abundance (peak OL). Norlupanes were detected in two biomarker rich oil samples using appropriate parent to daughter ions transitions and the lupanoid measured ratios range from 0.27 to 0.44(Table 5.20). A compound tentatively identified as taraxastane (Tar?), eluting before 17α-22S- homohopane, occurs as a significant peak. There is a low relative abundance of C_{35} pentakishomohopane, which may reflect highly oxygenated conditions and the nature of organic matter (hydrogen richness) of the source rock. Additionally, the oils

are very poor in tricyclic and tetracyclic terpanes: parameters that utilise these compounds could only be measured for a few samples.

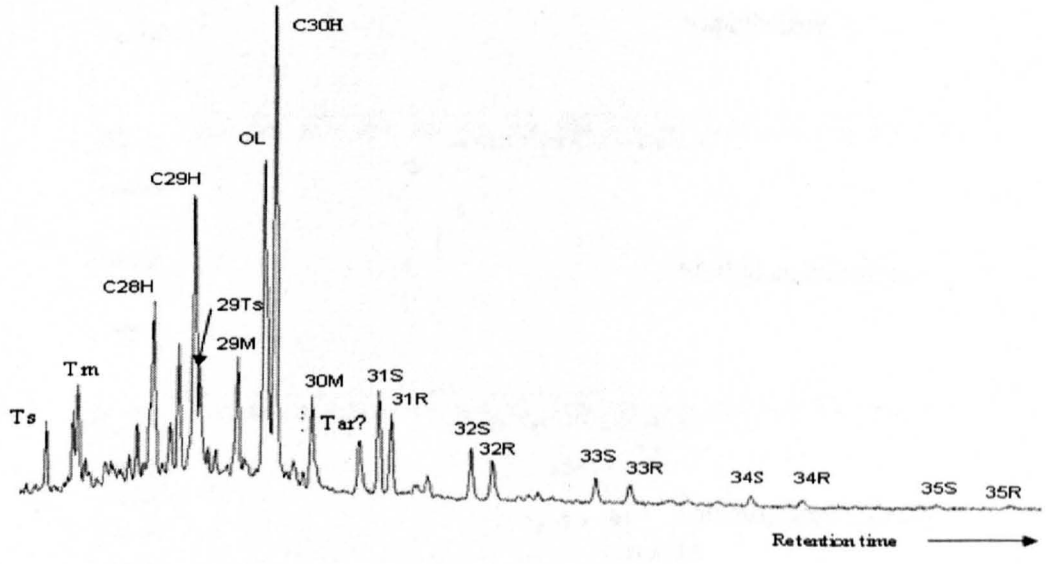

Figure 5.54. Partial m/z 191 mass chromatogram showing the distribution of terpanes in a representative Kutei oil sample (KT-5). Peak identities are provided in Appendix IIIb.

5.6.4. Aromatics

Only the alkylnaphthalenes, alkylphenanthrenes and alkyldibenzothiophenes were quantified and utilised for thermal maturity and organic source assessments. The data generated are presented in Table 5.21. Figure 5.55 and 5.56 show representative distributions of alkylnaphthalenes and alkylphenanthrenes in the Kutei Basin oil sample KT-5. Interestingly, despite low sterane and terpane concentration in most samples the, aromatics hydrocarbon fraction of these oils contain relatively high amounts of high molecular weight aromatic compounds, thus permitting the measurement of aromatic hydrocarbon thermal maturity data for most oil samples whose saturated hydrocarbon data could not be determined. On this basis the Kutei Basin oils were expelled from relatively mid-late mature source rocks (Table 5.20).

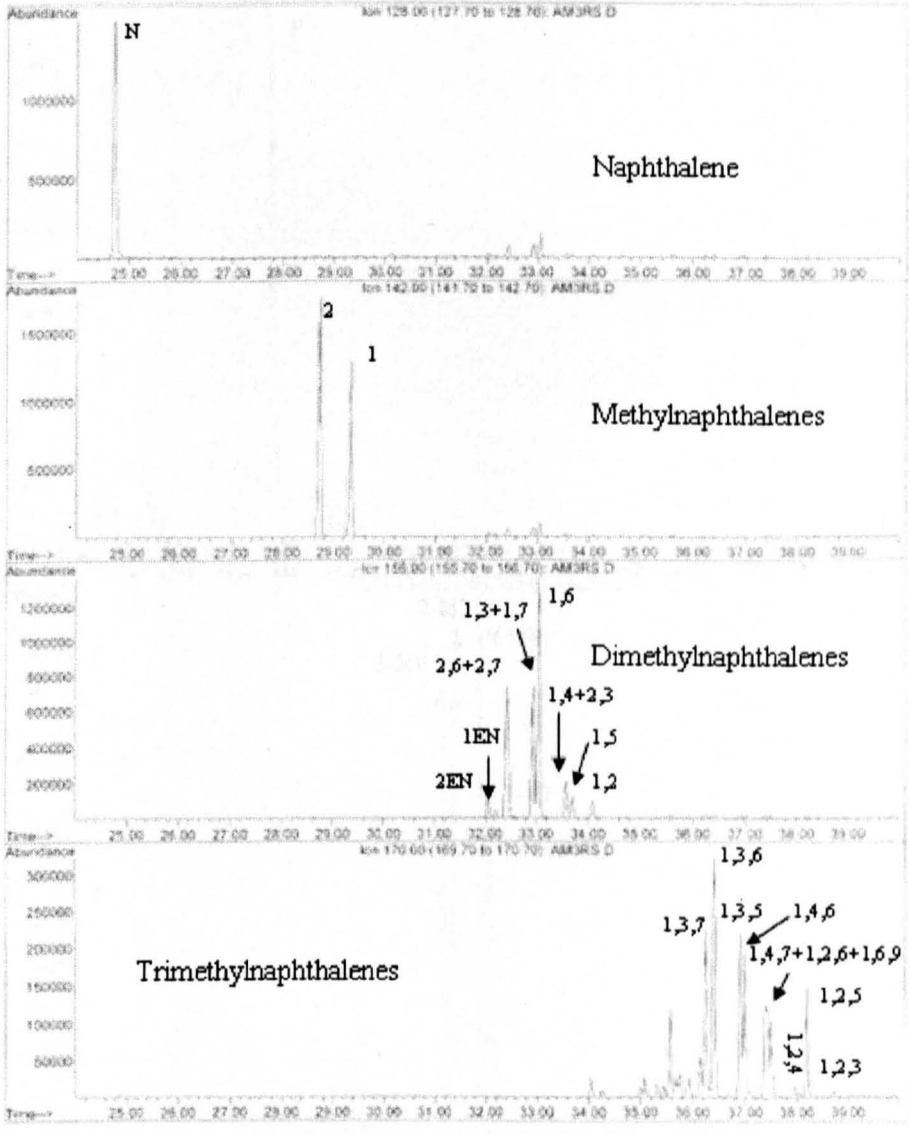

Figure 5.55. GC-MS m/z 128, 142, 156 and 170 mass chromatograms showing the distributions of naphthalene and alkylnaphthalenes in a representative oil (sample KT-5) from the Kutei Basin. Note integer denotes the position of alkylation in each isomer. EN represents ethylnaphthalene.

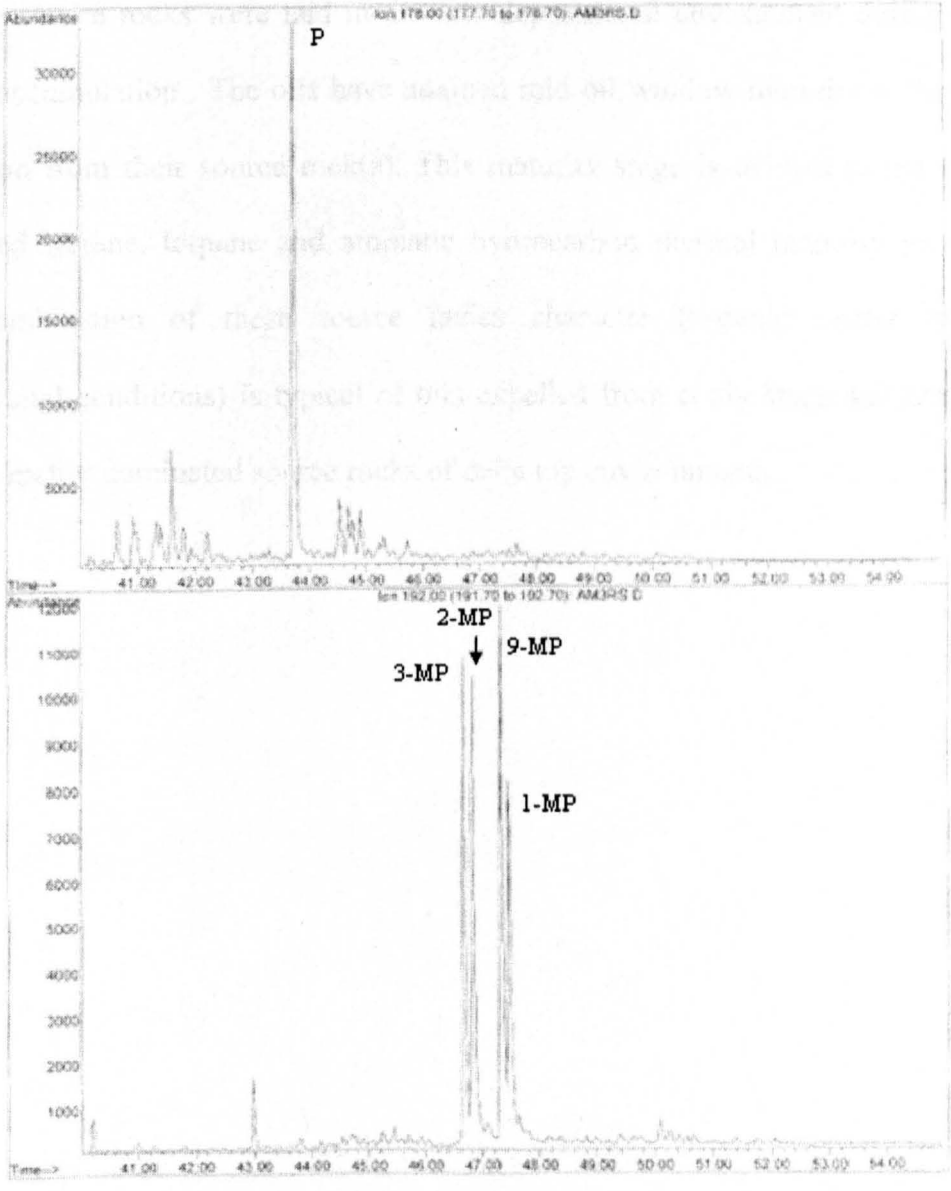

Figure 5.56. GC-MS m/z 178 and 192 mass chromatograms showing the distributions of phenanthrene and methylphenanthrenes in a representative oil (sample KT-5) from the Kutei Basin. P = phenanthrene, and 2-MP, 3-MP, 9-MP and 1-MP are methylphenanthrenes with the integers denoting the position of methyl substitution on the phenanthrene ring.

5.6.5. Summary of source facies and thermal maturity

On the basis of the molecular properties of the analysed Kutei oil/condensate samples in this study, the oils have been derived overwhelmingly from source rock facies that received abundant terrigenous higher plants organic input (abundant *n*-alkane >C_{21}), high C_{29} sterane content, oleanane index and absence of C_{30} 24-*n*-propylcholestane. Additionally, the high pr/ph ratios and absence of gammacerane in the oils suggest

that the source rocks were laid in an oxic depositional environment during organic matter accumulation. The oils have attained mid oil window maturity at the time of expulsion from their source rock(s). This maturity stage is evident in the ratios of measured sterane, terpane and aromatic hydrocarbon thermal maturity parameters. The combination of these source facies character (organic matter type and depositional conditions) is typical of oils expelled from coaly shale and terrigenous organic matter dominated source rocks of delta top environments.

Table 5.18. Sterane source and maturity parameters measured for the Kutei Basin oil set.

Sample	%C27	%C28	%C29	%C30	%C27 Dia	%C28 Dia	%C29 Dia	% C30 Dia	C29 αββ	C29 ααα	Dia/Reg	29/27
KT-1	0.00	0.00	0.00	0.00	0.00	0.00	0.00	0.00	0.00	0.00	0.00	0.00
KT-2	0.00	0.00	0.00	0.00	0.00	0.00	0.00	0.00	0.00	0.00	0.00	0.00
KT-3	0.00	0.00	0.00	0.00	0.00	0.00	0.00	0.00	0.00	0.00	0.00	0.00
KT-4	0.00	0.00	0.00	0.00	0.00	0.00	0.00	0.00	0.00	0.00	0.00	0.00
KT-5	2.81	5.38	91.81	0.00	2.88	6.28	90.84	0.00	0.39	0.33	2.70	32.67
KT-6	0.00	0.00	0.00	0.00	0.00	0.00	0.00	0.00	0.00	0.00	0.00	0.00
KT-7	9.92	16.12	73.96	0.00	11.78	17.43	70.79	0.00	0.43	0.44	3.97	7.45
KT-8	0.00	0.00	0.00	0.00	0.00	0.00	0.00	0.00	0.00	0.00	0.00	0.00
KT-9	0.00	0.00	0.00	0.00	0.00	0.00	0.00	0.00	0.00	0.00	0.00	0.00
KT-10	4.39	5.77	89.84	0.00	5.72	5.41	88.86	0.00	0.31	0.18	1.25	20.48

% C27 Reg = % C_{27} ααα sterane to sum 27-29 ααα regular steranes also calculated for C_{28}, C_{29} and C_{30} sterane; % C27Dia = %C_{27} to sum 27-29 13 β(H), 17α(H) – diasteranes. C_{29} αββ = 5α(H),14β(H), 17β(H) -20S +20R / 5α(H),14β(H), 17β(H) + 5α(H),14α(H), 17α(H)- 20 S+R C29 steranes. C_{29}ααα = 5 α(H),14α(H), 17α(H)- C_{29} 20S/20S+20R sterane isomerisation maturity parameter. Dia/ Reg = Sum of 13β(H), 17α(H) and 13 α(H), 17 β(H)- 20S+20R diasteranes/ sum of 5α(H), 14α(H), 17α(H) and 5α(H), 14β(H), 17β(H) -20S+20R for the 27,28 and 29 compounds obtained from GC-MS-MS. C29/C27 = ratio of C_{29}/C_{27} for 5 α(H),14 α(H), 17 α(H) -20R sterane. All data were obtained from appropriate GC-MS-MS transitions. 0.00 = no data due to either low level or absence of one or more of the compounds in the parameter.

Table 5.19. Terpane source and maturity parameters of the oils from the Kutei Basin

Sample	OL	Lup	Bicad	C_{35}/C_{34}	Ga/Hop	26T/25T	23T/24T	Tet/Hop	23T/21T	19T/23T	Tet/23T	C_{32} αβ	Ts/Ts+Tm	30αβ/30αβ +βα
KT-1	0.00	0.00	0.00	0.00	0.00	0.00	0.00	0.00	0.00	0.00	0.00	0.00	0.00	0.00
KT-2	0.00	0.00	0.00	0.00	0.00	0.00	0.00	0.00	0.00	0.00	0.00	0.00	0.00	0.00
KT-3	0.00	0.00	0.00	0.00	0.00	0.00	0.00	0.00	0.00	0.00	0.00	0.00	0.00	0.00
KT-4	0.00	0.00	0.00	0.00	0.00	0.00	0.00	0.00	0.00	0.00	0.00	0.00	0.00	0.00
KT-5	0.46	0.44	10.90	0.47	0.00	0.00	0.00	0.00	0.00	0.00	0.00	0.51	0.40	0.79
KT-6	0.00	0.00	0.00	0.00	0.00	0.00	0.00	0.00	0.00	0.00	0.00	0.00	0.00	0.00
KT-7	0.38	0.27	13.11	0.65	0.00	0.00	0.00	0.00	0.00	0.00	0.00	0.55	0.32	0.84
KT-8	0.00	0.00	0.00	0.00	0.00	0.00	0.00	0.00	0.00	0.00	0.00	0.00	0.00	0.00
KT-9	0.00	0.00	0.00	0.00	0.00	0.00	0.00	0.00	0.00	0.00	0.00	0.00	0.00	0.00
KT-10	0.41	0.00	0.00	0.56	0.00	0.00	0.00	0.00	0.00	0.00	0.00	0.54	0.55	0.83

OL = 18α(H)+18β(H) oleanane/C_{30} 17α(H), 21β(H)- hopane. LUP = lupanoid index; 10 *(17α(H) bisnorlupane+ 17β(H) bisnorlupane +Norlupnae)/ C_{30} 17α(H), 21β(H)-hopane. Bicad = sum 100* (T + T_1 + R C_{30} bicadinanes)/ (T+T_1+R bicadinanes +17α(H),21β(H) hopanes. 35/34 = ratio of 17α(H), 21β(H)-pentakishomohopane (22S+ 22R)/ 17α(H), 21β(H)- tetrakishomohopane (22S +22R). Ga /hop = 10*gammacerane / C_{30} 17α(H), 21β(H)- Hopane. 26T/25T = C_{26} tricyclic terpane/ C_{25} tricyclic terpane. 23T/24T= C_{23} tricyclic terpane/ C_{24} tricyclic terpane. Tet/Hop = tetracyclic terpane/ C_{30} 17α(H), 21β(H)-hopane.23T/21T = C_{23} tricyclic terpane/ C_{21} tricyclic. 19T/23T = C_{19} tricyclic terpane/ C_{23} tricyclic. Tet/ 23T = tetracyclic terpane (24-des-E-hopane)/ C_{23} tricyclic. C_{32}αβ = 17α(H), 21β(H)-bishomohopane 22S/ 22S+ 22R. Ts/Ts+Tm = 18α (H)- 22,29,30- Trisnorneohopane (Ts)/ 18α(H)-22,29,30-Trisnorneohopane (Ts) + 17α(H)- 22,29,30-trisnorhopane (Tm). 30αβ/30αβ+βα = 17α(H), 21β(H) hopane/ 17α(H), 21β(H) hopane = 17β(H), 21α(H) -hopane (moretane). 0.00 = no data because of low level/absence of one or all of the compounds used in calculating the parameter.

Table 5.20. Aromatic hydrocarbon thermal maturity and source indicators from the Kutei Basin oils

Sample	MPI-1	MPI-2	MNR	ENR	DNR-1	TNR-1	DBT/P	MDR	MDR-1
KT-1	0.61	0.64	1.61	3.14	9.64	0.81	0.14	7.82	0.08
KT-2	0.74	0.80	1.53	1.99	8.06	0.78	0.14	7.41	0.13
KT-3	0.42	0.49	1.69	2.52	8.94	0.83	0.15	4.02	0.23
KT-4	0.44	0.46	0.00	0.00	0.00	0.00	0.28	13.10	0.38
KT-5	0.79	0.79	1.24	1.94	5.57	0.77	0.00	0.00	0.00
KT-6	0.00	0.00	1.33	1.52	5.68	0.73	0.00	0.00	0.00
KT-7	0.90	0.90	1.11	2.31	4.67	0.72	0.17	6.37	0.20
KT-8	0.00	0.00	1.53	2.48	5.24	0.72	0.00	0.00	0.00
KT-9	0.73	0.68	1.65	3.06	9.80	0.77	0.36	8.94	0.11
KT-10	0.31	0.34	1.69	2.38	6.48	0.80	0.13	6.30	0.18

MPI-1= 1.5*(2-MP+ 3-MP)/ (P + 1-MP + 9-MP); Radke *et al.*, (1982a). MPI-2 = (3* 2-MP/ (P+ 1-MP + 9-MP); Radke *et al.*, (1982a). MNR = (2-MN/ 1-MN); Radke *et al.*, (1982b). ENR = 2-EN/1-EN; Radke *et al.*, (1982b). DNR-1 = (2,6-DMN+ 2,7-DMN)/ 1,5-DMN; Radke *et al.*, (1982b). TNR-1 = 2,3,6-TMN/ (1,4,6-TMN + 1,3,5-TMN); Alexander *et al.*, (1985).DBT/P = dibenzothiophene/ phenanthrene. MDR = 4-MDBT/1-MDBT; Radke *et al.*, (1986). MDR-1= 1-MDBT/DBT; Radke *et al.*, (1982a).

5.7. Comparative biomarker organofacies signals in the studied oils and their source implications

This section aims to integrate the results of molecular analyses performed on the crude oil samples from studied basins to enable a comparative discussion of their source rock organofacies (organic matter type and depositional environment) characteristics.

5.7.1. Source rock organic matter type

The source rock organic matter type (marine algae vs. terrigenous higher plants) is interpreted based on their sterane compositions (C_{27}-C_{30} compounds) as well as the angiosperm marker (oleanane) which appears to be present to some extent in all of the oils presently accumulated within Tertiary deltaic sediments. Different plant communities have one or more of C_{27}-C_{30} compounds being relatively abundant in their sterol composition and this is reflected in the sterane composition of kerogen formed from these plant residues upon maturation. Thus the crude oil expelled from such kerogen, if insignificantly altered, will carry this signal. Briefly, the C_{27} sterane is copiously derived from marine phytoplankton (Goodwin, 1973; Volkman *et al.*, 1998) while C_{29} sterane compounds reflect input mostly from terrigenous higher plants (Huang & Meinschein, 1979).

Figure 5.57 is a ternary diagram of the C_{27}–C_{29} sterane composition in oils from the case study basins. This plot provides the means of comparing the oils in terms of their source rocks organic matter provenance. Samples of oils from the Assam Delta generally cluster in the C_{29} apex of the Figure 5.57 and they constitute oils grouping in Zone 3 of Figure 5.58 thus suggesting oil expulsion from source units rich in terrigenous higher plant matter that exemplify typical intra-delta sourced oils of the

delta top coaly facies. This observation is in accordance with the reports from previous workers that the oils have been derived from coaly and shale source units of the Barail Coal Group with overwhelmingly terrigenous organic matter (e.g. Raju & Mathur, 1995; Goswami *et al.*, 2005).

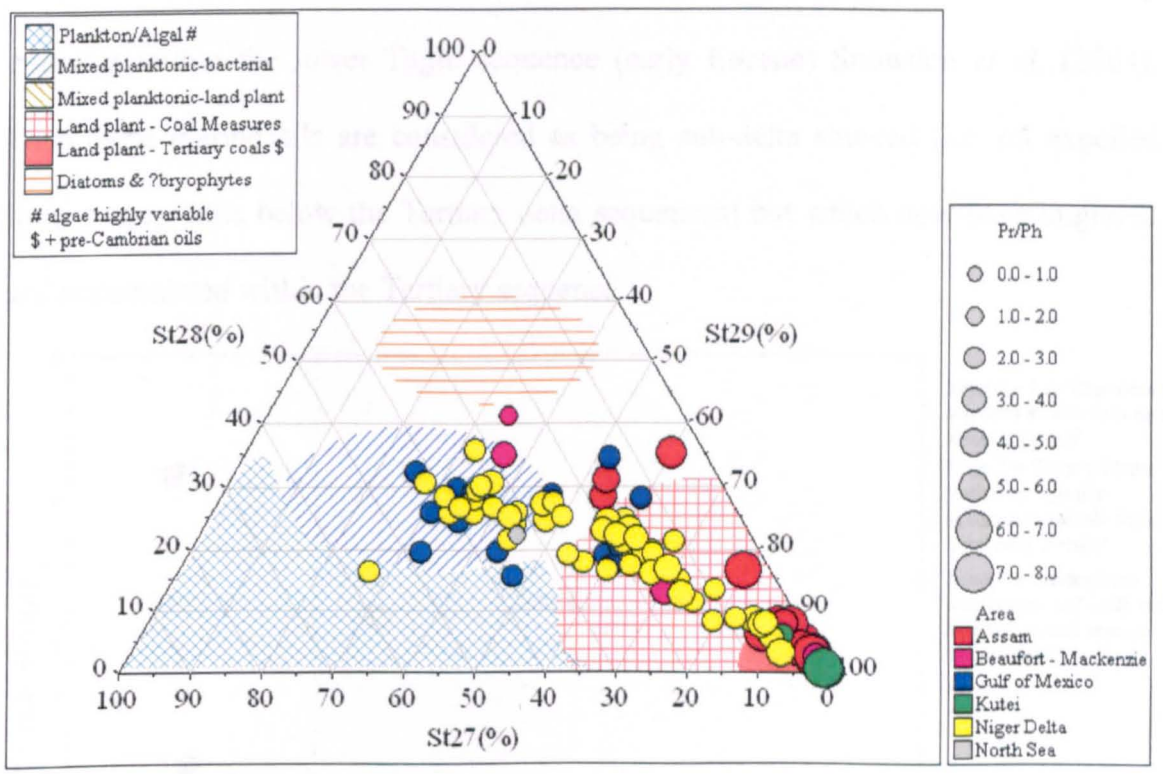

Figure 5.57. Ternary diagram showing the distribution of the 27, 28 and 29 carbon number regular steranes with 5α(H),14α(H),17α(H) 20R configuration from GC-MS-MS analyses of oils from the case study deltas. Interpretational overlay from IGI's p: IGI-2 software modified after Huang and Meinschein (1979). Note the North Sea oil permits a comparison of marine organofacies with the oils.

Conversely, samples of oils from the Beaufort-Mackenzie separate into two groups. The group plotting into the C_{29} sterane apex implicates expulsion from terrigenous higher plant organic matter source units while the oil group having higher C_{27} sterane contents are presumably expelled from source units with abundant marine algae input, which may not be within the Tertiary deltaic sequence but the oils are now reservoired within the Tertiary sands. The occurrence of marine and terrigenous end-member oils within oil accumulations in the Tertiary deltaic reservoir in Beaufort-Mackenzie Delta

has been reported by previous workers (e.g. Brooks, 1986a; Curiale, 1991; Li *et al.*, 2005) the marine oils are believed to have been expelled from Cretaceous source units, with the Late Cretaceous Smoking Hills and Boundary Creek formations as candidate source rocks, while the terrigenous oils are sourced from Tertiary source units within the Eocene Richards Formation (Brooks, 1986a; Curiale, 1991) and coaly intervals within the lower Taglu sequence (early Eocene) Snowdon *et al.* (2004). Thus these marine oils are considered as being sub-delta sourced (i.e. oil expelled from source units below the Tertiary delta sequences) but which now have migrated and accumulated within the Tertiary sequence.

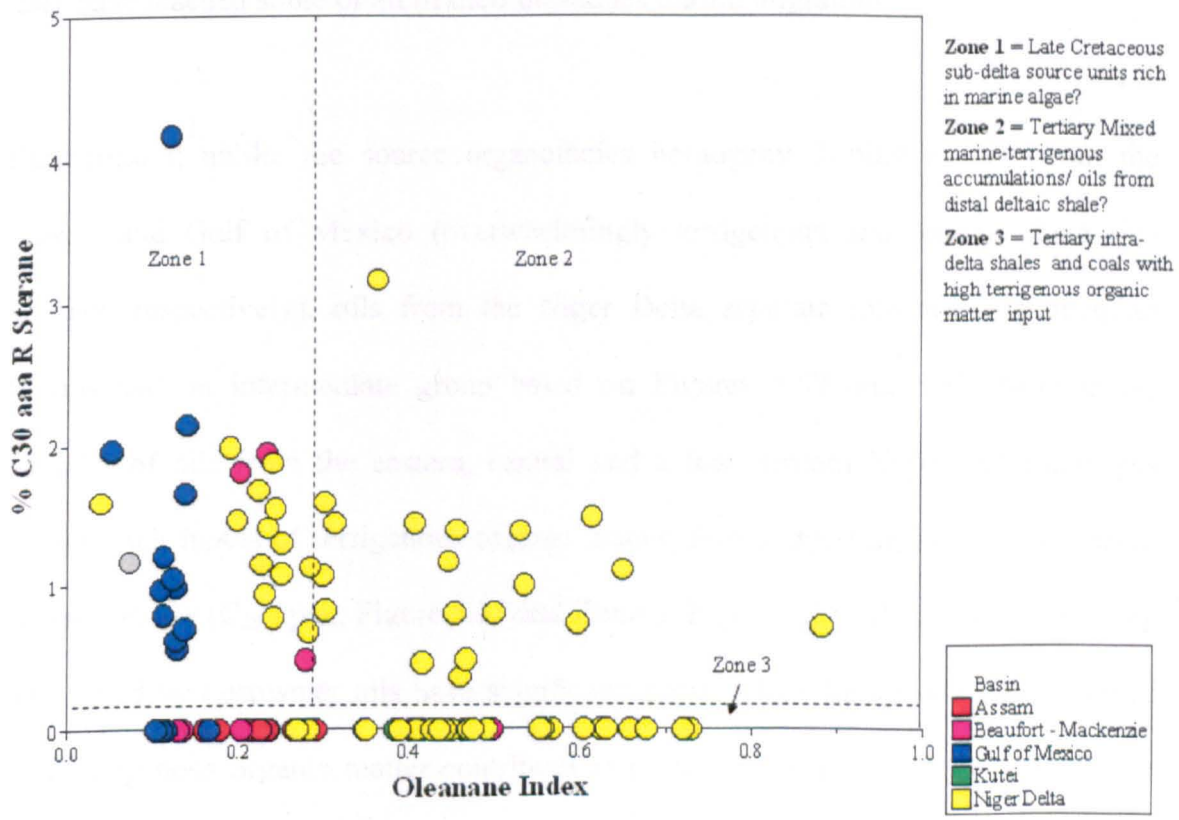

Figure 5.58. Novel plot of oleanane index against the C_{30} 24-*n*- propyl cholestane parameter defines oils into various zones determined by their primary source rock organic matter inputs.

Oils from Gulf of Mexico allegedly sourced from Tertiary deltaic or Late Jurassic Tithonian source rocks (Zumberge *et al.*, 1998) have mixed marine and terrigenous source signatures with high marine algae content (high C_{27} sterane and presence of

C_{30} 24-*n*- propylcholestane). The Gulf of Mexico oils in this dataset may therefore have been derived from source units that received significant marine algal input relative to terrigenous higher plants contribution. Additionally, their relatively high C_{30} 24-*n*-propylcholestane, particularly diasteranes, and low relative abundance of oleanane (oleanane index generally less than 0.2) suggests limited higher plant contribution and/or source rock age older than Late Cretaceous (Moldowan *et al.*, 1994). Most analysed oils from the Gulf of Mexico constitute the group in Zone 1 of Figure 5.58 (i.e marine, non-Tertiary sourced). It is possible that, given the evidence for migrational fractionation and the reservoir stratigraphy, the Gulf of Mexico oils may have leached some or all of their oleananes during migration.

Furthermore, unlike the source organofacies homogeny display by oils from the Assam and Gulf of Mexico (overwhelmingly terrigenous and marine algae rich kerogen respectively), oils from the Niger Delta separate into two end–member groups and an intermediate group based on Figures 5.57 and 5.58. Notable are samples of oils from the eastern, central and a few western Niger Delta acreages having high inputs of terrigenous organic matter, thus suggesting intra-delta derived accumulations (C_{29} apex, Figure 5.57 and Zone 3, Figure 5.58). Additionally, a group dominated by deepwater oils have significant marine algae inputs and they received less terrigenous organic matter contributions (Figure 5.57 and 5.58, Zone 1). These oils are considered to have been derived from sub-delta source units. Oils having intermediate marine and terrigenous organic matter source signatures (Figure 5.57 and Figure 5.58, Zone 2) reflect either mixed accumulations or expulsion from source rocks laid in distal deltaic setting (pro-delta shales) that received significant marine algae and terrigenous organic matter inputs.

Samples of oils from the Kutei generally constituted the region marked for oils derived from coals and shales with abundant terrigenous higher plants input (Figure 5.57 and Figure 5.58 Zone 3) are thus considered to be wholly intra-delta derived.

5.7.2. Source rock depositional environment

The environments of source rock deposition have been interpreted comparatively from the pr/ph ratios, gammacerane index and the pr/nC_{17} vs. ph/nC_{18} plots (Figures 5.59, 5.60 and 5.61 respectively). In general the source rock depositional conditions parallel the source rock organic matter type interpreted from sterane and oleanane compositions.

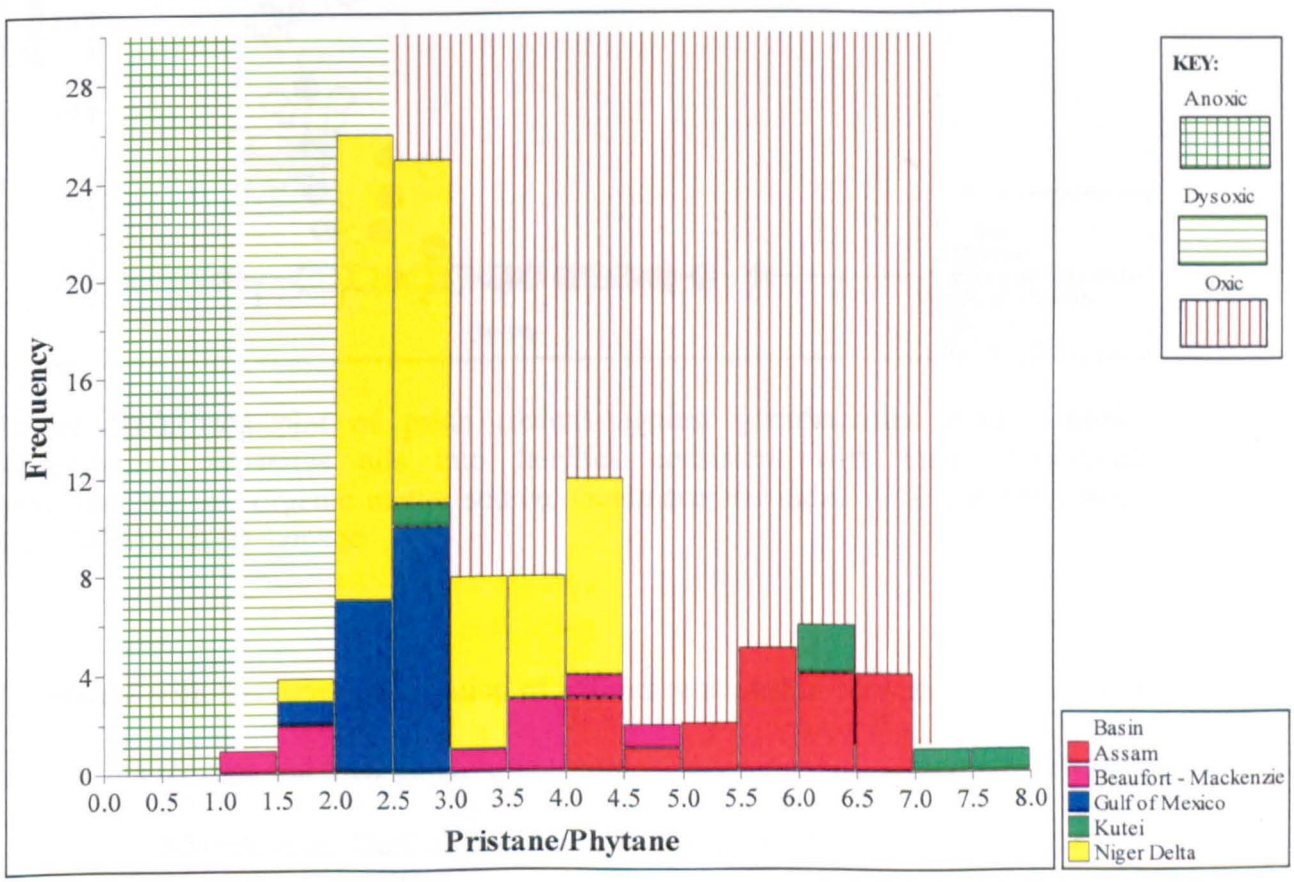

Figure 5.59. Source rock anoxia inferred from pr/ph ratios. The wide range of values for the crude oil samples reflects variable source rock depositional conditions for the oils.

For instance, oils reflecting expulsion from overwhelmingly terrigenous organic matter rich source units typical of delta top coals and carbonaceous shales (Assam and Kutei basin oils) have high pr/ph ratios (Figures 5.59, 5.60) and they lack gammacerane in their terpane distributions (Figure 5.60), thus suggesting source rock depositional conditions that are oxic and devoid of any water column stratifications.

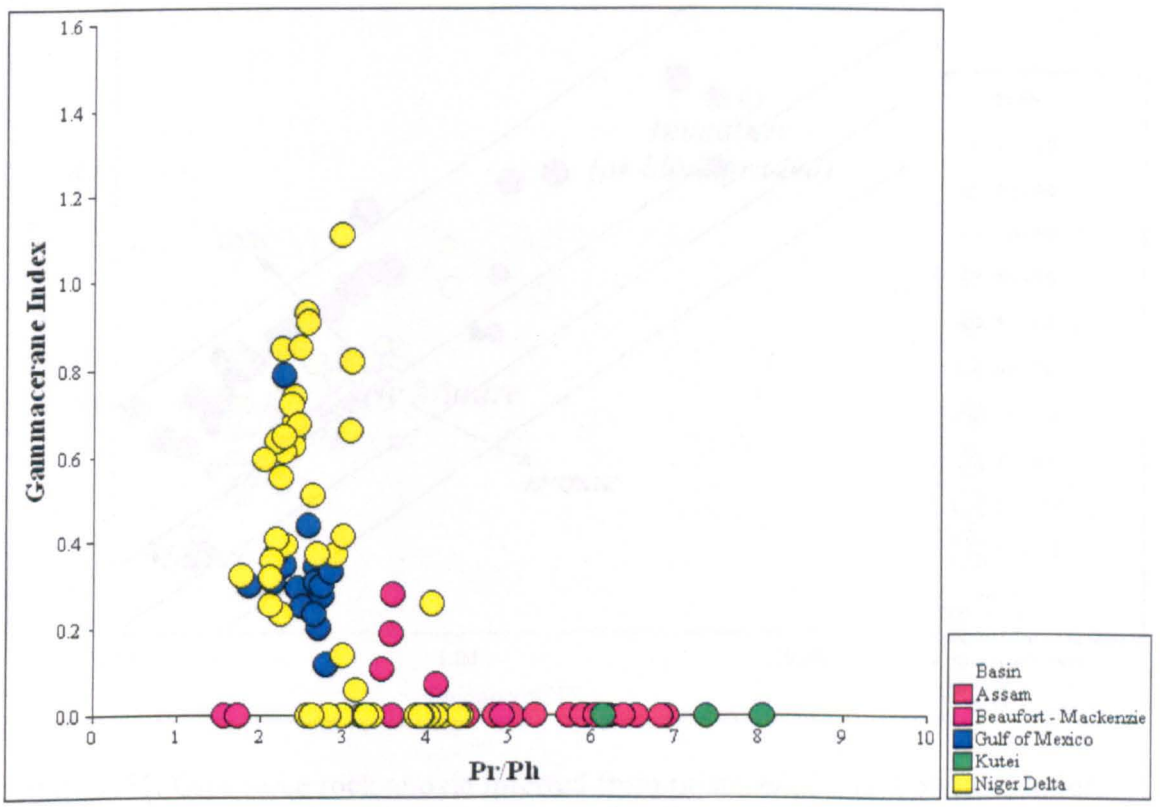

Figure 5.60.Cross plot of pr/ph (redox) against gammacerane index (salinity stratification) separates oils into families consistent with their depositional environments and organic matter source. Gammacerane index = 10*gammacerane / C_{30} 17α(H),21β(H) hopane

Consistent with the above observation of a direct relationship between oil source rock organic matter type and their putative depositional environments, samples of oils from the Beaufort-Mackenzie, Gulf of Mexico and the Niger Delta having high marine algae biomarker source signatures, generally show characteristics of source rock deposition in less oxygenated (low pr/ph ratios, less than 2.5; Figure 5.59, 5.60 and

5.61) and stratified water column conditions (presence of gammacerane, Figure 5.60) with exception being absence of detectable gammacerane in samples of oil from the Beaufort-Mackenzie Delta. Although a few samples plot as been immature or biodegraded based on Figure 5.61, these samples are not biodegraded based on their GC fingerprints.

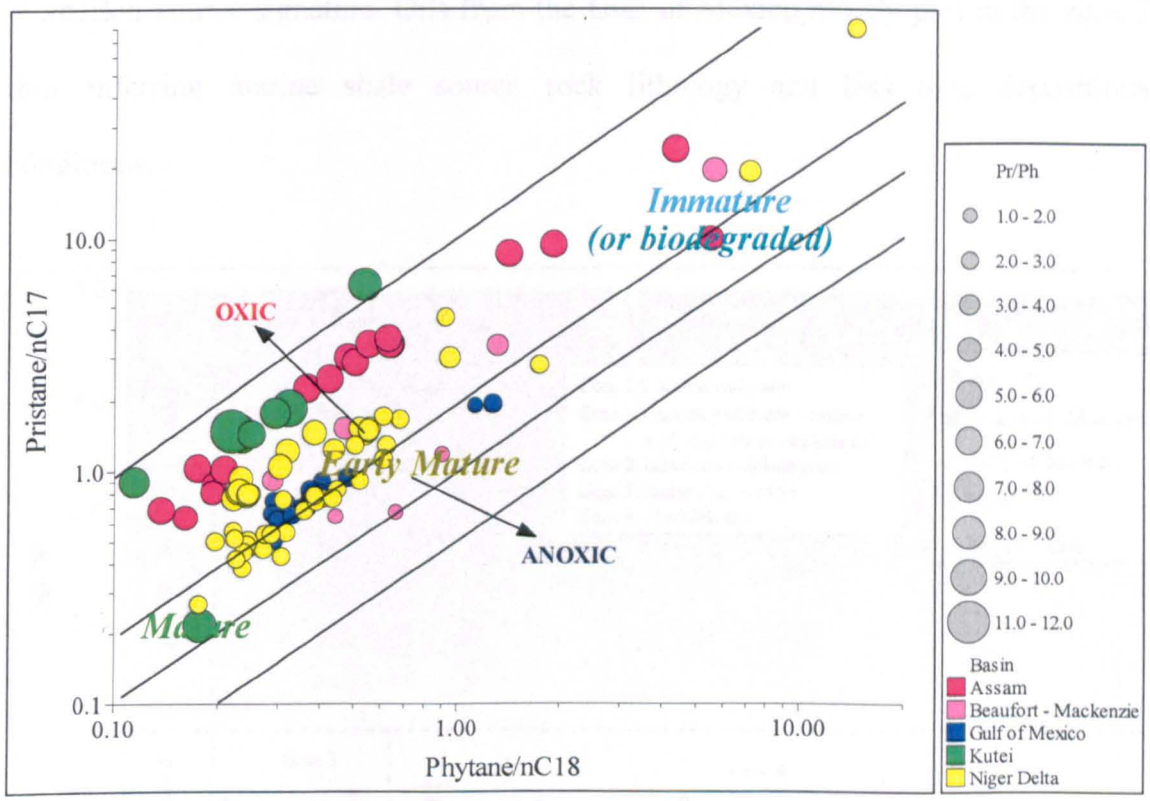

Figure 5.61. Oil source rock anoxia inferred from pristane/nC_{17} and ph/nC_{18} ratios. These parameters are sensitive to biodegradation (generally increase in values), thus biodegraded oils have been excluded from the plot.

More importantly, a cross plot of the ratio of dibenzothiophene/phenanthrene (DBT/P) versus the pristane/phytane ratio (pr/ph) (Figure 5.62) provides a means of making inference on the oils source rock depositional environments and lithology after Hughes *et al.* (1995). Note that all the samples of oils from the Kutei and Assam plot in the Zone 4 that is mostly associated (although not exclusive) with fluvial/deltaic depositional environments. However, oils from the Beaufort-Mackenzie Delta

separate into two groups (Zone 3 and Zone 4), the Zone 3 according to Hughes *et al.* (1995) is characterised by less oxygenated marine shale and other source rock depositional environments and lithology. One of the three Beaufort-Mackenzie oils plotting in this Zone 3 has terrigenous biomarker signature (sample BM-12) while the other two oils (sample BM4 and BM-10) are dominated by high marine algae biomarker source signature. Oils from the Gulf of Mexico mostly plot in the zone 3, thus inferring marine shale source rock lithology and less oxic depositional conditions.

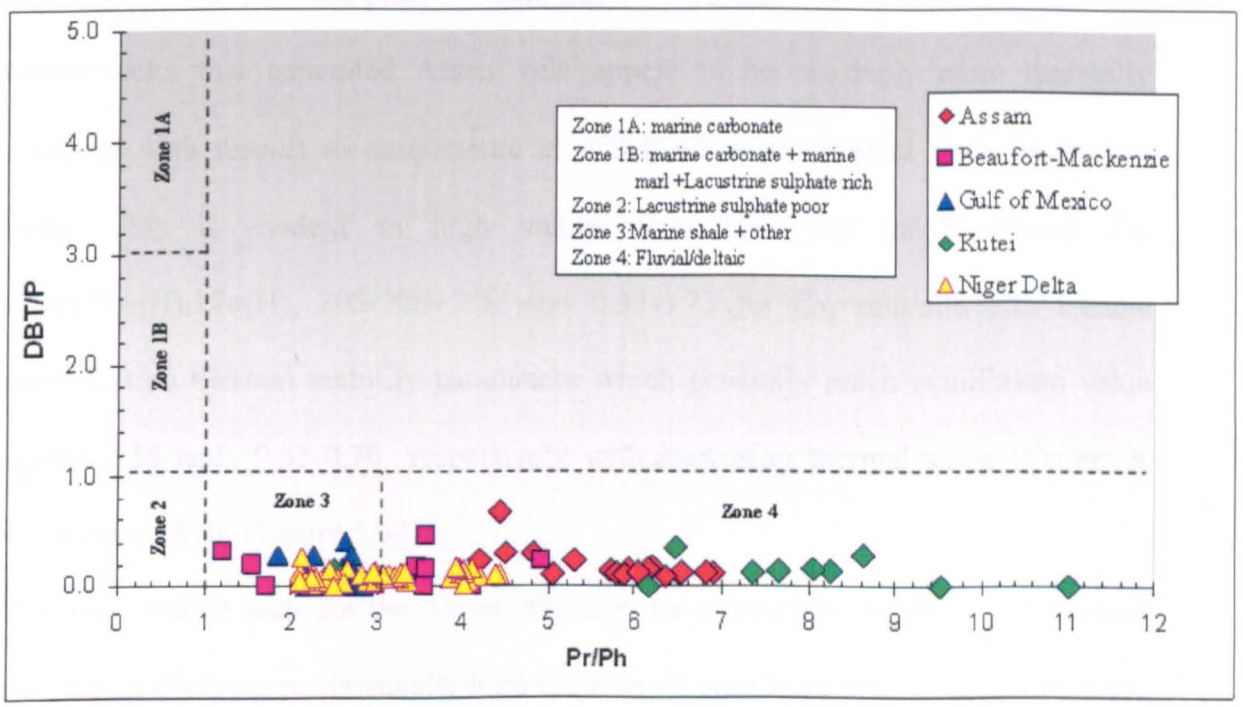

Figure 5.62. Cross plot of the ratio of dibenzothiophene/ Phenanthrene (DBT/P) versus the pristane/phytane ratio (pr/ph) provides a means of making inference on the oils source rock depositional environments and lithology after Hughes *et al.* (1995). Dotted fields are not fixed boundaries as exceptions can occur and each zone is as defined by Hughes *et al.* (1995).

In contrast, samples of oils from the Niger Delta show wide variability on this plot. However, they can be grouped according to the boundary divisions shown in Figure 5.62. The two groupings are; zone 3 (marine shale and less oxygenated depositional condition), and zone 4 (fluvial/deltaic), after Hughes *et al.* (1995). The deepwater

Niger Delta oils mainly plot in the Zone 3, while the bulk of the oils plotting in the Zone 4 (Figure 5.62) are constituted by the eastern and central terrigenous organic matter dominated shallow water Niger Delta oils. A significan number of the Niger Delta oils plot around the boundary of Zone 3 and Zone 4. Figure 5.62 thus provides a means to assess the source depositional conditions of these oils as well as the source rock lithology and it can be concluded from this plot that none of these oils have been generated from carbonate or lacustrine source rocks.

5.7.3. Thermal Maturity

Figures 5.63 and 5.64 are plots of some key thermal maturity biomarker ratios. The source rocks that generated Assam oils appear to be relatively more thermally advanced with respect to temperature at which oil were expelled from the source rocks. This is evident in high values (0.44-0.65) for the measured C_{29} 5α(H),14α(H),17α(H), 20S/20S+20R and 0.33-0.73 for C_{29} αββ/αββ+ααα sterane isomerisation thermal maturity parameters which generally reach equilibrium value around 0.55 and 0.65-0.70 respectively with increasing thermal stress (Seifert & Moldowan, 1986) (Figure 5.63).

The coaly source units for the Assam oils may be responsible for their high thermal maturity as coals characteristically hold their liquid petroleum until its micro-porosity are saturated before expulsion can take place (Hunt, 1991; Collinson *et al.*, 1994; Isaksen *et al.*, 1998), thus giving rise to delayed expulsion. On the other hand, oils from the Gulf of Mexico mostly have low values for the measured C_{29} 5α(H),14α(H),17α(H), 20S/20S+20R and C_{29} αββ/αββ+ααα sterane isomerisation thermal maturity parameters thus suggesting a high expulsion efficiency as the oils are presumably expelled from their source rock(s) under low-moderate thermal stress, typical of high organic rich shales.

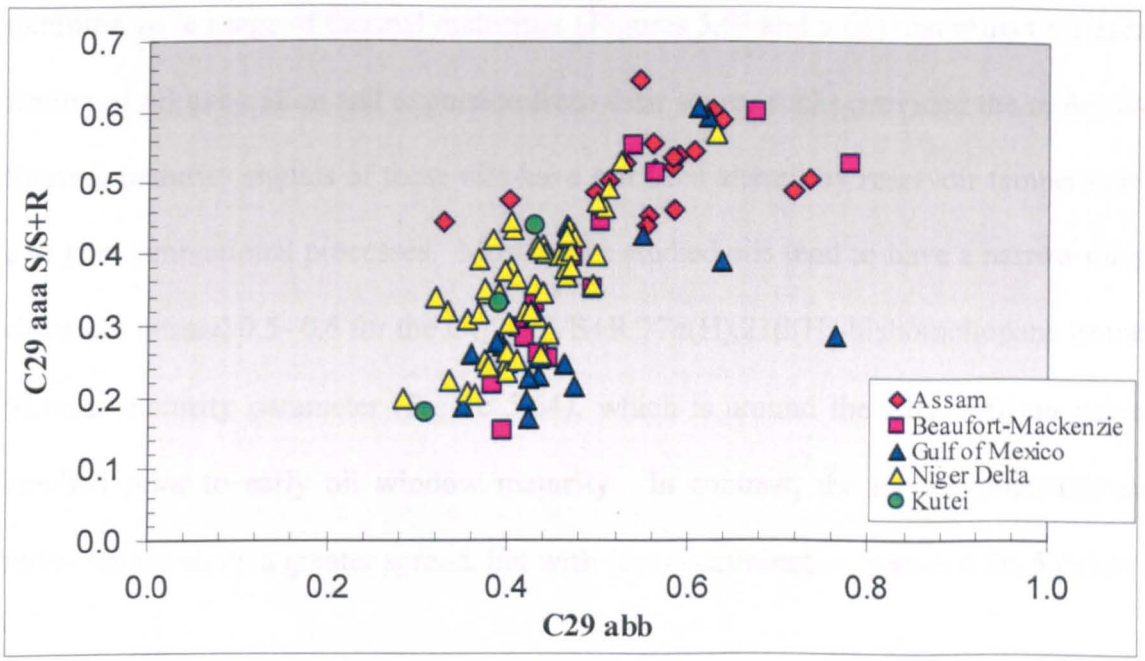

Figure 5.63. Plot of C29 abb (C_{29} αββ/αββ+ααα) against C29 aaa S/S+R (5α(H),14 α(H),17α(H)- ethyl cholestane 20S and 20R sterane thermal maturity parameters show the wide range of thermal maturity of the oils.

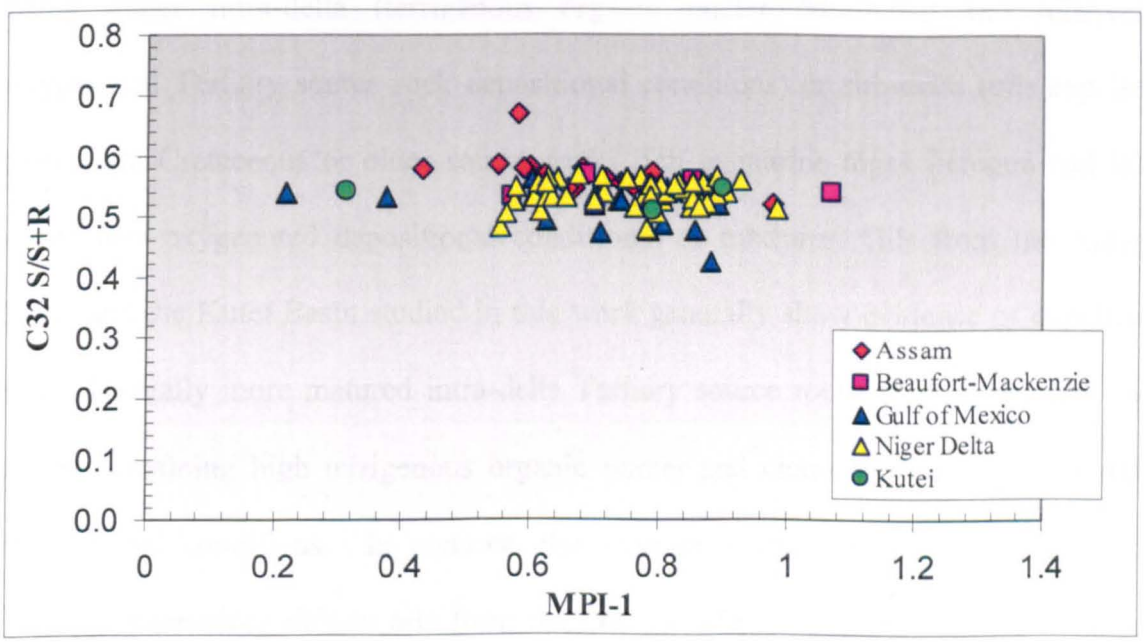

Figure 5.64. Plot of MPI-1= 1.5*(2-MP+ 3-MP)/ (P + 1-MP + 9-MP); Radke *et al.*, (1982a) versus C32 ab S/S+R (17α(H), 21β(H)-bishomohopane) thermal maturity parameters. Most oils tend to have narrow range of values for the bishomohopane parameter but there is a considerable variation in their MPI-1 values.

Furthermore, crude oils from the Beaufort-Mackenzie Delta and the Niger Delta exhibit a wide range of thermal maturities (Figures 5.63 and 5.64) that reflect different timing of oil generation and expulsion from their source rocks provided the molecular thermal maturity signals of these oils have not been altered by reservoir temperatures and post generational processes. Most of the studied oils tend to have a narrow range of values around 0.5- 0.6 for the C_{32} αβ S/S+R 17α(H),21β(H)-bishomohopane isomer thermal maturity parameter (Figure 5.64), which is around their equilibrium values reached prior to early oil window maturity. In contrast, the methyl phenanthrene index values show a greater spread, but with less discrimination between the 5 deltas

5.8. Conclusions

The biomarker source signatures in the oils from the Assam, Beaufort-Mackenzie, Gulf of Mexico, Kutei and Niger Deltas areas help to predict their source units as being either intra-delta (terrigenous organic matter dominated and relatively oxygenated Tertiary source rock depositional conditions) or sub-delta (oils expelled from Late Cretaceous or older source rocks rich in marine algae kerogen and laid under less oxygenated depositional conditions) or mixtures. Oils from the Assam Delta and the Kutei Basin studied in this work generally show evidence of expulsion from thermally more matured intra-delta Tertiary source rocks of the delta-top coal facies containing high terrigenous organic matter and characterized by highly oxic depositional conditions. In contrast, the biomarker characteristics of samples of Tertiary reservoired deltaic oils from the Gulf of Mexico suggests expulsion under lower thermal stress from sub-delta marine shale source rocks that received significant marine algae inputs and laid down under less oxygenated conditions. This source rock may be the organic rich and thick Tithonian marine clastic and marl source rock

recently intersected in up to five deepwater wells (Zumberge *et al.*, 1998; Cornford, C. Pers. Comm, 2007).

Additionally, on the basis of the biomarker organofacies source signatures (steranes and triterpanes mainly), oil accumulations in the Beaufort–Mackenzie Delta are separable into those sourced from mainly marine algae dominated source rock kerogen laid in less oxygenated depositional conditions (sub-delta) and a dominantly land-plant organic matter source rock deposited under oxic depositional conditions (intra-delta). Similarly, the Niger Delta oils can be grouped into intra-delta and sub-delta derived oils but with an intermediate (mixed?) oil accumulations. Based on biomarker compositions, the deepwater oils and a few western shallow water accumulations are considered to be derived from sub-delta source rocks laid in less oxygenated conditions and containing abundant marine algae organic matter while the intra-delta oils are characterised by dominant high terrigenous biomarker source signature and source rock deposition under relatively oxic conditions. An attempt will be made in Chapter Eight to correlate allegedly sub-delta sourced deepwater Niger Delta oils with the candidate source units in Late Cretaceous Araromi Formation in the margining Dahomey Basin, south-western Nigeria.

CHAPTER SIX

MOLECULAR GEOCHEMISTRY II: OIL CHARACTERIZATION USING NOVEL COMPOUNDS

Summary

One key objective of this study as outlined in Section 1.9 was to search for novel molecular markers that can be used to characterize oils derived principally from source rocks of Tertiary deltaic basins. The recognition of certain molecular compounds that represent specific biological and chemical processes and products in time and space over varying conditions in the geosphere and their successful linkage to their natural product precursors in the biosphere has permitted the use of compounds like oleanane, lupane, gammacerane and bicadinanes in characterising sedimentary organic matter and the petroleum derived from it. In this chapter, a series of compounds tentatively identified as compounds A_1, A_2, B_1, B_2 and C all occurring in Tertiary-reservoired oils of Assam, Beaufort-Mackenzie, Gulf of Mexico, Niger and Kutei basins are hereby reported. The presence and the relative distributions of compounds A_1, A_2, B_1, B_2 is systematic and correlate with the abundance of oleanane in these oils, thus suggestive a similar source among terrigenous higher plants of the angiosperm family. On the basis of mass spectral characteristics and laboratory synthesis experiments, the novel compounds A_1, A2, B1, and B_2 are tentatively identified as seco-oleananes, while compound C is a seco-hopane. The K-index, a parameter developed from these compounds and defined as $(A_1+ A_2+ B_1+ B_2)/C$, co-varies with oleanane index, thus permitting its use in discriminating organofacies among oils and perhaps the source rock stratigraphic age.

6.0. Introduction

The last three decades have seen advances in our understanding of the biosynthetic pathways of several organic molecules and their application to petroleum exploration and production. Because some of these compounds in the geosphere have unique and preserved carbon skeletons that maintain a link to a natural product in the biosphere, they are called biological markers (Mackenzie, 1984). Among such compounds are oleananes (Ekweozor *et al.*, 1979a,1979b; Grantham *et al.*, 1983; ten Haven & Rullkötter, 1988; Ekweozor & Udo, 1988), lupane and norlupanes (Wang & Simoneit, 1990; Curiale, 1991; Nytoft *et al.*, 2002; Curiale, 2006, and references therein), gammacerane (Venkatesan, 1989; ten Haven *et al.*, 1989; Sinninghe Damsté *et al.*, 1995); bicadinanes (Cox *et al.*, 1986; van Aarssen *et al.*, 1990), which characterise the sources of organic matter to sedimentary kerogen and the derived crude oil. In addition, some of these compounds are isomeric and because of the differential thermal stability of the isomers they are potential indicators of the thermal maturity of source rocks and oils (e.g. bicadinanes, Murray *et al.*, 1994; oleanane, Ekweozor & Telnaes, 1990). Besides the utility of these compounds in assessing organic input and thermal maturity of organic sediment and petroleum, considerable success has been achieved in their use in predicting the age of the petroleum source rock and the oils derived therefrom (e.g. oleanane index generally > 2.0 in sediments and oils is alleged to be characteristic of Late Cretaceous or younger source rock (Moldowan *et al.*, 1994)) as well as in providing proxies for deconvoluting complex processes like oil mixing and migration contamination (e.g. using lupanoids and norlupanoids; Curiale, 2006).

In an effort to characterize Tertiary deltaic oils on a global scale using representative crude oil samples, a series of GC-MS analyses was carried out in selected ion monitoring (SIM) mode and, interestingly, certain previously unreported triterpenoids showing remarkable distributions in all of the oils from the Assam, Beaufort-Mackenzie, Gulf of Mexico, Niger and Kutei basins were detected. The advantage offered by GC-MS-MS was utilized to selectively characterize these novel compounds. Several previously unknown triterpanes and their ring-degraded analogues have been reported in oils with significant terrigenous higher plant inputs, derived from Tertiary basins from the Niger Delta, Taiwan and Indonesia (e.g.Woolhouse *et al.*, 1992). However, none of these reports identified these novel compounds reported here.

This chapter reports a novel series of terpanes of as yet unconfirmed structures, called here compounds A_1, A_2, B_1, B_2 and C, occurring in crude oils from Tertiary deltaic petroleum systems with significant terrigenous organic matter inputs. The distribution and relative abundance of these novel compounds have potential utility as molecular markers of organic matter provenance and source rock age.

6.1. Samples

Representative samples of crude oils from Tertiary deltaic reservoirs of the Assam, Niger, Beaufort-Mackenzie, Mississippi Delta (Gulf of Mexico) and the Kutei basins were analysed, in addition to standard marine oils from the North Sea (Upper Jurassic) and the Tertiary Oropouche oilfield from Trinidad (Figure 6.1). Table 1 presents some of molecular thermal maturity and organic source parameters measured for the oil set using the GC-MS and GC-MS-MS analytical programs described in Sections 3.3 and 3.4.

6.2. Results and Discussion

6.2.1. Gas chromatographic characteristics

The compounds are best monitored selectively by m/z 414→123 parent to daughter ion transition GC-MS-MS analysis (Figure 6.2). Compound C elutes at about the retention time of C_{29} *n*-alkane, and between Ts and Tm. The presence and relative abundances of compounds A_1, A_2, B_1, B_2 is systematic and it is concomitant with the presence and abundance of oleanane in any oil in the sample set, thus suggesting a similar source among terrigenous higher plants of the angiosperm family. The compounds A and B series appear to be doublets, while compound C elutes as a single peak much later than the A and B isomers. Although several other minor compounds are detected in the m/z 414 →123 GC-MS-MS chromatograms (Figure 6.2), only peaks A_1, A_2, B_1, B_2 and C were quantified because of their consistent occurrence in measurable quantity in all the oils

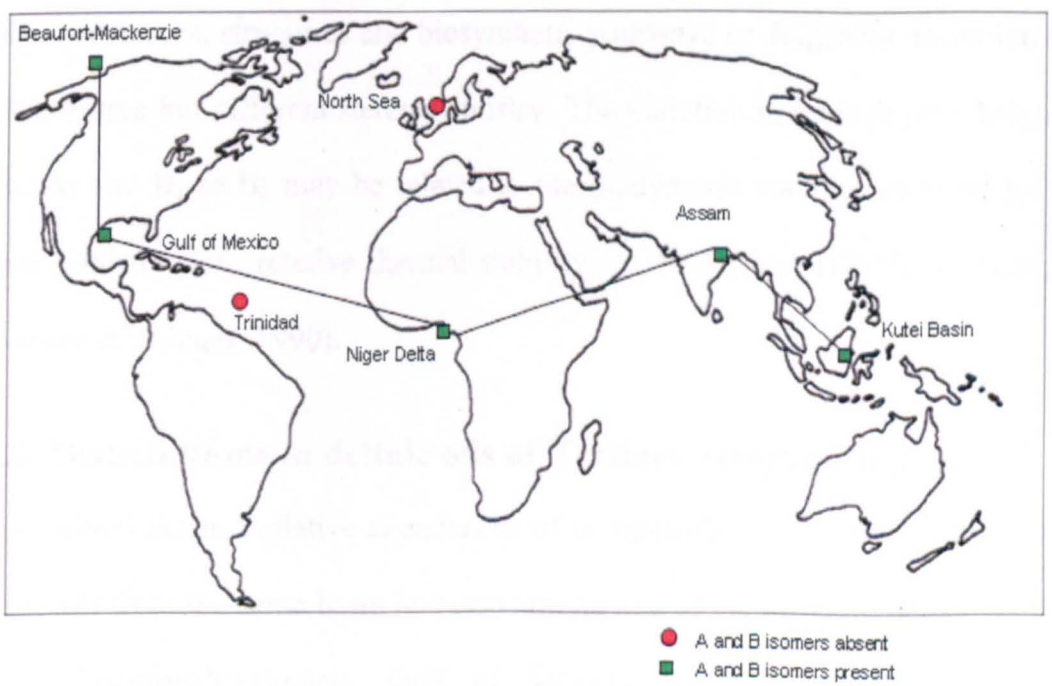

Figure 6.1. Map of the world showing the distribution of the Tertiary deltaic basins where the novel terpanes have been detected (block shape). Marine oils from Trinidad and North Sea basins lack A and B isomers (oval shape). Blank map taken from http://wps.ablongman.com/wps/media/objects/579/592970/BlankMaps/World%20Map.gif

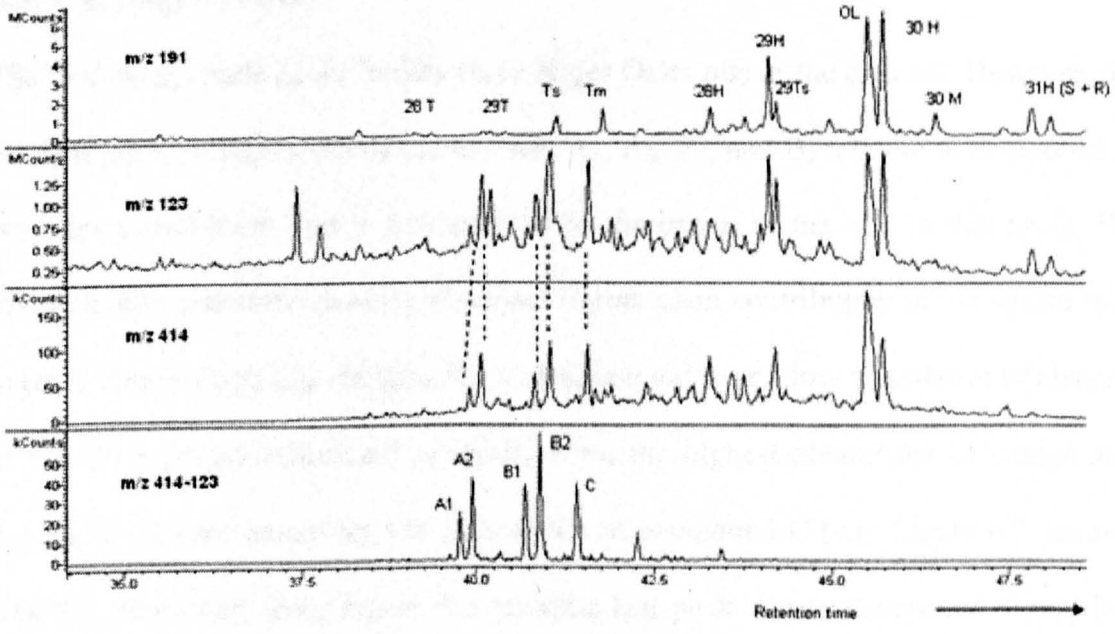

Figure 6.2. Representative mass chromatograms showing the distributions of compounds A_1, A_2, B_1, B_1 and C in m/z 123 and m/z 414 GC-MS mass chromatograms. The m/z 414→123 parent-daughter ion transitions GC-MS-MS (bottom chromatogram) afforded the selective monitoring of the compounds from interfering peaks. Note the absence or very low abundance of these novel compounds in the m/z 191 chromatogram. Peak identities are provided in Appendices IIIB and IIIC

The characteristic occurrence of A and B as doublets may suggest compounds with similar precursors, structures and biosynthetic pathways or diagenetic evolution from similar source but different stereochemistry. The variation in relative peak heights of A_1 to A_2 and B_1 to B_2 may be related to thermodynamic stability imposed by their stereochemistry. (cf.. relative thermal stability of 18α(H) and 18β(H) oleanane; e.g. Ekweozor & Telnaes, 1990).

6.2.2. Distributions in deltaic oils of Tertiary reservoir age

The distributions and relative abundances of compounds A_1, A_2, B_1, B_2 and C vary among oils from the same basin and also among oils of the different deltaic basins of Assam, Beaufort-Mackenzie, Gulf of Mexico, Niger Delta and Kutei. This distribution is discussed in the section below.

6.2.2.1. Niger Delta

The five compounds occur in fifty three Niger Delta oils in the data set. However, the distribution and abundance of compounds A_1, A_2, B_1, and B_2 relative to compound C provides information that is fundamental to the origin of the oils in this basin. For instance, oils generally showing abundant higher plant contribution to the source rock organic matter (high C_{29} steranes, high oleanane index and low abundance or absence of C_{30} 24-*n*-propylcholestane) generally have the highest abundance of compounds A_1, A_2, B_1, B_2 and relatively low abundance of compound C (e.g. Figure 6.3 sample ND006). However, from Figure 6.3 an abundant peak due to compound C and low level of compounds A_1, A_2, B_1, B_2 occur in oils of marine organofacies (e.g. sample ND023, a deepwater oil) containing low $\%C_{29}$ steranes and low oleanane index reflecting low level of angiosperm higher plant inputs (Ekweozor & Udo, 1988; Moldowan *et al.*, 1994), and significant amounts of C_{30} 24-*n*-propylcholestane that is diagnostic of marine algae (Moldowan *et al.*, 1990). Additionally, some shallow western Niger Delta oils having evidence of significant marine algal contribution to their source rocks show a distributions represented by sample ND30 in figure 6.3. Oils showing mixed organofacies characteristics, perhaps resulting either from mixing of oils from marine and terrigenous source facies or oils expelled from source rocks of mixed organofacies, show high contents of A_1, A_2, B_1, B_2 and C (e.g Figure 6.3, ND001). The distribution of the novel terpanes among this oil group appears intermediate between the terrigenous (ND006) and marine (ND023) organofacies distributions. Despite variation in relative abundance of the compounds A_1, A_2, B_1, B_2 and C among various oil groups, an apparent similarity occurs in all of the oils in the pattern of compounds A and B doublets. The similarity being that in all of the Niger

Delta oils studied, compound A_1 is less abundant than A_2 and similarly B_1 is lower in abundance compared to B_2 (e.g. Figure 6.3).

In order to understand the difference in the distribution and relative abundance of compounds A_1, A_2, B_1, B_2 and C for oils showing terrigenous and marine characteristics in Niger Delta, a sample of North Sea Vesselfrik oil, sourced from Upper Jurassic Kimmeridge Clay was introduced into the sample set. This sample does not contain oleanane, and interestingly there is absence of compounds of A_1, A_2, B_1, and B_2 in this oil (Figure 6.3, North Sea).

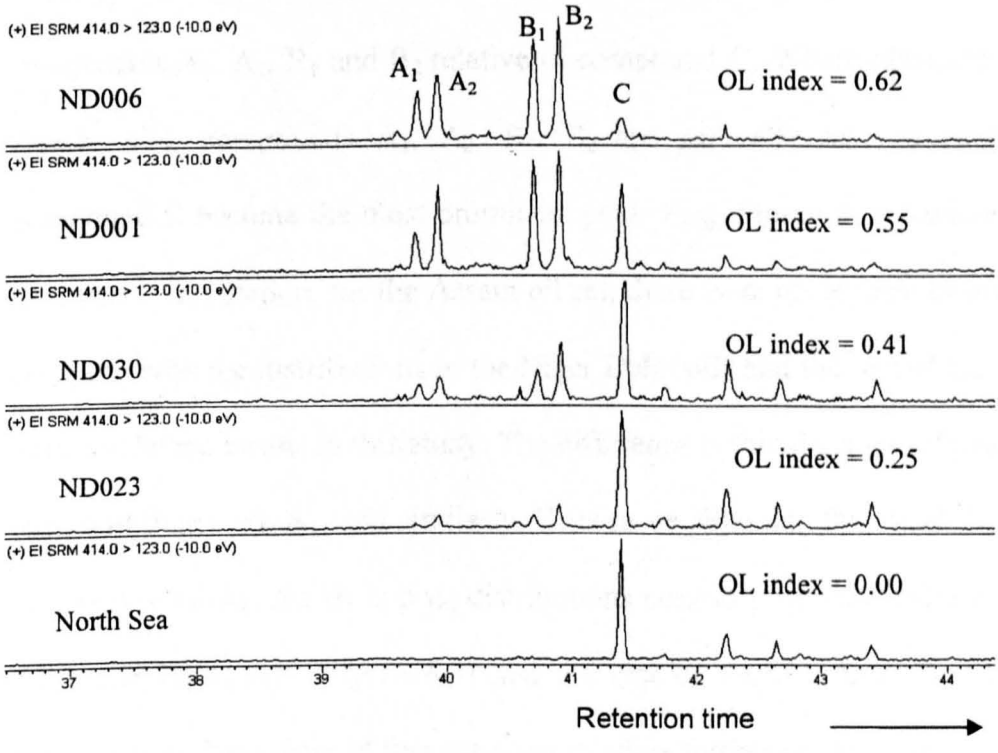

Figure 6.3. GC-MS-MS 414→123 transition MRM chromatograms showing the distribution of the novel terpanes in representative Niger Delta oils. The North Sea oil permits a comparison of the distribution of the compounds in non-oleanane bearing oil with those of the Niger Delta oils.

The absence of these compounds is consistent with the assumption that these compounds may be related to oleanane, and/or may have similar precursors in

angiosperm flowering plants as oleanane. Compound C appears ubiquitous in all the oils studied regardless of source rock age and oleanane occurrence, as it occurs in Tertiary marine oil from Trinidad and also in an Upper Jurassic Kimmeridge Clay sourced oil from the North Sea, despite absence of compounds A and B in that oil.

6.2.2.2. Assam Delta

The Assam oils in this study are mostly derived from coaly source rocks of the Barail group (Goswami *et al.*, 2005). The contribution of angiosperm flowering plants confering the oleanane precursor is relatively low in this oil set as evident in the low oleanane index (Table 1). Consistent with this observation, there is a low level of compounds A_1, A_2, B_1 and B_2 relative to compound C. Where oleanane is low, as in Assam oils, compounds A_1, A_2, B_1, B_2 are generally low in abundance, thus compound C become the most prominent peak (e.g. Figure 6. 4, sample AS-15) and vice versa. In addition, for the Assam oil set, there is an observable characteristic that contrasts with the distributions in the Niger Delta oils and the rest of the oils from the Tertiary deltaic basins in this study. The difference is that the areas of peak A_2 is more abundant than peak A_1, and similarly, B_1 is more abundant than peak B_2, this pattern of compounds A_1, A_2, B_1 and B_2 distributions contrasts with the pattern observed for the Niger Delta oils (Figure 6.3) and the rest of the oils from Tertiary basins of investigation. The origin of this variation requires further exploration, which is outside the scope of this study.

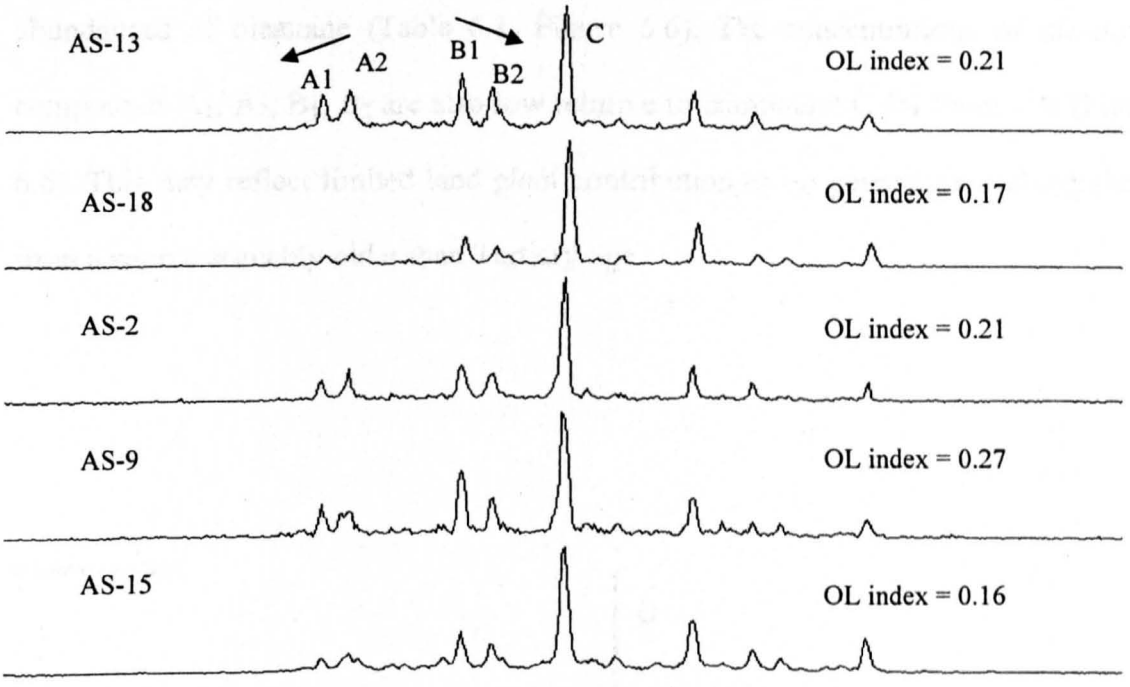

Figure 6.4. GC-MS-MS 414→123 transition showing the distribution of the novel terpanes in representative Assam oils. "OL" refers to oleanane.

6.2.2.3. Beaufort-Mackenzie Delta

Consistent with two organic source facies for oils from Beaufort-Mackenzie (based on terpane and sterane data presented in Sections 5.3.2 and 5.3.3), oils from Beaufort-Mackenzie show two distributions for compounds A_1, A_2, B_1, B_2 and C (Figure 6.5). Samples having marine organic facies characteristics based on terpane and steranes data show lower abundances to a near absence of compounds A_1, A_2, B_1, B_2 and relatively high amounts of compound C (Figure 6.5, BM-10), whereas oils of terrigenous characteristics have significant concentrations of compounds A_1, A_2, B_1, B_2 that are commensurate with their oleanane contents (e.g. Figure 6.5, BM-13).

6.2.2.4. Gulf of Mexico

Most oils from the Gulf of Mexico in this study show characteristics of expulsion from source rocks of marine organofacies affinity with low levels of higher plant inputs as reflected in the presence of C_{30} 24-*n*-propyl cholestane and very low

abundances of oleanane (Table 6.1, Figure 6.6). The concentrations of the novel compounds A_1, A_2, B_1, B_2 are also low relative to compound C for these oils (Figure 6.6). This may reflect limited land plant contribution or oil generation and expulsion from a source arguably older than Tertiary age.

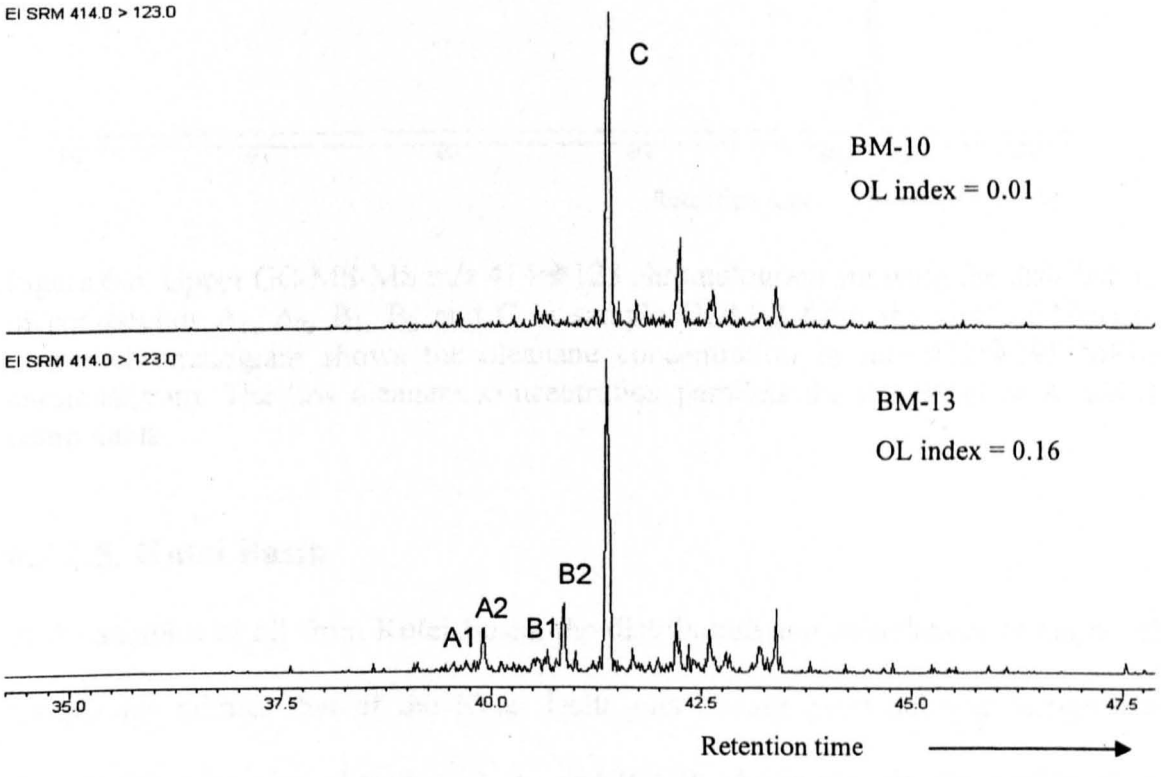

Figure 6.5. GC-MS-MS 414→123 transition chromatograms showing the distribution of the novel terpanes in two representative Beaufort-Mackenzie oils. The low oleanane concentration parallels the low relative abundance of A and B compounds.

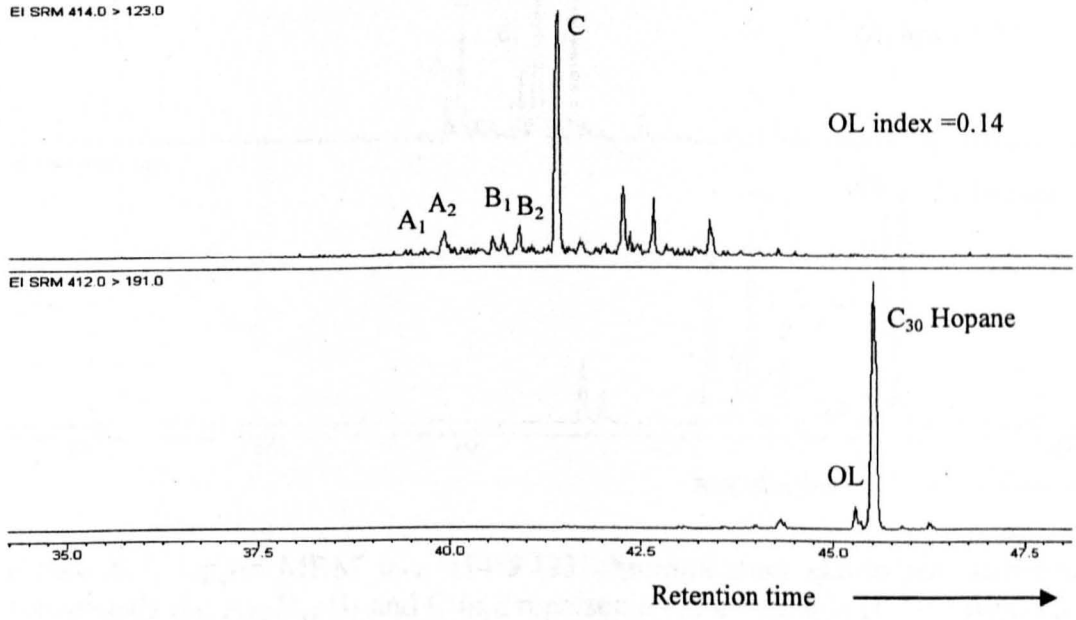

Figure 6.6. Upper GC-MS-MS m/z 414➔123 chromatogram showing the distribution of compounds A_1, A_2, B_1, B_2 and C in sample GOM-2 from the Gulf of Mexico. Lower chromatogram shows the oleanane concentration in m/z 412➔191 MRM chromatogram. The low oleanane concentration parallels the low level of A and B compounds.

6.2.2.5. Kutei Basin

In the samples of oil from Kutei Basin, the distribution and abundances of the novel compounds mimics that of the Niger Delta oils having overwhelming terrigenous characteristics i.e. area of peak $A_2 > A_1$, and $B_2 > B_1$. As previously observed in other oils, the concentration of the novel compounds A_1, A_2, B_1, B_2 also parallel oleanane abundance in these oils (Figure 6.7).

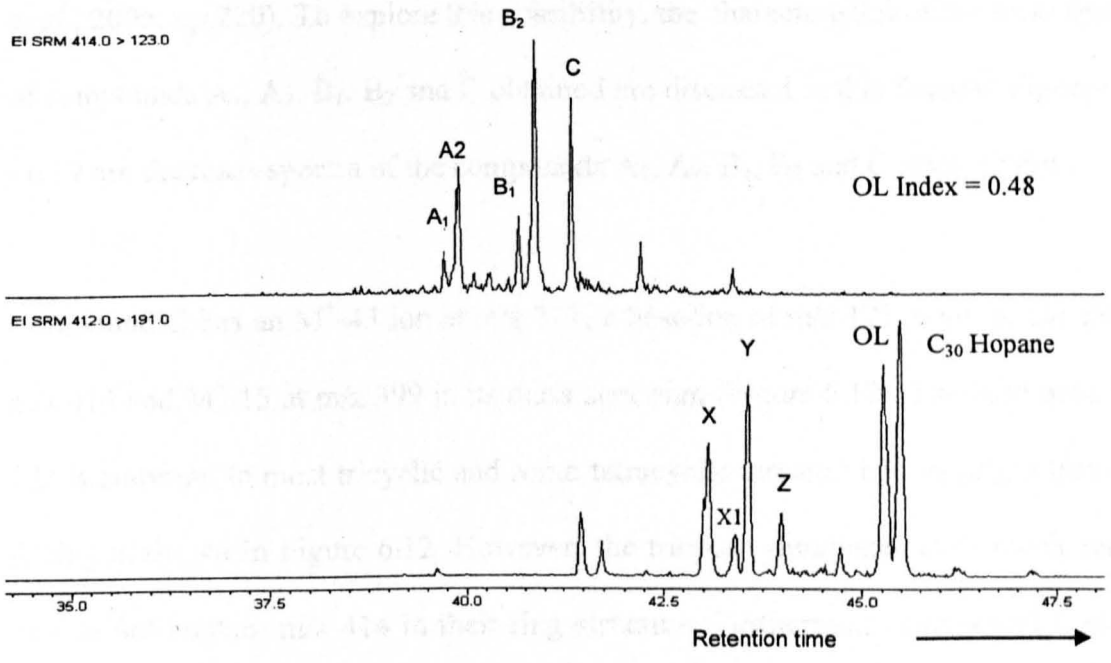

Figure 6.7. Upper MRM m/z 414→123 chromatogram shows the distribution of compounds A_1, A_2, B_1, B_2 and C in a representative oil sample (KT-5) from the Kutei Basin. Lower chromatogram shows the oleanane concentration in the MRM m/z 412→191 chromatogram. X,Y and Z = C_{30} pentacyclics triterpanes identified as peaks 10, 11 and 13 by Woolhouse *et al.* (1992). Peak OL refers to oleanane+lupine?

6.3. Structural Elucidation

In order to gain information on the origin of the compounds A_1, A_2, B_1, B_2 and C, a detailed knowledge of their structures is critical. As a preliminary approach to structural understanding, initial mass spectra data were obtained from GC-MS analyses of purified triterpane fractions containing the novel compounds separated by means of a high performance liquid chromatography (HPLC) technique as described in Section 3.10. Additional laboratory experiments were carried out by Dr. Peter Nytoft of the Geological Survey of Denmark and Greenland (GEUS) to synthesise the compounds A_1, A_2, B_1, B_2 and C.

6.3.1. Mass spectra characteristics of compounds A_1, A_2, B_1, B_2 and C

The mass spectrum of a compound often offers valuable information on the ring structure and its molecular weight, which can be used to identify a compound (Peters

et al., 2005, pp.220). To explore this possibility, the characteristics of the mass spectra of compounds A_1, A_2, B_1, B_2 and C obtained are discussed in this Section. Figures 6.8 - 6.12 are the mass spectra of the compounds A_1, A_2, B_1, B_2 and C respectively.

Compound C has an M^+-43 ion at m/z 371, a base ion of m/z 123, a molecular ion of m/z 414 and M^+-15 at m/z 399 in its mass spectrum (Figure 6.12). The base peak m/z 123 is common to most tricyclic and some tetracyclic terpanes and its origin from the A ring is shown in Figure 6.12. However, the tricyclic diterpanes elute much earlier and do not contain m/z 414 in their ring structure. Furthermore, compound C elutes just immediately after C_{29} *n*-alkane and its retention time is closer to that of 17α(H)-22,29,30-trisnorhopane (Tm) under the chromatography conditions used in this study. The presence of M^+-43 ions at m/z 371 suggests the occurrence of an isopropyl side chain in its terminal ring thus giving it a structural similarity to the hopanoids. Based on these mass spectral characteristics, a tetracyclic saturated C_{30} compound is thus predicted for compound C. Additionally, the mass spectrum of compound C is identical to that published as compound "i" by Rullkötter (1982). Similarly, the Peak K and synthetic seco-hopane standard reported by Schimtter *et al.* (1982) is also identical to the compound C. On these bases, compound C is tentatively identified as a C_{30} 8, 14-secohopane, with many isomers as shown by Schmitter *et al.* (1982), comprising 8α(H), 14β(H), 17α(H), 21β(H).

All the compounds contain the base peak m/z 123 ion and significant m/z 109 and m/z 137 ions. The presence of the base peak ion m/z 123 and molecular ion m/z 414 in the mass spectra for all of these compounds makes them comparatively similar to the onocerane I, II and III published by Kimble *et al.* (1974) and in subsequent reports of

onocerane I, by Curiale (1988) in the Oligocene shale of the Kinshenehn Formation in Montana, Oligocene shales of the Shahejie Formation in China by Wang *et al.* (1988) and Pindiga Formation shales of the Upper Benue Trough Nigeria by Pearson and Obaje (1999). The mass spectra of compounds A_1, A_2, B_1 and B_2 are just like that for the onocerane-I up to the m/z 191, not surprising given identical A and B-rings, any slight variation is attributable to instrumental factors. However, the presence of significant m/z 109 and m/z 137 ions are unlike those in the mass spectra previously reported for the onoceranes. The low abundance of m/z 191 ions explains why these novel compounds are difficult to identify in the m/z 191 GC-MS mass chromatograms. The A and B pairs are probably differing in their stereochemistry at one or more carbon number position in their ring structures and unlike compound C, the absence of M^+-43 ion at m/z 371 in their mass spectra suggests an oleanane-type structure for the compounds A_1, A_2, B_1 and B_2. Notable in their mass spectra characteristics are: A_1: m/z 193>191, A2: m/z 191≈193, B_1: m/z 193>191, B_2: m/z 193≈191 C: m/z 193≈191. More importantly, m/z 177<193 for A_1 and B_1, but 177≈193 for A_2 , B_2 and C. Also, $M^+ > M^{-15}$ for A_1 and B_1, but $M^+ \approx M^{-15}$ for A_2, B_2 and C.

It can thus be concluded that compounds A_1, A_2, B_1 and B_2 and C are all C30 tetracyclics with C- ring opened at C8(14), but A_1, A_2, B_1 and B_2 have an hexacyclic E ring. The stereochemistry at C-8 and C-14 may control m/z 191/193 ratio. If so, probably 8α(H), 14β(H) as with the secohopane, for A_2 and B_2 (191≈193)

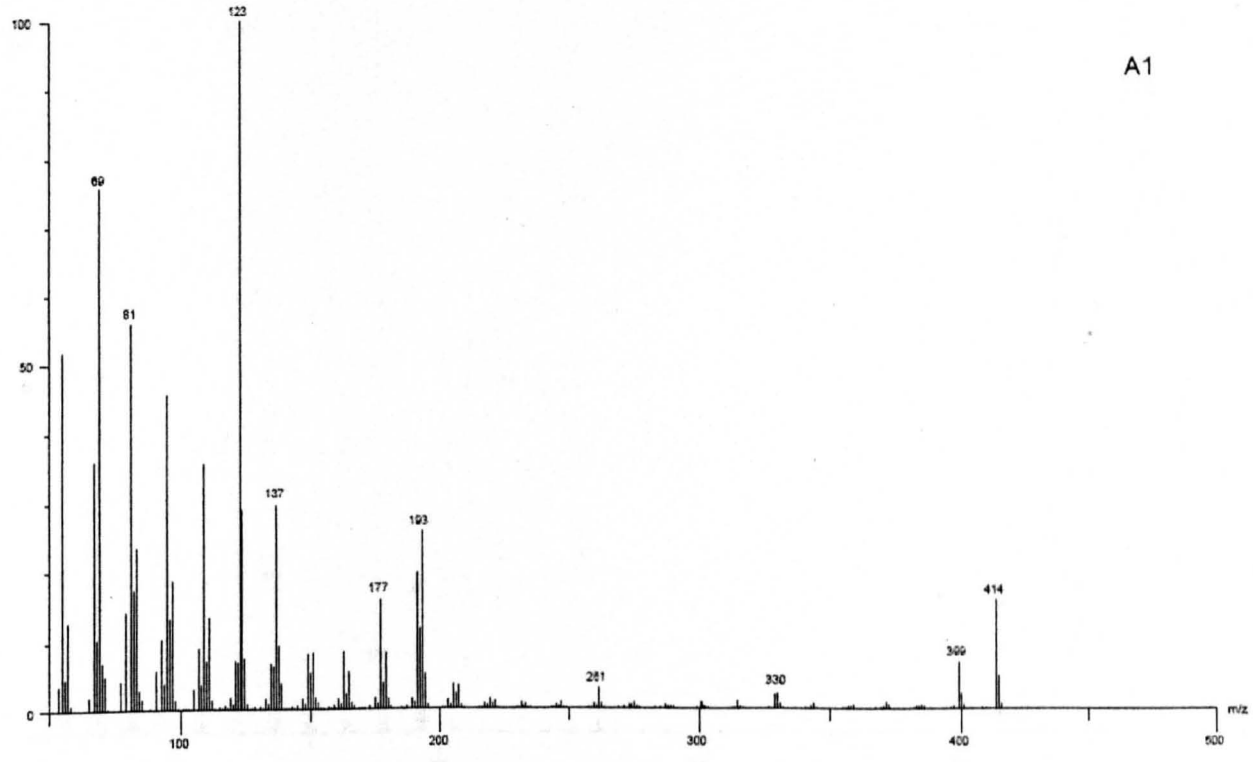

Figure 6.8. Mass spectrum of compound A_1.

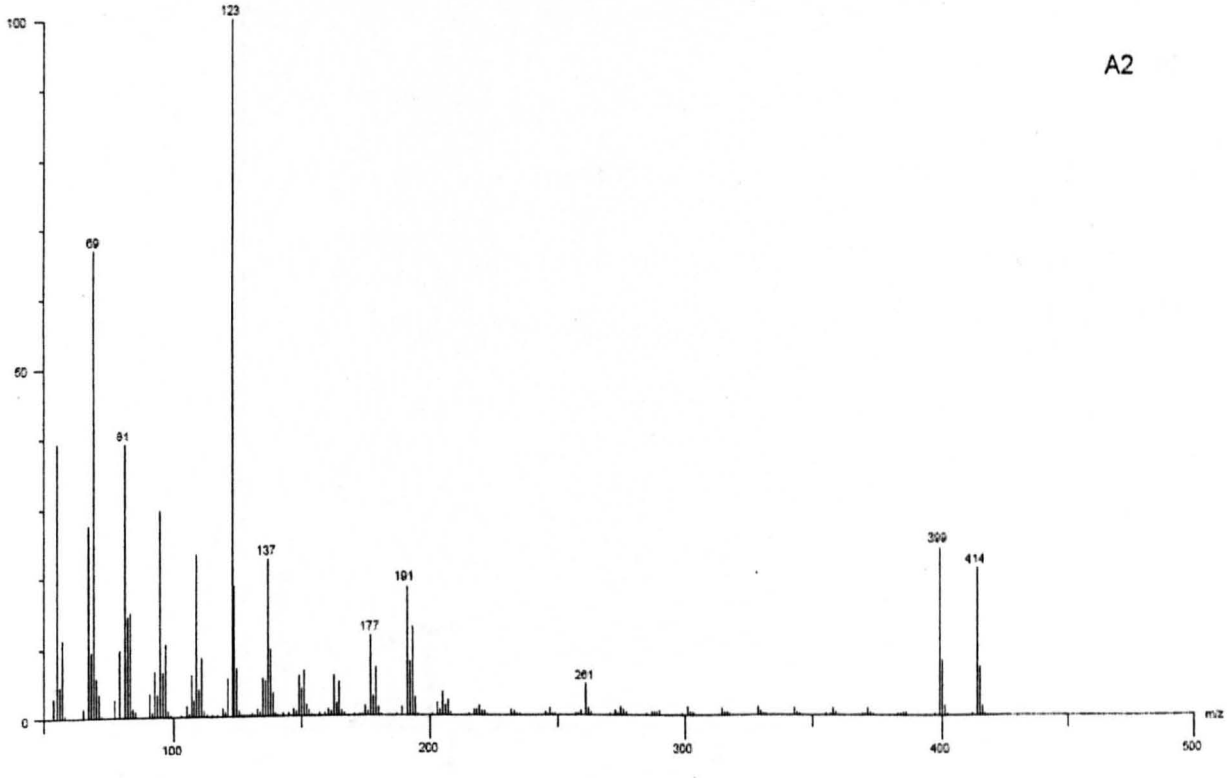

Figure 6.9. Mass spectrum of compound A_2.

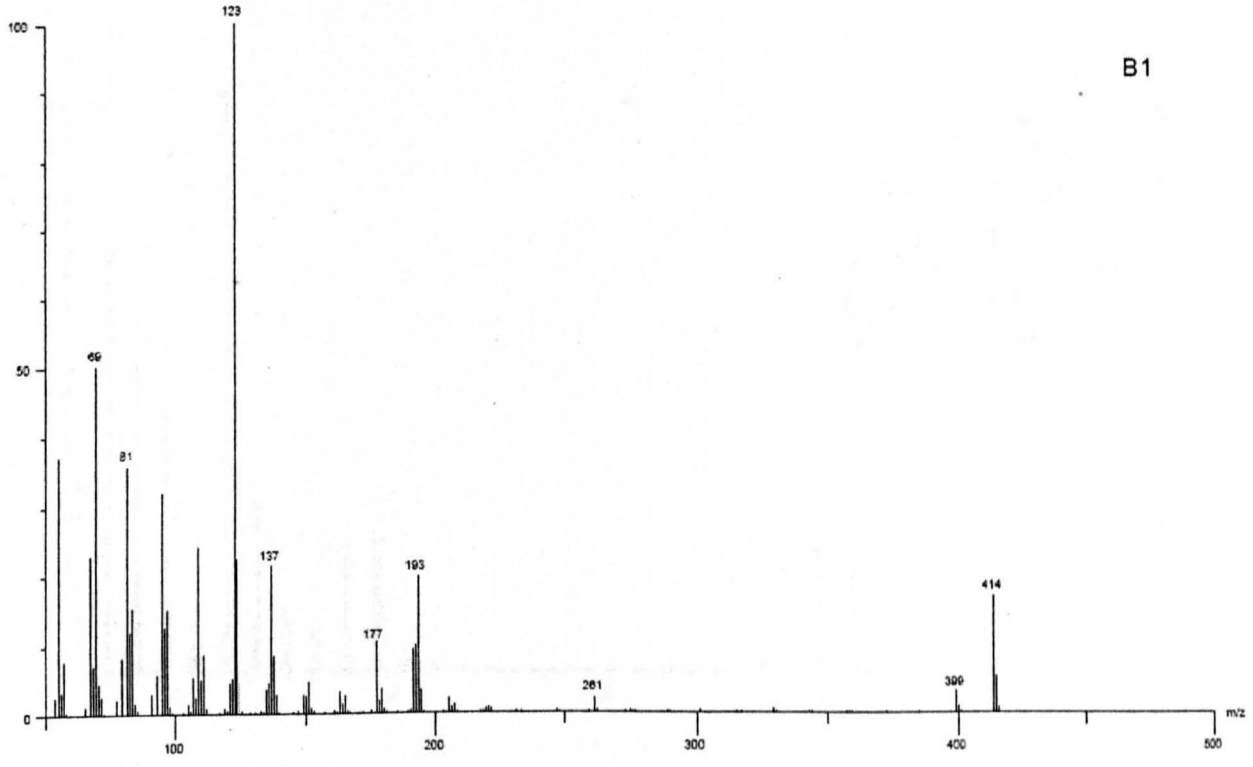

Figure 6.10. Mass spectrum of compound B_1.

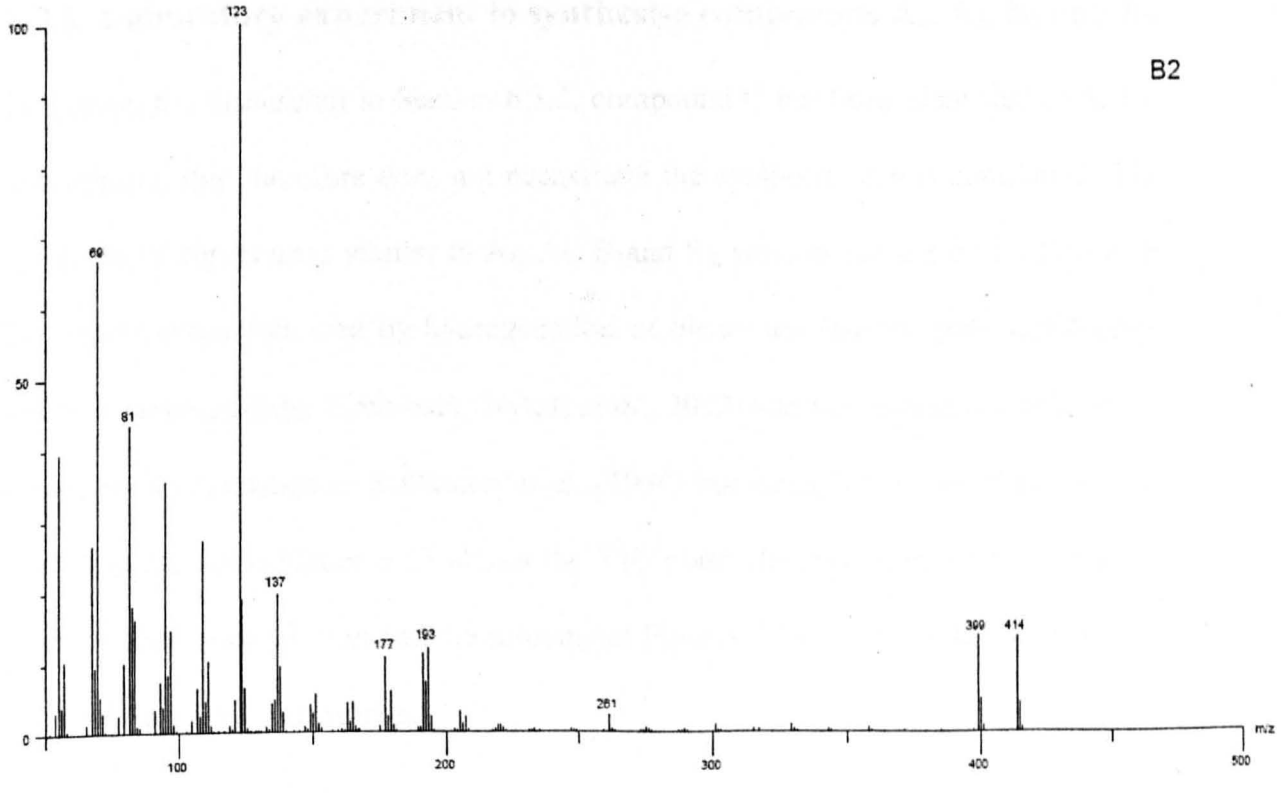

Figure 6.11.Mass spectrum of compound B_2.

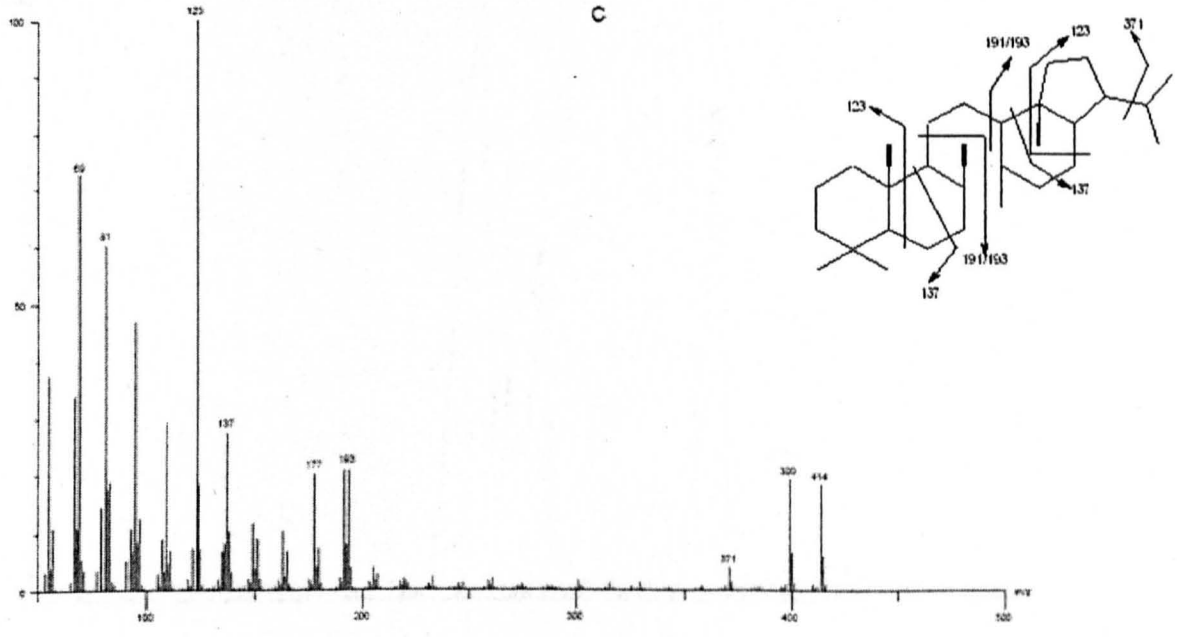

Figure 6.12. Mass spectrum of Compound C. Insert is the likely structure and the various fragmentation patterns to generate the mass spectrum ions.

6.3.2. Laboratory experiment to synthesise compounds A_1, A_2, B_1 and B_2

Following the discussion in Section 6.3.2, compound C has been identified as 8, 14-secohopane, this therefore does not necessitate the synthesis of this compound. The synthesis of compounds similar to A_1, A_2, $B_1$and B_2, was carried out by Dr P. Nytoft by isomerisation followed by hydrogenation of oleanenes. Briefly, pure lup-20(29)-ene was prepared from birch-bark (Nytoft *et al.*, 2002) and isomerised to a mixture of oleanenes as described in Rullkötter *et al.* (1994) but using 0.1 N Perchloric acid in glacial acetic acid. Figure 6.13 shows the TIC mass chromatogram of the oleanene mixture after isomerisation and the subsequent Figures 6.14 -6.17 are the mass spectra of the oleanenes in the mixture.

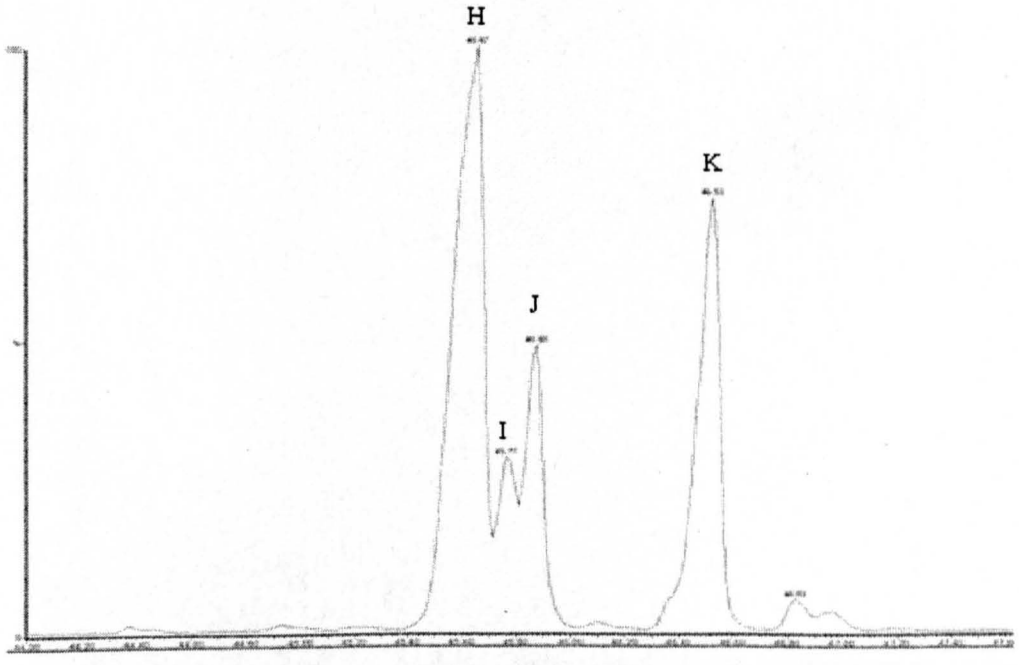

Figure 6.13. Total ion current (full scan) showing the mixtures of oleanenes formed after isomerisation. Peaks labelled H, I, J and K are olean-13(18)-ene, olean-12-ene, oleane-18-ene, and 18α-olean-12-ene respectively.

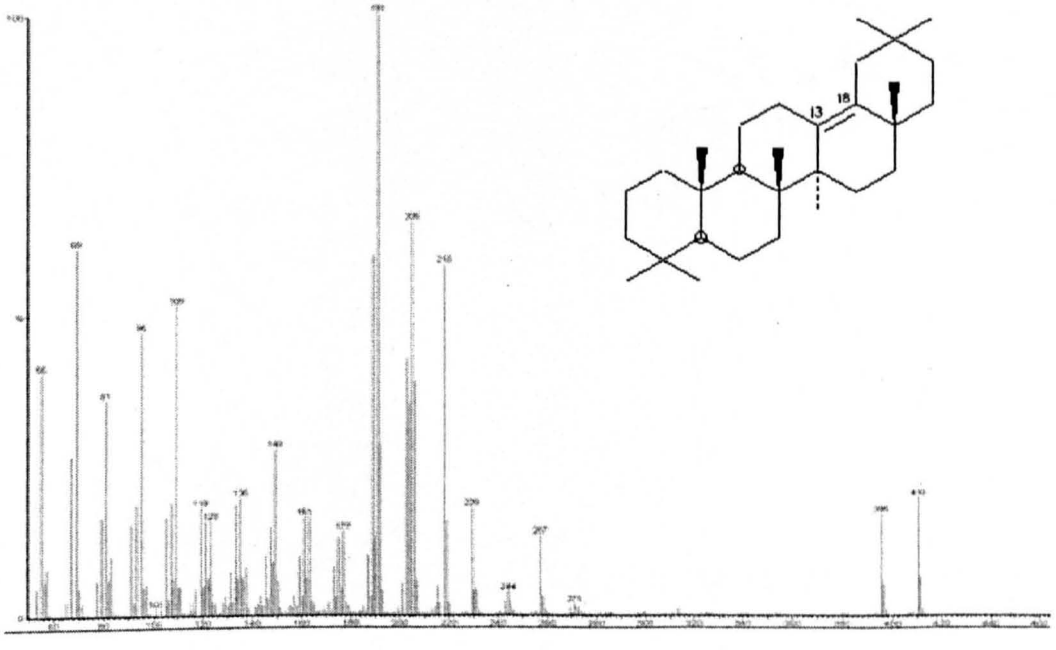

Figure 6.14. Mass spectrum of olean-13(18)-ene (peak H, Figure 6.13) obtained from isomerisation of lup-20(29)-ene from birch tree.

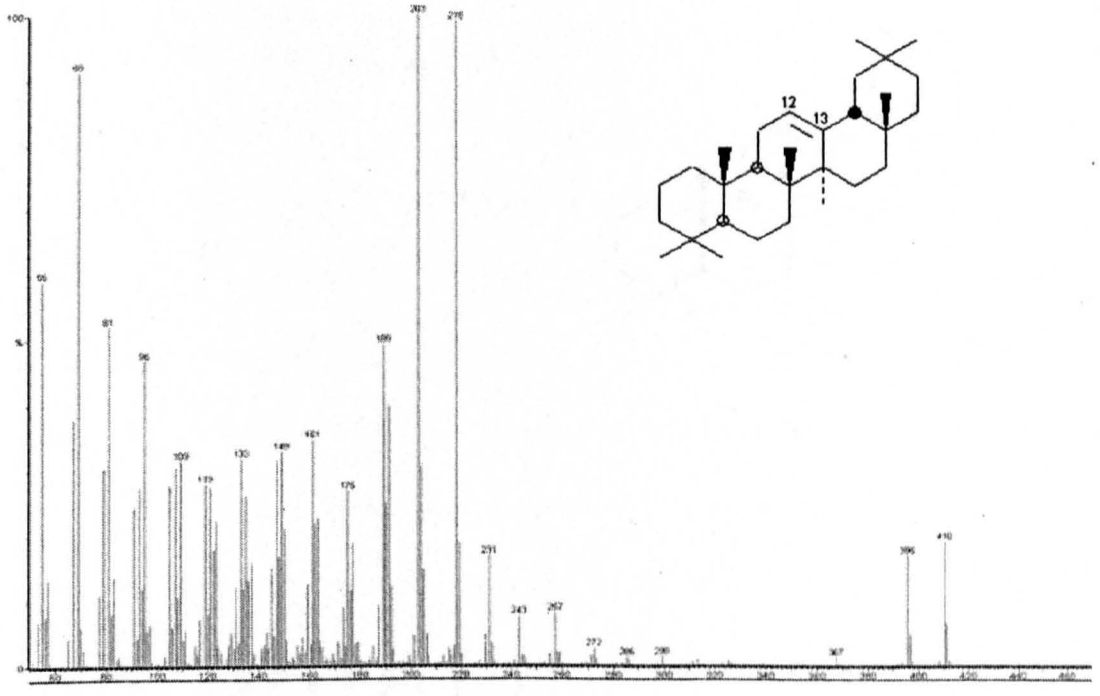

Figure 6.15. Mass spectrum of 18β-olean-12-ene (peak I, Figure 6.13) obtained from isomerisation reaction of lup-20(29)-ene from birch tree.

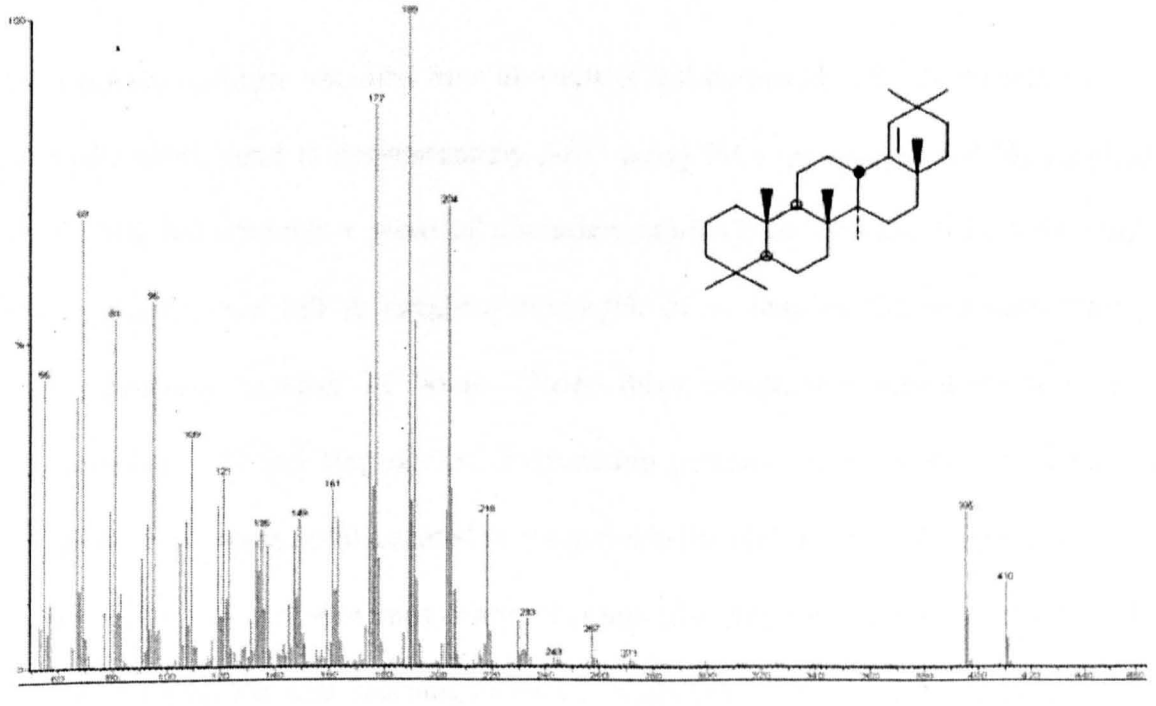

Figure 6.16. Mass spectrum of olean-18-ene (peak J, figure 6.13) obtained from isomerisation reaction of lup-20(29)-ene from birch tree.

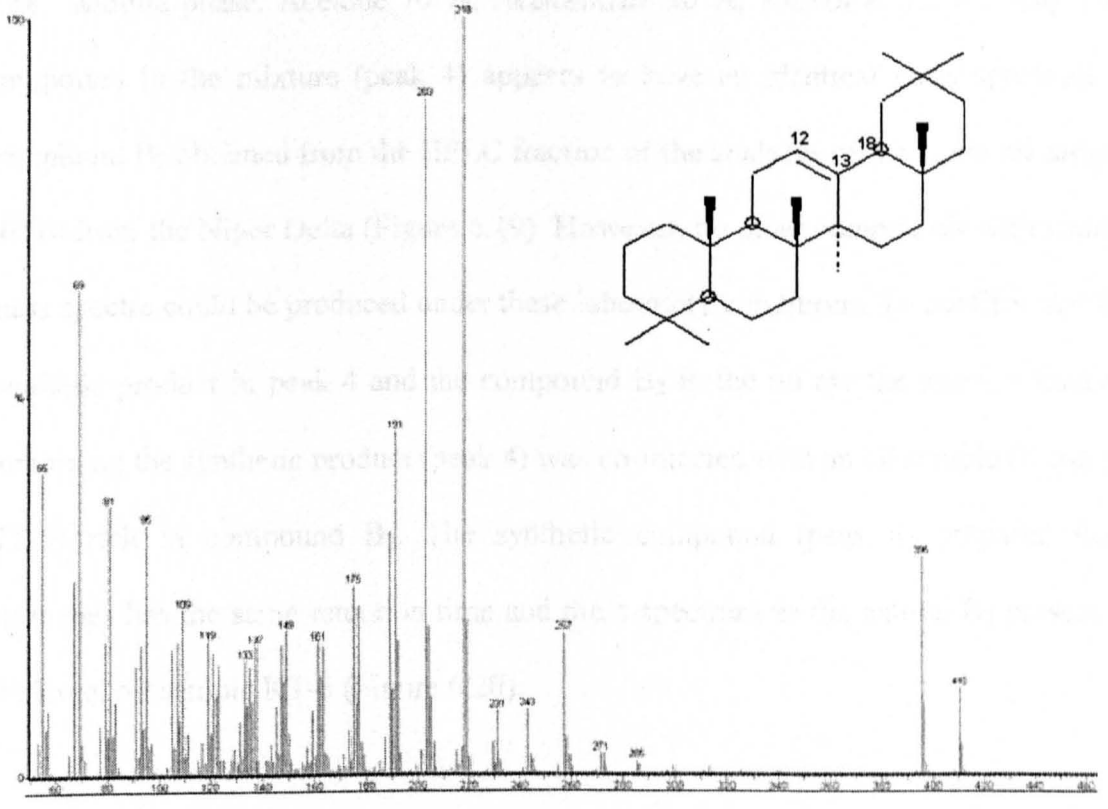

Figure 6.17. Mass spectrum of 18α-olean-12-ene (peak K, Figure 6.13) obtained from isomerisation reaction of lup-20(29)-ene from birch tree.

The oleanene mixture obtained from above was hydrogenated in 0.1 N Perchloric acid in glacial acetic acid at approximately 50°C using PtO_2 as catalyst and H_2 supplied from a balloon through a piece of discarded capillary GC-column (I.D. 0.53 mm). Hydrogenation was left to progress overnight, or as long as the hydrogen supply lasted, probably around 12 hours. Under these conditions, oleanenes were not hydrogenated whereas ring-opened degradation products from oleanenes (catalyst: perchloric acid) were hydrogenated to compounds thought to be 8, 14-seco-oleananes. Figure 6.18 is an m/z 414 mass chromatogram showing the mixture of compounds from hydrogenation and rearrangement of oleanenes. The mixture of compounds from the hydrogenation was separated using reverse phase HPLC similar to the final separation of triterpenoids from the ND10 oil (Column Vydac 201TP 4.6 x 250 mm,

C18. Mobile phase: Acetone 70 %, Acetonitrile 30 %, vol/vol at 0.8 ml/min). One compound in the mixture (peak 4) appears to have an identical mass spectrum to compound B_2 obtained from the HPLC fraction of the analyses of the crude oil sample ND10 from the Niger Delta (Figure 6.19). However, no other compounds with similar mass spectra could be produced under these laboratory conditions. To confirm that the synthetic product in peak 4 and the compound B_2 in the oil are the same, a fraction containing the synthetic product (peak 4) was co-injected with an oil sample (Kutei oil KT-5) rich in compound B_2. The synthetic compound (peak 4) prepared from oleanenes has the same retention time and mass spectrum as the natural B_2 present in the Kutei oil sample KT-5 (Figure 6.20).

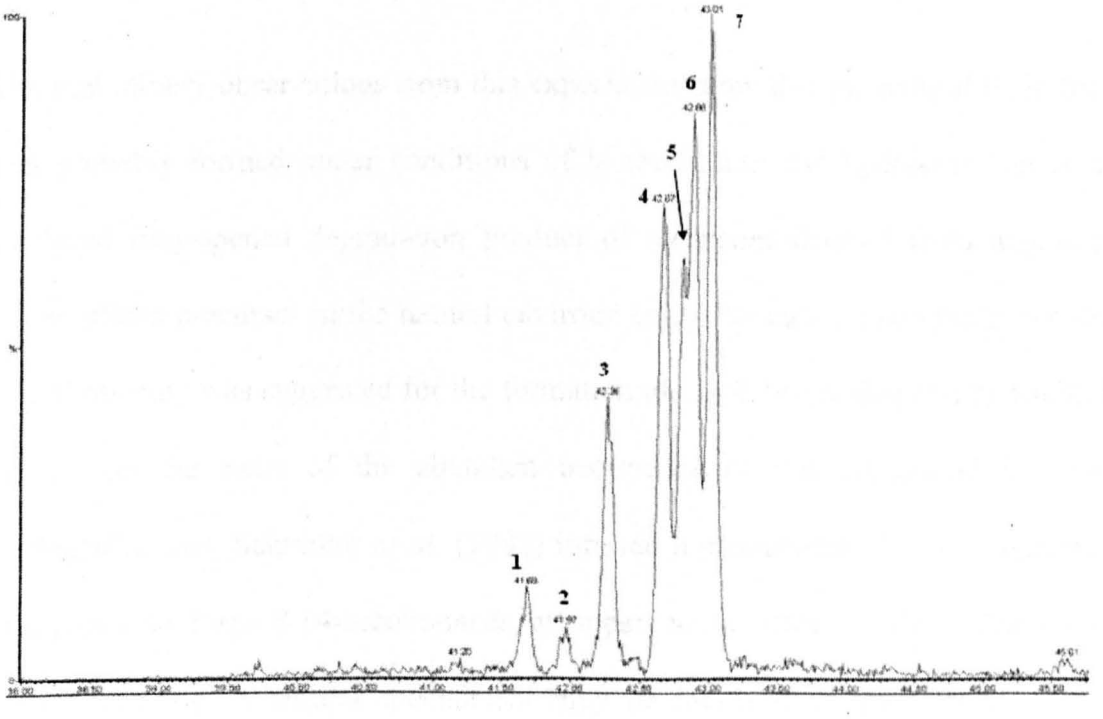

Figure 6.18. M/z 414 mass chromatogram showing the mixture of compounds formed from hydrogenation of oleanenes.

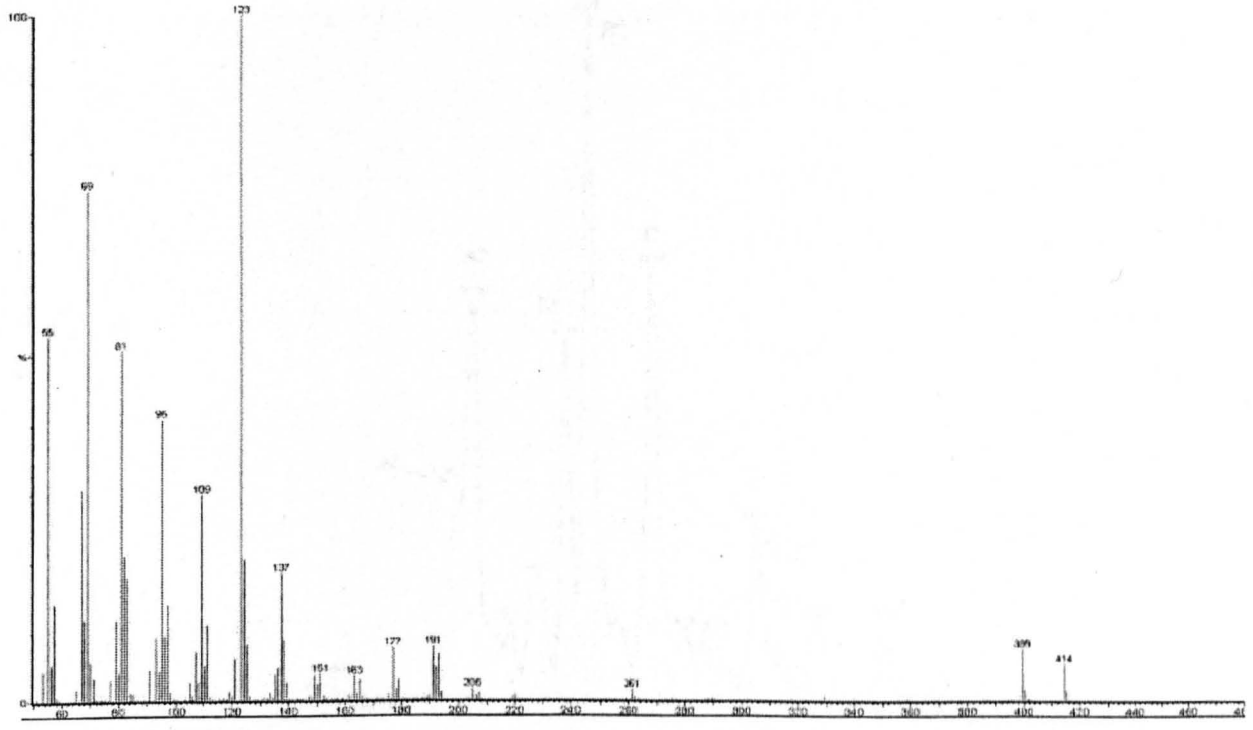

Figure 6.19. Mass spectrum of synthetic B2 (peak 4, Figure 6.18) obtained from hydrogenation of oleanane. Note the similarity of the spectrum with natural B2 in Niger Delta oil (Figure 6.11).

The preliminary observations from this experiment show that the natural B_2 in the oil was probably formed under conditions of isomerisation and hydrogenation of acid catalysed ring-opened degradation product of oleanenes derived from angiosperm higher plants precursor in the natural environment. Although, a microbially mediated ring C opening was suggested for the formation of C_{30} 8,14-secohopane by Rullkotter (1982), on the basis of the abundant occurrence of this compound in heavily biodegraded oils. Schmitter *et al.* (1982) inferred a mechanism of ring C opening in triterpanes to form 8,14-secohopanes at super acidic sites on clay minerals like montmorillonite. A similar mechanism may be involved in the formation of the supposed seco-oleananes in the deltaic oils considered here, but a microbially mediated transformation cannot be discounted.

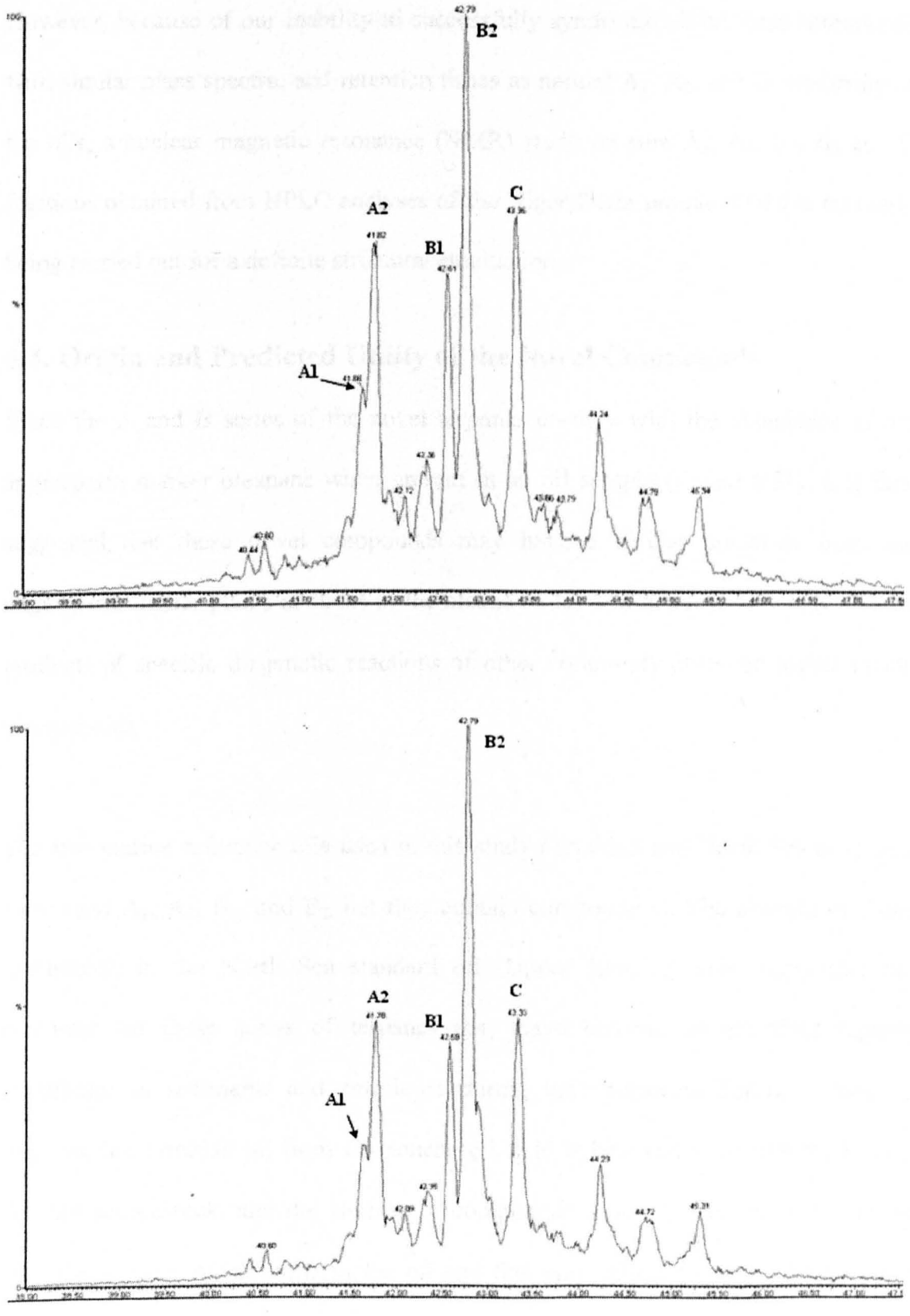

Figure 6.20. M/z 414➔123 mass chromatogram showing the distribution of compounds A_1, A_2, B_1, and B_2 in Kutei oil KT-5 (above) and similar distribution with co-injected synthetic B_2(below).Note the similarity of retention time between synthetic B_2 and natural B_2 and the increase in the area of peak B_2 in the lower chromatogram.

However, because of our inability to successfully synthesise all of these compounds with similar mass spectra, and retention times as natural A_1, A_2, and B_1 occurring in the oils, a nuclear magnetic resonance (NMR) study of pure A_1, A_2, B_1, B_2 and C fractions obtained from HPLC analyses of the Niger Delta sample ND10 is currently being carried out for a definite structural elucidation.

6.4. Origin and Predicted Utility of the Novel Compounds

Since the A and B series of the novel terpanes co-vary with the abundance of the angiosperm marker oleanane when present in an oil sample (Figure 6.21), it is thus suggested that these novel compounds may have a similar precursor from the angiosperm higher plants as those of the oleananoids. Additionally, they may also be products of specific diagenetic reactions of other commonly observed higher plants triterpenoids.

The two marine reference oils used in this study (Trinidad and North Sea oils) lack compound A_1, A_2, B_1, and B_2, but they contain compound C. The absence of these compounds in the North Sea standard oil (Upper Jurassic) may imply that the precursor for these series of terpanes may have become an abundant organic contributor to sediments and petroleum during the Cretaceous-Tertiary times. In addition, the Trinidad oil from Oropouche oil field is believed to be derived from a Tertiary source rock, and the absence of compounds A and B isomers is consistent with the absence of oleanane in the oil and this may reflect the limited land plant contribution to the source rock organic matter for this oil. Compound C occurs in measurable quantities in all samples and often remains the only significant peak in the MRM m/z 414 → 123 mass chromatograms of samples having marine organic matter characteristic (e.g. North Sea, Oropuche and some Beaufort-Mackenzie Delta and

deepwater Niger Delta oils), thus permitting a means to compare the abundance of the compounds A and B isomers.

Furthermore, based on the variation in the abundance and distribution of these compounds in samples of oils from each basin and variation among oils within the same basin, a parameter called K-Index, which sums the peak area of compounds A and B and normalised to compound C was generated and used as an indicator of level of terrigenous higher plant contribution to the source rock organic matter and perhaps stratigraphic age of the source rock: K-Index = $(A_1+A_2+B_1+B_2)/ C$. A plot of K- Index values against the oleanane indices (Figure 6.21) shows a striking positive correlation of these parameters, thus rendering tentative confirmation of a similar controlling factor. The controlling factor is suggested to be the precursor of the organic matter. In order to investigate the effect of thermal maturity on the characteristics abundance of compounds A_1, A_2, B_1, and B_2 relative to compound C, molecular thermal maturity data were generated (Table 6.1) and plots of K-Index against some of these thermal maturity parameters reveal no trend of increasing or decreasing K-index with thermal maturity (Figures 6.22 and 6.23), thus suggesting that the abundance of these compounds is not sensitive to the level of thermal evolution of the source rocks for these oils, but rather an influence imposed by original organic input and source rock age.

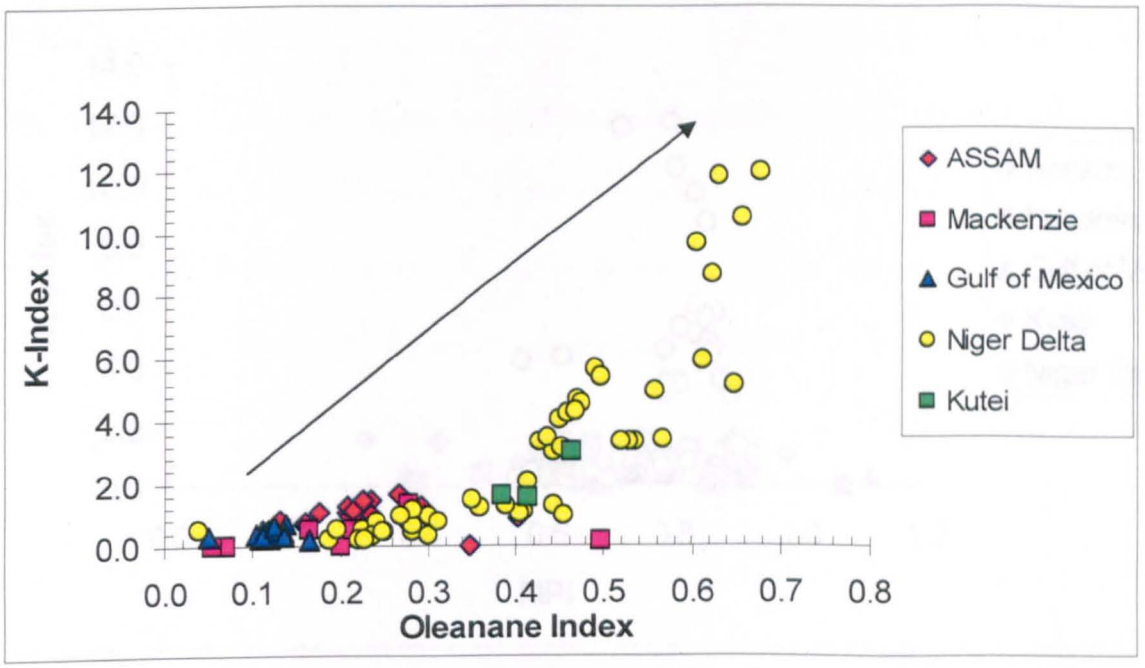

Figure 6.21. Cross plot of K-Index and Oleanane index shows a positive correlation.

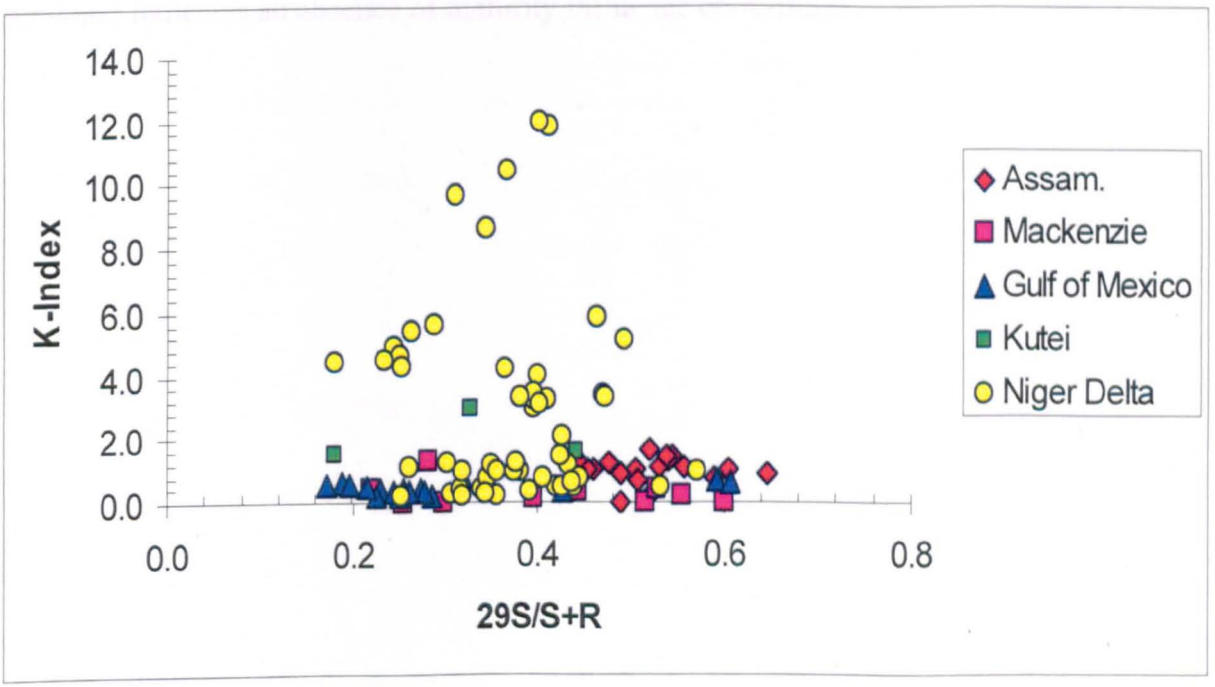

Figure 6.22. Plot of K-Index against C_{29} ααα (20S/20S+20R) sterane thermal maturity parameter reveals no data trend, thus suggesting no thermal maturity influence on K-Index.

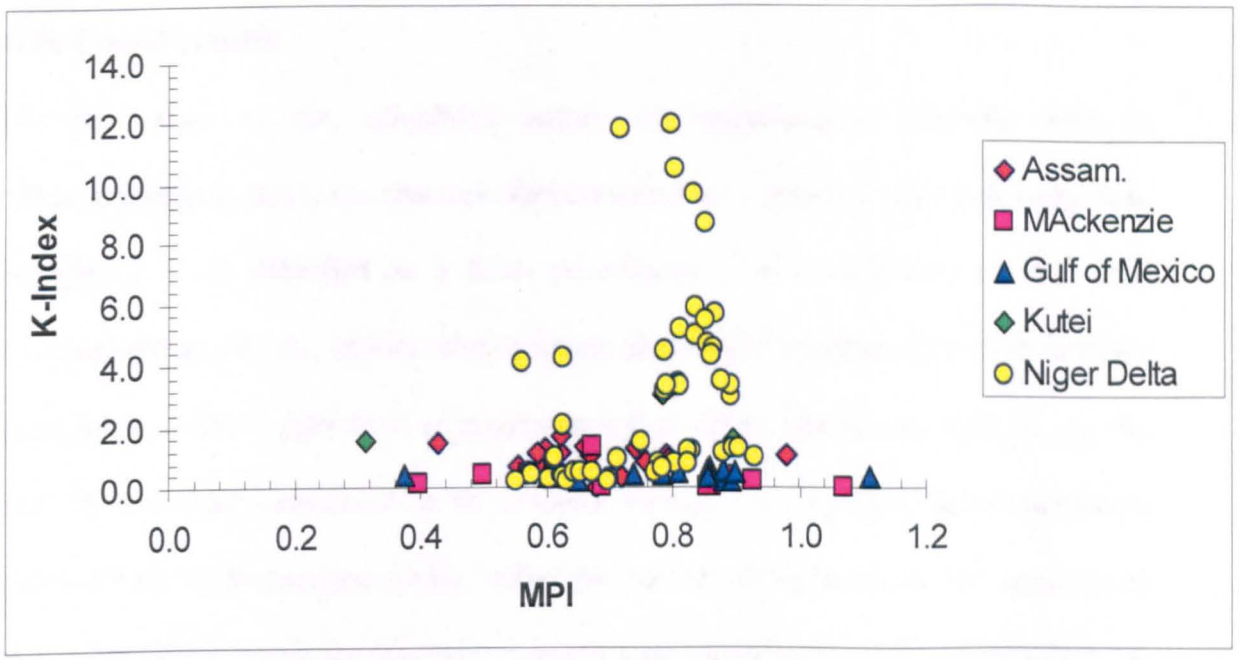

Figure 6.23. Plot of K-Index against methyl phenanthrene index (1.5*(2-MP+3-MP)/ phenanthrene+ 9-MP+1-MP) molecular thermal maturity parameter shows no data trend and indicates an absence of maturity influence on K-Index.

6.5. Conclusions

On the basis of the ubiquitous nature of compound C coupled with its chromatographic and mass spectral characteristics as compared with published data, compound C is identified as a 8,14- secohopane. The co-variance of the novel compounds A_1, A_2, B_1, and B_2 with oleanane abundance when present in oil samples suggests a similar origin from angiosperms higher plant. The compounds A_1, A_2, B_1, and B_2 are thus considered to be isomers formed by ring-opening isomerisation followed by hydrogenation of C_{30} triterpene natural components in the angiosperm flowering plants. From the laboratory experiments on oleananes, B_2 is probably 8,14-seco-oleanane. The distribution and relative concentrations of the compounds A and B isomers relative to C can be used as an indicator (K-index) of the level of land plant contribution for recognition of various source rock facies among oils in a basin. The variation in the relative abundance of A and B isomers eluting as doublets may be a thermodynamic stability control and if this is fully understood and explored using samples of source rocks, this relationship could be useful in the assessment of thermal maturity of sediments and oils. More work is suggested for the structure of these compounds in order to explore their full potential in petroleum correlation studies. An NMR analysis is currently being undertaken as part of such studies.

Table 6.1. Source and thermal maturity molecular parameters measured for the selected oils analysed for novel terpane compounds

SAMPLE	BASIN	K-Index	OL-Index	%C27	%C29	%C30	Pr/Ph	C_{29}S/S+R	$C_{29}\beta\beta$/ $\beta\beta+\alpha\alpha$	C_{32} S/S+R	MPI
AS-1	Assam	1.12	0.21	7.51	87.18	0.00	5.92	0.56	0.56	0.57	0.62
AS-2	Assam	0.93	0.21	4.44	78.65	0.00	6.52	0.65	0.55	0.56	0.79
AS-3	Assam	1.07	0.18	4.87	74.81	0.00	6.90	0.51	0.51	0.57	0.79
AS-4	Assam	0.68	0.16	7.92	64.41	0.00	6.20	0.51	0.73	0.59	0.55
AS-5	Assam	1.08	0.22	5.70	83.27	0.00	6.16	0.46	0.58	0.56	0.76
AS-6	Assam	1.07	0.22	8.31	72.25	0.00	5.92	0.60	0.63	0.52	0.98
AS-7	Assam	1.47	0.24	5.97	79.64	0.00	5.04	0.54	0.61	0.58	0.43
AS-8	Assam	1.03	0.23	1.38	88.30	0.00	5.71	0.45	0.56	0.55	0.67
AS-9	Assam	1.30	0.29	6.79	73.33	0.00	4.82	0.44	0.33	0.55	0.66
AS-10	Assam	0.33	0.12	14.35	70.68	0.00	6.53	0.52	0.58	0.56	0.72
AS-11	Assam	0.91	0.40	21.99	46.48	0.00	4.20	0.49	0.72	0.55	0.79
AS-12	Assam	1.27	0.28	7.89	52.56	0.00	5.31	0.48	0.40	0.58	0.60
AS-13	Assam	1.29	0.21	3.35	82.41	0.00	6.82	0.54	0.59	0.56	0.74
AS-14	Assam	0.83	0.13	13.14	64.22	0.00	5.78	0.44	0.55		0.76
AS-15	Assam	0.78	0.16	6.17	82.54	0.00	4.42	0.59	0.64	0.58	0.59
AS-16	Assam	1.14	0.22	6.22	80.07	0.00	5.88	0.53	0.53	0.67	0.58
AS-17	Assam	1.66	0.27	7.59	79.16	0.00	6.36	0.52	0.56	0.54	0.62
AS-18	Assam	1.47	0.23	4.29	82.40	0.00	6.04	0.54	0.58	0.56	0.75
AS-19	Assam		0.35	20.47	46.08	0.00	4.49	0.49	0.50	0.58	0.68
BM-1	Beaufort-Mackenzie	0.00	0.14	3.74	92.98	0.00	3.46	0.30	0.41	0.55	0.86
BM-2	Beaufort-Mackenzie	0.01	0.07	29.91	35.54	10.19	3.58	0.52	0.56	0.56	0.86
BM-3	Beaufort-Mackenzie	0.15	0.50	3.82	91.84	0.00	0.00	0.40	0.47	0.48	0.40
BM-4	Beaufort-Mackenzie	0.02	0.06	27.30	34.11	6.22	1.57	0.60	0.68	0.57	0.69
BM-5	Beaufort-Mackenzie	0.24	0.20	23.61	56.68	0.00	4.91	0.55	0.54		0.93
BM-6	Beaufort-Mackenzie	1.35	0.28	3.38	86.95	0.00	4.10	0.28	0.42	0.54	0.67
BM-7	Beaufort-Mackenzie	0.33	0.13	2.71	94.16	0.00	0.00	0.44	0.50	0.54	0.89
BM-9	Beaufort-Mackenzie	0.70	0.20	4.69	86.49	1.81	3.58	0.25	0.45	0.54	1.07
BM-10	Beaufort-Mackenzie	0.45	0.12	23.87	47.51	20.64	1.72	0.53	0.78	0.50	0.00
BM-11	Beaufort-Mackenzie	0.43	0.23	3.02	84.37	1.93	3.56	0.22	0.38	0.53	0.57

SAMPLE	BASIN	K-Index	OL-Index	%C27	%C29	%C30	Pr/Ph	C_{29}S/S+R	$C_{29}\beta\beta$/ $\beta\beta+\alpha\alpha$	C_{32} S/S+R	MPI
BM-13	Beaufort-Mackenzie	0.53	0.16	23.1	66.2	0.00	4.81	0.35	0.50	0.53	0.88
BM-14	Beaufort-Mackenzie	0.52	0.22	15.3	68.4	0.00	4.44	0.26	0.44	0.50	0.85
GOM- 1	Gulf of Mexico	0.45	0.13	36.42	40.16	0.57	2.73	0.23	0.44	0.53	0.38
GOM- 2	Gulf of Mexico	0.68	0.14	36.88	43.09	2.14	2.79	0.59	0.62	0.54	0.61
GOM- 3	Gulf of Mexico	0.43	0.14	26.62	49.27	1.65	2.27	0.27	0.39	0.48	0.78
GOM- 4	Gulf of Mexico	0.61	0.12	39.06	27.98	0.99	2.44	0.19	0.35	0.48	0.86
GOM- 5	Gulf of Mexico	0.58	0.13	36.19	32.88	0.62	2.65	0.20	0.42	0.52	0.86
GOM- 6	Gulf of Mexico	0.44	0.11	35.01	34.60	0.80	2.65	0.26	0.43	0.53	0.74
GOM- 7	Gulf of Mexico	0.24	0.12	26.91	50.56	4.17	2.49	0.00	0.64	0.53	0.88
GOM- 9	Gulf of Mexico	0.23	0.11	37.83	35.09	nm	2.70	0.23	0.42	0.52	0.89
GOM- 10	Gulf of Mexico	0.21	0.17	39.59	32.02	0.97	2.59	0.29	0.76	0.49	0.65
GOM- 12	Gulf of Mexico	0.49	0.12	42.79	33.72	0.00	2.57	0.22	0.48	0.49	0.81
GOM- 13	Gulf of Mexico	0.54	0.11	18.32	45.62	nm	2.19	0.17	0.42	0.43	0.88
GOM- 14	Gulf of Mexico	0.51	0.12	35.24	35.22	0.00	2.72	0.31	0.43	0.54	0.90
GOM- 15	Gulf of Mexico	0.37	0.10	24.26	48.26	0.00	2.65	0.28	0.39	0.54	0.86
GOM- 16	Gulf of Mexico	0.32	0.11	17.42	50.23	1.06	2.28	0.26	0.36	0.48	1.11
GOM- 17	Gulf of Mexico	0.62	0.13	32.41	47.78	0.00	2.15	0.61	0.61	0.56	0.60
GOM- 18	Gulf of Mexico	0.35	0.05	24.48	50.07	1.21	1.86	0.43	0.55	0.55	0.62
GOM- 19	Gulf of Mexico	0.33	0.14	27.69	41.67	3.07	2.85	0.25	0.46	0.52	nm
KT5	Kutei	2.99	0.46	2.81	91.81	1.96	6.14	0.33	0.39	0.51	0.79
KT7	Kutei	1.58	0.38	9.92	73.96	0.70	8.04	0.44	0.43	0.55	0.90
KT6	Kutei	1.55	0.41	4.39	89.84	0.00	7.37	0.18	0.31	0.54	0.31
NDO01	Niger Delta	4.43	0.55	17.04	65.89	0.00	2.67	0.18	0.31	0.54	0.79
NDO02	Niger Delta	3.41	0.57	22.36	51.69	0.00	2.99	0.47	0.50	0.53	0.81
NDO03	Niger Delta	10.48	0.66	13.55	72.32	0.00	3.87	0.37	0.47	0.54	0.80
NDO04	Niger Delta	5.85	0.61	21.95	54.17	1.49	3.22	0.46	0.51	0.55	0.84
NDO05	Niger Delta	5.14	0.65	21.20	53.26	1.11	3.34	0.49	0.51	0.55	0.81
NDO06	Niger Delta	8.64	0.62	14.98	75.38	0.00	4.42	0.34	0.39	0.52	0.85
NDO07	Niger Delta	3.32	0.53	21.48	49.33	1.00	3.00	0.47	0.50	0.54	0.80
NDO08	Niger Delta	11.83	0.63	14.05	68.29	0.00	4.20	0.41	0.44	0.54	0.72

SAMPLE	BASIN	K-Index	OL-Index	%C27	%C29	%C30	Pr/Ph	C_{29}S/S+R	$C_{29}\beta\beta$/ $\beta\beta+\alpha\alpha$	C_{32} S/S+R	MPI
NDOO9	Niger Delta	3.31	0.53	33.00	40.06	1.39	2.99	0.41	0.43	0.54	0.81
NDO10	Niger Delta	11.96	0.68	13.32	69.66	0.00	4.39	0.40	0.46	0.51	0.80
NDO12	Niger Delta	1.20	0.36	32.15	39.53	3.16		0.43	0.41	0.55	0.83
NDO13	Niger Delta	0.27	0.23	36.06	35.81	1.41	2.40	0.31	0.35	0.54	0.60
NDO14	Niger Delta	0.50	0.23	38.16	33.66	1.15	2.39	0.32	0.33	0.53	0.57
NDO15	Niger Delta	0.42	0.25	33.17	39.05	1.31	2.38	0.32	0.37	0.55	0.62
NDO16	Niger Delta	0.94	0.30	35.24	35.10	1.08	2.28	0.38	0.40	0.56	0.61
NDO17	Niger Delta	0.41	0.24	34.01	37.14	0.77	2.40	0.34	0.32	0.55	0.58
NDO18	Niger Delta	0.96	0.30	37.71	32.20	0.82	2.36	0.37	0.40	0.51	0.61
NDO19	Niger Delta	0.74	0.24	34.59	34.79	1.55	2.26	0.35	0.38	0.54	0.78
NDO20	Niger Delta	0.33	0.24	36.85	34.34	1.88	2.56	0.39	0.37	0.53	0.63
NDO21	Niger Delta	0.19	0.22	38.77	29.46	1.68	2.47	0.36	0.43	0.53	0.63
NDO22	Niger Delta	0.48	0.28	48.24	30.62	0.67	2.62	0.42	0.38	0.56	0.64
NDO23	Niger Delta	0.46	0.25	33.85	34.87	1.09	2.24	0.44	0.47	0.54	0.65
NDO24	Niger Delta	0.18	0.23	28.29	42.97	0.94	2.57	0.32	0.42	0.49	0.55
NDO25	Niger Delta	0.31	0.30	31.29	36.48	1.60		0.34	0.44	0.53	0.70
NDO26	Niger Delta	0.19	0.19	32.40	32.54	1.98	2.88	0.25	0.37	0.53	0.70
NDO28	Niger Delta	0.77	0.28	20.13	57.55	0.00	1.77	0.45	0.40	0.55	0.80
NDO29	Niger Delta	4.92	0.56	21.69	54.52	0.00	2.81	0.24	0.38	0.55	0.84
NDO30	Niger Delta	1.10	0.41	16.29	61.64	0.00	2.18	0.26	0.44	0.56	0.88
NDO31	Niger Delta	9.66	0.60	20.99	60.49	0.00	2.99	0.31	0.43	0.56	0.83
NDO33	Niger Delta	1.01	0.40	29.50	47.84	1.44	2.46	0.32	0.43	0.56	0.93
NDO34	Niger Delta	4.06	0.45	30.37	46.15	0.00	2.61	0.40	0.44	0.51	0.56
NDO35	Niger Delta	1.28	0.39	22.42	52.52	0.00	2.28	0.30	0.40	0.55	0.90
NDO36	Niger Delta	4.23	0.46	21.09	53.55	0.36	2.29	0.36	0.41	0.57	0.63
NDO39	Niger Delta	0.48	0.04	34.73	40.27	1.60		0.43	0.47	0.57	0.77
NDO40	Niger Delta	0.62	0.28	33.05	39.24	1.13	3.10	0.44	0.47	0.56	0.78
NDO41	Niger Delta	1.27	0.44	29.88	42.39	1.18	3.08	0.38	0.46	0.54	0.91
NDO42	Niger Delta	1.18	0.28	21.04	63.50	0.00	2.18	0.35	0.38	0.55	0.82
NDO43	Niger Delta	1.49	0.35	16.95	55.13	0.00	2.24	0.42	0.47	0.57	0.75

SAMPLE	BASIN	K-Index	OL-Index	%C27	%C29	%C30	Pr/Ph	C_{29}S/S+R	$C_{29}\beta\beta/\beta\beta+\alpha\alpha$	C_{32} S/S+R	MPI
NDO44	Niger Delta	0.95	0.45	27.92	44.31	1.40	2.04	0.57	0.63	0.55	
NDO45	Niger Delta	0.76	0.31	27.74	50.36	1.45	2.12	0.41	0.44	0.56	0.82
NDO46	Niger Delta	0.94	0.27	24.92	52.15	0.00	2.11	0.36	0.49	0.57	0.71
NDO47	Niger Delta	0.48	0.20	23.79	50.21	1.46	2.12	0.53	0.52	0.57	0.67
NDO48	Niger Delta	2.98	0.44	23.23	54.36	0.00	3.96	0.40	0.46	0.54	0.89
NDO49	Niger Delta	5.65	0.49	23.73	47.91	0.00	4.11	0.29	0.45	0.56	0.87
NDO50	Niger Delta	3.29	0.43	20.74	55.63	0.00	4.01	0.40	0.50	0.57	0.89
NDO51	Niger Delta	4.64	0.47	21.85	50.23	0.00	4.02	0.25	0.40	0.53	0.86
NDO52	Niger Delta	4.52	0.48	24.96	47.87	0.00	3.98	0.23	0.40	0.52	0.87
NDO53	Niger Delta	3.45	0.44	21.76	58.47	0.00	4.02	0.40	0.46	0.52	0.88
NDO54	Niger Delta	5.40	0.50	23.57	49.35	0.81	3.95	0.26	0.40	0.56	0.85
NDO55	Niger Delta	4.31	0.47	21.70	51.22	0.48	3.92	0.25	0.41	0.52	0.86
NDO56	Niger Delta	3.15	0.45	29.06	41.44	0.81	3.28	0.40	0.47	0.55	0.79
NDO57	Niger Delta	3.34	0.52	27.88	42.25	0.71	2.96	0.38	0.47	0.53	0.79
NDO58	Niger Delta	2.06	0.41	28.04	43.66	0.47	2.97	0.43	0.47	0.56	0.63
Oropouche	Trinidad	0.00	0.07	33.12	33.37	1.17		0.43	0.55	0.53	
VisselFrisk	North Sea, UK	0.00	0.00	33.63	40.76	5.49	1.49	0.51	0.63	0.58	

K-Index = sum compounds $(A_1+A_2+B_1+B_2)/C$. OL- index = 18α(H) + 18β(H) oleanane/C_{30} 17α(H), 21β(H) hopane. C_{29} S/S+R =5α(H),14α(H),17α(H) C_{29} 20S/20S+20R sterane thermal maturity parameter from GC-MS-MS analyses. %C27-%C30 = percentage of C27-C30 to sum 27-30 steranes for 5α(H), 14α(H), 21α(H) 20R sterane from GC-MS-MS. Pr/Ph = Pristane/phytane ratio from GC. $C_{29}\beta\beta/\beta\beta+\alpha\alpha$ =5α(H), 14β(H), 17β(H) 20S +20R / 5α(H), 14β(H), 17β(H) + 5α(H), 14α(H), 17α(H)- 20S+20R thermal maturity parameter for C_{29} steranes from GC-MS-MS analyses. C32 S/S+R =17α(H), 21β(H)-bishomohopane 22S/22S+22R isomerisation thermal maturity parameter. MPI = (methylphenanthrene index); 1.5*(2-methylphenanthrene + 3-methylphenanthrene) / (Phenanthrene + 1-methylphenanthrene + 9-methylphenanthrene).

CHAPTER SEVEN

ISOTOPE GEOCHEMISTRY

Summary

The stable isotope composition of a crude oil is primarily controlled by the isotopic composition of its source rock organic matter. Therefore, because of the source signature inherent in crude oil stable isotope compositions, stable isotope data in combination with biomarker data offer more reliable assessment of petroleum systems than either used alone. This chapter discusses the data for the bulk saturated and aromatic hydrocarbon fractions and compound specific stable carbon isotope analyses (CSIA) performed on representative crude oil samples from the Assam, Beaufort-Mackenzie, Gulf of Mexico, Niger and the Kutei basins. The stable carbon isotope data have been interpreted in the light of the oil source rock organic matter in each of the case study basins. In most cases, both the bulk and compound specific stable carbon isotope data are in agreement with the organofacies (marine vs. terrigenous organic matter sourced oils) indications from molecular data in Chapter Five. The original source rock kerogen proved to be the primary control on the *n*-alkane stable carbon isotope profiles in this study.

7.0. Introduction

Isotopes are atoms containing the same number of protons in their nuclei but different numbers of neutrons (Hoefs, 2004, pp.1; Peters *et al.*, 2005a, pp. 136). Atomic mass is related to the numbers of protons and neutrons while the atomic number is determined by the number of protons. In essence, isotopes have the same atomic numbers and hence chemical properties, but different atomic masses. The analyses of stable isotope ratios of certain elements (e.g. carbon $^{13}C/^{12}C$, sulphur $^{34}S/^{32}S$ and hydrogen $^{2}H/^{1}H$) is useful in petroleum exploration studies to establish genetic relationships among source rocks/sediments, kerogen, bitumen, crude oils and hydrocarbon gases as it relates to their organic provenance and depositional environment (e.g. Stahl & Carey, 1975; Fuex, 1977; Stahl, 1977; Schoell, 1984; Sofer, 1984; Peters *et al.*, 1986, 1993; Li *et al.*, 2005). Additionally, since the stable isotope composition of an oil is primarily controlled by the isotopic composition of its source rock organic matter, the stable isotope data in combination with biomarker data therefore offers a more reliable assessment of petroleum systems than biomarkers alone and they have become a necessary tool for successful oil-oil and oil-source rock correlations studies (e.g. Peters *et al.*, 1986; Scotchman *et al.*, 1998; Al-Arouri *et al.*, 1998; Peters *et al.*, 2000; Haack *et al.*, 2000; Curiale *et al.*, 2005; Kotarba *et al.*, 2007).

Of the stable isotopes in petroleum, stable carbon isotope measurements are routinely undertaken because of the relatively analytical ease of stable carbon isotope measurements made possible by the highest proportional occurrence of carbon among other elements in petroleum (Peters *et al.*, 2005a). A comprehensive discussion of principles, mechanisms of isotopic fractionation and their applications can be found in Kaplan (1975), Schoell (1984), and Hoefs (1997, 2004). In brief, isotope values are

represented as delta (δ) values which represent the deviation in parts per thousand (‰; permil) of the isotope abundance ratio of the heavy (^{13}C) and light (^{12}C) carbon isotopes of a sample from that in a known and acceptable standard (Hoefs, 1997, 2004; Peters *et al.*, 2005a). The more negative the delta value is, the more enriched in the lighter isotope (depleted in heavy isotope) is the sample relative to the standard and vice versa (Hoefs, 2004).

Stable isotope measurements are usually carried out on whole oil and bulk saturated and aromatic hydrocarbon fractions of the whole oil. However, notable is the fact that isotopic measurements performed on bulk hydrocarbon fractions can be significantly influenced by the presence and the relative abundance of certain compound classes (e.g. isoprenoid alkanes relative to other alkanes) having different isotopic compositions (either heavier or lighter than other compounds) within these petroleum fractions. In spite of this observation, useful applications have been made of stable isotope values of bulk saturated and aromatic hydrocarbon fractions in combination with biomarkers in various correlation studies (e.g. Sofer, 1984; Peters *et al.*, 1986; Peters *et al.*, 2000; Haack *et al.*, 2000).

However, as analytical capability has advanced over time, stable isotope measurements are now performed on individual abundant and well resolved compounds in crude oils and source rock bitumen extracts, thus reducing the likelihood of the isotope values of certain compound classes (e.g. saturated and aromatic) being influenced by a few compounds having significantly different isotopic compositions. This analytical technique is called compound specific isotope analysis (CSIA) (Mathew & Hayes, 1978; Hayes *et al.*, 1987, 1990; Freeman *et al.*,

1990). Compound specific stable carbon isotope analyses (CSIA), particularly of the *n*-alkanes, when combined with the analysis of a wide range of biological marker compounds (biomarkers), arguably offers a more reliable determination of organo-facies and correlation than isotope data from bulk saturated and aromatic hydrocarbon fractions.

Despite the proven robust utility of CSIA as a tool for reconstruction of ancient biogeochemical pathways (Hayes *et al.*, 1987; Freeman *et al.*, 1990), and its application in a number of basins such as the North Sea (Bjorøy *et al.*, 1991, 1994), this technique has not been applied as a complementary tool to better assess the oil systems in most Tertiary deltas, except for Miocene reservoired oils in Sulawesi assessed by Curiale and co workers (2005). CSIA data can also on its own merit help to unravel and quantify the degree of oil mixing (Rooney *et al.*, 1998). One challenge to CSIA data availability is indisputably that of analytical cost.

This chapter discusses the hydrocarbon fraction and compound specific stable carbon isotope measurements performed on representative crude oil samples from the Assam, Beaufort-Mackenzie, Gulf of Mexico, and Niger deltas.

7.1. Sample rationale

Considering the analytical cost inherent in stable isotope analyses, samples were selected for either bulk stable carbon isotopes of hydrocarbon fractions or CSIA using the rationale discussed in this Section. Following the previous discussions on molecular geochemistry (Chapter Five), the samples of oils from Assam are compositionally similar based on biomarkers and reflect dominantly terrigenous organic matter derived oils, and for this reason, bulk saturated and aromatic

hydrocarbon stable carbon isotope analyses were performed on this oil set and a few oils were only analysed for CSIA data to investigate if both analytical data sets were in agreement. Additionally, since most of the Gulf of Mexico Tertiary deltaic reservoired oils are compositionally similar in terms of their biomarker content, bulk saturated and aromatic hydrocarbon stable carbon isotope data was generated and only few samples were taken for CSIA to ascertain sample isotopic compositional homogeneity.

Conversely, where samples of oils separatedinto various organofacies groupings, as was the case for the Beaufort-Mackenzie and Niger Delta basins, end member oils were analysed only for their CSIA stable carbon isotope data in order to investigate whether the oil organofacies-defined families obtained based on molecular data were supported by the CSIA data. The analytical methods for the CSIA are as presented in Section in 3.5.

7.2. Bulk Stable Carbon Isotope Results and Discussion

7.2.1. Assam Delta

Bulk $\delta^{13}C$ stable carbon isotope values are presented in Table 7.1 From the measured $\delta^{13}C$ values of the saturated and aromatic hydrocarbon fractions, the Assam oils mostly separate into the non-marine region of Figure 7.1 as defined by the canonical variable (CV) line (CV is based on Sofer, 1984 = -2.53 ($\delta^{13}C$ sat) +2.22 ($\delta^{13}C$ arom) - 11.65). Nevertheless, despite the overwhelmingly terrigenous biomarker signature of the Assam oils, a few samples plot in the marine region of Figure 7.1. This observation has been made by previous workers (e.g. Peters *et al.*, 1986), that stable carbon isotope ratios of crude oil saturated and aromatic hydrocarbon fractions may

sometimes incorrectly classify a non-marine terrigenous organic provenance sourced oil (waxy) into marine (non-waxy) and vice versa. In an effort to investigate whether the bulk isotope fractions $\delta^{13}C$ values have actually downgraded the geochemical similarity in terms of source facies among the Assam oils, one of the two outlier Assam samples in Figure 7.1 was analysed by CSIA along with a few oils plotting in the non-marine region of Figure 7.1. The CSIA data (Figure 7.3) show significant variation in the $\delta^{13}C$ values of the crude oil *n*-alkanes in the region between C_{12}- C_{20} *n*-alkanes among these oils, other than this observation, the samples appear similar, thus attesting to the biomarker data that the source facies for these oils are overwhelmingly terrigenous organic matter of similar kerogen composition.

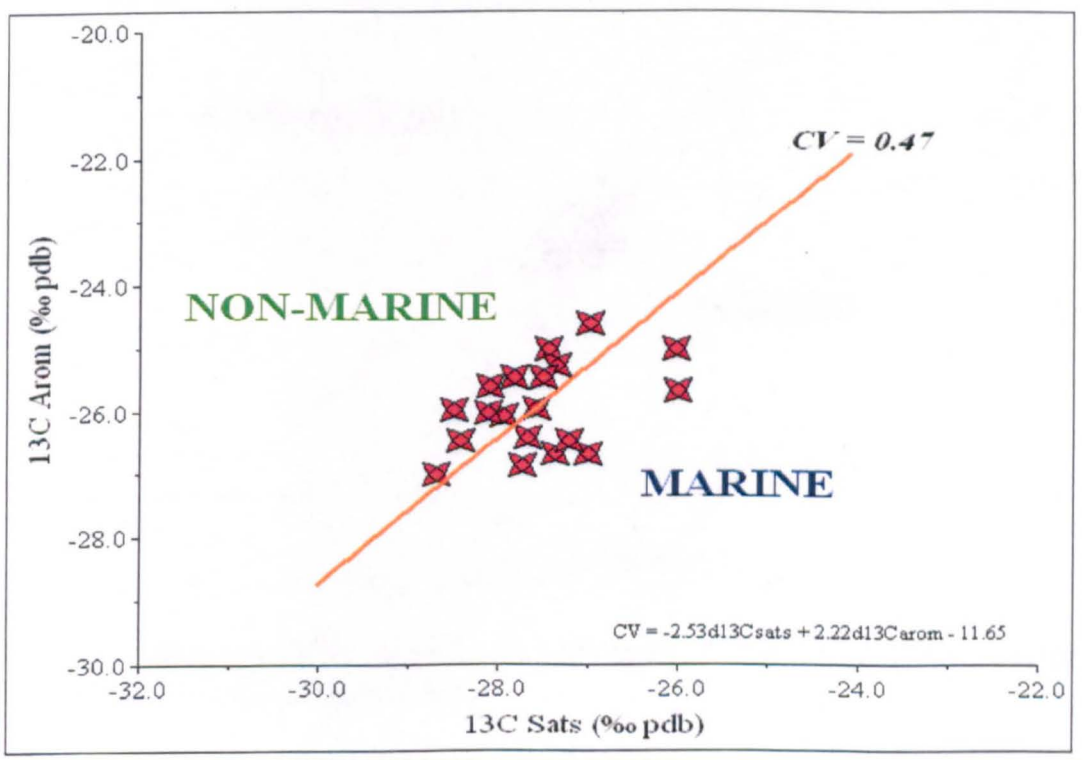

Figure 7.1. Plot of the $\delta^{13}C$ values of the bulk saturated and aromatic hydrocarbon fractions of the Assam oils.

7.2.2. Gulf of Mexico

The samples of oils from the Gulf of Mexico are compositionally similar in their saturated and aromatic hydrocarbon fractions $\delta^{13}C$ values as revealed by the clustering of data points in Figure 7.2. The oils plot in the marine region of the CV line. This geochemical homogeneity is in accord with the molecular data presented in section 5.4 of chapter five. Based on the Sofer (1984) interpretation, the $\delta^{13}C$ values of these oils thus suggests expulsion from a source rock rich in marine kerogen.

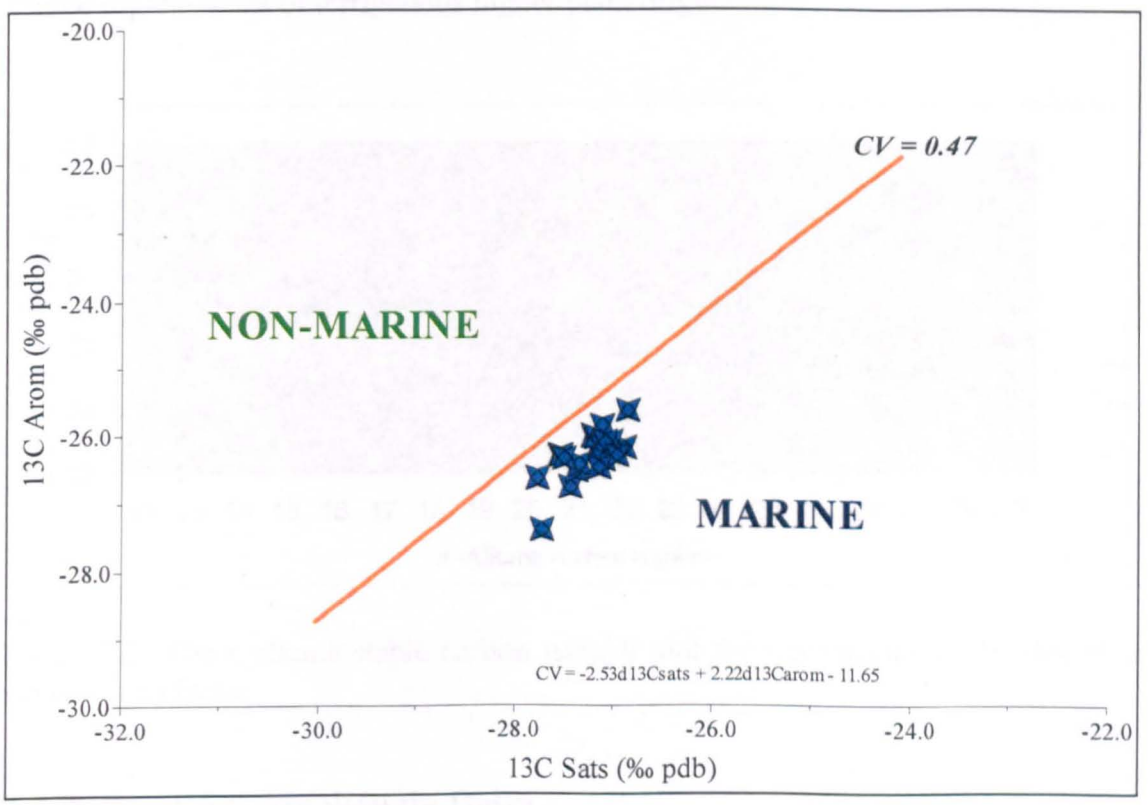

Figure 7.2. Plot of the $\delta^{13}C$ values of the bulk saturated and aromatic hydrocarbon fractions of the Gulf of Mexico oils.

7.3. Compound Specific Stable Carbon isotopes (CSIA)

7.3.1. Assam Delta

CSIA was performed on four samples of crude oil from the Assam sample set so as to investigate whether isotope compositional heterogeneity occur within this oil set as

the plot of the bulk saturated and aromatic hydrocarbon isotope data (Figure 7.1) suggests despite compositional uniformity at the molecular level. Figure 7.3 is a plot of the nC_{12} to nC_{30} *n*-alkane stable carbon isotope data. In general, the representative sample of oils analysed exhibit small variations in the $\delta^{13}C$ isotope values between nC_{12} to nC_{18} but are more similar in their $\delta^{13}C$ isotope values after the nC_{19} (figure 7.3). This deduction thus supports the molecular data as well as the bulk saturated and aromatic stable carbon isotope $\delta^{13}C$ values data that consigns the oils into similar source organofacies of terrigenous higher plant origin.

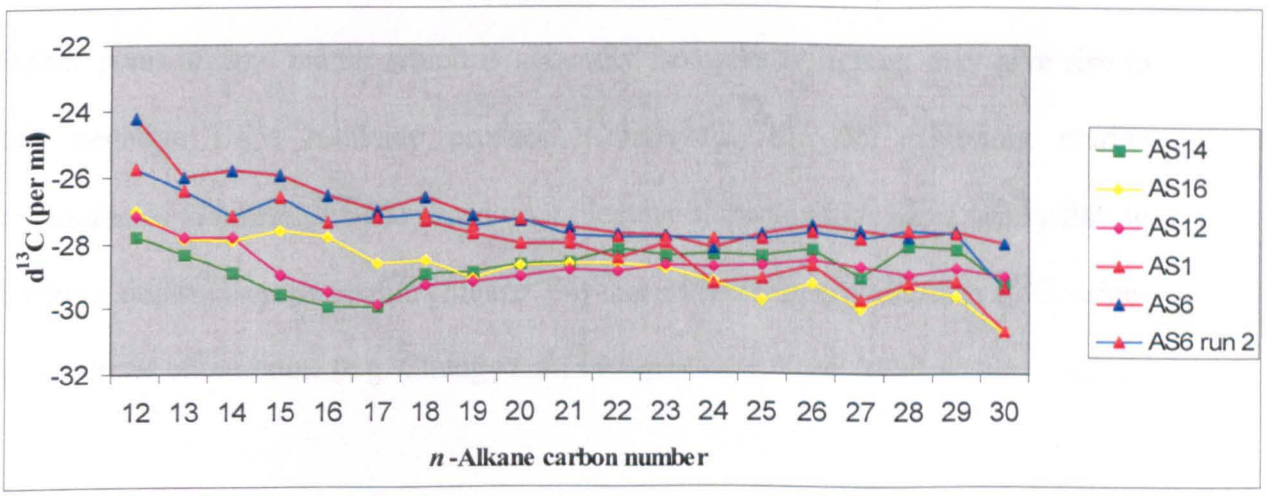

Figure 7.3. The *n*-alkane stable carbon isotope plot for representative samples of oil from Assam Delta.

7.3.2. Beaufort-Mackenzie Delta

Four oil samples (three of terrigenous and one of marine source facies, based on molecular data in Section 5.3) were analysed from the Beaufort–Mackenzie data set. The three oils with terrigenous molecular source facies exhibit similar *n*-alkane stable carbon isotope profiles of slightly negative slope resulting from more negative $\delta^{13}C$ values with increasing *n*-alkane chain length (Table 7.3, Figure 7.4). A characteristic negatively slope profile is commonly associated with oils and bitumen extracts derived from terrigenous deltaic organic matter mainly (Bjorøy *et al.*, 1991;

Wilhelms, *et al.*, 1994; Murray *et al.*, 1994; Xiong *et al.*, 2005; Samuel *et al.*, 2006b). The cause of this characteristic negative slope profile is not known for certain at present. Nonetheless, in addition to widespread variability in the stable carbon compositions among various terrigenous higher plant components, a likely factor for the observed negative isotope profiles is that algae and bacteria generally biosynthesise short chain lipid constituents and terrigenous higher plants generally produce long chain ones (Bray & Evans, 1961). Thus, it is thought in this thesis that combined sourcing of this shorter chain organic input from marine influenced algal-bacterial colonies, which is isotopically heavy and long chain input from terrigenous higher plant organic matter which is generally isotopically lighter, may give rise to this negative slope *n*-alkane profiles. Conversely, the oil exhibiting marine organofacies (Sample BM-10) based on molecular characteristics has a nearly flat to positive sloping isotope profile (Figure 7.4) that reflect a nearly uniform $\delta^{13}C$ values of the crude oil *n*-alkane (e.g. Chung *et al.*, 1994).

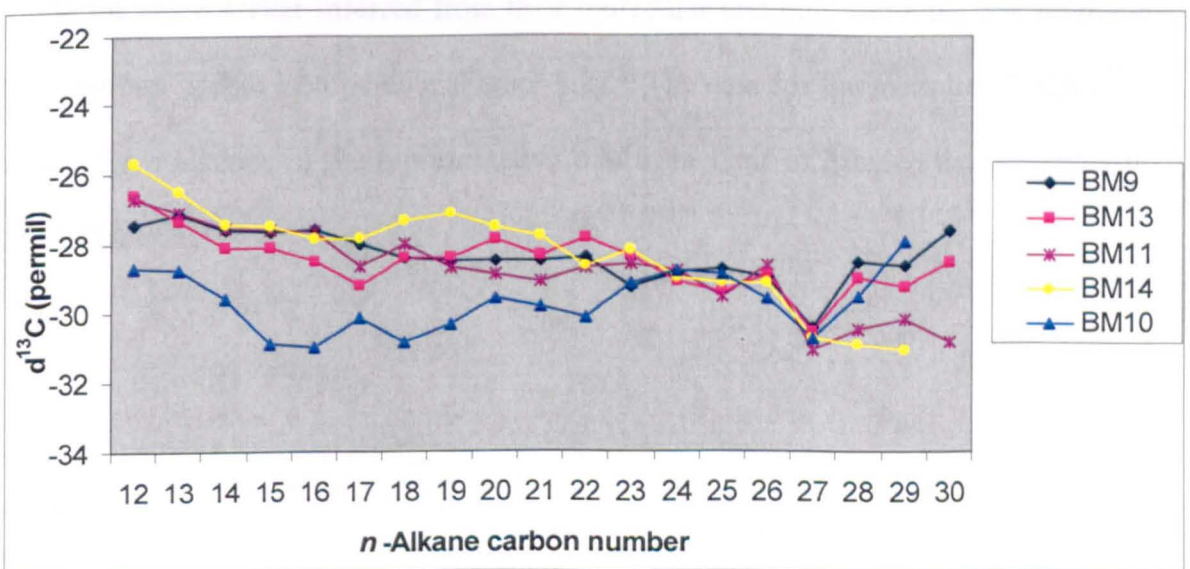

Figure 7.4. The *n*-alkane stable carbon isotope plot for representative samples of oil from the Beaufort-Mackenzie Delta.

7.3.3. Gulf of Mexico

The CSIA $\delta^{13}C$ profile of *n*-alkanes in representative crude oil samples from the Gulf of Mexico are presented in Figure 7.5. Apart from sample GOM-13, most of the analysed oils display a nearly flat profile that is commonly associated with crude oils expelled from source rocks rich in marine algae (Chung *et al.*, 1994; Murray *et. al.*, 1994). This flat profile resulting from homogeneity in the *n*-alkane $\delta^{13}C$ distribution is thought to be a result of derivation of organic carbon from a nearly uniform carbon pool, arguably algal-bacterial sources. This is probably because marine phytoplankton derives most of their organic carbon utilised during the metabolic reduction process of photosynthesis from the ocean in form of dissolved CO_2 (or more rarely HCO_3^-)and mixing of the ocean water could results in homogeneity in the carbon pool.

A closer look at the sample GOM-13 molecular data (e.g. Sections 5.42 and 5.43), shows that this oil sample contains mixed marine-terrigenous characteristics and has no detectable 24-*n*-propylcholestane. The similarity in the isotope profiles of most of the analysed Gulf of Mexico oils is not surprising as it corroborates source facies rich in marine algae earlier inferred from their molecular and bulk saturated and aromatic hydrocarbon stable isotope data (Figure 7.2). The data for the measured CSIA $\delta^{13}C$ values for *n*-alkanes in the representative oils from Gulf of Mexico are presented in Table 7.4.

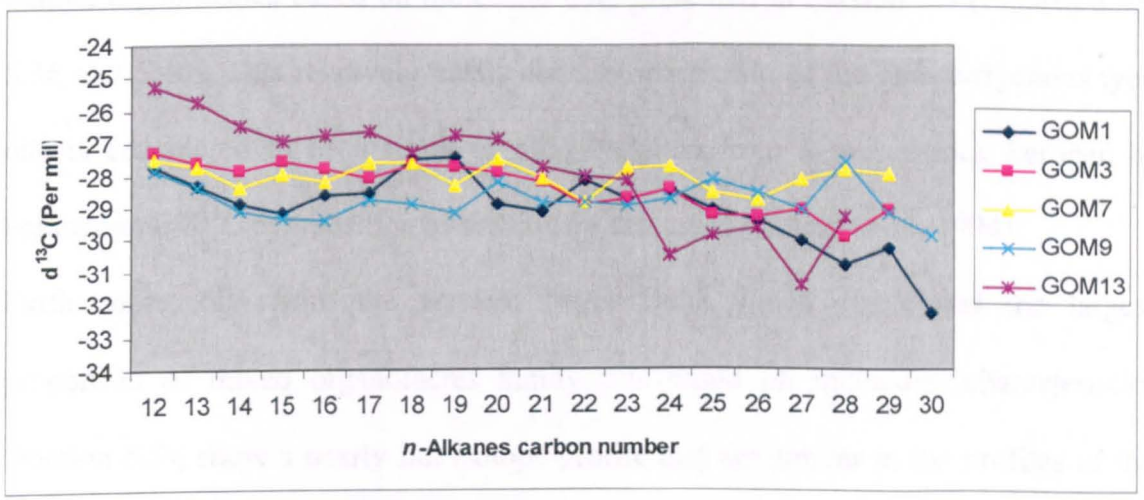

Figure 7.5. The *n*-alkane stable carbon isotope plot for representative samples of oil from the Gulf of Mexico.

7.3.3. Niger Delta

Table 7.5 shows data for representative Niger Delta crude oil samples analysed in this study. Two distinct isotope profiles were achieved from the Niger Delta data set (Figure 7.6 and 7.7). Figure 7.6 is a plot showing a negative sloping crude oil *n*-alkanes stable carbon isotope profile consisting mostly of samples from the central and eastern Niger Delta oil accumulations with a few western oils. The negative profile of this oil set, as earlier observed also for some Beaufort-Mackenzie oils, is a result of systematic depletion in the $\delta^{13}C$ composition (i.e. more negative $\delta^{13}C$ values) with increasing *n*-alkane chain length. This negative-slope fingerprint has been described in some published literature to be characteristic of deltaic and terrigenous crude oils e.g. from South Texas (Bjorøy *et al.*, 1991), Australia (Wilhelms *et al.*, 1994), Indonesia (Wilhelms *et al.*, 1994; Murray *et al.*, 1994), New Zealand and Philippines (Murray *et al.*, 1994).

In contrast, a nearly flat to positive slope profile was obtained for another oil group consisting of shallow water samples from the western acreage and some deepwater Niger Delta oils (Figure 7.7). Notably, this group is dominated by oils having more

marine organofacies based on molecular data presented in Section 5.5 (Figures 5.33, 5.36 and 5.40). This relatively nearly flat isotope profile of the non-terrigenous type oils is considered to be a result of oil generation from a source rock kerogen of homogenous $\delta^{13}C$ composition as previously discussed (Chung *et al.*, 1994).

Furthermore, oils from the western Niger Delta which constituted the largest proportion of mixed organofacies family oils based on molecular characteristics (Section 5.5), show a nearly flat isotope profile that are similar to the profiles of the deepwater oils (Figure 7.7). However, a closer look at the CSIA data reveal that these western shallow water oils are isotopically heavier than the deepwater oils and they display stable carbon isotope profiles that are not typical of oils derived from high terrigenous organic matter sources (i.e nearly flat n-alkane $\delta^{13}C$ profiles, as against commonly negative sloping profiles that characterise terrigenous organic matter sourced oils), despite mixed terrigenous and marine biomarker signals. This observation of disparate marine-type isotope profiles and mixed facies molecular characteristic of this group of western Niger Delta oils is interpreted to reflect a situation in which the marine organic matter probably contributed more than the terrigenous to the bulk oil generating organic carbon in the source rock kerogen. In support of this interpretation, it was noted that Eneogwe and Ekundayo (2003) measured stable carbon isotopes on saturated and aromatic hydrocarbon fractions of about sixty-six oils recovered from wells from the western shallow water accumulations and their data for most of the oils generally show a non-terrigenous (non-waxy) canonical variable (CV); this independent data is therefore consistent with the marine organic matter CSIA signatures of these western Niger Delta oil accumulations.

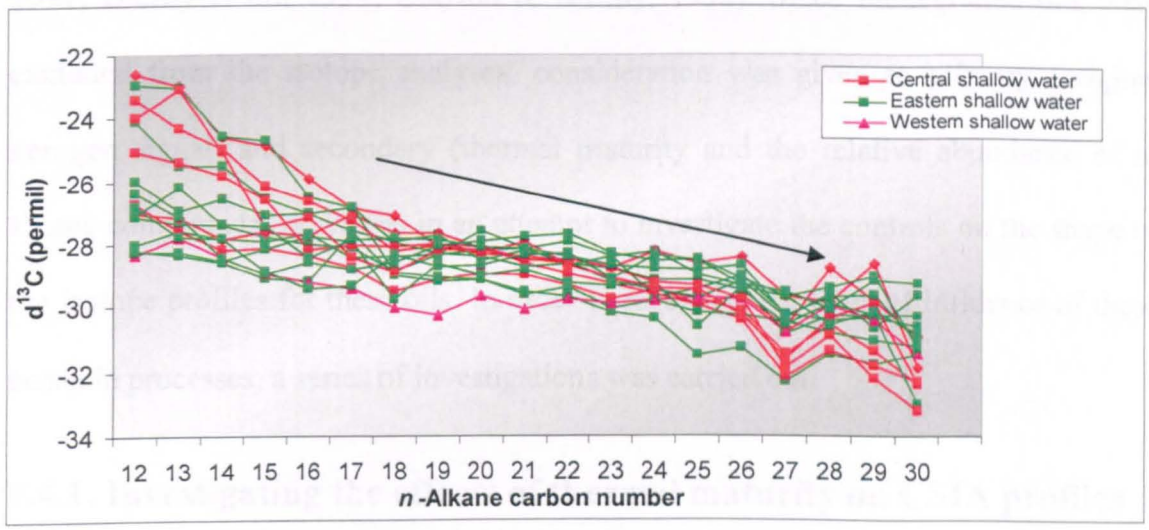

Figure 7.6. A negatively sloping *n*-alkane stable carbon isotope profile of samples of oil from the Niger Delta showing terrigenous source facies

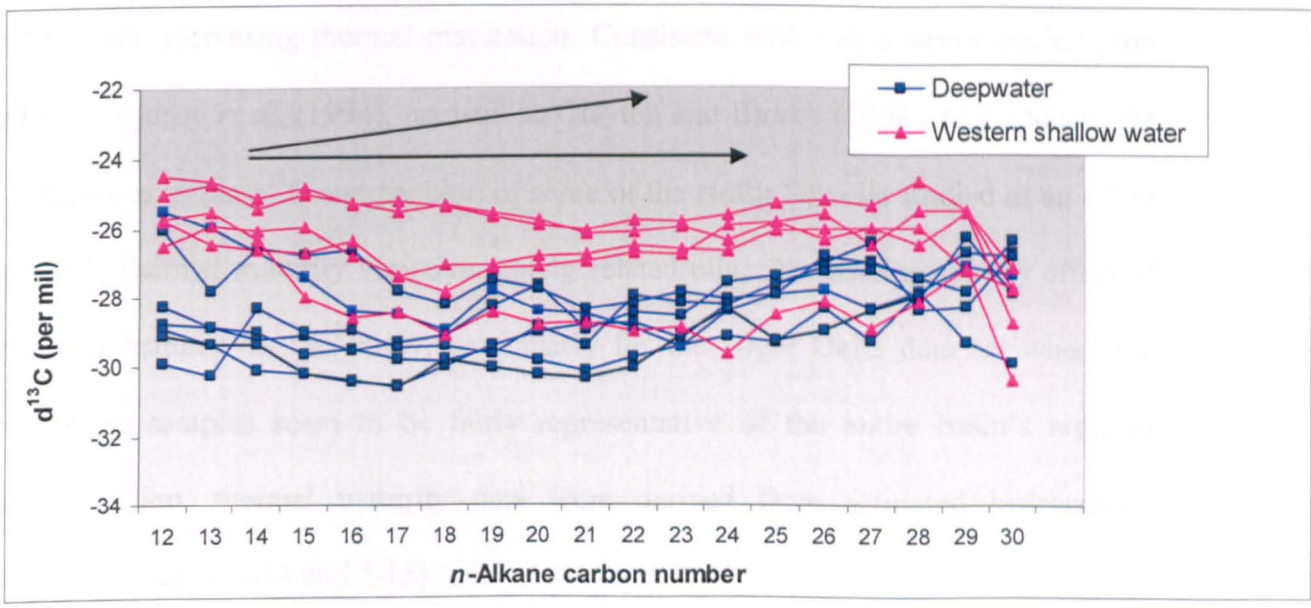

Figure 7.7. Nearly flat n-alkane stable carbon isotope profile of deepwater and some western shallow water Niger Delta oils typical of oils expelled from source rock rich in marine kerogen.

7.4. Controls on the shape of CSIA Plots

There is as yet no agreement on all the controls for the negatively sloping profiles observed for oils of terrigenous organofacies and the nearly flat profiles that usually characterises non-terrigenous source facies. Several processes (e.g. thermal maturity, biodegradation, fractionation, water washing and mixed accumulations) are known to influence isotopic compositions of oil (e.g. Chung *et al.*, 1981; Sofer, 1984; Clayton,

1991; Bjorøy *et al.*, 1994; Clayton & Bjorøy, 1994). Since biodegraded oils were excluded from the isotope analyses, consideration was given to primary (original kerogen signal) and secondary (thermal maturity and the relative abundance of *n*-alkane compounds) processes in an attempt to investigate the controls on the shape of the isotope profiles for these oils. In order to recognise the level of influence of these possible processes, a series of investigations was carried out.

7.4.1. Investigating the effects of thermal maturity on CSIA profiles

In a study of twenty Paleozoic oils from the Big Horn Basin, Wyoming, Chung *et al.* (1981) show that crude oils become enriched in the heavy isotope (more positive $\delta^{13}C$) with increasing thermal maturation. Consistent with this observation, Clayton (1991), Bjorøy *et al.* (1994), as well as Clayton and Bjorøy (1994), also account for differences in the $\delta^{13}C$ composition of some of the North Sea oils studied as an effect of wide thermal maturity variation among related oils. To investigate, any effect of thermal maturity in this study, particularly for the Niger Delta data set where the crude oil samples seem to be fairly representative of the entire basin's regional accumulation, thermal maturity data were derived from saturated hydrocarbon fractions (Tables 5.14 and 5.15).

From the molecular thermal maturity plots (in Figure 7.8 and 7.9), although the oils exhibit a range of thermal maturity, it is evident that thermal maturity has no effect on the observed stable carbon isotope signatures. It is in fact more interesting to add that the four eastern shallow water Niger Delta outlier samples, which are more mature than most of the oils in the data set (cf. Figure 7.8), generally display a negative isotope profile (i.e. more negative $\delta^{13}C$ values with increasing *n*-alkane chain length as seen in Figure 7.6), thus suggesting that enrichment of ^{13}C (more positive $\delta^{13}C$

expulsion from source rock kerogen. It thus seems that other processes may be responsible for this trend of negative slope isotope profile.

7.4.2. Effect of *n*-alkane abundance (short vs. long chain compounds) on CSIA profiles

Following from the previous Section, it is apparent that thermal maturity has no significant effect on the CSIA isotope profiles of the crude oils *n*-alkanes $\delta^{13}C$ values. Additionally, in order to demonstrate that the abundance of each *n*-alkane peak does not exert control on its absolute $\delta^{13}C$ composition and the overall isotope profile for oil. The GC chromatograms (Figure 7.10 and 7.11) of samples of representative end-member oils (marine (sample NDO13) and terrigenous (sample NDO10) based on biomarker data) showing nearly flat and a negative slope isotope profiles respectively were examined. From the peak area integrated data and visual inspection, despite the relatively low abundance of high molecular weight *n*-alkanes in the sample shown in Figure 7.10, the sample (NDO14) still displays a nearly flat $\delta^{13}C$ isotope profile of its *n*-alkanes, thus signalling a homogenous source of carbon. In Figure 7.11 there are relatively abundant long chain *n*-alkanes, but despite this, a negative slope isotope profile is seen that reflects primarily the source of carbon and not the abundance of each *n*-alkane compounds.

values) with maturity does not occur in this data set. Also, the only western Niger Delta outlier sample in Figures 7.8 and 7.9 displays a nearly flat profile (Figure 7.7) attesting to no systematic enrichment in ^{13}C with maturity. Indeed, Figure 7.8 confirms the previously reported utility of Ts/Ts+Tm parameter as both thermal maturity and source rock organofacies sensitive parameter (Moldowan *et al.*, 1986). In this plot, the deepwater and some western Niger Delta samples showing marine-type isotope profile tend to separate into the uppermost region of Figure 7.9, thus implicating a likelihood of similar source rock organofacies for these oils.

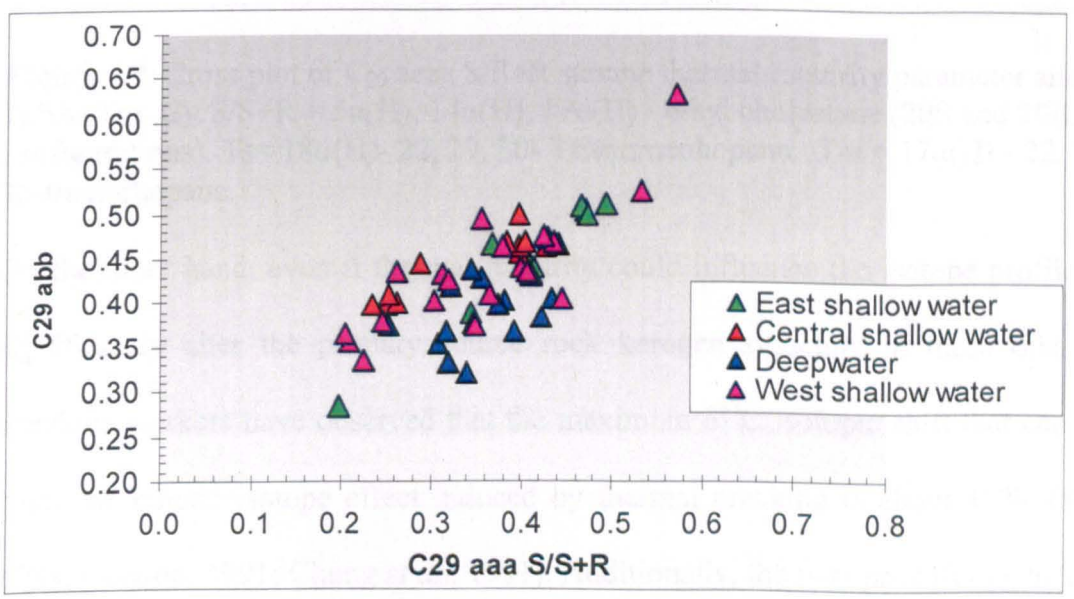

Figure 7.8. Plot of C_{29} S/S+R (5α(H), 14α(H), 17α(H) - ethyl cholestane (20S and 20R configurations) versus sterane C29 abb (5α(H),14β(H), 17β(H) 20S +20R / 5α(H),14β(H), 17β(H) + 5α(H),14α(H), 17α(H) 20S+20R for C_{29} steranes) thermal maturity parameters.

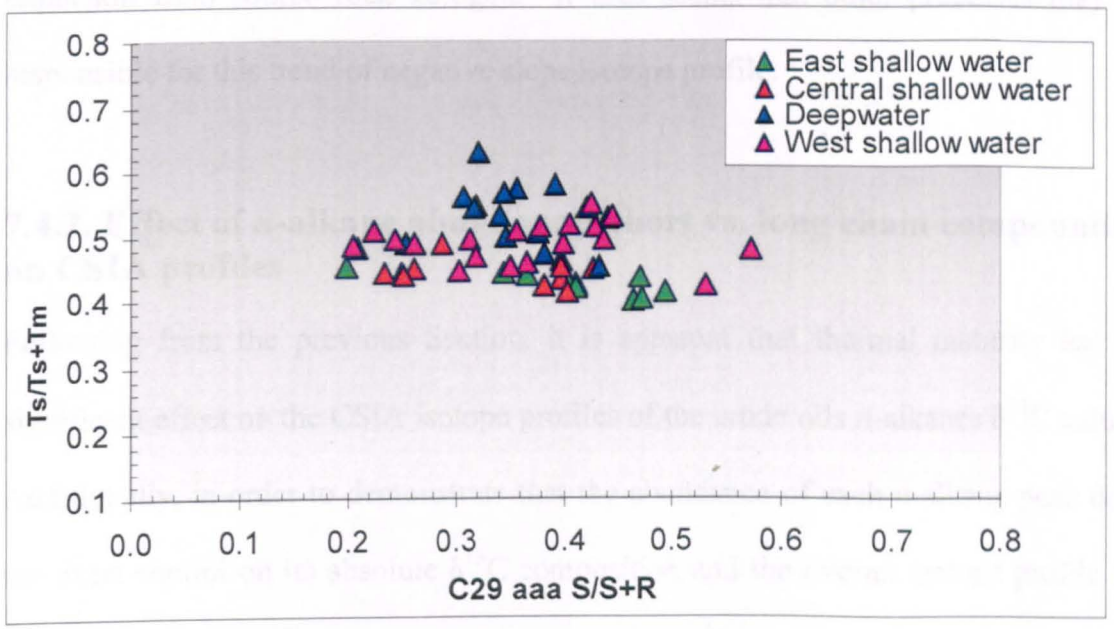

Figure 7.9. Cross plot of C_{29} aaaa S/S+R sterane thermal maturity parameter and Ts/Ts+Tm. C_{29} S/S+R = 5α(H), 14α(H), 17α(H) - ethyl cholestane (20S and 20R configurations). Ts= 18α(H)- 22, 29, 30- Trisnorneohopane. Tm = 17α(H) - 22, 29, 30-trisnorhopane.

On the other hand, even if thermal maturity could influence the isotope profile as to significantly alter the primary source rock kerogen signature in these oils, other previous workers have observed that the maximum $\delta^{13}C$ isotopic shift that can result from the kinetic isotope effect induced by thermal cracking is about ±2‰ (Shoell, 1984, Clayton, 1991; Chung *et al.*, 1991). Additionally, the isotope shift due to kinetic isotope effect during hydrocarbon generation from the source rock kerogen can not explain this observation as the trend is counter conventional since it is generally accepted in geochemical processes that the ^{12}C-^{12}C bond are preferentially cleaved because of their greater reaction rates made possible by weaker bond energies relative to the ^{13}C-^{12}C bond during kerogen maturation (Degens, 1969; Tissot & Welte, 1984; Galimov, 1985; Peters *et al.*, 2005a, pp.139). In effect, the early generated low molecular weight products (short chain *n*-alkanes) would be expected to be more depleted in $\delta^{13}C$ (more negative values) if the kinetic isotope effect is active during oil

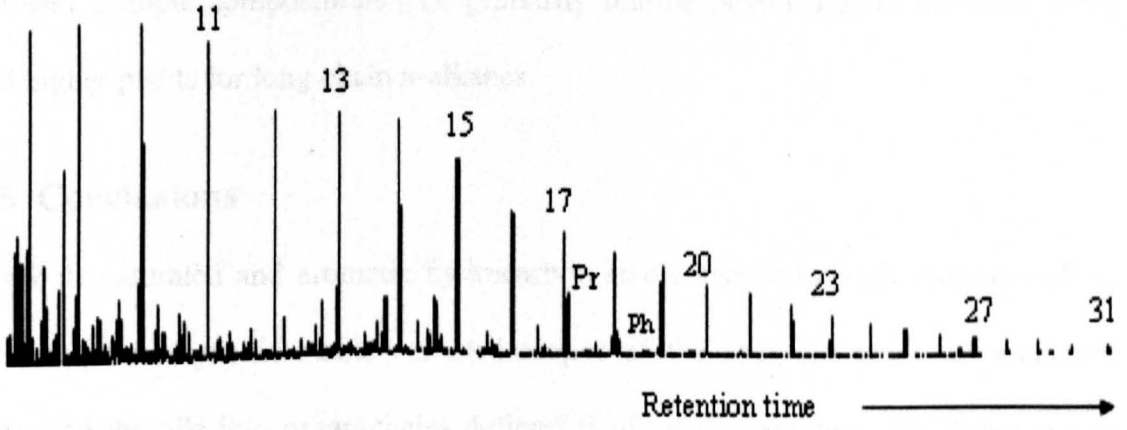

Figure 7.10. A gas chromatogram showing the n-alkane distribution in a representative deepwater Niger Delta crude oil (sample NDO14).

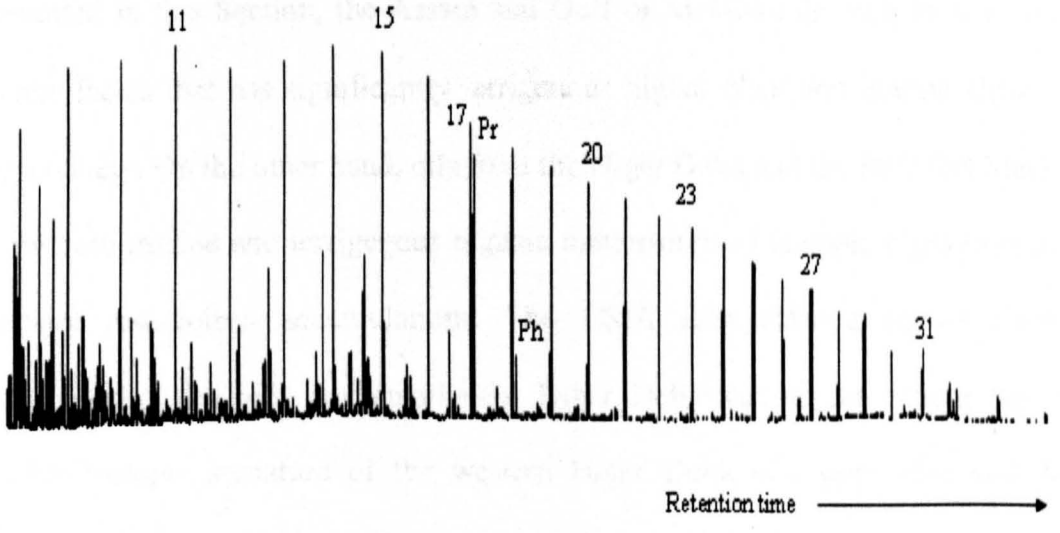

Figure 7.11. A gas chromatogram showing the *n*-alkane distribution in a representative terrigenous source facies, shallow water Niger Delta crude oil (sample NDO10).

7.4.3. Effect of original organic matter on CSIA profiles

Sofer *et al.* (1991) reported that the *n*-alkane $\delta^{13}C$ profile is controlled primarily by the source rock kerogen type. By extension of this reasoning and in the absence of any effects of secondary processes of biodegradation, fractionation as well as lack of significant effect resulting from thermal maturity and absolute *n*-alkane peak abundance on the *n*-alkane $\delta^{13}C$ composition as demonstrated so far, the *n*-alkane $\delta^{13}C$

isotope profiles presented in this work are assumed to reflect the influence of primary kerogen isotopic compositions.- i.e primarily marine phytoplankton for short chain and higher plants for long chain *n*-alkanes.

7.5. Conclusions

The bulk saturated and aromatic hydrocarbon stable carbon isotopic data as well as the compound specific stable carbon isotopes of the analysed crude oil *n*-alkanes separated the oils into organofacies defined families that are generally in agreement with the classification of terrigenous and marine organic matter derived oils earlier achieved using molecular data alone in Chapter Five. Based on stable isotope data presented in this Section, the Assam and Gulf of Mexico oils each have a common source facies that has significantly terrigenous higher plant and marine algae inputs respectively. On the other hand, oils from the Niger Delta and the Beaufort Mackenzie show both marine and terrigenous organic matter-derived isotopic signatures in their Tertiary reservoired accumulations. The CSIA data offer a robust means of characterising the oils, particularly the Niger Delta sample set, where the strong marine isotopic signature of the western Niger Delta oils were observed despite mixed-marine and terrigenous source signatures for these oil group within the Niger Delta sample set. Thus the CSIA data provides an independent assessment as well as a supportive tool to the molecular data in an appraisal of the petroleum systems of the basin.

Table 7.1. Bulk saturated and aromatic hydrocarbon fraction stable carbon isotope data for Assam and Gulf of Mexico oils.

Sample	Basin	$d^{13}C$ Sat	$d^{13}C$ Aro	CV
GOM- 1	Gulf of Mexico	-27.73	-27.37	-2.25
GOM- 2	Gulf of Mexico	-27.77	-26.62	-0.49
GOM- 3	Gulf of Mexico	-26.89	-26.18	-1.74
GOM- 4	Gulf of Mexico	-27.02	-26.09	-1.21
GOM- 5	Gulf of Mexico	-27.20	-26.00	-0.55
GOM- 6	Gulf of Mexico	-27.16	-26.20	-1.10
GOM- 7	Gulf of Mexico	-27.44	-26.74	-1.59
GOM- 8	Gulf of Mexico	-27.17	-26.02	-0.67
GOM- 9	Gulf of Mexico	-27.37	-26.50	-1.23
GOM- 10	Gulf of Mexico	-27.54	-26.29	-0.34
GOM- 11	Gulf of Mexico	-27.11	-25.84	-0.43
GOM- 12	Gulf of Mexico	-27.52	-26.28	-0.37
GOM- 13	Gulf of Mexico	-27.08	-26.09	-1.06
GOM- 14	Gulf of Mexico	-27.34	-26.42	-1.13
GOM- 15	Gulf of Mexico	-27.10	-26.35	-1.58
GOM- 16	Gulf of Mexico	-26.96	-26.28	-1.78
GOM- 17	Gulf of Mexico	-27.49	-26.32	-0.53
GOM- 18	Gulf of Mexico	-26.85	-25.62	-0.60
GOM- 19	Gulf of Mexico	-27.15	-26.46	-1.70
AS-1	Assam	-27.67	-26.40	-0.25
AS-2	Assam	-26.02	-25.00	-1.32
AS-3	Assam	-27.72	-26.86	-1.15
AS-4	Assam	-27.58	-25.92	0.58
AS-5	Assam	-28.49	-25.96	2.80
AS-6	Assam	-26.97	-24.58	2.02
AS-7	Assam	-26.00	-25.66	-2.84
AS-8	Assam	-28.42	-26.44	1.56
AS-9	Assam	-27.44	-25.00	2.27
AS-10	Assam	-28.70	-26.99	1.04
AS-11	Assam	-27.83	-25.44	2.28
AS-12	Assam	-28.10	-25.59	2.63
AS-13	Assam	-27.00	-26.67	-2.55
AS-14	Assam	-27.36	-26.66	-1.61
AS-15	Assam	-27.34	-25.26	1.44
AS-16	Assam	-27.95	-26.05	1.23
AS-17	Assam	-27.21	-26.44	-1.51
AS-18	Assam	-27.50	-25.44	1.45
AS-19	Assam	-28.12	-26.00	1.77

Table 7.2. Compound specific stable carbon isotope data of selected Assam crude oil samples

Sample	nC12	nC13	nC14	nC15	nC16	nC17	nC18	nC19	nC20	nC21	nC22	nC23	nC24	nC25	nC26	nC27	nC28	nC29	nC30
DKM 13	-27.17	-27.79	-27.80	-28.99	-29.47	-29.89	-29.28	-29.17	-29.01	-28.84	-28.86	-28.68	-28.71	-28.69	-28.54	-28.74	-28.95	-28.75	-29.02
SHM 5	-26.98	-27.88	-27.90	-27.60	-27.80	-28.61	-28.51	-29.06	-28.66	-28.62	-28.63	-28.76	-29.19	-29.74	-29.24	-29.98	-29.32	-29.63	-30.72
BHJ 4	-27.77	-28.31	-28.88	-29.51	-29.93	-29.92	-28.93	-28.88	-28.60	-28.58	-28.17	-28.37	-28.33	-28.35	-28.16	-29.03	-28.05	-28.14	-29.23
NHK 315							-27.30	-27.73	-27.99	-28.00	-28.45	-27.99	-29.24	-29.05	-28.68	-29.73	-29.24	-29.19	-30.68
KUM 2	-24.22	-25.97	-25.77	-25.95	-26.53	-26.98	-26.60	-27.15	-27.31	-27.50	-27.72	-27.76	-28.17	-27.72	-27.47	-27.59	-27.83	-27.68	-28.02
Kum 2 Run 2	-25.75	-26.41	-27.17	-26.60	-27.35	-27.21	-27.11	-27.47	-27.26	-27.76	-27.80	-27.80	-27.86	-27.88	-27.66	-27.84	-27.59	-27.68	-29.39

Table 7.3. Compound specific stable carbon isotope data of selected crude oil samples from Beaufort-Mackenzie Delta

Sample	nC12	nC13	nC14	nC15	nC16	nC17	nC18	nC19	nC20	nC21	nC22	nC23	nC24	nC25	nC26	nC27	nC28	nC29	nC30
BM9	-27.46	-27.17	-27.58	-27.67	-27.60	-28.00	-28.38	-28.51	-28.51	-28.48	-28.39	-29.25	-28.85	-28.73	-28.98	-30.43	-28.57	-28.63	-27.63
BM13	-26.58	-27.36	-28.12	-28.09	-28.50	-29.19	-28.42	-28.39	-27.88	-28.34	-27.83	-28.33	-29.10	-29.39	-28.91	-30.57	-28.99	-29.25	-28.54
BM11	-26.68	-27.10	-27.57	-27.58	-27.64	-28.67	-28.01	-28.69	-28.92	-29.08	-28.69	-28.59	-28.81	-29.57	-28.67	-31.10	-30.48	-30.21	-30.83
BM14	-25.69	-26.51	-27.45	-27.48	-27.85	-27.85	-27.37	-27.14	-27.55	-27.79	-28.65	-28.18	-29.00	-29.14	-29.17	-30.77	-30.97	-31.10	
BM10	-28.72	-28.76	-29.58	-30.88	-31.02	-30.15	-30.83	-30.33	-29.58	-29.87	-30.17	-29.13	-28.82	-28.91	-29.62	-30.76	-29.54	-27.95	

Table 7.4. Compound specific stable carbon isotope data of selected crude oil samples from the Gulf of Mexico

Sample	nC12	nC13	nC14	nC15	nC16	nC17	nC18	nC19	nC20	nC21	nC22	nC23	nC24	nC25	nC26	nC27	nC28	nC29	nC30
GOM1	-27.73	-28.34	-28.90	-29.15	-28.62	-28.53	-27.53	-27.45	-28.88	-29.11	-28.12	-28.70	-28.45	-29.08	-29.41	-30.05	-30.78	-30.29	-32.25
GOM3	-27.30	-27.64	-27.87	-27.58	-27.78	-28.09	-27.69	-27.72	-27.90	-28.20	-28.91	-28.69	-28.42	-29.26	-29.30	-29.08	-29.91	-29.08	
GOM7	-27.51	-27.76	-28.36	-27.98	-28.20	-27.64	-27.61	-28.33	-27.49	-28.08	-28.83	-27.82	-27.76	-28.54	-28.79	-28.13	-27.87	-27.96	
GOM9	-27.85	-28.37	-29.13	-29.33	-29.39	-28.78	-28.90	-29.15	-28.21	-28.81	-28.83	-28.92	-28.72	-28.13	-28.51	-29.05	-27.59	-29.17	-29.86
GOM13	-25.28	-25.72	-26.49	-26.91	-26.78	-26.65	-27.26	-26.77	-26.86	-27.75	-28.03	-28.11	-30.51	-29.85	-29.64	-31.39	-29.28		

Table 7.5. Compound specific stable carbon isotope data of selected Niger Delta crude oil samples

Sample	nC12	nC13	nC14	nC15	nC16	nC17	nC18	nC19	nC20	nC21	nC22	nC23	nC24	nC25	nC26	nC27	nC28	nC29	nC30
NDO01	-25.43	-25.33	-26.53	-26.82	-26.56	-26.56	-26.26	-26.51	-26.34	-26.81	-26.46	-26.26	-27.11	-26.82	-26.56	-27.46	-26.29	-26.57	-28.21
NDO02	-26.77	-27.75	-27.81	-28.86	-29.42	-29.30	-28.31	-28.69	-28.66	-28.35	-28.30	-29.07	-28.34	-28.51	-29.29	-29.50	-30.03	-29.15	-29.23
NDO03	-28.24	-28.25	-28.53	-28.13	-27.77	-27.92	-29.74	-28.61	-28.99	-28.81	-29.24	-29.35	-29.21	-30.59	-29.36	-29.67	-29.37	-29.01	-31.25
NDO04	-27.08	-26.16	-27.33	-27.45	-28.42	-27.87	-27.83	-27.84	-28.11	-28.16	-28.37	-28.64	-28.74	-28.82	-28.64	-30.26	-29.64	-29.60	-31.09
NDO05	-25.99	-26.93	-26.52	-27.04	-27.03	-26.81	-27.96	-28.30	-28.36	-28.71	-28.62	-28.73	-29.12	-29.13	-29.46	-30.56	-29.91	-30.23	-32.99
NDO06	-28.19	-28.32	-28.58	-29.08	-29.19	-27.63	-29.01	-29.18	-29.16	-29.59	-29.36	-30.05	-29.80	-30.17	-30.25	-30.46	-30.77	-31.00	-31.20
NDO07	-27.98	-27.58	-27.83	-27.89	-27.69	-28.41	-28.37	-28.35	-28.19	-28.15	-28.67	-28.37	-28.23	-28.93	-29.34	-30.84	-30.26	-30.27	-30.29
NDO09	-26.33	-27.10	-28.41	-28.96	-28.58	-28.83	-28.56	-28.02	-27.92	-27.77	-27.67	-28.28	-28.51	-28.48	-29.07	-29.67	-30.56	-30.12	-30.85
NDO10	-27.12	-27.34	-27.36	-27.75	-28.02	-28.10	-28.87	-28.34	-27.59	-28.17	-27.91	-28.38	-29.68	-29.41	-28.99	-30.24	-30.42	-30.32	-30.59
NDO11	-24.10	-25.50	-25.52	-26.53	-27.02	-27.55	-27.90	-27.72	-28.53	-28.21	-28.56	-29.17	-29.45	-29.70	-29.17	-30.33	-29.57	-30.65	-29.61
NDO13	-27.71	-28.44	-28.79	-28.98	-28.84	-28.75	-29.69	-29.48	-29.64	-30.14	-30.36	-30.54	-29.95	-29.67	-29.34	-30.97	-28.56	-29.22	-29.37
NDO14	-28.23	-28.85	-29.20	-29.10	-29.54	-29.28	-29.10	-28.27	-27.64	-28.96	-28.42	-28.56	-27.57	-27.37	-26.95	-26.37	-28.34	-28.26	-26.67
NDO15	-25.45	-25.96	-26.65	-27.39	-28.39	-28.50	-28.97	-27.78	-28.39	-28.52	-28.92	-29.44	-28.41	-27.90	-27.73	-28.28	-27.81	-27.06	-27.33
NDO16	-28.87	-29.35	-30.09	-30.18	-30.41	-30.51	-29.96	-29.39	-28.99	-28.78	-28.75	-29.20	-28.21	-27.58	-27.07	-26.89	-27.38	-26.65	-26.74
NDO18	-26.02	-27.78	-26.56	-26.75	-26.60	-27.79	-28.22	-27.50	-27.73	-28.35	-28.17	-27.85	-28.04	-27.90	-26.78	-26.94	-27.43	-27.80	-26.30
NDO19	-29.87	-30.23	-28.30	-28.99	-28.96	-29.42	-29.38	-29.62	-28.84	-29.40	-27.97	-28.16	-28.19	-27.63	-27.21	-27.17	-27.98	-26.22	-27.83
NDO22	-24.48	-24.63	-25.14	-24.84	-25.32	-25.20	-25.36	-25.66	-25.94	-26.04	-25.77	-25.83	-25.60	-25.30	-25.18	-25.30	-24.60	-25.45	-27.09
NDO26	-29.09	-29.35	-29.34	-30.16	-30.38	-30.56	-29.79	-30.03	-30.24	-30.34	-30.02	-29.11	-28.35	-29.26	-28.96	-28.37	-27.89	-28.88	-27.88
NDO31	-27.05	-26.47	-27.12	-27.34	-27.21	-27.77	-27.25	-27.57	-27.69	-27.53	-27.26	-27.12	-27.32	-27.32	-26.62	-27.45	-27.14	-27.85	-28.79
NDO33	-26.50	-25.93	-26.07	-25.95	-26.82	-27.38	-27.84	-27.17	-27.11	-26.98	-26.69	-26.77	-25.93	-25.81	-26.29	-25.98	-26.47	-25.51	-28.73
NDO36	-25.77	-26.45	-26.61	-26.73	-26.38	-27.42	-27.07	-27.04	-26.83	-26.75	-26.50	-26.62	-26.65	-26.06	-26.01	-25.98	-25.98	-27.18	-27.71
NDO40	-28.33	-27.83	-28.43	-28.96	-29.24	-29.42	-30.03	-30.26	-29.65	-30.09	-29.76	-29.87	-29.80	-29.68	-29.75	-30.80	-29.95	-30.42	-31.44
NDO45	-25.04	-24.71	-25.42	-25.65	-25.29	-25.61	-25.31	-25.57	-25.77	-26.18	-26.12	-25.98	-26.37	-25.80	-25.56	-26.46	-25.48	-25.47	-27.77
NDO46	-24.48	-24.63	-25.14	-24.84	-25.32	-25.20	-25.36	-25.66	-25.94	-26.04	-25.77	-25.83	-25.60	-25.30	-25.18	-25.30	-24.60	-25.45	-27.09
NDO47	-25.72	-25.55	-26.33	-27.99	-28.61	-28.44	-29.11	-28.46	-28.80	-28.77	-29.02	-28.90	-29.64	-28.48	-28.09	-28.92	-28.08	-27.09	-30.36
NDO49	-23.99	-23.09	-25.06	-27.47	-27.14	-28.42	-28.91	-28.19	-28.19	-28.51	-28.45	-28.78	-29.23	-29.31	-29.73	-31.87	-30.89	-32.22	-33.21

Sample	nC12	nC13	nC14	nC15	nC16	nC17	nC18	nC19	nC20	nC21	nC22	nC23	nC24	nC25	nC26	nC27	nC28	nC29	nC30
NDO53	-26.72	-27.55	-28.17	-28.13	-28.40	-28.75	-29.50	-29.12	-28.95	-29.01	-29.32	-29.77	-29.47	-29.75	-30.12	-31.43	-30.54	-31.35	-32.42
NDO54	-26.13	-28.68	-26.91	-27.80	-27.68	-28.27	-28.39	-28.32	-27.19	-27.72	-27.51	-27.51	-27.79	-27.86	-27.52	-28.49	-28.91	-28.69	-28.39
NDO55	-22.62	-22.97	-24.59	-24.90	-25.91	-26.86	-27.12	-28.10	-28.33	-28.40	-28.57	-29.20	-29.43	-29.95	-29.66	-30.66	-28.78	-29.79	-30.93
NDO56	-23.43	-24.30	-24.96	-26.14	-26.63	-27.22	-28.26	-28.06	-28.09	-28.60	-28.93	-29.27	-29.60	-29.95	-30.40	-32.18	-31.37	-31.85	-32.32
NDO57	-25.05	-25.39	-25.82	-26.57	-28.18	-28.06	-28.08	-28.00	-28.29	-27.94	-28.66	-29.11	-29.41	-29.46	-30.25	-31.58	-30.36	-29.83	-32.37
NDO58	-27.01	-27.14	-27.86	-27.60	-27.79	-27.04	-27.66	-27.69	-28.15	-28.46	-28.62	-28.73	-28.23	-28.61	-28.42	-29.65	-29.86	-28.61	-31.88

*n*C12- *n*C30 = *n*-alkane carbon numbers, e.g. *n*C12= dodecane.

CHAPTER EIGHT

THE SEARCH FOR SUB-DELTA SOURCE ROCKS: A NIGER DELTA CASE STUDY

Summary

This chapter presents the results and discussion of the geochemical characterization of candidate sub-delta source rock of the Araromi Formation in the Late Cretaceous sections of Dahomey Basin, southwestern Nigeria. The shale samples are characterised by TOC values ranging from 0.5 to 4.78 wt%, immature Tmax values generally less than 440 and HI values (2-327 mgHC/gTOC) that range from non-source rock to liquid hydrocarbon generation potentials. Bitumen extracts contain pr/ph ratios varying between 0.78 to 2.02, low oleanane index values (<0.22), high relative abundances of C_{27} steranes and significant 24-*n*-propylcholestane contents. Nearly flat *n*-alkane compound specific stable carbon isotope profiles are apparent for the analysed shale bitumen extracts. Despite the elevated oleanane concentration in the deepwater oils when compared to the Araromi shale extracts, the molecular and isotopic data of the Araromi shale extracts is comparable with the deepwater oils, thus leading to a proposal that similar source rock(s) organofacies may have expelled the deepwater oils.

8.0. Introduction

As exploration shifts to deepwater settings of the oceans, a detailed knowledge of the elements of the petroleum systems (particularly the source rocks) is critical to the success of the exploration projects. Incomplete knowledge of the regional and stratigraphic distributions of the sources rocks limits our ability to predict the volume, composition and phase of petroleum (liquid versus gas), let alone the oil quality in the deepwater setting (Katz & Robinson, 2006).

The source rocks for the sections of the Agbada and Akata formations studied by numerous workers have been shown to be dominated by terrigenous organic matter with vitrinite being the most abundant macerals (e.g. Ekweozor & Okoye, 1980; Bustin 1988). However, molecular and isotopic data presented in Chapters Five and Seven of this study suggest that the deepwater oils and some oil accumulations in the western section from the Niger Delta have been expelled from source rock(s) rich in marine kerogen and are compositionally different from oils from the other shallow water accumulations. This geochemical characteristic, as presented in Chapter Five and Seven is evident in the presence in the deepwater oils of relatively abundant C_{27} steranes, 24-*n*-propylcholestane and gammacerane, together with low oleanane index values and nearly flat C_{12} to C_{30} *n*-alkane stable carbon isotope profiles. However, the geochemistry of the deepwater Niger Delta oils is in contrast to some other deltaic provinces such as the deepwater Kutei Basin and associated Mahakam Delta, where land plant leaf waxes (liptinites transported down slope from hinterlands) in turbidite sands and deepwater shales, are proposed as the source of the organic matter for the deepwater oils, and the deepwater oils are compositionally consistent with the

overwhelmingly terrigenous characteristics of the shallow water oils (Saller *et al.*, 2006).

At present two schools of thought exist for the possible origin of deepwater oils in the Niger Delta.

I. Oil generation from Palaeogene section of the Tertiary delta

Katz (2006) argued in favour of a Palaeogene source rock containing mixed marine and terrigenous kerogen as a possible source rock for the deepwater Niger Delta oils. His view is built on the strength of similarity in biomarker characteristics (similar relative oleanane index, sterane distributions and C_{34}/C_{35} homohopane ratios) of the deepwater oils he studied and samples of cores recovered from the Palaeogene oil-prone section of the ODP site 959. One global norm which plagues oil-source rock understanding, and hence petroleum systems designation in deltas, is that the true source rocks may be deeply buried beyond present sampled intervals. If this holds true for Niger Delta, then the Palaeogene source rock age suggested for the deepwater Niger Delta oils by Katz (2006) may not have been sampled in wells drilled within the delta, despite most oil accumulations being largely reservoired in Miocene and younger sands.

II. Oil generation from discrete sub-delta units

Thoughts have been focused on the possibility of oil generation from Cretaceous source rocks in Dahomey Basin, which is located in the western margin of the delta. Haack *et al.* (2000) were in fact the first to speculate a possible Cretaceous unit contributing to the delta oil system. The concept of sub-delta sourcing was subsequently introduced and enunciated by Samuel *et al.* (2006b). Additionally,

Ekweozor (2004) suggested Cretaceous shales of the Lower Benue Trough, which margins the delta in the east, as likely sub-delta source rock candidates. The major controls on the ability of Cretaceous source rocks to contribute to the Tertiary delta oil system are arguably the expulsion (which depends on the source rock richness and thickness) and migration (dependent on connected conduits) efficiencies. Katz (2006) argued that Cretaceous source rocks, if present, may have generated and expelled liquid hydrocarbons prior to trap development within the Tertiary Niger Delta prograde, such that the only possibility of a sub-delta oil sourcing will result from re-migration of oils leaked from traps of the Cretaceous sequences. However, Katz and Robinson (2006) acknowledged the controls imposed by the combination of reduced overburden, lower sediment-water interface temperatures and lower heat flow values in the deepwater environments. As a result of the decrease in sediment overburden as compared to the shelf environments, deeper source rock burial will therefore be required for generation of oil from Tertiary source rocks (if any) in the deepwater setting, and in effect, the source rock intervals within the Akata and the overlying Agbada formations may not have been buried to a depth of active oil generation. If, on the other hand, oil generation occurs from the Akata and Agbada formations in the deepwater section, the expelled oils should reflect the dominance of terrigenous biomarker source signatures (e.g. predominance of C_{29} over C_{28} and C_{27} steranes; high pristane/phytane ratios, high oleanane index), given a compositionally uniform source rock organofacies. However, predominantly terrigenous biomarker characteristics have not been observed for the analysed deepwater oils in this study, thus implicating expulsion from source units that have yet to be identified.

In summary, because of the uncertainty in the ability to accurately predict the efficiency of both of the Agbada and Akata formations to generate oils in deep water sections of the delta, and the failure of the palynofacies characteristics, which are landplant dominated (Bustin, 1988) in the studied Niger Delta shale samples to account for the source of the marine oils, consideration is given in this thesis to Late Cretaceous sub-delta source rocks as possible source units for the deepwater oils. Such potential Late Cretaceous source rocks are mostly buried to depths of oil generation and are found in basins margining the delta to the west and east.

This chapter therefore has the following objectives:

1. To characterise candidate sub-delta source rocks of the Araromi Formation in the Late Cretaceous sections of Dahomey Basin, south western Nigeria.
2. Attempt to correlate the bitumen extract from these source rock samples with similar geochemical data from the deepwater Niger Delta oils using a combination of biomarker and compound specific stable carbon isotope data.

8.1. Samples

Core samples from the Gbekebo well drilled in the Dahomey Basin, west of the Niger Delta (Figure 8.1 and 8.2) were collected from the Geological Survey, Kaduna, Nigeria. The well penetrated the entire Upper Cretaceous Araromi Formation. Samples were analysed for their total organic content (TOC) and organic quality (HI) using standard geochemical Leco TOC Analyser and source rock pyrolysis techniques described in Section 3.7 and 3.8 respectively. Samples having high TOC values were soxhlet extracted to recover bitumen extracts for biomarker analyses. The GC, GC-MS and GC-MS-MS conditions used were the same as those reported for the analysed oils in Sections 3.2, 3.3 and 3.4 of Chapter Three. TOC, rock pyrolysis and biomarker data are presented in Table 8.1.

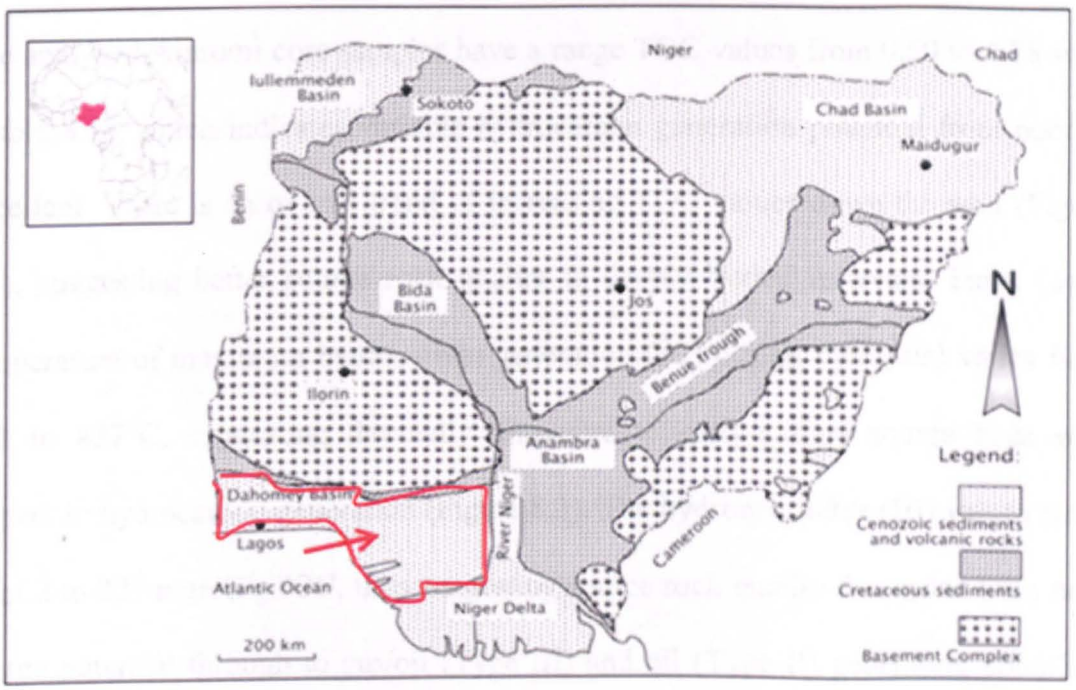

Figure 8.1. Map showing the sedimentary basins of Nigeria. The arrow points to location of the Dahomey Basin on the south-western margin of the Niger Delta. (modified after Adekeye, 2004).

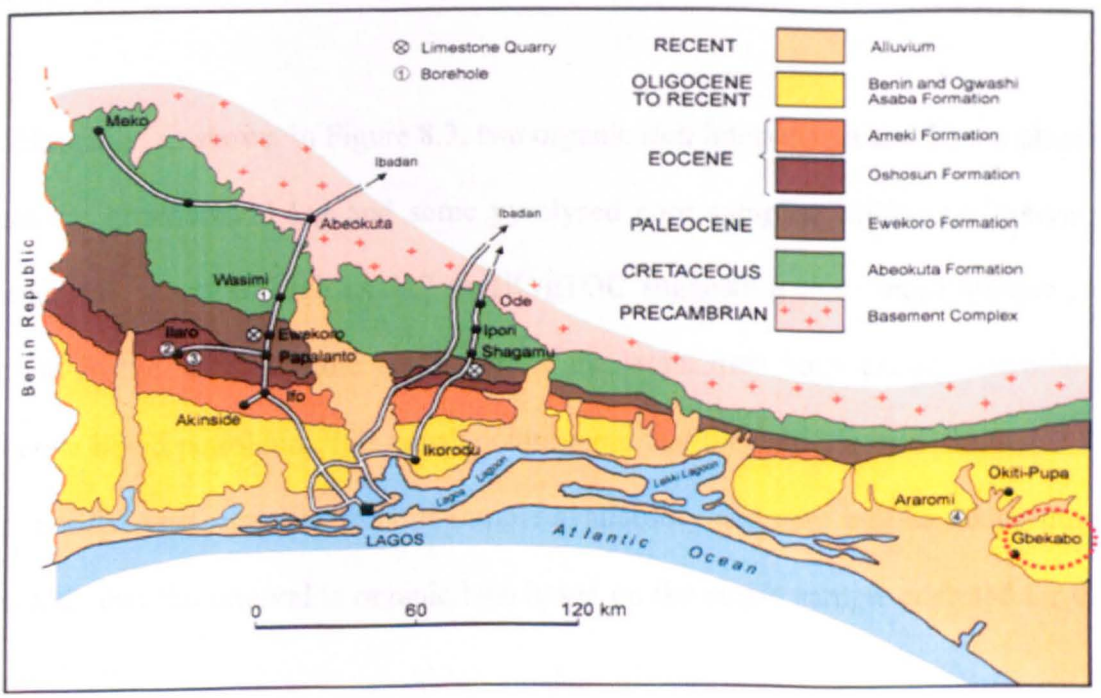

Figure 8.2. Outline Geological map of Dahomey Basin showing the location of the Gbekebo well (red dotted ring) on the eastern margin of Dahomey (west of the Niger Delta). Map modified after Adekeye (2004).

8.2. Hydrocarbon Source Potential

The analysed Araromi core samples have a range TOC values from 0.50 to 4.78 wt% (Table 8.1), which indicates variable hydrocarbon generation potential from poor to excellent. There is an overall trend of increasing TOC values down the well (Figure 8.3), suggesting better source rock quality in deeply buried intervals. Tmax (oven temperature of maximum hydrocarbon generation (S2) during pyrolysis) varies from 422 to 437°C, suggesting thermally immature to early-mature source beds with respect to hydrocarbon generation (Figure 8.3). The hydrogen index (HI) values range from 2 to 327 mgHC/gTOC, thus suggesting source rock quality that spans from non-source potential through to gas/oil (Type III) and oil (Type II) generating potentials (Figure 8.4). In general the organic matter is considered to be a mixture of Type II and Type III and a down-hole profile of increasing trend of HI concomitant with the TOC trend is apparent in the well log (Figure 8.3).

Additionally, as shown in Figure 8.3, two organic rich intervals (A and B) are obvious from the geochemical log and some pyrolysed core samples within the interval B contain HI values as high as 327 mgHC/gTOC suggesting that more organic rich section in the deep offshore equivalent of the strata may have greater potential to generate liquid petroleum. It is worth pointing out that the entire interval 3000 to 3200 ft is poorly represented interms of sample availability and care will be taking not to conclude that the interval is organic lean based on the single sample analysed for this interval.

Source rock[1]	TOC (%)	HI (mg HC /gTOC)	S_2 yield (kg/t)
A	2	200	4
B	4	300	12

[1] Averages, T_{max} = 432°C

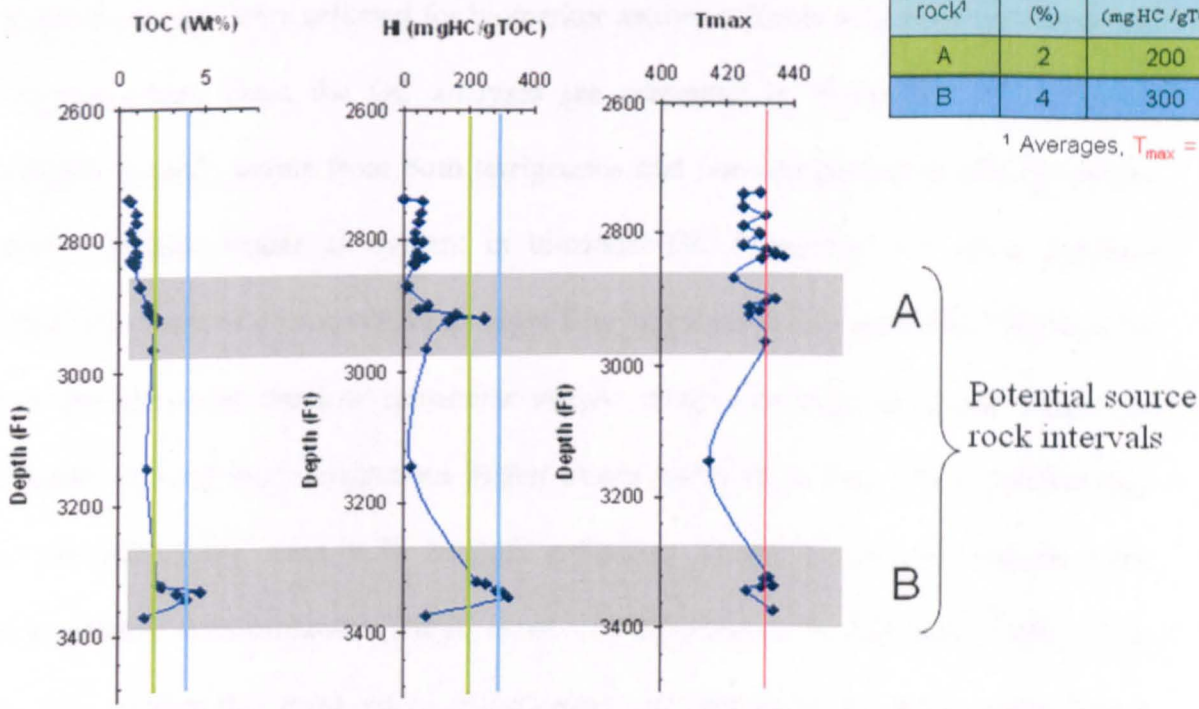

Figure 8.3. Geochemical log of the Gbekebo well covering the entire Araromi Formation. Two organic rich intervals are apparent (A and B). Only one sample within the interval "A" contain oleanane whereas most samples in the interval "B" contain oleanane, with oleanane index (OL in Table 8.1) values as high as 0.21, despite the high marine algae biomarker composition of interval B.

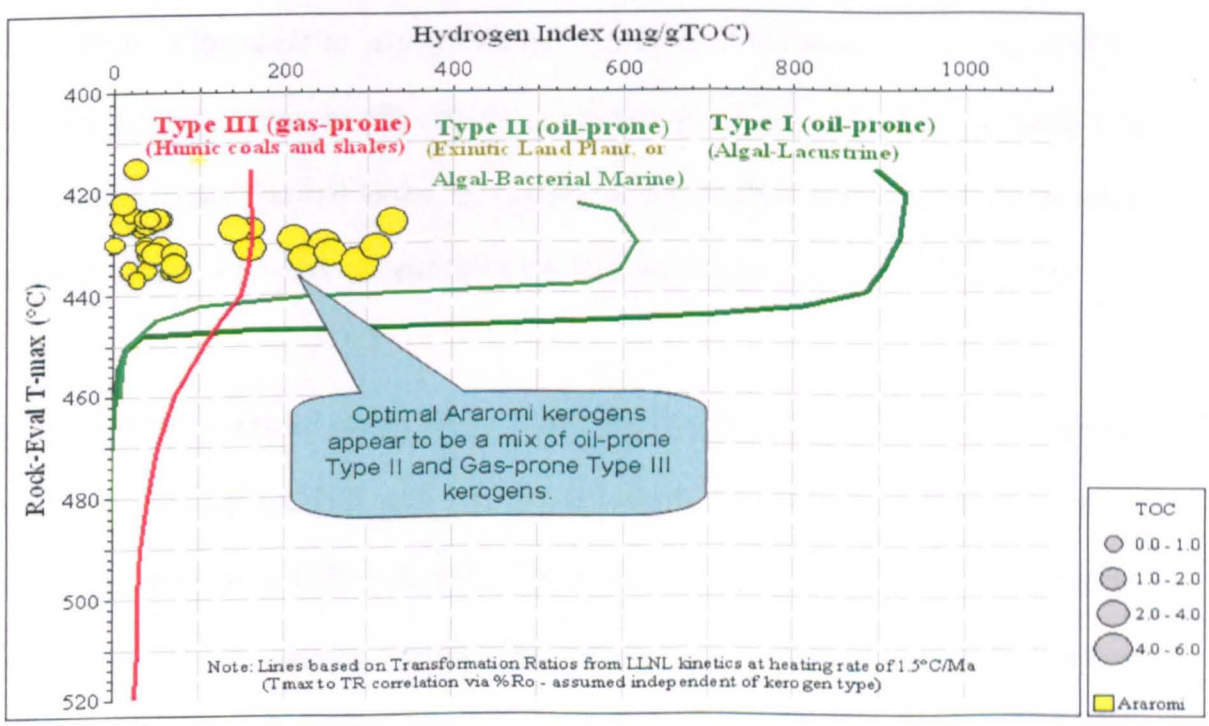

Figure 8.4. Plot of Rock-Eval HI against Tmax indicating the kerogen types and their respective hydrocarbon potentials in the analysed Araromi Formation sediments.

8.3. Comparison of biomarker compositions

Twelve samples were selected for biomarker analyses (Table 8.1). Representative gas chromatograms from the GC analyses are presented in Figure 8.5. The samples contain variable inputs from both terrigenous and non-terrigenous (probably marine algae) organic matter as evident in bi-modal GC fingerprints of some samples. However, there is a relatively high input from algal-bacterial precursors indicated by the abundance of the low molecular weight relative to high molecular weight *n*-alkanes derived from terrigenous higher plants (Bray & Evans, 1961). Additionally pr/ph ratios vary from 0.78 to 2.02 reflecting anoxic to sub-oxic source rock depositional environments (Didyk *et al.*, 1978;Volkman & Maxwell, 1986). It is worthy of note that pr/ph ratios in deepwater oils are generally in the range 2 to 3 (Table 5.14, Chapter Five), suggesting more oxic depositional conditions when compared with the Araromi Shales having range of 0.78-2.02. However, the low pr/ph ratios for the Araromi shale extract may also increase, giving sufficient thermal maturation of the shale to appropriate thermal level of oil generation (Tmax 440°C), by cleavage of carbon in phytane (C_{20} isoprenoid) to generate more pristane (C_{19} isoprenoid) under thermal stress. In essence, at oil window maturity, the pr/ph ratios of the Araromi expellable oil and the deepwater oil samples may be comparable.

Steranes in the saturated hydrocarbon fractions of the bitumen extracts of the Araromi shale analysed by GC-MS and GC-MS-MS show the C_{27}-C_{29} distribution to be nearing a ratio of 1.1:0.9:1.0, with higher C_{27} and C_{28} compounds on occasions relative to the C_{29} sterane homologues for the 5α(H),14α(H),17α(H) 20R isomers. Figures 8.6 and 8.7 show the comparison of the sterane distributions of the deepwater Niger Delta oils and the bitumen extracts from the Araromi shale. It is apparent that

Figures 8.6 and 8.7 show the comparison of the sterane distributions of the deepwater Niger Delta oils and the bitumen extracts from the Araromi shale. It is apparent that samples of deepwater oils and some of the shale extracts from Araromi Formation are comparable on the basis of their sterane compositions.

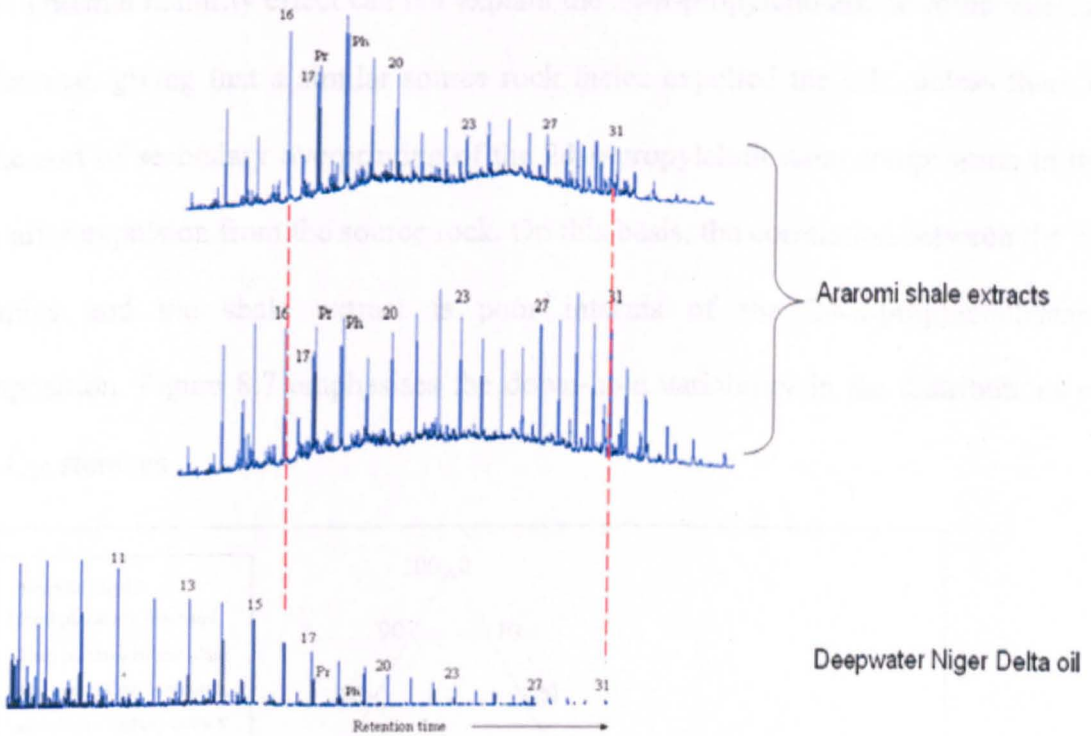

Figure 8.5. Representative gas chromatogram of the Araromi shale (samples GB314 and GB 307) extracts and a deepwater Niger Delta oil (sample NDO14) showing how *n*-alkane and isoprenoid distributions in the Araromi shale can vary as to resemble deepwater distributions upon maturation (upper chromatogram) and the apparent contrast in the distribution with the deepwater oils (lower Araromi shale extract chromatogram).

Additionally, the presence of the 24-*n*-propylcholestane, marker of chrysophyte marine algae contribution to source rock organic matter (Moldowan *et al.*, 1990) confirms the high marine algal contribution to the organic matter in the Araromi shales, as values of $\%C_{30}$ sterane range from 0.45 to as high as 5.23% even in oleanane rich intervals in Zone "B" in Figure 8.3. In general, some intervals within the shale have sterane distributions, which are similar to those of the deepwater oils

analysed in this study (Figure 8.6 and 8.7), samples with high HI values (GB 455 and 456) are among the Araromi samples that show reasonable correlation with the oils in the Figure 8.6. However, the majority of the Araromi shale extracts contain elevated 24-*n*-propylcholestane (2 to 5%) and this is generally less than 2% for the deepwater oils. Thermal maturity effect can not explain the 24-*n*-propylcholestane compositional difference, giving that a similar source rock facies expelled the oils, unless there is some sort of secondary overprinting of the 24-*n*-propylcholestane composition in the oils after expulsion from the source rock. On this basis, the correlation between the oil samples and the shale extract is poor interms of the 24-*n*-propylcholestane composition. Figure 8.7 emphasises the down-hole variability in the distributions of C_{27}-C_{29} steranes.

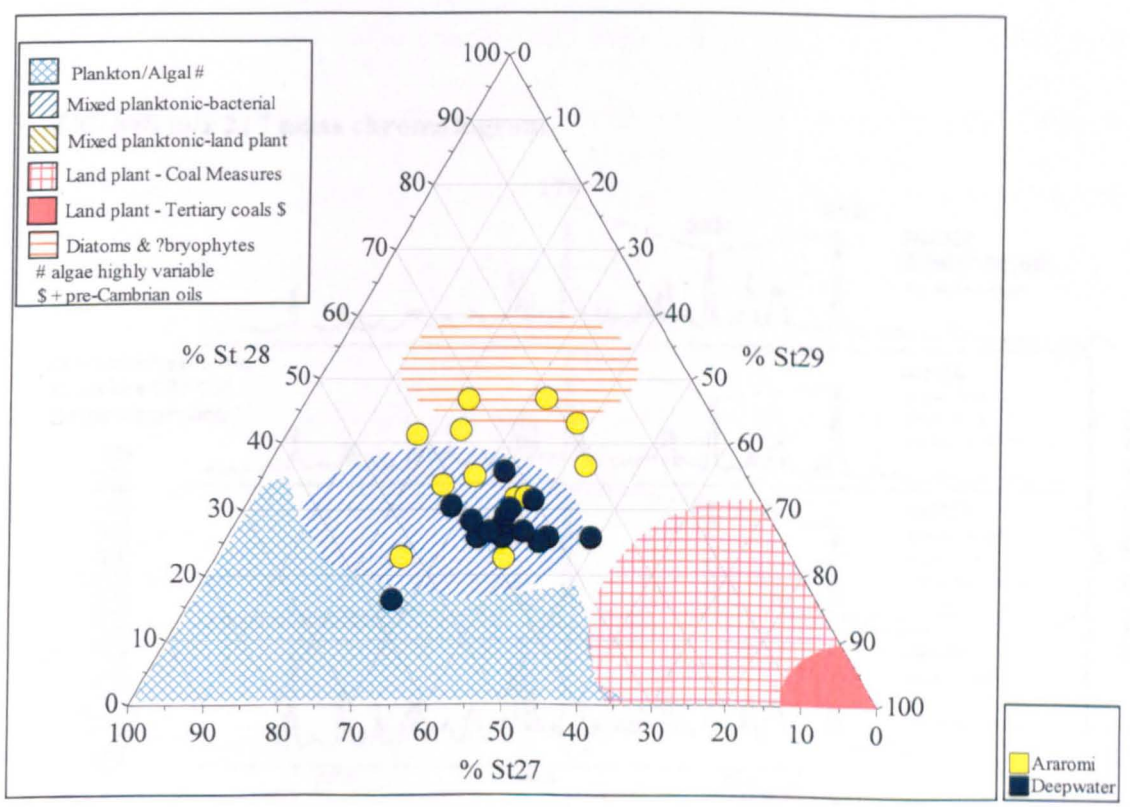

Figure 8.6. Ternary diagram showing the plot of C_{27} C_{28} and C_{29} steranes (based on 5α(H),14α(H),17α(H) 20R sterane peaks from appropriate GC-MS-MS transitions) interpreted in terms of likely kerogen precursor. Interpretational overlay from IGI's p: IGI-2 software modified after Huang and Meinschein (1979).

Furthermore, the terpane distributions in the m/z 191 mass chromatograms of the Araromi shale extracts are similar to the deepwater Niger Delta oils, except that the deepwater oils contain elevated oleanane, which may be related to thermal maturity effect compared with the shale extracts. The variability in the oleanane and 24-*n*-propylcholestane compositions is apparent in Figure 8.8. Notable is that oleanane in the shale extracts are comparably low except for two samples at the base of the well (samples GB 450 and GB 455), which have values as high as 0.2. One contrasting observation from Figure 8.8 is that samples GB 450 and 455, which have highest oleanane index, also contain the highest amount of the 24-*n*-propylcholestane. It can be concluded that in terms of sterane and oleanane compositions, samples in the interval B have reasonable correlation with the deepwater oils.

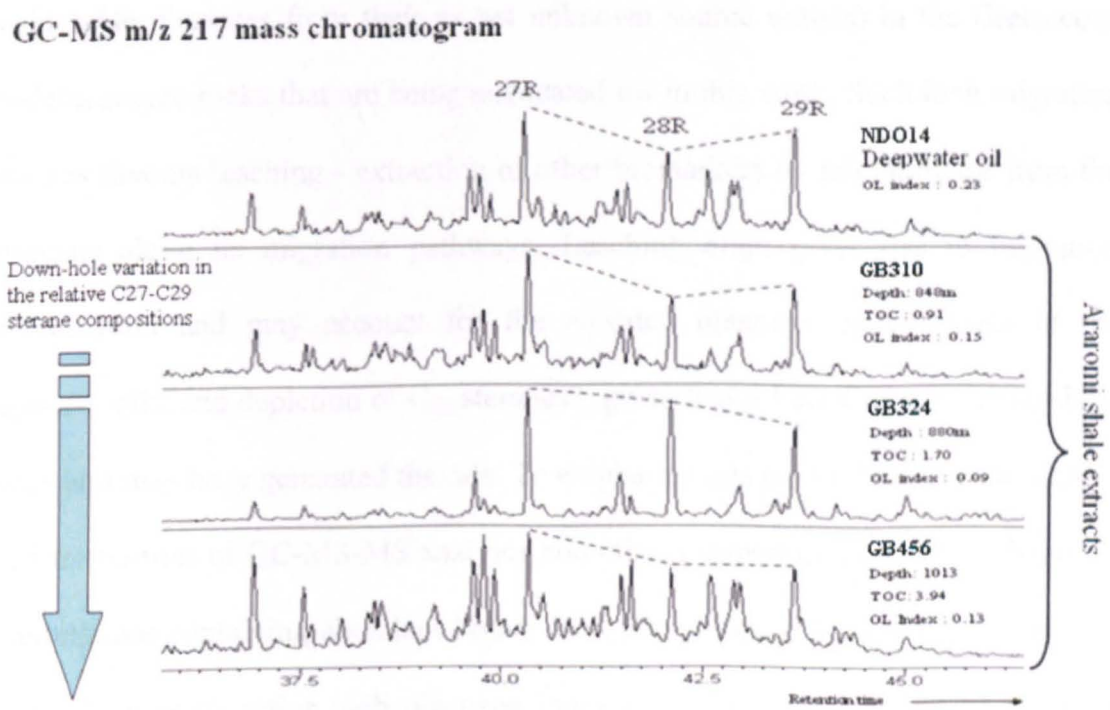

Figure 8.7. GCMS m/z 217 mass chromatograms showing the distribution of C_{27}-C_{29} steranes in representative intervals within the Araromi shale and a typical distribution in deepwater Niger Delta oil. Note the downhole variation in the sterane distributions within the Araromi shale extracts.

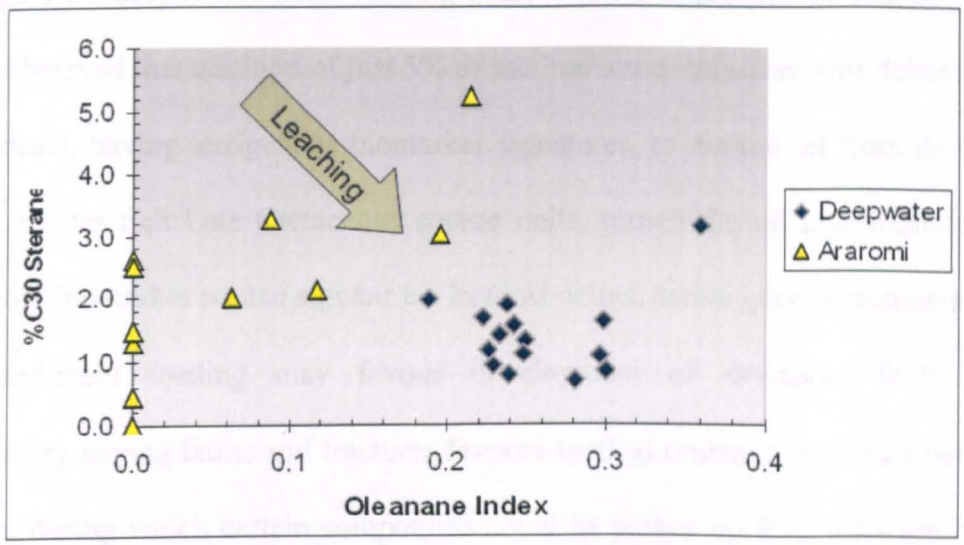

Figure 8.8. Plot of oleanane index (18α (H) + 18β(H)-oleanane/18α(H)+ 18β(H), oleanane + C_{30} -Hopane) versus 24-*n*-propylcholestane shows variability in the compositions of these biomarkers in the Araromi shale extracts. The oils and the shale extracts generally show poor correlation in the 24-*n*-propylcholestane composition which can not be explained by thermal maturity effect or leaching.

The deepwater oils are reservoired within the Tertiary sands and may have migrated considerable distances from their as yet unknown source units(s) in the Cretaceous sub-delta source rocks that are being advocated for in this work. Such long migration distances favours leaching - extraction of other biomarkers by migrating oil from the sediments along its migration pathways. Leaching often gives rise to migration contamination and may account for the elevated oleanane compositions in the deepwater oils, and depletion of C_{30} steranes?, given that a Late Cretaceous sub-delta source unit may have generated the oils. To emphasise this possibility, Li *et al.* (2007) noted from series of GC-MS-MS analyses and mixing experiments that significant oil accumulations containing abundant higher land plant biomarker signatures (high C_{29} sterane, high pr/ph ratios high oleanane index and significant amount of lupanoid hydrocarbons) in the Tertiary reservoirs of the Beaufort-Mackenzie Delta may in fact have been sourced from the Late Cretaceous Smoking Hills and Boundary Creek formations, whose shale extracts are contrastingly characterized by low/no oleanane

and high 24-*n*-propylcholestane. Using mass balance approach, Li and co-workers (2007) observed that addition of just 5% of the immature intra-reservoir deltaic source rock extract, having terrigenous biomarker signatures, to mature oil from the marine organic matter rich Late Cretaceous source units, turned the oil into"immature oil" with coaly biomarker source signatures. In most deltas, active gravity tectonics during rapid sediment loading may favour development of extensive faults. Good connectivity among faults and fractures favours vertical drainage in deltaic petroleum systems, during which certain compounds could be picked up from adjacent beds by migrating oil that can significantly alter the primary biomarker source signatures in the reservoired oils. Because of this, the presence of elevated oleanane concentration in the deepwater oils relative to the Araromi shale extracts is not sufficient evidence to downgrade the chances of sub-delta sourcing of these deepwater Niger delta oils.

8.4. Comparison of stable carbon isotope compositions

The CSIA data for the analysed Araromi shale extracts and the representative deepwater Niger Delta oils is presented are Table 8.2. Figure 8.9 shows the *n*-alkane CSIA profiles for the deepwater oils and the Araromi shale extracts. The Araromi bitumen extracts are mostly isotopically heavier at shorter chain lengths than the analysed deepwater oils but are similar at longer chain lenght. Although both the deepwater samples and the Araromi shale extracts display nearly flat profiles that have earlier been interpreted as a consequence of derivation of organic carbon from a nearly homogenous marine source (Chung *et al.*, 1994), the correlation between the shale extracts and the deepwater oils isotopic profiles is poor, because the trend of their profiles are not uniform i.e. the shale extracts are heavier (more positive $\delta^{13}C$

values) in the short *n*-alkane chain lengh and lighter (more negative $\delta^{13}C$ values) in the long *n*-alkane chain length (Figure 8.9).

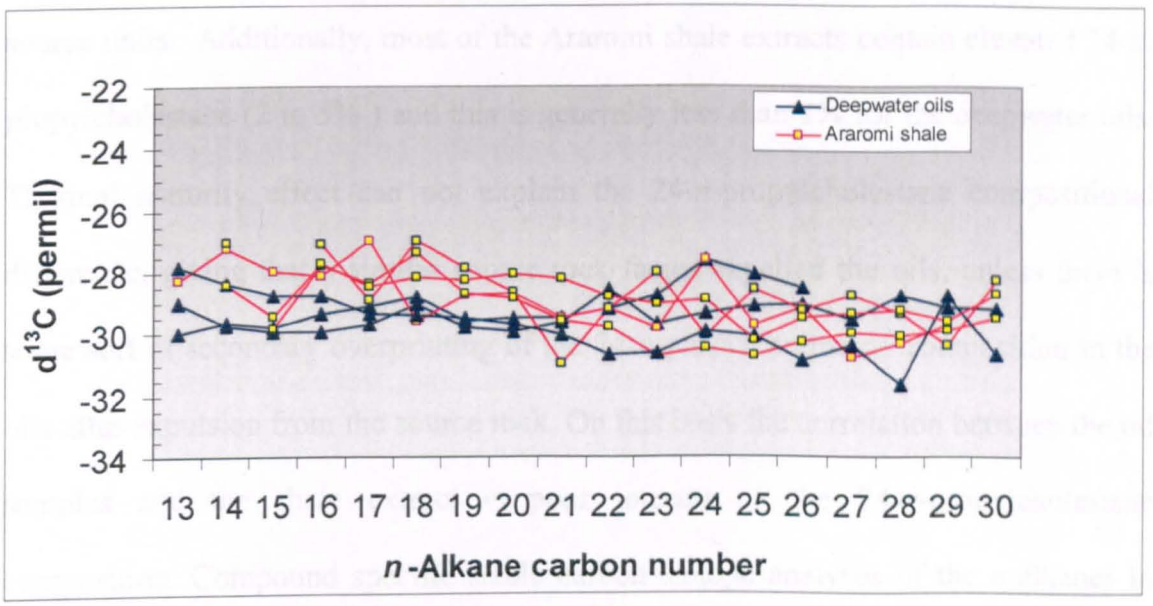

Figure 8.9. CSIA profile of *n*-alkanes in representative deepwater Niger Delta oils and the bitumen extracts of the Araromi shale.

8.5. Summary and source implications

The geochemical data presented for the representative samples from the Late Cretaceous Araromi Formation in the Dahomey Basin, south western Nigeria suggest fair to good source rock potentials with TOC values ranging from 0.5 to 4.78 wt % and having the potential to expel both gaseous and liquid hydrocarbon upon adequate maturation of the organic matter as a function of burial depth and temperature. Gas chromatographic analyses indicate a mixed marine algae and terrigenous higher plant organic matter input with more of marine algae contribution in some samples as revealed by their bimodal and unimodal *n*-alkane distributions and the C_{27}-C_{30} sterane carbon number compositions. The source rock organic matter accumulations probably occur under anoxic to sub-oxic conditions (pr/ph ratios range from 0.78 to 2.02). These biomarker characteristics do not compare well with the deepwater oils, where

pr/ph ratios are within the range of 2 to 3 and the oils conatin elevated oleanane index values, which may have been influenced by thermal maturity (i.e. addition of more oleanane) by leaching during migration of the deepwater oils from probable sub-delta source units. Additionally, most of the Araromi shale extracts contain elevated 24-*n*-propylcholestane (2 to 5%) and this is generally less than 2% for the deepwater oils. Thermal maturity effect can not explain the 24-*n*-propylcholestane compositional difference, giving that a similar source rock facies expelled the oils, unless there is some sort of secondary overprinting of the 24-*n*-propylcholestane composition in the oils after expulsion from the source rock. On this basis the correlation between the oil samples and the shale extract is poor interms of the 24-*n*-propylcholestane composition. Compound specific stable carbon isotope analyses of the *n*-alkanes in the urea adducted saturated hydrocarbon fractions of the Araromi shale extracts reveal a nearly flat carbon number isotopic profile that suggests derivation of organic carbon from uniform $\delta^{13}C$ composition of a probable marine algae source. These *n*-alkane CSIA profiles do not compare very well with those of the deepwater oils, with the shale samples being relatively isotopically heavier(more positive $\delta^{13}C$ values) in the short chain *n*-alkane and isotopically lighter (more negative $\delta^{13}C$ values) in long chain *n*-alkane region.

Notwitstanding the relatively overall poor geochemical fit between the deepwater oils and shale extracts from the Araromi Formation, a proposal that the deepwater oils are probably sourced from this formation or one of similar source facies that has been buried to depths of oil generation is being supported. Such Late Cretaceous sub-delta source units underlie the delta prograde.

Notable is the fact that an oil represents the natural average of the source rock organic facies from which it has been expelled and so therefore the vertical facies variation within a single well penetrating the Araromi Formation in the Dahomey Basin suggests how the expelled oil can vary compositionally, (though to a relatively small extent) when compared to the bulk geochemical composition of the candidate source rock samples. Peters *et al.* (1999) stated that poor sample representation in addition to the lateral and vertical variations in candidate source rocks geochemical compositions often make direct oil-source rocks correlations not possible. Furthermore, as oil fills Tertiary reservoirs, the compositional biomarker source signatures of the expelled oil undergo another compositional alteration by process of migration contamination, which occurs on a variable scale. This migration contamination can be subtle and give rise to elevated concentration of certain compounds, which are readily leached (e.g. the oleananoids) from the adjacent immature beds as the oil migrates from its source to trap.

In conclusion, this "subtle" migration contamination and thermal maturity difference may explain the elevated oleanane concentration in the deepwater oils as compared to their concentration in the Araromi shale extracts. Had the shale extracts of the Araromi Formation contained elevated oleanane relative to the deepwater oils; it would have proved difficult to propose an oil-source rock relationship. To this end, a sub-delta source facies is being proposed, instead of a Palaeogene source, as the source units for the deepwater Niger Delta oils.

Table 8.1. Bulk geochemical and selected biomarker parameters for the analysed Araromi shale in Dahomey Basin

Sample	Depth (ft)	TOC	S1	S2	Tmax	HI	PI	Pr/Ph	%C27	%C28	%C29	%C30	OL	C29S/S+R
GB 304	2735.7	0.50	0.00	0.01	430.00	2.00	0.00							
GB 305	2739	0.63	0.12	0.36	425.00	57.14	0.25							
GB 306	2758.8	1.02	0.14	0.51	425.00	50.00	0.22							
GB 307	2772	1.01	0.13	0.48	432.00	47.52	0.21	1.06	36.94	25.55	37.06	0.45	0.00	0.23
GB 309	2788.5	0.69	0.05	0.24	425.00	34.78	0.17							
GB 310	2798.4	0.91	0.04	0.34	430.00	37.36	0.11	1.28	45.28	26.62	28.09	0.00	0.00	0.18
GB 311	2801.7	0.99	0.06	0.55	430.00	55.56	0.10							
GB 312	2818.2	0.95	0.08	0.41	425.00	43.16	0.16							
GB 313	2824.8	1.00	0.28	0.42	432.00	42.00	0.40							
GB 314	2828.1	0.68	0.12	0.44	435.00	64.71	0.21	0.78	24.10	41.81	32.77	1.32	0.00	0.25
GB 315	2831.4	0.91	0.07	0.36	435.00	39.56	0.16	0.93	23.62	35.50	38.88	2.00	0.06	0.31
GB 316	2834.7	0.76	0.06	0.21	437.00	27.63	0.22							
GB 318	2838	0.82	0.06	0.30	431.00	36.59	0.17	1.18	22.16	39.74	36.59	1.51	0.00	0.26
GB 320	2867.7	1.24	0.06	0.15	422.00	12.10	0.29							
GB 323	2897.4	1.67	0.12	1.29	435.00	77.25	0.09							
GB 324	2904	1.70	0.06	0.83	432.00	48.82	0.07	1.25	31.95	41.15	24.29	2.61	0.00	0.31
GB 325	2910.6	1.87	0.27	3.01	427.00	160.96	0.08							
GB 326	2917.2	2.13	0.18	5.25	430.00	246.48	0.03		38.20	38.47	20.83	2.50	0.00	0.26
GB 327	2920.5	2.12	0.17	3.01	427.00	141.98	0.05							
GB 402	2963.4	1.97	0.21	1.39	432.00	70.56	0.13		31.39	31.00	33.51	4.11		0.23
GB 421	3144.9	1.66	0.28	0.42	415.00	25.30	0.40							
GB 450	3319.8	2.24	0.31	5.01	433.00	223.66	0.06	1.13	33.68	38.20	25.09	3.02	0.20	0.29
GB 451	3323.1	2.52	0.32	6.44	432.00	255.56	0.05							
GB 454	3333	4.78	0.81	13.75	434.00	287.66	0.06							
GB 455	3336.3	3.33	0.73	10.30	431.00	309.31	0.07	2.02	30.15	30.74	33.89	5.23	0.21	0.16
GB 456	3342.9	3.94	1.29	12.88	426.00	327.07	0.09	1.39	37.91	33.23	26.73	2.13	0.12	0.47
GB 460	3372.6	1.54	0.31	1.09	434.00	70.78	0.22	0.96	34.20	33.56	29.00	3.24	0.09	0.19

HI = Hydrogen index (100*S2/TOC). PI = production Index S1/(S1+S2). Pr/Ph = pristane/phytane. % C27-C30 = % C27-C30 ααα sterane to sum 27-29 ααα regular steranes. OL = 18α(H) + 18β(H) oleanane/C_{30} 17α(H), 21β(H)- Hopane. C29 S/S+R = ratio of 5α(H), 14 α(H), 21α(H)- sterane (20S+ 20R) thermal maturity parameter. The shaded areas are intervals A and B.

Table 8.2. Compound specific stable carbon isotope data for representative deepwater and oils and Araromi shale extracts.

Sample	nC13	nC14	nC15	nC16	nC17	nC18	nC19	nC20	nC21	nC22	nC23	nC24	nC25	nC26	nC27	nC28	nC29	nC30
	-27.82	-28.35	-28.74	-28.73	-29.34	-29.41	-29.48	-29.67	-30.02	-30.66	-30.62	-29.96	-30.06	-30.85	-30.37	-31.66	-28.73	-30.69
DA8	(0.27)	(0.12)	(0.09)	(0.42)	(1.09)	(0.93)	(0.27)	(0.45)	(0.21)	(0.51)	(0.39)	(0.38)	(0.74)	(0.37)	(0.54)	(0.51)	(0.68)	(0.91)
	-28.97	-29.73	-29.92	-29.92	-29.68	-29.05	-29.80	-29.92	-29.63	-28.54	-29.69	-29.34	-29.09	-29.03	-29.52	-28.75	-29.13	-29.17
DA3	(0.80)	(0.16)	(0.23)	(0.36)	(0.89)	(0.36)	(0.37)	(0.68)	(0.79)	(0.72)	(0.60)	(0.26)	(0.14)	(0.44)	(1.1)	(2.2)	0.70)	(1.1)
	-29.97	-29.63	-29.79	-29.34	-29.10	-28.81	-29.59	-29.50	-29.50	-29.18	-28.76	-27.61	-28.06	-28.51				
DA 7	(0.49)	(0.16)	(0.37)	(0.19)	(0.45)	(0.51)	(0.65)	(0.27)	(0.37)	(0.47)	(0.28)	(0.33)	(0.42)	(1.05)				
		-27.02		-27.05	-28.89	-26.95	-27.87	-28.64	-30.98	-29.18	-28.00	-30.08	-28.53	-29.25	-28.76	-29.34	-30.36	-28.24
GB 315		(1.3)		(0.52)	(0.56)	(0.95)	(0.92)	(0.63)	(0.67)	(1.80)	(0.69)	(1.60)	(1.9)	(0.43)	(0.54	(1.80)	(0.301	(0.95)
		-28.39	-29.43	-27.71	-28.45	-28.14	-28.24	-28.05	-28.17	-28.81	-29.03	-28.89	-30.22	-29.50	-29.36	-29.24	-29.59	-28.70
GB 324		(0.89)	(0.28)	(0.14)	(0.17)	(0.25)	(0.17)	(0.74)	(2.5)	(1.19)	(0.98)	(0.58)	(0.67)	(1.02)	(0.49)	(0.33)	(0.37)	(0.29)
			-29.83	-27.73	-28.33	-27.34	-28.69	-28.82	-29.59	-29.80	-30.74	-30.48	-30.74	-30.30	-29.97	-30.07	-29.89	-29.50
GB 326			(0.88)	(0.07)	(0.51)	(0.90)	(0.38)	(0.33)	(0.21)	(0.29)	(0.63)	(0.30)	(1.14)	(0.16)	(0.41)	(0.41)	(0.35)	(0.10)
	-28.25	-27.23	-27.95	-28.09	-26.96	-29.61	-28.74	-28.70	-29.49	-29.19	-29.85	-27.60	-29.72	-29.13	-30.77	-30.35	-29.68	
GB 455	(1.1)	(0.51)	(0.10)	(0.06)	(1.40)	(0.50)	(0.15)	(0.22)	(0.50)	(1.38)	(1.84)	(1.62)	(0.31)	(0.48)	(0.46)	(1.98)	(2.91)	

Note data reported are average of three analyses for each sample. Data in bracket are the standard deviation of replicate analyses. nC$_{13}$- nC$_{30}$ refers to n-alkane carbon number.

CHAPTER NINE

CONCLUSIONS AND FUTURE WORK

9.0. Introduction

The work in this thesis has been carried out with the primary objective of characterising the crude oils reservoired in Tertiary deltas in terms of their organic matter composition (algal-bacterial versus higher land plant), their depositional eH (oxic versus anoxic) and thermal maturity at expulsion. One of the main aims was to achieve an improved understanding of the petroleum systems producing the oils so as to resolve the geochemical paradox (i.e. why the Tertiary-reservoired oils and the candidate intra-delta source rock samples do not usually show good geochemical match) and their source ro between the oil accumulations in Tertiary deltas and their supposed source rocks. This chapter thus presents the overall conclusions drawn from the work (from the interpretation of literature data and from new geochemical analyses performed on the assembled global set of Tertiary deltaic oils) as well as suggesting further work to improve our knowledge of the complex petroleum systems operating worldwide in Tertiary deltas.

9.1. Biomarker compositions

Nearly all the deltaic oils analysed in this study contain oleanane, a terrigenous higher plant marker characterisitic of angiosperm land plants. The oleanane abundance is highly variable relative to the C_{30} hopane and may reflect primarily the level of higher plant contributions or favourable diagenetic conditions (marine influence) for oleanane formation at the expense of the other organic compounds and competing aromatisation reaction pathways that may have been formed from the β-Amyrin

precursor (Murray *et al.*, 1997; Killops and Killops, 2005, pp.194-195), or the extent of migration leaching in some of the oils. Unfortuantely aromatised terpenoids were not exermined in Chapter Five as likely compounds that may form at the expense of oleanane, particularly in samples having low oleanane index. However, the oleanane index compares positively with abundance of other terrigenous higher plant biomarkers (e.g. C_{29} steranes) in the oils, thus suggesting that in most of the oils, their oleanane abundance reflects more of the original angiosperms higher plant inputs. Other higher plant biomarkers like bicadinanes are present in the Assam oils, while bisnorlupanes were only detected in oils from Kutei and Beaufort-Mackenzie Delta. Unlike oleananes, the occurrence of these other higher plants biomarkers is not ubiquitous in the samples exermined in the study. Detailed discussions on crude oils biomarker compositions have been provided in Chapters Five and Six, a summary of the biomarker characterises of the oils are thus provided here. Table 9.1 provides summary of biomarker compositions for the oils from each Tertiary deltaic basin studied.

Assam Delta: The analysed Assam crude oils are very rich in *n*-alkanes $>C_{21}$ and over 90% of the crude oil samples analysed contain C_{29} sterane compositions >60% relative to the total C_{27}-C_{30} sterane carbon number compounds, high pristane/ phytane ratios (av.= 5.74) and absence of 24-*n*-propylcholestanes, which is diagnostic of marine chrysophyte algae contribution. These biomarker characteristics in addition to presence of significant oleanane and bicadinane angiosperms markers suggest that the source facies that expelled these oils contain dominantly terrigenous higher plant inputs and were deposited under relatively oxic depositional conditions typical of the coaly and carbonaceous shales of delta top to delta front environments.

Table 9.1. Summary of the Biomarker composition of oils from the Basins of study

	Assam	Beaufort-Mackenzie	Gulf of Mexico	Niger Delta	Kutei
Organic Matter Source Parameters					
nC_{17}/nC_{27}	0.9±0.43	0.17±0.103	0.14±0.098	0.32±0.16	0.24±0.29
$\%C_{27}$ sterane	8.34	11.7(27[a])	31.60	26.20(35.39*)	5.70
$\%C_{28}$ sterane	18.59	15.67(33.92[a])	27.33	25.38(35.39*)	9.09
$\%C_{29}$ sterane	73.08	72.56(39.05[a])	41.07	48.72(35.24*)	85.20
C_{29}/C_{27} steranes	13.97	17.09	1.44	2.20(1.02*)	20.20
$\%C_{30}$ 24-*n*-propylcholestane	0.00	12.35	1.17	0.7(1.41*)	0.00
Hopane/Sterane	3.20	0.32	0.24	2.26	2.24
Oleanane Index	0.22	0.17	0.12	0.42(0.26*)	0.42
Lupanoid Index	0.00	0.17	0.00	0.00	0.36
Bicadinane Index	1.86±2.31	0.00	0.00	0.00	12.00
26T/25T	nm	0.69	0.95	1.07	0.00
Depositional Condition Indicators					
Pristane/Phytane	5.74 ±0.81	3.08 (2.26[a])	2.5 ±0.26	2.93 (2.45*)	7.56±2.27
Pristane/nC17	4.37±5.56	3.57±6.41	0.87±0.39	1.27±0.76	1.68±1.70
Phytane/nC18	0.98±1.40	1.29±1.79	0.45±0.27	1.37±0.75	0.26±0.13
Diasteranes/Steranes	3.110.94	8.57	11.69	0.86	2.64
Gammacerane Index	0.00	0.06	0.32	0.17(0.80*)	0.00
DBT/P	0.19	0.14	0.19	1.26	0.14
Thermal Maturity Parameters					
C_{29} S/S+R	0.52	0.39	0.30	0.36	0.32
C_{29} abbS/S+R	0.56	0.51	0.48	0.43	0.38
C_{32} S/S+R	0.57	0.54	0.51	0.54	0.53
MPI-1	0.68	0.64	0.67	0.77	0.49
MNR	1.92	1.26	1.12	1.45	1.34
Ts/Ts+Tm	nm[2]	0.42	0.42	0.48	0.42

[a] = Values in bracket applies to Beaufort-Mackenzie Delta oils having marine organofacies biomarker characteristics. *= Values apply to deepwater Niger Delta sample sets only. Nm=not measured. nm[2]= Ts/Ts+Tm not measured for Assam oils because of the co-elution of Tm with some bicadinane peaks on the GC column utilised for the analyses. 0.00= no values for the sample set because of absence of one or more compounds in the calculation of the parameter. Full meanings of abbreviated biomarker parameters are as described in Chapter Five.

The Assam oils are comparatively thermally more advanced than most of the oils from other basins studied (Figures 5.63 and 5.64). The elevated thermal maturity of these oils is not surprising, as some of the Assam oils have been tentatively tied to the Oligocene Barail coal group and Eocene Kopili shale (Goswami *et al.*, 2005 and references therein). Coals and coal-shales are usually characterised by delayed petroleum fluid expulsion controlled by a combination of its micro-porosities and the chemistry of the dominant macerals.

Beaufort-Mackenzie: Beaufort-Mackenzie Delta crude oil samples analysed in this study are separable into two end-members based on their biomarker characteristics. The first end-member of oils is constituted by those containing elevated C_{27} sterane (marine algae marker) relative to the C_{29} homologues (mostly derived from terrigenous higher plants), comparatively low pristane/phytane ratios (mostly < 2.0), absence to low levels of oleanane and lupanoids and presence of abundant 24-*n*-propylcholestanes, (a marker of marine chrysophyte algal input). The biomarker characteristics of this group of oils suggest that the source rocks that expelled these oils contain abundant marine algae contribution relative to terrigenous higher plants. Additionally, these oils are thermally more mature than the second oil group (Figure 5.63) as revealed by the values of the C_{29} 5α(H),14α(H),17α(H) 20S/20S+20R and C_{29} αββ/αββ+ααα sterane isomerisation thermal maturity parameters (Seifert & Moldowan, 1986). Oils of the second end-member are characterised by presence of abundant terrigenous higher plant biomarkers such as their elevated C_{29} sterane composition, high pr/ph ratios (generally >2.5), very low to absence of 24-*n*-propylcholestane, elevated oleanane (mostly > 2.0) and lupanoid indices. These oils dominate the sample set and probably dominate the biomarker geochemistry of most

of the basin's Tertiary accumulations and they have lower sterane thermal maturity parameters. The relatively lower thermal maturity seen for the terrigenous organofacies oils of the Beaufort-Mackenzie oils is surprising as comparable terrestrial oils from Assam and Niger deltas are more mature. This anomaly could be due to high resinite content in the source rock organic matter as resinites have been suggested by to expel oils at low thermal maturity and are responsible for Tertiary-reservoired immature oils and condensates in the Beaufort-Mackenzie Basin (Snowdon, 1980b, Snowdon & Powell, 1982). These two distinct groups of Beaufort-Mackenzie oils were previously observed by Brooks (1986a) and Curiale (1991) and that the marine oils are likely sourced from the Late Cretaceous Smoking Hills and Boundary Creek formations, while the terrigenous oils are believed to have been expelled from Eocene Richards Formation and other Tertiary source units rich in terrigenous organic matter.

Gulf of Mexico: The crude oil samples from the Gulf of Mexico analysed in this study are sub-mature to mature (based on sterane and terpane thermal maturity parameters Figures 5.63 and 5.64) and they have similar biomarker compositions that depict a strong affinity to oils expelled from source rocks rich in marine algae and containing low levels of terrigenous higher plants inputs. The limited terrigenous higher plant contribution is apparent in the relatively low oleanane index (generally lower than 0.2) and significant 24-*n*-propylcholestanes indicative of a marine input. The low oleanane index could, in addition to being an indication of limited angiosperm contribution to the source rock kerogen, be a result of the source rock age. This combination is consistent with a Late Cretaceous sub-delta marine source rock filling reservoirs within the Tertiary sands. The source rock depositional environment

is inferred to be sub-oxic (average pr/ph ratios = 2.5) and occasionally under prevailing stratified water column conditions (presence of gammacerane).

Niger Delta: The molecular data presented in this study show that two different end-member oil families and an intermediate family, reflecting expulsion from at least two distinct source rock organofacies, are present within the Niger Delta oil accumulations.

One oil family, charged by a source rock rich in marine kerogen (low oleanane index <0.3, presence of significant quantity of 24-*n*-propylcholestanes, low to moderate pr/ph ratios (average= 2.4), presence of gammacerane, comparatively low C_{29} sterane composition), dominates oil accumulations in the deepwater and a few shallow water western Niger Delta fields. These data suggest that sub-delta Cretaceous source rocks rich in marine algal kerogen charge deepwater accumulations and envisaged as being laid down in sub-oxic depositional conditions. Stratigraphically, these conditions are met in the Late Cretaceous sections of Dahomey Basin on the Niger Delta's western margin, although the geochemical correlation between the candidate Araromi source rock samples and the deepwater oils is poor. Also, organic rich stratigraphic equivalent in the Anambra Basin on the eastern margin of the delta may also form part of the Cretaceous system. Both sequences have, in part, become overstepped by the prograding Tertiary delta. It is concluded from this present work based on the biomarker geochemistry of the deepwater oils, that these oils probably constitute the Late Cretaceous marine sub-delta oil system, which Haack *et al.* (2000) speculated will receive charges from marine source rock organofacies similar to the type described in the Epiya-1 well, on the Niger Delta north-western margin. The new data suggest that this organofacies will be the major source for liquid petroleum in the

deepwater section of the delta. The inability of Haack and co-workers to confirm this proposal with actual oil samples from within the Niger Delta has precluded their proposition from gaining general acceptance.

The oil family that constitutes the second end-member is terrigenous in organic matter character and it is pervasive in oil accumulations over the entire delta. This family is characterised by high oleanane index, high C_{29} sterane relative abundance, low abundance/absence of 24-*n*-propylcholestanes, high pr/ph ratios (average = 3.6) and absence of gammacerane. Oils of this family occur in the western, central and eastern Niger Delta oil accumulations. This terrigenous organic matter dominated oil family constitutes a petroleum system that is being charged by Tertiary intra-delta source rocks that are compositionally similar to the terrigenous organofacies described and generally accepted as the major source for Niger Delta oils.

An intermediate oil family also occurs, which may result from mixed accumulations charged by source rocks from both end-members or from oils expelled from source rocks containing mixed marine-terrigenous kerogen probably laid down under conditions that were less oxygenated (based on pr/ph ratios) and occasional water column stratification (presence of gammacerane in some of the oils) compared to those of overwhelming terrigenous characteristics. This oil family is most common in shallow water accumulations, especially in the western region of the Niger Delta. The biomarker compositions for these oils are intermediate between the two end-member oil families. On the basis of the biomarker compositions, particularly the distribution as well as abundance of the non-cheilanthanes-type tricyclic terpane compounds X and Y of unknown structures (Figures 5.41 and 5.42), the intermediate oil family is thought of as a distinct system charged by source rocks rich in a mix of marine algae and terrigenous organic matter. As previously observed by Haack *et al.* (2000) as well

as Eneogwe and Ekunadyo (2003), this oil system is localised and dominates accumulations in the western section of the delta.

The three oil families thus implicate the likelihood of three petroleum systems in the Niger Delta. Although, Haack *et al.* (2000) inferred the likelihood of a lower Cretaceous lacustrine oil system in the Niger Delta in addition to Tertiary terrigenous and Upper Cretaceous-Palaeocene marine systems, oils of this lacustrine system cannot be confirmed in this study based on the analysed shallow water and deepwater sample sets.

Kutei: On the basis of the molecular properties of the analysed Kutei oil/condensate samples in this study, the oils have been derived overwhelmingly from source rock facies that received abundant terrigenous higher plants organic input as evident in the high wax content (abundant *n*-alkanes $>C_{21}$), high C_{29} sterane composition, high oleanane index and absence of 24-*n*-propylcholestanes. Additionally, the high pr/ph ratios (average = 7.56) and absence of gammacerane in the oils (marker of stratified water column conditions) suggest that the source rock was deposited under an oxic and non-stratified water column. Based on measured sterane and terpane thermal maturities parameters, the oils are mid-mature (Figure 5.63 and 5.64). The combination of this source facies character is typical of coaly and carbonaceous shale dominated by terrigenous organic matter.

9.2. Novel terpane compounds

Two previously uncharacterised tricyclic terpane compounds X (C_{21})and Y (C_{25}), in m/z 191 mass chroatogram (Figure 5.41), which do not not belong to the cheilanthane series were detected. Based on the NMR structural characteristics, compound Y is a

C_{25} tricyclic terpane formed from degradation of rings A and B in a C_{30} pentacylic of the oleanane-type structure (Figure 5.45), while the C_{21} tricyclic terpane X probably has a similar structure with a shorter side chain (ethyl), this will be confirmed when an NMR result for compound X becomes available. Based on Compounds X and Y abundance, the Niger Delta oils were saparated into three groups that are sourcefacies related (Figure 5.42)

More importantly, four novel terpenoid compounds tentatively named as A_1, A_2, B_1, and B_2 were tentatively identified as 8,14-secotriterpanes, possibly 8,14-seco-oleananes in the analysed samples of oils from the basins studied. These compounds were monitored selectively from the other interfering terpanes using the GC-MS-MS parent to daughter ion transition m/z 414→123 (Figure 6.2). The tentative identification of these compounds as seco-oleananes was arrived at based on their their mass spectra characteristics, GC chromatographic behaviour (retention times as compared with other terpanes) and their co-variance with oleanane abundance when present in oil samples. Thus the same or a similar precursor to oleananes from the angiosperm higher plant family is highly favoured. In addition to these compounds, a compound (labelled "C" in this thesis) previously reported as 8, 14-secohopane (Rullkötter, 1982; Schimtter *et al.* 1982) also occurs in the oils. The distribution and relative concentrations of the compounds A and B isomers (seco-oleananes?) relative to compound "C" can be used as an index (defined as K-index= Sum of peak area of compounds A_1, A_2, B_1, and B_2 normalised to peak area of compound C) as an indicator of the level of land plant contribution to the source rock kerogen (Figure 6.21).

Additionally, compounds A_1, A_2, B_1, and B_2 occur in low abundances in the Niger Delta deepwater oils (e.g. NDO 23) and some western shallow water oils (e.g.ND30) having marine source rock organofacies (Figure 6.3). Whereas oils of the terrigenous family contain compounds A_1, A_2, B_1, and B_2 in high abundance (ND001 and ND006, Figure 6.3). This unique molecular signature among oils of these families provides a powerful tool for characterising the Niger Delta oil accumulations.

Based on laboratory experiments using pure lup-20(29)-ene prepared from Birch tree bark, the pathway for the formation of compounds A_1, A_2, B_1, and B_2 is proposed to commence by acid catalysed ring-opening, isomerisation followed by hydrogenation. The variation which occurs in the relative abundance (peak height or area) of compounds A_1 and A_2, similarly, B_1, and B_2, eluting as isomeric pairs in the oils from each basin, appears to be a control imposed by their stereochemistry. If this is fully explored using samples of source rocks, this relationship could be useful in the assessment of thermal maturity of sediments and oils. The co-occurrence of all the four isomers eluting as doublets (i.e. A_1, A_2, B_1, and B_2) suggests a single precursor molecule. More work is needed for the full structural elucidation of these compounds in order to explore their full application in petroleum correlation studies and for the purpose of confirming their tentative identities as seco-oleananes. A nuclear magnetic resonance (NMR) study is currently being undertaken as part of future work in order to elucidate the structures of these compounds.

9.3. Stable carbon isotopes characteristics

Compound specific stable carbon isotope analyses (CSIA) were performed on *n*-alkanes in the saturated hydrocarbon fractions of the representative oils from basins studied because of the method's greater interpretative strength as compared to bulk

stable carbon isotopes of saturated and aromatic hydrocarbon fractions. Nonetheless, bulk stable carbon isotopes of saturated and aromatic hydrocarbon fractions were measured for samples of oils from the Assam and the Gulf of Mexico in addition to the CSIA analyses of these oils.

Assam: The fairly representative sample of oils analysed exhibit small variations in their $\delta^{13}C$ isotope values between nC_{12} to nC_{18} but are comparatively similar in their $\delta^{13}C$ isotope values above the nC_{19}, and the oils are typified by gentle negative sloping nC_{12} to nC_{30} *n*-alkane CSIA profiles. This observation supports the biomarker data as well as the bulk saturated and aromatic stable carbon isotope $\delta^{13}C$ values data, which indicate that the Assam oils have been, expelled from similar source organofacies of terrigenous higher plant origin.

Beaufort-Mackenzie: The CSIA data for the analysed oils are in accordance with their biomarker compositions. The end-member oils with terrigenous biomarker source signatures exhibit similar *n*-alkane stable carbon isotope profiles of slightly negative slope (resulting from more negative $\delta^{13}C$ values with increasing *n*-alkane chain length) that commonly typify oils and source rock bitumen extracts derived from terrigenous deltaic organic matter mainly. Conversely, a representative sample of oil from the marine organofacies end-member (based on biomarker composition) has a nearly flat isotopic profile with *n*-alkane carbon number that reflects nearly uniform $\delta^{13}C$ values of crude oil *n*-alkanes typical of organic carbon derived from marine algae and containing relatively homogenous $\delta^{13}C$ composition usually associated with ocean carbon pool that undergoes periodic mixing. In summary, the CSIA isotopic data separates the oils into groupings that are in conformity with their biomarker compositions.

Gulf of Mexico: The CSIA $\delta^{13}C$ profile of *n*-alkanes in the analysed representative crude oil samples from the Gulf of Mexico exhibit a nearly flat profile that is commonly associated with crude oils expelled from source rocks rich in marine algae and containing homogenous $\delta^{13}C$ organic carbon composition. Additionally, the oils cluster on the marine CV (Sofer, 1984) side of the plot of the bulk saturated and aromatic hydrocarbon stable carbon $\delta^{13}C$ isotopes, thus supporting the inference drawn on the oils' source rock organofacies based on the CSIA data. The similarity in the isotope profiles of most analysed Gulf of Mexico oils corroborates similar marine algal-rich source rock organofacies earlier inferred from their biomarker compositions.

Niger Delta: Two distinct CSIA *n*-alkane $\delta^{13}C$ stable carbon isotope profiles were observed in the Niger Delta oil data set:

Negative sloping crude oil *n*-alkane $\delta^{13}C$ stable carbon isotope profiles, consisting mostly of samples from the central and eastern Niger Delta oil accumulations with a few western oils, and dominated by crude oils of the terrigenous biomarker family. The negative profile of this oil set as earlier observed also for some Beaufort-Mackenzie oils, is a result of systematic depletion in the $\delta^{13}C$ composition with increasing *n*-alkane chain length (more negative $\delta^{13}C$ values) typical of deltaic and terrigenous crude oils. On the contrary, a nearly flat to positive slope profile was obtained for another oil group consisting of shallow water samples from the western acreage and some deepwater Niger Delta oils. These profiles are constituted mainly by the deepwater oils and most western shallow water oils having mixed marine-terrigenous biomarker characteristics. This relatively nearly flat isotopic profile of the non-terrigenous type oils is considered to be a result of oil generation from a source rock kerogen rich in marine algae of homogenous $\delta^{13}C$ composition.

The western shallow water oils have a similar non-terrigenous type CSIA profiles to the deepwater oils despite their mixed biomarker compositions. They are isotopically heavier (less negative $\delta^{13}C$ values) than the deepwater oils. This observation of non-terrigenous type CSIA isotope profiles despite mixed marine-terrigenous oil biomarker characteristics for these western Niger Delta oils is interpreted to reflect that the marine organic matter probably contributed more to the *n*-alkane generating organic carbon in the source rock kerogen. Hence the resulting isotopic compositional signal in some of the expelled oils is biased towards a more marine stable carbon isotopic signature. These observation of a marine isotopic signature for these western Niger Delta shallow water oils based on their *n*-alkanes CSIA data agrees with previous bulk isotope composition interpretations reported for the western Niger Delta oils by Haack *et al.* (2000) as well as Eneogwe and Ekundayo (2003).

9.4. Model to explain source rock types charging Tertiary deltas as indicated by oil properties.

The assembled literature database of source rock and oil geochemical properties in addition to those of the analysed oils in this study provide evidence for four source rock groupings in Tertiary deltaic petroleum systems. Three of these source rock groups, namely delta top source rocks, sub-marine delta shelf source rocks, and pro-delta source rocks are classified as intra-delta because they are located within the Tertiary delta sequence. The fourth source rock group is classified as sub-delta because it occurs outside of the Tertiary delta sediment package and are necessarily older than the Tertiary delta. A summary of the geochemical characteristics and stratigraphic locations of these source rocks is provided in Figure 9.1.

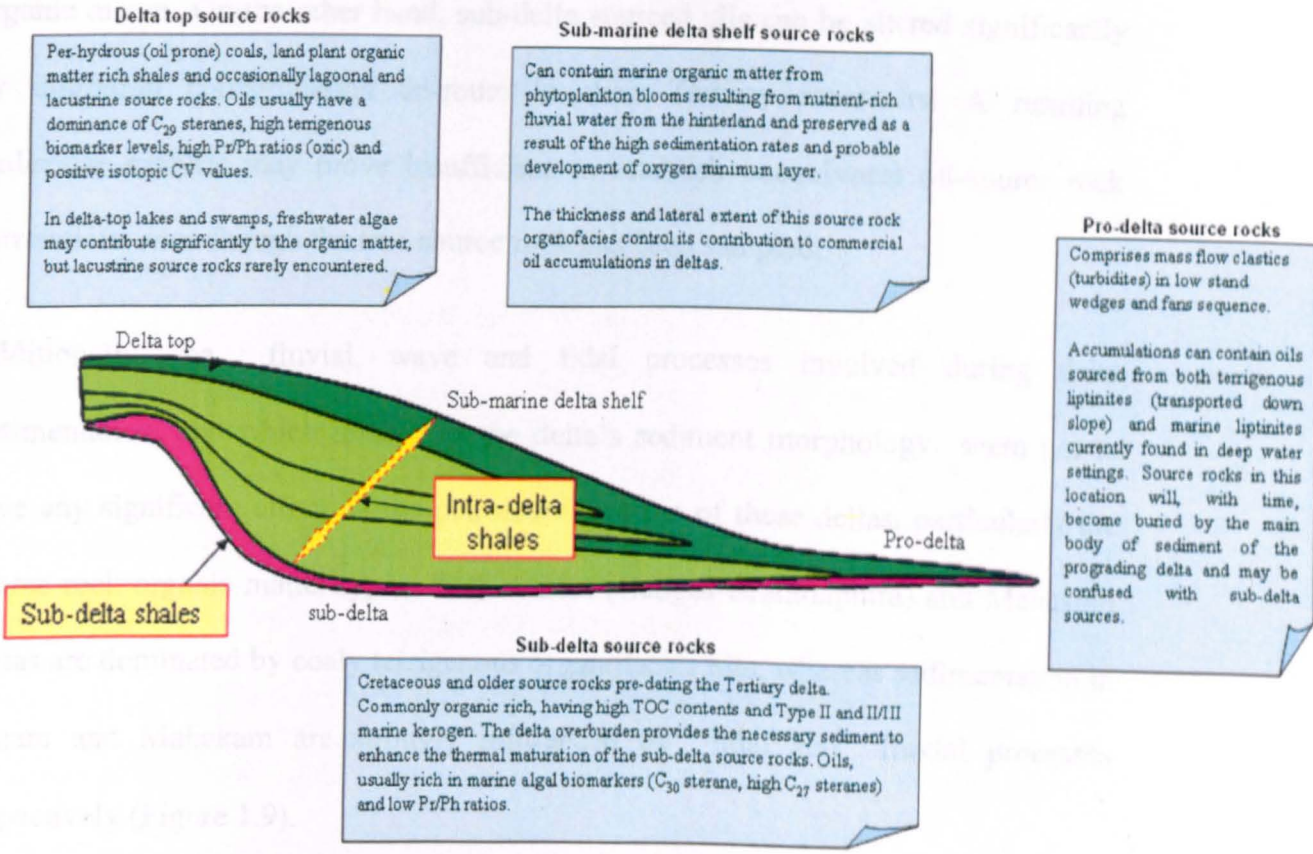

Figure 9.1. Model showing positions of various source rocks charging deltaic petroleum system, their stratigraphic relationships and the summary of their inferred geochemical properties.

Furthermore, an understanding of the fact that source rocks within a delta sequence can vary laterally and vertically in their organofacies depending on their location within the Tertiary delta prograde is necessary in order to undertake oil-source rock correlation studies in Tertiary deltaic systems. Each of the intra-delta source rock groups can be stratigraphically restricted and geographically remote, whereas their migrated oils can be found in other parts of the delta sequence. Therefore the appropriate source rock samples may prove difficult to locate in drilled wells. For instance, an oil expelled from pro-delta shale facies containing probably mixed marine-terrigenous kerogen may show poor correlation if compared with samples of source rocks from highstand, delta-top, source rock intervals rich in terrigenous

organic matter. On the other hand, sub-delta sourced oils can be altered significantly by migration contamination en-route to their Tertiary reservoirs. A resulting molecular analysis may prove insufficient to establish unequivocal oil-source rock correlations even though the true source rock has been sampled.

Additionally, the fluvial, wave and tidal processes involved during delta sedimentation, and which influences the delta's sediment morphology seem not to have any significant effect on the petroleum systems of these deltas, particularly the source rock organic matter types. Both Assam (Ganges Brahmaputra) and Mahakam deltas are dominated by coaly terrigenous organofacies oils, whereas sedimentation in Assam and Mahakam are strongly influenced by tidal and fluvial processes respectively (Figure 1.9).

Katz (2006) believes that the deepwater oils from Niger Delta are probably sourced from a Palaeogene section of the delta (lower Akata Formation), although the data presented in this thesis (Chapter Eight) does not make a case (based on poor biomarker data match and CSIA isotopic profiles), strong enough, to support the proposal that the deepwater Niger Delta accumulations receive charges predominantly from sub-delta Cretaceous source rocks in the marginal Araromi shale in Dahomey Basin, south-western Nigeria, a Late Cretaceous sub-delta source units rich in marine algae kerogen is still inferred herein. The expulsion and secondary migration of oils from Cretaceous sub-delta source rocks may have been made possible by propitious convergence of buoyancy and pressure-driven oil migration filling the Miocene reservoirs of the Tertiary delta via a 3-D network of connected sub-vertical listric faults and sub-horizontal interbeds of mud and sand (couplets) in the delta's stratigraphy. The timing of oil generation from the sub-delta source rock(s) is

predicted to be controlled by the prograding delta, the time being earlier in the proximal (early overburden development) and later in the distal locations where the delayed overburden results in later burial times.

Tertiary deltaic petroleum systems have remained poorly understood because of multiple source facies, sub-delta oil generation, mixing, and migration contamination of oils. Sub-delta generation of oil is substantially unacknowledged and evidence for the importance of this phenomenon has not been well demonstrated in published literature. A deltaic basin can be seen from two standpoints; an *acceptor* of hydrocarbon generated outside of the delta sequence (sub-delta) and a *donor* of hydrocarbon generated within its source rock intervals (intra-delta). Notwithstanding the poor geochemical match between the biomarker and stable carbon isotope geochemistry of the deepwater Niger Delta oils and bitumen extracts of the Late Cretaceous Araromi Formation on the delta's western margin, it is proposed that the sub-delta source rock facies could be one of the primary sources of oil in the deepwater systems of most deltas building on passive continental margins (e.g. Gulf of Mexico and Niger Delta).

Accurate recognition and categorising of sub-delta and intra-delta oil groups is critical to understanding petroleum generation history, source rock characteristics and the pattern of source rock distribution and occurrence in any deltaic basin and of course the success of the petroleum exploration and production in the progressively deepwater waters of Tertiary deltaic basins. A well-modelled pattern of source rock distribution is a particularly indispensable exploration tool, allowing exploration drilling to benefit from charge predictions in terms of direction, amount, type and

timing. A particularly pertinent current challenge is to predict ahead of drilling the characteristics of the oils in the deepwater of any delta. Accurate answers to these key questions will help focus exploration targets and reduce exploration uncertainties and petroleum system risking in deltaic basins.

9.5. Future work

While it is believed that an improved understanding of the Tertiary deltaic petroleum systems has been achieved by the work in this thesis, some gaps in knowledge could not be filled because of the limitations imposed by a combination of data and time. To this end some future work is suggested here to address these gaps.

More crude oil samples (especially sub-delta sources) should be acquired for each basin of study. The oil samples should be analysed concurrently with representative regional source rock samples of high quality (cores preferably, as ditch cuttings may be oil stained) for the purpose of oil-source rock correlation studies. Studies focused on microscopy and organic petrology of the regional source rock facies, particularly for the Niger Delta is highly recommended for the purpose of recognising organic matter origin in source rocks. The data from the regional microscopic studies can then be incorporated into the regional source rock modelling. Such modelling will take into account the lateral and spatial variations in source rock facies for the predictions of probable source facies and their organic matter character (marine vs. terrigenous), organic quality and quantity, effectiveness for oil generation and the nature of the petroleum products at various depths in the region and within the sub-basins.

Where oil- source rock studies have proved inadequate to identify possible sub-delta source units or to correlate even some of the terrigenous oils to the Tertiary delta

facies, as is the case in the Beaufort-Mackenzie Delta and the Kutei Basin (Curiale, 2006), a combination of geological, geophysical and geochemical data may help improve the level of the petroleum systems understanding.

Despite the elevated oleanane concentration and relatively lower 24-*n*-propyl cholestane in the deepwater Niger Delta oils, it was suggested in this work that there exists a probable geochemical relationship between the sub-delta Araromi shale extracts and the deepwater Niger Delta oils and that over reliance on oleanane as one single parameter could be misleading because of the possible effect of migration contamination. The concept of migration contamination thus requires more work that will be focused on:

1. To what extent can it occur in deltaic basins so as to overprint the primary oil-source biomarker signatures?
2. What is involved in the mechanism of the migration-contamination, such that only oleanenes and oleananes are extracted from "immature" and mature source beds respectively and leaving behind other olefins?

Although it is not clear exactly how these two questions can be answered, perhaps some laboratory migration experiments using immature organic-rich rocks rich in terrigenous markers, through which oil is passed, could be used

The need for quantitative biomarker work to give an idea of migration contamination i.e. comparing change in absolute concentration of altered sub-delta oil biomarker components with Tertiary-reservoired likely altered sub-delta oil sample. The need to look at aromatic diagenetic products of higher plant biomarkers is highly

recommended as this may help understand why oleanane was low in some oil samples (Assam), despite strong terrigenous biomarker content.

Elucidation of the structures of the proposed "seco-oleanane" compounds (compounds A_1, A_2 and B_1, B_2) is recommended as such structural information will shed light on their origin, geochemical significance and applications to petroleum exploration. Nuclear magnetic resonance (NMR) analyses of pure compounds A, B and C recovered from HPLC fractions has been proposed and this work is already underway in collaboration with Dr. Peter Nytoft of the Geological Survey of Denmark and Greenland (GEUS).

REFERENCES

ADEKEYE, O.A. 2004. Aspects of sedimentology, geochemistry and hydrocarbon potentials of Cretaceous-Tertiary sediments in the Dahomey Basin, south-western Nigeria. *Ph.D thesis, University of Ilorin, Ilorin, Nigeria*, 202 pp.

AKINLUA, A. & TORTO, N. 2006. Determination of selected metals in Niger delta oils by graphite furnace atomic absorption spectrometry. *Analytical Letter*, **39**, 1993-2005.

AKINLUA, A., AJAYI, T.R., JARVIE, D.M. & ADELEKE, B.B. 2005. A Re-Appraisal of the application of Rock-Eval pyrolysis to source rock studies in the Niger delta. *Journal of Petroleum Geology*, **28**, 39-48.

AKINLUA, A., AJAYI, T.R. & ADELEKE, B.B. 2006. Niger delta oil geochemistry: Insight from light hydrocarbons. *Journal of Petroleum Science and Engineering*, **50**, 308-314.

AKINLUA, A., TORTO, N. & AJAYI, T.R. 2007a. Oils in the NW Niger delta: aromatic hydrocarbons content and infrared spectroscopic characterization. *Journal of Petroleum Geology*, 30, 91-100.

AKINLUA, A., TORTO, N., AJAYI, T.R. & OYEKUNLE, J.A.O. 2007b. Trace metals characterisation of Niger delta kerogens. *Fuel*, **86**, 1358-1364.

ALAN, T. J., WENGER L.M., MELIA, M.B., ROSS, A.H. & KUMINECZ, C.P.1993.Recognition of a New Hydrocarbon Play in a Mature Exploration Area through Integration of Geochemical, Palynologic, Geologic, and Seismic interpretations (onshore Northern Rim of Gulf of Mexico). *American Association of Petroleum Geologists Annual Meeting*, New Orleans, Louisiana, April 25-28.

AL-AROURI, K.R., MCKIRDY, D.M. & BOREHAM, C.J.1998. Oil-source correlations as a tool in identifying the petroleum systems of the southern Taroom Trough, Australia.*Organic Geochemistry*, **29**, 713-734.

ALBRECHT, P. & OURISSON, G. 1969. Diagenese des hydrocarbures satures dans une serie sedimentaire epaisse (Douala, Cameroun). *Geochimica et Cosmochimica Acta*, **33**, 138-142.

ALBRECHT, P., VANDENBROUCKE, M. & MANDENGUÉ. M. 1976. Geochemical studies on the organic matter from the Douala Basin (Cameroon)-I. Evolution of the extractable organic matter and the formation of petroleum. *Geochimica et Cosmochimica Acta*, **40**, 791-799.

ALEXANDER, R., KAGI, R.I., ROLAND, S.J., SHEPPARD, P.N. & CHIRILA, T.V. 1985. The effects of thermal maturity on distributions of

dimethylnaphthalenes and trimethylnapthalenes in someancient sediments and petroleum. *Geochimica et Cosmochimica Acta*, **49**, 385-395.

ALLEN, P.A. & ALLEN, J.R. 2005. *Basin Analysis: Principles and Applications*. (2nd edition), Blackwell publishing, Oxford, United Kingdom. 549pp.

ALSHARHAN, A. S. & SALAH, M.G. 1997. A common source rock for Egyptian and Saudi hydrocarbons in the Red Sea. *American Association of Petroleum Geologists Bulletin*, **81**, 1640-1659.

AREF'YEV, O.A., RUSINOVA, G.V. & PETROV, A.A. 1996. Biomarkers of crude oils of eastern regions of Russia. *Petroleum Chemistry*, **36**, 289-302.

ARTHUR, M.A. & SAGEMAN, B.B. 2004. Sea level control on source rock development: perspectives from the Holocene Black Sea, the mid-Cretaceous western interior of North America, and the Late Devonian Appalachian Basin. In: Harris, N and Pradier, B. (eds.), *The Deposition of Organic Carbon-rich Sediments: Models, Mechanisms and Consequences*. SEPM Special Publications. Society for Sedimentary Geology, Tulsa, OK, pp. 35–59.

AVBOVBO, A. A. 1978. Tertiary Lithostratrigraphy of Niger Delta. *American Association of Petroleum Geologists Bulletin*, **62**, 295-300.

BAGGE, M.A. & KEELY, M.L. 1994. The oil potential of Mid-Jurassic Coals in northern Egypt. *In*: Scott, A.C. & Fleet, A.J. (eds.), *Coal and Coal-bearing Strata as Oil-prone Source Rocks, Geological Society Special Publication*, **77**, pp. 183-200.

BARAKAT, A. O., MOSTAFA, A., EL GAYAR, M.S. & OMAR, M.F. 1996. Source input and paleoenvironmental assessments using molecular biomark indicators of crude oils from the southern part of the Gulf of Suez, Egypt. *Proceedings of the 13th Egyptian Petroleum Conference*, 1, pp. 475-488.

BARKER, C. 1972. Aquathermal Pressuring--Role of Temperature in Development of Abnormal-Pressure Zones. *American Association of Petroleum Geologists Bulletin*, **56**, 2068-2071.

BENNET, B. & LARTER, S.R. 2000. Quantitative separation of aliphatic and aromatic hydrocarbon using silver ion-silica solid–phase extraction. *Analytical Chemistry*, **72**, 1039-1044.

BISSADA, K.K., KATZ, B.J., BARNICLE, S.C & SCHUNK, D.J. 1990. On the origin of hydrocarbons in the Gulf of Mexioc Basin-A reappraisal. *In*: Schumacher, D. & Perkins, B.F. (eds.), *Gulf Coast Oils and gases, proceedings of the 9th Annual Research Conference, Gulf Coast SEPM Foundation*, pp. 163-171.

BJORØY, M., HALL, P. B., GILLYON, P. & JUMEAU, J. 1991. Carbon isotope variations in *n*-alkanes and isoprenoids of whole oils. *Chemical Geology*, **93**, 13-20.

BJORØY, M., HALL, P.B. & MOE, R.P. 1994. Stable Carbon isotope Variation of *n*-alkanes in Central Graben oils. *Organic Geochemistry*, **22**, 355-381.

BOREHAM, C.J. & POWELL, T.G. 1993. Petroleum source rock potential of coal and associated sediments; Qualitative and Quantitative aspects. *In*: Law, B.E & Rice, D.D. (eds.), *Hydrocarbons from Coals, American Association of Petroleum Geologists Studies in Geology*, **38**, 203-218.

BOREHAM, C.J., BLEVIN, J.E., RADLINSKI, A.P. & TRIGG, K.R. 2003. Coal as a source of oil and gas: a case study from the Bass Basin, Australia. *Australian Petroleum Production and Exploration Association Journal*, **43**, 117-148.

BRAY, E.E. & EVANS, E.D. 1961. Distribution of *n*-paraffins as a clue to recognition of source beds. *Geochimica et Cosmochimica Acta*, **22**, 2-5.

BRINCATT, D. & ABBOTT, G. 2001. Some aspects of the molecular biogeochemistry of laminated and massive rocks from the Naples Beach Section (Santa Barbara-Ventura Basin). *In*: Isaacs, C.M. & Rullkötter, J. (eds.), *The Monterey Formation: from Rocks to Molecules*, Columbia University Press, New York, pp.140-149.

BROOKS, J.D., GOULD, K. & SMITH, J.W. 1969. Isoprenoid hydrocarbons in coal and petroleum. *Nature*, **222**, 257-259.

BROOKS, P.W. 1986a. Unusual biological marker geochemistry of oils and possible source rocks, offshore Beaufort-Mackenzie Delta, Canada. *Organic Geochemistry*, **10**, 401-406.

BROOKS, P.W. 1986b. Biological marker geochemistry of oils from the Beaufort-Mackenzie region, Artic Canada. *Bulletin of Canadian Petroleum Geology*, **34**, 490-505.

BURKE. K. 1972. Longshore drift, submarine canyons, and submarine fans in developmet of Niger Delta. *American Association of Petroleum Geologists Bulletin*, **56**, 1975-1983.

BURRUS, J. OSADETZ, K. GAULIER, J.M. BROSSE, E. DOLIGEZ, B. CHOPPIN de JANVRY, G. BARLIER, J. & VISSER, K. 1993. Source rock permeability and petroleum expulsion efficiency: modelling examples from the Mahakam Delta, the Williston Basin and the Paris Basin. In: J.R. Parker, J.R. (eds.), *Petroleum Geology of Northwest Europe: Proceedings of the 4th Conference on Petroleum Geology of NW. Europe*, Barbican Centre, London. Geological Society, London, pp. 1317-1333.

BUSTIN R. M. 1988. Sedimentology and characteristics of dispersed organic matter in Tertiary Niger Delta: origin of source rocks in deltaic environments. *American Association of Petroleum Geologists Bulletin*, **72**, 277-298.

CAILLET, G. & BATIOT, S. 2003. 2D modelling of hydrocarbon migration along and across growth faults: an example from Nigeria. *Petroleum Geoscience*, **9**, 113-124.

CAWLEY, S.J. & FLEET, A.J. 1987. Deltaic petroleum source rocks: a review. *In: abstracts of the Symposium on Deltas: Sites and Traps for Fossil fuels, Meeting of the Geological Society of London.*

CHAMBERS, J.L.C. & DALEY, T.E. 1995. A tectonic model for the onshore Kutei basin, east Kalimantan, based upon an integrated geological and geophysical interpretation. *Proceedings of the Indonesia Petroleum Association*, Jakarta, pp. 115-1130.

CHAPPE, B., ALBRECHT, P. & MICHAELIS, W. 1982. Polar lipids of archaebacteria in sediments and petroleums. *Science*, **217**, 65-66.

CHRISTIANSEN, F.G., BOJESEN-KOEFOED, J., DAM, G., PEDERSEN, A.K. & PULVERTAFT, T.C.R. 1994. Live oil onshore West Greenland: a new and encouraging discovery. *In: Proceedings of the American Association of Petroleum Geologists Annual Convention, Denver, Colorado*, pp.121.

CHRISTIANSEN, F.G., BOJESEN-KOEFOED, J., DAM, G., NYTOFT, H.P., LARSEN, L.M., PEDERSEN, A.K. & PULVERTAFT, T.C.R. 1996. The Marraat oil discovery on Nuussuag, West Greenland: Evidence for a Latest Cretaceous-Earliest Tertiary Oil Prone Source Rock in the Labarador Sea-Melville Bay Region. *Bulletin of Canadian Petroleum Geology*, **1996**, 39-54.

CHUNG, H.M., BRAND, S.W. & GIZZLE, P.L. 1981. Carbon isotope geochemistry of Palaeozoic oils from the Big Horn Basin. *Geochimica et Cosmochimica Acta*, **45**, 1803-1815.

CHUNG, H.M., ROONEY, M.A. & CLAYPOOL, G.E. 1991. Thermal maturity of oils. *In*: Manning, D. (ed.), *Organic Geochemistry- Advances and Applications in Energy and the Natural Environment*, Manchester University Press, Manchester, pp. 143-146.

CHUNG, H.M., CLAYPOOL, G.E., ROONEY, M.A. & SQUIRES, R.M., 1994. Source characteristics of marine oils as indicated by carbon isotopic ratios of volatile hydrocarbons. *American Association of Petroleum Geologists Bulletin*, **78**, 396-408.

CLARK, R.H. & ROUSE, J.T. 1971. A Closed System for Generation and Entrapment of Hydrocarbons in Cenozoic Deltas, Louisiana Gulf Coast. *American Association of Petroleum Geologists Bulletin, 55, 1170-1178*

CLAYPOOL, G.E. & MANCINI, E.A. 1989. Geochemical relationships of petroleum in Mesozoic reservoirs to carbonate source rocks of Jurassic Smackover Formation, southwestern Alabama. *American Association of Petroleum Geologists Bulletin*, **73**, 904-924.

CLAYTON, C. J. 1991. Effect of maturity on carbon isotope ratios of oils and condensates. *Organic Geochemistry*, **17**, 887-899.

CLAYTON, C.J. & BJORØY, M. 1994. Effect of maturity on $^{13}C/^{12}C$ ratios of individual compounds in North Sea oils. *Organic Geochemistry*, **21**, 737-750.

CLAYTON, J.L., RICE, D.D. & MICHAEL, G.E. 1991. Oil-generating coals of the San Juan Basin, New Mexico and Colorado, U.S.A. *Organic Geochemistry*, **17**, 735-742.

COLEMAN, J.M. 1976. *Deltas: Processes of Deposition and Models for Exploration.* Champaign: Continuing Education publishing Company Incorporation. 102 pp.

COLEMAN, J.M. & WRIGHT, L.D. 1971. Analysis of major river systems and their deltas, procedures and rationale, with two examples. *Louisiana State University Coastal Studies Institute Technical Report*, **95**, 125 pp.

COLEMAN, J.M. & PRIOR, D.B. 1980. Deltaic Sand Bodies: *American Association of Petroleum Geologist, Continuing Education Course Note Series*, **15**, 171 pp.

COLLINSON, M.E., van BERGEN, P.F., SCOTT, A.C. & de LEEUW, J.W. 1994. The oil generating-potential of plants from coal and coal-bearing strata through time: a review with new evidence from Carboniferous plants. *In*: Scott, A.C. & Fleet, A.J. (eds.), *Coal and Coal-bearing Strata as Oil-prone Source Rocks, Geological Society of London Special Publication*, **77**, 31-70.

COMBAZ, A. & de MATHAREL, M. 1978. Organic sedimentation and genesis of petroleum in Mahakam Delta, Borneo. *American Association of Petroleum Geologists Bulletin*, **62**, 1684-1695.

COMET, P.A. JANINA K. RAFALSKA, J.K. & BROOKS, J.M. 1993. Sterane and triterpane patterns as diagnostic tools in the mapping of oils, condensates and source rocks of the Gulf of Mexico region. *Organic Geochemistry*, **20**, 1265-1296.

CONNAN, J. & CASSOU, A. M. 1977. Properties of gases and petroleum liquids derived from terrestrial kerogen at various maturation levels. *Geochimica et Cosmochimica Acta*, **44**, 1-23.

CORNFORD, C. 2000. Risking petroleum systems. *In*: Garg, A.K., Banerjie, V. S.N., Swamy, S.N. &. Dwivedi, P. (eds.), *Proceedings of the fifth International Conference and Exhibition on Petroleum Geochemistry and Exploration in the Afro-Asian Region, New Delhi*, B.R. Publishing Corporation, Delhi, pp. 13-21.

CORREDOR, F., SHAW, J.H. & BILOTTI, F. 2005. Structural styles in the deep-water fold and thrust belts of the Niger Delta. *American Association of Petroleum Geologists Bulletin*, **89**, 753-780.

COX, H.C., de LEEUW, J.W., SCHENCK, P.A., Van KONINGSVELD, H., JANSEN, J.C., Van de GRAFF, B. van GEERESTEIN, V.J., KANTERS, J.A., KRUK, C. & JANS, A.W.H. 1986. Bicadinane, a C_{30}- pentacyclic isoprenoid hydrocarbon found in crude oil. *Nature,* **319,** 316-318.

CREANEY, S. 1980. The organic petrology of the Upper Cretaceous Boundary Creek Formation, Beaufort-Mackenzie basin. *Bulletin of Canadian Petroleum Geology*, **28**, 112-129.

CURIALE, J.A. 1988. Molecular genetic markers and maturity indices in intermontane lacustrine facies: Kinshenehn Formation, Montana. *Organic Geochemistry,* **13**, 633-638.

CURIALE, J. A. 1991. The petroleum geochemistry of Canadian Beaufort Tertiary "non-marine" oils. *Chemical Geology,* **93**, 21-45.

CURIALE, J.A. 1995. Saturated and olefinic terrigenous triterpanoid hydrocarbons in biodegraded Tertiary oil of northeast Alaska. *Organic Geochemistry*, **23,** 177-182.

CURIALE, J.A. 2002. A review of the occurrences and causes of migration-contamination in crude oils. *Organic Geochemistry,* **33**, 1389-1400.

CURIALE J.A. 2006. The occurrence of norlupanes and bisnorlupanes in oils of Tertiary deltaic basins. *Organic Geochemistry*, **37**, 1846-1856.

CURIALE, J.A. & BROMLEY, B.W. 1996. Migration of petroleum intoVermilion 14 Field, Gulf Coast, USA- molecular evidence. *Organic Geochemistry,* **24**, 563-79.

CURIALE, J.A. & FROLOV, E.B. 1998. Occurrence and origin of olefins in crude oils: a critical review. *Organic Geochemistry,* **29**, 397-408.

CURIALE, J., MORELOS, J., LAMBIASE, J. & MUELLER, W. 2000. Brunei Darussalem- characteristics of selected petroleums and source rocks. *Organic Geochemistry,* **31**, 1475-93.

CURIALE, J., LIN, R. & DECKER, J. 2005. Isotopic and molecular characteristics of Miocene-reservoired oils of the Kutei Basin, Indonesia. *Organic Geochemistry,* **36**, 405-424.

CURIALE, J., DECKER J., LIN, R. & MORLEY, R.J. 2006. Oils and oil- prone coals of the Kutei Basin, Indonesia. *Extended abstract, American Association of Petroleum Geologists International Conference, Perth, Australia. Nov. 5-8 2006.*

CURRY, D.J, EMMETT, J.K. & HUNT, J.W. 1994. Geochemistry of aliphatic-rich coals in the Cooper Basin, Australia and Taranaki Basin, New Zealand: Implication for the occurrence of potentially oil-generative coals. *In*: Scott,

A.C. & Fleet, A.J. (eds.), *Coal and Coal-bearing Strata as Oil-prone Source Rocks, Geological Society of London Special Publication*, **77**, 149-182.

CURTIS, M. D. 1982. Comparative Cenozoic petroleum geology of major deltas--Mississippi, Niger, and Mackenzie. *American Association of Petroleum Geologists Bulletin*, **66**, *1680-1680.*

CURTIS, D. M. 1986. Comparative Tertiary petroleum geology of the Gulf Coast, Niger and Beaufort-Mackenzie delta areas. *Geological Journal*, **21**, 225-255.

CURTIS, D.M. 1989. A conceptual model for sources of oils in Gulf Coast Cenozoic reservoirs. Gulf Coast Association Geological Society Transaction, **39**, 37-56.

CZOCHANSKA, Z., GILBERT, T.D., PHILP, R.P., SHEPPARD, C.M., WESTON, R.J., WOOD, T.A. & WOOLHOUSE, A.D.1988. Geochemical application of sterane and triterpane biomarkers to a description of oils from the Taranaki Basin in New Zealand. *Organic Geochemistry*, **12**, 123-135.

DEGENS, E.T. 1969.Biogeochemistry of stable carbon istotopes.*In*: Eglinton, G. & Murphy, M.T.J. (eds.), *Organic Geochemistry*, Springer, Berlin, pp.304-329.

DEMAISON, G.J., HUIZINGA, B.J. 1994. Genetic classification of petroleum systems using three factors: charge, migration, and entrapment. *In*: Magoon, L.B. & Dow, W.G. (eds.), *The Petroleum System- from Source to Trap. American Association of Petroleum Geologists, Memoir*, **60**, pp. 73-89.

DIDYK, B. M., SIMONEIT, B. R. T., BRASSELL, S. C. & ENGLINTON, G. 1978. Organic geochemical indicators of paleoenvironmental conditions of sedimentation. *Nature*, **272**, 216-222.

DIECKMANN, V., ERDMANN M., ONDRAK, R., SNOWDON, L. R. & HORSFIELD, B. 2005. Deep Basin Petroleum Formation from Neo-Formed Sources, the Mackenzie Delta, Canada. *Program abstract of the American Association of Petroleum Geologists Annual Meeting, Calgary, June 19-22, 2005.*

DIETRICH, J. R., DIXON, J., MCNEIL, D.H., MCINTYRE, D.J., SNOWDON, L. R. & CAMERON, A.R. 1989. The geology, biostratigraphy and organic geochemistry of the Natsek E-56 and Edlok N-56 wells, western Beaufort Sea, Arctic Canada, in Current research, part G. *Geological Survey of Canada Paper* **89**-1G, pp. 133-157.

DIXON J., DIETRICH, J.R., MCNEIL, D.H., MCINTYRE, D.J., SNOWDON, L.R. & BROOKS, P. 1985. Geology, biostratigraphy and organic geochemistry of Jurassic to Pleistocene strata, Beaufort-Mackenzie area, northwest Canada. *Canadian Society of Petroleum Geologists Course Notes*, 65pp.

DIXON, J., DIETRICH, J., SNOWDON, L. R., MORRELL, G. & MCNEIL, D.H. 1992. Geology and Petroleum Potential of Upper Cretaceous and Tertiary

Strata, Beaufort-Mackenzie Area, Northwest Canada (I). *American Association of Petroleum Geologists Bulletin*, **76**, 927-947.

DOBSON, L.M. & BUFFLER, R.T. 1997. Seismic Stratigraphy and Geologic History of Jurassic rocks, Northeastern Gulf of Mexico. *American Association of Petroleum Geologists Bulletin*, **81**,100-120.

DOUST, H. & OMATSOLA, E. 1990. Niger Delta. *In:* Edwards, J.D. & Santogrossi, P.A. (eds.), *Divergent/passive Margin Basins. American Association of Petroleum Geologists Memoir*, **4**, pp.239-248.

DURAND, B. 1983. Present trends in organic geochemistry in research on migration of hydrocarbons. *In*: Bjorøy, M., Albrecht, P., Conford, C. *et al.*, (eds.), *Advances in Organic Geochemistry 1981*, John Wiley & Sons, New York, pp. 117-28.

DURAND, B. & ESPITALIE, J. 1976. Geochemical studies on the organic matter from the Douala Basin (Cameroon)-II. Evolution of kerogen. *Geochimica et Cosmochimica Acta*, **40**, 801-808.

DURAND, B. & OUDIN, J. L. 1979. Exemple de migration des hydrocarbures dans une serie deltaique: le Delta de la Mahakam, Kalimantan, Indonesie. *Exploration, Supply and Demand, Proc. Bucharest, 10th World Petroleum Congress*, 2, pp. 3-11.

DURAND, B. & PARATTE, M. 1983. Oil potential of coals: a geochemical approach. *In*: Brooks, J. (ed.), *Petroleum Geochemistry and Exploration of Europe, Blackwell Scientific Publishing, Boston, MA*, pp. 255-65.

EJEDAWE, J.E. 1981.Patterns of Incidence of oil reserves in Niger Delta basin. *American Association of Petroleum Geologists Bulletin*, **65**, 1574-1585.

EJEDAWE, J.E. & OKOH, S.U. 1981 Prediction of optimal depths of petroleum occurrence in the Niger Delta basin. *Oil and Gas*, **79**, 190-204.

EJEDAWE J. E., COKER S. J. L., LAMBERT-AIKHIONBARE D. O., ALOFE K. B. & ADOH, F. O. 1984. Evolution of oil-generative window and oil and gas occurrence in Tertiary Niger Delta Basin. *American Association of Petroleum Geologists Bulletin*, **68**, 1744-1751.

EKWEOZOR, C. M. 2004. Source rocks of giant hydrocarbon deposits in deep offshore, Niger delta. Abstract: *Nigerian Association of Petroleum Explorationists and American Association of Petroleum Geologists Regional West Africa Deepwater Conference, Abuja, Nigeria.*

EKWEOZOR C. M. & DAUKORU, E. M. 1984. Petroleum source bed evaluation of the Tertiary Niger Delta--reply. *American Association of Petroleum Geologists Bulletin* **68**, 390-394.

EKWEOZOR C. M. & DAUKORU, E.M. 1994. Northern delta depobelt portion of the Akata-Agbada (!) petroleum system, Niger Delta, Nigeria. *In*: Magoon, L.B. & Dow, W.G. (eds.), *The Petroleum System-from Source to Trap. American Association of Petroleum Geologists Memoir*, **60**, pp. 599-614.

EKWEOZOR C. M. & OKOYE N. V. 1980. Petroleum source-bed evaluation of the Tertiary Niger Delta. *American Association of Petroleum Geologists Bulletin* **64**, 1251-1259.

EKWEOZOR, C.M. & TELNAES, N. 1990. Oleanane parameter: verification by quantitative study of the biomarker occurrence in sediments of the Niger Delta. *Organic Geochemistry*, **16**, 401-413.

EKWEOZOR, C.M. & UDO, O.T. 1988. The oleananes: origin, maturation and limits of occurrence in Southern Nigeria sedimentary basins. *In*: Mattavelli, L. & Novelli, L. (eds.), *Advances in Organic Geochemistry 1987*. Pergamon Press, Oxford, pp. 131-140.

EKWEOZOR C. M., OKOGUN J. I., EKONG D. E. U. & MAXWELL J. R. 1979a.Preliminary organic geochemical studies of samples from the Niger delta (Nigeria) I. Analyses of crude oils for triterpanes. *Chemical Geology*, **27**, 11-28.

EKWEOZOR C. M., OKOGUN J. I., EKONG D. E. U. & MAXWELL J. R. 1979b.Preliminary organic geochemical studies of samples from the Niger delta (Nigeria) : II. Analyses of shale for triterpenoid derivatives. *Chemical Geology*, **27**, 29-37.

ENACHESCU, M.E. 1990. Structural setting and validation of direct hydrocarbon indicators for Amauligak Oil Field, Canadian Beaufort Sea. *American Association of Petroleum Geologists Bulletin*, **74**, 41-59.

ENEOGWE C. I. 2003. The distribution of light hydrocarbons in western Niger Delta oils. *Journal of Petroleum Geology*, **26**, 479-488.

ENEOGWE C. I. 2004.The invariance ratio in isoheptanes: a powerful tool for oil-oil correlation in the Tertiary Niger Delta, Nigeria. *Organic Geochemistry*, **35**, 989-992.

ENEOGWE, C. & EKUNDAYO, O. 2003. Geochemical correlation of crude oils in the NW Niger Delta, Nigeria. *Journal of Petroleum Geology*, **26**, 95-103.

ENEOGWE, C., EKUNDAYO, O. & PATTERSON, B.A. 2002. Source-derived oleanenes identified in Niger Delta oils. *Journal of Petroleum Geology*, **25**, 83-95.

EVAMY B. D., J H., KAMERLING P., KNAAP W. A., MOLLOY F. A. & ROWLANDS P. H. 1978. Hydrocarbon habitat of Tertiary Niger Delta. *American Association of Petroleum Geologists Bulletin*, **62**, 277-298.

ERTEL, J. R. & HEDGES, J. 1980. A test of the melanoidin hypothesis. *American Association of Petroleum Geologists Bulletin*, **64**, 704 -704.

FAILS, T.G.1990.The Northern Gulf Coast Basin: a classic petroleum province. In: Brooks, J. (ed.), *Classic Petroleum Provinces, Geological Society Special Publication*, **50**, 221-248.

FAZEELAT, T., ALEXANDER, R. & KAGI, R. 1994. Extended 8, 14-secohopanes in some seep oils from Pakistan. *Organic Geochemistry*, **21**, 257-264.

FISHER, W.L., BROWN, F.J.R., SCOTT, A.J. & MCGOWEN, J.H. 1969. *Delta systems in the exploration for oil and gas:* A research colloquium, University of Texas Bureau of Economic Geology, Austin.

FRANKL, E.J. & CORDRY, E.A. 1967. The Niger Delta oil province-recent developments onshore and offshore: *7th World Petroleum Congress, Mexico City, Proceeding,* **1b**, pp.195-209.

FREEMAN, K.H., HAYES, J.M., TRENDEL, J.M. & ALBRECHT, P. 1990. Evidence from carbon istope measurements for diverse origins of sedimentary hydrocarbons. *Nature*, **343**, 254-256.

FUEX, A.N. 1977. The use of stable carbon isotopes in hydrocarbon exploration. *Journal of Geochemical Exploration*, **7**, 155-188.

GALIMOV, E. M. 1980. C13/C12 in kerogen. *In*: Durand, B (ed.), *Kerogen, Insoluble Organic Matter from Sedimentary Rocks*, Paris, Editions Technip, pp.271-299.

GALIMOV, E.M. 1985. *The Biological Fractionantion of Isotopes*. Academic Press, New York.

GALLOWAY, W.E. 1975. Process framework for describing the morphologic and stratigraphic evolution of deltaic depositional systems. *In*: Broussard, M.L, (ed.), *Deltas, Models for Exploration, Houston Geological Society, Houston, Texas*, 555pp.

GANZ, H., OBILAJA, S., LADIPO, K., OTOGHILE, C., ANEKE, U., ANOWAI, C., EJEDAWE, J. & LEHNER B. 2005. Integrated hydrocarbon system analysis in the Niger delta. *Extended book of abstracts, 22nd International Meeting of Organic Geochemistry, Seville-Spain, September 12-16, 2005.*

GLENNIE, K. W. 1997, *Petroleum Geology of the North Sea*. Oxford, Blackwell Science, 636 pp.

GOODWIN, T. W. 1973. Comparative Biochemistry of Sterols in eukaryotic Microorganisms. *In*: Erwin, J. A. (ed.), *Lipids and Biomembranes of Eukaryotic Micro organisms*, Academic Press, New York, pp. 1-40.

GOOSENS, H., De LEEUW, J.W., SCHENCK, P.A. & BRASSEL, S.C. 1984. Tocopherols as likely precursors of pristane in ancient sediments and crudeoils. *Nature*, **312**, 440-442.

GOSWAMI, B.G., BISHT, R.S., BHATNAGAR, A.K., KUMAR, D., PANGTEY, K.L., MITTAL, A.K., DATTA, G.C. & THOMAS, N.J. 2005. Geochemical characterization and source investigation of oils discovered in Khoraghat-Nambar structures of the Assam-Arakan basin, India. *Organic Geochemistry*, **36,** 161-181.

GRANTHAM, P.J., POSTTHUMA, J. & BAAK, A. 1983. Triterpanes in a number of Far-Eastern crude oils. *In*: Bjoroy, M., Albretch, C., Cornford, C., *et al.*, (eds.), *Advances in Organic Geochemitry 1981*, John Wiley & Sons, New York, pp. 675-683.

GREINER, G. & CHI, B. 1995. Canada. *In*: Kulke, H (ed.), *Regional Petroleum Geology of the World Part II: Africa, America, Australia and Antarctica.* Berlin, Gebru Borntraeger, pp. 279-334.

HAACK, R. C., SUNDARARAMAN, P., DIEDJOMAHOR, J.O., XIAO, H., GANT., N.J., MAY, E.D. & KELSCH, K. 2000. Niger Delta petroleum systems, Nigeria. *In*: Mello, M.R & Katz, B.J. (eds.), *Petroleum Systems of the South Atlantic Margins, American Association of Petroleum Geologists Memoir,* **73,** 213-231.

HAMILTON, W. 1979. Tectonics of the Indonesian region: *United States Geological Survey Professional Paper*, 1078, 345pp.

HARWOOD, R. J. 1977. Oil and gas generation by laboratory pyrolysis of kerogen. *American Association of Petroleum Geologists Bulletin*, **61**, 2082-2102.

HAYES, J.M., TAKIGIKU, R., OCAMPO, R., CALLOT, H.J. & ALBRECHT, P. 1987. Isotopic compositions and probable origins of organic molecules in the Eocene Messel shale. *Nature*, **329**, 48-51.

HAYES, J.M., FREEMAN, K.H., POPP, B.N. HOHAM, C.H. 1990. Compound specific isotopic analyses: a novel tool for reconstruction of ancient biogeochemical processes. *Organic Geochemistry*, **16,** 1115-1128.

HEYDARI, E., WADE, W.J. & ANDERSON, L.C. 1997. Depositional Environments, Organic Carbon Accumulation, and Solar-Forcing Cyclicity in Smackover Formation Lime Mudstones, Northern Gulf Coast. *American Association of Petroleum Geologists Bulletin*, **81**, 760-774.

HOEFS, J. 1997. *Stable Isotope Geochemistry.* (4th edition), Springer-Verlag, Berlin, 201pp.

HOEFS, J. 2004. *Stable Isotope Geochemistry.* (5th edition), Springer-Verlag, Berlin, 244pp.

HOFFMANN, C. F., MACKENZIE, A. S., LEWIS, C. A., MAXWELL, J. R., OUDIN, J. L., DURAND, B. & VANDENBROUCKE, M. 1984. A biological marker study of coals, shales and oils from the Mahakam Delta, Kalimantan, Indonesia. *Chemical Geology*, **42**, 1-23.

HORSFIELD, B., YORDY, K.L. & CRELLING, J.C. 1988. Determining the petroleum generation potential of coals using organic geochemistry and organic petrology. *Organic Geochemistry*, **13**, 121-129.

HUANG, W.Y., MEINSHEIN, W.G., 1979. Sterols as ecological indicators. *Geochimica et Cosmochimica Acta*, **43**, 739-745.

HUANG, Y., FREEMAN, K.H., WILKIN, R.T., ARTHUR, M.A. & JONES, A.D. 2000. Black Sea chemocline oscillations during the Holocene: molecular and isotopic studies of marginal sediments. *Organic Geochemistry*, **31**, 1525-1531.

HUC, A.Y., DURAND, B., ROUCACHET, J., VANDENBROUKE, M. & PITTION, J.L. 1986. Comparison of three series of organic matter of continental origin. *Organic Geochemistry*, **10**, 65-72.

HUGHES, W.B. & DZOU, L.I.P. 1995. Reservoir overprinting of crude oils. *Organic Geochemistry*, **23**, 905-914.

HUGHES, W.B. HOLBA, A.G. & DZOU, L.I.P. 1995. The ratio of dibenzothiophene to phenanthrene and pristane to phytane as indicators of depositional environment and lithology of petroleum source rocks. *Geochimica et Cosmochimica Acta*, **59**, 3581-3598.

HUNT, J. 1991. Generation of gas and oil from coal and other terrestrial organic matter. *Organic Geochemistry*, **17**, 673-680.

HUTCHINSON, C.S. 1989. *Geological Evolution of the South-East Asia.* Oxford, England, Oxford Science publications, 368pp.

ILLICH, H.A. 1983. Pristane, phytane and lower molecular weight isoprenoids distributions in oils. *American Association of Petroleum Geologists Bulletin*, **67**, 385-393.

ISAKSEN, G.H., CURRY, D.J., YEAKEL. J.D. & A.I. JENSSEN, A.I. 1998.Controls on the oil and gas potential of humic coals. *Organic Geochemistry*, *29, 23-44.*

ISSLER, D.R. & SNOWDON, L.R. 1990. Hydrocarbon generation kinetics and thermal modelling, Beaufort-Mackenzie Basin. *Bulletin of Canadian Petroleum Geology*, **38**, 1-16.

JAFFÉ, R., ALBRECTH, P. & OUDIN, J.L. 1988a. Carboxylic acids as indicators of oil migration. I. Occurrence and geochemical significance of C-22 diastereoisomers of the 17β(H), 21β(H) C_{30} hopanoic acid in geological samples. *Organic Geochemistry*, **13**, 483-488.

JAFFÉ, R., ALBRECTH, P. & OUDIN, J.L. 1988b. Carboxylic acids as indicators of oil migration. II. Case of the Mahakam Delta, Indonesia. *Geochimica et Cosmochimica Acta*, **52**, 2599-607.

JANARDHANAN, M., DAS, S.K., MAHESHWARI, S.C. & BARAPATRA, D.V. 2000. Three distinctly different source facies and conditions as evidenced by geochemical signatures of oils in southern Nagapattinam sub-basin, Cauvery Basin, India. In: Garg, A.K., Banerjie, V., Swamy, S.N.& Dwivedi, P. (eds.), *Proceedings of the Fifth International Conference and Exhibition on Petroleum Geochemistry and Exploration in the Afro-Asian Region*. B.R. Publishing Corporation, New Delhi, pp. 529-534.

JONES, R.W. 1987. Organic facies. *In*: Brooks, J. & Welte, D. (eds.), *Advances in Petroleum Geochemistry*, Academic Press, London, pp. 1-90.

KAPLAN, I.R. 1975. Stable isotopes as a guide to biogeochemical processes. *Proceedings of the Royal Society of London*, **189**, 183-211.

KATZ, B.J. 1994. An alternative view on indo-Australian coals as source of petroleum. *Australia Petroleum Exploration Association Journal*, 256-267.

KATZ, B.J. 2006. Significance of ODP results on deepwater hydrocarbon exploration- eastern equatorial Atlantic region. *Journal of African Earth Sciences*, **46**, 331-345.

KATZ, B.J. & ROBISON, V.D. 2006. Oil quality in deep-water settings: Concerns, perceptions, observations and reality. *American Association of Petroleum Geologists Bulletin*, **90**, 909-920.

KENNICUTT, M.C., MCDONALD, T.J., COMET, P.A., DENOUX, G.J. & BROOKS, J.M. 1992. The origins of petroleum in the northern Gulf of Mexico.*Geochimica et Cosmochimica Acta*, **56**, 1259-1280..

KENNICUTT, M.C., REQUEJO, A.G., SASSEN, R. & BROOKS, J. M. 1993.Oil Formation in the Northern Gulf of Mexico. Geochemical Evidence. *American Association of Petroleum Geologists Annual Meeting*, New Orleans, Louisiana, April 25-28, 1993.

KHAVARI-KHORASANI, G. 1987. Oil-prone coals of the Wallon Coal Measures, Surat Basin, Australia. *In*: Scott, A.C (ed.), *Coal and Coal- bearing Strata: Recent Advances, Geological Society of London Special Publications*, **32**, 303-310.

KILLOPS, S. D. & FREWIN, N.L. 1994. Triterpenoid diagenesis and cuticular preservation.*Organic Geochemistry*, **21**, 1193-1209.

KILLOPS, S.D. & KILLOPS, V.J. 2005. Introduction to organic geochemistry. 2nd edition. Blackwell Publishing, Oxford, UK. 393pp.

KILLOPS, S.D., WOOLHOUSE, A.D., WESTON, R.J. & COOK, R.A.1994. A Geochemical Appraisal of Oil Generation in the Taranaki Basin, New Zealand. *American Association of Petroleum Geologists Bulletin*, **78**, 1560-1585.

KILLOPS, S.D., RAINE, J.I., WOOLHOUSE, A.D. & WESTON, R.J. 1995. Chemostratigraphic evidence of higher-plant evolution in the Tranaki Basin, New Zealand. *Organic Geochemistry*, **23**, 429-445.

KILLOPS, S.D., FUNNELL, R.H., SUGGATE, R.P., SYKES, R., PETERS K.E., WALTERS, C., WOOLHOUSE, A.D., WESTON, R.J. & BOUDOU, J.P. 1998. Predicting generation and expulsion of paraffinic oil from vitrinite-rich coals. *Organic Geochemistry*, **29**, 1-21.

KIMBLE, B.J., MAXWELL, J.R., PHILP, R.P. & ENGLINTON, G. 1974. Identification of steranes and triterpanes in geolipid extracts by high-resolution gas chromatography and mass spectrometry. *Chemical Geology*, **14**, 173-198.

KNOX , G.J. & OMATSOLA, E.M. 1989. Development of the Cenozoic Niger Delta in terms of the 'Escalator Regression' model and impact on hydrocarbon distribution. *In*: van der Linden, W.J.M., Cloetingh, S.A.P.L., Kaasschieter, J.P.K., van der Graff, W. J E., Vandenberghe, J. & van der Gun, J.A.M. (eds.), *proceedings of the KNGMG Symposiums on Coastal Lowlands, Geology and Geotechnology*. Kluwer Academic Publishers, Amsterdam, pp. 181-202.

KOTARBA, M.J., WIĘCŁAW, D., KOLTUN,Y.V., MARYNOWSKI, L., KUŚMIEREK, J. & DUDOK, I.V. 2007. Organic geochemical study and genetic correlation of natural gas, oil and Menilite source rocks in the area between San and Stryi rivers (Polish and Ukrainian Carpathians. *Organic Geochemistry*, *38*, 1431-1456.

KULKE, H. 1995. Nigeria. *In*: Kulke, H. (ed.), *Regional Petroleum Geology of the World. Part II: Africa, America, Australia and Antartica*: Berlin, Gebru Borntraeger, p.143-172.

KVENVOLDEN, K.A., RAPP, J.B., HOSTETTLER, F.D. & SNAVELY, P.D. 1989. Preliminary evaluation of the petroleum potential of the Tertiary accretionary terrane, west side of the Olympic Peninsula, Washington, Comparison of molecular markers in oils and rock extracts. *United States Geological Survey Bulletin*, **1892**, pp. 19-35.

KVENVOLDEN, K.A., HOSTETTLER, F.D., RAPP, J.B., SNAVELY, P.D. 1991. Biomarkers in Tertiary mélange, Western Olympic Peninsula, Washington, USA. *Chemical Geology*, **93**, 101-110.

LANDRUM, J.H. & SUTTON, C. 1988.Organic Geochemical Analysis of Oils from Coastal Plain along Gulf of Mexico: Abstract. *American Association of Petroleum Geologists Bulletin*, **72**, 209-209.

LAMBERT-AIKHIONBARE, D. O. & IBE A. C. 1984. Petreoleum source-bed evaluation of the Tertiary Niger Delta: Discussion: *American Association of Petroleum Geologists Bulletin*, **61**, 961-981.

LAW, B.E. & RICE, D.D. 1993. Hydrocarbons from coal. *American Association of Petroleum Geologists Bulletin*, **71**, 207-214.

LAWVER, L. A. & SCOTESE, C.R. 1990. A review of tectonic models for the evolution of the Canada Basin. *In*: Grantz, A., Johnson, A.L. & Sweeney, J.F. (eds.), *The Arctic Ocean region: The Geology of North America, Geological Society of America*, **L**, pp. 593-618.

LI, M., XIONG, Y., SNOWDOWN, L. & ISSLER, D. 2005. Compound specific stable carbon and hydrogen isotope ratios as a diagnostic oil-source correlation tool in the Canadian Beaufort-Mackenzie Basin. *Extended abstracts, 22nd International Meeting of Organic geochemistry, Seville-Spain, September 12-16, 2005.*

LI, M, ZHANG, S., SNOWDON, L & ISSLER, D. 2007. Pitfalls and potential remedies of the current oil-source rock correlation approach: case studies in two of the world largest Tertiary deltaic systems. *In*: book of abstracts, *23rd International Meeting of Organic geochemistry, Torquay, England, September* 8-14, 2007.

MACGREGOR, D.S. 1994. Coal-bearing strata as source rocks- a global review. *In*: Scott, A.C. & Fleet, A.J. (eds.) *Coal and Coal-bearing Strata as Oil-prone Source Rocks, Geological Society of London Special Publication*, **77**, 107-116.

MACKENZIE, A.S. 1984. Applications of biological markers in petroleum geochemistry. *In*: Brooks, J. & Welte, D. (eds.), *Advances in Petroleum Geochemistry*, Academic Press, London, pp. 115-214.

MACRAE, G. 1991. Salt Tectonism in the Destin Dome Region, Northeastern Gulf of Mexico. *American Association of Petroleum Geologists meeting abstract,* Dallas, Texas, April 7-10, 1991.

MACRAE, G. & WATKINS, J.S. 1993.Basin architecture, salt tectonics, and Upper Jurassic structural styles, Desoto Canyon Salt Basin, Northeastern Gulf of Mexico. *American Association of Petroleum Geologists Bulletin*, **77**, 1809-1824.

MAGNIER, P H., OKI, T., & KARTAADIPUTRA, L. 1975. The Mahakam delta, Kalimantan, Indonésie. *Proceeding of the 9th World Petroleum Congress*, Tokyo, pp. 239-250.

MAGOON, L.B. 1988. The petroleum system- a classification scheme for research, exploration, and resource assessment. *In*: Magoon, L.B. (ed.), *Petroleum Systems of the United States, United States Geological Survey Bulletin*, **1870**, 2-15.

MAGOON, L.B. & Dow, W.G. 1994. The Petroleum System. *In*: Magoon, L.B. & Dow, W.G. (eds.), *The Petroleum System-From Source to Trap, American Association of Petroleum Geologists* Memoir, **60**, pp. 3-24.

MAGOON, L.B. & BEAUMONT, E.A. 1999. Petroleum systems. *In*: Beaumont, E.A & Foster, N.H. (eds.), *Handbook of Petroleum Geology: Exploring for oil and Gas Traps, American Association of Petroleum Geologists,* Washington Dc, pp.31-34.

MAGOON, L.B. & DOW, W.G. 2000. Mapping the petroleum system - an investigative technique to explore the hydrocarbon fluid system. *In*: Mello, M.R & Katz, B.J. (eds.), *Petroleum Systems of South Atlantic margins, American Association of Petroleum Geologists Memoir*, **73**, pp. 53-68.

MANGO, F.D. 1987. Invariance in the isoheptanes of petroleum. *Science*, **327**, 514-517.

MARTHUR, N., RAJU, S.V. & KULKANI, T.G 2001. Improved identification of pay zones through integration of geochemical and log data: A case study from Upper Assam Basin, India. *American Association of Petroleum Geologists Bulletin*, **85**, 309-324.

MATHEWS, D.E. & HAYES, J.M. 1978. Isotope-ratio monitoring gas chromatography-mass spectrometry. *Analytical Chemistry*, **50**, 1465-1473.

MCBRIDE, B.C., ROWAN, M.G. & WEIMER, P. 1998a. The Evolution of Allochthonous Salt Systems, Northern Green Canyon and Ewing Bank (Offshore Louisiana), Northern Gulf of Mexico. *American Association of Petroleum Geologists Bulletin*, **82**, 1013-1036.

MCBRIDE, B.C., PAUL WEIMER, P. &. ROWAN, M.G. (1998b).The Effect of Allochthonous Salt on the Petroleum Systems of Northern Green Canyon and Ewing Bank (Offshore Louisiana), Northern Gulf of Mexico. *American Association of Petroleum Geologists Bulletin*, **82**, 1083-1112.

McWHAE, J. R. 1986. Tectonic history of northern Alaska, Canadian Arctic, and Spitsbergen regions since early Cretaceous. *American Association of Petroleum Geologists Bulletin*, **70**, 430-450.

MELLO, M.R. & KATZ, B.J. 2000 (eds.), Petroleum Systems of the South Atlantic Margin. *American Association of Petroleum Geologists Memoir*, **73**, pp. 3-4.

MERKI, P.J. 1972. Structural geology of the Cenozoic Niger Delta: *In:* Dessauvagie, T.F.J & Whiteman, A.J. (eds.), *African Geology. University of Ibadan Press*, pp. 635-646.

MICHELSEN, J.K. & KHAVARI-KHORASANI, G. 1999. The physics and efficiency of petroleum expulsion from coal. *In*: Mastalerz, M., Gilkson, M. & Golding, S.D. (eds.), *Coalbed Methane: Scientific, Environmental and Economic Evaluation*, Kluwer Academic Publishers, Netherlands, pp. 517-543.

MOLDOWAN, J.M., SEIFERT, W.K. & GALLEGOS, E.J. 1985.Relationship between petroleum composition and depositional environment of petroleum source rocks. *American Association of Petroleum Geologists Bulletin*, **69**, 1255-1268.

MOLDOWAN, J.M., SUNDARARAMAN, P. & SCHOELL, M. 1986. Sensitivity of biomarker properties to depositional environment and/ or source input in the Lower Toarcian of S.W. Germany. *Organic Geochemistry*, **10**, 915-926.

MOLDOWAN, J. M., FAGO, F., LEE, C.Y., JACOBSON, S.R., WATT, D.S., SLOUGUI, N., JEGANATHAN, A. & YOUNG, D.C. 1990. Sedimentary 24-*n*-propylcholestanes, molecular fossils diagnostic of marine algae. *Science*, **247**, 309-312.

MOLDOWAN, J.M., DAHL, J., HUIZINGA, B.J., FAGO, F.J., HICKEY, L.J., PEAKMAN, T.M. & TAYLOR, D.W. 1994. The molecular fossil record of oleanane and its relation to angiosperms. *Science*, **265**, 768-771.

MOORE, G.T. & ASQUITH, D.O. 1971. Delta: Term and Concept. *Geological Society of America Bulletin*, **82**, 2563-2568.

MOSS, S.J., CHAMBERS, J., CLOKE, I, SATRIA, D., ALI J. R., BAKER, S., MILSOM, J. & CARTER A. 1997. New observations on the sedimentary and tectonic evolution of the Tertiary Kutai Basin, East Kalimantan. *In*: Fraser, A.J., Mathews, S.J. & Murphy, R.W. (eds.), *Petroleum Geology of Southeast Asia, Geological Society Special Publication*, **126**, pp. 395-416

MUKHOPADHYAY, P.K., GORMLEY, J.R. & ZUMBERGE, J.E. 1989. Generation of hydrocarbons from the Tertiary coals of Texas- Coal as a potential source rock for liquid hydrocarbons in a deltaic basin? *Organic Geochemistry*, **14**, 351-352.

MURCHISON, D.G. 1987. Recent advances in organic petrology and organic geochemistry: an overview with some reference to "oil from coal". *In*: Scott, A.C. (ed.), *Coal and Coal-bearing Strata: recent Advances, Geological Society of London Special Publication*, **32**, 257-303.

MURRAY, A.P., SUMMONS, R.E., BOREHAM, C.J. & DOWLING, L.M. 1994. Biomarker and *n*-alkane isotope profiles for Tertiary oils: relationship to source rock depositional setting. *Organic Geochemistry*, **22**, 521-542.

MURRAY, A. P., SOSROWIDJOJO, I. B., ALEXANDER, R., KAGI, R. I., NORGATE C. M. & SUMMONS R. E. 1997. Oleananes in oils and sediments: Evidence of marine influence during early diagenesis? *Geochimica et Cosmochimica Acta*, **61**, 1261-1276.

NEGLIA, S. 1980. Migration of fluids in sedimentary basins. Reply to R.E Chapman. *American Association of Petroleum Geologists Bulletin*, **64**, 1543-1547.

NEWMAN, J., BOREHAM, C.J., WARD, S.D., MURRAY, A.P. & BAL, A.A. 1999. Floral influences on the petroleum source potential of New Zealand coals. *In*: Mastalerz, M., Glikson, M. & Golding, S. (eds.), *Coalbed Methane: Scientific, Environmental and Economic Evaluation*, Kluwer, the Netherlands, pp. 461-492.

NEWTON, R. & BOTTRELL, S. H. 2007. Stable isotopes of carbon and sulphur as indicators of environmental change: past and present. *Journal of the Geological Society,* **164**, 691-708.

NWACHUKWU, J. I. & CHUKWURA, P. I. 1986. Organic matter of Agbada Formation, Niger Delta, Nigeria. *American Association of Petroleum Geologists Bulletin,* **70**, 48-55.

NWANGWU, U. 1995.A unique hydrocarbon trapping mechanism in the offshore Niger Delta. *In*: Oti, M.N. & Postma, G. (eds.), *Geology of Deltas, Rotterdam, A.A. Balkema*, pp. 269-278.

NYTOFT, H.P., BOJESEN-KOEFOED, J.A., CHRISTIANSEN, F.G. & FOWLER, M.G. 2002. Oleanane or lupane? Reappraisal of the presence of oleanane in Cretaceous-Tertiary oils and sediments. *Organic Geochemistry*, **33**, 1225-1240.

NYTOFT, H.P., BOJESEN-KOEFOED, J.A. & CHRISTIANSEN, F.G. 2005 Bicadinanes in high latitude oils. *Extended abstracts, 22nd International Meeting of Organic geochemistry, Seville-Spain, September 12-16, 2005*, pp. 245-246.

OEHLER, J. H. 1984. Carbonate source rocks in the Jurassic Smackover trend of Mississippi, Alabama and Florida. *In*: Palacas, J. G. (ed.), *Petroleum Geochemistry and Source Rock Potential of Carbonate Rocks, American Association of Petroleum Geologists Studies in Geology* **18**, pp. 63-69.

ONDRAK, R., DIECKMANN, V., SNOWDON, L. R., STASIUK, L. & HORSFIELD, B. 2005. Modelling the Burial and Temperature History of the Beaufort-Mackenzie Basin with Respect to Hydrocarbon generation. *Program abstract, American Association of Petroleum Geologists Annual Meeting, Calgary, June 19-22, 2005.*

OUDIN, J. L. & PICARD, P. F. 1982. Genesis of hydrocarbons in the Mahakam Delta and the relationship between their distribution and the over-pressure zones. *Proceedings of 11th Annual Convention of the Indonesian Petroleum Association.*

PALACA, J.G. 1984. Petroleum Geochemistry and Source Rock Potential of Carbonate Rocks. *American Association of Petroleum Geologists Studies in Geology*, **18**.

PALACAS, J.G., KING, J.D., CLAYPOOL, G.E. & MAGOON, L.B. 1984a. South Florida Basin- a prime example of carbonate-source rocks of petroleum. *In:* Palacas, J. G. (ed.), *Petroleum Geochemistry and Source Rock Potential of Crabonate Rocks. American Association of Petroleum Geologists Studies,* **18,** 71-96.

PALACAS, J.G., KING, J.D., CLAYPOOL, G.E. & MAGOON, L.B. 1984b. Origin of asphalt and adjacent oil stains in Lower Cretaceous limestone, deep Sea

Drilling Project Leg 77. In: Buffler, R.T. & Schager, W. (eds.), *Initial Reports of the Deep Sea Drilling Project*, pp. 477-488.

PANDE A., UNIYAL, A. K. & CHANDRA, K. 1994. Genetic correlation of biodegraded crude oils from Lower Assam, India using biomarker compositions. *Organic Geochemistry*, **21**, 971-977.

PEARSON, M.J. & OBAJE, N.G. 1999. Onocerane and other triterpenoids in Late Cretaceous sediments from the Upper Benue Trough, Nigeria: tectonic and paleoenvironmental implications. *Organic Geochemistry*, **30**, 583-592.

PEDERSEN, G. K., ANDERSEN, L. A., LUNDSTEEN, E. B., PETERSEN, H. I., BOJESEN-KOEFOED, J. A. & NYTOFT, H. P. 2006. Depositional environments, organic maturity and petroleum potential of the Cretaceous coal-bearing Atane Formation at Qullissat, Nuussuaq Basin, West Greenland. *Journal of Petroleum Geology*, **29**, 3-26.

PEPPER, A.S. 1991. Estimating the petroleum expulsion behaviour of source rocks; a novel quantitative approach. *In*: England, W.A & Fleet, A.J. (eds.), *Petroleum Migration, Geological Society London Special Publication*, **59**, 9-32.

PEPPER, A.S. & CORVI, P.J. 1995. Simple kinetic models of petroleum formation. Part III: modelling an open system. *Marine and Petroleum Geology*, **12**, 417-403.

PERRODON, A. 1992. Petroleum systems: models and applications. *Journal of Petroleum Geology*, **15**, 319-326.

PETERS, K.E., MOLDOWAN J.M., SCHOELL, M. & HEMPKIN, W.B. 1986. Petroleum isotopic and biomarker composition related to source rock organic matter and depositional environment. Organic Geochemistry, 10, 17-27.

PETERS, K.E., KONTOROVICH, A.E., MOLDOWAN, J.E., ANDRUSEVICH, V.E., HUIZINGA, B. J., DEMAISON, G. J. & STASOVA, O. F. 1993. Geochemistry of selected oils and rocks from the central portion of the West Siberian Basin, Russia. *American Association of Petroleum Geologists Bulletin*, **77**, 863-887.

PETERS, K.E., FRASER, T.H., AMRIS, W., RUSTANTO, B. & HERMANTO, E. 1999. Geochemistry of crude oils from Eastern Indonesia. *American Association of Petroleum Geologists Bulletin*, **83**, 1927-1942.

PETERS, K.E., SNEDDEN, J.W., SULAEMAN, A., SARG, J.F. & ENRICO, R.J. 2000. A new geochemical sequence Stratigraphic model for Mahakam Delta and Makasssar slope, Kalimantan, Indonesia. *American Association of Petroleum Geologists Bulletin*, **84**, 12-44.

PETERS, K.E., WALTERS, C.C. & MOLDOWAN, J.M. 2005a. *The Biomarker Guide*, (2nd edition) Volume 1, Cambridge University Press, Cambridge, 471 pp.

PETERS, K.E., WALTERS, C.C. & MOLDOWAN, J.M. 2005b. *The Biomarker Guide*, (2nd edition), Volume 2, Cambridge University Press, Cambridge, 1155 pp.

PETERSEN, H. I. 2002. A re-consideration of the "oil window" for humic coal and kerogen type III source rocks. *Journal of Petroleum Geology*, **25**, 407-432.

PETERSEN, H.I., ANDSBJERG, J., BOJESEN-KOEFOED, J.A. & NYTOFT, H.P. 2000.Coal-generated oil: source rock evaluation and petroleum geochemistry of the Lulita oilfield, Danish North Sea. *Journal of Petroleum Geology*, **23**, 55-90.

PETERSEN, H. I., TRU, V., NIELSEN, L. H., DUC, N. A.& NYTOFT H. P. 2005. Source rock properties of lacustrine mudstones and coals (Oligocene Dong ho Formation), onshore Song Hong Basin, northern Vietnam. *Journal of Petroleum Geology*, **28**, 19-38.

PETERSEN H. I., FOOPATTHANAKAMOL, A. & RATANASTHIEN, B. 2006. Petroleum potential, thermal maturity and the oil window of oil shales and coals in Cenozoic rift basins, central and northern Thailand. *Journal of Petroleum Geology*, **29**, 337-360.

PIETERS, P.E. ABIDIN, H.Z. & SUDANA, D. 1993. *Geology of the long Pahangai sheet area, Kalimantan 1: 250 000*. GRDC, Bandung, Indonesia

PIGGOT, N. & ABRAMS, M.A. 1996. Near-surface coring in the Beaufort and Chukchi Seas, Northern Alaska. *In*: Schumacher, D. & Abrams, M.A. (eds.), *Hydrocarbon Migration and its Near-surface Expression, American Association of Petroleum Geologists Memoir*, **66**, 385-399.

PILGER, R.H. 1981. The opening of the Gulf of Mexico: Implications for the Tectonic Evolution of the Northern Gulf Coast. *Gulf Coast Association of Geological Societies Transactions*, **31**, 377-382.

PINDELL, J.L. 1985. Alleghenian reconstruction and subsequent Evolurtion of the Gulf of Mexico, Bahamas and Proto-Carribean. *Tectonics*, **4**, 1-39.

POWELL, T.G & MCKIRDY, D.M. 1973. Relationship between ratio of pristane to phytane, crude oil composition and geological environement in Australia. *Nature*, **243**, 37-39.

POWELL, T. G. & SNOWDON, L. R. 1975. Geochemistry of oils and condensates from the Mackenzie Delta basin, NWT, in Current research. *Geological Survey of Canada Paper* **75-1C**, pp. 41-43.

POWELL, T.G. & BOREHAM, C.J. 1994. Terrestrially sourced oils: where do they exist and what are our limits of knowledge? - a geochemical perspective. *In*: Scott, A.C. & Fleet, A.J. (eds.), *Coal and Coal-bearing Strata as Oil-prone Source Rocks, Geological Society of London Special Publication*, **77**, 11-29.

RADKE, M. WELTE, D.H. & WILLSCH, H. 1982a. Geochemical study on a well in the Western Canada Basin: relation of the aromatic distribution pattern to maturity of organic matter. *Geochimica et Cosmochimica Acta*, **46**, 1-10.

RADKE, M. WILLSCH, H. & LEYTHASEUR, D. 1982b. Aromatic components of coal: relation of distribution pattern to rank. *Geochimica et Cosmochimica Acta*, **46**, 1831-48.

RADKE, M. WELTE, D.H. & WILLSCH, H. 1986. Maturity parameters based on aromatic hydrocarbons: influence of organic matter type. *Organic Geochemistry*, **10**, 51-63.

RAJU, S.V. & MATHUR, N. 1995. The Petroleum geochemistry of a part of upper Assam basin, India: brief overview. *Organic Geochemistry*, **23**, 55-70.

RASHID, M. A. 1985. *Geochemistry of marine humic compounds.* New York, Springer-Verlag, 300 pp.

REED, K.J. 1969. Environment of Deposition of Source Beds of High-Wax Oil. *American Association of Petroleum Geologists Bulletin,* **53**, 1502-1506.

REINECK, H.E. & SINGH, I.B. 1980. *Depositional Sedimentary Environments.* (2nd edition), Springer-Verlag, Berlin. Heidelberg, 549pp.

ROBINSON, A. 1987. An overview of source rocks in Indonesia: *Proceedings of the Indonesian petroleum Association, Jakarta*, pp.97-122.

ROHMER, M., KOKKE, W.C., FENICAL, W.& DJERASSI, C. 1980. Isolation of two new C_{30} sterols, (24E)-24-*n*-propylidenecholesterol and 24(E)-24-*n*-proprylcholesterol from a cultured marine chrysophyte. *Steroids*, **35**, 219-231.

ROHRBACK, B. G. 1983. Crude oil geochemistry of the Gulf of Suez. *In*: Bjorøy, M. *et al.*, (eds.), *Advances in organic geochemistry 1981,* Chichester, Wiley, pp. 39-48.

ROONEY, M.A., VULETICH, A.K. & GRIFFITH, C.E., 1998. Compound-specific isotope analysis as a tool for characterizing mixed oils: an example from the West of Shetlands area. *Organic Geochemistry*, **29,** 241-254.

ROSÉ, R. & HARTONO, P. 1978. Geological Evolution of the Tertiary Kutei-Melwai basin, Kalimantan, Indonesia: *Proceedings of the Indonesian Petroleum Association 7th Annual Convention, Jakarta*, pp. 225-237.

ROWAN, M.G., RATLIFF, R.A., TRUDGILL, B.D. & DUARTE, J.B. 2001. Emplacement and evolution of the Mahogany salt body, central Louisiana outer shelf, northern Gulf of Mexico. *American Association of Petroleum Geologists Bulletin,* **85**, 947-969.

ROWLAND, S.J. 1990. Production of acyclic isoprenoids hydrocarbons by laboratory maturation of methanogenic bacteria. *Organic Geochemistry*, **15**, 9-16.

RUBISTEIN, I., SIESKIND, O. & ALBRECHT, P. 1975. Rearranged sterenes in a shale: occurence and simulated froamtion. *Journal of Chemical Society, Perkin Transaction*, **I**, 1833-1836.

RULLKÖTTER, J. 1982. Microbial alteration of 17α (H)-hopanes in Madagascar asphalts: removal of C-10 methyl group and ring opening. *Geochimica et Cosmochimica Acta*, **46**, 1545-1553.

RULLKÖTTER, J., PEAKMAN, T.M. & Ten HAVEN, H.L. 1994. Early diagenesis of terrigenous triterpenoids and its implications for petroleum geochemistry. *Organic Geochemistry*, **21**, 215-233.

SALLER, A., LIN, R. & DUNHAM, J. 2006. Leaves in turbidite sands: The main source of oil and gas in the deep water Kutei Basin, Indonesia. *American Association of Petroleum Geologists Bulletin*, **90**, 1585-1608.

SALVADOR, A. 1987. Late Triassic-Jurassic Paleogeography and Origin of Gulf of mexico Basin. *American Association of Petroleum Geologists Bulletin*, **71**, 419-451.

SALVADOR, A. 1991. Triassic-Jurassic. *In*: Salvador, A. (ed.), *The Gulf of Mexico Basin.* Boulder, Colorado, Geological Society America, The Geology of North America, **J**, pp.131-180.

SAMUEL, A., KNELLER, B., RASLAN, S., SHARP, A. & PARSONS. C. 2003. Prolific deep-marine slope channels of the Nile Delta, Egypt. *American Association of Petroleum Geologists Bulletin*, **87**, 541-560.

SAMUEL, O.J., JONES D.M. & CORNFORD, C. 2006a. Intra-delta versus sub-delta sourcing of petroleum: a global review. *Extended abstract, American Association of Petroleum Geologists International Conference*, Perth, Australia. Nov. 5-8 2006.

SAMUEL, O.J., JONES D.M., CORNFORD, C. & PRATT, L.M. 2006b. Evidence for sub-delta sourcing of petroleum in the Tertiary Niger delta: can this explain the geochemical paradox between some tertiary reservoired oils and the delta source rocks? *Book of abstract, 24th Annual International Conference, Nigerian Association of Petroleum Explorationists*, Abuja, Nigeria. Nov. 13-17th 2006.

SASSEN, R.1989 Migration of crude oil from Smackover source rock to Jurassic and Cretaceous reservoirs of the northern Gulf Rim. *Organic Geochemistry*, **14**, 51-60.

SASSEN, R. 1990a. Lower Tertiary and Upper Cretaceous source rocks in Louisiana and Mississippi.: Implications to Gulf of Mexico crude oil. *American Association of Petroleum Geologists Bulletin*, **74**, 857-878.

SASSEN, R. 1990b. Geochemistry of Carbonate source rocks and crude oils in Jurassic salt basins of the Gulf Coast. *In*: Schumacher, D. & Perkins, B.F. (eds.), *Gulf Coast Oils and Gases, proceedings of the 9th Annual Research Conference, Gulf Coast SEPM Foundation*, pp. 11-22.

SASSEN, R., MOORE, C.H. & MEENDSEN, F.C. 1987a. Distribution of hydrocarbon source potential in the Jurassic Smackover Formation. *Organic Geochemistry*, **11**, 379-383.

SASSEN, R, TYE, R.S., CHINN, E.W. & LEMOINE, R.C. 1988. Origin of crude oil in the Wilcox Trend of Louisiana and Mississippi: evidence of long-range migration. *Gulf Coast Association Geological Society Transactions*, **38**, 27-34.

SAXBY, J.D. & SHIBAOKA, M. 1986. Coals and coal macerals as source rocks for oil and gas. *Applied Geochemistry*, **1**, 25-36.

SENGUPTA, S., 1974. The effects of temperature and pressure on lycopodium clavatum spores. *In*: *Advances in Organic Geochemistry* 1973, pp. 305-306.

SEIFERT, W.K. & MOLDOWAN, J.M. 1986. Use of biological markers in petroleum Exploration. *In*: Johns, R.B. (ed.), *Methods in Geochemistry and Geophysics*, **24**, Elsevier, Amsterdam, pp. 261-290.

SCHMITTER, J. M., SUCROW, W. & ARPINO, P.J. 1982. Occurrence of Novel tetracyclic geochemical markers: 8, 14-seco-hopanes in a Nigerian crude oil. *Geochimica et Cosmochimica Acta*, **46**, 2345-2350.

SCHOELL, M. 1984. Recent advances in petroleum isotope geochemistry. *Organic Geochemistry*, **6**, 645-663.

SCHOELL, M., TESCHNER, M., WEHNER, H., DURAND, B. & OUDIN, J.L. 1983. Maturity related biomarker and stable isotope variations and their application to oil/source rock correlation in the Mahakam Delta, Kalimantan. *In*: Bjorøy, M. (ed.), *Advances in Organic Geochemistry 1981*, Chichester, Wiley, pp. 156-163.

SCHUMACHER, D. & PERKINS, B.F. 1990. *Gulf Coast Oils and Gases*. Editors, Proceedings of the 9th Annual Research Conference, Gulf Coast SEPM Foundation.

SCOTCHMAN, I.C., GRIFFITH, C.E., HOLMES, A.J. & JONES, D.M. 1998. The Jurassic petroleum system north and west of Britain: a geochemical oil-source correlation study. *Organic Geochemistry*, **29**, 671-700.

SHANMUGAM, G. 1985. Significance of coniferous rain forests and related organic matter in generating commercial quantities of oil, Gippsland Basin, Australia. *American Association of Petroleum Geologists Bulletin*, **69**, 1241-1254.

SHARAF, L. M. 2003. Source rock evaluation and geochemistry of condensates and natural gases, offshore Nile delta, Egypt. *Journal of Petroleum Geology*, **26**, 189–209.

SHARP, Z., 2006. *Principles of Stable Isotope Geochemistry*. (First edition), Pearson Prentice Hall, Pearson Educational Inc., New Jersey, 344 pp.

SHORT, K.C. & STAUBLE, A.J. 1967. Outline of geology of Niger Delta. *American Association of Petroleum Geologists Bulletin*, **51**, 761-779.

SINNINGHE DAMSTÉ, J.S., KENIG, F., KOOPMANS, M.P., KÖSTER, J., SCHOUTEN, S., HAYES, J.M.& De LEEUW, J.W. 1995. Evidence for gammacerane as an indicator of water column stratification. *Geochimica et Cosmochimica Acta*, **59**, 1895-1900.

SMITH, J.W., GOULD, K.W. & RIGBY, D. 1982. The stable isotope geochemistry of Australian coals. *Organic Geochemistry*, **3**, 111-131.

SNOWDON, L. R. 1978. Organic geochemistry of the Upper Cretaceous/Tertiary delta complexes of the Beaufort-Mackenzie sedimentary basin, northern Canada. Ph.D. thesis, Rice University, Houston, Texas, 130pp.

SNOWDON, L. R. 1980. Petroleum source potential of the Boundary Creek Formation, Beaufort-Mackenzie basin. *Bulletin of Canadian Petroleum Geology*, **28**, 46-58.

SNOWDON, L. R. 1984. Organic geochemical data for the Eocene Richards Formation, Beaufort-Mackenzie basin. *Geological Survey of Canada Open File Report 1007*, 129pp.

SNOWDON, L. R. 1987. Organic properties and source potential of two early Tertiary shales, Beaufort-Mackenzie basin. *Bulletin of Canadian Petroleum Geology*, **35**, 212-232.

SNOWDON, L. R. 1988. Hydrocarbon migration in Mackenzie delta sediments. *Bulletin of Canadian Petroleum Geology*, **36**, 407-412.

SNOWDON, L. R. 1990. Rock-Eval/TOC results from 29 Beaufort-Mackenzie wells. *Geological Survey of Canada Open File Report*, **2192**, 209 pp.

SNOWDON, L.R. 1991. Oil from Type III organic matter: resinite revisited. *Organic Geochemistry*, **17**, 743-747.

SNOWDON, L. R. & POWELL, T.G. 1979. Families of crude oils and condensates in the Beaufort-Mackenzie basin. *Bulletin of Canadian Petroleum Geology*, **27**, 139-162.

SNOWDON, L. R. & POWELL, T.G. 1982. Immature oil and condensate-modification of hydrocarbon generation model for terrestrial organic matter. *American Association of Petroleum Geologists Bulletin*, **66**, 775-788.

SNOWDON, L.R., STASIUK, L.D., ROBINSON, R., DIXON, J., DIETRICH, J. & MCNEIL, D.H. 2004. Organic geochemistry and organic petrology of a potential source rock of early Eocene age in the Beaufort–Mackenzie Basin. *Organic Geochemistry*, **36**, 1039-1052.

SOFER, Z. 1984. Stable carbon isotopic compositions of crude oils: application to source depositional environments and petroleum alteration. *American Association of Petroleum Geologists Bulletin*, **68**, 31-49.

SOFER, Z., BJORØY, M. & HUSTAD, E. 1991. Isotopic composition of individual *n*-alkanes in oils. *In*: Manning, D. (ed.), *Organic Geochemistry- Advances and Applications in Energy and the Natural Environment*, Manchester University Press, Manchester, pp. 207-211.

SOSROWIDJOJO, I.B., ALEXANDER, R. KAGI, R.I. 1993. Identification of novel diaromatic secobicadinanes and tricadinanes in crude oils. *In*: Øygard, K (ed.), *Proceedings of the 16th International metting on Organic Geochemistry*, September 20-24, Stavanger, Norway, Falch Hurtigtrykk, pp. 481-484

STACHER P. 1995. Present Understanding of the Niger Delta hydrocarbon habitat. *In:* Oti, M.N. & Postma, G. (eds.), *Geology of Deltas, Rotterdam, A.A. Balkema*, pp. 257-267.

STAHL, W. 1977. Carbon and nitrogen isotopes in hydrocarbon research and exploration. *Chemical Geology*, **20**, 121-149.

STAHL, W. & CAREY, B.D. 1975. Source-rock identification by isotope analyses of natural gases from fields in the Val and Delaware Basins, West Texas. *Chemical Geology*, **16**, 257-267.

SUPRITANA, S. 1990. *Geology of the Muara Wahau Sheet area, Kalimantan, 1: 250 000*. GRDC, Bandung, Indonesia.

SYKES, R. 2004. Peat biomass and early diagenetic controls on the paraffinic oil potential of humic coals, Caterbury Basin, New Zealand. *Petroleum Geoscience*, **10**, 283 -303.

SYKES, R. & SNOWDOWN, L.R. 2002. Guidelines for assessing the petroleum potential of coaly source rocks using Rock- Eval pyrolysis. *Organic Geochemistry*, **33**, 1441-1455.

SYKES, R., SNOWDOWN, L.R. & JOHANSEN, P.E 2004. Leaf Biomass- a new paradigm for sourcing the terrestrial oils of Taranaki Basin. *Petroleum Exploration Society of Australia (PESA), Eastern Australasian basins Symposium II, Adelaide*, pp 1-22.

TANG, J. & LERCHE, I. 1991. Analysis of the Beaufort-Mackenzie Basin, Canada: burial, thermal and hydrocarbon histories. *Marine and Petroleum Geology*, **9**, 510-526.

TEN HAVEN, H.L. & RULLKÖTTER, J. 1988. The diagenetic fate of taraxer-14-ene and oleanene isomers. *Geochimica et Cosmochimica Acta*, **52**, 2543-2548.

TEN HAVEN, H. L., ROHMER, M., RULLKÖTTER, J. & BISSERET, P. 1989. Tetrahymanol, the most likely precursor of gammacerane, occurs ubiquitously in marine sediments. *Geochimica et Cosmochimica Acta*, **53**, 3073-3079.

THOMAS, B.M. 1982. Land-plant source rocks for oil and their significance in Australian basin. *Australian Petroleum Exploration Association Journal*, **22**, 164-178.

THOMPSON, K.F.M. & KENNICUTT, M.C. II. 1992. Correlations of Gulf Coast petroleum on the basis of isoprenoid biomarkers. *Organic Geochemistry*, **18**, 103-119.

THOMPSON, K.F.M., KENNICUTT, M. & BROOKS, J.M. 1990.Classification of offshore Gulf of Mexico oil and Gas Condensates. *American Association of Petroleum Geologists Bulletin*, **74**, 187-198.

THOMPSON, S., COOPER, B.S., MORELY, R.J. & BARNARD, P.C. 1985. Oil-generating coals. *In*: Thomas, B.M. (ed.), *Petroleum Geochemistry in Exploration of the Norwegian Shelf*, Graham and Trotman, pp. 59-73.

TISSOT, B.P. 1984. Recent Advances in Petroleum Geochemistry Applied to Hydrocarbon Exploration. *American Association of Petroleum Geologists Bulletin*, **68**, 545-563.

TISSOT, B.P. & WELTE, D.H. 1984. *Petroleum Formation and Occurrence*. Springer-Verlag, New York, 699pp.

TISSOT, B.P, DURAND, B., ESPITALIE, J. & COMBAZ, A. 1974. Influence of nature and diagenesis of organic matter in formation of Petroleum. *American Association of Petroleum Geologists Bulletin*, **58**, 499-506.

TRENDEL, J.M., GRAFF, R., ALBRECHT, P., RIVA, A. 1991. 24, 28-Dinor-18α-oleanane, a novel demethylated higher plant derived triterpane hydrocarbon in petroleum. *Tetrahedron Letters*, **32**, 2959-2962.

TUTTLE M.L.W., CHARPENTIER, R.R. & BROWNFIELD, M.E. 1999.Tertiary Niger Delta (Akata-Agbada) Petroleum System (No. 719201), Niger Delta Province, Nigeria, Cameroon, and Equatorial Guinea, Africa . *A US Geological Survey World Energy Assessment Project*: http://greenwood.cr.usgs.gov/energy/ WorldEnergy/OF99-50H/ChapterA.html#TOP. Date accessed: 20/11/ 2005.

UDO, O.T., EKWEOZOR, C.M. & OKOGUN, J.I. 1988. Petroleum geochemistry of an ancient clay-filled canyon in the western Niger delta, Nigeria. *Nigerian Association of Petroleum Explorationists Bulletin*, **3**, 8-25.

United State Energy Information Administration (EIA). 2007. http://www.eia.doe.gov. Date accessed: 25/04/ 2007.

United State Geological Survey web database (USGS). 2003 http://www.usgs.gov/pubprod/. Date accessed 05/06/ 2003.

VAN ARSSEN, B.G.K., COX, H.C., HOOGENDOORN, P. & de LEEUW, J.W. 1990. A cadinene biopolymer present in fossil and extant dammar resins as a source for cadinanes and bicadinanes in crude oils from south East Asia. *Geochimica et Cosmochimica Acta*, **54**, 3021-3031.

VAN BEMMELEN, R.W.1949. *The Geology of Indonesia.* Government printing office, The Hague, 732pp.

VANDENBROUCKE, M., ALBRECHT, P. & DURAND. B. 1976. Geochemical studies on the organic matter from the Douala Basin (Cameroon)-III. Comparison with the Early Toarcian shales, Paris Basin, France. *Geochimica et Cosmochimica Acta*, **40**, 1241-1246.

VAN KREVELEN, D. W. 1993. *Coal-Typology, Physics, Chemistry, Constitution.* 3rd (revised) edition, Elsevier, Amsterdam, 979 pp.

VAN KREVELEN, D. W & SCHUYER, J. 1957. *Coal Science: aspects of coal constitution.* Elsevier, Amsterdam, 352pp.

VAN de WEERD, A.A. & ARMIN, R.A. 1992. Origin and evolution of the Tertiary hydrocarbon bearing basins in Kalimantan (Borneo), Indonesia. *American Association of Petroleum Geologist Bulletin*, **76**, 1778-1803

VENKATESAN, M.I. 1989. Tetrahymanol: its widespread occurrence and geochemical significance. *Geochimica et Cosmochimica Acta*, **53**, 3095-3101.

VERDIER, A.C., OKI T. & SUARDY, A. 1979. Geology of the Handil Field (East Kalimantan- Indonesia). *In*: Halbouty, M.T (ed.), *Giant Oil and Gas Fields of the Decade 1968-1978. American Association of Petroleum Geologists Memoir*, **30**, 399-421.

VOLKMAN, J.K. & MAXWELL, J.R 1986. Acyclic isoprenoids as biological markers. *In*: Johns, R.B. (ed.), *Biological markers in sedimentary record*, Elsevier, New York, pp. 1-42.

VOLKMAN, J.K., BARRETT, S.M., BLACKBURN, S.I., MANSOUR, M.P., SIKES, E.L. & GELIN, F. 1998. Microalgal biomarkers: a review of recent research developments. *Organic Geochemistry*, **29**, 1163-1179

WADE, W.J. & MOORE, C.H.1993.Sequence Stratigraphy of Middle and Upper Jurassic Strata of Southwestern Alabama. *Meeting abstract, American Association of Petroleum Geologists/ SEPM Gulf Coast Sections* (GCAGS), Shreveport, Louisiana, October 20-22, 1993.

WANDREY, C.J. 2004. Sylhet-Kopili/Barail-Tipam composite petroleum system, Assam Geological Province, India. *In:* Wandrey, C, J. (ed.), *Petroleum systems and related geologic studies in region 8, South Asia, United States Geological Survey Bulletin* **2208-D**, 25pp.

WANG, T., FAN, P. & SWAIN, F.M. 1988. Geochemical characteristics of crude oils and source beds in different continental facies of four oil-bearing basins, China. *In*: Fleet, A.J., Kelts, K. & Talbot, M.R. (eds.), *Lacustrine Petroleum Source Rocks. Geological Society of London*, London, pp. 309-325.

WANG, T.G. & SIMONEIT, B.R.T. 1990. Organic geochemistry and coal petrology of Tertiary brown coal in the Zhoujing mine, Baise Basin, South Chiuna.2. Biomarker assemblage and significance. *Fuel*, **69**, 12-20.

WEBER, K.J. 1987. Hydrocarbon distribution patterns in Nigeria growth fault structures controlled by structural style and stratigraphy. *Journal of Petroleum Science and Engineering*, **1**, 91-104.

WEBER, K. J. & DAUKORU, E. M. 1975. Petroleum geology of the Niger Delta. Proceedings of the Ninth World Petroleum Congress, Volume 2, Geology: London, *Applied Science Publishers Limited*, pp. 210-221.

WEIMER, P., ROWAN, M.G., MCBRIDE, B.C. & KLIGFIELD, R. 1998. Evaluating the Petroleum Systems of the Northern Deep Gulf of Mexico through integrated basin Analysis: An overview. *American Association of Petroleum Geologists Bulletin*, **82**, 865-877.

WENGER, L.M., SASEEN, R & SCHUMACHER, D.1990. Molecular characteristics of Smackover, Tuscaloosa and Wilcox-reservoired oils in the east Gulf Coast. *In*: Schumacher, D. & Perkins, B.F. (eds.), *Gulf Coast Oils and Gases, proceedings of the 9th Annual Research Conference, Gulf Coast SEPM Foundation*, pp. 37-57.

WEVER, H. E. 2000. Petroleum and Source Rock Characterization Based on C_7 Star Plot Results: Examples from Egypt. *American Association of Petroleum Geologists Bulletin*, **84**, 1041-1054.

WHITEMAN, A. 1982. *Nigeria: Its Petroleum Geology, Resources and Potential.* London, Graham and Trotman, 394pp.

WILHELMS, A., LARTER, S.R. & HALL, K. 1994. A comparative study of the stable carbon isotopic composition of crude oil alkanes and associated crude oil asphaltene pyrolysate alkanes. *Organic Geochemistry*, **21**, 751-759

WILKINS, R.W.T. & GEORGE, S.C. 2002. Coal as a source rock for oil: a review. *International Journal of Coal Geology*, **50**, 317-361.

WILLIAMS, D.F & LERCHE, I. 1988. Organic-Rich Source Beds and Hydrocarbon Production in Gulf Coast Region. *Meeting abstract, American Association of Petroleum Geologists*, **72**, 1126-1126.

WINKER, C. D. & BOOTH, J.R. 2000. Sediment dynamics of the salt-dominated continental slope, Gulf of Mexico: Integration of observations from the seafloor, near-surface, and deep subsurface. *Gulf Coast Section Society of Sedimentary Geologist (SEPM) Foundation 20th Annual Research Conference on Deep-Water reservoirs of the World,* December 3- 6, 2000, pp. 1059- 1086.

WOOLHOUSE, A. D., OUNG, J.N., PHILP, R. P. & WESTON, R. J. 1992. Triterpanes and ring-A degraded triterpanes as biomarkers characteristic of Tertiary oils derived from predominantly higher plant sources. *Organic Geochemistry*, **18**, 23-31.

WRIGHT, L.D. 1985. River deltas. *In*: Davis, R. A. (ed.) *Coastal Sedimentary Environments.* (2nd edition), Springer Verlag, New York, pp. 1-76.

XIONG, Y., LI, M., SNOWDON, L. & ISSLER, D. 2005. Compound-Specific C and H Isotope Ratios as an Oil-Source Correlation Tool in the Beaufort-Mackenzie Basin. *Program abstract of the American Association of Petroleum Geologists Annual Meeting, Calgary, June 19-22, 2005.*

YOUNG, F. G. 1975. Upper Cretaceous stratigraphy, Yukon coastal plain and northwestern Mackenzie delta. *Geological Survey of Canada Bulletin,* **249**, 83 pp.

YOUNG, F. G., MYHR, D.W. & YORATH, C.J. 1976. Geology of the Beaufort-Mackenzie basin: *Geological Survey of Canada Paper,* **76-11**, 63 pp.

ZHOU, Y., SHENG, G., FU, J., GENG, A., CHEN, J., XIONG, Y., ZHANG, Q. 2003. Triterpane and sterane biomarkers in the YA13-1 condensates from Qiongdongnan Basin, South China Sea. *Chemical Geology*, **199**, 343-359.

ZUMBERGE, J., ILLICH, H., PRATSCH, C., BROWN, S. & CAMERON, N. 1998. Origin of oil in the Gulf of Mexico: exploration significance. *PESGB Petex 98 Conference Proceedings, Expanded Lecture Abstracts, London*, Paper E5.

APPENDIX I

Appendix IA: Table of published bulk, biomarker and stable carbon isotope data of Assam oils.

Sample	Depth (m)	Formation	API	% Sul	Pr/Ph	Pr/nC17	Ph/nC18	MPI (1)	d13C sat	d13 C aro	CV	Reference
AB-1	3112-3117	Sylhet	35.6		4.5	0.9	0.2	0.82	-27.3	-25	2.19	Goswami et. al. 2005
AB-2	2387-2392	Bokabil	51.4		5.2	1.5	0.35	0.75	-28.7	-26	3.24	Goswami et. al. 2005
AB-3	2023-2025	Bokabil	29.6		4.5	1.3	0.33	0.72	-28.4	-26.1	2.26	Goswami et. al. 2005
AB-4	2454-2457	Bokabil	27.8		4.6	1.2	0.31	0.76	-28.7	-25.8	3.68	Goswami et. al. 2005
AB-5	1820-1823	Bokabil	39.8		5.4	2.2	0.47	0.58	-28.4	-26.1	2.26	Goswami et. al. 2005
AB-6	2502-2516	Bokabil			5.1	1.4	0.34	0.68	-27.9	-26.1	1	Goswami et. al. 2005
AB-7	2545-2547	Bokabil	27									Goswami et. al. 2005
AB-8	2459-2465	Bokabil	30.2		5	1.5	0.38	0.74	-28.2	-26.2	1.53	Goswami et. al. 2005
AB-9	2488-2503	Bokabil	30.9									Goswami et. al. 2005
BA-1	2221-2225	Bokabil	34.6		4.8	1.6	0.39	0.66	-28.8	-26.1	3.27	Goswami et. al. 2005
BA-1	2173-2177	Bokabil	35.2		5.2	1.4	0.35	0.71	-28.9	-26	3.75	Goswami et. al. 2005
BA-1	2142-2145	Bokabil	34.5		4.5	1.7	0.44	0.69	-28.4	-26.2	2.04	Goswami et. al. 2005
BA-1	2114-2122	Bokabil	33.7		5.3	1.5	0.34	0.74	-28.2	-26.3	1.31	Goswami et. al. 2005
MRN-1	3373	Barail	34.4	0.1	6	3.4	0.6					Raju & Mathur 1994
SAL-5	3201	Barail	0	0.08	5.6	3.3	0.6					Raju & Mathur 1994
N-1	2934	Barail	34.3	0.13	6	2.4	0.4					Raju & Mathur 1994
N-31	3972	Barail	32	0.07	5.7	3.4	0.6					Raju & Mathur 1994
N-373	2401	Tipam	26.6	0.25	6.1	6.7	1.2					Raju & Mathur 1994
N-22	2988	Barail	33.2	0.16	6.5	2.4	0.4					Raju & Mathur 1994
JN-4	2330	Tipam	28.5	0.33	3.9	17	4.3					Raju & Mathur 1994
N-355	3062	Barail	32.4	0.14	6.3	2.1	0.3					Raju & Mathur 1994
DGB_1	0	Tipam	0	0.11	6.6	2.5	0.3					Raju & Mathur 1994

API= API gravity. % sulphur= Wt % elemental sulphur in oil. Pr/ph= pristane/phytane. Pr/nC17 = pristane/ C17 *n*-alkane. Ph/ nC18 =phytane/ C18 *n*-alkane. MPI(1)= Methyl Phenanthrene Index(1.5*(2-MP+ 3-MP)/ (P + 1-MP + 9-MP); Radke *et al.*, (1982a)). d13C Sat= $\delta^{13}C$ of saturated hydrocarbon fractions. d13CAro =$\delta^{13}C$ of aromatic hydrocarbon fractions. CV= canonical variable (CV = -2.53(δ13C sat.) + 2.22(δ13C arom.)-11.65).

Sample	Depth (m)	Ts/ Ts+Tm	OL Index	Bicad/ Hop	C32 S/S+R	Hop/St	C29 20S/ S+R	C29αββ	%C27	%C28	%C29	C29/C27	Reference
AB-1	3112-3117	0.13	0.09	0.09	0.6	6.02	0.54	0.52	17	28	55	3.23	Goswami et. al. 2005
AB-2	2387-2392	0.34	0.38	0.87	0.6	4.02	0.52	0.48	24	17	59	2.46	Goswami et. al. 2005
AB-3	2023-2025	0.26	0.35	0.74	0.6	3.87	0.52	0.49	22	14	64	2.91	Goswami et. al. 2005
AB-4	2454-2457				0.6	3.83	0.52	0.5	25	16	59	2.36	Goswami et. al. 2005
AB-5	1820-1823												Goswami et. al. 2005
AB-6	2502-2516												Goswami et. al. 2005
AB-7	2545-2547												Goswami et. al. 2005
AB-8	2459-2465	0.27	0.33	0.76	0.6	3.87	0.5	0.51	18	23	59	3.28	Goswami et. al. 2005
AB-9	2488-2503												Goswami et. al. 2005
BA-1	2221-2225	0.37	0.35	0.85	0.6	4.53	0.54	0.48	25	15	60	2.40	Goswami et. al. 2005
BA-1	2173-2177	0.34	0.38	0.82	0.6	4.28	0.53	0.5	22	20	58	2.64	Goswami et. al. 2005
BA-1	2142-2145	0.31	0.42	0.93	0.6	4.46	0.54	0.51	26	15	59	2.27	Goswami et. al. 2005
BA-1	2114-2122	0.32	0.32	0.89	0.6	3.89	0.54	0.52	22	19	59	2.68	Goswami et. al. 2005
MRN-1	3373	0.06	0.38			1.6	0.44		5	20	70	14.00	Raju & Mathur 1994
SAL-5	3201	0.17	0.31			2.5	0.5		4	23	73	18.25	Raju & Mathur 1994
N-1	2934	0.08	0.4			1.5	0.52		6	26	68	11.33	Raju & Mathur 1994
N-31	3972	0.26	0.35			3.5	0.52		3	20	77	25.67	Raju & Mathur 1994
N-373	2401	0.06	0.24			1.7	0.49		5	18	77	15.40	Raju & Mathur 1994
N-22	2988	0.17	0.38			2.2	0.46		3	20	77	25.67	Raju & Mathur 1994
JN-4	2330	0.11	0.31			2.5	0.47		5	18	77	15.40	Raju & Mathur 1994
N-355	3062	0.23	0.33			2.6	0.53		5	22	74	14.80	Raju & Mathur 1994
DGB_1	0	0.16	0.09			8	0.44		4	20	76	19.00	Raju & Mathur 1994

Ts/Ts+Tm = 18α(H)- 22,29,30- Trisnorneohopane (Ts)/ 18α(H)- 22,29,30- Trisnorneohopane (Ts) + 17α(H)- 22,29,30-trisnorhopane (Tm). OL index= 18α (H) + 18β(H) oleanane/(18α(H) + 18β(H) oleanane + 17α(H), 21β(H) hopane. Bicad/Hop= sum of all bicadinane isomers/ 17α(H), 21β(H) hopane. C32 S/S+R =. 17α(H), 21β(H)-bishomohopane 22S/ 22S+ 22R thermal maturity parameter. Hop/St= 17α(H), 21β(H) hopane / sum C27-C29 steranes. C_{29}20S/S+R= 5α(H),14α(H), 17α(H)- C_{29} 20S/20S+20R sterane isomerisation maturity parameter.C29 αββ = C_{29} αββ/αββ+ααα sterane isomerisation thermal maturity parameter. % C27, %C28 and %C29 = C_{27}, C_{28}, C_{29} as a percentage of sum 27-29 for 5α(H),14α(H), 17α(H)- 20R sterane. C29/C27= ratio of C29/C27 sterane for the 5α(H),14α(H), 17α(H)- 20R configuration.

Appendix IB: Table of published bulk, biomarker and stable carbon isotope data of oils from Beaufort-Mackenzie Delta, Canada.

Sample	Well name	Depth (ft)	Reservoir	% Sul	V (ppm)	Ni (ppm)	V/ V+Ni	d13C oil	d13C Sat	d13C Aro	CV	%C27	% C28	% C29	C29/ C27	C 29S /S+R	C32 S/S+R	Lup/ Hop	Hop/ Ster	OL/Hop	References
AP6209-1	ADLARTOK P-09	5361	Moose Channel	0.117	0.6	0	0	-25.09	-26.88	-25.06	0.72	7.00	13.00	80.00	11.43	0.36	0.57	1.60	6.67	0.13	Curiale, 1991
AP6209-2	ADLARTOK P-09	5479	Moose Channel	0.037	0.5	0	0	-26.03	-27.21	-25.2	1.25	8.00	13.00	79.00	9.88	0.36	0.57	1.49	5.89	0.14	Curiale, 1991
AP6209-3	ADLARTOK P-09	5623	Moose Channel	0.034	0.5	0	0	-25.85	-26.96	-25.1	0.84	7.00	12.00	81.00	11.57	0.34	0.57	1.52	5.55	0.15	Curiale, 1991
AP6209-4	ADLARTOK P-09		Moose Channel ?	0.025	0.5	0	0	-26.57	-27.5	-25.38	1.58	7.00	12.00	81.00	11.57	0.35	0.57	2.20	5.26	0.16	Curiale, 1991
AP6209-5	AMAULIGAK I-65		Kugmallit	0.08	0.1	0	0	-27.43	-28.18	-26.28	1.30	7.00	20.00	73.00	10.43	0.31	0.52	35.82	5.26	0.21	Curiale, 1991
AP6209-6	AMAULIGAK I-65	12241	Kugmallit	0.052	0.2	0	0	-27.58	-28.07	-26.42	0.71	9.00	20.00	71.00	7.89	0.30	0.53	31.94	8.33	0.18	Curiale, 1991
AP6209-7	AMAULIGAK I-65		Kugmallit	0.058	0.2	0	0	-27.65	-28.12	-26.43	0.82	16.00	19.00	65.00	4.06	0.32	0.56	47.76	7.69	0.20	Curiale, 1991
AP6209-8	AMAULIGAK I-65	11427	Kugmallit	0.113	0.2	0	0	-27.6	-28.09	-26.51	0.57	7.00	20.00	73.00	10.43	0.30	0.57	37.61	7.69	0.19	Curiale, 1991
AP6209-9	AMAULIGAK I-65		Kugmallit	0.154	0.2	0.4	0.33	-27.32	-28.06	-26.47	0.58	5.00	20.00	75.00	15.00	0.29	0.51	36.89	7.69	0.19	Curiale, 1991
AP6209-10	AMAULIGAK I-65B	15325	Kugmallit	0.15	0.3	0.8	0.27	-27.69	-28.32	-26.55	1.06	5.00	22.00	73.00	14.60	0.37	0.52	36.22	9.09	0.18	Curiale, 1991
AP6209-11	ATKINSON H-25	5775	Cretaceous	0.912	8.9	3	0.75	-27.55	-28.09	-26.69	0.17	36.00	28.00	37.00	1.03	0.43	0.57		8.33	0.07	Curiale, 1991
AP6209-12	ISSUNGNAK I-65B	11281	Kugmallit	0.088	0	0	0	-27.36	-28.02	-26.28	0.90	4.00	17.00	79.00	19.75	0.31	0.52	48.78	9.09	0.20	Curiale, 1991
AP6210-2	KOAKOAK-O22	12805	Kugmallit	0.075	0	0	0	-27.36	-28.09	-26.73	0.08	8.00	15.00	77.00	9.63	0.12	0.38	203.75	1.38	0.76	Curiale, 1991
AP6210-3	KOAKOAK-O22		Kugmallit	0.05	0.1	0	0	-27.82	-28.03	-26.58	0.26	8.00	12.00	80.00	10.00	0.13	0.34	168.78	1.38	1.43	Curiale, 1991
AP6210-4	KOPANAOR 2I-44		Kugmallit ?	0.037	0.2	0.5	0.29	-28.49	-28.28	-26.63	0.78	4.00	19.00	77.00	19.25	0.24	0.53	64.19	4.54	0.30	Curiale, 1991
AP6210-5	KOPANAOR 2I-44	9711	Richards ?	0.054	0.2	0.6	0.25	-28.28	-28.18	-26.54	0.73	10.00	17.00	74.00	7.40	0.18	0.54	64.22	3.85	0.28	Curiale, 1991
AP6210-6	KOPANAOR M-13		Kugmallit	0.053	0.4	0	0	-28.74	0	-26.51	0.00	24.00	29.00	48.00	2.00	0.33	0.00			0.00	Curiale, 1991
AP6210-7	KOPANAOR M-13	11604	Kugmallit	0.195	0.4	0.8	0.33	-28.12	-28.37	-26.83	0.56	13.00	19.00	68.00	5.23	0.23	0.48	54.47	4.00	0.26	Curiale, 1991
AP6210-8	KUGPIK L-24	8152	Cretaceous	0.052	0	0	0	-28.25	-29.03	-26.41	3.17	43.00	25.00	32.00	0.74	0.54	0.57		2.50	0.00	Curiale, 1991
AP6210-9	KUGPIK L-24	7406	Cretaceous	0.083	0.1	0	0	-27.1	-29.85	-28.01	1.69	40.00	26.00	34.00	0.85	0.51	0.58	2.10	7.69	0.00	Curiale, 1991
AP6210-10	KUMAK J-06	7560	Reindeer	0.069	0	0.6	0	-27.29	-27.94	-26.87	-0.61	8.00	16.00	76.00	9.50	0.46	0.57	3.12	7.14	0.22	Curiale, 1991
AP6210-11	KUMAK K-16	4936	Reindeer	0.143	0.2	0	0	-27.26	-27.16	-26.05	-0.77	11.00	16.00	74.00	6.73	0.44	0.50	11.17	7.14	0.13	Curiale, 1991
AP6210-12	KUMAK K-16	9732	Reindeer ?	0.024	0	0	0	-26.42	-27.67	-25.95	0.75	14.00	19.00	67.00	4.79	0.48	0.54	0.00	9.09	0.12	Curiale, 1991
AP6211-1	NIGLINTGAK M-19	4547	Reindeer	0.092	0.2	0.6	0.25	-27.15	-27.12	-26.1	-0.98	6.00	16.00	79.00	13.17	0.45	0.58	0.00	6.25	0.13	Curiale, 1991
AP6211-2	NIGLINTGAK M-19	5647	Reindeer	0.005	0	0	0	-26.29	0	0	-11.65	24.00	17.00	59.00	2.46	0.38	0.54	0.37	11.10	0.16	Curiale, 1991
AP6211-3	NIGLINTGAK M-19	5730	Reindeer	0.108	0.1	0.5	0.17	-25.77	-27.13	-25.98	-0.69	6.00	16.00	78.00	13.00	0.44	0.55	8.66	6.67	0.12	Curiale, 1991
AP6211-4	NIGLINTGAK M-19	4409 (?)	Reindeer	0.055	0	0	0	-27.36	-27.8	-25.94	1.10	10.00	15.00	75.00	7.50	0.47	0.60	0.00	7.69	0.11	Curiale, 1991
AP6211-5	PITSIULAK A-05	5520	Kugmallit	0.108	0.1	1.5	0.06	-27.68	-28.19	-26.66	0.49	14.00	17.00	69.00	4.93	0.15	0.52	23.45	2.85	0.26	Curiale, 1991
AP6211-7	TARSIUT A-25	4880	Kugmallit	0.137	0.1	0	0	-27.01	-27.44	-26.35	-0.72	7.00	12.00	81.00	11.57	0.19	0.00	62.41	3.23	0.33	Curiale, 1991
AP6211-8	E. TARSUIT N-44	5552	Kugmallit	0.08	0	0	0	-27.85	-27.79	-26.37	0.12	9.00	17.00	74.00	8.22	0.30	0.54	27.07	5.88	0.29	Curiale, 1991
AP6211-9	UVILUK P-66		RIchards	0.143	0.2	0.5	0.29	-28.02	-28.41	-26.47	1.46	26.00	26.00	48.00	1.85	0.43	0.59	36.73	9.09	0.13	Curiale, 1991
	IMNAK J-29 (DST5)	9346										22.00	33.00	46.00	2.09	0.46				0.00	Brooks, 1986a
	ATKINSON H-25 (DST1)	5760										21.00	37.00	43.00	2.05	0.41				0.00	Brooks, 1986a
	W. ATKINSON L17 (DST3)	7766										28.00	29.00	43.00	1.54	0.44				0.00	Brooks, 1986a
	MAYOGIAK (DST 12)	9582										22.00	38.00	39.00	1.77	0.54				0.00	Brooks, 1986a
	KUGPIK L-24 (DST 2)	8164										33.00	27.00	40.00	1.21	0.43				0.00	Brooks, 1986a
	WAGNARK C23 (DST 7)	3543										0.00	0.00	0.00	0.00	0.81				0.00	Brooks, 1986a
	KAMIK (DST3)	9403										9.00	16.00	75.00	8.33	0.50				0.00	Brooks, 1986a
	PARSONS D-20 (DST3)	11818										8.00	16.00	76.00	9.50	0.48				0.00	Brooks, 1986a
	PULLEN E-17 (FT1)	11781										4.00	9.00	87.00	21.75	0.23				0.23	Brooks, 1986a
	KOAKOAK O-22 (DST 4A)	12841										5.00	22.00	73.00	14.60	0.17				0.82	Brooks, 1986a
	KOPANOAR M-13 (DST 5A)	11624										2.00	10.00	88.00	44.00	0.21				0.14	Brooks, 1986a
	TAGLU-C42 (DST3)	10630										16.00	20.00	64.00	4.00	0.46				0.22	Brooks, 1986a
	IVIK K-54 (DST 4)	8280										5.00	22.00	73.00	14.60	0.40				0.15	Brooks, 1986a
	TARSIUT A-25	5040										3.00	16.00	81.00	27.00	0.43				0.35	Brooks, 1986a
	KUMAK J-26 (DST 10)	4473										2.00	9.00	89.00	44.50	0.41				0.04	Brooks, 1986a
	NIGLIATGAK M-19 (DST9)	7155										5.00	10.00	85.00	17.00	0.44				0.12	Brooks, 1986a
	ADGO P-25 (DST2)	4438										1.90	22.70	75.40	39.68	0.39				0.00	Brooks, 1986a
	ISSUNGNAK 20-61 (DST4)	11480										8.10	6.70	85.20	10.52	0.40				0.20	Brooks, 1986a

% sulphur= Wt % elemental sulphur in oil. V= concentration of vanadium metal in parts per million of oil. Ni = concentration of nickel metal in parts per million of oil. V/V+Ni = ratio of vanadium/ vanadium + nickel metal. d13C oil= $\delta^{13}C$ of whole oil. d13C Sat= $\delta^{13}C$ of saturated hydrocarbon fractions. d13CAro =$\delta^{13}C$ of aromatic hydrocarbon fractions. CV= canonical variable (CV = -2.53(δ13C sat.) + 2.22(δ13C arom.)-11.65). % C27, %C28 and %C29 = C_{27}, C_{28}, C_{29} as a percentage of sum 27-29 for 5α(H),14α(H), 17α(H)- 20R sterane. C29/C27= ratio of C29/C27 sterane for the 5α(H),14α(H), 17α(H)- 20R configuration. C29 St 20S/R= 5α(H),14α(H), 17α(H)- C_{29} 20S/20S+20R sterane isomerisation maturity parameter. C32 S/S+R =. 17α(H), 21β(H)-bishomohopane 22S/ 22S+ 22R thermal maturity parameter. Lup/Hop= sum of lupanoids/ 17α(H), 21β(H) hopane. Hop/St= 17α(H), 21β(H) hopane / sum C27-C29 steranes. OL/Hop= 18α(H) + 18β(H) oleanane/ 17α(H), 21β(H) hopane

Appendix IC: Table of bulk, biomarker and stable carbon isotope data from the Gulf of Mexico (USA). Data from Geomark Research Inc

Sample	Well	Depth (ft)	Formation	Age	API	% Sulphur	Ni (ppm)	V (ppm)	V/ V+Ni	% Sat	% Arom	% NSO
LA0002	B.Freeman 1	12455	Alliance	Oligocene	46.6	0.05	0.3	0	0.000	79.2	16.9	3.9
LA0003	H.Reese C-4	9660		Oligocene	39.4	0.06	7.5	0	0.000	79.1	15.7	5.2
LA0066		6161		Pliocene	37.4	0.14	0.1	0	0.000	69.3	21.5	9.2
LA0099	10-D	11573		Neogene	39.2	0.09	3.2	0.1	0.030	81.1	14.9	4
LA0100		8598		Miocene	43.6	0.06	0.9	0	0.000	81	14	5
LA0140		13242	F-2	Neogane	34.6	0.1	0.5	0	0.000	74.3	17.6	8.2
LA0141		8491	P6- sands	Neogene	33.6	0.2	40.2	0.4	0.010	64.4	24.7	11
LA0268	A-7	9616		Pleistocene	31.9	0.13	0	0	0.000	80	14.3	5.8
LA0273	OCS-G-7699 A-4 ST1	15555	MG Sand	Neogene	39.8	0.06	0	0	0.000	77.1	16.7	6.2
LA0275	A-3	14299	(Textularia X)	Lower Pliocene	50.2	0.03	0.1	0	0.000	79.3	15.5	5.2
LA0313	OCS-G-0310 76		GAS	Miocene	31.9	0.83	0.7	0	0.000	78	17	4.9
LA0354	OCS-G-4444 1	13208	BF-2	Miocene	46	0.06	7	8	0.533	76.3	14.3	9.5
LA0360	OCS-G-2099 5	15456	13000 Sand	Miocene	46.3	0.05	5	3	0.375	76	14.5	9.5
LA0380	OCS-G-1192 1	8522	8900 Sand	Pliocene	41.3	0.08	5	2	0.286	74.5	17.2	8.3
LA0382	OCS-G-3401 CA-01-D	12212	11900 sand	Pliocene	31.4	0.21	7	2	0.222	69.1	23.1	7.9
LA0392	OCS-G-2076 A-15	10742	10250 Sand	Pliocene	33.8	0.18	4	5	0.556	76.3	18.1	5.6
LA0393	OCG-G-3543 12	15348	A-04 Sand	Miocene	36.7	0.11	4	6	0.600	76.2	20	3.8
LA0402	OSC-G-3148 5	13578	13500 Sand	Miocene	36.7	0.08	4	8	0.667	82	13.8	4.3
LA0431	OSC-G-0787 1			Pliocene	36.3	0.13	5	3	0.375	78.2	16.5	5.2

API= API gravity. % sulphur= Wt % elemental sulphur in oil. Ni = concentration of nickel metal in parts per million of oil. V= concentration of vanadium metal in parts per million of oil. V/V+Ni = ratio of vanadium/ vanadium + nickel metal. % Sat = percentage of saturated hydrocarbon in the whole oil. % Arom= percentage of aromatic hydrocarbon in the whole oil. %NSO = percentage of non- hydrocarbon fractions of the whole oil.

Sample.	Pr/Ph	Pr/nC17	Ph/nC18	d13C sat	d13 C aro	CV	Ts/Tm	Ol/C30 Hop	St/Terp	C29 St 20S/R	Dia/ Reg Ster	%C27	%C28	%C29	C29/C27
LA0002	2.82	0.82	0.35	-27.73	-27.37	-2.25	0.7	0.11	0.27	0.40	1.72	28.10	34.10	37.80	1.35
LA0003	2.96	0.72	0.26	-27.77	-26.62	-0.49	1.09	0.14	0.21	0.65	2.48	28.00	32.50	39.50	1.41
LA0066	2.3	1.63	0.96	-26.89	-26.18	-1.74	0.68	0.12	0.4	0.35	1.49	29.90	34.70	35.40	1.18
LA0099	2.19	0.66	0.35	-27.02	-26.09	-1.21	0.58	0.1	0.56	0.28	1.07	31.00	34.30	34.70	1.12
LA0100	2.52	0.67	0.34	-27.2	-26	-0.55	0.7	0.13	0.56	0.31	1.65	31.60	34.20	34.20	1.08
LA0140	2.48	0.72	0.32	-27.16	-26.2	-1.1	0.79	0.12	0.56	0.36	2.07	32.10	34.70	33.20	1.03
LA0141	2.35	0.81	0.43	-27.44	-26.74	-1.59	0.88	0.14	0.62	0.47	2.79	31.10	34.00	35.00	1.13
LA0268	2.13	0.5	0.25	-27.17	-26.02	-0.67	0.62	0.08	0.59	0.29	0.53	27.60	34.00	38.40	1.39
LA0273	2.65	0.78	0.36	-27.37	-26.5	-1.23	0.65	0.11	0.66	0.31	1.98	32.00	35.40	32.50	1.02
LA0275	2.81	0.65	0.31	-27.54	-26.29	-0.34	0.98	0.15	0.59	0.53	4.16	32.10	33.70	34.20	1.07
LA0313	2.03	0.52	0.27	-27.11	-25.84	-0.43	0.55	0.07	0.37	0.43	1.38	30.40	32.90	36.70	1.21
LA0354	2.8	0.55	0.24	-27.52	-26.28	-0.37	0.88	0.13	0.66	0.40	2.30	30.40	34.80	34.80	1.14
LA0360	2.39	0.45	0.23	-27.08	-26.09	-1.06	0.52	0.12	0.5	0.25	0.95	30.20	34.50	35.30	1.17
LA0380	2.79	0.83	0.4	-27.34	-26.42	-1.13	0.72	0.12	0.59	0.35	1.88	29.40	36.40	34.20	1.16
LA0382	2.58	0.77	0.35	-27.1	-26.35	-1.58	0.78	0.11	0.48	0.42	1.86	30.00	36.50	33.50	1.12
LA0392	2.27	0.66	0.32	-26.96	-26.28	-1.78	0.65	0.11	0.47	0.36	1.30	29.90	34.70	35.40	1.18
LA0393	2.21	0.57	0.29	-27.49	-26.32	-0.53	0.97	0.14	0.42	1.01	4.55	27.4	33.6	39.00	1.42
LA0402	1.77	0.38	0.23	-26.85	-25.62	-0.6	0.67	0.14	0.65	0.35	1.48	29.60	34.20	36.30	1.23
LA0431	2.9	0.78	0.32	-27.15	-26.46	-1.7	0.73	0.1	0.6	0.35	2.00	30.40	35.30	34.30	1.13

Pr/ph= pristane/phytane. Pr/nC17 = pristane/ C17 *n*-alkane. Ph/ nC18 =phytane/ C18 *n*-alkane. d13C Sat= $\delta^{13}C$ of saturated hydrocarbon fractions. d13CAro =$\delta^{13}C$ of aromatic hydrocarbon fractions. CV= canonical variable (CV = -2.53(δ13C sat.) + 2.22(δ13C arom.)-11.65). Ts/Tm = 18α(H)- 22,29,30- Trisnorneohopane (Ts)/17α(H)- 22,29,30-trisnorhopane (Tm). Ol/C30 Hop= 18α(H) + 18β(H) oleanane/ 17α(H), 21β(H) hopane. St/Terp= sum of all C27-C29 steranes / C27-C30 terpanes. C29 St 20S/R= 5α(H),14α(H), 17α(H)- C_{29} 20S/20S+20R sterane isomerisation maturity parameter. Dia/Reg Ster = sum of all C27-29 27-29 βα+ ββ diasteranes /ααα steranes. % C27, %C28 and %C29 = C_{27}, C_{28}, C_{29} as a percentage of sum 27-29 for 5α(H),14α(H), 17α(H)- 20R sterane. C29/C27= ratio of C29/C27 sterane for the 5α(H),14α(H), 17α(H)- 20R configuration.

Appendix ID: table of biomarker data for Miocene reservoired oils in Kutei Basin, Indonesia.

Sample	Pr/Ph	OL index	Bicad	C29 20S/ S+R	%C27	%C28	%C29	C27/C28	C29/C27	Reference
S3	4.36	16.3	47.4	0.62	14	29	57	0.48	4.07	Curiale et al 2005
S5	0	16.8	43.4	0.46	36	24	40	1.50	1.11	Curiale et al 2005
S6	0	12.6	38.9	0.45	11	19	71	0.58	6.45	Curiale et al 2005
S7	5.81	17.9	51.4	0.41	9	20	71	0.45	7.89	Curiale et al 2005
S9	1.86	11.7	57.5	0.49	36	27	38	1.33	1.06	Curiale et al 2005
S10	0	17.8	45.9	0.4	28	29	43	0.97	1.54	Curiale et al 2005
S35	4.66	39.6	71.9	0.33	14	26	60	0.54	4.29	Curiale et al 2005
S36	5.13	39.2	52.1	0.16	19	31	50	0.61	2.63	Curiale et al 2005
S38	5.6	45.2	66.2	0.25	11	27	62	0.41	5.64	Curiale et al 2005
S39	5.37	49.8	57.1	0.18	26	20	54	1.30	2.08	Curiale et al 2005
S51	2.06	26.8	50.3	0.37	12	23	66	0.52	5.50	Curiale et al 2005
S54	0	58.9	89.7	0	13	18	69	0.72	5.31	Curiale et al 2005
S55	0	64.9	95.1	0.42	19	18	64	1.06	3.37	Curiale et al 2005
S56	0	65.6	94	0.31	7	15	78	0.47	11.14	Curiale et al 2005
S57	0	67.3	93.5	0.25	7	16	77	0.44	11.00	Curiale et al 2005
S58	5.16	58.2	92.4	0.33	9	16	75	0.56	8.33	Curiale et al 2005
S59	4.86	61.1	92.9	0.31	10	16	74	0.63	7.40	Curiale et al 2005
S60	6.03	56.6	86.7	0.24	15	18	67	0.83	4.47	Curiale et al 2005
S61	0	79.2	87	0.11	15	20	65	0.75	4.33	Curiale et al 2005
S62	0	79	95.7	0.51	11	17	73	0.65	6.64	Curiale et al 2005
S63	0	82.2	94.6	0.5	8	15	77	0.53	9.63	Curiale et al 2005
S67	10.03	56.6	70.1	0.37	15	18	67	0.83	4.47	Curiale et al 2005
S68	5.8	62	66.2	0.32	20	21	59	0.95	2.95	Curiale et al 2005
S69	7.19	10.5	23.9	0.48	7	21	72	0.33	10.29	Curiale et al 2005
S70	4.19	22.9	22.8	0.4	13	22	65	0.59	5.00	Curiale et al 2005
S71	9	9.8	12	0.46	28	29	44	0.97	1.57	Curiale et al 2005
S72	5.32	22.6	36.5	0.39	11	21	68	0.52	6.18	Curiale et al 2005
S73	6.53	30.3	30.9	0.29	11	21	68	0.52	6.18	Curiale et al 2005
S74	0	53.6	96.6	0.15	16	31	53	0.52	3.31	Curiale et al 2005
S75	0	58.2	94.8	0.34	20	29	51	0.69	2.55	Curiale et al 2005
S76	0	64.2	94.3	0.32	13	23	64	0.57	4.92	Curiale et al 2005
S77	0	60.4	89.1	0.41	9	23	69	0.39	7.67	Curiale et al 2005

Pr/ph= pristane/phytane. OL index = 100* 18α(H) + 18β(H) oleanane/(18α(H) + 18β(H) oleanane + 17α(H), 21β(H) hopane. Bicad= 100* sum of all bicadinane isomers normalized to C30 αβ hopne. C_{29}20S/S+R= 5α(H),14α(H), 17α(H)- C_{29} 20S/20S+20R sterane isomerisation maturity parameter. % C27, %C28 and %C29 = C_{27}, C_{28}, C_{29} as a percentage of sum 27-29 for 5α(H),14α(H), 17α(H)- 20R sterane. C27/C28= ratio of C27 an C28 sterane for the 5α(H),14α(H), 17α(H)- 20R . C29/C27= ratio of C29/C27 sterane for the 5α(H),14α(H), 17α(H)- 20R configuration.

Appendix IE: Table of published bulk, biomarker and stable carbon isotopes of oils from Mahakam Delta, Indonesia

Field	Depth (ft')	Res. Age	API	wt % Sulphur	Pr/Ph	Pr/ nC17	Ph/ nC18	d13C Sat	d13 C Aro	CV	OL Index	Bicad/ Hop	C32 S/S+R	C29 20S /S+R	C29 St αββ	%C27	%C28	%C29	C29/ C27	% C30	Reference
Apar-1	8416	Middle Miocene	m/u	<0.1	5.33	1.43	0.27	-29.45	-27.22	2.43	91	4.2	0.59	0.48	0.51	11.3	22.8	65.9	5.83	0.00	Peters et al 2000
Attaka		late Miocene	40.4	<0.1	6.9	1.62	0.3	-29.38	-27.45	1.74	44	6.78	0.59	0.35	0.34	15.2	27.5	57.3	3.77	0.00	Peters et al 2000
Attaka		late Miocene	40.4	0.027	7.11	1.67	0.29	-29.5	-27.58	1.76	44	6.92	0.66	0.38	0.38	13.3	29.5	57.2	4.30	0.00	Peters et al 2000
Badak-122	6808	late Miocene	49.5	0.001	0	1.77	0	-28.06	-29.46	-6.06	29	4.26	0.56	0.46	0.54	37.5	33	29.5	0.79	5.00	Peters et al 2000
Badak-417	9992	Middle Miocene	45.7	0.001	0	1.83	0	-28.13	-27.13	-0.71	28	4.55	0.64	0.42	0.55	36.5	37.2	26.3	0.72	5.00	Peters et al 2000
Bekapai-B9	7511	late Miocene	34	<0.1	6.09	1.78	0.27	-29.58	-27.78	1.52	45	9.32	0.58	0.40	0.42	13.6	28.7	57.7	4.24	0.00	Peters et al 2000
Bekapai-BH1	4992	late Miocene	34.7	0.001	7.31	2	0.35	-29.4	-27.47	1.75	50	6.32	0.6	0.30	0.29	14.1	26.3	59.6	4.23	0.00	Peters et al 2000
Bekapai-BJ1	6406	late Miocene	m/u	0.001	6.1	1.79	0.31	-29.48	-27.82	1.17	46	5.09	0.58	0.26	0.19	14.3	26.4	59.3	4.15	0.00	Peters et al 2000
Bekapai-BK3	7888	late Miocene	31.8	0.001	6.95	1.86	0.32	-29.27	-27.6	1.13	46	6.22	0.59	0.33	0.30	15.8	26.3	57.9	3.66	0.00	Peters et al 2000
Bekapai-G7	8039	late Miocene	34	<0.1	6.25	1.64	0.27	-29.46	-27.84	1.08	45	8.6	0.57	0.32	0.35	14.2	26.7	59.1	4.16	0.00	Peters et al 2000
Bekapai-B11-DST1	12405	Middle Miocene	27.4	0.03	5.04	1.23	0.27	-28.92	-27.09	1.38	39	5.44	0.58	0.58	0.59	18	20.6	61.4	3.41	0.00	Peters et al 2000
Bekapai-B11-DST3	11342	late Miocene	34.3	0.001	6.02	1.43	0.24	-29.82	-27.18	3.45	48	13.07	0.56	0.43	0.42	14.6	28.5	56.9	3.90	0.00	Peters et al 2000
Bekapai-B4-DST1	7400	late Miocene	30.9	0.001	5.85	1.85	0.32	-29.42	-27.49	1.75	49	9.31	0.56	0.37	0.34	15.8	29.4	54.8	3.47	0.00	Peters et al 2000
Bekapai-B4-DST5	4339	late Miocene	45.2	0.001	3.79	0.83	0.23	-26.88	-26.07	-1.52	25	3.3	0.61	0.49	0.54	37.9	29.1	33	0.87	2.30	Peters et al 2000
Handil-H2	7505	Middle Miocene	m/u	<0.1	6.38	1.96	0.29	-30.17	-27.71	3.16	41	9.34	0.57	0.50	0.60	6	26.2	67.8	11.30	0.00	Peters et al 2000
Handil-H501 DST2	7095	late Miocene	m/u	0.001	5.7	1.86	0.36	-29.88	-27.19	3.58	43	13.86	0.59	0.55	0.69	8.9	23.6	67.5	7.58	0.00	Peters et al 2000
Handil -H6	8157	Middle Miocene	m/u	m/u	5.94	1.96	0.31	-30.1	-27.4	3.67	26	7.61	0.56	0.50	0.64	4.4	22.7	72.9	16.57	0.00	Peters et al 2000
Handil-H6	8567	Middle Miocene	m/u	0.001	5.61	1.73	0.28	-30.01	-27.36	3.54	38	6.74	0.56	0.53	0.66	6	25.7	68.3	11.38	0.00	Peters et al 2000
Handil-H6 DST3A	8344	Middle Miocene	35.8	0.001	7.07	1.53	0.25	-29.53	-27.09	2.92	34	13.58	0.6	0.60	0.71	22.2	32	45.8	2.06	0.00	Peters et al 2000
Handil-H-6 DST5	7364	late Miocene	34.7	0.001	6.97	1.69	0.29	-29.36	-27.11	2.45	39	15.21	0.59	0.50	0.63	12.5	30.3	57.2	4.58	0.00	Peters et al 2000
Handil-HB365 DST1	3831	Pliocene	m/u	0.001	6.41	1.95	0.32	-29.62	-27.25	2.79	41	11.06	0.6	0.52	0.63	8.1	24.8	67.1	8.28	0.00	Peters et al 2000
Handil-HB365 DST3	3070	Pliocene	m/u	0.001	6.61	2.55	0.41	-29.67	-27.33	2.74	40	9.8	0.59	0.48	0.59	7.4	24.7	67.9	9.18	0.00	Peters et al 2000
Handil-HCB252S DST3	4923	late Miocene	33.9	0.001	6.22	1.76	0.29	-29.98	-27.35	3.48	39	11.88	0.6	0.50	0.62	7.3	26.4	66.3	9.08	0.00	Peters et al 2000
Handil-HI385 DST1	10995	Middle Miocene	m/u	m/u	6.05	2.2	0.36	-29.86	-27.25	3.4	26	9.39	0.6	0.55	0.71	8.8	22.6	68.6	7.80	0.00	Peters et al 2000
Handil-HL263S DST2	3142	Pliocene	m/u	m/u	6.43	2.45	0.4	-29.95	-27.35	3.41	39	9.99	0.59	0.52	0.59	6.2	24.7	69.1	11.15	0.00	Peters et al 2000
Handil-HN190 DST1	7774	Middle Miocene	m/u	0.001	5.57	1.71	0.28	-29.86	-27.19	3.53	40	10.91	0.59	0.52	0.62	8.9	22.7	68.4	7.69	0.00	Peters et al 2000
Handil-HQ2S	3346	Pliocene	33	<0.1	7.51	1.96	0.27	-29.96	-27.57	2.94	40	10.63	0.57	0.50	0.60	9.2	26.5	64.3	6.99	0.00	Peters et al 2000
Handil-HY1 DST1	3546	Pliocene	m/u	0.001	6.94	2.05	0.32	-29.61	-27.23	2.81	40	10.65	0.59	0.51	0.58	6.5	25	68.5	10.54	0.00	Peters et al 2000
Handil-HL275s	1479	Pliocene	m/u	<0.1	7.43	2.94	0.37	-29.79	-27.67	2.29	39	9.75	0.57	0.49	0.60	7.8	27.5	64.7	8.29	0.00	Peters et al 2000
HandilKerbau-2	12897	Middle Miocene	m/u	<0.1	6.47	2.29	0.3	-30.31	-27.74	3.45	24	8.14	0.59	0.56	0.73	9.8	27.5	62.7	6.40	0.00	Peters et al 2000
Mutiara-41	3470	late Miocene	41	0.016	5.71	1.51	0.26	-29.58	-27.13	2.96	26	12.02	0.63	0.57	0.70	19.9	42.3	37.8	1.90	0.00	Peters et al 2000
Mutiara-48	2144	late Miocene	35.7	0.023	3.89	0.73	0.2	-26.45	-26.16	-2.81	39	8.85	0.6	0.52	0.59	28.4	31	40.6	1.43	2.90	Peters et al 2000
Nilam-130L	12288	Middle Miocene	32.5	0.035	5.87	1.86	0.29	-29.71	-27.16	3.22	41	16.73	0.61	0.53	0.60	13.9	44	42.1	3.03	0.00	Peters et al 2000
Nilam-164	10564	Middle Miocene	m/u	m/u	5.74	1.88	0.36	-30.24	-27.44	3.94	32	12.59	0.6	0.49	0.55	8	36.7	55.3	6.91	0.00	Peters et al 2000
Nilam-N19U D-59	8843	Middle Miocene	m/u	0.001	5.43	1.31	0.26	-29.9	-27.2	3.61	42	11.77	0.58	0.56	0.63	6.9	28.9	64.2	9.30	0.00	Peters et al 2000
Peciko	0	late Miocene	41.7	0.001	10.87	12.43	1.81	-29.57	-27.76	1.53	20	28.58	0.6	0.50	0.32	18.4	32.7	48.9	2.66	0.00	Peters et al 2000
Perintis-1 DST3	10509	Middle Miocene	50.2	0.03	6.33	1.52	0.26	-28.3	-27.5	-1.1	42	10.85	0.58	0.34	0.28	15.3	24.1	60.6	3.96	0.00	Peters et al 2000
Ragat-1 DST 3	8079	late Miocene	30.8	0.08	5.38	1.52	0.3	-28.8	-27.8	-0.5	56	9.72	0.58	0.30	0.31	14.3	23.8	61.9	4.33	0.00	Peters et al 2000
Seguni	0	Middle Miocene	42.4	0.001	6.36	1.85	0.35	-28.98	-27.25	1.17	56	13.35	0.56	0.44	0.41	11.4	29.8	58.8	5.16	0.00	Peters et al 2000
Semanlu-1	10155	Middle Miocene	32	<0.1	6.2	1.77	0.28	-29.71	-27.62	2.2	46	10.92	0.59	0.48	0.52	7.3	27.4	65.3	8.95	0.00	Peters et al 2000
Semberah-037	7590	Middle Miocene	42.6	0.001	4.59	1.18	0.24	-29.63	-26.76	3.91	32	15.57	0.58	0.60	0.72	10.2	34.5	55.3	5.42	0.00	Peters et al 2000
semberah-31L	10596	Middle Miocene	m/u	0.001	0	0	0	-26.62	-27.22	-4.73	0	0	0	0.48	0.59	32.6	32.7	34.7	1.06	5.10	Peters et al 2000
Sepinggan	0	Middle Miocene	33.8	0.041	5.98	1.89	0.38	-28.86	-27.13	1.14	40	10.62	0.65	0.36	0.34	11.8	39	49.2	4.17	0.00	Peters et al 2000
Sepinggan	0	Middle Miocene	30.8	0.001	5.81	1.95	0.39	-28.72	-27.09	0.87	40	12.22	0.58	0.29	0.31	12	28.2	59.8	4.98	0.00	Peters et al 2000
Serang	0	late Miocene	39.2	0.043	6.9	1.75	0.31	-29.55	-27.83	1.33	40	5.03	0.66	0.34	0.32	14.2	30.5	55.3	3.89	0.00	Peters et al 2000
sisi-1 DST 3	10867	late Miocene	34.3	0.06	6.65	1.68	0.29	-29.2	-27.5	1.18	51	16.48	0.56	0.44	0.45	13.1	25.4	61.5	4.69	0.00	Peters et al 2000
Tambora-T19	9840	Middle Miocene	40	<0.10	7.24	1.94	0.26	-30.19	-27.68	3.28	30	7.19	0.57	0.52	0.66	9.4	26.2	64.4	6.85	0.00	Peters et al 2000
Tambora-T11bis	9299	Middle Miocene	38	<0.10	7.99	3.36	0.41	-30.32	-27.97	2.97	32	5.45	0.58	0.52	0.57	5.9	26.7	67.4	11.42	0.00	Peters et al 2000
Tunu-T5	11306	late Miocene	m/u	<0.10	5.76	1.57	0.25	-30.05	-27.62	3.06	51	18.72	0.59	0.48	0.51	9.2	25.5	65.3	7.10	0.00	Peters et al 2000
Tunu-TN5 DST3	12015	late Miocene	35.5	0.001	6.51	2.14	0.36	-29.77	-27.43	2.77	38	10.48	0.59	0.51	0.42	7.4	22	70.6	9.54	0.00	Peters et al 2000
Tunu-TN5 DST5	10621	late Miocene	43.9	0.001	7.3	2.09	0.33	-29.47	-27.41	2.06	57	17.56	0.57	0.47	0.38	14.6	30.5	54.9	3.76	0.00	Peters et al 2000
Tunu-TNW10 DST2	14088	Middle Miocene	m/u	0.001	6.04	1.6	0.37	-29.71	-27.39	2.71	40	10.15	0.59	0.58	0.61	11.3	24.2	64.5	5.71	0.00	Peters et al 2000
Tunu-TNW2 DST1	11936	late Miocene	42.6	0.001	6.32	1.72	0.29	-28.92	-27.1	1.36	49	15.41	0.58	0.54	0.48	11.3	26.9	61.8	5.47	0.00	Peters et al 2000
Tunu-TNW2 DST2	11592	late Miocene	42.8	0.001	6.15	1.17	0.26	-29.22	-27.1	2.11	40	17.24	0.58	0.48	0.43	11.4	30.8	57.8	5.07	0.00	Peters et al 2000
Tunu-TNW3 DST2 BIS	13074	Middle Miocene	26.6	0.001	5.31	1.27	0.31	-29.16	-26.84	2.54	39	11.46	0.59	0.59	0.63	9.1	25.1	65.8	7.23	0.00	Peters et al 2000

Appendix IE continued.

Field	Depth (ft)	Res. Age	API	wt % Sulphur	Pr/Ph	Pr/ nC17	Ph/ nC18	d13C Sat	d13 C Aro	CV	OL Index	Bicad/ Hop	C32 S/S+R	C29 20S /S+R	C29 St αββ	%C27	%C28	%C29	C29/ C27	% C30	Reference
Tunu-TNW3 DST2 BIS	13074	Middle Miocene	26.6	0.001	5.31	1.27	0.31	-29.16	-26.84	2.54	0	0	0	0.58	0.60	10.1	25.9	64	6.34	0.00	Peters et al 2000
Tunu-TNW3 DST3	12333	Middle Miocene	30.2	0.001	6.27	1.6	0.32	-29.66	-27.37	2.63	41	12.49	0.58	0.51	0.42	6.4	19.2	74.4	11.63	0.00	Peters et al 2000
Tunu-TNW4 DST1	12070	late Miocene	35.3	0.001	6.68	1.65	0.34	-29.46	-27.45	1.94	29	8.89	0.59	0.52	0.42	10.1	24	65.9	6.52	0.00	Peters et al 2000
Tunu-TNW7 DST1	12366	Middle Miocene	36.1	0.001	6.76	1.94	0.36	-29.38	-27.32	2.03	46	18.41	0.57	0.52	0.46	18.3	23.8	57.9	3.16	0.00	Peters et al 2000
Tunu-TNW9 DST1 TER	12969	Middle Miocene	38.5	0.001	6.39	1.3	0.28	-29.71	-27.25	3.02	40	5.97	0.59	0.53	0.55	12.3	22.6	65.1	5.29	0.00	Peters et al 2000
Tunu-TNW9 DST2	12808	Middle Miocene	37.5	0.001	6.89	2.14	0.42	-29.64	-27.59	2.09	24	18.92	0.6	0.60	0.49	13.9	37.6	48.5	3.49	0.00	Peters et al 2000
Merah- Besar-6 DST 1	8537	Late Miocene	35.5	0.035	6.25	2.37	0.4	-29.08	-27.67	0.49	55	0	0.57	0.17	0.17	11.6	29.6	58.8	5.07	0.00	Peters et al 2000
Merah- Besar-6 DST 3	6810	Late Miocene	56.4	0.013	15.42	3.75	0.43	-31.3	-27.51	6.47	29	0	0.65	0.09	0.09	14.7	29.6	55.7	3.79	0.00	Peters et al 2000

API= API gravity. % sulphur= Wt % elemental sulphur in oil. Pr/ph= pristane/phytane. Pr/nC17 = pristane/ C17 *n*-alkane. Ph/ nC18 =phytane/ C18 *n*-alkane. d13C Sat= $\delta^{13}C$ of saturated hydrocarbon fractions. d13CAro =$\delta^{13}C$ of aromatic hydrocarbon fractions. CV= canonical variable (CV = -2.53(δ13C sat.) + 2.22(δ13C arom.)-11.65). OL index = 100* 18α(H) + 18β(H) oleanane/(18α(H) + 18β(H) oleanane + 17α(H), 21β(H) hopane. Bicad= sum of all bicadinane isomers/ 17α(H), 21β(H) hopane. C32 S/S+R =. 17α(H), 21β(H)-bishomohopane 22S/ 22S+ 22R thermal maturity parameter. C_{29}20S/S+R= 5α(H),14α(H), 17α(H)- C_{29} 20S/20S+20R sterane isomerisation maturity parameter. C29 αββ = C_{29} αββ/αββ+ααα sterane isomerisation thermal maturity parameter % C27, %C28 and %C29 = C_{27}, C_{28}, C_{29} as a percentage of sum 27-29 for 5α(H),14α(H), 17α(H)- 20R sterane. C29/C27= ratio of C29/C27 sterane for the 5α(H),14α(H), 17α(H)- 20R configuration. %C30= C30 to sum C27-C30 for 5α(H),14α(H), 17α(H)- 20R steranes expressed as a percentage.

Appendix IF: Table of published biomarker and stable carbon isotope data for western Niger Delta oils, Nigeria

Sample	Field	Depth	d13C Sat	d13 C aro	CV	Ts/(Ts+Tm)	Dia/(Dia + Reg	C29 abb	%C27	%C28	%C29
A1	A	5811	-25.87	-25.87	-2.69	48.97	29.64	36.08	31.48	33.33	35.19
A2		6221	-26.34	-26.34	-3.61	47.66	28.30	37.41	31.62	33.90	34.48
A3		6297	-26.44	-26.44	-4.67	47.72	30.07	37.60	33.38	33.99	32.62
A4		6654	-25.83	-25.83	-2.98	45.56	30.12	36.23	29.04	41.92	29.04
A5		6693	-25.81	-25.81	-2.11	45.18	26.75	33.00	32.03	38.59	29.37
A6		7172	-26.01	-26.01	-4.32	50.34	23.57	35.94	33.03	33.62	33.35
A7		7257	-25.65	-25.65	-3.83	51.81	24.14	36.67	37.26	32.23	30.51
A8		7516	-25.72	-25.72	-3.55	52.11	20.73	36.75	32.12	32.95	34.93
A9		7565	-25.88	-25.88	-1.91	47.72	27.45	39.05	33.66	32.06	34.28
A10		8175	0	0	0.00	44.28	25.70	33.59	32.44	33.50	34.06
A11		8195	0	0	0.00	44.09	22.16	33.21	29.22	34.05	36.73
A12		8365	0	0	0.00	44.65	26.97	36.27	33.77	35.15	31.08
B1	B	6820	-25.98	-25.98	-2.76	50.15	24.50	32.48	25.35	33.23	41.42
B2		5558	-25.9	-25.9	-3.34	51.48	28.70	34.66	31.59	30.76	37.65
B3		6021	-25.88	-25.88	-3.67	51.91	32.53	37.21	31.44	31.49	37.07
B4		6100	-25.7	-25.7	-1.91	47.62	25.64	31.05	26.12	33.99	39.89
B5		6175	-25.89	-25.89	-3.32	50.17	31.09	38.05	32.49	30.41	37.10
B6		6886	-26.15	-26.15	-1.27	56.78	39.29	46.21	23.55	41.07	35.38
B7		6081	-25.83	-25.83	-2.38	49.09	30.22	33.66	29.33	31.20	39.47
B8		8602	-26.07	-26.07	-3.16	48.90	30.50	37.01	33.45	31.37	35.17
B9		8733	-25.74	-25.74	-2.28	48.12	27.05	37.19	29.77	32.60	37.62
C1	C	5351	-26.07	-26.07	-2.56	50.70	26.82	32.45	22.07	39.13	38.80
C2		5994	-26	-26	-0.15	50.38	23.67	38.09	23.54	26.99	49.47
C3		6580	-25.93	-25.93	-0.02	49.62	30.26	28.52	23.88	38.21	37.90
C4		7075	-25.9	-25.9	0.68	51.86	30.66	54.87	23.17	31.55	45.28
C5		7246	-25.9	-25.9	-0.05	48.38	28.85	33.38	20.67	40.70	38.64
C6		9140	-26.02	-26.02	-1.94	43.74	23.74	25.91	20.90	25.71	53.00
C7		9991	-26.27	-26.27	0.59	47.91	28.15	33.52	26.37	28.54	45.09
D1	D	7186	-25.56	-25.56	-2.06	46.09	29.60	37.85	41.18	29.41	29.41
D2		6984	-25.59	-25.59	-2.76	46.47	18.56	34.24	33.20	32.27	34.53
D3		7002	-25.67	-25.67	-3.06	46.34	20.19	34.00	33.36	33.75	32.90
D4		8151	-25.57	-25.57	-4.08	47.27	28.76	37.56	32.30	33.03	34.67
D5		7072	-25.63	-25.63	-2.92	45.85	21.36	31.22	35.05	33.63	31.32
D6		8045	0	0	0.00	48.98	18.80	33.97	31.85	32.80	35.34
D7		7843	0	0	0.00	43.04	17.08	34.44	35.63	32.63	31.75
E1	E	6100	-25.69	-25.69	-2.04	45.97	19.43	27.69	34.09	30.17	35.74
E2		6030	-25.84	-25.84	2.63	45.60	20.34	33.35	34.83	28.47	36.70
E3		6180	-25.93	-25.93	-2.32	45.81	18.78	31.79	33.53	29.01	37.46
E4		8713	-25.89	-25.89	-2.21	47.46	20.73	34.28	32.76	31.91	35.33
E5		8523	-25.85	-25.85	-2.19	45.42	22.11	30.57	37.58	32.01	30.41
E6		8774	-25.82	-25.82	-2.18	45.37	21.14	32.34	29.90	33.33	36.77
F1	F	8270	-25.8	-25.8	0.27	50.74	30.01	31.81	20.18	28.35	51.47
F2		6990	-25.83	-25.83	-0.33	46.64	23.80	28.26	25.79	27.02	47.18
F3		7399	-25.79	-25.79	-3.50	48.99	27.20	35.28	19.82	40.13	40.05
F4		7585	-25.93	-25.93	-1.61	45.40	27.68	30.19	19.12	46.92	33.97
F5		8085	-25.73	-25.73	-0.43	45.45	27.96	25.17	17.94	36.77	45.29
F6		10460	-25.74	-25.74	0.02	50.03	30.72	36.95	27.60	27.80	44.60
G1	G	6272	-25.76	-25.76	-2.45	46.77	17.90	33.75	31.69	33.76	34.55
G2		6421	-25.67	-25.67	-2.12	46.91	17.31	31.04	30.71	32.19	37.11
G3		6625	-26.03	-26.03	-2.82	49.09	28.42	36.58	41.65	31.49	26.85
G4		7649	-26.06	-26.06	-3.27	49.04	21.57	34.46	32.07	31.80	36.12
G5		7381	-25.69	-25.69	-3.15	54.93	22.04	41.12	30.78	31.37	37.85
G6		8205	-25.9	-25.9	-4.03	61.00	23.57	40.83	30.81	31.84	37.35
G7		8505	-25.81	-25.81	-4.69	59.08	24.27	41.01	32.09	29.84	38.07
H1	H	6493	-25.47	-25.47	-5.55	58.56	28.82	45.75	31.71	29.52	38.77
H2		6761	-25.47	-25.47	-6.06	58.21	31.45	41.75	31.72	29.26	39.02
H3		6867	-25.47	-25.47	-6.51	60.68	33.45	45.15	31.71	30.65	37.64
H4		9619	-25.81	-25.81	-7.39	65.67	39.93	50.21	31.82	28.88	39.30
I1	I	8061	-27.33	-27.33	-2.72	46.20	27.64	31.57	25.66	35.80	38.54
I2		8702	-27.22	-27.22	-1.39	49.79	30.93	44.50	14.32	18.00	67.00
I3		9302	-27.42	-27.42	-1.71	41.56	28.02	41.95	31.85	31.15	37.00
J1	J	6544	-25.94	-25.94	-2.82	53.84	22.14	41.84	37.21	37.62	25.18
J2		10894	-25.74	-25.74	-2.91	50.06	24.79	37.92	33.86	30.39	35.75
	K	4586	-25.63	-25.63	-2.21	51.18	24.78	40.32	35.34	31.87	32.79
		4601	-25.88	-25.88	-4.74	52.06	21.74	39.19	30.55	31.20	38.26

d13C Sat= $\delta^{13}C$ of saturated hydrocarbon fractions. d13CAro =$\delta^{13}C$ of aromatic hydrocarbon fractions. CV= canonical variable (CV = -2.53(δ13C sat.) + 2.22(δ13C arom.)-11.65). Ts/Ts+Tm = 18α(H)- 22,29,30- Trisnorneohopane (Ts)/ 18α(H)- 22,29,30- Trisnorneohopane (Ts) + 17α(H)- 22,29,30-trisnorhopane (Tm). Dia/ Dia+reg = sum of all C27-29 27-29 βα+ ββ diasteranes / C27-29 27-29 βα+ ββ diasteranes + αββ and ααα steranes. C29 abb= C_{29} αββ/αββ+ααα sterane isomerisation thermal maturity parameter. % C27, %C28 and %C29 = C_{27}, C_{28}, C_{29} as a percentage of sum 27-29 for 5α(H),14α(H), 17α(H)- 20R sterane.

Appendix IIIA

Peak	Peak Identity
1.	C_{27} 13β(H), 17α(H)- diasterane (20S)
2.	C_{27} 13β(H), 17α(H)- diasterane (20R)
3.	C_{27} 13α(H), 17β(H)- diasterane (20S)
4.	C_{27} 13α(H), 17β(H)- diasterane (20R)
5.	C_{27} 5α(H), 14α(H), 17α(H)- sterane (20S)
6.	C_{27} 5α(H), 14β(H), 17β(H)- sterane (20S+ 20R)
7.	C_{27} 5α(H), 14α(H), 17α(H)- sterane (20R)
8.	C_{28} 13β(H), 17α(H)- diasterane (24S+24R)
9.	C_{28} 13β(H), 17α(H)- diasterane (24S+24R)
10.	C_{28} 13α(H), 17β(H)- diasterane (20S)
11.	C_{28} 13α(H), 17β(H)- diasterane (20R)
12.	C_{28} 5α(H), 14α(H), 17α(H)- sterane (20S)
13.	C_{28} 5α(H), 14β(H), 17β(H)- sterane (20S+ 20R)
14.	C_{28} 5α(H), 14α(H), 17α(H)- sterane (20R)
15.	C_{29} 13β(H), 17α(H)- diasterane (20S)
16.	C_{29} 13β(H), 17α(H)- diasterane (20R)
17.	C_{29} 13α(H), 17β(H)- diasterane (20S)
18.	C_{29} 13α(H), 17β(H)- diasterane (20R)
19.	C_{29} 5α(H), 14α(H), 17α(H)- sterane (20S)
20.	C_{29} 5α(H), 14β(H), 17β(H)- sterane (20S+ 20R)
21.	C_{29} 5α(H), 14α(H), 17α(H)- sterane (20R)
22.	C_{30} 13β(H), 17α(H)- diasterane (20S)
23.	C_{30} 13β(H), 17α(H)- diasterane (20R)
24.	C_{30} 13α(H), 17β(H)- diasterane (20S)
25.	C_{30} 13α(H), 17β(H)- diasterane (20R)
26.	C_{30} 5α(H), 14α(H), 17α(H)- sterane (20S)
27.	C_{30} 5α(H), 14β(H), 17β(H)- sterane (20S+ 20R)
28.	C_{30} 5α(H), 14α(H), 17α(H)- sterane (20R)

Appendix IIIB

Peak	Peak Identity
Ts	18α(H)- 22,29,30- Trisnorneohopane (Ts)
Tm + T-Bicad	17α(H)- 22,29,30-trisnorhopane (Tm) + trasn-trans-trans bicadinanes
30T S,R	C_{30} tricyclic terpane (24S+24R)- cheilanthane series
28H	17α(H), 21β(H)-norhopane
29H	17α(H), 21β(H)-norhopane
29Ts	18α(H) – norneohopane
D30	17α(H) - diahopane
29M	17β(H), 21α(H)-normoratane
OL	18α(H) + 18β(H)-oleananes
30H	17α(H), 21β(H)-hopane
30M	17β(H), 21α(H)-moratane
T	19α(H)-taraxastane
31S	17α(H), 21β(H)-homohopane (22S)
31R	17α(H), 21β(H)-homohopane (22R)
31S, R MOR	17β(H), 21α(H)-homomoratane (22S+22R)
32S	17α(H), 21β(H)-bidhomohopane (22S)
32R	17α(H), 21β(H)-bishomohopane (22R)
33S	17α(H), 21β(H)-trishomohopane (22S)
33R	17α(H), 21β(H)-trishomohopane (22R)
34S	17α(H), 21β(H)-tetrakishomohopane (22S)
34R	17α(H), 21β(H)-tetrakishomohopane (22R)
35S	17α(H), 21β(H)-pentakishomohopane (22S)
35R	17α(H), 21β(H)-pentakishomohopane (22R)

Appendix IIIC

Peak	Peak Identity
19T	C_{19} Tricyclic terpane- cheilanthane series
20T	C_{20} Tricyclic terpane- cheilanthane series
X	Unknown C_{21} Tricyclic terpane
21T	C_{21} Tricyclic terpane- cheilanthane series
22T	C_{22} Tricyclic terpane- cheilanthane series
23T	C_{23} Tricyclic terpane - cheilanthane series
24T	C_{24} Tricyclic terpane- cheilanthane series
Y	Unknown C_{25} Tricyclic terpane
Y1	10β-des-A-oleanane (C_{24} tetracyclic terpane)
25T	C_{25} Tricyclic terpane (22S+22R) - cheilanthane series
Z	10β-des-A-ursane (C_{24} tetracyclic terpane)
Tet	Tetracyclic terpane – 24-de-E-hopane
26T	C_{26} Tricyclic terpane (22S+22R)-cheilanthane series
Z1	unknown C_{27} terpane
28T	C_{28} Tricyclic terpane (22S+22R) - cheilanthane series
29T	C_{29} Tricyclic terpane (22S+22R) - cheilanthane series